



UNIVERSIDADE D
COIMBRA

Pedro Manuel da Costa Gomes Brandão

**ISATIN AND MULTICOMPONENT REACTIONS:
SUSTAINABLE CATALYTIC SYNTHESIS OF NOVEL
BIOACTIVE OXINDOLE DERIVATIVES**

Tese no âmbito do Doutoramento em Química, ramo de Catálise e Sustentabilidade, orientada pela Professora Doutora Marta Piñeiro Gómez, coorientada pelo Professor Doutor Anthony J. Burke e pelo Doutor Maxim L. Kuznetsov e apresentada ao Departamento de Química da Faculdade de Ciências e Tecnologia da Universidade de Coimbra.

Dezembro de 2021



UNIVERSIDADE D
COIMBRA

Pedro Manuel da Costa Gomes Brandão

**ISATIN AND MULTICOMPONENT REACTIONS:
SUSTAINABLE CATALYTIC SYNTHESIS OF NOVEL
BIOACTIVE OXINDOLE DERIVATIVES**

**Tese no âmbito do Doutoramento em Química, ramo de Catálise e Sustentabilidade,
orientada pela Professora Doutora Marta Piñeiro Gómez, coorientada pelo
Professor Doutor Anthony J. Burke e pelo Doutor Maxim L. Kuznetsov e apresentada
ao Departamento de Química da Faculdade de Ciências e Tecnologia da
Universidade de Coimbra**

Dezembro de 2021

À minha Avó Alice,
por tudo o que me ensinou
(*in memoriam*)

Agradecimentos

A viagem foi complexa, repleta de momentos de grande entusiasmo contrabalançados com momentos de quase desespero, mas tudo isto são sentimentos que fazem parte do desenvolvimento científico... A viagem chega agora ao seu destino, materializado na forma desta Tese. Este objetivo, que eu havia estabelecido há mais de 10 anos, dependeu sempre da minha capacidade de resiliência, persistência e adaptação. No entanto, estas características nunca teriam sido suficientes para me fazer chegar até aqui, e as (pocas) palavras que se seguem, são o meu sentido e singelo agradecimento a todos aqueles que, de forma direta ou indireta, me ajudaram a atingir este objetivo.

As minhas primeiras palavras são, invariavelmente, dedicadas aos meus orientadores, impulsionadores deste projeto que eu agarrei com toda a minha dedicação.

À Professora Doutora Marta Piñeiro Gómez, agradeço a orientação científica, a transmissão de conhecimentos, e a constante capacidade para me manter otimista, mesmo nos momentos em que esta viagem se tornava mais atribulada. Agradeço-lhe a confiança que sempre depositou em mim, e por sempre me ter dado espaço para dar as minhas opiniões e contributos para tornar este projeto o melhor possível, sempre estimulando o meu espírito crítico sobre cada decisão, com uma boa dose de bom humor.

Ao Professor Doutor Anthony J. Burke, pela orientação científica e transmissão de conhecimentos, e pela constante motivação para levar as ideias do projeto mais além, tornando-o mais inovador, robusto e relevante. Agradeço também pelos desafios que me lançou na área da escrita científica e da participação na organização de eventos (ISySyCat 2017, 2019 e 2021), experiências profissionalmente e pessoalmente muito enriquecedoras.

Ao Professor Doutor Maxim Kuznetsov, pela orientação científica e transmissão de conhecimentos na área deste doutoramento onde eu tinha menos experiência, a química computacional. Agradeço todo o esforço e recursos que colocou ao meu dispor para poder aprender mais sobre este ramo da química.

À Professora Doutora Teresa Pinho e Melo, enquanto Coordenadora do Grupo de Química Orgânica do Centro de Química de Coimbra, agradeço pela fácil integração no grupo e pelos desafios que me lançou, nomeadamente na área da química de fluxo.

Às colaborações que foram estabelecidas para os ensaios biológicos, essenciais para o estudo da relevância das novas moléculas por mim sintetizadas, agradeço ao

Professor Doutor José M. Padrón, ao Professor Doutor Óscar López, ao Professor Doutor Holger Stark, à Professora Doutora Eugénia Pinto e à Professora Doutora Gabriela Silva, a quem dirijo um agradecimento especial por ter aberto as portas do seu laboratório da Faculdade de Farmácia da Universidade de Coimbra, o que me permitiu relembrar os tempos das aulas de Microbiologia.

À Dr.^a Sílvia Gramacho pelo contributo nas análises de GC-MS e pela sua boa disposição, e ao Dr. Pedro Cruz pela valiosa ajuda para a obtenção dos espectros de RMN.

Agradeço o apoio financeiro da Fundação para a Ciência e Tecnologia (FCT) através da bolsa de doutoramento do Programa Doutoral CATSUS (PD/BD/128490/2017), assim como à direção deste programa doutoral, por me ter selecionado para o integrar e pelas oportunidades para desenvolver o meu trabalho. Agradeço ainda a todos os meus colegas do CATSUS, pelas trocas de experiências e conhecimentos.

Voltar ao meu país e à academia, depois de quase dois anos a viver num outro país, numa outra cultura, a trabalhar em áreas totalmente distintas, e começar de novo numa cidade que apenas conhecia enquanto turista, longe de tudo e de todos os que conhecia, foi sem dúvida o primeiro grande desafio deste doutoramento. O modo como fui recebido no Lab029 da Universidade de Évora facilitou, em muito, esta transição. Assim, agradeço a todos os que me receberam com uma boa dose de bom humor e com um enorme companheirismo. Tenho de destacar a Doutora Elisabete Carreiro e a Doutora Carolina Marques, pela disponibilidade, amizade, momentos de convívio, paciência para me ouvir e pelos muitos conselhos que me deram, mesmo a quilómetros de distância, durante todo o meu doutoramento e a escrita desta Tese, e por embarcarem nos meus desafios de escrita dos artigos de revisão. Um particular agradecimento à Carolina pela ajuda valiosa com os estudos da reação de Petasis.

A mudança para Coimbra trouxe uma nova jornada de adaptação a um novo grupo e a um novo laboratório. Agradeço a todos os colegas do Grupo de Química Orgânica pelo companheirismo ao longo destes anos. Em particular agradeço à Nélia Tavares (parceira de edição do CATSUS, e todos os desafios administrativos que isso implicou), à Carla Grosso, ao João Ribeiro, ao Nuno Alves, à Ana Mata, ao Américo Alves, à Carla Gomes e à Cláudia Alves pelas discussões científicas salutares e risadas do quotidiano. Agradeço também a valiosa ajuda sempre prestada pela D. Lurdes. Agradeço ainda a todo o corpo docente associado ao laboratório, assim como à Doutoradas Ana Lúcia Cardoso Lopes, à Doutora Susana Martins Lopes e à Doutora Isabel Soares pela ajuda prestada no meu processo de adaptação a este novo laboratório e pela constante partilha de conhecimentos.

Pelas amizades que o Departamento de Química da Universidade de Coimbra me trouxe, durante as produtivas horas de almoço a discutir tudo e mais alguma coisa, por todas as risadas, por todos os conselhos, por todas as conversas antes, durante e depois do confinamento, agradeço a cumplicidade e sinceridade da Daniela, da Estefanía e da Catarina.

Às amizades que a Ciência me trouxe, e que há muitos anos me apoiam nestes caminhos, muitas vezes tortuosos, e que apesar dos quilómetros de distância, oceanos pelo meio, eu sei que estão sempre lá, agradeço à Manu, à Gisela e à Dr^a Sara.

Aos amigos que fiz ao longo do meu percurso, dos tempos da ESE, da FFUP, da Farmácia Mag, da TCS, agradeço pelos valiosos contributos para a minha construção enquanto individuo e profissional.

Por fim tenho de agradecer aqueles que fazem de mim quem eu sou, o meu porto seguro e a minha maior base de apoio, que me deram todas as ferramentas para eu poder voar, sabendo que por mais turbulência que possa encontrar, tenho sempre um local seguro onde voltar, a minha Família. Ao meu Pai, José Manuel, e à minha Mãe, Laura, agradeço todo o amor, a educação, as oportunidades que me deram e o constante apoio para que eu possa realizar os meus sonhos e objetivos e tornar-me um melhor ser humano. À minha Irmã, Sofia, pelo companheirismo desde sempre, por ser minha amiga desde o meu 1^o dia, por estar sempre disponível para me ouvir e aconselhar, e por me incentivar a concretizar os meus sonhos.

À Petra, o Amor da minha vida e a minha melhor amiga, eu agradeço por toda a paciência e dedicação. Agradeço-lhe por ser sempre a primeira a encorajar-me a alcançar os meus sonhos e o meu potencial, muitas vezes acreditando mais nas minhas capacidades que eu próprio. Por me ter incentivado desde o momento em que recebi o e-mail de seleção para o programa doutoral a embarcar nesta aventura, apesar do impacto que isso teria nas nossas vidas, e pelas mudanças que fez na sua vida para me acompanhar nesta reta final da escrita da Tese, dificultada com a presença de uma pandemia, estarei para sempre grato. Pela paciência e pelo amor que sempre demonstrou enquanto eu me dediquei ao trabalho apresentado nesta dissertação, devo-lhe um futuro que agora é nosso, a tornar reais os nossos sonhos e os nossos objetivos. Agradeço também à família dela, por toda a paciência e apoio que sempre nos deram.

Table of Contents

	Page
Abstract.....	xxi
Resumo.....	xxiii
Abbreviations, Acronyms and Symbols.....	xxv
List of Publications Related to the Scientific Topic of the Thesis.....	xxviii
List of Figures, Schemes and Tables.....	xxxix
Chapter 1: General Introduction.....	1
1.1. Getting Inspired by History and Nature in the Quest for New Drug Candidates.....	3
1.2. Selecting Privileged Scaffolds as Starting Point for Drug Discovery.....	5
1.2.1. From Bacteria to Humans: Isatin is Ubiquitous in Nature.....	7
1.2.1.1. Oxindole Derivatives: from Drug Discovery to Clinical Practice.....	10
1.2.1.1.1. Oxindole-Based Drugs Reaching Clinical Trials: Successes and Failures.....	10
1.2.1.1.2. Oxindole-Based Drug Candidates: a Clear Trend.....	13
1.2.1.2. From Nature to the Laboratory: Isatin in Synthetic Organic Chemistry...15	
1.2.2. Tryptanthrin: the Golden-Yellow Alkaloid.....	18
1.2.2.1. Tryptanthrin Derivatives in Drug Discovery.....	22
1.2.2.2. Synthesis and Chemical Transformation of the Tryptanthrin Scaffold...23	
1.3. Selecting Tools for the Discovery of New Potential Bioactive Molecules.....	24
1.3.1. Green Chemistry and Sustainable Chemistry: are They Synonyms?.....	24
1.3.1.1. How to Measure the Sustainability of a Chemical Process?.....	27
1.3.1.2. Green Chemistry in Drug Discovery and Development.....	29
1.3.2. Druglikeness in Drug Discovery.....	31
1.3.3. Multicomponent Reactions: Conscientious Fast-Track for Structural Diversity and Sustainability.....	37
1.3.3.1. Ugi Reaction: a Versatile Isocyanide-Based MCR.....	44
1.3.3.2. Petasis Reaction: Organoboron Reagents in MCRs.....	52
1.4. Bringing Together Privileged Scaffolds and Sustainable Tools: State of the Art and Setting Up the Goals.....	55
1.5. References.....	58

	Page
Chapter 2: In the Quest for New Bioactive Oxindole Derivatives: Engaging Isatin in the U4CR	99
2.1. Introduction.....	101
2.2. Isatin-Based U4CR.....	102
2.2.1. Reaction Conditions Optimization.....	102
2.2.2. Library I Synthesis.....	105
2.2.3. Theoretical Study: Insights into Isatin-Imine Formation.....	110
2.2.4. Druglikeness Evaluation.....	112
2.2.5. Biological Activity Evaluation.....	116
2.2.6. The Passerini Adducts – Druglikeness and Biological Activity.....	122
2.3. Conclusions.....	124
2.4. References.....	126
Chapter 3: U4c3CR as an Efficient Tool for Oxindole-Lactam Hybrids in Drug Discovery	131
3.1. Introduction.....	133
3.2. U4c3CR for the Synthesis of Oxindole-Lactam Hybrids.....	135
3.3. Druglikeness Evaluation.....	139
3.4. Biological Activity Evaluation.....	142
3.4.1. Cholinesterase Inhibition.....	142
3.4.2. Monoamine Oxidase Inhibition.....	144
3.4.3. Antibacterial Activity.....	146
3.5. Conclusions.....	147
3.6. References.....	149
Chapter 4: A New Route to Tryptanthrin and its Petasis Adducts	157
4.1. Introduction.....	159
4.2. A New Route for the Synthesis of Tryptanthrin from Indigo and Isatin.....	160
4.3. What's Next? Engaging Tryptanthrin in MCRs.....	168
4.3.1. Tryptanthrin and the Ugi Reaction.....	169
4.3.2. Engaging Tryptanthrin in the Petasis MCR.....	173
4.3.2.1. Library III Synthesis.....	173

	Page
4.3.2.2. Enantioselective Version of the Tryptanthrin-Based Petasis Reaction.....	177
4.3.2.3. Druglikeness Evaluation.....	179
4.3.2.4. Biological Activity Evaluation.....	184
4.4. Conclusions.....	186
4.5. References.....	188
Chapter 5: Final Remarks and Future Perspectives.....	193
Chapter 6: Experimental Section.....	199
6.1. General Remarks.....	201
6.1.1. Solvents and reagents.....	201
6.1.2. Detection, characterization and purification of the synthesized compounds and other relevant equipment.....	201
6.2. General Procedures.....	202
6.2.1. General procedure for the synthesis of 3,3-disubstituted oxindoles obtained via Ugi4CR (Chapter 2 – Library I).....	202
6.2.1.1. Synthesis of <i>N</i> -(<i>tert</i> -butyl)-3-(<i>N</i> -butyl-2-chloroacetamido)-1- methyl-2-oxoindoline-3-carboxamide (I.5aaaa).....	202
6.2.1.2. Synthesis of <i>N</i> -(<i>tert</i> -butyl)-3-(<i>N</i> -butyl-2-chloroacetamido)-2- oxoindoline-3-carboxamide (I.5baaa).....	203
6.2.1.3. Synthesis of <i>N</i> -(<i>tert</i> -butyl)-3-(<i>N</i> -butyl-2-chloroacetamido)-2- oxo-1-phenylindoline-3-carboxamide (I.5caaa).....	204
6.2.1.4. Synthesis of 1-Benzyl- <i>N</i> -(<i>tert</i> -butyl)-3-(<i>N</i> -butyl-2-chloro- acetamido)-2-oxoindoline-3-carboxamide (I.5daaa).....	204
6.2.1.5. Synthesis of <i>N</i> -(<i>tert</i> -butyl)-3-(<i>N</i> -butyl-2-chloroacetamido)-2- oxo-1-(prop-2-yn-1-yl)indoline-3-carboxamide (I.5eaaa).....	205
6.2.1.6. Synthesis of 5-Bromo- <i>N</i> -(<i>tert</i> -butyl)-3-(<i>N</i> -butyl-2-chloro- acetamido)-2-oxoindoline-3-carboxamide (I.5faaa).....	206
6.2.1.7. Synthesis of <i>N</i> -(<i>tert</i> -butyl)-3-(<i>N</i> -butyl-2-chloroacetamido)- 5-iodo-2-oxoindoline-3-carboxamide (I.5gaaa).....	206
6.2.1.8. Synthesis of <i>N</i> -(<i>tert</i> -butyl)-3-(<i>N</i> -butyl-2-chloroacetamido)- 5-nitro-2-oxoindoline-3-carboxamide (I.5haaa).....	207

	Page
6.2.1.9. Synthesis of <i>N</i> -(<i>tert</i> -butyl)-3-(<i>N</i> -butyl-2-chloroacetamido)-5,7-dimethyl-2-oxoindoline-3-carboxamide (I.5iaaa).....	207
6.2.1.10. Synthesis of <i>N</i> -(<i>tert</i> -butyl)-3-(<i>N</i> -butyl-2-chloroacetamido)-2-oxo-7-(trifluoromethyl)indoline-3-carboxamide (I.5jaaa).....	208
6.2.1.11. Synthesis of 3-(<i>N</i> -butyl-2-chloroacetamido)- <i>N</i> -cyclohexyl-1-methyl-2-oxoindoline-3-carboxamide (I.5aaab).....	209
6.2.1.12. Synthesis of 3-(<i>N</i> -butyl-2-chloroacetamido)- <i>N</i> -cyclohexyl-2-oxoindoline-3-carboxamide (I.5baab).....	209
6.2.1.13. Synthesis of 3-(<i>N</i> -butyl-2-chloroacetamido)-1-methyl-2-oxo- <i>N</i> -(2,4,4-trimethylpentan-2-yl)indoline-3-carboxamide (I.5aaac).....	210
6.2.1.14. Synthesis of <i>N</i> -benzyl-3-(<i>N</i> -butyl-2-chloroacetamido)-1-methyl-2-oxoindoline-3-carboxamide (I.5baad).....	210
6.2.1.15. Synthesis of 3-(2-chloro- <i>N</i> -propylacetamido)- <i>N</i> -cyclohexyl-2-oxoindoline-3-carboxamide (I.5bbab).....	211
6.2.1.16. Synthesis of <i>N</i> -(<i>tert</i> -butyl)-3-(2-chloro- <i>N</i> -propylacetamido)-1-methyl-2-oxoindoline-3-carboxamide (I.5abaa).....	212
6.2.1.17. Synthesis of 3-(2-chloro- <i>N</i> -ethylacetamido)- <i>N</i> -cyclohexyl-2-oxoindoline-3-carboxamide (I.5bcab).....	212
6.2.1.18. Synthesis of 3-(2-chloro- <i>N</i> -isobutylacetamido)- <i>N</i> -cyclohexyl-2-oxoindoline-3-carboxamide (I.5bdab).....	213
6.2.1.19. Synthesis of <i>N</i> -(<i>tert</i> -butyl)-3-(2-chloro- <i>N</i> -isobutylacetamido)-2-oxoindoline-3-carboxamide (I.5bdaa).....	214
6.2.1.20. Synthesis of 3-(<i>N</i> -benzyl-2-chloroacetamido)- <i>N</i> -(<i>tert</i> -butyl)-1-methyl-2-oxoindoline-3-carboxamide (I.5aeaa).....	214
6.2.1.21. Synthesis of 3-(<i>N</i> -benzyl-2-chloroacetamido)- <i>N</i> -(<i>tert</i> -butyl)-2-oxoindoline-3-carboxamide (I.5beaa).....	215
6.2.1.22. Synthesis of <i>N</i> -(<i>tert</i> -butyl)-3-(2-chloro- <i>N</i> -phenylacetamido)-2-oxoindoline-3-carboxamide (I.5bfaa).....	215
6.2.1.23. Synthesis of 3-(2-Chloro- <i>N</i> -(furan-2-ylmethyl)acetamido)- <i>N</i> -cyclohexyl-2-oxoindoline-3-carboxamide (I.5bhab).....	216
6.2.1.24. Synthesis of 3-(2-Chloro- <i>N</i> -(thiophen-2-ylmethyl)acetamido)- <i>N</i> -cyclohexyl-2-oxoindoline-3-carboxamide (I.5biab).....	216

	Page
6.2.1.25. Synthesis of 3-(2-Bromo- <i>N</i> -butylacetamido)- <i>N</i> -(<i>tert</i> -butyl)-1-methyl-2-oxoindoline-3-carboxamide (I.5aaba).....	217
6.2.1.26. Synthesis of 3-(2-Bromo- <i>N</i> -butylacetamido)- <i>N</i> -(<i>tert</i> -butyl)-2-oxoindoline-3-carboxamide (I.5baba).....	218
6.2.1.27. Synthesis of 3-(2-Bromo- <i>N</i> -butylacetamido)- <i>N</i> -cyclohexyl-2-oxoindoline-3-carboxamide (I.5babb).....	218
6.2.1.28. Synthesis of 3-(2-Bromo- <i>N</i> -propylacetamido)- <i>N</i> -(<i>tert</i> -butyl)-2-oxoindoline-3-carboxamide (I.5bbba).....	219
6.2.1.29. Synthesis of 3-(<i>N</i> -butyl-2-fluoroacetamido)- <i>N</i> -cyclohexyl-2-oxoindoline-3-carboxamide (I.5bacb).....	219
6.2.1.30. Synthesis of <i>N</i> -(<i>tert</i> -butyl)-3-(<i>N</i> -butyl-2,2,2-trifluoroacetamido)-1-methyl-2-oxoindoline-3-carboxamide (I.5aada).....	220
6.2.1.31. Synthesis of 3-(<i>N</i> -butyl-2,2,2-trifluoroacetamido)- <i>N</i> -cyclohexyl-2-oxoindoline-3-carboxamide (I.5badb).....	221
6.2.1.32. Synthesis of <i>N</i> -(<i>tert</i> -butyl)-1-methyl-2-oxo-3-(2,2,2-trifluoro- <i>N</i> -((tetrahydrofuran-2-yl)methyl)acetamido)indoline-3-carboxamide (I.5agda).....	221
6.2.1.33. Synthesis of <i>N</i> -(<i>tert</i> -butyl)-1-methyl-2-oxo-3-(2,2,2-trifluoro- <i>N</i> -(furan-2-ylmethyl)acetamido)indoline-3-carboxamide (I.ahda).....	222
6.2.1.34. Synthesis of <i>N</i> -(<i>tert</i> -butyl)-1-methyl-2-oxo-3-(2,2,2-trifluoro- <i>N</i> -(thiophen-2-ylmethyl)acetamido)indoline-3-carboxamide (I.5aida).....	222
6.2.1.35. Synthesis of 3-(<i>N</i> -butyl-2,2,2-trichloroacetamido)- <i>N</i> -cyclohexyl-2-oxoindoline-3-carboxamide (I.5baeb).....	223
6.2.1.36. Synthesis of <i>N</i> -(<i>tert</i> -butyl)-3-(<i>N</i> -butyl-4-chlorobenzamido)-1-methyl-2-oxoindoline-3-carboxamide (I.5aafa).....	224
6.2.1.37. Synthesis of 3-(<i>N</i> -butyl-4-chlorobenzamido)- <i>N</i> -cyclohexyl-2-oxoindoline-3-carboxamide (I.5bafb).....	224
6.2.2. Identification of side products isolated during the synthesis of I.5bfaa.....	225
6.2.2.1. Side product (<i>E</i>)-3-(Phenylimino)indolin-2-one (I.6a).....	225
6.2.2.2. Side product 2-Chloro- <i>N</i> -phenylacetamide (I.6b).....	225
6.2.3. Identification of Passerini adducts.....	225
6.2.3.1. Passerini adduct 3-(Cyclohexylcarbamoyl)-1-methyl-2-oxoindolin-3-yl benzoate (I.7a).....	226

	Page
6.2.3.2. Passerini adduct 3-(<i>tert</i> -Butylcarbamoyl)-1-methyl-2-oxindolin-3-yl 2-phenylacetate (I.7b).....	226
6.2.3.3. Passerini adduct 3-(<i>tert</i> -Butylcarbamoyl)-2-oxindolin-3-yl cinnamate (I.7c).....	226
6.2.3.4. Passerini adduct 3-(Cyclohexylcarbamoyl)-2-oxindolin-3-yl 4-chlorobenzoate (I.7d).....	227
6.2.4. General procedure for the synthesis of β -lactam-oxindole hybrids obtained via Ugi4c3CR (Chapter 3 – Library II).....	227
6.2.4.1. Synthesis of <i>N</i> -(<i>tert</i> -Butyl)-2-oxo-3-(2-oxoazetidin-1-yl)indoline-3-carboxamide (II.4aaa).....	228
6.2.4.2. Synthesis of <i>N</i> -(<i>tert</i> -Butyl)-1-methyl-2-oxo-3-(2-oxoazetidin-1-yl)-indoline-3-carboxamide (II.4baa).....	228
6.2.4.3. Synthesis of <i>N</i> -(<i>tert</i> -Butyl)-2-oxo-3-(2-oxoazetidin-1-yl)-1-(prop-2-yn-1-yl)indoline-3-carboxamide (II.4caa).....	229
6.2.4.4. Synthesis of <i>N</i> -(<i>tert</i> -Butyl)-2-oxo-3-(2-oxoazetidin-1-yl)-1-phenylindoline-3-carboxamide (II.4daa).....	229
6.2.4.5. Synthesis of 1-Benzyl- <i>N</i> -(<i>tert</i> -butyl)-2-oxo-3-(2-oxoazetidin-1-yl)-indoline-3-carboxamide (II.4eaa).....	230
6.2.4.6. Synthesis of 5-Bromo- <i>N</i> -(<i>tert</i> -butyl)-2-oxo-3-(2-oxoazetidin-1-yl)-indoline-3-carboxamide (II.4faa).....	230
6.2.4.7. Synthesis of <i>N</i> -(<i>tert</i> -Butyl)-5-iodo-2-oxo-3-(2-oxoazetidin-1-yl)-indoline-3-carboxamide (II.4gaa).....	231
6.2.4.8. Synthesis of <i>N</i> -(<i>tert</i> -Butyl)-5-nitro-2-oxo-3-(2-oxoazetidin-1-yl)-indoline-3-carboxamide (II.4haa).....	231
6.2.4.9. Synthesis of <i>N</i> -(<i>tert</i> -Butyl)-5,7-dimethyl-2-oxo-3-(2-oxoazetidin-1-yl)indoline-3-carboxamide (II.4iaa).....	232
6.2.4.10. Synthesis of <i>N</i> -(<i>tert</i> -Butyl)-2-oxo-3-(2-oxoazetidin-1-yl)-7-(trifluoromethyl)indoline-3-carboxamide (II.4jaa).....	232
6.2.4.11. Synthesis of <i>N</i> -Cyclohexyl-2-oxo-3-(2-oxoazetidin-1-yl)indoline-3-carboxamide (II.4aba).....	233
6.2.4.12. Synthesis of 2-Oxo-3-(2-oxoazetidin-1-yl)- <i>N</i> -(2,4,4-trimethylpentan-2-yl)indoline-3-carboxamide (II.4aca).....	233

	Page
6.2.4.13. Synthesis of <i>N</i> -Benzyl-2-oxo-3-(2-oxoazetidin-1-yl)indoline-3-carboxamide (II.4ada).....	234
6.2.4.14. Synthesis of 1-Benzyl-2-oxo-3-(2-oxoazetidin-1-yl)- <i>N</i> -(2,4,4-trimethylpentan-2-yl)indoline-3-carboxamide (II.4eca).....	234
6.2.4.15. Synthesis of <i>N</i> -Benzyl-2-oxo-3-(2-oxoazetidin-1-yl)-1-(prop-2-yn-1-yl)indoline-3-carboxamide (II.4cda).....	235
6.2.4.16. Synthesis of <i>N</i> -Cyclohexyl-1-methyl-2-oxo-3-(2-oxoazetidin-1-yl)indoline-3-carboxamide (II.4bba).....	235
6.2.4.17. Synthesis of 1-Methyl-2-oxo-3-(2-oxoazetidin-1-yl)- <i>N</i> -(2,4,4-trimethyl-pentan-2-yl)indoline-3-carboxamide (II.4bca).....	236
6.2.5. General procedure for the synthesis of γ -lactam-oxindole hybrids obtained via Ugi4c3CR (Chapter 3 – Library II).....	236
6.2.5.1. Synthesis of <i>N</i> -(<i>tert</i> -Butyl)-2-oxo-3-(2-oxopyrrolidin-1-yl)indoline-3-carboxamide (II.5aab).....	237
6.2.5.2. Synthesis of <i>N</i> -(<i>tert</i> -Butyl)-1-methyl-2-oxo-3-(2-oxopyrrolidin-1-yl)indoline-3-carboxamide (II.5bab).....	237
6.2.5.3. Synthesis of <i>N</i> -(<i>tert</i> -Butyl)-2-oxo-3-(2-oxopyrrolidin-1-yl)-1-phenylindoline-3-carboxamide (II.5dab).....	238
6.2.5.4. Synthesis of 1-Benzyl- <i>N</i> -(<i>tert</i> -butyl)-2-oxo-3-(2-oxopyrrolidin-1-yl)indoline-3-carboxamide (II.5eab).....	238
6.2.5.5. Synthesis of 5-Bromo- <i>N</i> -(<i>tert</i> -butyl)-2-oxo-3-(2-oxopyrrolidin-1-yl)indoline-3-carboxamide (II.5fab).....	239
6.2.5.6. Synthesis of <i>N</i> -(<i>tert</i> -Butyl)-5-iodo-2-oxo-3-(2-oxopyrrolidin-1-yl)indoline-3-carboxamide (II.5gab).....	239
6.2.5.7. Synthesis of <i>N</i> -(<i>tert</i> -Butyl)-5-nitro-2-oxo-3-(2-oxopyrrolidin-1-yl)indoline-3-carboxamide (II.5hab).....	240
6.2.5.8. Synthesis of <i>N</i> -(<i>tert</i> -Butyl)-5,7-dimethyl-2-oxo-3-(2-oxopyrrolidin-1-yl)indoline-3-carboxamide (II.5iab).....	240
6.2.5.9. Synthesis of <i>N</i> -(<i>tert</i> -Butyl)-2-oxo-3-(2-oxopyrrolidin-1-yl)-7-(trifluoromethyl)indoline-3-carboxamide (II.5jab).....	241
6.2.5.10. Synthesis of <i>N</i> -Cyclohexyl-2-oxo-3-(2-oxopyrrolidin-1-yl)indoline-3-carboxamide (II.5abb).....	241

	Page
6.2.5.11. Synthesis of 2-Oxo-3-(2-oxopyrrolidin-1-yl)- <i>N</i> -(2,4,4-trimethylpentan-2-yl)indoline-3-carboxamide (II.5acb).....	242
6.2.5.12. Synthesis of <i>N</i> -Benzyl-2-oxo-3-(2-oxopyrrolidin-1-yl)indoline-3-carboxamide (II.5adb).....	242
6.2.5.13. Synthesis of 1-Methyl-2-oxo-3-(2-oxopyrrolidin-1-yl)- <i>N</i> -(2,4,4-trimethylpentan-2-yl)indoline-3-carboxamide (II.5bcb).....	243
6.2.5.14. Synthesis of <i>N</i> -Benzyl-2-oxo-3-(2-oxopyrrolidin-1-yl)-1-(prop-2-yn-1-yl)indoline-3-carboxamide (II.5cdb).....	243
6.2.6. General procedure for the synthesis of tryptanthrin and brominated tryptanthrins using iodine/DMF/NaH trio (Chapter 4).....	244
6.2.6.1. Synthesis of tryptanthrin.....	244
6.2.6.2. Synthesis of 3,9-dibromo-tryptanthrin.....	244
6.2.6.3. Synthesis of 2,4,8,10-tetrabromo-tryptanthrin.....	245
6.2.7. Procedures for the synthesis of precursors for the Petasis MCR.....	245
6.2.7.1. General procedure for the synthesis of brominated tryptanthrins (III.1a-1d).....	245
6.2.7.1.1. Synthesis of 8-Bromo-tryptanthrin (8-bromoindolo[2,1- <i>b</i>]quinazoline-6,12-dione) (III.1a).....	246
6.2.7.1.2. Synthesis of 2-Bromo-tryptanthrin (2-bromoindolo[2,1- <i>b</i>]quinazoline-6,12-dione) (III.1b).....	246
6.2.7.1.3. Synthesis of 8-Bromo-2-fluoro-tryptanthrin (8-bromo-2-fluoroindolo[2,1- <i>b</i>]quinazoline-6,12-dione) (III.1c).....	246
6.2.7.1.4. Synthesis of 2-Bromo-8-fluoro-tryptanthrin (2-bromo-8-fluoroindolo[2,1- <i>b</i>]quinazoline-6,12-dione) (III.1d).....	247
6.2.7.2. General procedure for the synthesis of boronate-tryptanthrins (III.2a- III.2d).....	247
6.2.7.2.1. Synthesis of 8-(5,5-dimethyl-1,3,2-dioxaborinan-2-yl)indolo[2,1- <i>b</i>]quinazoline-6,12-dione (III.2a).....	247
6.2.7.2.2. Synthesis of 2-(5,5-dimethyl-1,3,2-dioxaborinan-2-yl)indolo[2,1- <i>b</i>]quinazoline-6,12-dione (III.2b).....	248
6.2.7.2.3. Synthesis of 8-(5,5-dimethyl-1,3,2-dioxaborinan-2-yl)-2-fluoroindolo[2,1- <i>b</i>]quinazoline-6,12-dione (III.2c).....	248

	Page
6.2.7.2.4. Synthesis of 2-(5,5-dimethyl-1,3,2-dioxaborinan-2-yl)-8-fluoroindolo[2,1- <i>b</i>]quinazoline-6,12-dione (III.2d).....	249
6.2.8. General procedure for the synthesis of tryptanthrin-based Petasis adducts (Chapter 4 – Library III).....	249
6.2.8.1. Synthesis of 8-((2-hydroxyphenyl)(morpholino)methyl)indolo[2,1- <i>b</i>]quinazoline-6,12-dione (III.5aaa).....	250
6.2.8.2. Synthesis of 8-((2-hydroxyphenyl)(piperidin-1-yl)methyl)indolo[2,1- <i>b</i>]quinazoline-6,12-dione (III.5aca).....	250
6.2.8.3. Synthesis of 8-((3,4-dihydroisoquinolin-2(1H)-yl)(2-hydroxyphenyl)methyl)indolo[2,1- <i>b</i>]quinazoline-6,12-dione (III.5ada).....	251
6.2.8.4. Synthesis of 8-((3,5-di- <i>tert</i> -butyl-2-hydroxyphenyl)(morpholino)methyl)indolo[2,1- <i>b</i>]quinazoline-6,12-dione (III.5aac).....	252
6.2.8.5. Synthesis of 8-((5-bromo-2-hydroxyphenyl)(morpholino) methyl)indolo[2,1- <i>b</i>]quinazoline-6,12-dione (III.5aad).....	252
6.2.8.6. Synthesis of 8-((3-ethoxy-2-hydroxyphenyl)(morpholino) methyl)indolo[2,1- <i>b</i>]quinazoline-6,12-dione (III.5aaf).....	253
6.2.8.7. Synthesis of 8-((2-hydroxy-3-methoxyphenyl)(morpholino) methyl)indolo[2,1- <i>b</i>]quinazoline-6,12-dione (III.5aag).....	253
6.2.8.8. Synthesis of 8-((3-(<i>tert</i> -butyl)-2-hydroxyphenyl)(morpholino) methyl)indolo[2,1- <i>b</i>]quinazoline-6,12-dione (III.5aai).....	254
6.2.8.9. Synthesis of 2-((2-hydroxyphenyl)(morpholino)methyl)indolo[2,1- <i>b</i>]quinazoline-6,12-dione (III.5baa).....	254
6.2.8.10. Synthesis of 2-((2-hydroxyphenyl)(piperidin-1-yl)methyl)indolo[2,1- <i>b</i>]quinazoline-6,12-dione (III.5bca).....	255
6.2.8.11. Synthesis of 2-((benzyl(methyl)amino)(2-hydroxyphenyl)methyl)indolo[2,1- <i>b</i>]quinazoline-6,12-dione (III.5bea).....	256
6.2.8.12. Synthesis of 2-((3,5-di- <i>tert</i> -butyl-2-hydroxyphenyl)(morpholino)methyl)indolo[2,1- <i>b</i>]quinazoline-6,12-dione (III.5bac).....	256
6.2.8.13. Synthesis of 2-((5-bromo-2-hydroxyphenyl)(morpholino)methyl)indolo[2,1- <i>b</i>]quinazoline-6,12-dione (III.5bad).....	257
6.2.8.14. Synthesis of 2-((3-ethoxy-2-hydroxyphenyl)(morpholino)methyl)indolo[2,1- <i>b</i>]quinazoline-6,12-dione (III.5baf).....	257

	Page
6.2.8.15. Synthesis of 2-((2-hydroxy-3-methoxyphenyl)(morpholino) methyl)indolo[2,1- <i>b</i>]quinazoline-6,12-dione (III.5bag).....	258
6.2.8.16. Synthesis of 2-fluoro-8-((2-hydroxyphenyl)(morpholino)methyl) indolo[2,1- <i>b</i>]quinazoline-6,12-dione (III.5caa).....	259
6.2.8.17. Synthesis of 8-((3-(<i>tert</i> -butyl)-2-hydroxyphenyl)(morpholino) methyl)-2-fluoroindolo[2,1- <i>b</i>]quinazoline-6,12-dione (III.5cai).....	259
6.2.8.18. Synthesis of 8-fluoro-2-((2-hydroxyphenyl)(morpholino) methyl)indolo[2,1- <i>b</i>]quinazoline-6,12-dione (III.5daa).....	260
6.2.8.19. Synthesis of 8-fluoro-2-((2-hydroxyphenyl)(piperidin-1-yl)methyl) indolo[2,1- <i>b</i>]quinazoline-6,12-dione (III.5dca).....	260
6.2.8.20. Synthesis of 2-((5-bromo-2-hydroxyphenyl)(morpholino)methyl)- 8-fluoroindolo[2,1- <i>b</i>]quinazoline-6,12-dione (III.5dad).....	261
6.2.9. General procedure for the asymmetric version of the tryptanthrin-based Petasis adducts (Chapter 4 – (S)- III.5aaa).....	261
6.3. Biological activity assays.....	262
6.3.1. Antiproliferative activity evaluation.....	262
6.3.2. Cholinesterase inhibition evaluation.....	262
6.3.3. Monoamine oxidase inhibition evaluation.....	263
6.3.4. Antimicrobial activity evaluation.....	264
6.4. Computational details.....	264
6.5. References.....	266
Appendices	269
Appendix 1.....	271
Appendix 2.....	272
Appendix 3.....	273
Appendix 4.....	274
Appendix 5.....	275
Appendix 6.....	276
Appendix 7.....	277
Appendix 8.....	278
Appendix 9.....	279

	Page
Appendix 10.....	280
Appendix 11.....	281
Appendix 12.....	282
Appendix 13.....	283
Appendix 14.....	284
Appendix 15.....	285

Abstract

The central goal of the work presented in this doctoral dissertation was to showcase multicomponent reactions and catalytic processes as sustainable tools for the efficient synthesis of structurally diverse libraries with potential biological activity and promising druglike properties. This approach is particularly valuable when privileged scaffolds are used as starting materials of the multicomponent reactions. Isatin and tryptanthrin are two related compounds, known for possessing great interest in the fields of medicinal chemistry and drug discovery and were selected as key components for library generation.

Among the various multicomponent reactions described in the literature, the Ugi reaction is known for being widely applied in the synthesis of active pharmaceutical ingredients and other biologically active compounds. The interest on this reaction is motivated by its robustness, reliability, and for the ability to generate, in one single step, two new amide bonds, a functional group known to be present in several pharmacologically active compounds.

The Ugi four component reaction, its most classic version, was applied for the synthesis of new oxindole derivatives bearing two linear amides (Library I). Thorough optimization of the synthetic methodology enabled us to select the Lewis acid indium (III) trichloride as a safe, easy to use, cheap, and green catalyst. This approach, the first to be reported on an isatin-based Ugi four component reaction, was suitable for a wide range of substrate scope, allowing the preparation of new compounds with considerable structural diversity. Limitations for the methodology were also identified, such as the relevance of the carboxylic acid component pK_a for reaction selectivity. Library I was evaluated *in vitro* against several tumor cell lines, with promising results, including low and sub-micromolar range of antiproliferative activity. *In silico* druglikeness evaluation of this library also validated the potential of these molecules as drug candidates.

Using another version of the Ugi reaction, the Ugi four-center three component reaction, a molecular hybridization approach was considered for the synthesis of a library of oxindole-lactam hybrids (Library II). Using isatin as starting material, a series of oxindole-lactam hybrids was obtained, aiming to inhibit cholinesterases, relevant therapeutic targets in Alzheimer's disease. The resulting library proved to be selective inhibitors of butyrylcholinesterase, with three compounds presenting inhibition values below 10 micromolar. The *druglikeness* evaluation of Library II *in silico* indicate the ability of two of these most active compounds to cross the blood-brain barrier by passive diffusion, and therefore might be an excellent point for the development of selective

butyrylcholinesterase inhibitors, a therapeutic option so far unavailable in clinical practice. This catalyst-free approach proved to be suitable for a wide range of substrates and therefore enabled great structural diversity.

The serendipity discovery of a new synthetic methodology to prepare the valuable alkaloid tryptanthrin from isatin and indigo, using $I_2/NaH/DMF$ as oxidant trio, is also reported. This approach, promoted under microwave irradiation, proved to be time-efficient and a green alternative for the synthesis of tryptanthrin. Next, we decided to engage this tetracyclic bioactive compound in multicomponent reactions, a poorly explored research field. Our first efforts focused on the Ugi reaction, however all the attempts performed were unsuccessful. Computational studies were performed in order to understand the reactivity differences between isatin and tryptanthrin. Indeed, in the first step of the Ugi reaction (imine formation), the process is favored when using isatin, whereas the energetic barrier is higher when tryptanthrin is applied as starting material. Then, the Petasis multicomponent reaction was selected as model reaction, in order to further explore the reactivity of this molecule (namely, its aryl bromide derivatives). The tryptanthrin derivatives (Library III) were successfully prepared using BINOL as organocatalyst, and an asymmetric version using (*R*)-BINOL lead to excellent enantioselectivity. The Petasis adducts were then evaluated for their antimicrobial activity, and one compound exhibited moderate fungicidal activity, selective against dermatophyte fungal strains.

The outputs of the work presented in this doctoral dissertation corroborate the impact of multicomponent reactions in the field of sustainable drug discovery and medicinal chemistry, especially when privileged scaffolds are employed. Several bioactive compounds were identified, targeting pathologies with great public health and socio-economic impact, such as cancer, neurodegenerative diseases and infectious diseases.

Keywords: Isatin, Tryptanthrin, Multicomponent reactions, Ugi reaction, Petasis reaction, Oxindole hybrids, Sustainable Green Chemistry

Resumo

O principal objetivo do trabalho apresentado nesta dissertação de doutoramento visa demonstrar a relevância das reações multicomponente e de processos catalíticos enquanto ferramentas para a síntese sustentável de bibliotecas de compostos com diversidade estrutural, com potencial atividade biológica e propriedades *druglike* promissoras. Esta abordagem é particularmente relevante quando estruturas privilegiadas são usadas como materiais de partida das reações multicomponente. A isatina e a triptantrina são dois compostos conhecidos por terem um grande interesse para as áreas da química medicinal e de descoberta de fármacos, e foram por isso selecionadas como componentes-chave para a preparação de bibliotecas de compostos.

Entre as várias reações multicomponente descritas na literature, a reação de Ugi é conhecida por ser abundantemente utilizada na síntese de substâncias ativas e de outros compostos com atividade biológica. O interesse nesta reação é amplamente motivado pela sua robustez, segurança e pela sua capacidade de gerar, num só passo reacional, duas novas ligações amida, um grupo funcional amplamente presente em compostos com atividade farmacológica.

A reação de Ugi quatro componentes, a versão mais clássica desta reação, foi usada para a síntese de derivados oxindólicos com amidas lineares (biblioteca I). Uma otimização cuidada da metodologia de síntese levou-nos a selecionar o ácido de Lewis tricloreto de índio (III) enquanto catalisador seguro, fácil de utilizar, barato e amigo do ambiente. Esta abordagem, que constitui o primeiro exemplo de reação de Ugi quatro componentes usando isatina como material e partida, permitiu a utilização de vários substratos para a síntese de novos compostos, com elevado grau de diversidade estrutural. Limitações a esta metodologia também foram identificadas, nomeadamente no que diz respeito aos requisitos do pK_a do ácido carboxílico para que a reação seja seletiva. A biblioteca I foi avaliada *in vitro* contra várias linhas celulares tumorais, com resultados promissores, incluindo atividade antiproliferativa em concentrações sub-micromolares. Avaliação *in silico* das propriedades de *druglikeness* da biblioteca também validam o seu potencial enquanto candidatos a fármacos.

Usando uma outra versão da reação de Ugi, a reação de Ugi de quatro-centros três componentes, uma abordagem de hibridização molecular foi aplicada para a síntese de uma biblioteca de híbridos oxindole-lactama (biblioteca II). Através da utilização de isatina enquanto material de partida, vários híbridos oxindole-lactâmas foram obtidos, com o objetivo de inibir colinesterases, importantes alvos terapêuticos para a doença de

Alzheimer. Os híbridos demonstraram possuir capacidade de inibição seletiva da butirilcolinesterase, com três dos compostos a apresentar atividade menor que 10 micromolar. A avaliação *in silico* das propriedades *druglike* demonstraram que dois dos três compostos mais ativos apresentam potencial para atravessar a barreira hematoencefálica por difusão passiva, e por estes motivos podem ser um excelente ponto de partida para o desenvolvimento de novos inibidores seletivos da butirilcolinesterase, uma opção terapêutica ainda não disponível na prática clínica. A metodologia sintética, que ocorre na ausência de catalisador, demonstrou ser suscetível de ser aplicada a um vasto número de reagentes e, assim, permitir uma grande diversidade estrutural.

A descoberta por serendipismo de uma nova rota sintética para a obtenção do alcaloide triptantrina a partir de isatina ou indigo, usando $I_2/NaH/DMF$ como trio oxidativo, é também aqui descrita. Este processo, promovido por radiação micro-ondas, demonstrou permitir poupanças em tempo de reação e constituir uma alternativa sustentável para a síntese de triptantrina. De seguida, decidimos utilizar este composto tetracíclico, que apresenta várias atividades biológicas, em reações multicomponente, uma vez que esta área de investigação se encontra subexplorada. Os nossos primeiros esforços foram focados na reação de Ugi, mas sem sucesso. Estudos computacionais permitiram perceber as diferenças de reatividade entre isatina e triptantrina, demonstrando que o primeiro passo reacional da reação de Ugi (formação da imina) é favorecido com a isatina, enquanto que uma maior barreira energética é descrita quando triptantrina é usada como material de partida. Assim, selecionamos a reação de Petasis para novos estudos, de modo a explorar a reatividade desta molécula de novas formas. A biblioteca de derivados da triptantrina (biblioteca III) foi sintetizada utilizando BINOL como organocatalisador, e uma versão assimétrica com recurso ao (*R*)-BINOL foi também desenvolvida com sucesso, apresentando excelente enantiosseletividade. Os produtos da reação de Petasis foram avaliados quanto à sua atividade antimicrobiana, sendo que um dos novos derivados possui atividade fungicida moderada, seletiva contra dermatófitos.

Os resultados obtidos nesta dissertação de doutoramento permitem corroborar a importância das reações multicomponente na área da descoberta sustentável de novos fármacos e da química medicinal, em particular quando têm por base estruturas privilegiadas. Foram identificados vários novos compostos com atividade biológica, visando patologias com grande impacto socioeconómico e na saúde pública, como o cancro, as doenças neurodegenerativas e as doenças infecciosas.

Palavras-chave: Isatina, Triptantrina, Reações multicomponente, Reação de Ugi, Reação de Petasis, Híbridos oxindólicos, Química verde sustentável

Abbreviations, Acronyms and Symbols

A β – Amyloid- β

AChE – Acetylcholinesterase

ACS GCIPR – American Chemical Society Green Chemistry Institute

Pharmaceutical Roundtable

ADMET - Absorption, distribution, metabolism, excretion, and toxicity

ALS – Amyotrophic lateral sclerosis

AMP – Antimicrobial peptides

ANP – Atrial natriuretic peptide

API(s) – Active pharmaceutical ingredient(s)

AUC – Area under the curve

BBB – Blood-brain barrier

BINOL – 1,1'-Bi-2-naphthol

B₂NPG₂ – Bis(neopentyl glycolato)diboron

BOILED-Egg model – Brain or intestinal estimated permeation method

BuChE – Butyrylcholinesterase

CCK₁ – Cholecystokinin A

β -CD – β -Cyclodextrin

CFU – Colony-forming unit

CLSI – Clinical and Laboratory Standards Institute

CNS – Central nervous system

COX-2 – Cyclooxygenase-2

DES(s) – deep-eutectic solvent(s)

DFT – Density functional theory

DMF – Dimethylformamide

DOS – Diversity-oriented synthesis

DT – Diisopropyl tartrate

DTPU – *N,N'*-diphenylthiourea

EEA – European Environment Agency

EPA – United States Environmental Protection Agency

ERK – Extracellular-signal-regulated kinase (ERK)

FDA – Food and Drug Administration

Fsp³ – Fraction of sp³ carbon atoms

GABA_A – γ -Aminobutyric acid type A

GBB3CR – Groebke-Blackburn-Bienaymé three component reaction

GC-MS – Gas-chromatography-mass spectrometry
GMP – Guanosine monophosphate
HBA – Hydrogen bond acceptors
HBD – Hydrogen bond donors
HDM2/MDM2 – Human double minute 2/Mouse double minute 2
HO-1 – Heme oxygenase 1
HSBM – High-speed ball-milling
HTS – High-throughput screening
IDO1 – Indoleamine 2,3-dioxygenase 1
IMI – Innovative Medicines Initiative
IMCR(s) – Isocyanide-based multicomponent reaction(s)
InhA – Enoyl-acyl carrier protein reductase
IUPAC – International Union of Pure and Applied Chemistry
LAG – Liquid-assisted grinding
5-LOX – 5-Lipoxygenase
MAO A – Monoamine oxidase A
MAO B – Monoamine oxidase B
MAOS – Microwave-assisted organic synthesis
MCR(s) – Multicomponent reaction(s)
MDR1 – Multidrug resistance protein 1
2-MeTHF – 2-methyltetrahydrofuran
MIC(s) – Minimum inhibitory concentration(s)
MLC(s) – Minimal lethal concentration(s)
MOF(s) – Metal-organic framework(s)
MPTP – 1-Methyl-4-phenyl-1,2,3,6-tetrahydropyridine
MR – Molar refractivity
MRSA – Methicillin-resistant *Staphylococcus aureus*
MS – Molecular sieves
MW – Molecular weight
NMDA – *N*-Methyl-*D*-aspartate
NMR – nuclear magnetic resonance
Nrf2 – Nuclear factor erythroid 2-related factor 2
NSAID(s) – Non-steroid anti-inflammatory drug
O3CR – Orru three component reaction
OECD – Organization for Economic Co-operation and Development
P3CR – Passerini three component reaction
P-gp – P-glycoprotein

PAINS – Pan-assay interference compounds
PEG(s) – polyethylene glycol polymers
R&D – Research and development
RB – Rotatable bonds
RLS – Restless leg syndrome
SARS-CoV-2 – Severe acute respiratory syndrome coronavirus 2
scCO₂ – Supercritical carbon dioxide
SDG(s) – United Nations' Sustainable Development Goal(s)
SMILES – Simplified molecular-input line-entry system
TDO – Tryptophan 2,3-dioxygenase
TFE – 2,2,2-trifluoroethanol
TMV – Tobacco mosaic virus
TOS – Target-oriented synthesis
TPSA – Topological polar surface area
TSLP – Thymic stromal lymphopoietin
TNF α – Tumor necrosis factor- α
U3CR – Ugi three component reaction
U4CR – Ugi four component reaction
U4c3CR – Ugi four-center three component reaction
U5c4CR – Ugi five-center four component reaction
UHP – Urea-hydrogen peroxide

List of Publications Related to the Scientific Topic of the Thesis

Manuscripts published in international journals with peer review process

1. Pedro Brandão, Adrián Puerta, José M. Padrón, Maxim L. Kuznetsov, Anthony J. Burke, Marta Pineiro “*Ugi adducts of isatin as promising antiproliferative agents with druglike properties*”, Asian Journal of Organic Chemistry, **2021**, in press (DOI: 10.1002/ajoc.202100684).
2. Pedro Brandão, Óscar López, Luisa Leitzbach, Holger Stark, José G. Fernández-Bolaños, Anthony J. Burke, Marta Pineiro “*Ugi Reaction Synthesis of Oxindole–Lactam Hybrids as Selective Butyrylcholinesterase Inhibitors*”, ACS Medicinal Chemistry Letters, **2021**, 12 (11), 1718–1725 (DOI: 10.1021/acsmchemlett.1c00344).
3. Pedro Brandão, Carolina Marques, Eugénia Pinto, Marta Pineiro, Anthony J. Burke “*Petasis adducts of tryptanthrin – synthesis, biological activity evaluation and druglikeness assessment*”, New Journal of Chemistry, **2021**, 45, 14633-14649 (DOI: 10.1039/D1NJ02079J).
4. Pedro Brandão, Carolina S. Marques, Elisabete P. Carreiro, Marta Pineiro, Anthony J. Burke “*Engaging Isatins in Multicomponent Reactions (MCRs) – Easy Access to Structural Diversity*”, The Chemical Record, **2021**, 21 (4), 924-1037 (DOI: 10.1002/tcr.202000167).
5. Pedro Brandão, Carolina S. Marques, Anthony J. Burke, Marta Pineiro “*The application of isatin-based multicomponent-reactions in the quest for new bioactive and druglike molecules*”, European Journal of Medicinal Chemistry, **2021**, 211, 113102 (DOI: 10.1016/j.ejmech.2020.113102).
6. Pedro Brandão, Anthony J. Burke, Marta Pineiro “*A Decade of Indium-Catalyzed Multicomponent Reactions (MCRs)*”, European Journal of Organic Chemistry, **2020**, 2020, 34, 5501-5513 (DOI: 10.1002/ejoc.202000596).
7. Daniela Pinheiro, Marta Pineiro, João Pina, Pedro Brandão, Adelino M. Galvão, J. Sérgio Seixas de Melo “*Tryptanthrin from indigo: Synthesis, excited state deactivation routes and efficient singlet oxygen sensitization*”, Dyes and Pigments, **2020**, 175, 108125 (DOI: 10.1016/j.dyepig.2019.108125).
8. Pedro Brandão, Daniela Pinheiro, J. Sérgio Seixas de Melo, Marta Pineiro “*I₂/NaH/DMF as oxidant trio for the synthesis of tryptanthrin from indigo or isatin*”, Dyes and Pigments, **2020**, 173, 107935 (DOI: 10.1016/j.dyepig.2019.107935).

9. Pedro Brandão, Anthony J. Burke “*Catalytic Ugi Reactions: Current Advances, Future Challenges - Part 1*”, *Chimica Oggi – Chemistry Today: Monographic Special Issue – Catalysis & Biocatalysis*, **2019**, 37 (4), 21-25.

10. Pedro Brandão, Anthony J. Burke “*Catalytic Ugi Reactions: Current Advances, Future Challenges - Part 2*”, *Chimica Oggi – Chemistry Today*, **2019**, 37 (4), 18-21.

11. Pedro Brandão, Anthony J. Burke “*Recent advances in the asymmetric catalytic synthesis of chiral 3-hydroxy and 3-aminooxindoles and derivatives: Medicinally relevant compounds*”, *Tetrahedron*, 2018, 74 (38), 4927-4957 (DOI: 10.1016/j.tet.2018.06.015).

Manuscripts published in national journals with peer review process

1. Daniela Pinheiro, Pedro Brandão, J. Sérgio Seixas de Melo, Marta Pineiro “*Triptantrina: da Natureza ao Laboratório*”, *Química*, **2021**, 45 (162), 195-200 (DOI: 10.52590/M3.P697.A30002440).

2. Pedro Brandão, Anthony J. Burke, Marta Pineiro “*Reações Multicomponente - Uma Ferramenta Valiosa na Descoberta e Produção de Fármacos*”, *Química*, **2020**, 44 (159), 264-276 (DOI: 10.52590/M3.P694.A30002331).

Submitted manuscripts:

1. Pedro Brandão, Marta Pineiro, Anthony J. Burke “*Tryptanthrin and its derivatives in drug discovery: synthetic insights*”, under review.

List of Figures, Schemes and Tables

	Page
Figure 1.1. Examples of bioactive compounds obtained from natural sources.....	4
Figure 1.2. Chemical structures of isatin, tryptanthrin, and indigo.....	7
Figure 1.3. Endogenous production of isatin from dietary <i>L</i> -tryptophan ingestion, via gut flora conversion to indole and hepatic oxidation to oxindole and isatin...8	8
Figure 1.4. Examples of bioactive natural oxindole alkaloids and respective biological activities.....	9
Figure 1.5. Oxindole-based drugs reaching clinical trials.....	11
Figure 1.6. Evolution of the number of publications in the last two decades concerning bioactive isatin/oxindole derivatives (data was collected using Web of Science, with keywords “isatin” or “oxindole” combined with “medicinal chemistry” or “drug”).....	14
Figure 1.7. Explored pharmacological activities of the oxindole core.....	15
Figure 1.8. Chemical transformations of the isatin scaffold.....	17
Figure 1.9. Main biological activities and pharmacokinetic profile features of tryptanthrin.....	20
Figure 1.10. Examples of recently reported bioactive tryptanthrin derivatives.....	22
Figure 1.11. Chemical transformations performed in the tryptanthrin scaffold.....	24
Figure 1.12. Twelve principles of green chemistry and United Nations’ Sustainable Development Goals.....	26
Figure 1.13. Overview of the main stakeholders and respective contributions to make the drug discovery and development process more sustainable.....	30
Figure 1.14. Pharmacodynamic and pharmacokinetic potential of drug candidates as equally determinant for clinical application success.....	33
Figure 1.15. Advantages of using druglikeness in drug candidates’ selection during the drug discovery and development process.....	34
Figure 1.16. Main descriptors of five of the most relevant druglikeness filters.....	34
Figure 1.17. Outputs of the SwissADME web-based tool.....	36
Figure 1.18. BOILED-Egg model of tryptanthrin and isatin.....	37
Figure 1.19. Evolution of the number of publications on MCRs between 2000-2020...39	39
Figure 1.20. MCRs compliance with green chemistry principles.....	40
Figure 1.21. Comparison between TOS, combinatorial chemistry and DOS.....	42
Figure 1.22. Examples of APIs obtained using MCRs.....	43

	Page
Figure 1.23. Examples of IMCRs.....	44
Figure 1.24. Central role of amide functional group in drug discovery and development.....	46
Figure 1.25. Catalytic Ugi reaction and indium catalysis advantages and disadvantages.....	49
Figure 1.26. Variations of the U4CR.....	50
Figure 1.27. Examples of variations of the U3CR.....	52
Figure 1.28. Examples of APIs synthesized using Petasis MCR.....	53
Figure 1.29. BINOL and BINOL derivatives applied as efficient asymmetric Petasis MCR.....	55
Figure 1.30. Trend on isatin-based MCRs.....	56
Figure 1.31. Thesis outline.....	57
Figure 2.1. Reagent scope for the U4CR.....	105
Figure 2.2. Library of oxindole derivatives obtained via U4CR.....	106
Figure 2.3. pK_a scale of the carboxylic acid components ²¹ used in the screening of the U4CR.....	109
Figure 2.4. Energy profile of imine formation.....	112
Figure 2.5. Calculated HBA, HBD and RB for the new oxindole-peptoid hybrids.....	113
Figure 2.6. Correlation between MW and CLogP of the synthesized compounds.....	114
Figure 2.7. BOILED-Egg model for the oxindole derivatives obtained via U4CR.....	115
Figure 2.8. GI_{50} range plot against human solid tumor cell lines.....	118
Figure 2.9. Structure-activity relationship for the synthesized library obtained via U4CR and bioavailability radar of the most active compounds.....	121
Figure 2.10. BOILED-Egg model of Passerini adducts I.7a-d and bioavailability radar of compound I.7a.....	123
Figure 2.11. Summary of the main results of this Chapter.....	125
Figure 3.1. Examples of advantages of the application of molecular hybridization in drug discovery.....	133
Figure 3.2. Examples of oxindole and lactam derivatives with ChE inhibition activity as the base for the rationale of oxindole-lactam hybrids.....	135
Figure 3.3. Isatin, isocyanide and amino acid components scope for the U4c3CR.....	137
Figure 3.4. Library of oxindole- β -lactam and oxindole- γ -lactam hybrids.....	138
Figure 3.5. Calculated hydrogen bond acceptors, hydrogen bond donors, and rotatable bonds for the synthesized library of oxindole-lactam hybrids.....	139
Figure 3.6. Relation between MW and CLogP of the synthesized hybrids.....	141

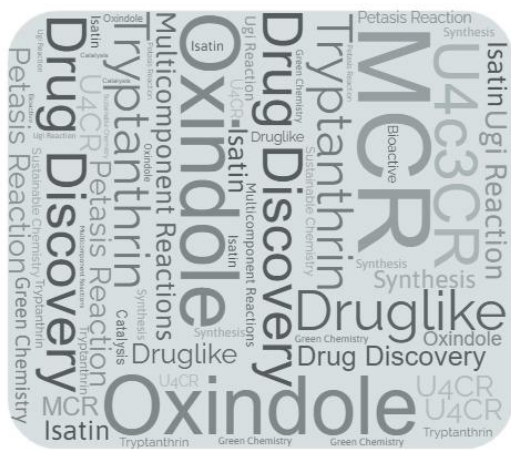
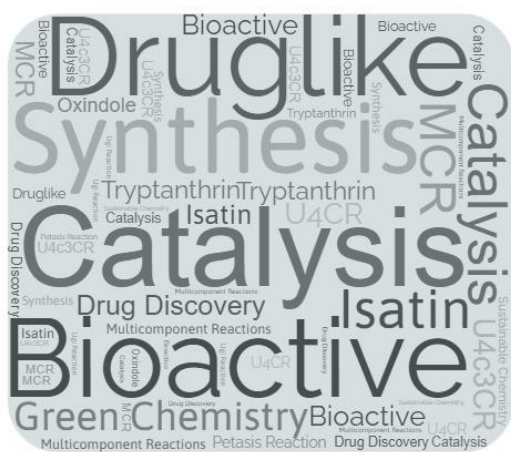
	Page
Figure 3.7. BOILED-Egg model for the oxindole-lactam hybrids obtained <i>via</i> U4c3CR.....	141
Figure 3.8. Structure-activity relationship of the oxindole-lactam hybrids as selective BuChE inhibitors, and bioavailability radars of the two most promising compounds.....	145
Figure 3.9. Structures of known MAO inhibitors.....	145
Figure 3.10. Summary of the main results for Chapter 3.....	147
Figure 4.1. GC-MS chromatograms of the products obtained for the synthesis of tryptanthrin from indigo and isatin, and the mass spectra of the four relevant compounds.....	162
Figure 4.2. Green metrics evaluation of contemporary approaches using iodine-promoted synthesis of tryptanthrin.....	168
Figure 4.3. Reagent scope for the Petasis multicomponent reaction.....	175
Figure 4.4. Calculated hydrogen bond acceptors, hydrogen bond donors, and rotatable bonds for the synthesized tryptanthrin derivatives.....	179
Figure 4.5. MW and CLogP correlation of the synthesized compounds and their placement according to the main filters upper limits.....	181
Figure 4.6. BOILED-Egg model for the new tryptanthrin derivatives.....	182
Figure 4.7. Highlights of Chapter 4.....	187
Figure 5.1. Examples of research opportunities created by the work reported in this thesis.....	196
Scheme 1.1. Concepts in Medicinal Chemistry: privileged scaffold, frequent hitters, promiscuous compounds and PAINS.....	6
Scheme 1.2. Main synthetic routes for the synthesis of the isatin scaffold.....	16
Scheme 1.3. Common methods for the preparation of the oxindole nucleus.....	17
Scheme 1.4. Possible biosynthetic pathways for tryptanthrin in different organisms.....	19
Scheme 1.5. Common methodologies for the preparation of tryptanthrin.....	24
Scheme 1.6. Classic U4CR mechanism.....	48
Scheme 1.7. Classic U3CR mechanism.....	51
Scheme 1.8. Petasis 3CR mechanism.....	54
Scheme 2.1. Reported examples of isatin-based U3CR and U4c3CR.....	102
Scheme 2.2. Side-products attained when aniline is used in this isatin-based U4CR.....	107
Scheme 2.3. Passerini adducts obtained when screening benzoic acid, phenyl-acetic acid and cinnamic acid as carboxylic acid component of the U4CR.....	108

	Page
Scheme 2.4. Exploring the U4CR using <i>p</i> -chlorobenzoic acid achieves both the Ugi and Passerini adducts of isatin.....	109
Scheme 2.5. Ball-and-stick representation of OC, transition states, intermediaries and F.....	111
Scheme 3.1. Synthetic approach for the U4c3CR to attain oxindole-lactam hybrids..	136
Scheme 4.1. Proposed mechanism for the indigo transformation to isatin and further oxidation to isatoic anhydride.....	165
Scheme 4.2. Contemporary iodine-promoted approaches for the synthesis of tryptanthrin.....	166
Scheme 4.3. Reported examples of tryptanthrin-based MCRs.....	169
Scheme 4.4. Attempted approaches at performing the Ugi reaction on tryptanthrin and phaitantrins.....	171
Scheme 4.5. Optimized structures of INT2tr, TS3tr, INT2ph and TS3ph.....	172
Scheme 4.6. Tryptanthrin synthesis from isatin and consecutive borylation.....	174
Scheme 4.7. Library of tryptanthrin derivatives obtained via a Petasis MCR.....	176
Scheme 4.8. Proposed mechanism for the (<i>R</i>)-BINOL-catalyzed asymmetric reaction.....	178
Table 2.1. Optimization of the U4CR conditions.....	103
Table 2.2. Compliance of the synthesized oxindole derivatives with the five evaluated druglikeness filters.....	116
Table 2.3. GI ₅₀ obtained for the new oxindole derivatives obtained via U4CR.....	117
Table 2.4. GI ₅₀ obtained for the Passerini adducts isolated.....	123
Table 3.1. <i>In silico</i> calculation of several physical-chemical properties of the synthesized oxindole-lactam hybrids.....	140
Table 3.2. ChE inhibition results.....	143
Table 3.3. MAO A and MAO B preliminary screening for compounds II.4caa, II.4cda and II.5cdb.....	146
Table 4.1. Microwave-assisted tryptanthrin synthesis using indigo as starting material.....	161
Table 4.2. Microwave-assisted tryptanthrin synthesis using isatin as starting material.....	164
Table 4.3. Optimization of the Petasis reaction conditions.....	175
Table 4.4. Asymmetric Petasis 3-MCR using borylated tryptanthrin (III.2a), morpholine (III.3a) and salicylaldehyde (III.4a): catalyst evaluation.....	178

	Page
Table 4.5. <i>In silico</i> calculation of several physical-chemical properties of the synthesized tryptanthrin derivatives.....	180
Table 4.6. Druglikeness filters compliance for the new tryptanthrin derivatives.....	183
Table 4.7. Antifungal activity (MIC and MLC) of the tryptanthrin derivatives against dermatophytes fungi strains.....	185

Chapter 1

General Introduction



1.1. Getting Inspired by History and Nature in the Quest for New Drug Candidates

“You have to know the past to understand the present.”

Carl Sagan

Since antiquity, mankind evolution has been intertwined with its social behavior. As recent evidence show, since prehistoric times, individuals and groups make efforts to treat and heal their peers in need, instead of looking to injured or sick individuals as liabilities.¹ Over the millennia, folk medicine was an always evolving field, highly dependent on information passed throughout generations, trial and error, and even trends which emerged through times. Although some practices can now be considered as bizarre or torture under 21st century scientific knowledge, there is evidence of how the social behavior of helping those in need is a crucial part of what makes us humans. These practices were also important to develop the scientific method and knowledge that we continue to implement and improve in the present times, and for the continuous improvement in the drug discovery field.^{2,3}

Over the centuries, the use of plant extracts or crude medicines isolated from naturally occurring sources was the common practice in therapeutics. These practices often led to relevant scientific breakthroughs, e.g., bark extracts were used for its antipyretic properties in Europe since the early of the 17th century, but its active substance, quinine, was only isolated and used in its pure form for the treatment of malaria in the 19th century.⁴⁻⁶ Inorganic compounds, such as arsenic trioxide (**Figure 1.1**), used in folk Chinese medicine for over 5000 years, is now approved for the treatment of leukemia, with its mechanism of action only being unveiled in the turn of this century.⁷⁻¹⁰ These are classic examples of empirical use of natural products to treat a pathology through the centuries, despite the lack of knowledge of how the disease or the treatment actually work.

The shift of mindset from the use of extracts to pure compounds was driven by Swiss physician Paracelsus in the early 16th century. The evolution of chemical knowledge, in particular focused on natural products, techniques of extraction and isolation of pure compounds from natural sources, exponentially increased the availability of drugs which are still used today in clinical practice, such as morphine and caffeine. This burst of knowledge emerged in the 19th century. At the same time, another important field emerged, which was going to revolutionize therapeutics – synthetic organic chemistry. This scientific breakthrough was carried by the German chemist

Friedrich Wöhler, who reported the first synthesis of an organic molecule, urea.^{11, 12} With such a discovery, a new door for the development of new therapeutic alternatives was open. The evolution of chemical knowledge allowed drug preparation to grow from local apothecaries and magistral formulations of medicines to large-scale pharmaceutical production of drugs, making them more accessible for a larger portion of the population.^{13, 14} A good example to illustrate the synergic effect between chemical knowledge of natural products and synthetic organic chemistry is the case of salicylic acid (**Figure 1.1**). It was known that the extract of *Salix alba* (willow) bark possesses antipyretic properties. Further studies led to the isolation of salicylic acid as the compound responsible for this relevant bioactivity. However, this compound, due to its acid nature, was also corrosive and irritating to the gastric mucosa when swallowed. Synthetic organic chemistry provided an alternative, by leading to the synthesis of acetylsalicylic acid in 1897, commercialized as Aspirin®, a non-steroid anti-inflammatory drug (NSAID) possessing antipyretic and analgesic properties, without the undesired gastric effects in short-term treatments. Nevertheless, salicylic acid is still used nowadays in several dermatological formulations, due to its keratolytic properties, showcasing the versatility and importance of the concomitant use of synthetic organic chemistry and natural product chemistry knowledge in present clinical practice.^{15, 16}

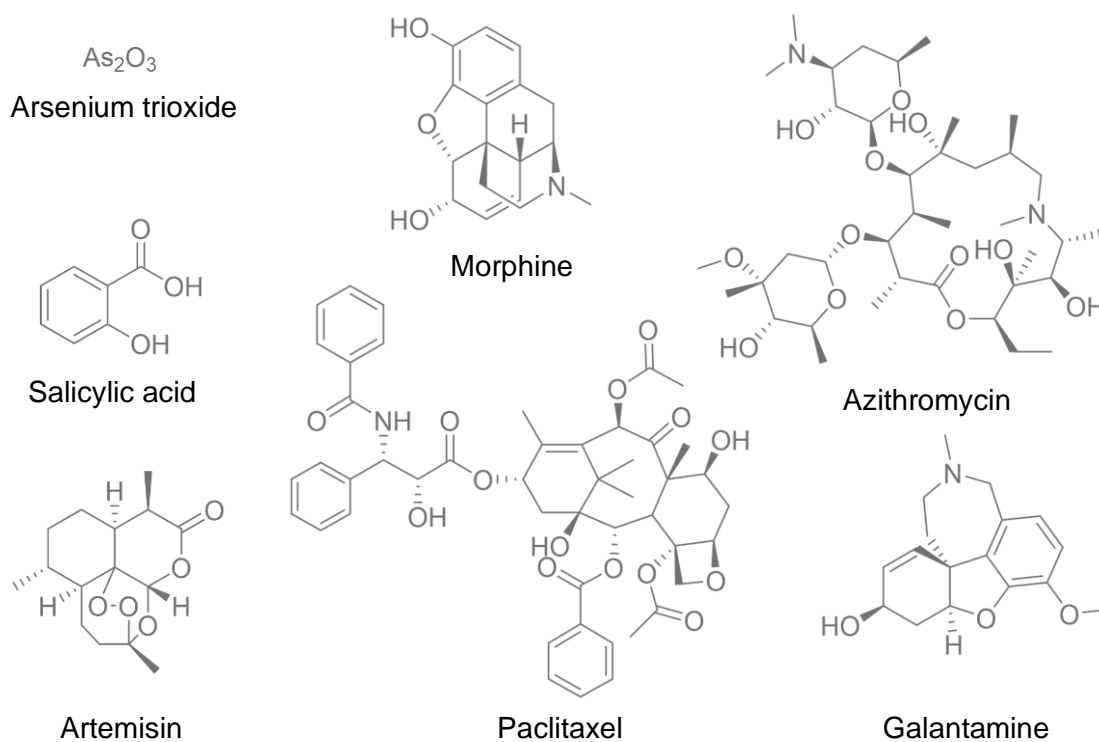


Figure 1.1. Examples of bioactive compounds obtained from natural sources.

With the development of scientific knowledge, many other natural products gained the status of commercial drugs, including morphine, galantamine, paclitaxel, artemisin, azithromycin, just to name a few (**Figure 1.1**). However, the complexity of some of these structures, makes their total synthesis a big challenge to synthetic organic chemists, and often it takes decades to achieve a synthetic route to achieve the desired drug. Nonetheless, the synthetic pathways developed are often very extensive, tedious, and not as straightforward as desirable for a commercial product. This often leads to very expensive drugs or for the need of using a natural product with a high level of complexity as starting material (semi-synthetic drugs). However, many times these starting materials, by being natural sources, are available at specific geographical locations, with interruptions in the supply chain or price fluctuations becoming a possibility at any point due to multiple factors (political tensions, natural disasters, wars, etc.). This might constitute an attrition cause for the investigation of natural products as drugs, but several alternatives are available in the medicinal and synthetic organic chemists' toolbox.¹⁷⁻²¹

1.2. Selecting Privileged Scaffolds as Starting Point for Drug Discovery

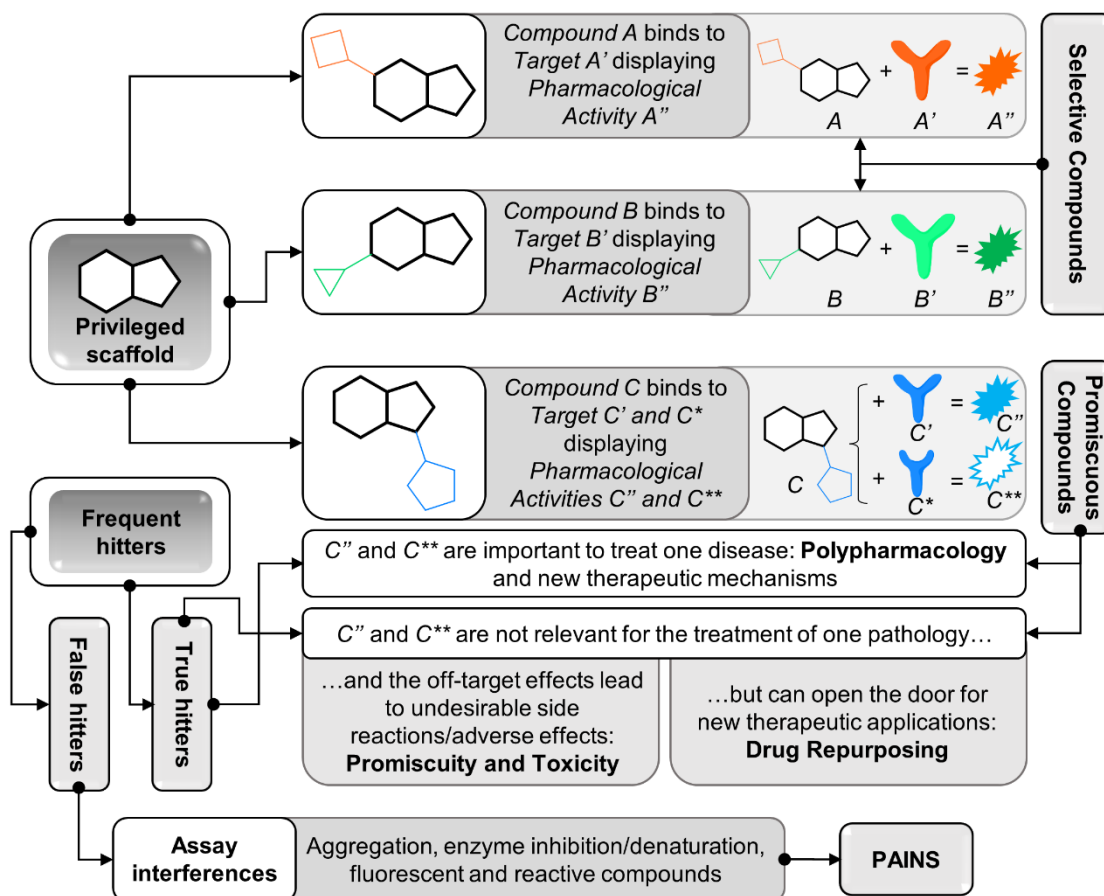
“I consider nature a vast chemical laboratory in which all kinds of composition and decompositions are formed.”

Antoine-Laurent de Lavoisier

In 1988, Evans *et al.* developed a research work through chemical modifications of benzodiazepines, known for their anxiolytic activity. Classically, benzodiazepines exert their therapeutic effect by interacting with γ -aminobutyric acid type A (GABA_A) receptors in the central nervous system.^{22, 23} But in their innovative work, potent and selective cholecystinin antagonists were achieved, targeting peripheral receptor CCK₁,²⁴ a receptor present in the gastrointestinal tract and mediating a series of physiological processes.²⁵ The presence of the benzodiazepine heterocycle in different compounds exhibiting significantly different pharmacological effects in different targets, led the authors to introduce the concept of “privileged structures”, as chemical motifs which “are capable of providing useful ligands for more than one receptor and that judicious modifications of such structures could be a viable alternative in the search for new receptor agonists and antagonists”.²⁴

The concept of privileged structure should not be confused with other concepts commonly used in the field of medicinal chemistry, such as frequent hitters,^{26, 27}

promiscuous binders,^{28, 29} or pan-assay interference compounds (PAINS)^{30, 31} (Scheme 1.1).³²



Scheme 1.1. Concepts in medicinal chemistry: privileged scaffold, frequent hitters, promiscuous compounds and PAINS.

Drug discovery programmes based on the development of novel bioactive small molecules often use privileged scaffolds as starting point for library generation. This choice is due to the higher chances of success which can be attained by introducing these chemical motifs in frameworks of new drug candidates.^{33, 34} Besides the established potential to interact with biological targets, privileged scaffolds often bring to the table a set of physico-chemical features which might be determinant for the success of the novel molecules pharmacodynamic and pharmacokinetic profiles.^{35, 36} The selection of the appropriate privileged structure can be a pivotal task for new drug candidates design, as it might determine if the library to be synthesized can actually stand a chance in moving on in the drug discovery and development pipeline. Several methodologies to help in this selection have been developed throughout the years. Recently, technologies involving machine learning and artificial intelligence started to operate in the detection and evaluation of privileged scaffolds and decision-making of

which molecules should be evaluated for their pharmacological interest.^{37, 38} More classic approaches for the identification and selection of privileged scaffolds involve the analysis of the chemical structures of marketed drugs,³⁹⁻⁴² and bioactive natural products.^{17, 43, 44} Indeed, the structural diversity and remarkable pharmacological potential of natural products make this collection of compounds a great starting-point for hand-picking privileged scaffolds.⁴⁵ Among the numerous families of natural products, alkaloids can be a great family for the development of new drug candidates.⁴⁶⁻⁴⁹ In this work, two alkaloids will take center stage for the development of new drug candidates, isatin and tryptanthrin (**Figure 1.2**). The reasons behind their choice, as well as their properties and pharmacological relevance will be addresses in the next sections.

1.2.1. From Bacteria to Humans: Isatin is Ubiquitous in Nature

Isatin was first reported in 1840, by the German chemist Otto Linné Erdmann and by the French chemist Auguste Laurent, while developing work with the dye indigo (**Figure 1.2**).⁵⁰⁻⁵³ Their work reveals that there is a powerful connection between these three key molecules - isatin, tryptanthrin and indigo.

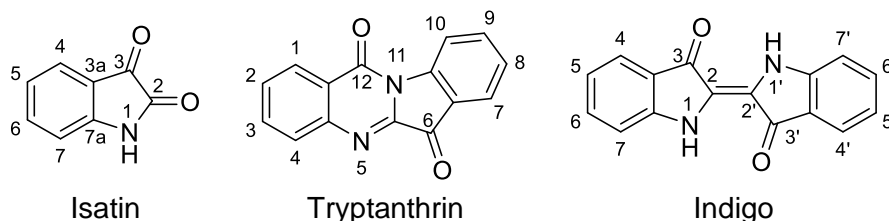


Figure 1.2. Chemical structures of isatin, tryptanthrin, and indigo.

Despite its discovery being made through a chemical reaction, isatin (chemically, indoline-2,3-dione) occurs in many natural sources, including bacteria where it is a biosynthetic metabolic intermediate or decomposition product of other valuable natural organic molecules, such as violacein (produced by *Chromobacterium violaceum*),⁵⁴ indirubin (produced by *Comamonas* sp. from indole),⁵⁵ and indigo (produced by *Pseudomonas* sp. and *Acinetobacter* sp., using indole as metabolic precursor).⁵⁶

In the kingdom Plantae, isatin is also a relevant biosynthetic intermediate for the synthesis of multiple pigments, such as indigo, indirubin, isoindirubin and isoindigo. Plants from the *Isatis* genus are the most prominent examples of isatin sources in the Plantae kingdom.⁵⁷ Isatin was also isolated from *Calanthe* species (*Orchidaceae* family),⁵⁸ and from *Couroupita guianensis* (*Lecythidaceae* family).⁵⁹

Despite plants being the main origin for traditional folk medicine preparations, some animal-based products were also used over the centuries. The dried venom of the parotoid glands of *Bufo* toads, namely the *Bufo bufo gargarizans*, is used in Asian folk medicine since almost one millennium B.C., under the names of Chansu (Chinese traditional medicine) and Senso (Japanese traditional medicine), for the treatment of pain and inflammatory diseases. In this complex mixture, isatin was also identified as one of its components.^{60, 61}

In the late 1980's, a new biomarker for anxiety and stress in humans was reported under the name of tribulin, possessing endogenous monoamine oxidase inhibitory activity, as well as the ability to bind to the benzodiazepine receptors. While some authors use the name tribulin and isatin interchangeably, for others isatin is just the main component of a more complex mixture.⁶²⁻⁶⁴ There are multiple possibilities for the origin of isatin in humans, as this heterocycle was already found in the brain tissue (showing ability to cross the blood-brain barrier (BBB)), with non-homogenic distribution,⁶⁵ and also in the heart, peripheral tissues, serum and urine. It is hypothesized that isatin can be a metabolic product of phenylalanine,⁶⁶ adrenaline,^{63, 64} or *L*-tryptophan (**Figure 1.3**).⁶⁷⁻⁷²

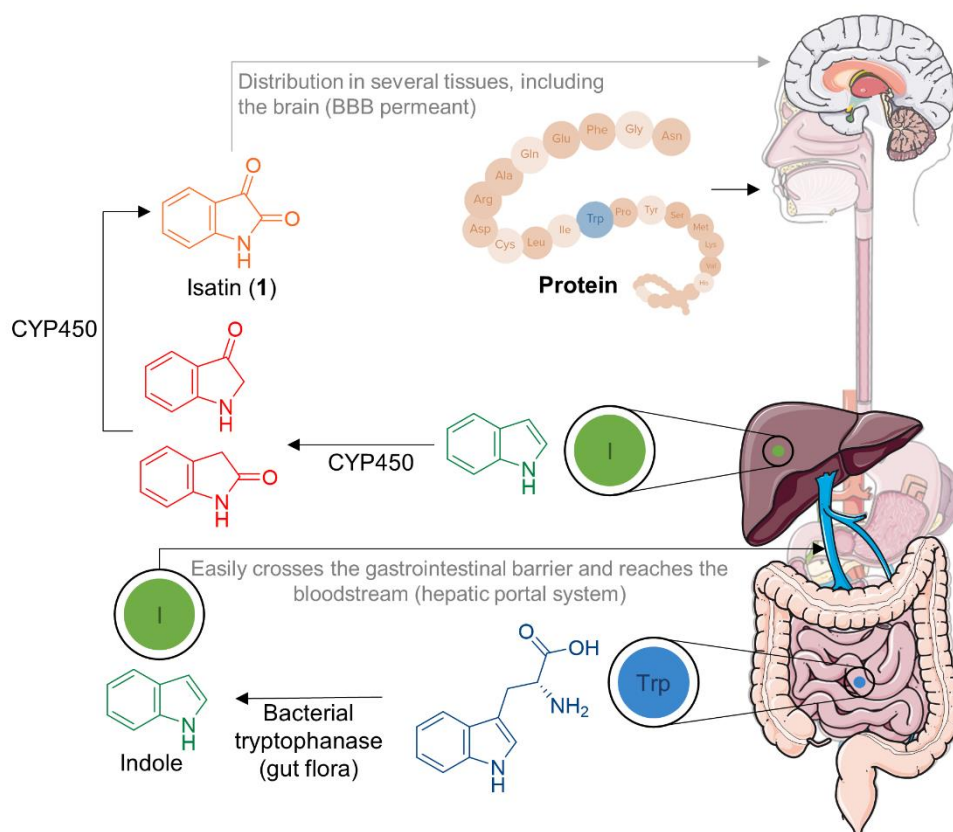


Figure 1.3. Endogenous production of isatin from dietary *L*-tryptophan ingestion, via gut flora conversion to indole and hepatic oxidation to oxindole and isatin.

Isatin endogenous roles appear to be multifactorial and complex, interacting with multiple intracellular isatin-binding proteins, and therefore it is likely responsible to operate as a regulator of complex protein networks in both physiological and pathological conditions. At physiological concentrations, it is known that isatin inhibits monoamine oxidase B (MAO-B) and atrial natriuretic peptide (ANP) receptors, preventing the generation of a second messenger, cyclic guanosine monophosphate (GMP). At higher concentrations, isatin increases the levels of monoamine neurotransmitters and it appears to interact with NO signaling pathways. It possesses angiogenic properties, attenuates parkinsonism induced by neurotoxin 1-methyl-4-phenyl-1,2,3,6-tetrahydropyridine (MPTP), and it can also influence certain apoptosis-related genes.⁷²⁻⁷⁵ This endogenous role of isatin shows the existence of potential targets to this compound, as well as its analogues and/or derivatives.

The vast potential pharmacological activities displayed by oxindole-containing alkaloid compounds range from antimicrobial, antioxidant, immunomodulatory, antiproliferative, central nervous system (CNS) (including sedative, hypnotic, anti-ischemic, anti-dementia, and neuroprotective effects), cardiovascular (including antihypertensive, antiarrhythmic, and antithrombotic effects), and anti-inflammatory activities (**Figure 1.4**), with several compounds presenting more than one bioactivity,

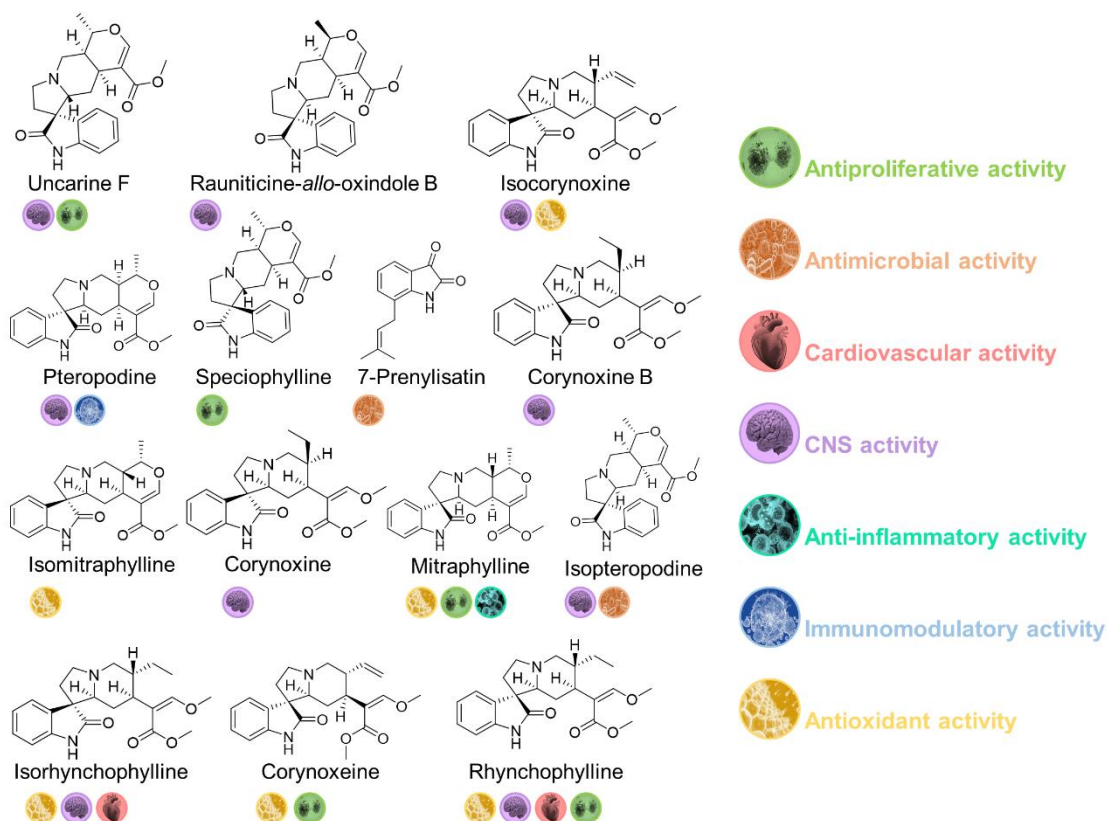


Figure 1.4. Examples of bioactive natural oxindole alkaloids and respective biological activities.

indicating the potential of oxindole-bearing compounds to bind to multiple targets, in significant contexts of polypharmacology.⁷⁶⁻⁸¹

1.2.1.1. Oxindole Derivatives: From Drug Discovery to Clinical Practice

The potential of the oxindole and the isatin scaffolds to operate as versatile starting materials for several chemical transformations, makes them valuable candidates to play a central role in drug discovery programmes. Furthermore, several compounds bearing the oxindole scaffold reached clinical trials and/or are currently commercialized, showcasing the interest of performing chemical transformations on the isatin core to discover new drug candidates.

1.2.1.1.1. Oxindole-Based Drugs Reaching Clinical Trials: Successes and Failures

A total of 15 molecules bearing the oxindole scaffold reached humans. This puts into evidence the privileged nature of this bicyclic chemical moiety, especially because these compounds were introduced for multiple therapeutic applications (**Figure 1.5**). The outcomes are quite variable with some being widely used in therapeutics, while others have been removed due to lack of therapeutic efficacy, toxicity issues, or even because they became unnecessary.

Methisazone was one of the first oxindole based drug candidates to reach clinical trials. Developed in the 1960s, methisazone was used in clinical practice for smallpox prophylaxis.⁸²⁻⁸⁴ Due to the success of vaccination programmes which lead to the eradication of smallpox in 1980, it became redundant in the clinical practice context.⁸⁵ Nowadays, bioterrorism and the emergence of poxviruses able to cause human disease, combined with the loss of protection against smallpox by the community, places this molecule at the center of the development of new agents for prophylaxis and treatment of these viral diseases.⁸⁶⁻⁸⁹

Oxyphenisatin and related compounds were widely used as laxative/purgative agent. Severe hepatotoxicity led regulatory authorities to withdraw this molecule from the market,^{90, 91} being now included in the list of “do not compound” drug products by the Food and Drug Administration (FDA) and other regulatory authorities.^{92, 93} Tenidap, designed as a NSAID for the treatment of rheumatoid arthritis, had its approval rejected by FDA due to toxic effects.⁹⁴⁻⁹⁶ Indolidan, evaluated for the treatment of congestive heart

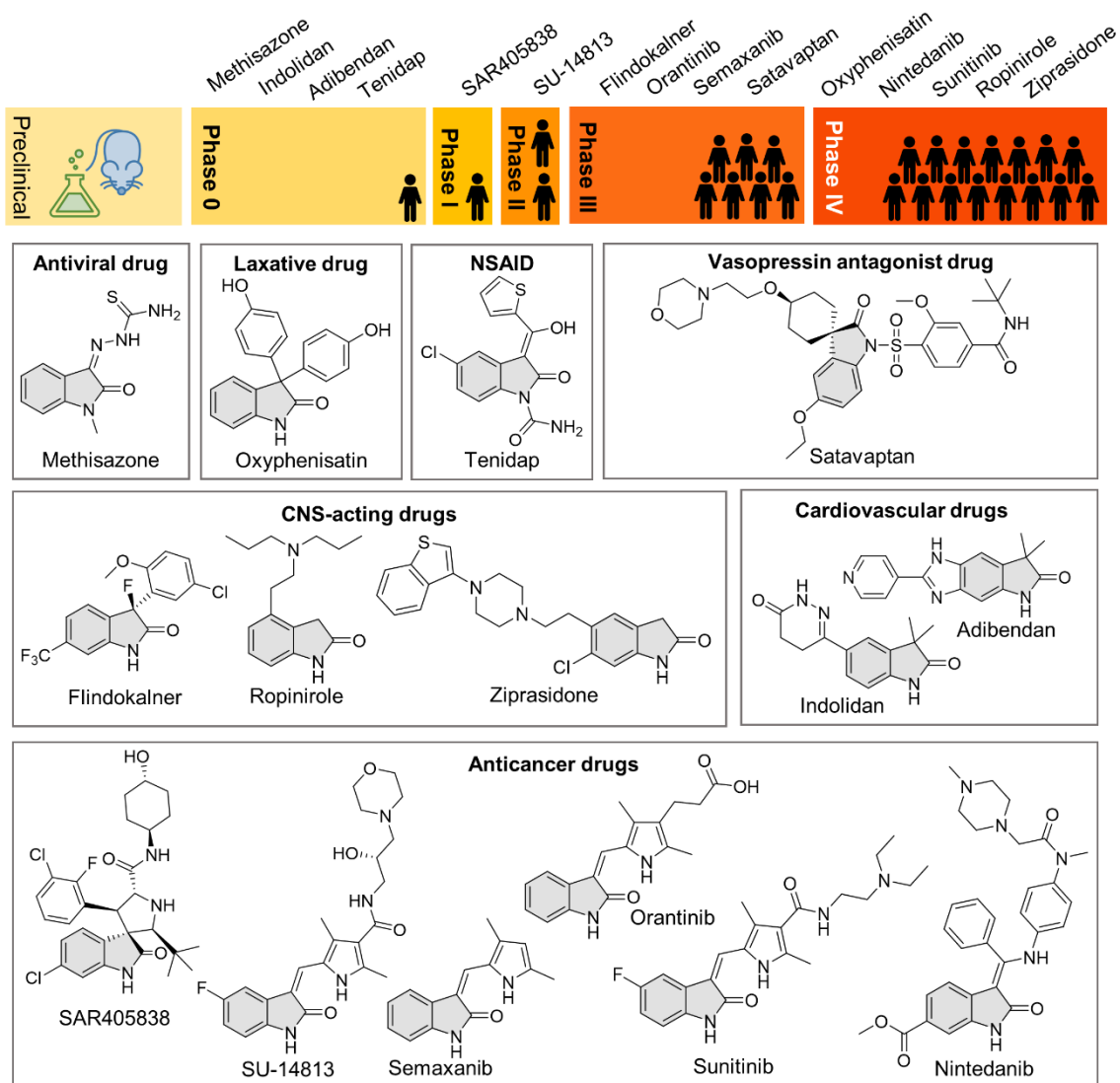


Figure 1.5. Oxindole-based drugs reaching clinical trials.

failure (phosphodiesterase IV inhibitor) proved to be effective only in acute administration, but not during chronic therapeutic treatments. Furthermore, arrhythmias were identified as an undesired side-effect, especially harmful in the target population.^{97, 98} The other drug developed for cardiovascular pathologies, adibendan, was experimentally used in the late 1980s and early 1990s in patients with severe congestive heart failure, due to its activity as a positive inotropic phosphodiesterase III inhibitor.⁹⁹⁻¹⁰²

Satavaptan, a vasopressin receptor-2 antagonist, reached Phase III clinical trials for the treatment of hyponatremia and ascites.¹⁰³⁻¹⁰⁵ Approval was not granted, as the overall risk benefit balance was negative.¹⁰⁶

Some of best examples of success of oxindole-based drugs can be observed in pathologies affecting the CNS. Flindokalner is a potent opener of the large conductance calcium-activated K^+ channels and applied in clinical trials for the treatment of cerebral ischemia/stroke. Despite no significant toxicity was observed for this drug candidate, its

development was stopped due to lack of efficacy when compared with placebo. Nevertheless, it is currently in preclinical studies for other pathologies, including clinical manifestations affecting the CNS (anxiety, migraine, depression), smooth muscle (preterm labor, constipation, bladder instability, angina pectoris), as well as ear pathologies (such as tinnitus or salicylate-induced ototoxicity).¹⁰⁷⁻¹⁰⁹ Ropinirole, on the other hand, is widely used in the therapeutics of Parkinson's disease, since it is a dopamine receptor agonist. It is also approved for the treatment of restless legs syndrome (RLS) and some evidence exists on its potential to treat psychiatric disorders, tremor, Tourette's syndrome, and amyotrophic lateral sclerosis (ALS).¹¹⁰⁻¹¹² The third molecule, ziprasidone, is an atypical antipsychotic drug, used worldwide for the treatment of schizophrenia, bipolar disorder and acute mania. Its mechanism of action is multifactorial, binding to several receptors present in the CNS.¹¹³⁻¹¹⁵

The largest number of oxindole derivatives reaching clinical trials is observed for anticancer agents. SAR405838 is a new orally bioavailable HDM2 antagonist, disrupting the p53-HDM2 interaction, leading to p53-dependent cell cycle arrest and apoptosis. It recently reached phase I clinical trials with promising results in combination therapy to treat solid tumors.¹¹⁶⁻¹¹⁸ The remaining five molecules are tyrosine-kinase inhibitors, exhibiting different levels of selectivity towards different kinases, as there are over 90 tyrosine kinases reported in humans.¹¹⁹ SU-14813 was used in phase I clinical trials for the treatment of advanced solid malignancies and moved on to phase II for the treatment of metastatic breast cancer. This molecule also displays anti-angiogenic potential, and therefore might be a useful therapeutic option.¹²⁰⁻¹²² Semaxanib reached phase III clinical trials, for the treatment of advanced colorectal cancer, but further development was dropped due to discouraging results, combined with the emergence of more promising tyrosine kinase inhibitors.^{123, 124} Orantinib also reached phase III clinical trials for the treatment of unresectable hepatocellular carcinoma recently, however the results shown no significant improvement in the overall survival of the patients.¹²⁵⁻¹²⁷

Nintedanib and sunitinib are two marketed drugs bearing the oxindole unit used in clinical practice. They are both orally available, improving therapeutic compliance and patients' comfort. However, their therapeutic applications are quite different. Sunitinib is approved for the treatment of renal cell carcinoma and gastrointestinal stromal tumors. In addition, several clinical trials are currently underway to study the effect of this drug, isolated or in combination therapy, in other cancer types,¹²⁸⁻¹³¹ despite some toxicity concerns.^{132, 133} Nintedanib is used as anticancer agent in non-small cell lung cancer,^{134, 135} but it is also approved for the treatment of idiopathic pulmonary fibrosis. It is one of the few pharmacological therapeutic options available for patients suffering of this condition, which evidences the relevance of this oxindole-based drug. It is currently

under numerous clinical trials for further therapeutic uses, including for advanced pancreatic cancer and fibrotic lung disease after severe acute respiratory syndrome coronavirus 2 (SARS-CoV-2) related pneumonia.¹³⁶⁻¹³⁸

Another molecule worth mentioning is toceranib, relevant in veterinary medicine. It is also a tyrosine kinase inhibitor and used to treat mastocytoma in dogs. This molecule was developed in parallel with sunitinib, but ended up being approved for veterinary use, being one of the few examples of dog-specific anticancer agents.^{139, 140}

1.2.1.1.2. Oxindole-Based Drug Candidates: A Clear Trend

Over the past two decades, the number of publications reporting oxindole and isatin-based derivatives with a wide range of biological activities has been increasing (**Figure 1.6**). Among the most commonly reported bioactivities, anticancer, antimicrobial, antiviral, antioxidant and anti-inflammatory are the most relevant. The already mentioned isatin scaffold potential to undergo multiple chemical transformation in various positions, as well as the considerable number of bioactive oxindole-derived natural products and drugs, inspired several research groups to develop drug discovery research and development projects around this family of compounds.¹⁴¹⁻¹⁴⁸ It is therefore expected that more molecules bearing this scaffold will reach clinical trials in the upcoming years.

Notoriously inspired by the structures of oxindole-based natural products, several efforts have been made in the synthesis and biological activity evaluation of novel spirooxindole derivatives.¹⁴⁹⁻¹⁵¹ Several approaches were also established to promote asymmetric version to access enantioselectivity, usually at position 3 of the oxindole unit.^{152, 153} Less common, but also gaining attention in several fronts is the synthesis of 3,3-disubstituted oxindole derivatives. These compounds, from both natural (*e.g.*, maremycins, TMC-95A-D) or synthetic (*e.g.*, flindokalner) origins, also exhibit relevant pharmacological properties, and more attention has been provided for these compounds, from the synthetic and medicinal chemistry point of view.¹⁵⁴⁻¹⁵⁶ The asymmetric catalytic synthesis of 3,3-disubstituted oxindole derivatives was recently reviewed by us (see **Appendix 1**).¹⁵⁷

The biological activity reported by oxindole based drug candidates is highly dependent on the isatin inherent reactivity, as well as the availability of commercially available isatin building blocks. The unique reactivity displayed by the carbonyl group at position 3 of isatin, as well as the wide availability of commercial 5-substituted isatins explain that these two positions are the most widely explored in the generation of new libraries in drug discovery context. Several molecules are currently under preclinical

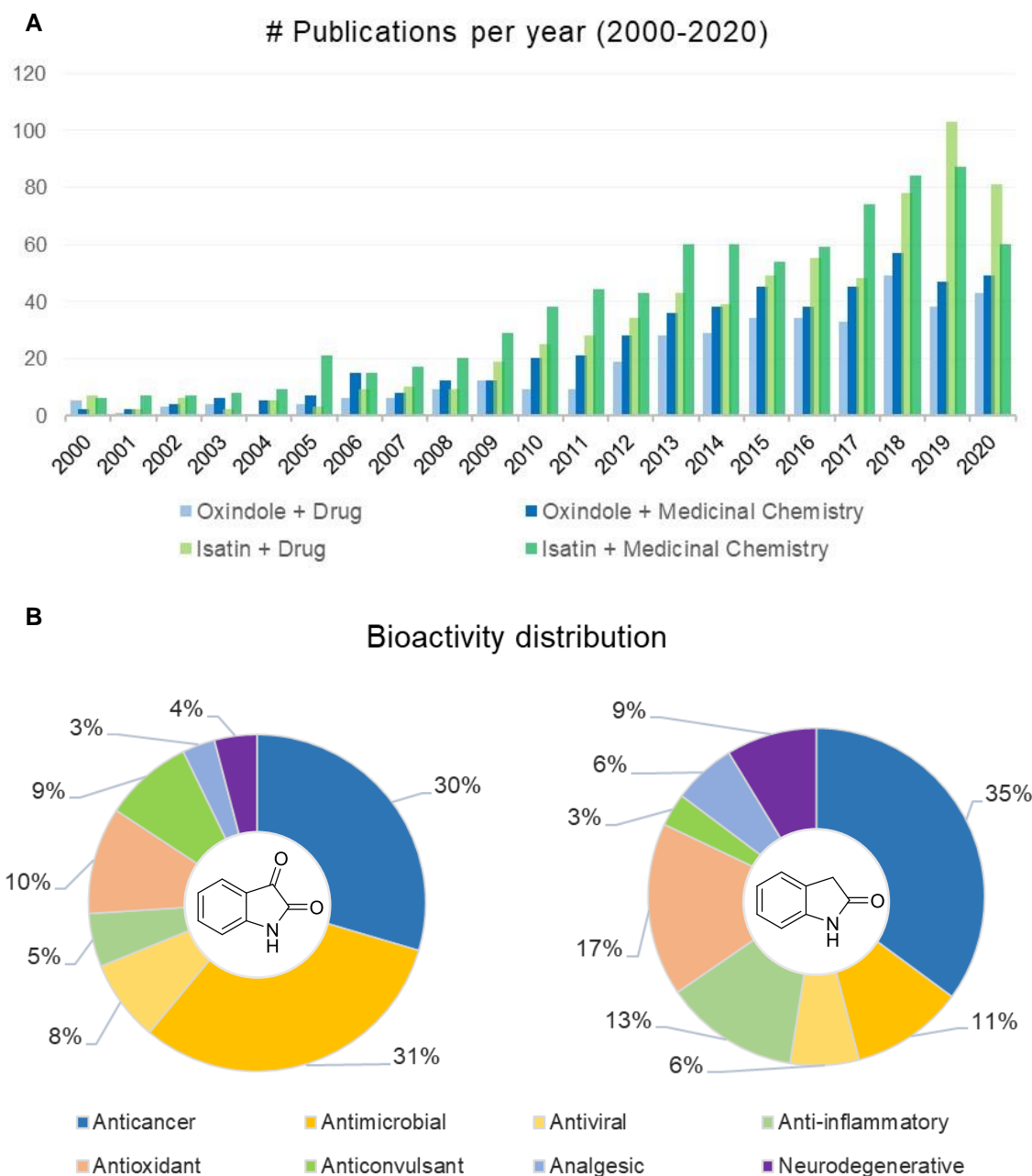


Figure 1.6. Evolution of the number of publications in the last two decades concerning bioactive isatin/oxindole derivatives (data was collected using *Web of Science*, with keywords “isatin” or “oxindole” combined with “medicinal chemistry” or “drug”) (A). Most common bioactivities reported for isatin (left) and oxindole (right) derivatives in the same time period (B).

development due to their pharmacological potential, and the wide diversity of biological activities reported put in evidence the privileged nature of the oxindole scaffold (Figure 1.7).^{158, 159}

It is noteworthy that due to the importance of the oxindole scaffold, several of these new derivatives first undergo phenotypic assays, and then the most promising

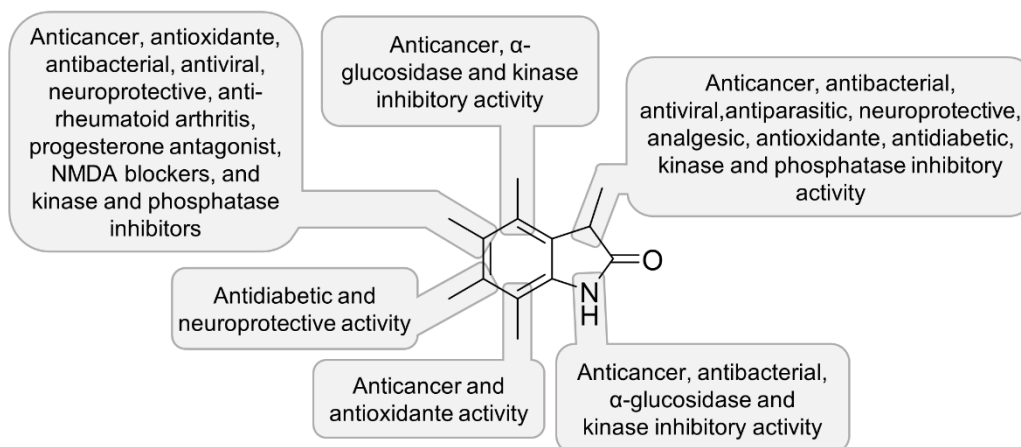


Figure 1.7. Explored pharmacological activities of the oxindole core.

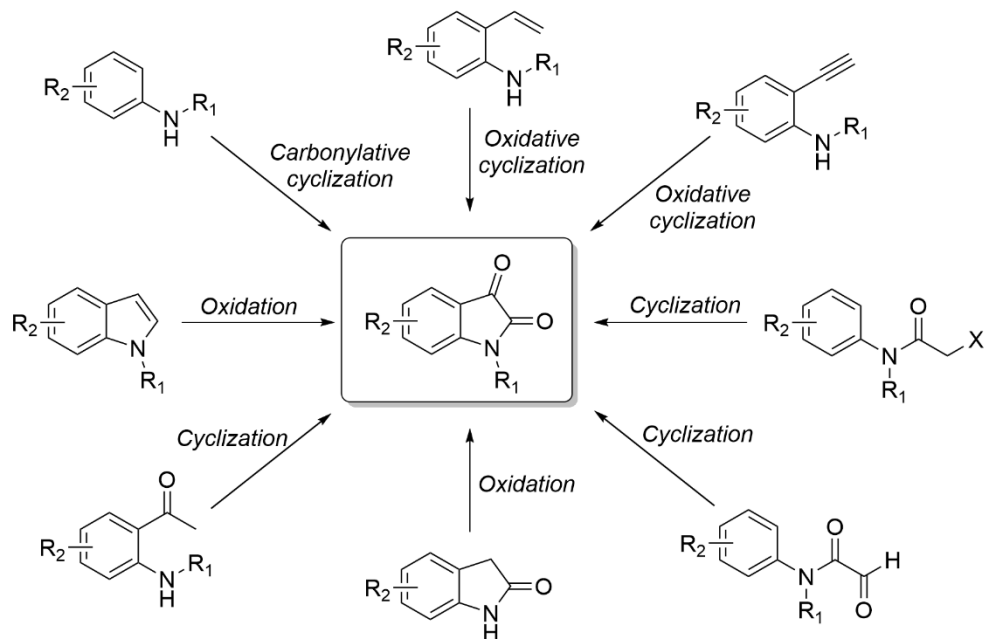
compounds are evaluated in what concerns their mechanism of action and molecular target.^{158, 159} Indeed, phenotypic drug discovery is regaining relevance over target-based screening, which became the “golden-rule” with the advent of computational docking studies. Phenotypic assays can help to overcome constraints caused by the complexity of the disease when appropriate disease models are employed (it can provide a more holistic and complete approach of the physiopathological process of the disease, while target-based screening can be too simplistic) and help to unveil new possible targets and mechanisms of action (allosteric binding sites, for example). Phenotypic drug discovery also possesses some drawbacks, since it can make it harder to properly identify hit compounds, as well as to determine the drug target and mechanism of action.^{160, 161}

The endogenous presence of oxindole and isatin related to physiological processes, combined with the pharmacological activity displayed by several of its natural and synthetic derivatives, including several compounds reaching clinical practice, makes isatin a valuable starting point for chemical library design and oxindole a privileged structure in drug discovery.

1.2.1.2. From Nature to the Laboratory: Isatin in Synthetic Organic Chemistry

Over recent years, a lot of attention has been given to the synthesis of novel oxindole derivatives from isatin. Despite its current widely commercial availability, several efforts have been developed for the preparation of isatin in synthetic organic chemistry laboratories, since these methodologies are able to unlock new substitution patterns in the isatin core. Common approaches are the oxidation of indole derivatives (using iodine oxidants, ruthenium-catalyzed oxidation reactions, among others), the

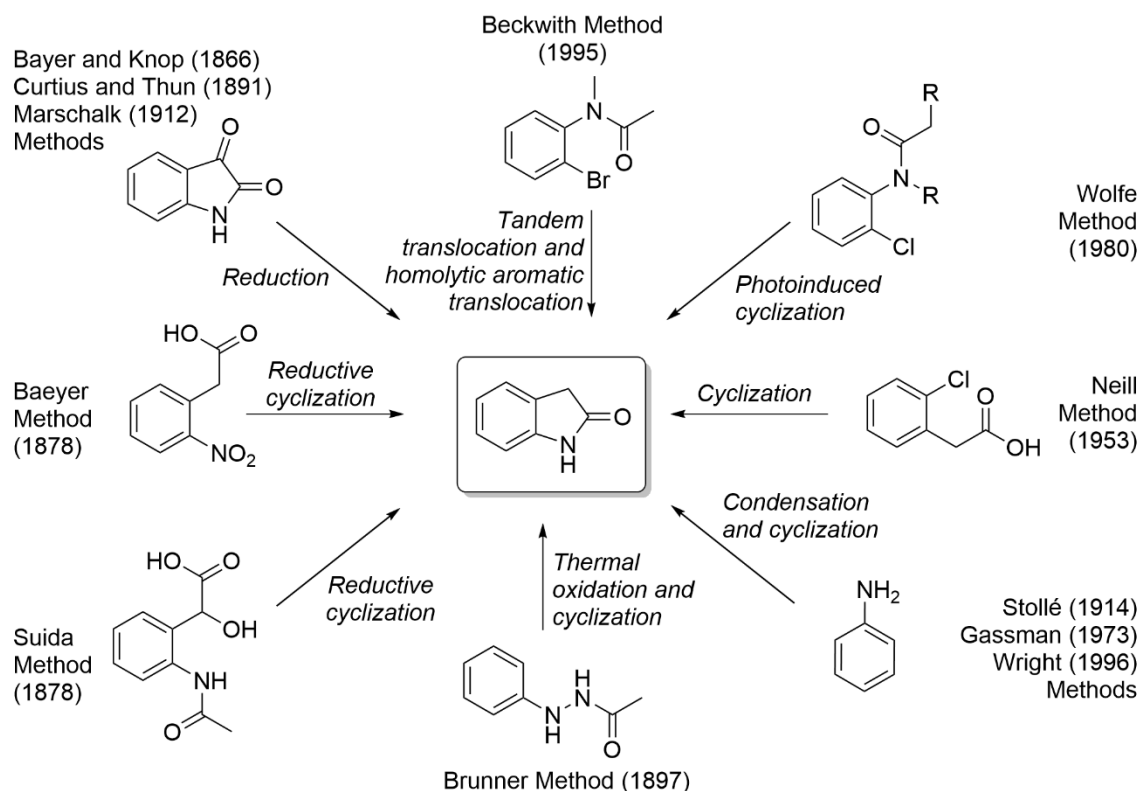
oxidation of oxindoles, 2-alkynyl or 2-alkenyl-anilines, the cyclization of *o*-aminoacetophenones or *N*-acylanilines, and direct carbonylation of anilines (**Scheme 1.2**).¹⁶²



Scheme 1.2. Main synthetic routes for the synthesis of the isatin scaffold.

The oxindole core can be also prepared via a wide range of chemical transformations, including using isatin as starting point. Shortly after the laboratorial synthesis of isatin in 1840, Bayer and Knop used this compound for the preparation of oxindole, via reduction reaction with sodium amalgam in the presence of a base, followed by treatment with tin and mineral acids. Several other chemists followed this path, and different reductive conditions were successfully employed to convert isatin to oxindole. Alternative commonly used methods to afford the oxindole core require 2-nitrophenylacetic acid (in the presence of tin and hydrochloric acid as reducing agents), 2-acetaminomandelic acid, β -acetylphenyl hydrazine, α -halogenated acid chloride condensation with aniline, and *o*-chloro-phenylacetic acid (heated in the presence of concentrated ammonium hydroxide and copper powder). All these methods were developed throughout the 19th century until the early 1950s, showing the relevance of the oxindole core in synthetic organic chemistry since its early years. More recent developments comprise the Gassman and Wright methodologies from aniline, the Wolfe method involving photoinduced cyclization of *N*-acyl-*o*-chloroanilines, and the Beckwith method from *o*-bromo-*N*-methylanilides (**Scheme 1.3**).¹⁶³⁻¹⁷⁴

Both the oxindole and the isatin scaffolds can undergo a wide variety of chemical transformations, creating high added-value molecules (**Figure 1.8**). In the isatin case, its unique reactivity at the carbonyl at position C3 is of great interest for the generation of



Scheme 1.3. Common methods for the preparation of the oxindole nucleus.

new libraries, withstanding a considerable range of modifications. Imine derivatives, thiosemicarbazones, spirooxindoles, 3,3-disubstituted oxindoles, as well as different heterocyclic families can be synthesized, the late one based on isatin ring-opening reactions. Substitutions in the aromatic ring, at position 1 (NH group) are also common strategies explored by several research groups. Reactivity of the amide carbonyl group at position C2 can lead to the preparation of relevant molecules, such as indigo and indirubin, as well as to some spiro compounds.¹⁷⁵⁻¹⁷⁸

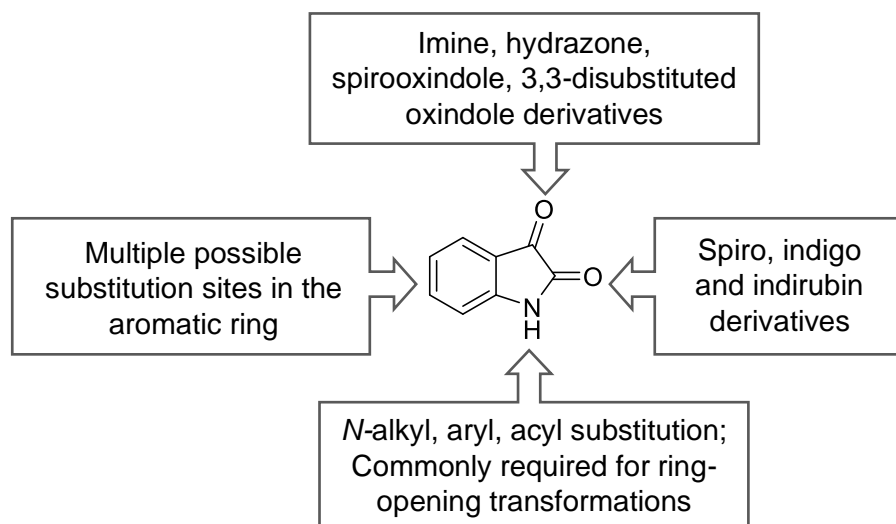


Figure 1.8. Chemical transformations of the isatin scaffold.

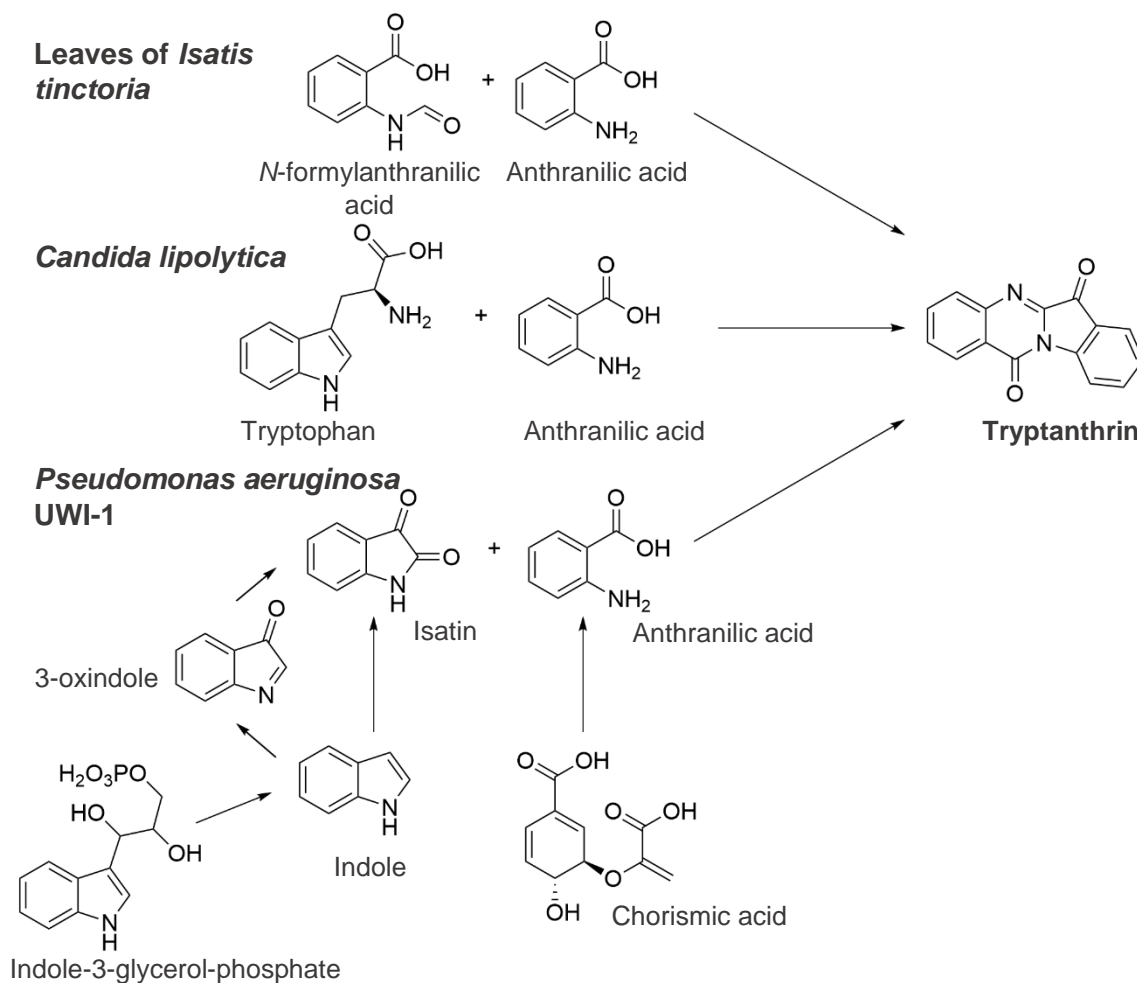
1.2.2. Tryptanthrin: the Golden-Yellow Alkaloid

Tryptanthrin (indolo[2,1-*b*]quinazoline-6,12-dione) is a indoloquinazoline alkaloid which has been around organic chemists labs since the beginning of its days, back in the 19th century. While its laboratorial preparation can date back to 1822, its presence has been indicated in multiple occasions throughout the 19th century and the early 20th century by chemists working with indigo, who often described golden-yellow needles/crystals as a product of indigo oxidation.^{179, 180} However, the tryptanthrin structure was only proposed in 1915, by Friedländer and Roschdestwensky, who prepared this alkaloid from air oxidation of indigo at high temperatures and also from the chemical reaction between isatin and anthranilic acid. At this stage, the name given to this tetracyclic alkaloid was anhydro- α -isatinanthranilide.¹⁸¹ The name tryptanthrin was later coined in 1971, when the compound was isolated from the culture of the yeast *Candida lipolytica* grown in the presence of high concentrations of tryptophan.¹⁸² The crystal structure was confirmed a few years later.¹⁸³

In the same decade, tryptanthrin was isolated from different natural sources, including the leaves of *Strobilanches cusia*, used in asian folk medicine for multiple purposes,¹⁸⁴ including *tinea pedis*, widely known as athlete's foot disease.¹⁸⁵ At this stage, the alkaloid was screened against a wide range of microorganisms, demonstrating specificity against dermatophytes as a fungistatic agent.¹⁸⁶ Later on, tryptanthrin was isolated from other plant species, including *Persicaria tinctoria* (commonly known as Chinese or Japanese indigo), *Isatis tinctoria* (also referred as *Isatis indigotica*, commonly named woad), *Couroupita guianensis* (commonly known as cannonball tree), *Wrightia* spp. and *Calanthe* spp., indicating a wide natural distribution of the compound across different genus of the kingdom *Plantae*, as well as in different geographical regions. In some of the cases, however, tryptanthrin might be formed during the treatment of the natural sources (drying, fermentation, oxidation) rather than existing in big quantities in the natural sources.^{58, 59, 187-189}

The exact biosynthetic pathway of tryptanthrin in plants remains unknown.¹⁹⁰ Studies performed in microorganisms which produce tryptanthrin, namely *Candida lipolytica* and *Pseudomonas aeruginosa* UWI-1, indicate its biosynthesis occurs from anthranilic acid and tryptophan,^{191, 192} or from anthranilic acid (generated from chorismic acid) and isatin (generated from oxidation of indole, a product from the metabolism of indole-3-glycerol-phosphate), respectively.¹⁹³ Further studies performed in leaves of *Isatis tinctoria* based on the incorporation of isotopically labeled compounds suggest anthranilic acid and *N*-formylanthranilic acid as the primary biosynthetic precursors of tryptanthrin (**Scheme 1.4**). Its presence in plants can be triggered by external

aggression, suggesting an ecological role, as it seems that tryptanthrin production is induced by contact with microorganisms, namely fungi, working as a phytoalexin (*i.e.*, a compound produced by a plant as a mechanism of defense against parasites).¹⁹⁴



Scheme 1.4. Possible biosynthetic pathways for tryptanthrin in different organisms.

Tryptanthrin has also been isolated from other microorganisms, including alphaproteobacterium *Oceanibulbus indolifex*, isolated from the north sea,¹⁹⁵ *Cytophaga* sp. strain AM13.1,¹⁹⁶ and fungi *Schizophyllum commune* (isolated from a patient with allergic bronchopulmonary mycosis)¹⁹⁷ and *Leucopaxillus cerealis*.¹⁹⁸ There are also two accounts indicating the presence of tryptanthrin in mammals, namely in the urine of *Elephas maximus* (Asian elephant),¹⁹⁹ and in the wing sac liquids of *Saccopteryx bilineata* (greater sac-winged bat).²⁰⁰

The presence of tryptanthrin in folk medicine formulations, as well as the early reports on its pharmacological relevance, led to several studies being conducted in order to explore the potential of this alkaloid as a drug candidate. Tryptanthrin has shown to exhibit several relevant biological activities, *in silico*, *in vitro* and *in vivo* (**Figure 1.9**).

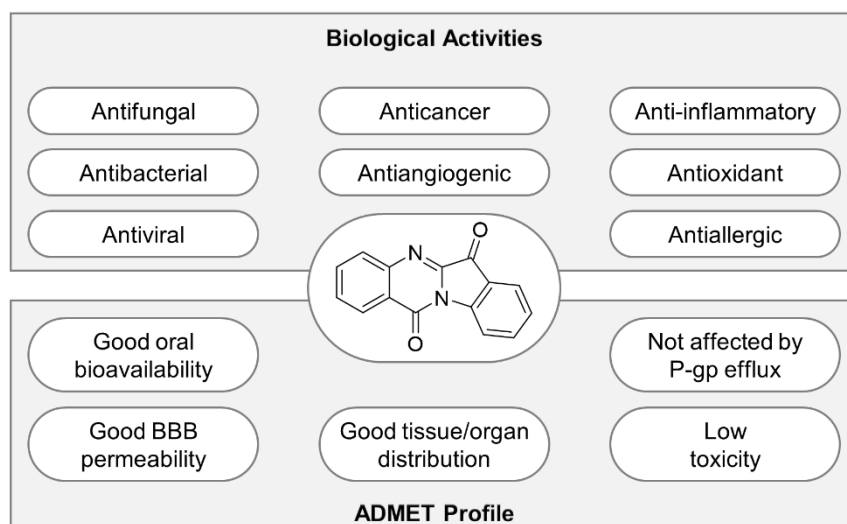


Figure 1.9. Main biological activities and pharmacokinetic profile features of tryptanthrin.

The antibacterial properties of tryptanthrin have been explored against several bacteria strains. Docking studies indicate the potential of this alkaloid to inhibit the enoyl carrier protein reductase (InhA) of *Mycobacterium tuberculosis*, the target of drugs such as isoniazid, which is facing growing drug resistance.²⁰¹ *In vitro*, it has shown moderate to good antibacterial activity against both Gram positive, including methicillin-resistant *Staphylococcus aureus* (MRSA), and Gram negative bacteria.^{193, 202} Its activity has also been assessed against *Helicobacter pylori*, both *in vitro* and *in vivo* (using infected *Meriones unguiculatus*, commonly known as Mongolian gerbils), with promising results.²⁰³ Tryptanthrin has very recently been described as a potential antiviral agent, namely against *Influenza A* virus and coronavirus (HCoV-NL63).²⁰⁴⁻²⁰⁶

The previously discussed antifungal activity, namely against dermatophyte pathogens, has been recently further explored *in vitro*, in order to better understand the mechanism of action (using fibroblasts and keratinocytes infected with *Trichophyton benhamiae*). Tryptanthrin was capable to fully prevent fungi-induced damage to dermal fibroblasts, and considerably reduced it in epidermal keratinocytes, via down-regulation of pro-inflammatory cytokines and antimicrobial peptides (AMP) expression promotion, being a good indicator of the dual activity of tryptanthrin, as a strong antifungal compound and as an innate immune response modulator.²⁰⁷

Tryptanthrin also exhibits a remarkable anti-inflammatory activity, in an ideal polypharmacology context, as it can interact with multiple targets linked with the inflammation process. This alkaloid is able to inhibit prostaglandin synthesis, being selective against cyclooxygenase-2 (COX-2), as well as to inhibit leukotriene synthesis by 5-lipoxygenase (5-LOX).^{208, 209} Other pro-inflammatory factors, such as cytokine IL-6

and tumor necrosis factor- α (TNF α), can also get their signaling pathways interrupted by the administration of tryptanthrin.²¹⁰ This anti-inflammatory activity has been explored *in vivo*, using disease models of colitis and pleurisy, with the advantage that tryptanthrin was active even after oral administration.^{211, 212} Tryptanthrin has also shown activity against neuroinflammatory conditions *in vivo*, using BV2 microglial cell line, and therefore present potential to treat neurodegenerative and other neuropathological processes, such as those which tend to occur after ischemic stroke. This activity is mediated via suppression of pro-inflammatory cytokines, namely *via* suppression of the nuclear factor erythroid 2-related factor 2 (Nrf2)/heme oxygenase 1 (HO-1), NF- κ B, and p38 signaling pathways.²¹³⁻²¹⁵ Recent studies also reported tryptanthrin as a useful regulator of the toll-like receptor 3 (TLR3)-mediated vascular inflammation.²¹⁶

The anti-inflammatory properties of tryptanthrin can also be employed in the treatment of skin diseases involving pro-inflammatory processes, such as atopic dermatitis and psoriasis. This effect can be translated in the down-regulation of thymic stromal lymphopoietin (TSLP), *via* MDM2 expression inhibition and p38 expression promotion, as well as several other regulators of this skin diseases, including histidine decarboxylase, IL-1 β , IL-4, IL-6, and TNF α .²¹⁷⁻²¹⁹ Tryptanthrin also down-regulates apelin promoter activity, an angiogenic factor, leading to an antiangiogenic effect in endothelial cells, a key pathological step of psoriasis.²²⁰

Tryptanthrin interferes with the production of cytokine IL-4, as well as prevents IgE-mediated degranulation *in vitro*, indicating its potential to inhibit type I allergic events.²²¹

The interaction of tryptanthrin with the immune system also makes it a great anticancer drug candidate. Positively, several examples can be found in the literature reporting tryptanthrin effectiveness against several solid tumors, and leukemia. Among the tumors evaluated, non-melanoma skin cancer, breast adenocarcinoma, gastric cancer, lung cancer, and neuroblastoma are some of those displaying more relevant results. The mechanism of antitumoral activity is correlated with tryptanthrin anti-inflammatory, antiangiogenic, and antioxidant activities, as it can suppress carcinogenesis and cell growth, and induce cell differentiation and apoptosis.^{190, 222-227}

The pharmacological potential of tryptanthrin already led to more detailed pharmacokinetic studies on this quinazoline alkaloid, using Sprague-Dawley rats and Kunming mice, exploring intravenous and oral administration route, respectively. The results show a good pharmacokinetic profile, being well distributed in the plasma after oral administration, indicating good oral absorption, and it tends to be found in higher concentrations in the liver, kidney, and lung. Lower concentrations were attained in spleen, heart, and brain. Nevertheless, the ability of tryptanthrin to reach the brain is also confirmed by several *in vitro* models indicating the potential to cross the BBB. *In vitro*

evaluation also showed that tryptanthrin is not a substrate of P-glycoprotein (P-gp), an efflux pump highly correlated with drug resistance in chemotherapy.^{228, 229}

The therapeutic potential and the promising pharmacokinetic profile of tryptanthrin, places this molecule well ahead in the pre-clinical pipeline, and might in the near future start to be used in human clinical trials.

1.2.2.1. Tryptanthrin Derivatives in Drug Discovery

The privileged nature of the tryptanthrin scaffold is put into evidence with the wide variety of recent reports on novel tryptanthrin derivatives bearing various bioactivities (**Figure 1.10**). Anticancer activity has been reported for several tryptanthrin derivatives,^{230, 231} and several potential targets and mechanisms of action have been identified, including inducing caspase dependent apoptosis through extracellular-signal-regulated kinase (ERK) up regulation,²³² topoisomerases I and II inhibition,²³³⁻²³⁵ multidrug resistance protein 1 (MDR1) down-regulation,²³⁴ and indoleamine 2,3-dioxygenase 1 (IDO1) and tryptophan 2,3-dioxygenase (TDO) inhibition.²³⁶⁻²³⁹

Other derivatives displayed relevant potential as new antimicrobial agents, including against MRSA and *Mycobacterium tuberculosis*.²⁴⁰⁻²⁴² Antiparasitic activity against *Plasmodium falciparum* and *Toxoplasma gondii* has also been reported for tryptanthrin derivatives.²⁴³⁻²⁴⁵

Tryptanthrin-6-oxime derivatives showed great potential as anti-inflammatory agents, operating as c-Jun *N*-terminal kinase inhibitors.²⁴⁶ Recent *in vitro* and *in vivo*

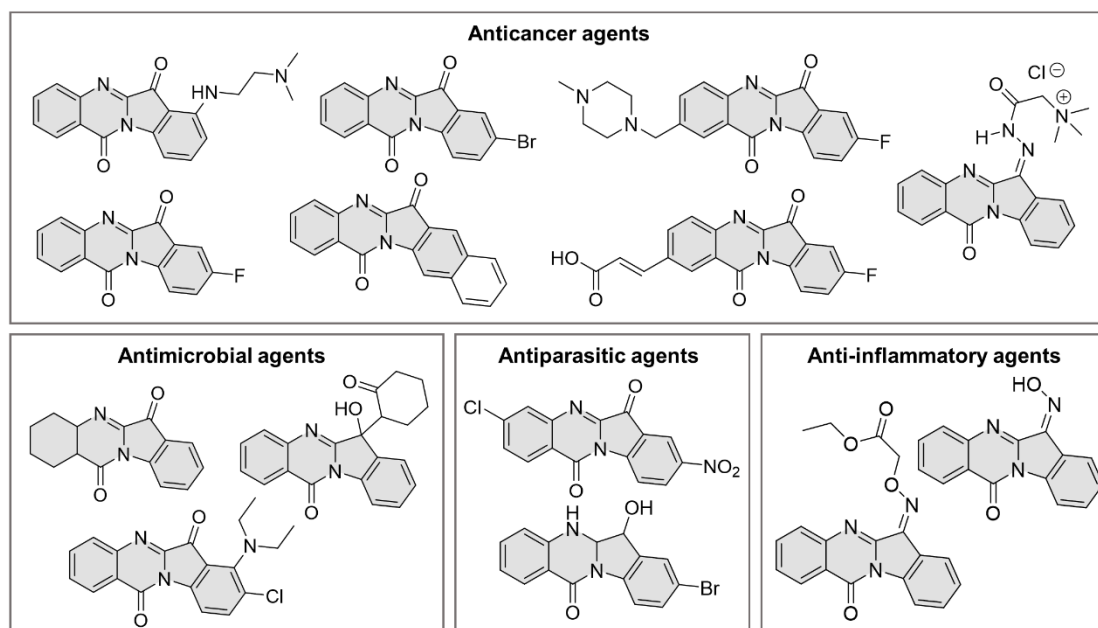


Figure 1.10. Examples of recently reported bioactive tryptanthrin derivatives.

studies indicate the potential of these derivatives to be suitable drug candidates for complex auto-immune and pro-inflammatory pathologies, such as rheumatoid arthritis.²⁴⁷

Also worth mentioning is a recent example where tryptanthrin derivatives were studied in what concerns their potential application as agrochemicals. Some of these derivatives exhibited good potential against plant pathogens, including tobacco mosaic virus (TMV) and the fungus *Physalospora piricola*.²⁴⁸ These findings open the door for further potential applications of tryptanthrin and its derivatives for the protection and quality improvement of crops. For more detailed information, the review “Tryptantrina: da Natureza ao Laboratório” can be consulted, as it explores the potential applications of tryptanthrin and its derivatives (see **Appendix 2**).²⁴⁹

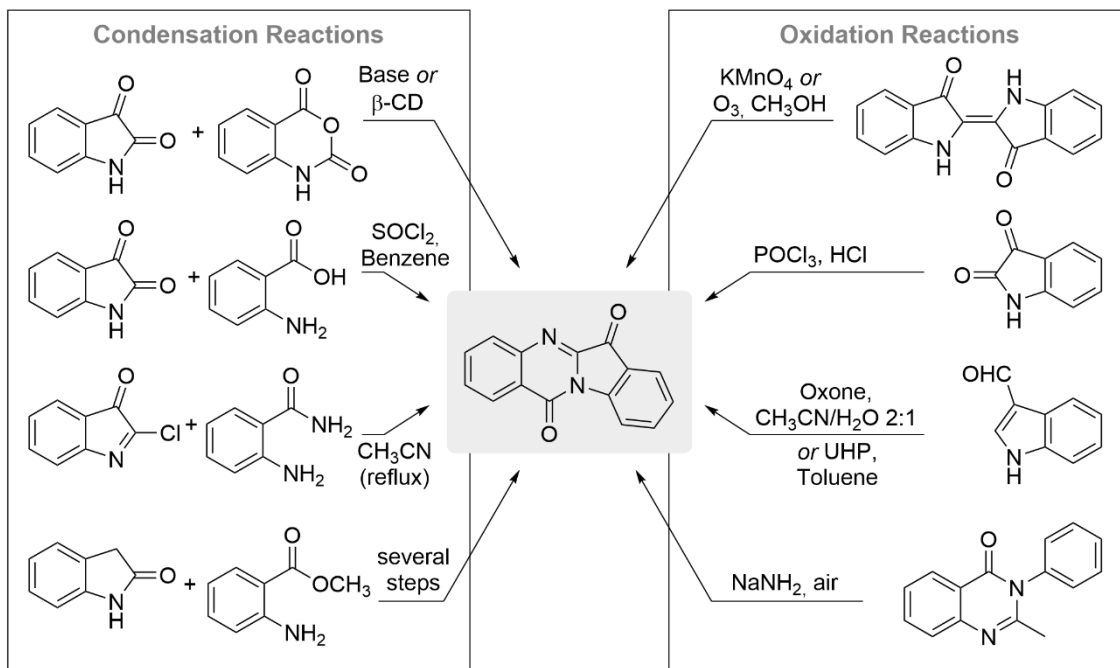
1.2.2.2. Synthesis and Chemical Transformations of the Tryptanthrin Scaffold

The potential applications of tryptanthrin got the attention of several research groups, which developed several synthetic methodologies to attain this tetracyclic alkaloid. These approaches can be divided into two main groups, the condensation reactions and the oxidation reactions. In the first case, the condensation between isatin or oxindole derivatives with anthranilic acid derivatives, namely isatoic anhydride, is widely explored, with a wide range of catalysts and reaction conditions reported in the literature. The oxidation reactions usually require indigo or isatin as starting materials in the presence of strong oxidants, but other reaction conditions have also been described. These processes usually start by oxidizing indigo to isatin and isatoic anhydride (or isatin to isatoic anhydride), followed by their respective condensation.^{179, 250, 251} **Scheme 1.5** summarizes some of these approaches, as well as some of the reaction conditions required for the synthesis of tryptanthrin.

The development of tryptanthrin derivatives is also a growing field in synthetic organic chemistry, in the quest for new molecules with different potential applications (dyes, bioactive products) and the development of synthetic routes for the preparation of tryptanthrin-based natural products, such as phaitantrins A-E, methylisatoid, candidine²⁵², and ophiuroidine.²⁵³ Among the most explored synthetic methodologies applied to modify the tryptanthrin core, aromatic substitutions and reactions involving the carbonyl group at position 6 are the most commonly reported and are summarized in **Figure 1.11**.

At this point, the selection of isatin and tryptanthrin as privileged structures and starting points for the synthesis of new molecules with potential biological activity

emerges as a promising approach. In the next section, the tools used to achieve these molecules will be discussed.



Scheme 1.5. Common methodologies for the preparation of tryptanthrin.

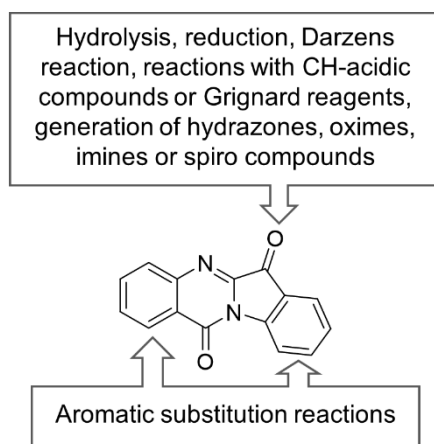


Figure 1.11. Chemical transformations performed in the tryptanthrin scaffold.

1.3. Selecting Tools for the Discovery of New Potential Bioactive Molecules

“Equipped with his five senses, man explores the universe around him and calls the adventure Science.”

Edwin Powell Hubble

1.3.1. Green Chemistry and Sustainable Chemistry: are They Synonyms?

As highlighted in the first paragraphs of this introduction, mankind has always devoted attention to the health and well-being of its communities. Nowadays, it became clear that the efforts made to develop new therapeutic options need to take into account the impact on ecosystems and environment of such actions, in a true One-Health approach.^{254, 255} This has been translated to the attention given by regulatory authorities and the pharmaceutical industry to develop guidelines to help to put into practice green chemistry and sustainable chemistry approaches. Although often used interchangeably, it is becoming more prominent the assumption that these two fields, despite highly overlapped, represent two different things.

Out of the two, green chemistry emerges has the one having a more solid definition. One of the possibilities, shared by the European Environment Agency (EEA)²⁵⁶ and the United States Environmental Protection Agency (EPA),²⁵⁷ defines green chemistry as the “design of chemical products and processes that reduce or eliminate the use and generation of hazardous substances”, a definition based on the work developed by Paul T. Anastas and co-workers in the turn of the century.^{258, 259} However, EPA also enunciates that “green chemistry is also known as sustainable chemistry”.²⁵⁷ In the year 2000, the Working Party on Synthetic Pathways and Processes in Green Chemistry of the IUPAC (International Union of Pure and Applied Chemistry) presented an alternative definition, stating that green chemistry is “the invention, design, and application of chemical products and processes to reduce or to eliminate the use and generation of hazardous substances”.^{260, 261} The two definitions are very similar, although the second becomes more embracing, by including the invention and application steps into the definition. A clearer picture of what green chemistry comprises is given by its twelve principles, depicted in **Figure 1.12** – top.

On the other hand, the definition of sustainable chemistry is often more “loosely” given and remains somehow unclear. Different authors, policy makers, and regulatory authorities tend to use their self-made definition of sustainable chemistry, which even gave rise to recent political actions by the United States Congress.²⁶² Although as mentioned before, the EPA uses the two terms as synonyms, the Congress hearing on the topic indicates that sustainable chemistry should be considered as a wider field, although green chemistry remains as a core component of it.^{263, 264} This broader sense of sustainable chemistry is translated into one of its definitions, provided by OECD (Organization for Economic Co-operation and Development), which defines sustainable chemistry as “a scientific concept that seeks to improve the efficiency with which natural resources are used to meet human needs for chemical products and services.” It “encompasses the design, manufacture and use of efficient, effective, safe and more environmentally benign chemical products and processes”, being also a “process that

stimulates innovation across all sectors to design and discover new chemicals, production processes, and product stewardship practices that will provide increased

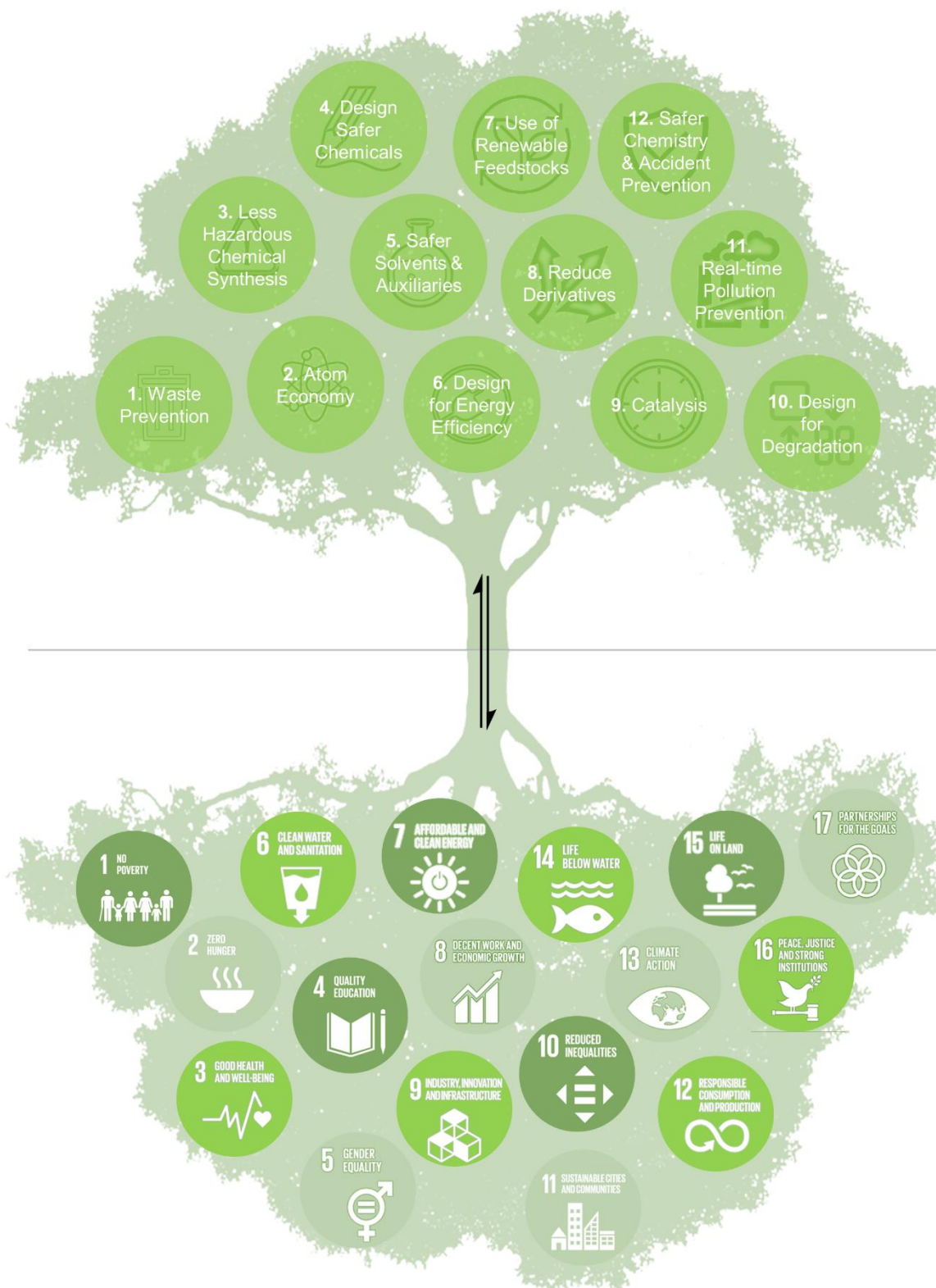


Figure 1.12. Twelve principles of green chemistry (top) and United Nations' Sustainable Development Goals (bottom).

performance and increased value while meeting the goals of protecting and enhancing human health and the environment".²⁶⁵ In 2018, Paul T. Anastas and Julie B. Zimmerman published another possible definition, more simplistic, for sustainable chemistry, as something that "promotes, advances, enables, and empowers the implementation of the chemistry of sustainability".²⁶⁶

The differences between green chemistry and sustainable chemistry can be pictured this way: while the first is a fast-growing scientific field, guided by scientific principles focused on chemical innovation, the second provides a more holistic interpretation, which takes into consideration other dimensions, such as the economic and social impact of sustainable practices. The United Nations' Sustainable Development Goals (SDGs) (**Figure 1.12**- bottom) are, at least in part, intrinsically connected to the principles of green chemistry and the vision of sustainable chemistry. This is put into evidence by the United Nations Environment Programme, which developed important guidelines for countries, policy makers, regulatory agencies, industries, and other relevant stakeholders, to better understand and facilitate the advance of green and sustainable chemistry.²⁶⁷ Out of the seventeen SDGs, green and sustainable chemistry can have an impact on eleven of them, directly or indirectly (SDGs 1, 2, 3, 6, 7, 8, 11, 12, 14, 15, and 17).^{268, 269} Green and sustainable chemistry are also highly connected with other relevant concepts, such as circular economy.²⁷⁰

1.3.1.1. How to Measure the Sustainability of a Chemical Process?

As a relatively new scientific field, green chemistry, due to its urgent need, is rapidly growing in the past 30 years. Several approaches emerged to transmit the relevant information comprised in green chemistry and its twelve principles, dissecting each one of them into its different tools, outputs, challenges, etc. Two great examples are the "Green ChemisTREE", developed by Anastas and co-workers,²⁷¹ and the "periodic table of the elements of green and sustainable chemistry", reported by Anastas and Zimmerman.²⁷² At the same time, measuring the greenness of a chemical process can be quite challenging. Different metrics have been developed in order to verify the compliance of chemical transformations with the twelve principles of green chemistry. The selection of appropriate metrics to identify and describe a given chemical process, in a "real-world" context, is very important and a very complex decision, as no single metric can provide the entire context of synthetic greenness and efficiency.²⁷³⁻²⁷⁵ In this work, attention will be given to three different metrics: E-Factor, Atom Economy and EcoScale.

One of the first metrics to have an impact on industrial waste reduction was the Environmental Factor, commonly known as E-Factor, developed by Roger Sheldon.²⁷⁶ This metric quantifies the amount of waste produced in a chemical process, with waste being defined as everything involved in the chemical process which is not the desired product. It is calculated as the ratio between the mass of waste residues and the mass of product:

$$E - Factor = \frac{m (waste) (kg)}{m (product) (kg)}$$

and therefore, despite leading the way for several industries, in particular fine chemicals and pharmaceutical industry to pay more attention to the generated waste in each chemical process, it has a major drawback, as it does not take into account the nature of the waste produced.^{277, 278}

Also in the early 1990s, Barry M. Trost developed another important concept, Atom Economy.²⁷⁹ This metric system is crucial to evaluate what happens at a molecular level during a synthetic process, as it measures how much of the reactants are converted into the final product, and can be calculated by determining the molecular weight ratio of the final product divided by the sum of all reactants:

$$Atom Economy = \frac{MW (product)}{\Sigma MW (reactants)}$$

where it is considered as reactant every material that is incorporated into an intermediate or product during the synthetic process. Solvents, reagents or materials used in catalytic quantities are not considered. However, the simplicity of atom economy might not mirror other important synthetic procedures components and their impact, namely solvent, catalyst recovery, energy use, toxicity, etc.^{280, 281}

Already in the 2000s, Van Aken and co-workers introduced EcoScale as a post-synthetic metric, which is more qualitative in nature. This post-synthetic semi-quantitative tool evaluates the quality of the organic preparation based on different parameters, namely yield, cost, safety, conditions, and ease of workup and purification. This tool is more versatile, as chemists can assign different relative penalty points to certain parameters. It provides a more holistic measurement of the synthetic process greenness and is ideal for comparison of different approaches to obtain the same molecule, as it evaluates the safety, economical, and ecological features of such processes.²⁸²⁻²⁸⁴

The wide application of the described metrics, as well as others already described or to emerge in the future, will influence decision making processes and will help to assess the economic viability of different products and processes. Ultimately, science and innovation are now establishing a new approach on research and development, where a green by design outlook starts at the molecular level and leads to a positive impact on the global scale.²⁸⁵⁻²⁸⁸

1.3.1.2. Green Chemistry in Drug Discovery and Development

Green chemistry plays a central role in the 21st century chemistry landscape, embracing areas such as analytical chemistry, materials chemistry, food chemistry, and organic and medicinal chemistry, which means different researchers, often with very distinct mindsets, tackle green chemistry and its principles, as well as its challenges, in a different perspective. The current society perception of climate change also took the public perception and awareness on sustainable chemistry to a new level, pressuring regulatory authorities and political players to have a stronger position in such matters.²⁸⁹

The pharmaceutical industry, as one of the most highly regulated productive areas, had to adapt and evolve into more sustainable practices and develop systems and approaches to overcome different challenges they face during the discovery and development of new drugs under sustainable conditions. This is of major importance, as fine chemical industries are among those which produce more waste per ton of product. This implies an ongoing cooperation between Research and Development (R&D) laboratories, regulatory authorities, policy makers and the pharmaceutical industry itself (**Figure 1.13**). In order to make the drug discovery and development pipeline more sustainable, research institutions and the pharmaceutical industry cooperate for the development of new innovative approaches to increase their processes eco-friendliness.²⁹⁰ One great example of such cooperation is the American Chemical Society Green Chemistry Institute Pharmaceutical Roundtable (ACS GCIPR), where several stakeholders from the pharmaceutical industry and academia encourage innovation for the integration of green chemistry and green engineering into the pharmaceutical industry.^{291, 292} In Europe, the Innovative Medicines Initiative (IMI), comprises six pharmaceutical companies, ten universities and five small to medium enterprises, and aims to support sustainable projects and train future generations of scientists for sustainability goals.²⁹³⁻²⁹⁵

Over recent years, several outputs have been reported from the efforts undertaken by academia and industry. The percipient selection of solvents through selection guides,

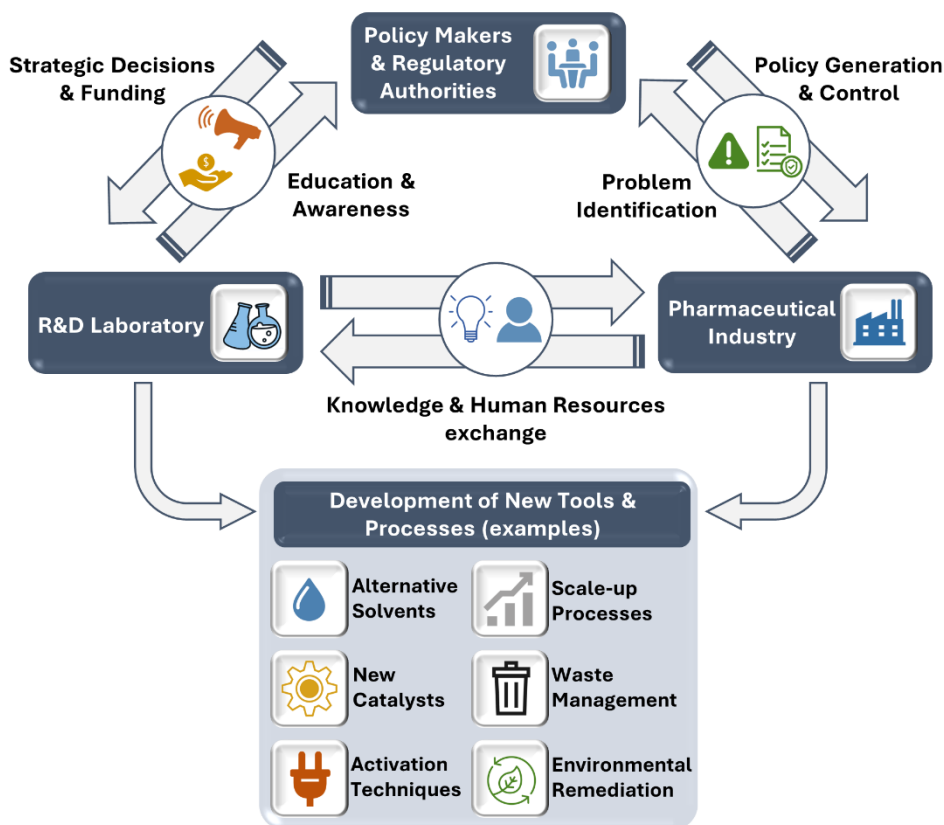


Figure 1.13. Overview of the main stakeholders and respective contributions to make the drug discovery and development process more sustainable.

supporting the use of less harmful solvents in both lab scale and industrial scale processes;²⁹⁶⁻²⁹⁸ the development of more sustainable and efficient catalytic processes, supporting the use of non-toxic and recyclable catalysts;^{299, 300} the application of new activation techniques and reactor setups, where mechanochemistry³⁰¹⁻³⁰⁴ and flow chemistry³⁰⁵⁻³⁰⁸ have shown an exponential growth in the past few years; waste minimization, monitoring, management and the creation of environmental remediation facilities^{309, 310} are some of the recent developments towards sustainability in drug discovery and development.^{311, 312}

Reaction telescoping or the use of multicomponent reactions (MCRs) in medicinal chemistry is also a very desirable approach for the generation of libraries of new molecules in a sustainable fashion. This type of reaction often improves synthetic pathways sustainability, by reducing reaction steps, derivatization processes (protection/deprotection), use of auxiliaries, energy requirements, and solvent use in both reaction and workup processes and, at the same time, allows the generation of structurally diverse libraries, a cornerstone of medicinal chemistry.³¹³ Nevertheless, as the sustainable toolkit expands, often the amount of compounds that can be obtained also expands, which might have a negative impact on sustainability. Nowadays, one of

the biggest challenges in medicinal chemistry is to refine and select from what can be made to what should be made. Reducing the number of compounds to be synthesized, as well as the number of steps required for their preparation, in order to reduce the resources, time, and workforce invested to achieve a new drug candidate is therefore an ongoing challenge in sustainable medicinal chemistry.³¹⁴

1.3.2. Druglikeness in Drug Discovery

Druglikeness^a plays a central role in drug discovery. Any given drug presents several features, which can be divided into structural, physicochemical, biochemical, pharmacokinetic, and toxicity features. These features will determine the way the drug will interact with the organism, from the absorption, distribution, metabolism, excretion, and toxicity (ADMET) profile (pharmacokinetic profile) to the drug-target interaction and consequent pharmacological activity (pharmacodynamic profile). While a clear definition of druglike or druglikeness remains elusive,³¹⁵ the one provided by Christopher A. Lipinski is worth mentioning. He states that druglike molecules are “defined as those compounds that have sufficiently acceptable ADMET properties and sufficiently acceptable toxicity properties to survive through the completion of human phase I clinical trials”,³¹⁶ and therefore druglikeness “is defined by a range of molecular properties and descriptors that can discriminate between drugs and non-drugs for such characteristics”.³¹⁷

While traditionally the drug discovery phase was highly focused on discovery of new molecules with the ability to exert a pharmacological activity by interacting with a certain target, with pharmacokinetic parameters being evaluated and optimized in later stages, during drug development, in the 1990s there was a shift in this mindset, giving this task for medicinal chemists during the drug discovery process, and therefore enhance the druglike properties of new drug candidates at an earlier stage of the drug discovery and development pipeline, which is in line with a green by design strategy and sustainable practices in medicinal chemistry.^{314, 318} This was highly driven by the development of druglikeness evaluation tools, conceived through the thorough analysis of drug databases in order to find common key descriptors to develop rules to apply in early drug discovery context, reducing attrition rates, and R&D time and costs.³¹⁹ It was verified that the pharmaceutical industry could profit from this change of mindset, as in the late 1980s the attrition rates due to pharmacokinetic and bioavailability issues were

^a This concept can be found in the literature in two forms: druglike and drug-like (as well as their derivatives druglikeness and drug-likeness). It was decided to employ “druglike/druglikeness”, as the suffix “-like” is hyphenated only when a) the root word is three or more syllables; b) the root word ends with double “L”; or c) the root word is a proper noun.

up to 39% and by the 2000 it had declined to 10%.³²⁰ In the decade 2000-2010, the percentage of compounds halted due to pharmacokinetic and bioavailability causes was 5%. These approaches translated to a decrease in failure rates at later stages of drug development, including in clinical trials.³²¹

An analysis of data collected from several programmes developed at Pfizer for phase II drug candidates, led to the development of the concept of “three pillars of survival” for drug candidates undergoing phase II clinical trials. The pillars are: 1) exposure at the target site of action, 2) binding to the pharmacological target as expected for its mode of action, and 3) expression of pharmacological activity commensurate with the demonstrated target and exposure and target binding.³²² The compliance with these pillars, as well as the bidirectional development of drug candidates in both the pharmacodynamic (activity) and pharmacokinetic (druglike) profiles is of utmost importance for the chances of success in introducing a new drug in the market (**Figure 1.14**).³²²⁻³²⁴

Molecules displaying good druglike properties bring several benefits to drug discovery and development programmes (**Figure 1.15**). Therefore, druglikeness concepts, and in particular druglikeness filters, are very important at early stages of research and in decision making in medicinal chemistry.³²⁴⁻³²⁶

There are multiple features of interest for organic and medicinal chemists working in drug discovery: a) structural properties, which are inherent to the compound (lipophilicity, topological polar surface area (TPSA), number of hydrogen bond acceptors (HBA) and donors (HBD), ionization constant, molecular weight (MW), 3D structure, molar refractivity (MR), and reactivity); b) physicochemical properties, related to the behaviour of the compound in the media where it is placed (solubility, permeability, and chemical stability); c) biochemical properties, corresponding to the way the compound interact with a living organism (metabolic stability, substrate of transporters, permeation to barriers (namely BBB), and plasma stability); d) safety, concerning potential drawbacks of the interaction of the compound with the organism (possibility of drug-drug interactions, existence of reactive metabolites, mutagenicity, cytotoxicity, and teratogenicity); and more classic e) pharmacokinetic parameters, including measurements that can be performed in what concerns the route the drug takes in the organism (clearance, volume of distribution, area under the curve (AUC), half-life, and bioavailability).³²⁴

The experimental determination of each of these properties for each compound developed in a drug discovery programme would be quite time- and resources-consuming, and therefore the development of tools that can estimate druglikeness in early stages of drug discovery are of utmost relevance, as they can filter out molecules

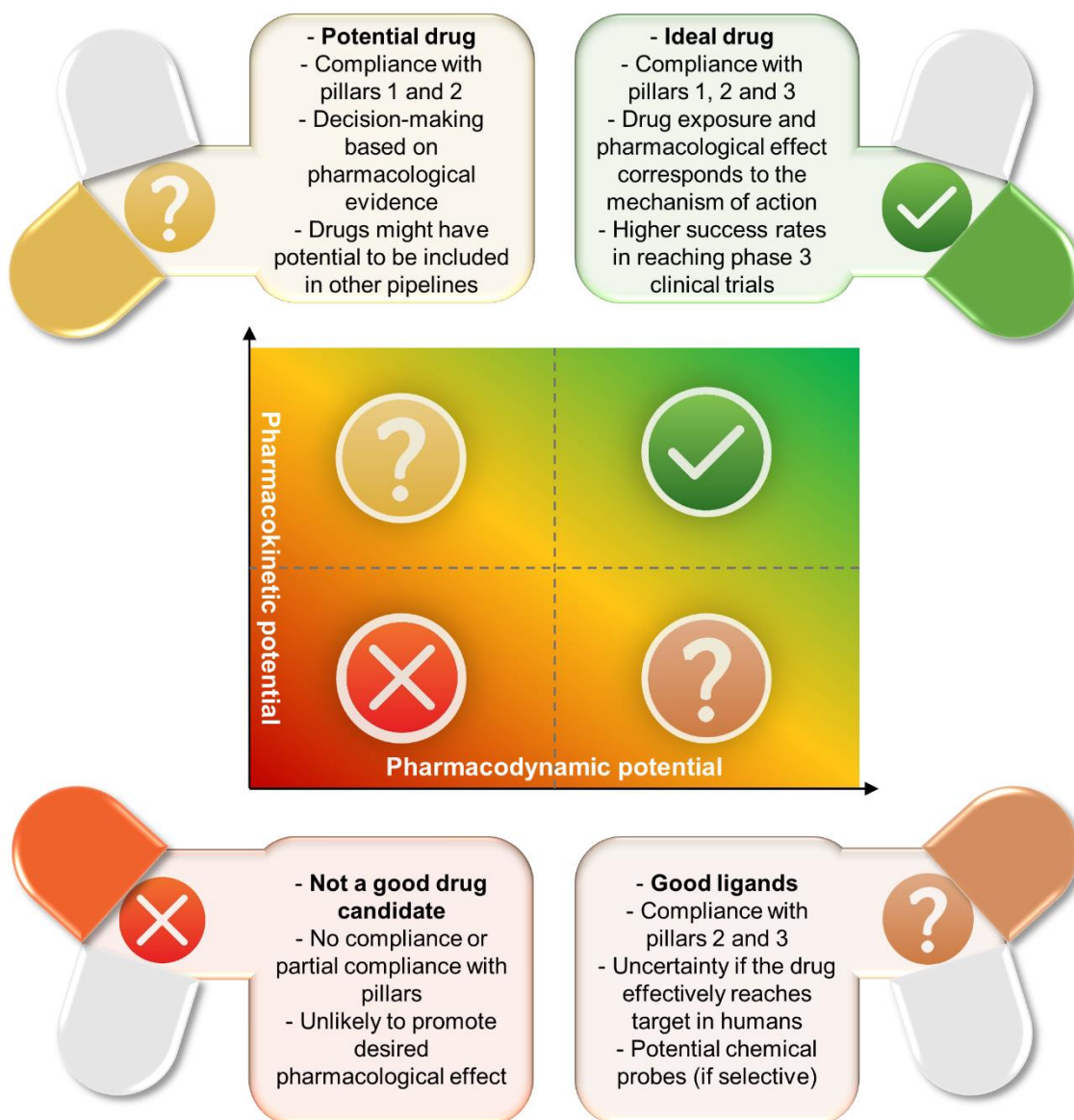


Figure 1.14. Pharmacodynamic and pharmacokinetic potential of drug candidates as equally determinant for clinical application success.

with potential to display undesirable properties and bring forward the molecules with more likelihood for success and, at the same time, improve sustainability, by promoting the rational use of resources.³²⁷ Considering the vast diversity of chemical space, and knowing that not all the theoretically postulated compounds can be synthetically attained with contemporary knowledge, it is also highly considered that bioactive compounds, as well as druglike compounds, are present in specific regions of the chemical space, and ideal drugs are likely to be located in regions of intersection of the ADMET region and a certain bioactivity region.³¹⁷

Most of druglikeness evaluation tools were developed to be applied in small molecule-based drug discovery platforms, which are still the most common class of drugs reaching market approval.⁴² The most popular example of a druglikeness filter is the one

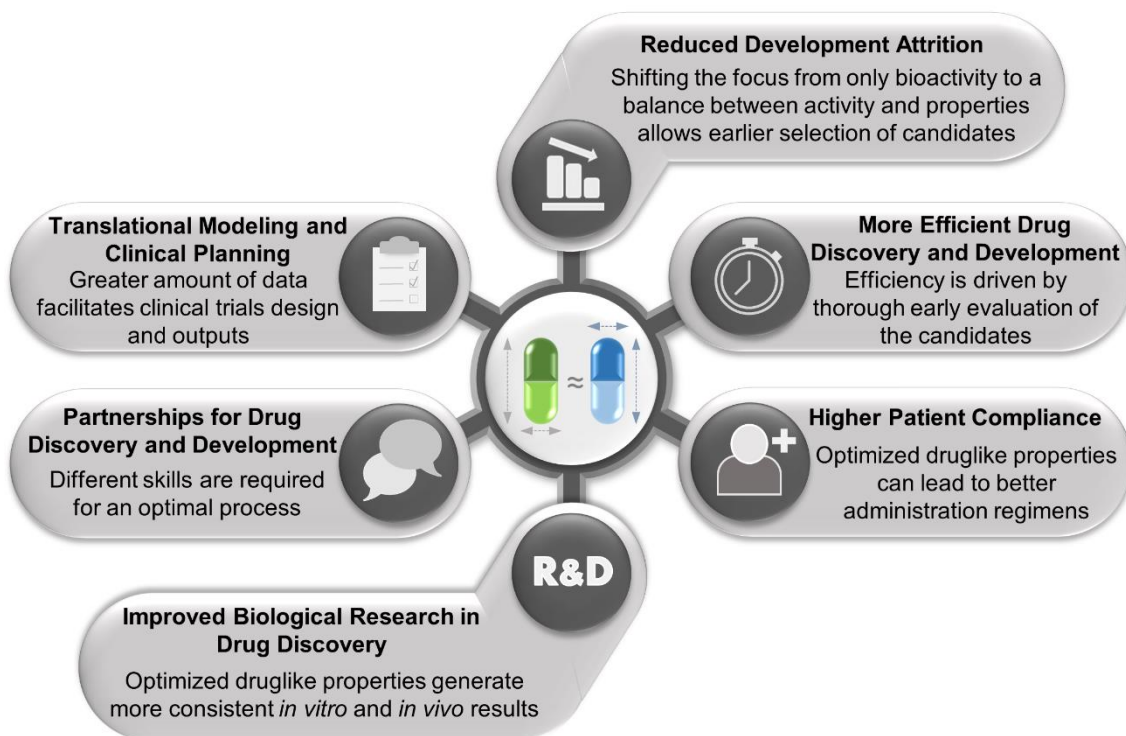


Figure 1.15. Advantages of using druglikeness in drug candidates' selection during the drug discovery and development process.

developed by Lipinski and co-workers, at Pfizer, which become known as Lipinski's rule, or Lipinski's rule of 5.³²⁸ But since then, several other researchers in the pharmaceutical industry and academia attempted to develop other filters, often to try to simplify as much as possible the rules to be complied by the drug candidate (**Figure 1.16**)³²⁸⁻³³⁴

Recent efforts in simplifying the rules, or constraining the chemical space to explore, have been made, such as the GSK 4/400 filter (MW < 400 Da and cLogP < 4),³³⁵ the Pfizer 3/75 filter, the golden triangle filter, or the fraction of sp³ carbon atoms (Fsp³), as a good indicator of molecular 3D complexity.³³⁵⁻³⁴¹ Researchers also focused their attention in developing rules to evaluate compounds which do not fall within the boundaries of the Lipinski filter, namely macrocycles and other high molecular weight drug candidates.³⁴²⁻³⁴⁵ Another approach is to address the target organ as the focus of

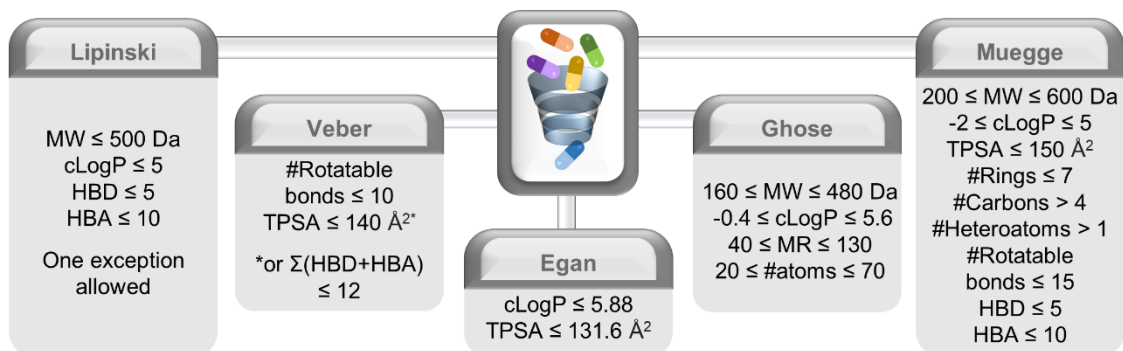


Figure 1.16. Main descriptors of five of the most relevant druglikeness filters.

the filter, which is particularly interesting for compounds targeting the CNS, which usually present lower MW than the average MW of drugs, and higher lipophilicity, required to cross the BBB.^{346, 347} New trends are also emerging to shift the chemical areas covered, by using deep learning and artificial intelligence to generate druglikeness filters,³⁴⁸ or even to generate target-specific druglikeness filters, in order to improve the outputs of target-based drug discovery programmes.³⁴⁹

Despite the inherent advantages of druglikeness filters, they also present some limitations. It is important to take into consideration that most of the rules contained in these filters are based on statistics, and therefore they must be evaluated as a probability, and not as a dogma. Active management of the druglike properties of drug candidates since the early stages of drug discovery is an essential step to reduce attrition. But molecules that do not comply with druglikeness filters should not be removed from the pipeline, especially when alternatives are not found, keeping in mind that if the pipeline is highly populated with these “exception” molecules, the risk of failure is also expected to increase proportionally. Furthermore, several molecules, namely natural products (e. g. cyclosporin, steroids, vitamins) are located in a chemical space region different than orally bioavailable synthetic drugs, and still remain suitable for oral administration. Furthermore, compounds displaying poor gastrointestinal absorption, for example, can be suitable for oral administration if properly formulated, and the drug delivery systems research field is also an expanding field of knowledge.^{315, 350-352}

In order to make the determination of the different parameters and verify the compliance with different filters, chemoinformatics has developed several *in silico* tools to assist researchers in these tasks, including web-based free tools, which are user friendly and can screen a wide number of molecules, based on their structures or using the simplified molecular-input line-entry system (SMILES).³⁵³⁻³⁵⁵ Popular examples of these tools are DrugMint,³⁵⁶ FAF-Drugs4,³⁵⁷ ADME-Space,³⁵⁸ ADMETlab,³⁵⁹ admetSAR,³⁶⁰ DRUDIT,³⁶¹ and SwissADME.³⁶² For this work, and based in recent comparative studies on different tools available,³⁵⁴ focus is given to SwissADME, since it is a robust tool that provides a wide range of physicochemical properties calculations, ADMET evaluations, druglikeness filters compliance, as depicted in **Figure 1.17**, in which isatin was used as an example.

Among the different properties predicted by this tool, in the druglikeness section, besides the five filters already described in **Figure 1.16**, it also displays a value designated as the bioavailability score. This filter was developed in the Abbott Laboratories, with the goal of predicting the probability of a compound to display at least 10% oral bioavailability. The bioavailability score takes into account the charge at physiological pH and the TPSA value. In the example shown, as isatin is compliant with

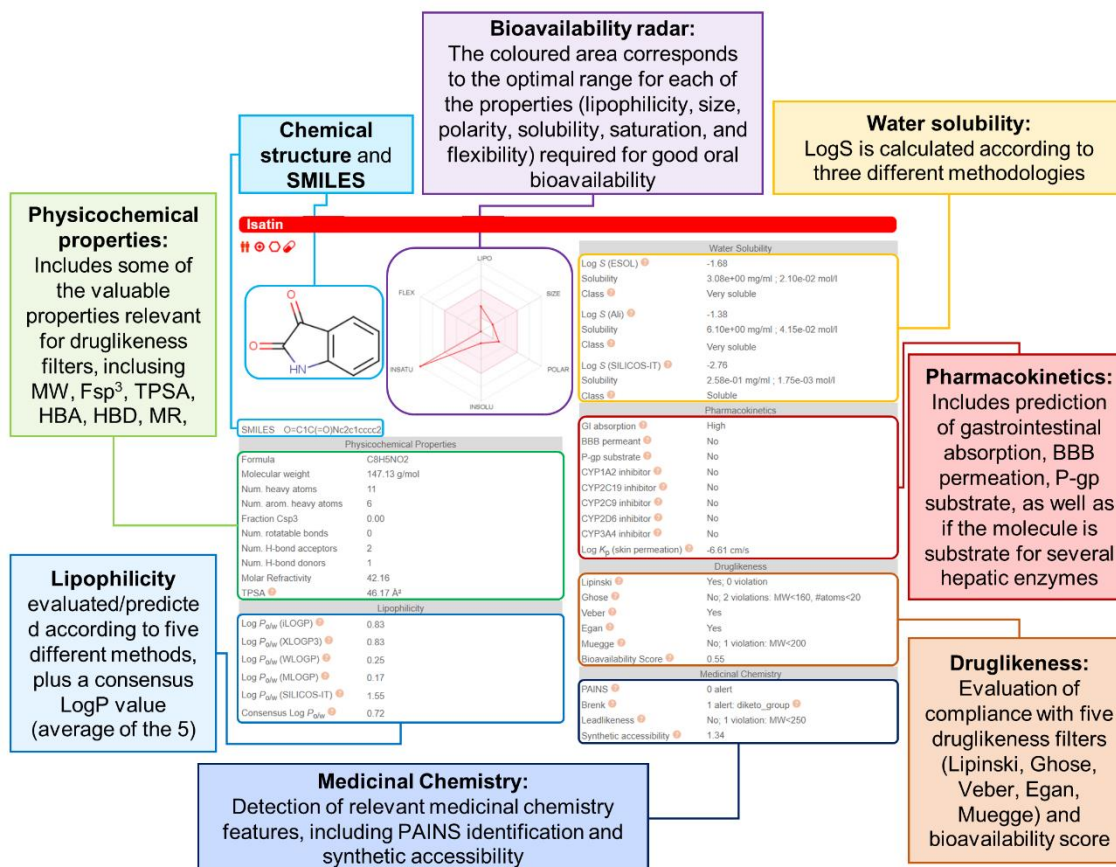


Figure 1.17. Outputs of the SwissADME web-based tool.

the Lipinski filter, it automatically gets a score of 0.55. Anions with high TPSA ($> 150 \text{ \AA}^2$) exhibit the lower score (0.11), whereas the highest score (0.85) is attributed to molecules exhibiting lower TPSA ($< 75 \text{ \AA}^2$).³⁶³

In the medicinal chemistry section, two relevant outputs is the PAINS alert³⁰ and the Brenk alert,³⁶⁴ both aiming to highlight the presence of unwanted groups which might hinder further development of a given drug candidate, due to their likelihood to generate pharmacokinetic development attrition, or pharmacodynamic concerns, due to promiscuous binding to multiple targets, or biological activity screening problems (see **Scheme 1.1**).³⁶⁵⁻³⁶⁸

Besides the bioavailability radar, which provides a good visual clue on the druglikeness potential of a drug candidate, another visual output can be obtained using SwissADME, namely a Brain Or Intestinal Estimated permeation method (BOILED-Egg model). This consists on a graphic representation of the relationship between lipophilicity (the value WLogP, obtained using the Wildman and Crippen methodology)³⁶⁹ and TPSA (calculated using the method reported by Ertl and co-workers),³⁷⁰ where the placement of the drug candidate within the yellow region (“egg yolk”) represents potential to cross the BBB by passive diffusion, while the placement in the white region of the graphic (“egg white”) indicates passive gastrointestinal absorption. A compound located outside these

regions indicates poor potential for oral administration.³⁷¹ **Figure 1.18** shows the example of the BOILED-Egg model for isatin and tryptanthrin.

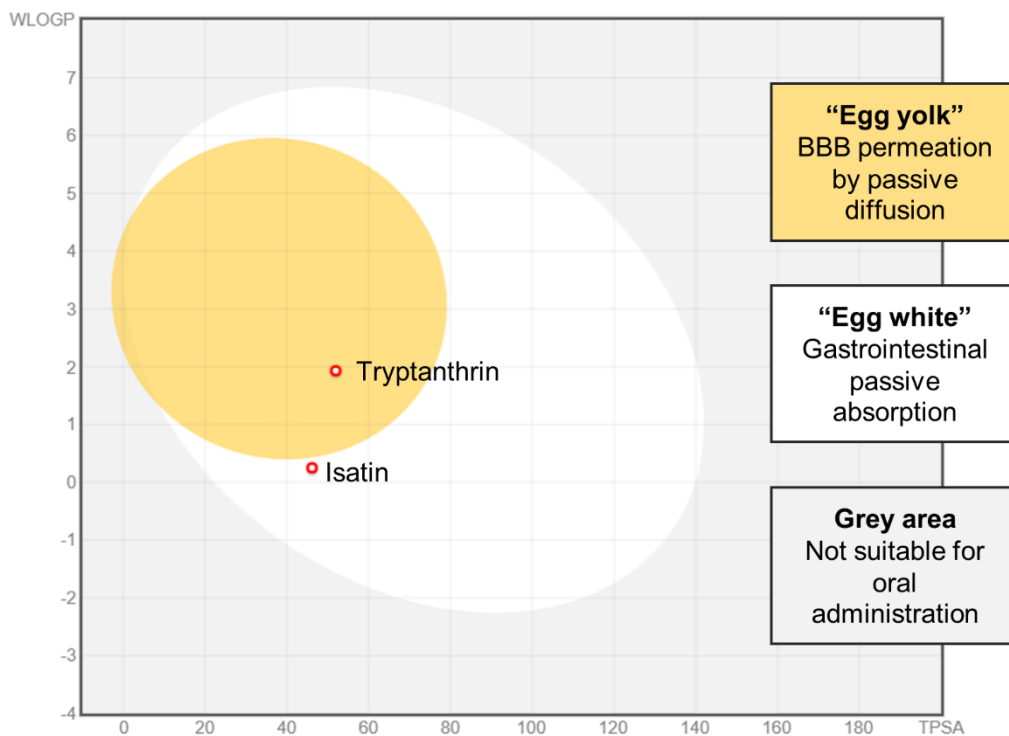


Figure 1.18. BOILED-Egg model of tryptanthrin and isatin.

As supported by scientific evidence and previously discussed in section 1.2.2, tryptanthrin is correctly predicted to cross the BBB. In the case of isatin, although it falls within the white region, it is very close to the BBB permeation parameters. It is known that isatin reaches the brain,³⁷² but in this case the possibility for active transport to cross the BBB cannot be excluded.

1.3.3. Multicomponent Reactions: Conscientious Fast-Track for Structural Diversity and Sustainability

MCRs are usually described as reactions in which three or more components are added simultaneously to one reaction vessel, leading to a final product that contains most of the atoms present in the starting reagents. This type of reaction encloses, from the mechanistic perspective, a sequence of more than one chemical transformation without the need to change reaction conditions after each chemical transformation. These features put in center stage two main advantages of multicomponent reactions: 1) easy access to structural diversity; and 2) less time and effort required to attain small molecule libraries when compared with step-by-step approaches.³⁷³ However many

more advantages can be listed from the use of MCRs, especially for sustainable drug discovery purposes, as it will be further addressed in this section.

Although MCRs have been around since the 19th century, their role in organic synthesis, and in particular in drug discovery and development has been growing more significantly since the turn to the 21st century. Indeed, looking to the publications made in this field in the last two decades, a 10-fold increase can be observed, as depicted in **Figure 1.19 A**. MCRs have in common the fact that they get the name of the researcher(s) who first reported them. One of the first MCRs described was the Strecker reaction (1850),³⁷⁴ followed by the Hantzsch reaction (1882)³⁷⁵ and the Biginelli reaction (1893)³⁷⁶ still in the 19th century. In the 20th century, one of the first MCRs reported was the Mannich reaction (1912).³⁷⁷ Remarkably, these four MCRs are in the top 5 of most commonly used MCRs in the first two decades of the 21st century (**Figure 1.19 B**). Several other reactions followed,³⁷⁸⁻³⁸³ until the Ugi reaction was first reported in 1959,³⁸⁴ and it still remains in the present as one of the most explored, especially in medicinal chemistry context. The next decades, all the way until the 21st century, continued to provide new MCRs,³⁸⁵⁻³⁹³ as presented chronologically in **Figure 1.19 C**.

Despite MCRs being around for over a century, the majority of contemporary organic chemistry textbooks and teaching programmes focus their attention on one- and two-component reactions, as well as in polymerization reactions. Therefore, the high value of MCRs is not adequately represented in the vast majority of academic settings, despite their remarkable applications in chemistry.³⁹⁴ However, a clear trend is gaining momentum, with academic chemists renewing their interest in MCRs, highly driven by pharmaceutical industry, which has fueled this resurgence due to the increasing need to assemble libraries of structurally complex molecules for drug discovery purposes in a sustainable way.³⁹⁵

Notwithstanding the wide diversity of MCRs, they share some common features. For example, MCRs are convergent, as several starting materials are combined in one reaction to achieve one product, an integrative nature which is very attractive when an increase in molecular diversity is required/desired. MCRs also exhibit a high bond-forming-index, with several bonds being formed in one synthetic transformation.^{396, 397}

But how do MCRs correlate with sustainability? The typical convergence MCRs display, as well as their time and resources savings are good indicators of MCRs inherent sustainability. But a more detailed analysis between MCRs features and green chemistry twelve principles can help to illustrate this relationship in a more efficient manner (**Figure 1.20**). Principles 1 and 2 are by far the ones which are more inherently correlated with MCRs sustainability. By allowing shorter synthetic routes and inducing great levels of chemo- and regioselectivity, with the production of few to no by-products (and often

innocuous, such as water), MCRs display a great deal of atom economy and waste

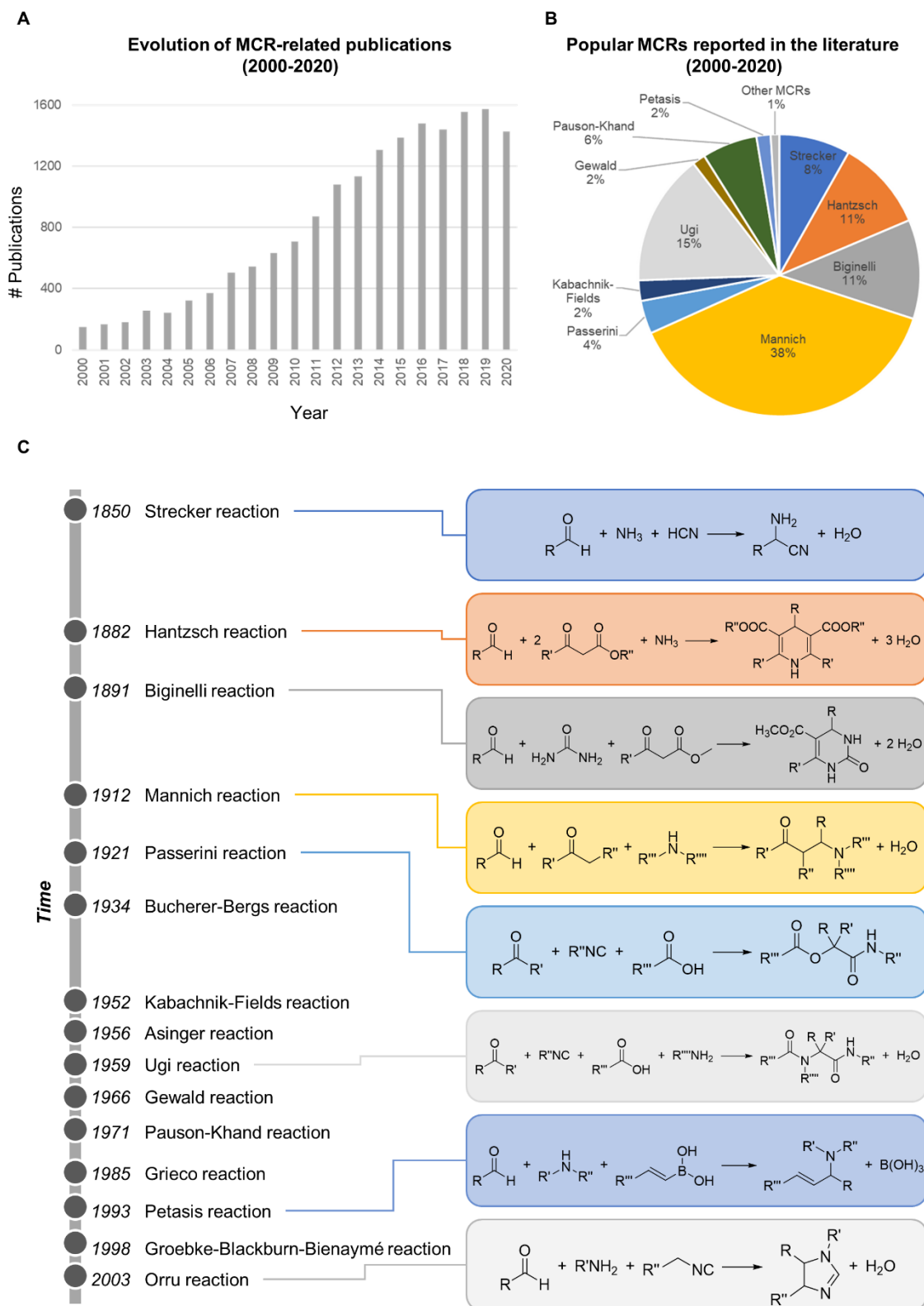


Figure 1.19. Evolution of the number of publications on MCRs between 2000-2020 (A) and popular MCRs reported between 2000-2020 (B) and timeline of the discovery of some MCRs (C). (A was obtained in *Web of Science* (25/09/2021) and “multicomponent reaction” as topic; B was obtained in *Web of Science* (25/09/2021) using the MCR name as topic).

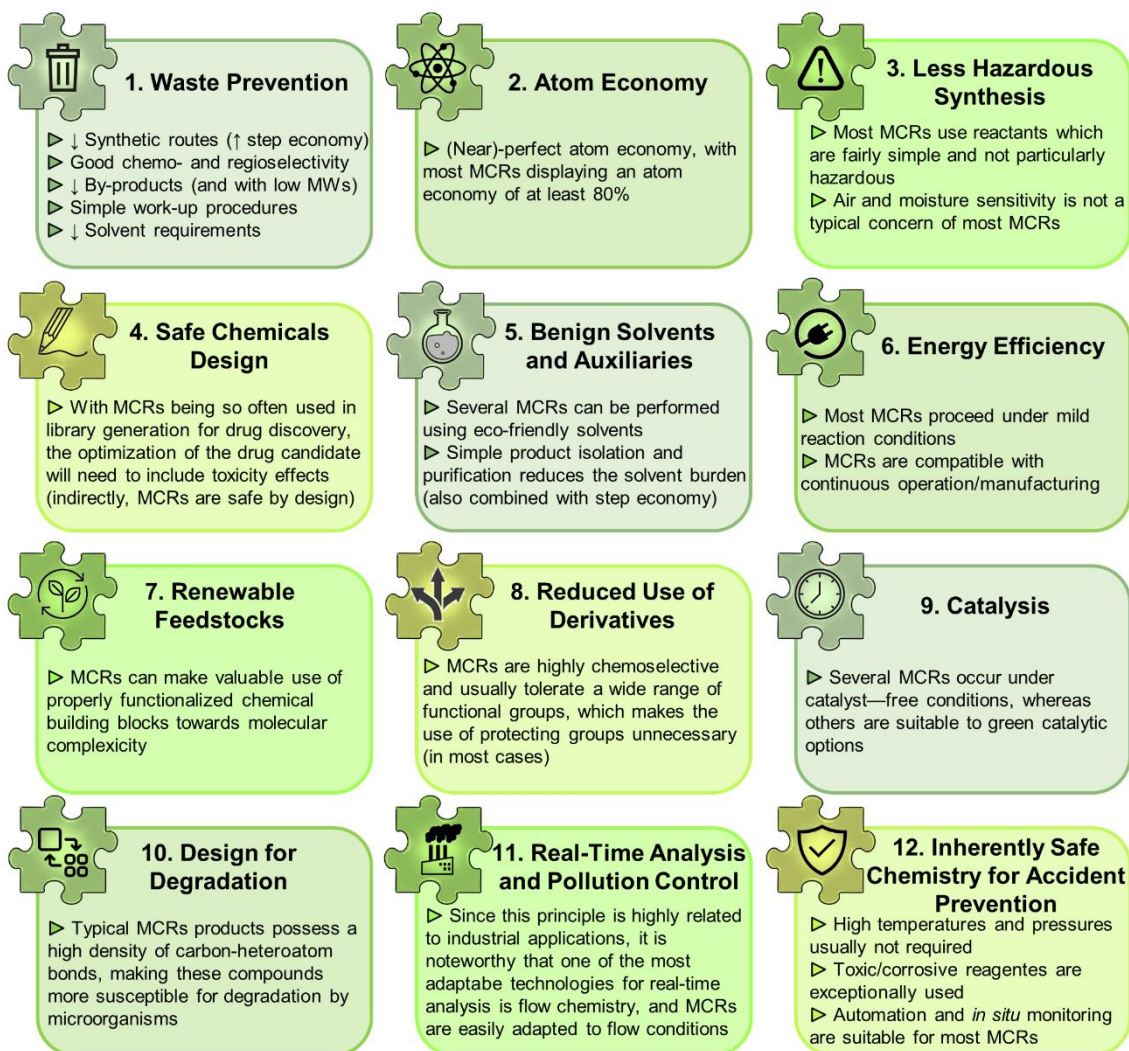


Figure 1.20. MCRs compliance with green chemistry principles.

prevention. High yields and simple work-up procedures (chromatography-free protocols) give a valuable contribution to reduce solvent requirements as well. In what concerns principle 3, most starting material employed in MCRs are not particularly hazardous and tend to be stable. Moisture and air sensitivity are also not typical concerns of MCRs, helping to comply with the less hazardous synthesis green chemistry principle (isocyanide-based MCRs can often be viewed as an exception for this trend, but as will be discussed later in the section, it is not necessarily true). Principle 4, as well as principle 10, are more oriented to the final product than the synthetic process itself, and therefore it is harder to draw conclusions correlating MCRs with these two principles. However, as MCRs are often used in drug discovery process, and drug candidates are thoroughly evaluated in what concerns their toxicity, it can be inferred that MCRs are indirectly safe by design. In what concerns the degradation of the final MCR products, as most bonds generated are carbon-heteroatom bonds, they are more prone for microorganism degradation.³⁹⁸

In what concerns principle 5, besides the aforementioned solvent savings allowed by MCRs due to their step economy and simple work-up procedures, recent advances have shown that several MCRs can be performed using eco-friendly solvent options (including water, ionic liquids, deep-eutectic solvents (DESs), polyethylene glycol polymers (PEGs), supercritical carbon dioxide (scCO₂), bio-derived solvents) or even under neat conditions.³⁹⁹⁻⁴⁰¹ Compliance with principle 6 is accomplished by MCRs *per se*, since most MCRs proceed under mild reaction conditions (ambient temperatures and pressures), but also due to their great capability to be coupled with other valuable sustainable tools, such as continuous flow chemistry,^{402, 403} microwave irradiation,^{404, 405} ultrasound irradiation,⁴⁰⁶⁻⁴⁰⁸ and mechanochemistry.⁴⁰⁹ In what concerns the compliance of MCRs with principle 7, it is a growing area of expertise. As the output of circular economy approaches and biomass introduces more molecules as promising starting materials, with more suitable functional groups, more can be applied in MCRs.^{410, 411} The overall high tolerance to different functional groups and high chemoselectivity makes MCRs less prone to the use of protecting groups, making them highly adaptable to green chemistry principle 8. Catalysis plays a key role in green chemistry and, although many MCRs occur under catalyst-free conditions, several examples can be found in the literature on advantages of use of different catalysts in different MCRs. Among the most commonly applied catalysts in MCRs, Brønsted and Lewis acids, organocatalysts, metal complexes, heterogeneous catalysts,⁴¹² biocatalysts,⁴¹³ and nanoparticles⁴¹⁴ proved to be sustainable catalytic options for several MCRs and, therefore, demonstrate the compliance with green chemistry principle 9.³⁹⁸ The compliance with green chemistry principles 11 and 12 have a great application for industrial settings, and MCRs proved to be suitable to comply with these principles, as they tend to be robust, scalable, and operationally simple, as they usually do not require high temperature or pressure setting and corrosive/toxic reagents are not commonly applied. Runaway reactions are also not commonly associated with MCRs. The opportunity to associate MCRs with automation and flow processes help to improve the success of compliance with these two principles.³⁹⁸

As previously discussed, MCRs are a fast-track to attain structural diversity. In other words, MCRs allow the synthesis of the highest number of compounds for the least synthetic effort. These features, place MCRs in the core of diversity-oriented synthesis (DOS), a common strategy in medicinal chemistry to find new drug candidates and selective biological probes.⁴¹⁵ This concept was first introduced by Stuart L. Schreiber in 2000,⁴¹⁶ as an alternative to target-oriented synthesis (TOS) and as a way to overcome combinatorial chemistry drawbacks. The differences between these three approaches

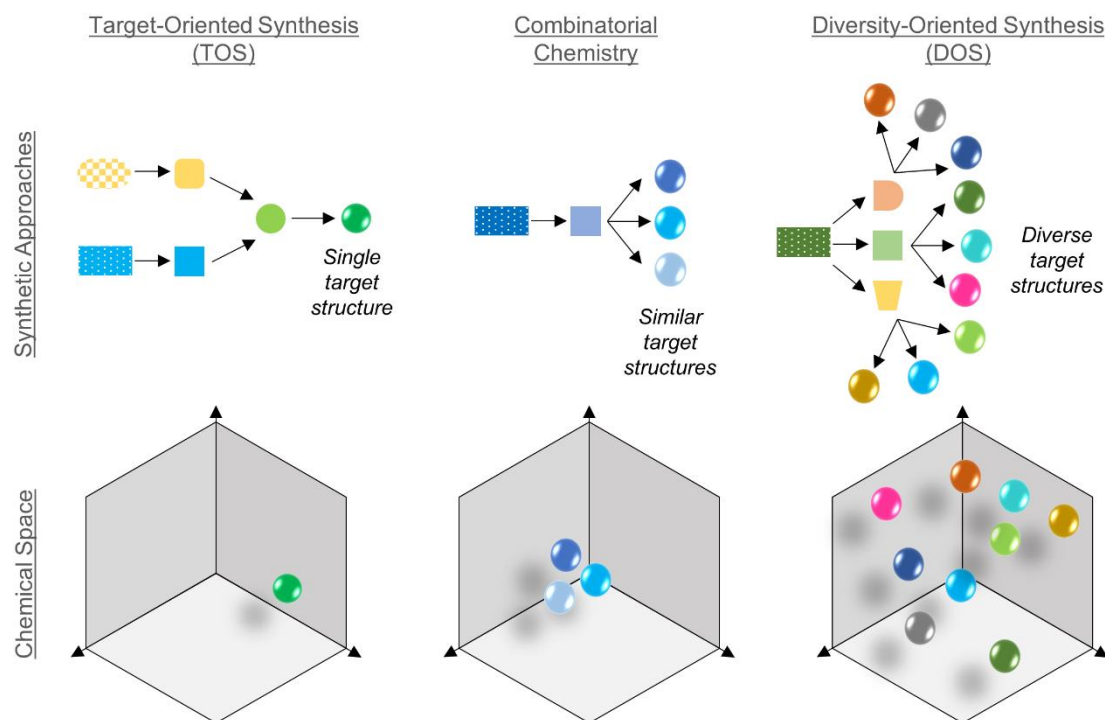


Figure 1.21. Comparison between TOS, combinatorial chemistry and DOS.

are depicted in **Figure 1.21**. TOS is used in drug discovery mainly in target-based drug discovery. The synthetic efforts are undertaken in order to produce a molecule which will effectively interact with a preselected protein target, and for this reason, it comprises a great deal of retrosynthetic planning. Combinatorial chemistry explores a dense region of the chemical space in the vicinity of the chemical space occupied by a known molecule of interest. Hence, retrosynthetic analysis plays a key role in this approach.⁴¹⁷ In DOS, a forward synthetic analysis is undertaken to achieve structural diversity. The main goal is to use simple starting materials and transform them, in an efficient manner, to structurally diverse and more complex molecular structures and therefore explore a wider region of the chemical space.^{418, 419} For these reasons, DOS is a suitable approach to apply in high-throughput screening (HTS) and phenotypic assay drug discovery programmes, facilitating the discovery of new hit compounds, and even potentially the discovery of new therapeutic targets and mechanisms of action.^{420, 421} While DOS can be attained in stepwise synthetic routes, it became clear that MCR can play a major role in generating DOS libraries with remarkable structural diversity in an efficient, sustainable and time- and cost-saving way.⁴²²⁻⁴²⁴

The application of MCRs in drug discovery and development programmes caught the attention of several researchers, in both academia and industry. Besides the described impact in achieving structural diversity and therefore being a great tool for the generation of complex molecular libraries, allowing the preparation of numerous new

compounds using minimum costs and efforts, MCRs can also be easily employed for hit-to-lead optimization purposes, and even to improve the sustainability of synthetic routes to achieve known molecules, including active pharmaceutical ingredients (APIs).⁴²⁵⁻⁴²⁷ As shown in **Figure 1.22** several examples of APIs, with a wide range of structural complexity, have been prepared using one (or more) MCR(s) in their synthetic pathway.⁴²⁸⁻⁴³⁷ Indeed, the Ugi MCR is one of the most versatile reactions to be applied in drug discovery and pharmaceutical production, as will be further discussed in this work. Its value for APIs production is demonstrated in the number, structural diversity, and complexity of molecules depicted in **Figure 1.22**.^{436, 438-447}

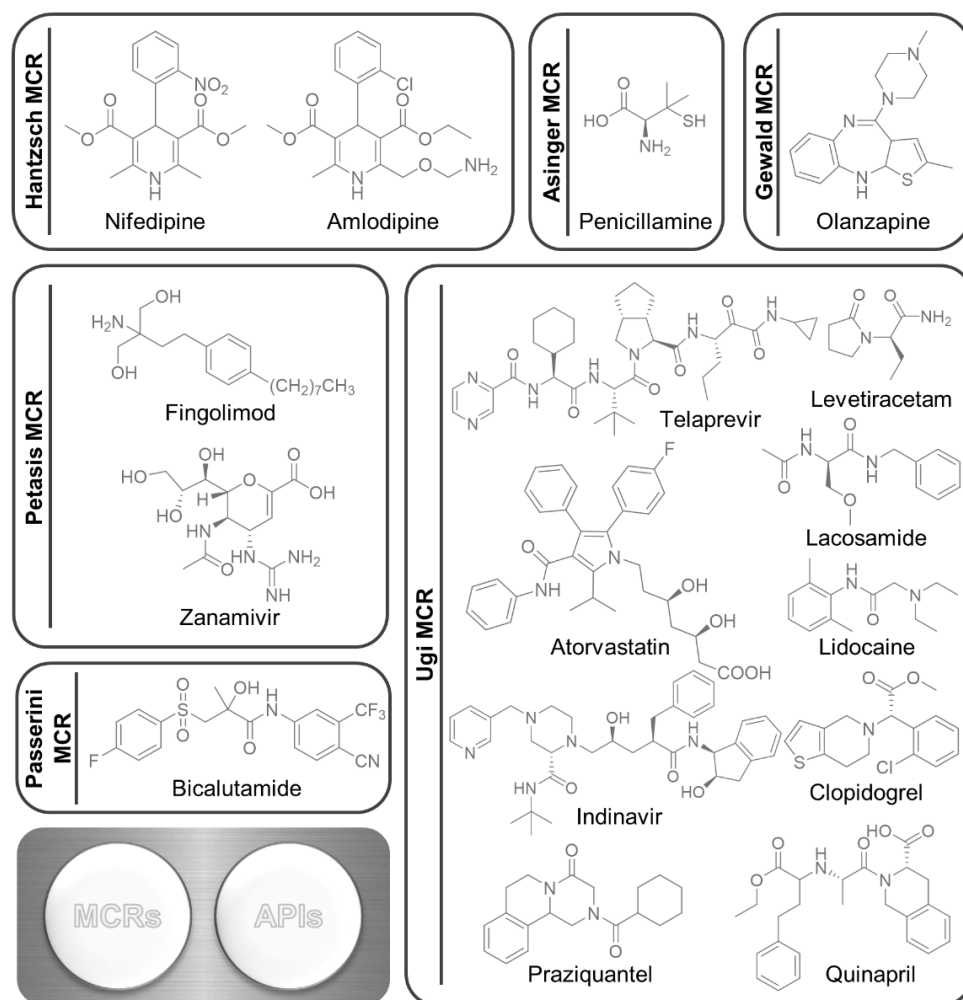


Figure 1.22. Examples of APIs obtained using MCRs.

The fast generation of structurally diverse compounds allowed by MCRs makes them a valuable tool for synthetic organic chemists and medicinal chemists working in the quest for new bioactive drug candidates.⁴⁴⁸⁻⁴⁵⁰ The application of MCRs in the synthesis of APIs and in medicinal chemistry has been reviewed by us in 2020 (see **Appendix 3**).⁴⁵¹

1.3.3.1. Ugi Reaction: A Versatile Isocyanide-Based MCR

Isocyanides play a central role in MCRs (**Figure 1.23**). The Passerini 3 component reaction (P3CR), the Ugi four component reaction (U4CR), the Groebke-Blackburn-Bienaymé 3 component reaction (GBB3CR), and the Orru three component reaction (O3CR) are some examples of isocyanide-based MCRs (IMCRs), although new reactions continue to emerge in the literature showcasing the versatility of isocyanides for MCR chemistry.⁴⁵²⁻⁴⁵⁵ This research field has been highly prolific, as the design of novel MCRs, the development of experimental improvements (new catalysts, enantioselectivity, etc.), the exploration of mechanistic insights, and possible applications (drug discovery, material science, agrochemicals development, bioconjugates synthesis) is quite challenging.⁴⁵⁶

The unique and chameleonic chemistry displayed by the isocyanide functional group is the main reason for the versatility of this type of reagent in MCRs. Isocyanides can act as nucleophiles (attacking activated electrophiles), as an electrophile (being intercepted by nucleophiles), as a carbene (taking part in formal [4+1] cycloaddition), and as a radical acceptor (generating imidoyl radical reaction intermediates). The lone pair

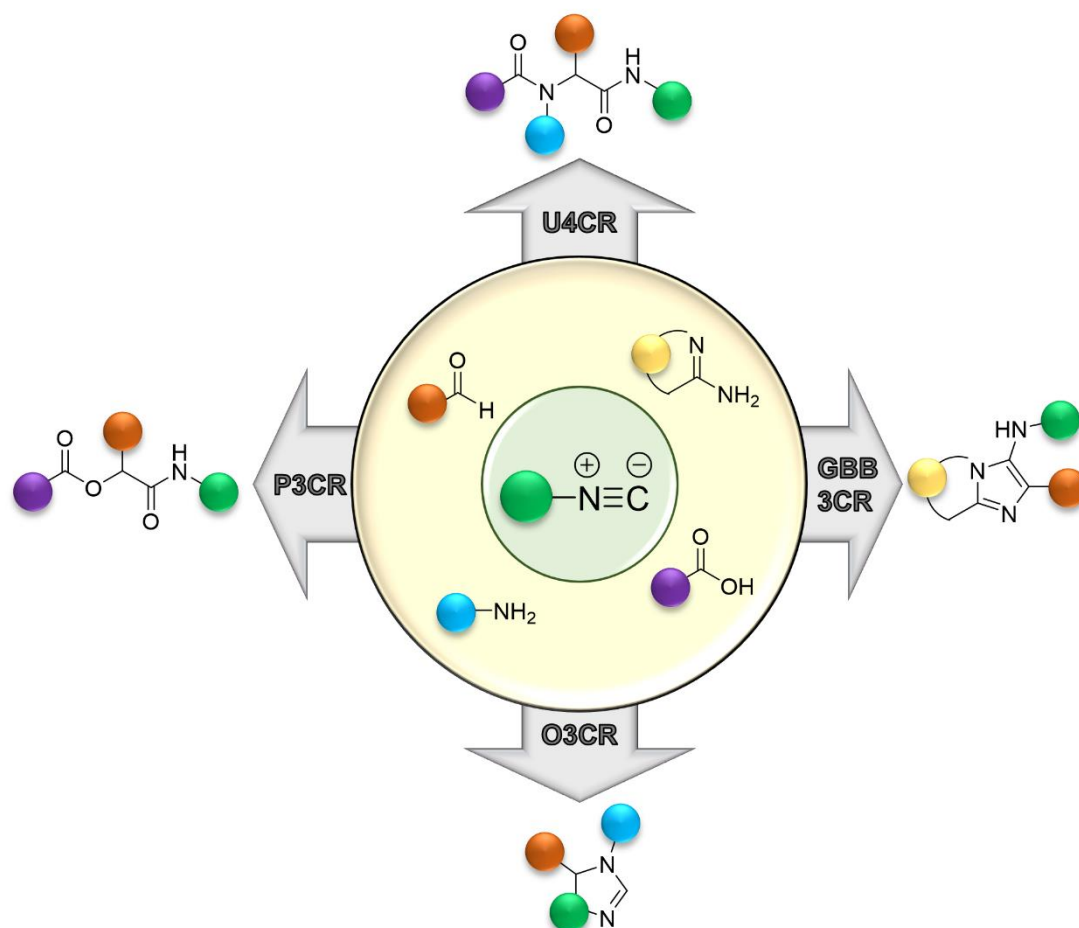


Figure 1.23. Examples of IMCRs.

of electrons present in the terminal carbon also explain the strong metal coordinative properties displayed by isocyanides. Their chemistry and reactivity are also explained by this functional group resonance structures, one bearing a triple bond between the nitrogen and carbon (and respective formal charges), and one with a double bond between the two atoms. This linear functional group acts as a potential dipole, but it can also form hydrogen bonds at the carbon terminal atom, although these types of bond do not activate the functional group for a nucleophilic attack.^{457, 458} Despite their versatility, the number of cheap commercially available isocyanides is somehow underwhelming, which explains the growing interest in discovering new synthetic methodologies to give these valuable building blocks for MCRs.^{440, 459}

Nevertheless, and despite their remarkable value for drug discovery programmes, concerns on isocyanides safety and sustainability are often raised. One of the most easily recognized drawbacks of working with isocyanides is their atrocious smell, mostly displayed by low molecular and volatile isocyanides. Higher molecular weight or sterically hindered isocyanides tend to be odorless and chemically stable.⁴⁵⁸ The unpleasant odour, as well as the name of this family of compounds (similar to cyanides and nitriles), tend to give a bad reputation to isocyanides.³⁹⁸ However, most isocyanides do not deserve to be associated with toxicity. Ugi and co-workers, while working in Bayer in the 1960's, performed a comprehensive investigation on isocyanide safety, and verified that most isocyanides do not display appreciable toxicity for mammals after oral and subcutaneous administration (in doses as high as up to 5 g/kg in mice).⁴⁶⁰ From the operational point of view, this class of compounds also display hazard concerns within the reasonable limits, and comparable to several other categories of chemicals, with no particular demands in what concerns transportation, storage and handling. Their destruction can also be easily achieved via acid work-up procedures.³⁹⁸

As previously stated, the Ugi reaction plays a prominent role among the different IMCRs, especially in what concerns drug discovery programmes. Its potential of application in the pharmaceutical industry is undeniable, with so many APIs synthesized using this reaction as a key step, but its advantages for early-stage drug discovery programmes is also well documented. The already mentioned structural diversity and the inherent sustainability are unspecific advantages of MCRs. But the Ugi reaction unveils specific advantages, including i) high flexibility, since it is suitable to be performed using different functional groups, ii) high versatility, since the different components of the U4CR can be replaced by different functional groups with similar reactivity, allowing a fine tuning of the structures achieved, iii) generating libraries which are prone to post-Ugi modifications, increasing the number and scaffold diversity of the structures which can be synthesized.⁴⁶¹ The most remarkable advantage of the Ugi reaction in medicinal

chemistry might as well be the type of bonds formed during this reaction – two new amide bonds are present in the final α -aminoacyl amides. Indeed, the amide functional group plays a pivotal role in drug discovery and development, as showcase in **Figure 1.24**.

The previously mentioned ACS GCIPR, back in 2007, voted amide bond formation – a reaction that avoids poor atom economy reagents - as the top priority transformation used by pharmaceutical companies, although better reagents are still required.²⁹¹ Recently, the key green chemistry research areas have been revisited, and a new (and reshaped) voting system (where no distinction between “current issues” and “desired, enabling transformations” was made) still place amide bond formation a top 10 key green chemistry research area, displayed as “general methods for catalytic/sustainable (direct) amide or peptide formation”.⁴⁶² A great deal of research and innovation has been made in developing new and more sustainable stoichiometric and catalytic methods for amide bond formation,⁴⁶³⁻⁴⁶⁷ galvanized by the fact that amide bond formation still remains the most popular reaction in medicinal chemistry and drug discovery.⁴⁶⁸ The interest in this type of reaction is easily understood, if we consider that the amide functional group is present in up to 54.5% of bioactive compounds and in about 2/3 of drug candidates.^{466, 469} In the last three decades, “amide” has been constantly ranked in the top 2 of the popularity of functional groups, spending most of the time as number 1, although in some years it was surpassed by the ether functional

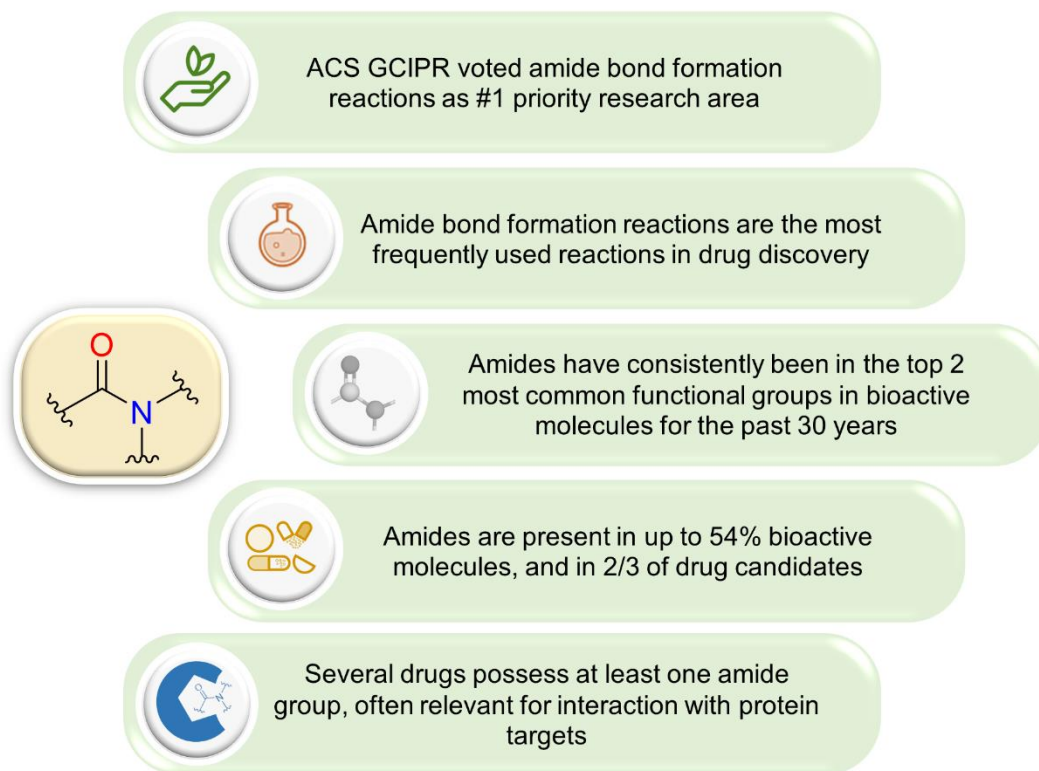


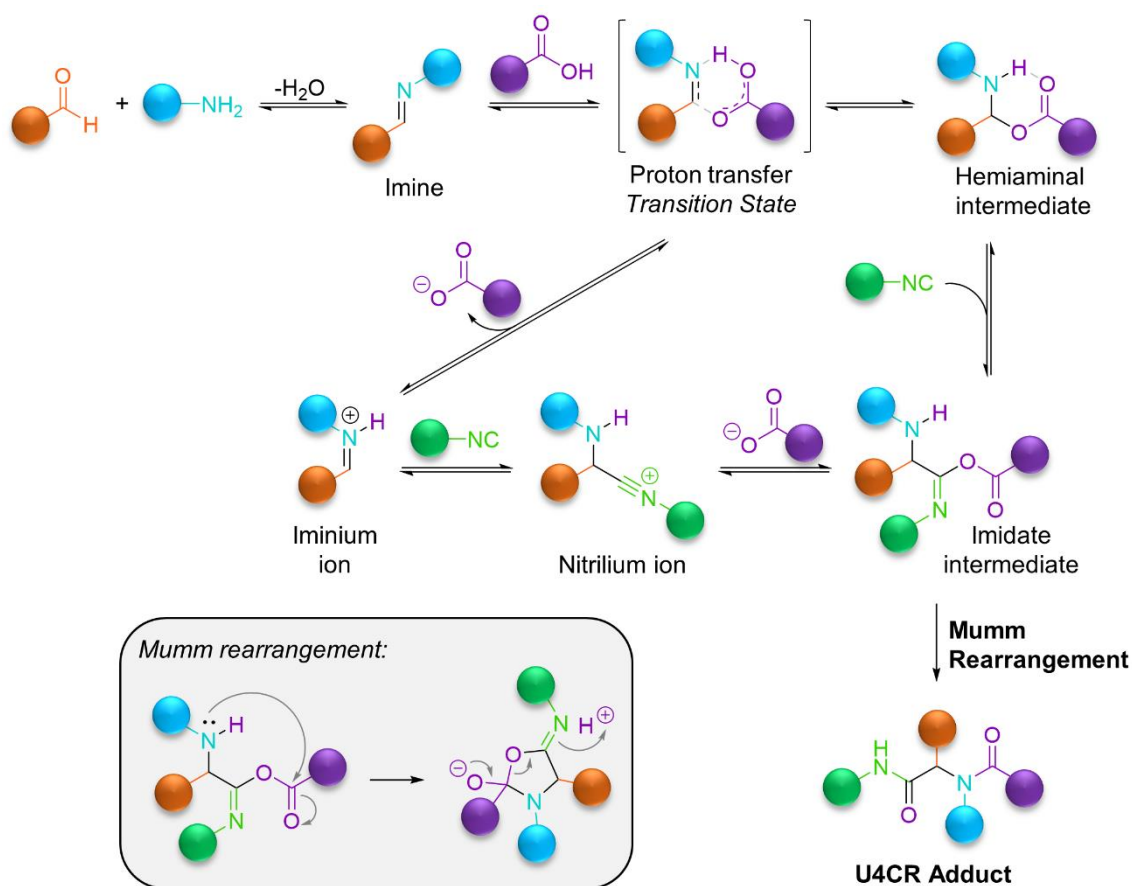
Figure 1.24. Central role of amide functional group in drug discovery and development.

group.⁴⁷⁰ For all these reasons, and although a plethora of synthetic methods for accessing amide bonds are now available, including several reported coupling reagents, the Ugi reaction has emerged as a viable sustainable alternative, often overlooked in reviews on amide bond synthesis, even though two new amide bonds are formed in a single step.³⁹⁸

Nevertheless, the Ugi reaction still presents some challenges. One of these challenges, shared with several other MCRs, is the limited information of their reaction mechanism. If compared to traditional reactions, the existence of two or more concurrent reaction pathways, as well as the greater number of possible intermediates in MCRs, make the study of their reaction mechanisms a trickier task and more open to debate, and therefore might constrain the development of more efficient MCRs.⁴⁷¹⁻⁴⁷³ Ivar Karl Ugi himself recognized this challenge in the early 2000s, over forty years after he first reported the now known as Ugi reaction, stating that “the reaction mechanisms of the MCRs cannot be investigated by the usual methods. Some essential mechanistic information of a MCR can be obtained from combinations of several methods, but not all of the usual detailed information can be expected”.⁴⁷⁴ Nevertheless, the synthetic value of MCRs continue to be praised due to their ability to afford a major final product, even if, mechanistically, they proceed in an “all roads lead to Rome” fashion, as recently reviewed by A. D. Neto and co-workers.⁴⁷²

The U4CR also shows great uncertainty like the other common MCRs from a mechanistic point of view. It is widely accepted that the first step consists in the formation of an imine, from the reaction between the carbonyl compound (usually an aldehyde, although ketones can also be employed) and the primary amine. After this stage, two possible pathways are currently viable. In the classical route, established when the reaction was first discovered, and highly supported by recent mass spectrometry investigations,⁴⁷⁵ the imine is protonated to generate the iminium ion, followed by isocyanide addition to afford the nitrilium ion which, after carboxylic acid addition, affords the imidate intermediate. Computational studies challenged this pathway, suggesting an alternative path via the formation of a hemiaminal intermediate after the proton transfer, which is then followed by isocyanide insertion, converging to the same imidate intermediate.⁴⁷⁶ The imidate intermediate then undergoes Mumm rearrangement to afford the final U4CR adduct.⁴⁷⁷ The overall mechanistic approach of a classic U4CR, including the two possible paths currently being debated, is depicted in **Scheme 1.6**.

General Introduction



Scheme 1.6. Classic U4CR mechanism.

The complexity of the reaction mechanism allows us to understand one of the biggest challenges faced by academia and industry in what concerns the Ugi reaction – enantioselectivity.⁴⁷⁸ Indeed, there is only one very recent example of enantioselective U4CR, using chiral phosphoric acid organocatalysts. Surprisingly, this approach required atypical solvents for the Ugi reaction (cyclohexane and dichloromethane), which is usually promoted in the presence of polar protic solvents, such as methanol, ethanol, or trifluoroethanol.⁴⁷⁹ This discovery is a milestone in IMCRs research area, and might unlock several future applications of the U4CR in the fields of medicinal chemistry and chemical biology.^{480, 481}

But despite the novelty that asymmetric catalytic Ugi reaction affords, catalytic transformations have been developed in order to further expand the scope, sustainability, and efficiency of the Ugi reaction. A review (divided into two parts) on the recent developments in the catalytic Ugi reaction was published during this PhD (see **Appendices 4 and 5**).^{482, 483} Among the most popularly used catalysts are Lewis acids, such as indium(III)⁴⁸⁴⁻⁴⁸⁷ and zinc⁴⁸⁸⁻⁴⁹¹ salts. Phosphorous-based catalysts,⁴⁹²⁻⁴⁹⁵ surfactant catalysts,⁴⁹⁶ metal-organic frameworks (MOFs) catalysts,⁴⁹⁷ nanocatalysts,⁴⁹⁸ and even biocatalysts,⁴⁹⁹⁻⁵⁰¹ are among some of the new trends observed for catalytic

Ugi transformations. Amid these catalysts, indium has to be highlighted, as this catalyst will play a central role in Chapter 2. As widely revised in the scientific literature, indium is a very versatile post-transition metal, widely used in the field of organic synthesis and catalysis due to the Lewis acidity of its metal complexes and salts.⁵⁰²⁻⁵⁰⁶ However, some of its most recent synthetic applications are in the field of MCRs, as reviewed during the development of the work reported in this thesis (see **Appendix 6**).⁵⁰⁷ What makes indium a multifaceted catalyst is its stability to air and moisture (it can be used in reactions in the presence of water), its safety, and the fact that it is very easy-to-handle.⁵⁰⁷ The main downfall of the use of indium is actually its abundance on Earth. Often collected as a by-product of zinc mining, indium demand has increased over recent years due to its application in the construction of solar panels and touchscreens. Indeed, indium is considered to be an “endangered” element, and therefore appropriate disposal and recyclability of electronic components containing indium, as well as the development of alternative technologies “indium-free” might improve the sustainability of its use (**Figure 1.25**).^{269, 508-510}

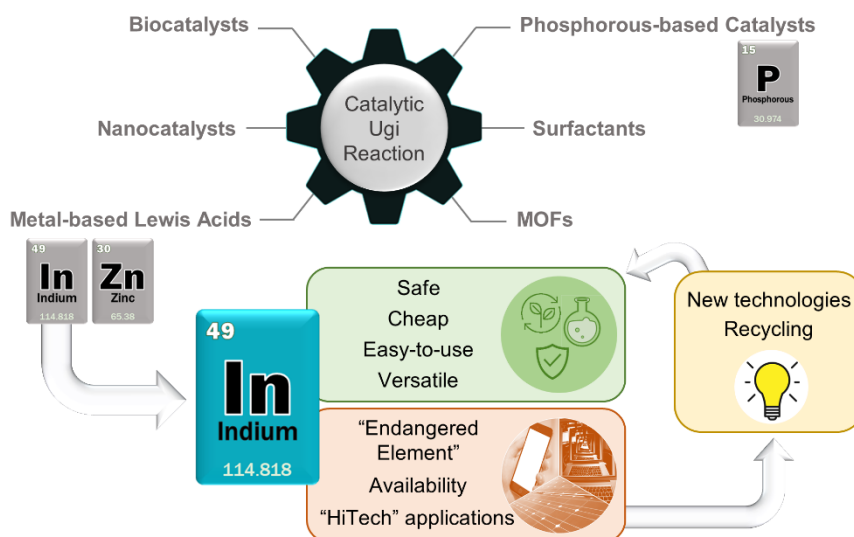


Figure 1.25. Catalytic Ugi reaction and indium catalysis advantages and disadvantages.

Besides the mentioned efforts in developing new and more efficient catalytic systems for the Ugi reaction, a clear trend for improving the sustainability of the chemical processes is to perform the reaction using eco-friendly activation techniques, such as microwave irradiation,⁴⁸⁵ and mechanochemistry,^{409, 486} green solvents, namely water⁵¹¹ or DESs,⁵¹² or even to perform the Ugi reaction under continuous flow.⁵¹³⁻⁵¹⁵

Nevertheless, the nature of the components themselves have an impact on the reaction outcome, especially in what concerns yields and reaction times. With regard to

the amine component, higher basicity and nucleophilicity usually improve the reaction outcome, as it facilitates the formation of the iminium ion. The carbonyl component is often depicted as an aldehyde, as both aliphatic and aromatic aldehydes easily react in the U4CR. Aliphatic ketones, although less reactive than aldehydes, work better than aryl ketones. For the acid component, higher acidity leads to higher yields and shorter reaction times, as the protonation of the imine to afford the iminium intermediate is facilitated.⁵¹⁶

Advances in the studies of the Ugi reaction take the exploration of the components out of the conventional approach model. While the isocyanide is a constant, and the scope of the carbonyl compound is restricted to aldehydes and ketones, the carboxylic acid component and the primary amine component can be replaced by other isosteres, as depicted in **Figure 1.26**.^{457, 491, 517}

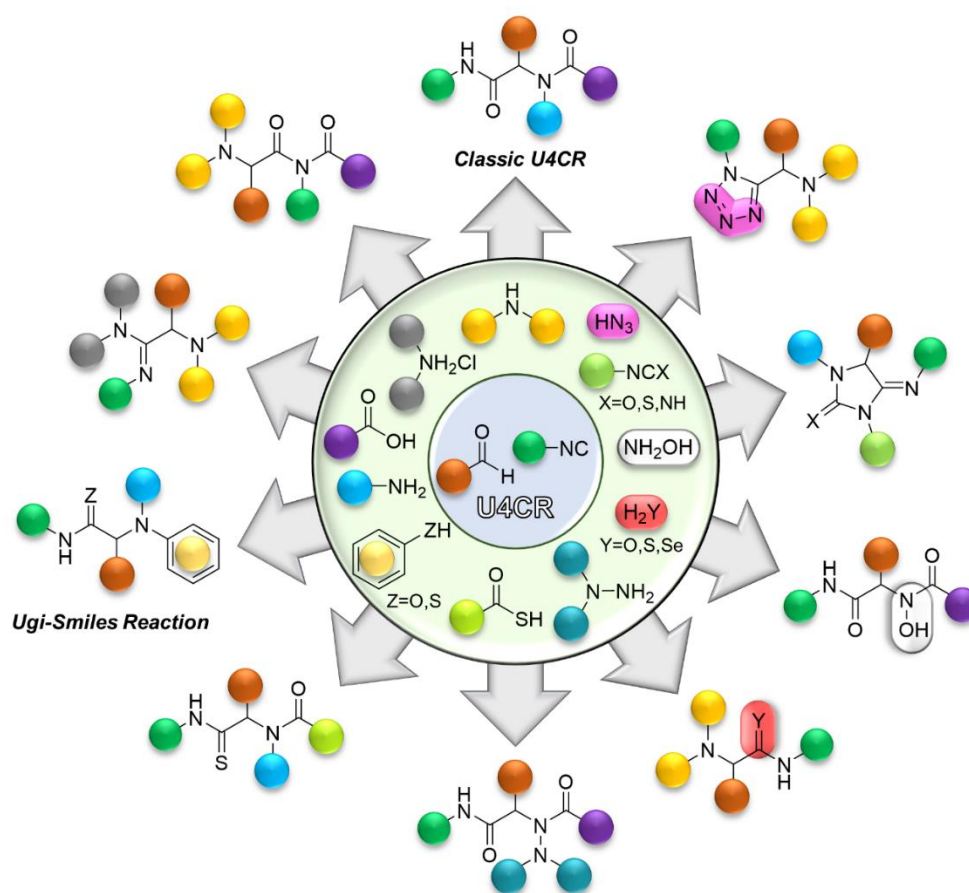
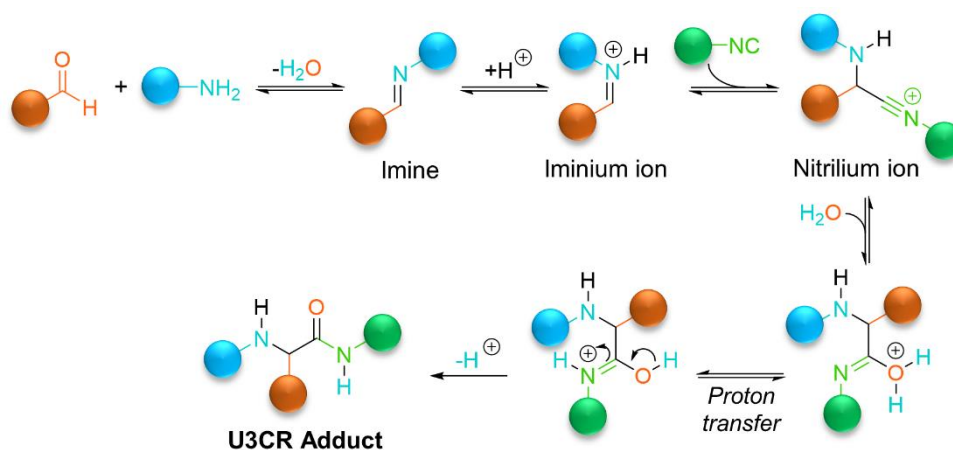


Figure 1.26. Variations of the U4CR.

Noteworthy, while most of the variations did not acquire a specific name, the replacement of the carboxylic acid by a phenol acquired the name Ugi-Smiles reaction, as the final step consists in the Smiles rearrangement, instead of the Mumm rearrangement which occurs in the classic U4CR.⁵¹⁸

Alternatively, Ugi 3 component reactions (U3CRs), can also constitute an effective way to achieve structural diversity. In its classic version, an U3CR comprises the reaction between a carbonyl component, an isocyanide, and a primary amine, affording an α -aminoamide. An acid is required as a catalyst, to promote the protonation of the imine to iminium, while the water released in the formation of the imine is later in the mechanism required to trap the nitrilium ion, with a proton transfer determining the formation of the final product (**Scheme 1.7**).^{519, 520}



Scheme 1.7. Classic U3CR mechanism.

Similarly to U4CRs, a myriad of U3CR have been described, according to different features and dependent on the starting building blocks features (**Figure 1.27**).^{393, 519-527} One U3CR in particular, which mechanistically undergoes the U4CR path, is the Ugi 4 center 3 component reaction (U4c3CR). In this approach, the four moieties required for the U4CR are present in three starting materials, and therefore requires the use of amino acids, oxoacids, isocyanoaldehydes, or isocyanoacids as starting material. The U4c3CR proved to be suitable to attain several valuable heterocycles,⁵²⁸ and this approach will be focus of further exploration in Chapter 3.

The use of reagents bearing functional groups that can undergo further chemical transformations, in a sequential or tandem manner open the door for post-Ugi chemical transformations and allow to attain even greater structural diversity. Other alternatives that also showcase the versatility of the Ugi reaction in organic synthesis is, similarly to what occurs with the GBB3CR, to use structural motifs in the starting materials that, upon formation of the nitrilium intermediate, will intercept/trap it, evading the attack by the carboxylate and leading to a thriving research field, the interrupted Ugi reaction.^{519, 529} Polyfunctionalized starting material employed in the Ugi reaction can also promote the formation of complex structures, such as the ones occurring using the Ugi 5 center 4 component reaction (U5c4CR),⁵³⁰ or even polymers.^{531, 532}

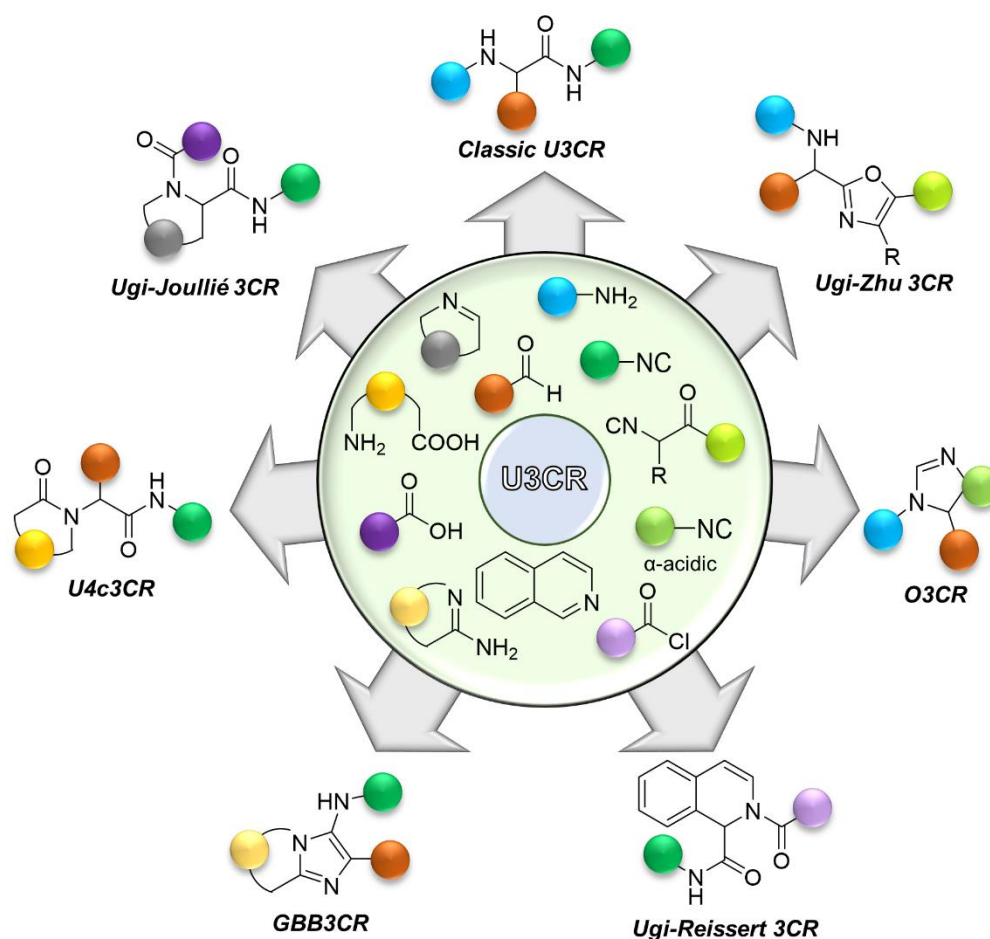


Figure 1.27. Examples of variations of the U3CR.

1.3.3.2. Petasis Reaction: Organoboron Reagents in MCRs

The Petasis MCR, also known as Petasis Borono-Mannich MCR, was first reported by Nicos A. Petasis and I. Akritopoulou in 1993 and it showed applicability for drug discovery and development since the beginning, as one of the compounds synthesized in this first report was naftifine (**Figure 1.28**),³⁸⁹ commercialized in several countries as a topical antifungal agent.⁵³³ And even more recently, besides the application of the Petasis MCR in the synthesis of APIs fingolimod and zanamivir (see **Figure 1.22**), it also proved to be of valuable interest for the synthesis of acalabrutinib (**Figure 1.28**), a drug approved in 2017 by FDA for the treatment of mantle cell lymphoma in adults.⁵³⁴

At the first approach, Petasis reported this reaction as a versatile and efficient way to afford allylamines, as vinyl boronic acids can participate as nucleophiles in the Mannich reaction involving formaldehyde and secondary amines, as using primary

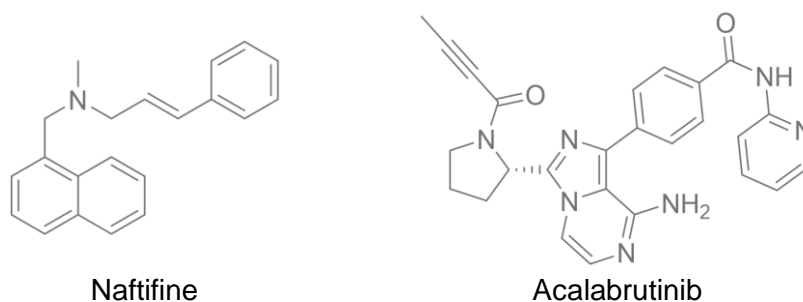
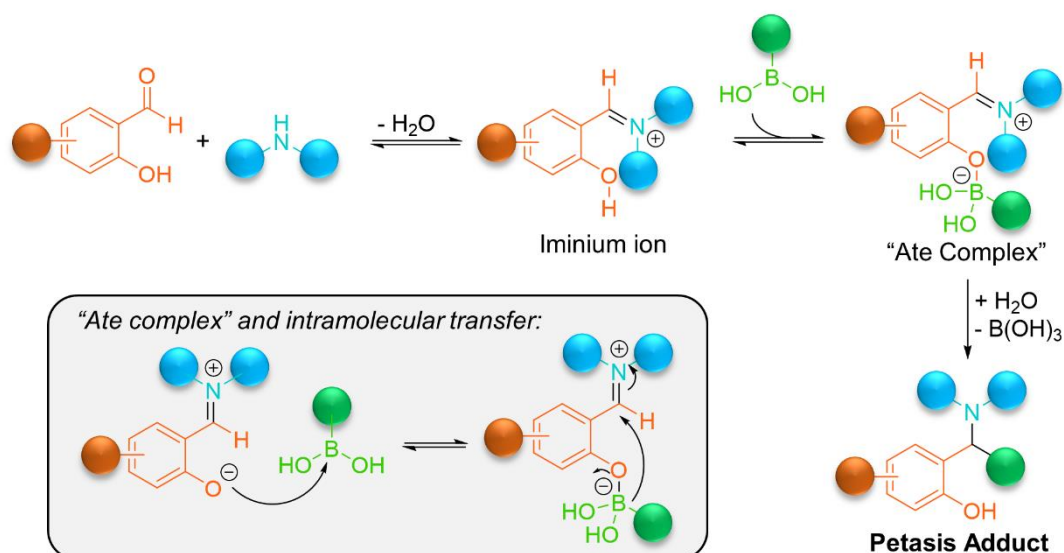


Figure 1.28. Examples of APIs synthesized using Petasis MCR.

amines led to lower yields. The authors also reported preliminary studies with aryl boronic acids showing that these could also be employed to afford benzylamines, but in a less efficient manner under the explored conditions (dioxane or toluene as solvent, at 90 °C).³⁸⁹ Later, in 2001, Petasis and Boral reported the construction of a library using several boronic acids (alkenyl, aryl, and heteroaryl), amines and salicylaldehydes.⁵³⁵ Nowadays, most examples of the application of the Petasis 3CR involve aldehydes with a heteroatom (hydroxy, phenol, or carboxylic acid) adjacent to the functional group (e.g. glyoxylic acid, salicylaldehydes, α -hydroxyaldehydes) to achieve good results; secondary and primary amines are suitable for the chemical transformation, although the first ones usually lead to better results; vinyl and aryl boronic acids appear as the most efficient for the MCR.⁵³⁶

Mechanistically, it shares with the Ugi reaction the fact that it evolves through several reversible steps in equilibrium, ending in an irreversible step, which drives the reaction to completion. But, similarly to several MCRs, the full reaction mechanism is not totally known. To the best of contemporary knowledge, and based on experimental and theoretical data, an iminium ion is attained by reacting the aldehyde and the amine components (to illustrate, a salicylaldehyde derivative and a secondary amine will be used in **Scheme 1.8**). Then, the phenol functional group activates the boronic acid, forming a tetrahedral boronate salt, usually designated as “ate complex”, which is capable of transferring the boron substituent to the iminium moiety, affording the final Petasis adduct (**Scheme 1.8**).⁵³⁷⁻⁵³⁹

The Petasis MCR possesses several advantages, which includes a) requiring mild reaction conditions and being robust (it is not air or moisture sensitive); b) easy access to a wide range of reaction substrates; c) not requiring the use of protecting groups in most cases; d) often occurring under catalyst-free conditions; e) being suitable for catalytic asymmetric transformations; and f) allowing the preparation of high-added value products, such as APIs, drug candidates, and natural products. On the other hand, some limitations can also be drawn for the Petasis MCR, namely the need for activated



Scheme 1.8. Petasis 3CR mechanism.

carbonyl components, or carbonyls bearing a suitable boron-activating group, and the fact that only vinyl or arylboronic acids tend to provide high reaction yields.⁵⁴⁰ The scope and applicability of the Petasis MCR has also expanded over recent years, especially due to the development of Petasis-type cascade reactions (usually involving intramolecular Diels-Alder or ring-closing metathesis reactions) and the four component Petasis-type reaction (which affords organoboron products, with an alcohol intervening as the fourth component).⁵⁴¹

While for the U4CR, despite being described decades earlier than the Petasis MCR, it is still finding its path to develop efficient asymmetric catalytic versions, several examples can be found in the literature concerning enantioselective versions of the Petasis MCR. Among the reports, a clear trend can be established, with organocatalysts playing a major role in the success of the enantioselectivity. This field has a remarkable impact in drug discovery and development, as recently shown by the attribution of the Nobel Prize in Chemistry 2021 to Benjamin List and David MacMillan "for the development of asymmetric organocatalysis".⁵⁴² For the Petasis MCR, chiral diols, especially the derivatives of chiral 1,1'-bi-2-naphthol (BINOL), are among the most commonly reported to attain great results in what concerns enantioselectivity and yields (**Figure 1.29**).⁵⁴³⁻⁵⁴⁷ The applicability of these catalysts in this asymmetric chemical transformation is based on the ability of the phenolic hydroxyl groups to coordinate with the Lewis acidic sites of reagents or substrates (in the case of the Petasis MCR, it can coordinate with the iminium ion and, at the same time, help to transfer the boronic acid substituent), creating a chiral environment for the asymmetric transformation.⁵⁴⁸⁻⁵⁵⁰

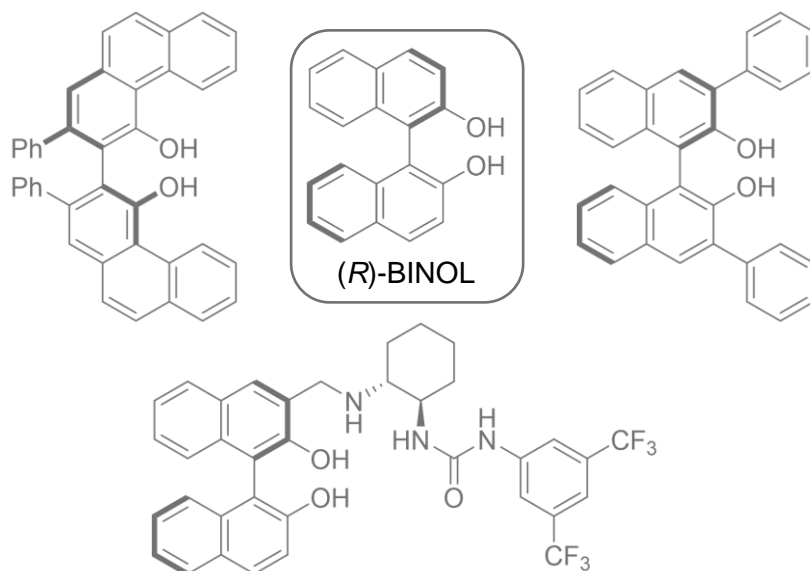


Figure 1.29. BINOL and BINOL derivatives applied as efficient asymmetric Petasis MCR.

1.4. Bringing Together Privileged Scaffolds and Sustainable Tools: State of the Art and Setting Up the Goals

“A scientist in his laboratory is not a mere technician: he is also a child confronting natural phenomena that impress him as though they were fairy tales.”

Marie Skłodowska Curie

In this work, isatin and tryptanthrin take center stage as privileged scaffolds in drug discovery. Making medicinal chemistry greener depends on the thorough selection of the appropriate sustainable tools. MCRs are valuable tools to generate libraries of compounds for screening in a fast, efficient, and sustainable manner.

Taking a closer look to the state of the art in what concerns engaging isatin in MCRs, it is noteworthy the remarkable application of this heterocycle to attain structural diverse libraries. A thorough review on this topic was recently published, addressing the developments on this topic between 2013-2019 (see **Appendix 7**).⁵⁵¹ Two main observations could be drawn from this systematic analysis (**Figure 1.30**): a) the vast majority of approaches comprise the generation of spirooxindole-based libraries (>78%); b) IMCRs, despite their high-value in medicinal chemistry and drug discovery, remain considerably unexplored (only 3.7% of the MCRs consisted of IMCRs).

And while in many of these reports, the challenge relies on the synthetic organic chemistry development (unlock the synthesis of new compounds, develop new catalysts,



Figure 1.30. Trend on isatin-based MCRs.

explore new reaction media, etc.), in some cases the biological activity of the synthesized libraries was also evaluated. A review on the recent developments reported in the literature on this topic was made during the development of this work and recently published (see **Appendix 8**). The application of isatin-based MCRs proved to be suitable for the development of bioactive molecules.⁵⁵² However, while most of the bioactive compounds result of chemical modifications at the C3 position of the isatin scaffold, the vast majority are spirooxindole derivatives, with the remaining chemical space, especially regions occupied by 3,3-disubstituted oxindoles which can be attained via MCR, remaining fairly unexplored. Furthermore, as depicted in **Figure 1.30**, isatin-based IMCRs are also sparsely reported. While checking for the application of isatin in the Passerini and Ugi reactions, two of the most explored IMCRs in drug discovery, we could find out that they were poorly explored, with only two examples, published in 2013, of the isatin-based Passerini-reaction,^{553, 554} and two examples concerning the use of the Ugi reaction,^{555, 556} which will be further discussed in Chapter 2.

Shifting the attention to the tryptanthrin scaffold, its application in MCRs is rare, with only few recent examples being reported⁵⁵⁷⁻⁵⁶⁰ as will be further discussed in Chapter 4.

The chemical space occupied by 3,3-disubstituted oxindole derivatives with potential bioactivity remains underexplored, especially those concerning Ugi-based approaches. In the case of tryptanthrin, it is clear that this molecule is just starting to be used as starting point for MCRs. As delineated in the title of this PhD thesis, the main goal of this work is the sustainable development of isatin and tryptanthrin bioactive derivatives, using green by design strategies. As part of the CATSUS PhD Programme, catalysis and sustainability played a central role in experimental design and reaction optimization, in an effort to improve the approaches efficiency and eco-friendliness. The outline of thesis is summarized in **Figure 1.31**.

In chapter 2, the aim is to obtain a structurally diverse library based from isatin (library I), in a sustainable fashion. By engaging isatin in a catalytic U4CR, the chemical space of 3,3-disubstituted oxindole derivatives can be expanded, based on sustainable

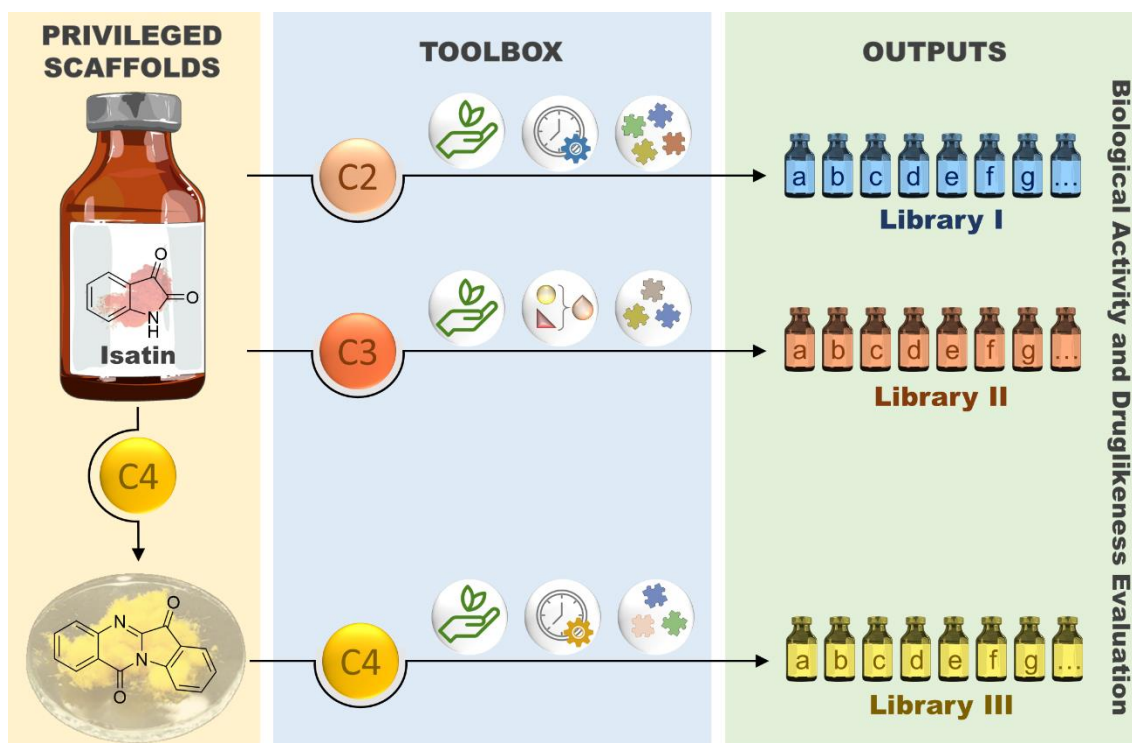


Figure 1.31. Thesis outline (C2=chapter 2; C3=chapter 3; C4=chapter 4).

methodologies. The obtained library is evaluated in what concerns its druglikeness properties and antiproliferative activity.

In chapter 3, the goal was to develop a library of oxindole-lactam hybrids (library II), based on the U4c3CR, with potential bioactivity. In this case, a rational drug design based on molecular hybridization was performed, to attain compounds to inhibit specific targets – cholinesterases – which are key players in Alzheimer's disease pathophysiology. Druglikeness of the resulting compounds was also evaluated, in order to determine the potential of these hybrids to be further studied.

A different approach was used in Chapter 4. Starting from the discovery and optimization of novel synthetic routes to attain tryptanthrin, followed by the exploration of its potential to be used as substrate of MCRs, to the organocatalyzed synthesis of library III, using a tryptanthrin-based Petasis MCR. The new derivatives were screened for their antimicrobial activity, namely antibacterial and antifungal.

1.5. References

1. Borgel, S.; Latimer, B.; McDermott, Y.; Sarig, R.; Pokhojaev, A.; Abulafia, T.; Goder-Goldberger, M.; Barzilai, O.; May, H., Early Upper Paleolithic human foot bones from Manot Cave, Israel. *Journal of Human Evolution*, **2019**, 102668.
2. Riddle, J. M., Folk Tradition and Folk Medicine: Recognition of Drugs in Classical Antiquity. *Pharmacy in History*, **2013**, 55 (2), 64-87.
3. Zanders, E. D., Laying the Foundations: Drug Discovery from Antiquity to the Twenty-First Century. Springer International Publishing, **2020**, pp 57-91.
4. Bruce-Chwatt, L. J., Cinchona and Quinine: A Remarkable Anniversary. *Interdisciplinary Science Reviews*, **1990**, 15 (1), 87-93.
5. Achan, J.; Talisuna, A. O.; Erhart, A.; Yeka, A.; Tibenderana, J. K.; Baliraine, F. N.; Rosenthal, P. J.; D'Alessandro, U., Quinine, an old anti-malarial drug in a modern world: role in the treatment of malaria. *Malaria Journal*, **2011**, 10 (1), 144.
6. Permin, H.; Norn, S.; Kruse, E.; Kruse, P. R., On the history of Cinchona bark in the treatment of Malaria. *Dan Medicinhist Arbog*, **2016**, 44, 9-30.
7. Zhang, T.-D.; Chen, G.-Q.; Wang, Z.-G.; Wang, Z.-Y.; Chen, S.-J.; Chen, Z., Arsenic trioxide, a therapeutic agent for APL. *Oncogene*, **2001**, 20 (49), 7146-7153.
8. Davison, K.; Mann, K. K.; Miller, W. H., Arsenic trioxide: Mechanisms of action. *Seminars in Hematology*, **2002**, 39 (2, Supplement), 3-7.
9. Miller, W. H.; Schipper, H. M.; Lee, J. S.; Singer, J.; Waxman, S., Mechanisms of Action of Arsenic Trioxide. *Cancer Research*, **2002**, 62 (14), 3893-3903.
10. Lengfelder, E.; Hofmann, W. K.; Nowak, D., Impact of arsenic trioxide in the treatment of acute promyelocytic leukemia. *Leukemia*, **2012**, 26 (3), 433-442.
11. Wöhler, F., Ueber künstliche Bildung des Harnstoffs. *Annalen der Physik*, **1828**, 88 (2), 253-256.
12. Cohen, P. S.; Cohen, S. M., Wöhler's Synthesis of Urea: How Do the Textbooks Report It? *Journal of Chemical Education*, **1996**, 73 (9), 883.
13. Pearson, G. J., Evolution in the practice of pharmacy - not a revolution! *Canadian Medical Association Journal*, **2007**, 176 (9), 1295-1296.
14. Hacker, M., Chapter 1 - History of Pharmacology—From Antiquity to the Twentieth Century. In *Pharmacology*, Hacker, M.; Messer, W.; Bachmann, K., Eds. Academic Press, San Diego, USA, **2009**, pp 1-7.
15. Desborough, M. J. R.; Keeling, D. M., The aspirin story - from willow to wonder drug. *British Journal of Haematology*, **2017**, 177 (5), 674-683.
16. Montinari, M. R.; Minelli, S.; De Caterina, R., The first 3500 years of aspirin history from its roots – A concise summary. *Vascular Pharmacology*, **2019**, 113, 1-8.
17. Newman, D. J.; Cragg, G. M., Natural product scaffolds as leads to drugs. *Future Medicinal Chemistry*, **2009**, 1 (8), 1415-1427.

18. de Fatima, A.; Silva Terra, B.; Moreira da Silva, C.; Leite da Silva, D.; Pereira Araujo, D.; da Silva Neto, L.; Anderson Nascimento de Aquino, R., From Nature to Market: Examples of Natural Products that Became Drugs. *Recent Patents on Biotechnology*, **2014**, 8 (1), 76-88.
19. Newman, D. J., Developing natural product drugs: Supply problems and how they have been overcome. *Pharmacology & Therapeutics*, **2016**, 162, 1-9.
20. Mathur, S.; Hoskins, C., Drug development: Lessons from nature. *Biomedical Reports*, **2017**, 6 (6), 612-614.
21. Prakash, B.; Kujur, A.; Yadav, A., Chapter 2 - Drug synthesis from natural products: a historical overview and future perspective. In *Synthesis of Medicinal Agents from Plants*, Tewari, A.; Tiwari, S., Elsevier, **2018**, pp 25-46.
22. Walters, R. J.; Hadley, S. H.; Morris, K. D. W.; Amin, J., Benzodiazepines act on GABA_A receptors via two distinct and separable mechanisms. *Nature Neuroscience*, **2000**, 3 (12), 1274-1281.
23. Sigel, E.; Ernst, M., The Benzodiazepine Binding Sites of GABA_A Receptors. *Trends in Pharmacological Sciences*, **2018**, 39 (7), 659-671.
24. Evans, B. E.; Rittle, K. E.; Bock, M. G.; DiPardo, R. M.; Freidinger, R. M.; Whitter, W. L.; Lundell, G. F.; Veber, D. F.; Anderson, P. S.; Chang, R. S. L.; Lotti, V. J.; Cerino, D. J.; Chen, T. B.; Kling, P. J.; Kunkel, K. A.; Springer, J. P.; Hirshfield, J., Methods for drug discovery: development of potent, selective, orally effective cholecystokinin antagonists. *Journal of Medicinal Chemistry*, **1988**, 31 (12), 2235-2246.
25. Herranz, R., Cholecystokinin antagonists: Pharmacological and therapeutic potential. *Medicinal Research Reviews*, **2003**, 23 (5), 559-605.
26. Roche, O.; Schneider, P.; Zuegge, J.; Guba, W.; Kansy, M.; Alanine, A.; Bleicher, K.; Danel, F.; Gutknecht, E.-M.; Rogers-Evans, M.; Neidhart, W.; Stalder, H.; Dillon, M.; Sjögren, E.; Fotouhi, N.; Gillespie, P.; Goodnow, R.; Harris, W.; Jones, P.; Taniguchi, M.; Tsujii, S.; Von Der Saal, W.; Zimmermann, G.; Schneider, G., Development of a Virtual Screening Method for Identification of "Frequent Hitters" in Compound Libraries. *Journal of Medicinal Chemistry*, **2002**, 45 (1), 137-142.
27. Yang, Z.-Y.; He, J.-H.; Lu, A.-P.; Hou, T.-J.; Cao, D.-S., Frequent hitters: nuisance artifacts in high-throughput screening. *Drug Discovery Today*, **2020**, 25 (4), 657-667.
28. Mendgen, T.; Steuer, C.; Klein, C. D., Privileged Scaffolds or Promiscuous Binders: A Comparative Study on Rhodanines and Related Heterocycles in Medicinal Chemistry. *Journal of Medicinal Chemistry*, **2012**, 55 (2), 743-753.
29. Schneider, P.; Röthlisberger, M.; Reker, D.; Schneider, G., Spotting and designing promiscuous ligands for drug discovery. *Chemical Communications*, **2016**, 52 (6), 1135-1138.
30. Baell, J. B.; Holloway, G. A., New Substructure Filters for Removal of Pan Assay Interference Compounds (PAINS) from Screening Libraries and for Their Exclusion in Bioassays. *Journal of Medicinal Chemistry*, **2010**, 53 (7), 2719-2740.
31. Baell, J.; Walters, M. A., Chemistry: Chemical con artists foil drug discovery. *Nature*, **2014**, 513 (7519), 481-483.

32. Schneider, P.; Schneider, G., Privileged Structures Revisited. *Angewandte Chemie International Edition*, **2017**, *56* (27), 7971-7974.
33. Kim, J.; Kim, H.; Park, S. B., Privileged Structures: Efficient Chemical “Navigators” toward Unexplored Biologically Relevant Chemical Spaces. *Journal of the American Chemical Society*, **2014**, *136* (42), 14629-14638.
34. Wu, G.; Zhao, T.; Kang, D.; Zhang, J.; Song, Y.; Namasivayam, V.; Kongsted, J.; Pannecouque, C.; De Clercq, E.; Poongavanam, V.; Liu, X.; Zhan, P., Overview of Recent Strategic Advances in Medicinal Chemistry. *Journal of Medicinal Chemistry*, **2019**, *62* (21), 9375-9414.
35. Welsch, M. E.; Snyder, S. A.; Stockwell, B. R., Privileged scaffolds for library design and drug discovery. *Current Opinion in Chemical Biology*, **2010**, *14* (3), 347-361.
36. Leite, A. C. L.; Espíndola, J. W. P.; Cardoso, M. V. d. O.; Gevanio Bezerra de Oliveira Filho, G. B. d., Privileged Structures in the Design of Potential Drug Candidates for Neglected Diseases. *Current Medicinal Chemistry*, **2019**, *26* (23), 4323-4354.
37. Hinkson, I. V.; Madej, B.; Stahlberg, E. A., Accelerating Therapeutics for Opportunities in Medicine: A Paradigm Shift in Drug Discovery. *Frontiers in Pharmacology*, **2020**, *11* (770).
38. Lai, J.; Hu, J.; Wang, Y.; Zhou, X.; Li, Y.; Zhang, L.; Liu, Z., Privileged Scaffold Analysis of Natural Products with Deep Learning-based Indication Prediction Model. *Molecular Informatics*, **2020**, *39* (11), 2000057.
39. Vitaku, E.; Smith, D. T.; Njardarson, J. T., Analysis of the Structural Diversity, Substitution Patterns, and Frequency of Nitrogen Heterocycles among U.S. FDA Approved Pharmaceuticals. *Journal of Medicinal Chemistry*, **2014**, *57* (24), 10257-10274.
40. Giordanetto, F.; Jin, C.; Willmore, L.; Feher, M.; Shaw, D. E., Fragment Hits: What do They Look Like and How do They Bind? *Journal of Medicinal Chemistry*, **2019**, *62* (7), 3381-3394.
41. Brown, D. G.; Wobst, H. J., A Decade of FDA-Approved Drugs (2010–2019): Trends and Future Directions. *Journal of Medicinal Chemistry*, **2021**, *64* (5), 2312-2338.
42. Bhutani, P.; Joshi, G.; Raja, N.; Bachhav, N.; Rajanna, P. K.; Bhutani, H.; Paul, A. T.; Kumar, R., U.S. FDA Approved Drugs from 2015–June 2020: A Perspective. *Journal of Medicinal Chemistry*, **2021**, *64* (5), 2339-2381.
43. Jones, A. M., 2.05 - Privileged Structures and Motifs (Synthetic and Natural Scaffolds). In *Comprehensive Medicinal Chemistry III*, Chackalamannil, S.; Rotella, D.; Ward, S. E., Elsevier, Oxford, **2017**, pp 116-152.
44. Newman, D. J., Natural Products as Leads to Potential Drugs: An Old Process or the New Hope for Drug Discovery? *Journal of Medicinal Chemistry*, **2008**, *51* (9), 2589-2599.
45. Davison, E. K.; Brimble, M. A., Natural product derived privileged scaffolds in drug discovery. *Current Opinion in Chemical Biology*, **2019**, *52*, 1-8.
46. Kuramoto, M.; Arimoto, H.; Uemura, D., Bioactive Alkaloids from the Sea: A Review. *Marine Drugs*, **2004**, *2* (1), 39-54.

47. Kochanowska-Karamyan, A. J.; Hamann, M. T., Marine Indole Alkaloids: Potential New Drug Leads for the Control of Depression and Anxiety. *Chemical Reviews*, **2010**, *110* (8), 4489-4497.
48. Amirkia, V.; Heinrich, M., Alkaloids as drug leads – A predictive structural and biodiversity-based analysis. *Phytochemistry Letters*, **2014**, *10*, xlviii-lviii.
49. Debnath, B.; Singh, W. S.; Das, M.; Goswami, S.; Singh, M. K.; Maiti, D.; Manna, K., Role of plant alkaloids on human health: A review of biological activities. *Materials Today Chemistry*, **2018**, *9*, 56-72.
50. Laurent, A., Recherches sur l'indigo. *Annales de Chimie et de Physique*, **1840**, *3* (3), 393-434.
51. Erdmann, O. L., Untersuchungen über den Indigo. *Journal für Praktische Chemie*, **1840**, *19* (1), 321-362.
52. Forster, S.; Christie, R., The significance of the introduction of synthetic dyes in the mid 19th century on the democratisation of western fashion. *JAIC - Journal of the International Colour Association*, **2013**, *11*.
53. Hagan, E.; Poulin, J., Statistics of the early synthetic dye industry. *Heritage Science*, **2021**, *9* (1).
54. Durán, N.; Antonio, R. V.; Haun, M.; Pilli, R. A., Biosynthesis of a trypanocide by *Chromobacterium violaceum*. *World Journal of Microbiology and Biotechnology*, **1994**, *10* (6), 686-690.
55. Qu, Y.; Zhang, X.; Ma, Q.; Ma, F.; Zhang, Q.; Li, X.; Zhou, H.; Zhou, J., Indigo biosynthesis by *Comamonas* sp. MQ. *Biotechnology Letters*, **2012**, *34* (2), 353-357.
56. Wang, J.; Zhang, X.; Fan, J.; Zhang, Z.; Ma, Q.; Peng, X., Indigoids Biosynthesis from Indole by Two Phenol-Degrading Strains, *Pseudomonas* sp. PI1 and *Acinetobacter* sp. PI2. *Applied Biochemistry and Biotechnology*, **2015**, *176* (5), 1263-1276.
57. Maugard, T.; Enaud, E.; Choisy, P.; Legoy, M. D., Identification of an indigo precursor from leaves of *Isatis tinctoria* (Woad). *Phytochemistry*, **2001**, *58* (6), 897-904.
58. Yoshikawa, M.; Murakami, T.; Kishi, A.; Sakurama, T.; Matsuda, H.; Nomura, M.; Matsuda, H.; Kubo, M., Novel Indole S,O-Bisdesmoside, Calanthoside, the Precursor Glycoside of Tryptanthrin, Indirubin, and Isatin, with Increasing Skin Blood Flow Promoting Effects, from Two *Calanthe* Species (Orchidaceae). *Chemical and Pharmaceutical Bulletin*, **1998**, *46* (5), 886-888.
59. Bergman, J.; Lindström, J.-O.; Tilstam, U., The structure and properties of some indolic constituents in *Couroupita guianensis* aubl. *Tetrahedron*, **1985**, *41* (14), 2879-2881.
60. Wei, L.; Wang, Q.; Liu, X., Application of thin-layer chromatography in quality control of Chinese medicinal preparations. II. Qualitative analysis of some Chinese medicinal preparations of Chansu. *Yaowu Fenxi Zazhi*, **1982**, *2* (5), 288-291.
61. Qi, J.; Zulfiker, A.; Li, C.; Good, D.; Wei, M., The Development of Toad Toxins as Potential Therapeutic Agents. *Toxins*, **2018**, *10* (8), 336.
62. Sandler, M.; Clow, A.; Watkins, P. J.; Fibiol, V. G., Tribulin — an endocoid marker for anxiety in man. *Stress Medicine*, **1988**, *4* (4), 215-219.

63. d'Ischia, M.; Palumbo, A.; Prota, G., Adrenalin oxidation revisited. New products beyond the adrenochrome stage. *Tetrahedron*, **1988**, *44* (20), 6441-6446.
64. Palumbo, A.; d'Ischia, M.; Misuraca, G.; Prota, G., A new look at the rearrangement of adrenochrome under biomimetic conditions. *Biochimica et Biophysica Acta (BBA) - General Subjects*, **1989**, *990* (3), 297-302.
65. Medvedev, A.; Buneeva, O.; Gnedenko, O.; Ershov, P.; Ivanov, A., Isatin, an endogenous nonpeptide biofactor: A review of its molecular targets, mechanisms of actions, and their biomedical implications. *BioFactors*, **2018**, *44* (2), 95-108.
66. Medvedev, A. E.; Clow, A.; Sandler, M.; Glover, V., Isatin: A link between natriuretic peptides and monoamines? *Biochemical Pharmacology*, **1996**, *52* (3), 385-391.
67. Gillam, E. M. J.; Notley, L. M.; Cai, H.; De Voss, J. J.; Guengerich, F. P., Oxidation of Indole by Cytochrome P450 Enzymes†. *Biochemistry*, **2000**, *39* (45), 13817-13824.
68. Sandler, M.; Przyborowska, A.; Halket, J.; Watkins, P.; Glover, V.; Coates, M. E., Urinary but Not Brain Isatin Levels Are Reduced in Germ-Free Rats. *Journal of Neurochemistry*, **1991**, *57* (3), 1074-1075.
69. Carpenedo, R.; Mannaioni, G.; Moroni, F., Oxindole, a Sedative Tryptophan Metabolite, Accumulates in Blood and Brain of Rats with Acute Hepatic Failure. *Journal of Neurochemistry*, **2002**, *70* (5), 1998-2003.
70. Riggio, O.; Mannaioni, G.; Ridola, L.; Angeloni, S.; Merli, M.; Carlà, V.; Salvatori, F. M.; Moroni, F., Peripheral and Splanchnic Indole and Oxindole Levels in Cirrhotic Patients: A Study on the Pathophysiology of Hepatic Encephalopathy. *The American Journal of Gastroenterology*, **2010**, *105* (6), 1374-1381.
71. Moroni, F., Tryptophan metabolism and brain function: focus on kynurenine and other indole metabolites. *European Journal of Pharmacology*, **1999**, *375* (1-3), 87-100.
72. Medvedev, A.; Buneeva, O.; Glover, V., Biological targets for isatin and its analogues: Implications for therapy. *Biologics*, **2007**, *1* (2), 151-162.
73. Glover, V.; Bhattacharya, S. K.; Chakrabarti, A.; Sandler, M., The psychopharmacology of isatin: a brief review. *Stress Medicine*, **1998**, *14* (4), 225-229.
74. Medvedev, A.; Igosheva, N.; Crumeyrolle-Arias, M.; Glover, V., Isatin: Role in stress and anxiety. *Stress*, **2005**, *8* (3), 175-183.
75. Igosheva, N.; Lorz, C.; Oconner, E.; Glover, V.; Mehmet, H., Isatin, an endogenous monoamine oxidase inhibitor, triggers a dose- and time-dependent switch from apoptosis to necrosis in human neuroblastoma cells. *Neurochemistry International*, **2005**, *47* (3), 216-224.
76. Wu, C.; Du, C.; Gubbens, J.; Choi, Y. H.; Van Wezel, G. P., Metabolomics-Driven Discovery of a Prenylated Isatin Antibiotic Produced by *Streptomyces* Species MBT28. *Journal of Natural Products*, **2015**, *78* (10), 2355-2363.
77. Wang, Z.-Y.; Liu, J.-Y.; Yang, C.-B.; Malampati, S.; Huang, Y.-Y.; Li, M.-X.; Li, M.; Song, J.-X., Neuroprotective Natural Products for the Treatment of Parkinson's Disease by Targeting the Autophagy-Lysosome Pathway: A Systematic Review. *Phytotherapy Research*, **2017**, *31* (8), 1119-1127.

78. Batiha, G. E.-S.; Magdy Beshbishy, A.; Wasef, L.; Elewa, Y. H. A.; Abd El-Hack, M. E.; Taha, A. E.; Al-Sagheer, A. A.; Devkota, H. P.; Tufarelli, V., *Uncaria tomentosa* (Willd. ex Schult.) DC.: A Review on Chemical Constituents and Biological Activities. *Applied Sciences*, **2020**, *10* (8), 2668.
79. Kushida, H.; Matsumoto, T.; Ikarashi, Y., Properties, Pharmacology, and Pharmacokinetics of Active Indole and Oxindole Alkaloids in *Uncaria Hook.* *Frontiers in Pharmacology*, **2021**, *12* (1769).
80. Ahmad, A.; Pandurangan, A.; Singh, N.; Ananad, P., A mini review on chemistry and biology of *Hamelia Patens* (Rubiaceae). *Pharmacognosy Journal*, **2012**, *4* (29), 1-4.
81. Ahmad, R.; Salim, F., Chapter 12 - Oxindole Alkaloids of *Uncaria (Rubiaceae, Subfamily Cinchonoideae)*: A Review on Its Structure, Properties, and Bioactivities. In *Studies in Natural Products Chemistry*, Atta ur, R., Elsevier, **2015**, Vol. 45, pp 485-525.
82. Landsman, J. B.; Grist, N. R., Controlled trial of Marboran on group vaccinated against smallpox. *The Lancet*, **1964**, *283* (7328), 330.
83. Bauer, D. J., Clinical experience with the antiviral drug Marboran® (1-methylisatin 3-thiosemicarbazone). *Annals of the New York Academy of Sciences*, **1965**, *130* (1), 110-117.
84. Bianchini, C., Methisazone (Marboran) in the prevention of smallpox and in the treatment of the complications of smallpox vaccination. *Archivio Italiano di Scienze Mediche Tropicali e di Parassitologia*, **1969**, *50* (1), 29-38.
85. Strassburg, M. A., The global eradication of smallpox. *American Journal of Infection Control*, **1982**, *10* (2), 53-59.
86. Neyts, J.; Clercq, E. D., Therapy and short-term prophylaxis of poxvirus infections: historical background and perspectives. *Antiviral Research*, **2003**, *57* (1-2), 25-33.
87. McFadden, G., Poxvirus tropism. *Nature Reviews Microbiology*, **2005**, *3* (3), 201-213.
88. Morand, A.; Delaigue, S.; Morand, J. J., Review of poxvirus: emergence of monkeypox. *Médecine et Santé Tropicales*, **2017**, *27* (1), 29-39.
89. Olson, V.; Shchelkunov, S., Are We Prepared in Case of a Possible Smallpox-Like Disease Emergence? *Viruses*, **2017**, *9* (9), 242.
90. Baeyer, A.; Lazarus, M. J., Ueber Condensations producte des Isatins. *Berichte der Deutschen Chemischen Gesellschaft*, **1885**, *18* (2), 2637-2643.
91. Hubacher, M. H.; Doernberg, S.; Horner, A., Laxatives: Chemical structure and potency of phthaleins and hydroxyanthraquinones. *Journal of the American Pharmaceutical Association*, **1953**, *42* (1), 23-30.
92. Food and Drug Administration, Public Health Service., U.S. Department of Health and Human Services, FDA Expands List of "Do Not Compound" Drug Products. *Journal of Pain & Palliative Care Pharmacotherapy*, **2017**, *31* (1), 76-78.
93. United Nations, Consolidated List of Products - Whose Consumption and/or Sale Have Been Banned, Withdrawn, Severely Restricted or Not Approved by Governments, Twelfth Issue - Pharmaceuticals. United Nations Ed., New York, USA, **2005**.

94. Kadin, S. B., EP 0156603 A3, 3-Substituted 2-oxindole-1-carboxamides as analgesic and anti-inflammatory agents. **1989**.
95. Wylie, G.; Appelboom, T.; Bolten, W.; Breedveld, F. C.; Feely, J.; Leeming, M. R.; Le Loët, X.; Manthorpe, R.; Marcolongo, R.; Smolen, J., A comparative study of tenidap, a cytokine-modulating anti-rheumatic drug, and diclofenac in rheumatoid arthritis: a 24-week analysis of a 1-year clinical trial. *British Journal of Rheumatology*, **1995**, *34* (6), 554-63.
96. Prupas, H. M.; Loose, L. D.; Spindler, J. S.; Dietz, A. J.; Gum, O. B.; Weisman, M. H.; Gordon, G.; Wolf, R. E.; Turner, R. A.; Collins, R. L.; Germain, B. F.; Katz, P.; Ballou, S. P.; Wolfe, F.; Daniels, J. C.; April, P. A.; Willkens, R. F.; Pariser, K.; Hepburn, B.; Zizic, T. M.; Ting, N.; Mehrban, M., Tenidap in Patients with Rheumatoid Arthritis. *Scandinavian Journal of Rheumatology*, **1996**, *25* (6), 345-351.
97. Kauffman, R. F.; Robertson, D. W.; Franklin, R. B.; Sandusky Jr., G. E.; Dies, F.; McNay, J. L.; Hayes, J. S., Indolidan: A Potent, Long-Acting Cardiotonic and Inhibitor of Type IV Cyclic AMP Phosphodiesterase. *Cardiovascular Drug Reviews*, **1990**, *8* (4), 303-322.
98. Corder, C. N.; Puls, A.; Wilson, M., Clinical effect of indolidan in congestive heart failure. *International Journal of Clinical Pharmacology, Therapy, and Toxicology*, **1992**, *30* (10), 405-409.
99. Voelker, W.; Mauser, M.; Preisack, M.; Karsch, K. R., Acute hemodynamic effects of adibendan, a new phosphodiesterase inhibitor, for severe congestive heart failure. *American Journal of Cardiology*, **1989**, *64* (5), 390-392.
100. Peters, P.; Saborowski, F.; May, E.; Schneider, M., Central hemodynamics of a new positive inotropic substance, adibendan. Data from a dose-finding study. *Arzneimittelforschung*, **1990**, *40* (6), 666-668.
101. Rauch, B.; Zimmermann, R.; Kapp, M.; Haass, M.; Von Molitor, S.; Neumann, F. J.; Kübler, W.; Dietz, R.; Tillmanns, H.; Smolarz, A., Hemodynamic and neuroendocrine response to acute administration of the phosphodiesterase inhibitor BM 14.478 in patients with congestive heart failure. *Clinical Cardiology*, **1991**, *14* (5), 386-396.
102. Von Der Leyen, H.; Mende, U.; Meyer, W.; Neumann, J.; Nose, M.; Schmitz, W.; Scholz, H.; Starbatty, J.; Stein, B.; Wenzlaff, H.; Döring, V.; Kalmir, P.; Haverich, A., Mechanism underlying the reduced positive inotropic effects of the phosphodiesterase III inhibitors pimobendan, adibendan and saterinone in failing as compared to nonfailing human cardiac muscle preparations. *Naunyn-Schmiedeberg's Archives of Pharmacology*, **1991**, *344* (1), 90-100.
103. Soupart, A.; Gross, P.; Legros, J.-J.; Alföldi, S.; Annane, D.; Heshmati, H. M.; Decaux, G., Successful Long-Term Treatment of Hyponatremia in Syndrome of Inappropriate Antidiuretic Hormone Secretion with Satavaptan (SR121463B), an Orally Active Nonpeptide Vasopressin V2-Receptor Antagonist. *Clinical Journal of the American Society of Nephrology*, **2006**, *1* (6), 1154-1160.

104. Ginès, P.; Wong, F.; Watson, H.; Milutinovic, S.; Ruiz Del Arbol, L.; Olteanu, D., Effects of satavaptan, a selective vasopressin V₂ receptor antagonist, on ascites and serum sodium in cirrhosis with hyponatremia: A randomized trial. *Hepatology*, **2008**, *48* (1), 204-213.
105. Wong, F.; Watson, H.; Gerbes, A.; Vilstrup, H.; Badalamenti, S.; Bernardi, M.; Ginès, P., Satavaptan for the management of ascites in cirrhosis: efficacy and safety across the spectrum of ascites severity. *Gut*, **2012**, *61* (1), 108-116.
106. European Medicines Agency (EMA), Withdrawal assessment report for Aquilda. In *Pre-authorisation Evaluation of Medicines for Human Use*, European Medicines Agency, London, UK, **2008**, Vol. EMEA/CHMP/316130/2008.
107. Mackay, K. B., BMS-204352 (Bristol Myers Squibb). *Current Opinion in Investigational Drugs*, **2001**, *2* (6), 820-823.
108. Jensen, B. S., BMS-204352: A Potassium Channel Opener Developed for the Treatment of Stroke. *CNS Drug Reviews*, **2006**, *8* (4), 353-360.
109. Minnerup, J.; Wersching, H.; Schilling, M.; Schäbitz, W. R., Analysis of early phase and subsequent phase III stroke studies of neuroprotectants: outcomes and predictors for success. *Experimental & Translational Stroke Medicine*, **2014**, *6* (1), 2.
110. Matheson, A. J.; Spencer, C. M., Ropinirole - A Review of its Use in the Management of Parkinson's Disease. *Drugs*, **2000**, *60* (1), 115-137.
111. Varga, L. I.; Ako-Agugua, N.; Colasante, J.; Hertweck, L.; Houser, T.; Smith, J.; Watty, A. A.; Nagar, S.; Raffa, R. B., Critical review of ropinirole and pramipexole - putative dopamine D₃-receptor selective agonists - for the treatment of RLS. *Journal of Clinical Pharmacy and Therapeutics*, **2009**, *34* (5), 493-505.
112. Okano, H.; Yasuda, D.; Fujimori, K.; Morimoto, S.; Takahashi, S., Ropinirole, a New ALS Drug Candidate Developed Using iPSCs. *Trends in Pharmacological Sciences*, **2020**, *41* (2), 99-109.
113. Greenberg, W. M.; Citrome, L., Ziprasidone for Schizophrenia and Bipolar Disorder: A Review of the Clinical Trials. *CNS Drug Reviews*, **2007**, *13* (2), 137-177.
114. Nemeroff, C. B.; Lieberman, J. A.; Weiden, P. J.; Harvey, P. D.; Newcomer, J. W.; Schatzberg, A. F.; Kilts, C. D.; Daniel, D. G., From clinical research to clinical practice: a 4-year review of ziprasidone. *CNS Spectrums*, **2005**, *10* (Suppl. 17), 1-20.
115. Montes, J. M., Use of ziprasidone in patients with schizophrenia in four European countries. *European Psychiatry*, **2011**, *26* (1, Supplement 1), 29-37.
116. Wang, S.; Sun, W.; Zhao, Y.; McEachern, D.; Meaux, I.; Barrière, C.; Stuckey, J. A.; Meagher, J. L.; Bai, L.; Liu, L.; Hoffman-Luca, C. G.; Lu, J.; Shangary, S.; Yu, S.; Bernard, D.; Aguilar, A.; Dos-Santos, O.; Besret, L.; Guerif, S.; Pannier, P.; Gorge-Bernat, D.; Debussche, L., SAR405838: An Optimized Inhibitor of MDM2-p53 Interaction That Induces Complete and Durable Tumor Regression. *Cancer Research*, **2014**, *74* (20), 5855-5865.
117. Bill, K. L. J.; Garnett, J.; Meaux, I.; Ma, X.; Creighton, C. J.; Bolshakov, S.; Barriere, C.; Debussche, L.; Lazar, A. J.; Prudner, B. C.; Casadei, L.; Braggio, D.; Lopez, G.; Zewdu, A.; Bid, H.; Lev, D.; Pollock, R. E., SAR405838: A Novel and Potent Inhibitor of the MDM2:p53

- Axis for the Treatment of Dedifferentiated Liposarcoma. *Clinical Cancer Research*, **2016**, *22* (5), 1150-1160.
118. De Weger, V. A.; De Jonge, M.; Langenberg, M. H. G.; Schellens, J. H. M.; Lolkema, M.; Varga, A.; Demers, B.; Thomas, K.; Hsu, K.; Tuffal, G.; Goodstal, S.; Macé, S.; Deutsch, E., A phase I study of the HDM2 antagonist SAR405838 combined with the MEK inhibitor pimasertib in patients with advanced solid tumours. *British Journal of Cancer*, **2019**, *120* (3), 286-293.
119. Prakash, C. R.; Theivendren, P.; Raja, S., Indolin-2-Ones in Clinical Trials as Potential Kinase Inhibitors: A Review. *Pharmacology & Pharmacy*, **2012**, *3* (1), 62-71.
120. Patyna, S.; Laird, A. D.; Mendel, D. B.; O'Farrell, A.-M.; Liang, C.; Guan, H.; Vojtkovsky, T.; Vasile, S.; Wang, X.; Chen, J.; Grazzini, M.; Yang, C. Y.; Haznedar, J. Ö.; Sukbuntherng, J.; Zhong, W.-Z.; Cherrington, J. M.; Hu-Lowe, D., SU14813: a novel multiple receptor tyrosine kinase inhibitor with potent antiangiogenic and antitumor activity. *Molecular Cancer Therapeutics*, **2006**, *5* (7), 1774-1782.
121. Fiedler, W.; Giaccone, G.; Lasch, P.; Van Der Horst, I.; Brega, N.; Courtney, R.; Abbattista, A.; Shalinsky, D. R.; Bokemeyer, C.; Boven, E., Phase I trial of SU14813 in patients with advanced solid malignancies. *Annals of Oncology*, **2011**, *22* (1), 195-201.
122. Pfizer Study Of The Efficacy And Safety Of SU-014813 In Patients With Metastatic Breast Cancer (NCT00322517). <https://clinicaltrials.gov/ct2/show/study/NCT00322517> (accessed 25/08/2021).
123. Hoff, P. M.; Wolff, R. A.; Bogaard, K.; Waldrum, S.; Abbruzzese, J. L., A Phase I Study of Escalating Doses of the Tyrosine Kinase Inhibitor Semaxanib (SU5416) in Combination with Irinotecan in Patients with Advanced Colorectal Carcinoma. *Japanese Journal of Clinical Oncology*, **2006**, *36* (2), 100-103.
124. Mita, M. M.; Rowinsky, E. K.; Forero, L.; Eckhart, S. G.; Izbicka, E.; Weiss, G. R.; Beeram, M.; Mita, A. C.; De Bono, J. S.; Tolcher, A. W.; Hammond, L. A.; Simmons, P.; Berg, K.; Takimoto, C.; Patnaik, A., A phase II, pharmacokinetic, and biologic study of semaxanib and thalidomide in patients with metastatic melanoma. *Cancer Chemotherapy and Pharmacology*, **2007**, *59* (2), 165-174.
125. Fabbro, D.; Manley, P. W., Su-6668. SUGEN. *Current Opinion in Investigational Drugs*, **2001**, *2* (8), 1142-1148.
126. Yorozyuya, K.; Kubota, T.; Watanabe, M.; Hasegawa, H.; Ozawa, S.; Kitajima, M.; Chikahisa, L. M.; Yamada, Y., TSU-68 (SU6668) inhibits local tumor growth and liver metastasis of human colon cancer xenografts via anti-angiogenesis. *Oncology Reports*, **2005**, *14* (3), 677-682.
127. Kudo, M.; Cheng, A.-L.; Park, J.-W.; Park, J. H.; Liang, P.-C.; Hidaka, H.; Izumi, N.; Heo, J.; Lee, Y. J.; Sheen, I. S.; Chiu, C.-F.; Arioka, H.; Morita, S.; Arai, Y., Orantinib versus placebo combined with transcatheter arterial chemoembolisation in patients with unresectable hepatocellular carcinoma (ORIENTAL): a randomised, double-blind, placebo-controlled, multicentre, phase 3 study. *The Lancet Gastroenterology & Hepatology*, **2018**, *3* (1), 37-46.

128. Hao, Z.; Sadek, I., Sunitinib: the antiangiogenic effects and beyond. *OncoTargets and Therapy*, **2016**, *9*, 5495-5505.
129. Christensen, J. G., A preclinical review of sunitinib, a multitargeted receptor tyrosine kinase inhibitor with anti-angiogenic and antitumour activities. *Annals of Oncology*, **2007**, *18* (Supplement 10), x3-x10.
130. Moran, M.; Nickens, D.; Adcock, K.; Bennetts, M.; Desscan, A.; Charnley, N.; Fife, K., Sunitinib for Metastatic Renal Cell Carcinoma: A Systematic Review and Meta-Analysis of Real-World and Clinical Trials Data. *Targeted Oncology*, **2019**, *14* (4), 405-416.
131. Chow, L. Q. M.; Eckhardt, S. G., Sunitinib: From Rational Design to Clinical Efficacy. *Journal of Clinical Oncology*, **2007**, *25* (7), 884-896.
132. Aqsa, A.; Droubi, S.; Amarnath, S.; Al-Moussawi, H.; Abergel, J., Sunitinib-Induced Acute Liver Failure. *Case Reports in Gastroenterology*, **2021**, *15* (1), 17-21.
133. Vallina, C.; Ramirez, L.; Torres, J.; Casanas, E.; Hernandez, G.; Lopez-Pintor, R., Osteonecrosis of the jaws produced by sunitinib: a systematic review. *Medicina Oral Patología Oral y Cirugía Bucal*, **2019**, e326-e338.
134. Caglevic, C.; Grassi, M.; Raez, L.; Listi, A.; Giallombardo, M.; Bustamante, E.; Gil-Bazo, I.; Rolfo, C., Nintedanib in non-small cell lung cancer: from preclinical to approval. *Therapeutic Advances in Respiratory Disease*, **2015**, *9* (4), 164-172.
135. Shiratori, T.; Tanaka, H.; Tabe, C.; Tsuchiya, J.; Ishioka, Y.; Itoga, M.; Taima, K.; Takashi, S.; Tasaka, S., Effect of nintedanib on non-small cell lung cancer in a patient with idiopathic pulmonary fibrosis: A case report and literature review. *Thoracic Cancer*, **2020**, *11* (6), 1720-1723.
136. Richeldi, L.; Du Bois, R. M.; Raghu, G.; Azuma, A.; Brown, K. K.; Costabel, U.; Cottin, V.; Flaherty, K. R.; Hansell, D. M.; Inoue, Y.; Kim, D. S.; Kolb, M.; Nicholson, A. G.; Noble, P. W.; Selman, M.; Taniguchi, H.; Brun, M.; Le Maulf, F.; Girard, M.; Stowasser, S.; Schlenker-Herceg, R.; Disse, B.; Collard, H. R., Efficacy and Safety of Nintedanib in Idiopathic Pulmonary Fibrosis. *New England Journal of Medicine*, **2014**, *370* (22), 2071-2082.
137. Wollin, L.; Wex, E.; Pautsch, A.; Schnapp, G.; Hostettler, K. E.; Stowasser, S.; Kolb, M., Mode of action of nintedanib in the treatment of idiopathic pulmonary fibrosis. *European Respiratory Journal*, **2015**, *45* (5), 1434-1445.
138. Ogata, H.; Nakagawa, T.; Sakoda, S.; Ishimatsu, A.; Taguchi, K.; Kadowaki, M.; Moriwaki, A.; Yoshida, M., Nintedanib treatment for pulmonary fibrosis after coronavirus disease 2019. *Respirology Case Reports*, **2021**, *9* (5), e00744
139. London, C. A.; Malpas, P. B.; Wood-Follis, S. L.; Boucher, J. F.; Rusk, A. W.; Rosenberg, M. P.; Henry, C. J.; Mitchener, K. L.; Klein, M. K.; Hintermeister, J. G.; Bergman, P. J.; Couto, G. C.; Mauldin, G. N.; Michels, G. M., Multi-center, Placebo-controlled, Double-blind, Randomized Study of Oral Toleranib Phosphate (SU11654), a Receptor Tyrosine Kinase Inhibitor, for the Treatment of Dogs with Recurrent (Either Local or Distant) Mast Cell Tumor Following Surgical Excision. *Clinical Cancer Research*, **2009**, *15* (11), 3856-3865.

140. Gustafson, T. L.; Biller, B., Use of Toceranib Phosphate in the Treatment of Canine Bladder Tumors: 37 Cases. *Journal of the American Animal Hospital Association*, **2019**, *55* (5), 243-248.
141. Pakravan, P.; Kashanian, S.; Khodaei, M. M.; Harding, F. J., Biochemical and pharmacological characterization of isatin and its derivatives: from structure to activity. *Pharmacological Reports*, **2013**, *65* (2), 313-335.
142. Zaryanova, E. V.; Lozinskaya, N. A.; Beznos, O. V.; Volkova, M. S.; Chesnokova, N. B.; Zefirov, N. S., Oxindole-based intraocular pressure reducing agents. *Bioorganic & Medicinal Chemistry Letters*, **2017**, *27* (16), 3787-3793.
143. Gupta, A. K.; Tulsyan, S.; Bharadwaj, M.; Mehrotra, R., Systematic Review on Cytotoxic and Anticancer Potential of N-Substituted Isatins as Novel Class of Compounds Useful in Multidrug-Resistant Cancer Therapy: *In Silico* and *In Vitro* Analysis. *Topics in Current Chemistry*, **2019**, *377* (3), 15.
144. Guo, H., Isatin derivatives and their anti-bacterial activities. *European Journal of Medicinal Chemistry*, **2019**, *164*, 678-688.
145. Nath, R.; Pathania, S.; Grover, G.; Akhtar, M. J., Isatin containing heterocycles for different biological activities: Analysis of structure activity relationship. *Journal of Molecular Structure*, **2020**, *1222*, 128900.
146. Dhokne, P.; Sakla, A. P.; Shankaraiah, N., Structural insights of oxindole based kinase inhibitors as anticancer agents: Recent advances. *European Journal of Medicinal Chemistry*, **2021**, *216*, 113334.
147. Ferraz de Paiva, R. E.; Vieira, E. G.; Rodrigues da Silva, D.; Wegermann, C. A.; Costa Ferreira, A. M., Anticancer Compounds Based on Isatin-Derivatives: Strategies to Ameliorate Selectivity and Efficiency. *Frontiers in Molecular Biosciences*, **2021**, *7* (511), 627272.
148. Nath, P.; Mukherjee, A.; Mukherjee, S.; Banerjee, S.; Das, S.; Banerjee, S., Isatin: A Scaffold with Immense Biodiversity. *Mini-Reviews in Medicinal Chemistry*, **2021**, *21* (9), 1096-1112.
149. Xia, M.; Ma, R.-Z., Recent Progress on Routes to Spirooxindole Systems Derived from Isatin. *Journal of Heterocyclic Chemistry*, **2014**, *51* (3), 539-554.
150. Siva, S. P.; Rachel, A. J.; Praveen, B.; Prabhu, P. M., Spirooxindoles as Potential Pharmacophores. *Mini-Reviews in Medicinal Chemistry*, **2017**, *17* (16), 1515-1536.
151. Zhou, L.-M.; Qu, R.-Y.; Yang, G.-F., An overview of spirooxindole as a promising scaffold for novel drug discovery. *Expert Opinion on Drug Discovery*, **2020**, *15* (5), 603-625.
152. Cheng, D.; Ishihara, Y.; Tan, B.; Barbas, C. F., Organocatalytic Asymmetric Assembly Reactions: Synthesis of Spirooxindoles via Organocascade Strategies. *ACS Catalysis*, **2014**, *4* (3), 743-762.
153. Mei, G.-J.; Shi, F., Catalytic asymmetric synthesis of spirooxindoles: recent developments. *Chemical Communications*, **2018**, *54* (50), 6607-6621.

154. Peddibhotla, S., 3-Substituted-3-hydroxy-2-oxindole, an Emerging New Scaffold for Drug Discovery with Potential Anti-Cancer and other Biological Activities. *Current Bioactive Compounds*, **2009**, 5 (1), 20-38.
155. Cao, Z.-Y.; Zhou, F.; Zhou, J., Development of Synthetic Methodologies via Catalytic Enantioselective Synthesis of 3,3-Disubstituted Oxindoles. *Accounts of Chemical Research*, **2018**, 51 (6), 1443-1454.
156. Ziarani, G. M.; Javadi, F.; Mohajer, F., The Molecular Diversity Scope of Oxindole Derivatives in Organic Synthesis. *Current Organic Chemistry*, **2021**, 25 (7), 779-818.
157. Brandão, P.; Burke, A. J., Recent advances in the asymmetric catalytic synthesis of chiral 3-hydroxy and 3-aminooxindoles and derivatives: Medicinally relevant compounds. *Tetrahedron*, **2018**, 74 (38), 4927-4957.
158. Kaur, M.; Singh, M.; Chadha, N.; Silakari, O., Oxindole: A chemical prism carrying plethora of therapeutic benefits. *European Journal of Medicinal Chemistry*, **2016**, 123, 858-894.
159. Khetmalis, Y. M.; Shivani, M.; Murugesan, S.; Chandra Sekhar, K. V. G., Oxindole and its derivatives: A review on recent progress in biological activities. *Biomedicine & Pharmacotherapy*, **2021**, 141, 111842.
160. Moffat, J. G.; Vincent, F.; Lee, J. A.; Eder, J.; Prunotto, M., Opportunities and challenges in phenotypic drug discovery: an industry perspective. *Nature Reviews Drug Discovery*, **2017**, 16 (8), 531-543.
161. Quancard, J.; Bach, A.; Cox, B.; Craft, R.; Finsinger, D.; Guéret, S. M.; Hartung, I. V.; Laufer, S.; Messinger, J.; Sbardella, G.; Koolman, H. F., The European Federation for Medicinal Chemistry and Chemical Biology (EFMC) Best Practice Initiative: Phenotypic Drug Discovery. *ChemMedChem*, **2021**, 16 (11), 1737-1740.
162. Bogdanov, A. V.; Mironov, V. F., Advances in the Synthesis of Isatins: A Survey of the Last Decade. *Synthesis*, **2018**, 50 (08), 1601-1609.
163. Kaur, M., Chapter 6 - Oxindole: A Nucleus Enriched With Multitargeting Potential Against Complex Disorders. In *Key Heterocycle Cores for Designing Multitargeting Molecules*, Silakari, O., Elsevier, **2018**, pp 211-246.
164. Curtius, T.; Thun, K., Einwirkung von Hydrazinhydrat auf Isatin und auf Phenole. *Journal für Praktische Chemie*, **1891**, 44 (1), 187-191.
165. Marschalk, C., Überführung des Oxindols in Isocumaranon. *Berichte der Deutschen Chemischen Gesellschaft*, **1912**, 45 (1), 582-585.
166. Baeyer, A., Synthese des Oxindols. *Berichte der Deutschen Chemischen Gesellschaft*, **1878**, 11 (1), 582-584.
167. Suida, W., Ueber das Isatin und seine Derivate. *Berichte der Deutschen Chemischen Gesellschaft*, **1878**, 11 (1), 584-587.
168. Brunner, K., Über Indolinone. *Monatshefte für Chemie*, **1897**, 18 (1), 95-122.
169. Stollé, R., Über Phenyl-oxindol. *Berichte der Deutschen Chemischen Gesellschaft*, **1914**, 47 (2), 2120-2122.

170. Gassman, P. G.; Van Bergen, T. J., General method for the synthesis of oxindoles. *Journal of the American Chemical Society*, **1973**, *95* (8), 2718-2719.
171. Wright, S. W.; McClure, L. D.; Hageman, D. L., A convenient modification of the Gassman oxindole synthesis. *Tetrahedron Letters*, **1996**, *37* (27), 4631-4634.
172. Neill, A. B., A New Synthesis of Oxindole. *Journal of the American Chemical Society*, **1953**, *75* (6), 1508-1508.
173. Wolfe, J. F.; Sleevi, M. C.; Goehring, R. R., Photoinduced cyclization of mono- and dianions of N-acyl-o-chloranilines. A general oxindole synthesis. *Journal of the American Chemical Society*, **1980**, *102* (10), 3646-3647.
174. Beckwith, A. L. J.; Storey, J. M. D., Tandem radical translocation and homolytic aromatic substitution: a convenient and efficient route to oxindoles. *Journal of the Chemical Society, Chemical Communications*, **1995**, *9*, 977.
175. Ziarani, G. M.; Gholamzadeh, P.; Lashgari, N.; Hajiabbasi, P., Oxindole as starting material in organic synthesis. *Arkivoc*, **2013**, *2013* (1), 470-535.
176. Moradi, R.; Ziarani, G. M.; Lashgari, N., Recent applications of isatin in the synthesis of organic compounds. *Arkivoc*, **2017**, *2017* (1), 148-201.
177. Varun, V.; Sonam, S.; Kakkar, R., Isatin and its derivatives: a survey of recent syntheses, reactions, and applications. *MedChemComm*, **2019**, *10* (3), 351-368.
178. Chauhan, G.; Pathak, D. P.; Ali, F.; Bhutani, R.; Kapoor, G.; Khasimbi, S., Advances on Synthesis, Derivatization and Bioactivity of Isatin: A Review. *Current Organic Synthesis*, **2020**.
179. Jahng, Y., Progress in the studies on tryptanthrin, an alkaloid of history. *Archives of Pharmacal Research*, **2013**, *36* (5), 517-535.
180. von Sommaruga, E., Ueber die Moleculargröße des Indigos. *Justus Liebig's Annalen der Chemie*, **1879**, *195* (3), 302-313.
181. Friedländer, P.; Roschdestwensky, N., Über ein Oxydationsprodukt des Indigblaus. *Berichte der Deutschen Chemischen Gesellschaft*, **1915**, *48* (2), 1841-1847.
182. Schindler, F.; Zähner, H., Stoffwechselprodukte von Mikroorganismen 91. Mitteilung * Tryptanthrin, ein von Tryptophan abzuleitendes Antibioticum aus *Candida lipolytica*. *Archiv für Mikrobiologie*, **1971**, *79* (3), 187-203.
183. Fedeli, W.; Mazza, F., Crystal structure of tryptanthrin (indolo[2,1-b]quinazoline-6,12-dione). *Journal of the Chemical Society, Perkin Transactions 2*, **1974**, (13), 1621.
184. Yu, H.; Li, T.-N.; Ran, Q.; Huang, Q.-W.; Wang, J., *Strobilanthes cusia* (Nees) Kuntze, a multifunctional traditional Chinese medicinal plant, and its herbal medicines: A comprehensive review. *Journal of Ethnopharmacology*, **2021**, *265*, 113325.
185. Honda, G.; Tabata, M., Isolation of antifungal principle tryptanthrin, from *Strobilanthes cusia* O. Kuntze. *Planta Medica*, **1979**, *36* (1), 85-90.
186. Honda, G.; Tabata, M.; Tsuda, M., The antimicrobial specificity of tryptanthrin. *Planta Medica*, **1979**, *37* (2), 172-4.

187. Honda, G.; Tosirisuk, V.; Tabata, M., Isolation of an Antidermatophytic, Tryptanthrin, from Indigo Plants, *Polygonum tinctorium* and *Isatis tinctoria*. *Planta Medica*, **1980**, *38* (03), 275-276.
188. Garcellano, R. C.; Moinuddin, S. G. A.; Young, R. P.; Zhou, M.; Bowden, M. E.; Renslow, R. S.; Yesiltepe, Y.; Thomas, D. G.; Colby, S. M.; Chouinard, C. D.; Nagy, G.; Attah, I. K.; Ibrahim, Y. M.; Ma, R.; Franzblau, S. G.; Lewis, N. G.; Aguinaldo, A. M.; Cort, J. R., Isolation of Tryptanthrin and Reassessment of Evidence for Its Isobaric Isostere Wrightiadione in Plants of the *Wrightia* Genus. *Journal of Natural Products*, **2019**, *82* (3), 440-448.
189. Oberthür, C.; Hamburger, M., Tryptanthrin Content in *Isatis tinctoria* Leaves - A Comparative Study of Selected Strains and Post-Harvest Treatments. *Planta Medica*, **2004**, *70* (07), 642-645.
190. Speranza, J.; Miceli, N.; Taviano, M. F.; Ragusa, S.; Kwiecień, I.; Szopa, A.; Ekiert, H., *Isatis tinctoria* L. (Woad): A Review of Its Botany, Ethnobotanical Uses, Phytochemistry, Biological Activities, and Biotechnological Studies. *Plants*, **2020**, *9* (3), 298.
191. Fiedler, E.; Fiedler, H. P.; Gerhard, A.; Keller-Schierlein, W.; König, W. A.; Zähler, H., Stoffwechselprodukte von Mikroorganismen. *Archiv für Mikrobiologie*, **1976**, *107* (3), 249-256.
192. Schrenk, D.; Riebinger, D.; Till, M.; Vetter, S.; Fiedler, H.-P., Tryptanthrins: A novel class of agonists of the aryl hydrocarbon receptor. *Biochemical Pharmacology*, **1997**, *54* (1), 165-171.
193. Ramkissoo, A.; Seepersaud, M.; Maxwell, A.; Jayaraman, J.; Ramsubhag, A., Isolation and Antibacterial Activity of Indole Alkaloids from *Pseudomonas aeruginosa* UWI-1. *Molecules*, **2020**, *25* (16), 3744.
194. Pedras, M. S. C.; Abdoli, A.; To, Q. H.; Thapa, C., Ecological Roles of Tryptanthrin, Indirubin and N-Formylanthranilic Acid in *Isatis indigotica*: Phytoalexins or Phytoanticipins? *Chemistry & Biodiversity*, **2019**, *16* (3), e1800579.
195. Wagner-Döbler, I.; Rheims, H.; Felske, A.; El-Ghezal, A.; Flade-Schröder, D.; Laatsch, H.; Lang, S.; Pukall, R.; Tindall, B. J., *Oceanibulbus indolifex* gen. nov., sp. nov., a North Sea alphaproteobacterium that produces bioactive metabolites. *International Journal of Systematic and Evolutionary Microbiology*, **2004**, *54* (4), 1177-1184.
196. Shaaban, M.; Maskey, R. P.; Wagner-Döbler, I.; Laatsch, H., Pharacine, a Natural p-Cyclophane and Other Indole Derivatives from *Cytophaga* sp. Strain AM13.1. *Journal of Natural Products*, **2002**, *65* (11), 1660-1663.
197. Hosoe, T.; Nozawa, K.; Kawahara, N.; Fukushima, K.; Nishimura, K.; Miyaji, M.; Kawai, K.-I., Isolation of a new potent cytotoxic pigment along with indigotin from the pathogenic basidiomycetous fungus *Schizophyllum commune*. *Mycopathologia*, **1999**, *146* (1), 9-12.
198. Jarrah, M. Y.; Thaller, V., 300 MHz ¹H NMR spectra of indolo[2,1-b]quinazoline-6,12-dione, tryptanthrine, and its 2- and 8-chloro-derivatives. *Journal of Chemical Research - Synopses*, **1980**, *186*, 2601.

199. Rasmussen, L. E. L.; Lee, T. D.; Daves, G. D.; Schmidt, M. J., Female-to-male sex pheromones of low volatility in the Asian elephant, *Elephas maximus*. *Journal of Chemical Ecology*, **1993**, *19* (10), 2115-2128.
200. Caspers, B.; Franke, S.; Voigt, C. C., The Wing-Sac Odour of Male Greater Sac-Winged Bats *Saccopteryx bilineata* (Emballonuridae) as a Composite Trait: Seasonal and Individual Differences. In *Chemical Signals in Vertebrates 11*, Hurst, J. L.; Beynon, R. J.; Roberts, S. C.; Wyatt, T. D., Springer, New York, USA, **2008**, pp 151-160.
201. Tripathi, A.; Wadia, N.; Bindal, D.; Jana, T., Docking studies on novel alkaloid tryptanthrin and its analogues against enoyl-acyl carrier protein reductase (InhA) of *Mycobacterium tuberculosis*. *Indian Journal of Biochemistry & Biophysics*, **2012**, *49* (6), 435-441.
202. Costa, D. C. M.; Azevedo, M. M. B. d.; Silva, D. O. e.; Romanos, M. T. V.; Souto-Padrón, T. C. B. S.; Alviano, C. S.; Alviano, D. S., *In vitro* anti-MRSA activity of *Couroupita guianensis* extract and its component Tryptanthrin. *Natural Product Research*, **2017**, *31* (17), 2077-2080.
203. Kataoka, M.; Hirata, K.; Kunikata, T.; Ushio, S.; Iwaki, K.; Ohashi, K.; Ikeda, M.; Kurimoto, M., Antibacterial action of tryptanthrin and kaempferol, isolated from the indigo plant (*Polygonum tinctorium* Lour.), against *Helicobacter pylori*-infected Mongolian gerbils. *Journal of Gastroenterology*, **2001**, *36* (1), 5-9.
204. Xu, L.; Jiang, W.; Jia, H.; Zheng, L.; Xing, J.; Liu, A.; Du, G., Discovery of Multitarget-Directed Ligands Against Influenza A Virus From Compound Yizhihao Through a Predictive System for Compound-Protein Interactions. *Frontiers in Cellular and Infection Microbiology*, **2020**, *10* (16).
205. Tsai, Y.-C.; Lee, C.-L.; Yen, H.-R.; Chang, Y.-S.; Lin, Y.-P.; Huang, S.-H.; Lin, C.-W., Antiviral Action of Tryptanthrin Isolated from *Strobilanthes cusia* Leaf against Human Coronavirus NL63. *Biomolecules*, **2020**, *10* (3), 366.
206. Mani, J. S.; Johnson, J. B.; Steel, J. C.; Broszczak, D. A.; Neilsen, P. M.; Walsh, K. B.; Naiker, M., Natural product-derived phytochemicals as potential agents against coronaviruses: A review. *Virus Research*, **2020**, *284*, 197989.
207. Hesse-Macabata, J.; Morgner, B.; Elsner, P.; Hipler, U.-C.; Wiegand, C., Tryptanthrin promotes keratinocyte and fibroblast responses *in vitro* after infection with *Trichophyton benhamiae* DSM6916. *Scientific Reports*, **2020**, *10* (1).
208. Danz, H.; Stoyanova, S.; Wippich, P.; Brattström, A.; Hamburger, M., Identification and Isolation of the Cyclooxygenase-2 Inhibitory Principle in *Isatis tinctoria*. *Planta Medica*, **2001**, *67* (05), 411-416.
209. Danz, H.; Stoyanova, S.; Thomet, O. A. R.; Simon, H.-U.; Dannhardt, G.; Ulbrich, H.; Hamburger, M., Inhibitory Activity of Tryptanthrin on Prostaglandin and Leukotriene Synthesis. *Planta Medica*, **2002**, *68* (10), 875-880.
210. Wang, Z.; Wu, X.; Wang, C.-L.; Wang, L.; Sun, C.; Zhang, D.-B.; Liu, J.-L.; Liang, Y.-N.; Tang, D.-X.; Tang, Z.-S., Tryptanthrin Protects Mice against Dextran Sulfate Sodium-

- Induced Colitis through Inhibition of TNF- α /NF- κ B and IL-6/STAT3 Pathways. *Molecules*, **2018**, 23 (5), 1062.
211. Agafonova, I. G.; Moskovkina, T. V., Studies on Anti-Inflammatory Action of Tryptanthrin, Using a Model of DSS-Induced Colitis of Mice and Magnetic Resonance Imaging. *Applied Magnetic Resonance*, **2015**, 46 (7), 781-791.
212. Pergola, C.; Jazzar, B.; Rossi, A.; Northoff, H.; Hamburger, M.; Sautebin, L.; Werz, O., On the inhibition of 5-lipoxygenase product formation by tryptanthrin: mechanistic studies and efficacy *in vivo*. *British Journal of Pharmacology*, **2012**, 165 (3), 765-776.
213. Kwon, Y.-W.; Cheon, S. Y.; Park, S. Y.; Song, J.; Lee, J.-H., Tryptanthrin Suppresses the Activation of the LPS-Treated BV2 Microglial Cell Line via Nrf2/HO-1 Antioxidant Signaling. *Frontiers in Cellular Neuroscience*, **2017**, 11, 18.
214. Jung, E. H.; Jung, J. Y.; Ko, H. L.; Kim, J. K.; Park, S. M.; Jung, D. H.; Park, C. A.; Kim, Y. W.; Ku, S. K.; Cho, I. J.; Kim, S. C., Tryptanthrin prevents oxidative stress-mediated apoptosis through AMP-activated protein kinase-dependent p38 mitogen-activated protein kinase activation. *Archives of Pharmacal Research*, **2017**, 40 (9), 1071-1086.
215. Lee, S.; Kim, D.-C.; Baek, H. Y.; Lee, K.-D.; Kim, Y.-C.; Oh, H., Anti-neuroinflammatory effects of tryptanthrin from *Polygonum tinctorium* Lour. in lipopolysaccharide-stimulated BV2 microglial cells. *Archives of Pharmacal Research*, **2018**, 41 (4), 419-430.
216. Kawaguchi, S.; Sakuraba, H.; Kikuchi, H.; Numao, N.; Asari, T.; Hiraga, H.; Ding, J.; Matsumiya, T.; Seya, K.; Fukuda, S.; Imaizumi, T., Tryptanthrin suppresses double-stranded RNA-induced CXCL10 expression via inhibiting the phosphorylation of STAT1 in human umbilical vein endothelial cells. *Molecular Immunology*, **2021**, 129, 32-38.
217. Han, N.-R.; Moon, P.-D.; Kim, H.-M.; Jeong, H.-J., Tryptanthrin ameliorates atopic dermatitis through down-regulation of TSLP. *Archives of Biochemistry and Biophysics*, **2014**, 542, 14-20.
218. Han, N.-R.; Kim, H.-M.; Jeong, H.-J., Tryptanthrin reduces mast cell proliferation promoted by TSLP through modulation of MDM2 and p53. *Biomedicine & Pharmacotherapy*, **2016**, 79, 71-77.
219. Cheng, H.-M.; Kuo, Y.-Z.; Chang, C.-Y.; Chang, C.-H.; Fang, W.-Y.; Chang, C.-N.; Pan, S.-C.; Lin, J.-Y.; Wu, L.-W., The anti-TH17 polarization effect of *Indigo naturalis* and tryptanthrin by differentially inhibiting cytokine expression. *Journal of Ethnopharmacology*, **2020**, 255, 112760.
220. Chang, H.-N.; Yeh, Y.-C.; Chueh, H.-Y.; Pang, J.-H. S., The anti-angiogenic effect of tryptanthrin is mediated by the inhibition of apelin promoter activity and shortened mRNA half-life in human vascular endothelial cells. *Phytomedicine*, **2019**, 58, 152879.
221. Iwaki, K.; Ohashi, E.; Arai, N.; Kohno, K.; Ushio, S.; Taniguchi, M.; Fukuda, S., Tryptanthrin inhibits Th2 development, and IgE-mediated degranulation and IL-4 production by rat basophilic leukemia RBL-2H3 cells. *Journal of Ethnopharmacology*, **2011**, 134 (2), 450-459.

222. Miao, S.; Shi, X.; Zhang, H.; Wang, S.; Sun, J.; Hua, W.; Miao, Q.; Zhao, Y.; Zhang, C., Proliferation-Attenuating and Apoptosis-Inducing Effects of Tryptanthrin on Human Chronic Myeloid Leukemia K562 Cell Line *in Vitro*. *International Journal of Molecular Sciences*, **2011**, *12* (6), 3831-3845.
223. Zeng, Q.; Luo, C.; Cho, J.; Lai, D.; Shen, X.; Zhang, X.; Zhou, W., Tryptanthrin exerts anti-breast cancer effects both in vitro and in vivo through modulating the inflammatory tumor microenvironment. *Acta Pharmaceutica*, **2021**, *71* (2), 245-266.
224. Shankar G, M.; Alex, V. V.; Nisthul A, A.; Bava, S. V.; Sundaram, S.; Retnakumari, A. P.; Chittalakkottu, S.; Anto, R. J., Pre-clinical evidences for the efficacy of tryptanthrin as a potent suppressor of skin cancer. *Cell Proliferation*, **2020**, *53* (1), e12710.
225. Liao, X.; Leung, K. N., Tryptanthrin induces growth inhibition and neuronal differentiation in the human neuroblastoma LA-N-1 cells. *Chemico-Biological Interactions*, **2013**, *203* (2), 512-521.
226. Liao, X.; Zhou, X.; Mak, N.-K.; Leung, K.-N., Tryptanthrin Inhibits Angiogenesis by Targeting the VEGFR2-Mediated ERK1/2 Signalling Pathway. *PLoS ONE*, **2013**, *8* (12), e82294.
227. Feng, X.; Liao, D.; Liu, D.; Ping, A.; Li, Z.; Bian, J., Development of Indoleamine 2,3-Dioxygenase 1 Inhibitors for Cancer Therapy and Beyond: A Recent Perspective. *Journal of Medicinal Chemistry*, **2020**, *63* (24), 15115-15139.
228. Jähne, E. A.; Eigenmann, D. E.; Sampath, C.; Butterweck, V.; Culot, M.; Cecchelli, R.; Gosselet, F.; Walter, F. R.; Deli, M. A.; Smieško, M.; Hamburger, M.; Oufir, M., Pharmacokinetics and *In Vitro* Blood-Brain Barrier Screening of the Plant-Derived Alkaloid Tryptanthrin. *Planta Medica*, **2016**, *82* (11/12), 1021-1029.
229. Zhang, X.; Xia, J.; Zhang, W.; Luo, Y.; Sun, W.; Zhou, W., Study on pharmacokinetics and tissue distribution of single dose oral tryptanthrin in Kunming mice by validated reversed-phase high-performance liquid chromatography with ultraviolet detection. *Integrative Medicine Research*, **2017**, *6* (3), 269-279.
230. Popov, A.; Klimovich, A.; Styshova, O.; Moskovkina, T.; Shchekotikhin, A.; Grammatikova, N.; Dezhenkova, L.; Kaluzhny, D.; Deriabin, P.; Gerasimenko, A.; Udovenko, A.; Stonik, V., Design, synthesis and biomedical evaluation of mostotrin, a new water soluble tryptanthrin derivative. *International Journal of Molecular Medicine*, **2020**.
231. Matveevskaya, V. V.; Pavlov, D. I.; Sukhikh, T. S.; Gushchin, A. L.; Ivanov, A. Y.; Tennikova, T. B.; Sharoyko, V. V.; Baykov, S. V.; Benassi, E.; Potapov, A. S., Arene-Ruthenium(II) Complexes Containing 11*H*-Indeno[1,2-*b*]quinoxalin-11-one Derivatives and Tryptanthrin-6-oxime: Synthesis, Characterization, Cytotoxicity, and Catalytic Transfer Hydrogenation of Aryl Ketones. *ACS Omega*, **2020**, *5* (19), 11167-11179.
232. Pathania, A. S.; Kumar, S.; Guru, S. K.; Bhushan, S.; Sharma, P. R.; Aithagani, S. K.; Singh, P. P.; Vishwakarma, R. A.; Kumar, A.; Malik, F., The Synthetic Tryptanthrin Analogue Suppresses STAT3 Signaling and Induces Caspase Dependent Apoptosis via ERK Up Regulation in Human Leukemia HL-60 Cells. *PLoS ONE*, **2014**, *9* (11), e110411.

233. Liang, J. L.; Park, S.-E.; Kwon, Y.; Jahng, Y., Synthesis of benzo-annulated tryptanthrins and their biological properties. *Bioorganic & Medicinal Chemistry*, **2012**, *20* (16), 4962-4967.
234. Jun, K.-Y.; Park, S.-E.; Liang, J. L.; Jahng, Y.; Kwon, Y., Benzo[*b*]tryptanthrin Inhibits MDR1, Topoisomerase Activity, and Reverses Adriamycin Resistance in Breast Cancer Cells. *ChemMedChem*, **2015**, *10* (5), 827-835.
235. Catanzaro, E.; Betari, N.; Arencibia, J. M.; Montanari, S.; Sissi, C.; De Simone, A.; Vassura, I.; Santini, A.; Andrisano, V.; Tumiatti, V.; De Vivo, M.; Krysko, D. V.; Rocchi, M. B. L.; Fimognari, C.; Milelli, A., Targeting topoisomerase II with tryptanthrin derivatives: Discovery of 7-((2-(dimethylamino)ethyl)amino)indolo[2,1-*b*]quinazoline-6,12-dione as an antiproliferative agent and to treat cancer. *European Journal of Medicinal Chemistry*, **2020**, *202*, 112504.
236. Yang, S.; Li, X.; Hu, F.; Li, Y.; Yang, Y.; Yan, J.; Kuang, C.; Yang, Q., Discovery of Tryptanthrin Derivatives as Potent Inhibitors of Indoleamine 2,3-Dioxygenase with Therapeutic Activity in Lewis Lung Cancer (LLC) Tumor-Bearing Mice. *Journal of Medicinal Chemistry*, **2013**, *56* (21), 8321-8331.
237. Zhang, S.; Qi, F.; Fang, X.; Yang, D.; Hu, H.; Huang, Q.; Kuang, C.; Yang, Q., Tryptophan 2,3-dioxygenase inhibitory activities of tryptanthrin derivatives. *European Journal of Medicinal Chemistry*, **2018**, *160*, 133-145.
238. Yang, D.; Zhang, S.; Fang, X.; Guo, L.; Hu, N.; Guo, Z.; Li, X.; Yang, S.; He, J. C.; Kuang, C.; Yang, Q., *N*-Benzyl/Aryl Substituted Tryptanthrin as Dual Inhibitors of Indoleamine 2,3-Dioxygenase and Tryptophan 2,3-Dioxygenase. *Journal of Medicinal Chemistry*, **2019**, *62* (20), 9161-9174.
239. Li, Y.; Zhang, S.; Wang, R.; Cui, M.; Liu, W.; Yang, Q.; Kuang, C., Synthesis of novel tryptanthrin derivatives as dual inhibitors of indoleamine 2,3-dioxygenase 1 and tryptophan 2,3-dioxygenase. *Bioorganic & Medicinal Chemistry Letters*, **2020**, *30* (11), 127159.
240. Hwang, J. M.; Oh, T.; Kaneko, T.; Upton, A. M.; Franzblau, S. G.; Ma, Z.; Cho, S. N.; Kim, P., Design, synthesis, and structure-activity relationship studies of tryptanthrins as antitubercular agents. *Journal of Natural Products*, **2013**, *76* (3), 354-67.
241. Deryabin, P. I.; Moskovkina, T. V.; Shevchenko, L. S.; Kalinovskii, A. I., Synthesis and antimicrobial activity of tryptanthrin adducts with ketones. *Russian Journal of Organic Chemistry*, **2017**, *53* (3), 418-422.
242. Zheng, X.; Hou, B.; Wang, R.; Wang, Y.; Wang, C.; Chen, H.; Liu, L.; Wang, J.; Ma, X.; Liu, J., Synthesis of substituted tryptanthrin via aryl halides and amines as antitumor and anti-MRSA agents. *Tetrahedron*, **2019**, *75* (48), 130351.
243. Krivogorsky, B.; Nelson, A. C.; Douglas, K. A.; Grundt, P., Tryptanthrin derivatives as *Toxoplasma gondii* inhibitors—structure–activity-relationship of the 6-position. *Bioorganic & Medicinal Chemistry Letters*, **2013**, *23* (4), 1032-1035.
244. Onambele, L. A.; Riepl, H.; Fischer, R.; Pradel, G.; Prokop, A.; Aminake, M. N., Synthesis and evaluation of the antiplasmodial activity of tryptanthrin derivatives. *International Journal of Parasitology: Drugs and Drug Resistance*, **2015**, *5* (2), 48-57.

245. Olson, J. A.; Terryn, R. J.; Stewart, E. L.; Baum, J. C.; Novak, M. J., New insight into the action of tryptanthrins against *Plasmodium falciparum*: Pharmacophore identification via a novel submolecular QSAR descriptor. *Journal of Molecular Graphics and Modelling*, **2018**, *80*, 138-146.
246. Schepetkin, I. A.; Khlebnikov, A. I.; Potapov, A. S.; Kovrizhina, A. R.; Matveevskaya, V. V.; Belyanin, M. L.; Atochin, D. N.; Zanoza, S. O.; Gaidarzhy, N. M.; Lyakhov, S. A.; Kirpotina, L. N.; Quinn, M. T., Synthesis, biological evaluation, and molecular modeling of 11*H*-indeno[1,2-*b*]quinoxalin-11-one derivatives and tryptanthrin-6-oxime as c-Jun *N*-terminal kinase inhibitors. *European Journal of Medicinal Chemistry*, **2019**, *161*, 179-191.
247. Kirpotina, L. N.; Schepetkin, I. A.; Hammaker, D.; Kuhs, A.; Khlebnikov, A. I.; Quinn, M. T., Therapeutic Effects of Tryptanthrin and Tryptanthrin-6-Oxime in Models of Rheumatoid Arthritis. *Frontiers in Pharmacology*, **2020**, *11* (1145).
248. Hao, Y.; Guo, J.; Wang, Z.; Liu, Y.; Li, Y.; Ma, D.; Wang, Q., Discovery of Tryptanthrins as Novel Antiviral and Anti-Phytopathogenic-Fungus Agents. *Journal of Agricultural and Food Chemistry*, **2020**, *68* (20), 5586-5595.
249. Pinheiro, D.; Brandão, P.; Seixas de Melo, J. S.; Pineiro, M., Triptantrina: da Natureza ao Laboratório. *Química*, **2021**, *45* (162), 195-200.
250. Tucker, A. M.; Grundt, P., The chemistry of tryptanthrin and its derivatives. *Arkivoc*, **2012**, *2012* (1), 546-569.
251. Kaur, R.; Manjal, S. K.; Rawal, R. K.; Kumar, K., Recent synthetic and medicinal perspectives of tryptanthrin. *Bioorganic & Medicinal Chemistry*, **2017**, *25* (17), 4533-4552.
252. Jao, C.-W.; Lin, W.-C.; Wu, Y.-T.; Wu, P.-L., Isolation, Structure Elucidation, and Synthesis of Cytotoxic Tryptanthrin Analogues from *Phaius mishmensis*. *Journal of Natural Products*, **2008**, *71* (7), 1275-1279.
253. Utkina, N. K.; Denisenko, V. A., Ophiuroidine, the first indolo[2,1-*b*]quinazoline alkaloid from the Caribbean brittle star *Ophiocoma riisei*. *Tetrahedron Letters*, **2007**, *48* (25), 4445-4447.
254. Destoumieux-Garzón, D.; Mavingui, P.; Boetsch, G.; Boissier, J.; Darriet, F.; Duboz, P.; Fritsch, C.; Giraudoux, P.; Le Roux, F.; Morand, S.; Paillard, C.; Pontier, D.; Sueur, C.; Voituron, Y., The One Health Concept: 10 Years Old and a Long Road Ahead. *Frontiers in Veterinary Sciences*, **2018**, *5*, 14.
255. Mackenzie, J. S.; Jeggo, M., The One Health Approach—Why Is It So Important? *Tropical Medicine and Infectious Disease*, **2019**, *4* (2), 88.
256. European Environment Agency (EEA), EEA Glossary: Green Chemistry, available in <https://www.eea.europa.eu/help/glossary/eea-glossary/green-chemistry> (accessed 09/09/2021).
257. United States Environmental Protection Agency (USEPA), Definition of green chemistry, available in <https://www.epa.gov/greenchemistry/basics-green-chemistry#definition> (accessed 09/09/2021).

258. Anastas, P. T.; Warner, J. C., *Green chemistry : theory and practice*. Oxford University Press, New York, USA, **1998**.
259. Anastas, P. T.; Lankey, R. L., Life cycle assessment and green chemistry: the yin and yang of industrial ecology. *Green Chemistry*, **2000**, 2 (6), 289-295.
260. Tundo, P.; Anastas, P.; Black, D.; Breen, J.; Collins, T.; Memoli, S.; Miyamoto, J.; Polyakoff, M.; Tumas, W., Synthetic pathways and processes in green chemistry. Introductory overview. *Pure and Applied Chemistry*, **2000**, 72, 1207-1228.
261. International Union of Pure and Applied Chemistry (IUPAC), Sustainable Chemistry, available in <https://iupac.org/who-we-are/committees/sustainable-chemistry/> (accessed 09/09/2021).
262. Hogue, C., Definition of “sustainable chemistry” unclear, report from U.S. Congress says. *Chemical & Engineering News*, **2018**, 96 (12), 14.
263. Hogue, C. Differentiating between green chemistry and sustainable chemistry in Congress, available in <https://cen.acs.org/environment/green-chemistry/Differentiating-between-green-chemistry-sustainable/97/web/2019/07> (accessed 09/09/2021).
264. United States House of Representatives Committee on Science, Space, & Technology: Subcommittee on Research and Technology, Benign by design: innovations in sustainable chemistry, available in <https://science.house.gov/hearings/benign-by-design-innovations-in-sustainable-chemistry> (accessed 09/09/2021).
265. Organisation for Economic Co-operation and Development (OECD), Sustainable Chemistry, available in <https://www.oecd.org/chemicalsafety/risk-management/sustainablechemistry.htm> (accessed 09/09/2021).
266. Anastas, P. T.; Zimmerman, J. B., The United Nations sustainability goals: How can sustainable chemistry contribute? *Current Opinion in Green and Sustainable Chemistry*, **2018**, 13, 150-153.
267. Halpaap, A., *Green and Sustainable Chemistry: Framework Manual*. United Nations, **2020**, United Nations Environment Programme Ed.
268. United Nations Environment Programme, Green and Sustainable Chemistry, available in <https://www.unep.org/explore-topics/chemicals-waste/what-we-do/policy-and-governance/green-and-sustainable-chemistry> (accessed 09/09/2021).
269. Poliakoff, M.; Licence, P.; George, M. W., UN sustainable development goals: How can sustainable/green chemistry contribute? By doing things differently. *Current Opinion in Green and Sustainable Chemistry*, **2018**, 13, 146-149.
270. Chen, T.-L.; Kim, H.; Pan, S.-Y.; Tseng, P.-C.; Lin, Y.-P.; Chiang, P.-C., Implementation of green chemistry principles in circular economy system towards sustainable development goals: Challenges and perspectives. *Science of The Total Environment*, **2020**, 716, 136998.
271. Erythropel, H. C.; Zimmerman, J. B.; De Winter, T. M.; Petitjean, L.; Melnikov, F.; Lam, C. H.; Lounsbury, A. W.; Mellor, K. E.; Janković, N. Z.; Tu, Q.; Pincus, L. N.; Falinski, M. M.; Shi, W.; Coish, P.; Plata, D. L.; Anastas, P. T., The Green ChemistTREE: 20 years after taking root with the 12 principles. *Green Chemistry*, **2018**, 20 (9), 1929-1961.

272. Anastas, P. T.; Zimmerman, J. B., The periodic table of the elements of green and sustainable chemistry. *Green Chemistry*, **2019**, 21 (24), 6545-6566.
273. Dicks, A. P.; Hent, A., Green Chemistry and Associated Metrics. In *Green Chemistry Metrics - A guide to determining and evaluating process greenness*, Springer, London, UK, **2015**, pp 1-15.
274. Anastas, P.; Eghbali, N., Green Chemistry: Principles and Practice. *Chemical Society Reviews*, **2010**, 39 (1), 301-312.
275. Sheldon, R. A., Fundamentals of green chemistry: efficiency in reaction design. *Chemical Society Reviews*, **2012**, 41 (4), 1437-1451.
276. Sheldon, R. A., Organic synthesis-past, present and future. *Chemistry and Industry*, **1992**, (23), 903-906.
277. Dicks, A. P.; Hent, A., The E Factor and Process Mass Intensity. In *Green Chemistry Metrics: A Guide to Determining and Evaluating Process Greenness*, Springer, Toronto, ON, Canada, **2015**, pp 45-67.
278. Sheldon, R. A., The E Factor: fifteen years on. *Green Chemistry*, **2007**, 9 (12), 1273-1283.
279. Trost, B. M., The Atom Economy - A Search for Synthetic Efficiency. *Science*, **1991**, 254 (5037), 1471-1477.
280. Dicks, A. P.; Hent, A., Atom Economy and Reaction Mass Efficiency. In *Green Chemistry Metrics: A Guide to Determining and Evaluating Process Greenness*, Springer, Toronto, ON, Canada, **2015**, pp 17-44.
281. Constable, D. J. C.; Curzons, A. D.; Cunningham, V. L., Metrics to 'green' chemistry— which are the best? *Green Chemistry*, **2002**, 4 (6), 521-527.
282. Van Aken, K.; Streckowski, L.; Patiny, L., EcoScale, a semi-quantitative tool to select an organic preparation based on economical and ecological parameters. *Beilstein Journal of Organic Chemistry*, **2006**, 2, 3.
283. Dach, R.; Song, J. J.; Roschangar, F.; Samstag, W.; Senanayake, C. H., The Eight Criteria Defining a Good Chemical Manufacturing Process. *Organic Process Research & Development*, **2012**, 16 (11), 1697-1706.
284. Dicks, A. P.; Hent, A., Selected Qualitative Green Metrics. In *Green Chemistry Metrics: A Guide to Determining and Evaluating Process Greenness*, Springer, Toronto, ON, Canada, **2015**; pp 69-79.
285. Sheldon, R. A., Metrics of Green Chemistry and Sustainability: Past, Present, and Future. *ACS Sustainable Chemistry & Engineering*, **2018**, 6 (1), 32-48.
286. Maertens, A.; Plugge, H., Better Metrics for "Sustainable by Design": Toward an *in Silico* Green Toxicology for Green(er) Chemistry. *ACS Sustainable Chemistry & Engineering*, **2018**, 6 (2), 1999-2003.
287. Li, J.; Albrecht, J.; Borovika, A.; Eastgate, M. D., Evolving Green Chemistry Metrics into Predictive Tools for Decision Making and Benchmarking Analytics. *ACS Sustainable Chemistry & Engineering*, **2018**, 6 (1), 1121-1132.

288. Zimmerman, J. B.; Anastas, P. T.; Erythropel, H. C.; Leitner, W., Designing for a green chemistry future. *Science*, **2020**, 367 (6476), 397-400.
289. Marion, P.; Bernela, B.; Piccirilli, A.; Estrine, B.; Patouillard, N.; Guilbot, J.; Jérôme, F., Sustainable chemistry: how to produce better and more from less? *Green Chemistry*, **2017**, 19 (21), 4973-4989.
290. Moors, E. H. M.; Cohen, A. F.; Schellekens, H., Towards a sustainable system of drug development. *Drug Discovery Today*, **2014**, 19 (11), 1711-1720.
291. Constable, D. J. C.; Dunn, P. J.; Hayler, J. D.; Humphrey, G. R.; Leazer, J. J. L.; Linderman, R. J.; Lorenz, K.; Manley, J.; Pearlman, B. A.; Wells, A.; Zaks, A.; Zhang, T. Y., Key green chemistry research areas—a perspective from pharmaceutical manufacturers. *Green Chemistry*, **2007**, 9 (5), 411-420.
292. American Chemical Society (ACS), ACS Green Chemistry Institute Pharmaceutical Roundtable, available in <https://www.acsgcipr.org/> (accessed 24/09/2021).
293. Hughes, V., Europe pledges billions to solve its drug development woes. *Nature Medicine*, **2008**, 14 (2), 107-107.
294. Goldman, M., The Innovative Medicines Initiative: A European Response to the Innovation Challenge. *Clinical Pharmacology & Therapeutics*, **2012**, 91 (3), 418-425.
295. Innovative Medicines Initiative (IMI), IMI - Europe's partnership for health, available in <https://www.imi.europa.eu/> (accessed 24/09/2021).
296. Prat, D.; Wells, A.; Hayler, J.; Sneddon, H.; McElroy, C. R.; Abou-Shehada, S.; Dunn, P. J., CHEM21 selection guide of classical- and less classical-solvents. *Green Chemistry*, **2016**, 18 (1), 288-296.
297. Isoni, V.; Wong, L. L.; Khoo, H. H.; Halim, I.; Sharratt, P., Q-SAVESS: a methodology to help solvent selection for pharmaceutical manufacture at the early process development stage. *Green Chemistry*, **2016**, 18 (24), 6564-6572.
298. Jordan, A.; Stoy, P.; Sneddon, H. F., Chlorinated Solvents: Their Advantages, Disadvantages, and Alternatives in Organic and Medicinal Chemistry. *Chemical Reviews*, **2021**, 121 (3), 1582-1622.
299. Sheldon, R. A., Engineering a more sustainable world through catalysis and green chemistry. *Journal of The Royal Society Interface*, **2016**, 13 (116), 20160087.
300. Beletskaya, I. P.; Kustov, L. M., Catalysis as an important tool of green chemistry. *Russian Chemical Reviews*, **2010**, 79 (6), 441-461.
301. Stolle, A.; Szuppa, T.; Leonhardt, S. E. S.; Ondruschka, B., Ball milling in organic synthesis: solutions and challenges. *Chemical Society Reviews*, **2011**, 40 (5), 2317.
302. Do, J.-L.; Friščić, T., Mechanochemistry: A Force of Synthesis. *ACS Central Science*, **2017**, 3 (1), 13-19.
303. Andersen, J.; Mack, J., Mechanochemistry and organic synthesis: from mystical to practical. *Green Chemistry*, **2018**, 20 (7), 1435-1443.

304. Pérez-Venegas, M.; Juaristi, E., Mechanochemical and Mechanoenzymatic Synthesis of Pharmacologically Active Compounds: A Green Perspective. *ACS Sustainable Chemistry & Engineering*, **2020**, *8* (24), 8881-8893.
305. Brandão, P.; Pineiro, M.; Pinho e Melo, T. M. V. D., Flow Chemistry: Towards A More Sustainable Heterocyclic Synthesis. *European Journal of Organic Chemistry*, **2019**, *2019* (43), 7188-7217.
306. Newman, S. G.; Jensen, K. F., The role of flow in green chemistry and engineering. *Green Chemistry*, **2013**, *15* (6), 1456.
307. Vaccaro, L.; Lanari, D.; Marrocchi, A.; Strappaveccia, G., Flow approaches towards sustainability. *Green Chemistry*, **2014**, *16* (8), 3680-3704.
308. Hessel, V.; Escribà-Gelonch, M.; Bricout, J.; Tran, N. N.; Anastasopoulou, A.; Ferlin, F.; Valentini, F.; Lanari, D.; Vaccaro, L., Quantitative Sustainability Assessment of Flow Chemistry—From Simple Metrics to Holistic Assessment. *ACS Sustainable Chemistry & Engineering*, **2021**, *9* (29), 9508-9540.
309. Clark, J. H.; Pfaltzgraff, L. A.; Budarin, V. L.; Hunt, A. J.; Gronnow, M.; Matharu, A. S.; Macquarrie, D. J.; Sherwood, J. R., From waste to wealth using green chemistry. *Pure and Applied Chemistry*, **2013**, *85* (8), 1625-1631.
310. Higuera, P. L.; Sáez-Martínez, F. J.; Lefebvre, G.; Moillon, R., Contaminated sites, waste management, and green chemistry: new challenges from monitoring to remediation. *Environmental Science and Pollution Research*, **2019**, *26* (4), 3095-3099.
311. Alfonsi, K.; Colberg, J.; Dunn, P. J.; Fevig, T.; Jennings, S.; Johnson, T. A.; Kleine, H. P.; Knight, C.; Nagy, M. A.; Perry, D. A.; Stefaniak, M., Green chemistry tools to influence a medicinal chemistry and research chemistry based organisation. *Green Chemistry*, **2008**, *10* (1), 31-36.
312. Beach, E. S.; Cui, Z.; Anastas, P. T., Green Chemistry: A design framework for sustainability. *Energy & Environmental Science*, **2009**, *2* (10), 1038-1049.
313. Bryan, M. C.; Dillon, B.; Hamann, L. G.; Hughes, G. J.; Kopach, M. E.; Peterson, E. A.; Pourashraf, M.; Raheem, I.; Richardson, P.; Richter, D.; Sneddon, H. F., Sustainable Practices in Medicinal Chemistry: Current State and Future Directions. *Journal of Medicinal Chemistry*, **2013**, *56* (15), 6007-6021.
314. Aliagas, I.; Berger, R.; Goldberg, K.; Nishimura, R. T.; Reilly, J.; Richardson, P.; Richter, D.; Sherer, E. C.; Sparling, B. A.; Bryan, M. C., Sustainable Practices in Medicinal Chemistry Part 2: Green by Design. *Journal of Medicinal Chemistry*, **2017**, *60* (14), 5955-5968.
315. Gleeson, M. P.; Leeson, P. D.; van de Waterbeemd, H., Chapter 1: Physicochemical Properties and Compound Quality. In *The Handbook of Medicinal Chemistry: Principles and Practice*, RSC Publishing, Cambridge, UK, **2015**, pp 1-31.
316. Lipinski, C. A., Drug-like properties and the causes of poor solubility and poor permeability. *Journal of Pharmacological and Toxicological Methods*, **2000**, *44* (1), 235-249.
317. Lipinski, C.; Hopkins, A., Navigating chemical space for biology and medicine. *Nature*, **2004**, *432* (7019), 855-861.

318. Di, L.; Kerns, E. H., Chapter 1 - Introduction. In *Drug-Like Properties (Second Edition)*, Di, L.; Kerns, E. H., Elsevier Ed., Oxford, UK, **2016**, pp 1-3.
319. Mignani, S.; Rodrigues, J.; Tomas, H.; Jalal, R.; Singh, P. P.; Majoral, J.-P.; Vishwakarma, R. A., Present drug-likeness filters in medicinal chemistry during the hit and lead optimization process: how far can they be simplified? *Drug Discovery Today*, **2018**, *23* (3), 605-615.
320. Kola, I.; Landis, J., Can the pharmaceutical industry reduce attrition rates? *Nature Reviews Drug Discovery*, **2004**, *3* (8), 711-716.
321. Waring, M. J.; Arrowsmith, J.; Leach, A. R.; Leeson, P. D.; Mandrell, S.; Owen, R. M.; Pairaudeau, G.; Pennie, W. D.; Pickett, S. D.; Wang, J.; Wallace, O.; Weir, A., An analysis of the attrition of drug candidates from four major pharmaceutical companies. *Nature Reviews Drug Discovery*, **2015**, *14* (7), 475-486.
322. Morgan, P.; Van Der Graaf, P. H.; Arrowsmith, J.; Feltner, D. E.; Drummond, K. S.; Wegner, C. D.; Street, S. D. A., Can the flow of medicines be improved? Fundamental pharmacokinetic and pharmacological principles toward improving Phase II survival. *Drug Discovery Today*, **2012**, *17* (9-10), 419-424.
323. Shih, H.-P.; Zhang, X.; Aronov, A. M., Drug discovery effectiveness from the standpoint of therapeutic mechanisms and indications. *Nature Reviews Drug Discovery*, **2018**, *17* (1), 19-33.
324. Di, L.; Kerns, E. H., Chapter 2 - Benefits of Property Assessment and Good Drug-Like Properties. In *Drug-Like Properties (Second Edition)*, Di, L.; Kerns, E. H., Elsevier Ed., Oxford, UK, **2016**, pp 5-13.
325. Leeson, P. D.; Springthorpe, B., The influence of drug-like concepts on decision-making in medicinal chemistry. *Nature Reviews Drug Discovery*, **2007**, *6* (11), 881-890.
326. Di, L.; Kerns, E. H.; Carter, G. T., Drug-Like Property Concepts in Pharmaceutical Design. *Current Pharmaceutical Design*, **2009**, *15* (19), 2184-2194.
327. Ursu, O.; Rayan, A.; Goldblum, A.; Oprea, T. I., Understanding drug-likeness. *WIREs Computational Molecular Science*, **2011**, *1* (5), 760-781.
328. Lipinski, C. A.; Lombardo, F.; Dominy, B. W.; Feeney, P. J., Experimental and computational approaches to estimate solubility and permeability in drug discovery and development settings. *Advanced Drug Delivery Reviews*, **1997**, *23* (1-3), 3-25.
329. Lipinski, C. A., Lead- and drug-like compounds: the rule-of-five revolution. *Drug Discovery Today: Technologies*, **2004**, *1* (4), 337-341.
330. Ghose, A. K.; Viswanadhan, V. N.; Wendoloski, J. J., A Knowledge-Based Approach in Designing Combinatorial or Medicinal Chemistry Libraries for Drug Discovery. 1. A Qualitative and Quantitative Characterization of Known Drug Databases. *Journal of Combinatorial Chemistry*, **1999**, *1* (1), 55-68.
331. Veber, D. F.; Johnson, S. R.; Cheng, H.-Y.; Smith, B. R.; Ward, K. W.; Kopple, K. D., Molecular Properties That Influence the Oral Bioavailability of Drug Candidates. *Journal of Medicinal Chemistry*, **2002**, *45* (12), 2615-2623.

332. Egan, W. J.; Merz, K. M.; Baldwin, J. J., Prediction of Drug Absorption Using Multivariate Statistics. *Journal of Medicinal Chemistry*, **2000**, *43* (21), 3867-3877.
333. Muegge, I.; Heald, S. L.; Brittelli, D., Simple Selection Criteria for Drug-like Chemical Matter. *Journal of Medicinal Chemistry*, **2001**, *44* (12), 1841-1846.
334. Muegge, I., Selection criteria for drug-like compounds. *Medicinal Research Reviews*, **2003**, *23* (3), 302-321.
335. Gleeson, M. P., Generation of a Set of Simple, Interpretable ADMET Rules of Thumb. *Journal of Medicinal Chemistry*, **2008**, *51* (4), 817-834.
336. Hughes, J. D.; Blagg, J.; Price, D. A.; Bailey, S.; Decrescenzo, G. A.; Devraj, R. V.; Ellsworth, E.; Fobian, Y. M.; Gibbs, M. E.; Gilles, R. W.; Greene, N.; Huang, E.; Krieger-Burke, T.; Loesel, J.; Wager, T.; Whiteley, L.; Zhang, Y., Physicochemical drug properties associated with *in vivo* toxicological outcomes. *Bioorganic & Medicinal Chemistry Letters*, **2008**, *18* (17), 4872-4875.
337. Yukawa, T.; Naven, R., Utility of Physicochemical Properties for the Prediction of Toxicological Outcomes: Takeda Perspective. *ACS Medicinal Chemistry Letters*, **2020**, *11* (2), 203-209.
338. Johnson, T. W.; Dress, K. R.; Edwards, M., Using the Golden Triangle to optimize clearance and oral absorption. *Bioorganic & Medicinal Chemistry Letters*, **2009**, *19* (19), 5560-5564.
339. Lovering, F.; Bikker, J.; Humblet, C., Escape from Flatland: Increasing Saturation as an Approach to Improving Clinical Success. *Journal of Medicinal Chemistry*, **2009**, *52* (21), 6752-6756.
340. Ivanenkov, Y. A.; Zagribelnyy, B. A.; Aladinskiy, V. A., Are We Opening the Door to a New Era of Medicinal Chemistry or Being Collapsed to a Chemical Singularity? *Journal of Medicinal Chemistry*, **2019**, *62* (22), 10026-10043.
341. Wei, W.; Cherukupalli, S.; Jing, L.; Liu, X.; Zhan, P., Fsp³: A new parameter for drug-likeness. *Drug Discovery Today*, **2020**, *25* (10), 1839-1845.
342. Giordanetto, F.; Kihlberg, J., Macrocyclic Drugs and Clinical Candidates: What Can Medicinal Chemists Learn from Their Properties? *Journal of Medicinal Chemistry*, **2014**, *57* (2), 278-295.
343. Doak, B. C.; Zheng, J.; Dobritsch, D.; Kihlberg, J., How Beyond Rule of 5 Drugs and Clinical Candidates Bind to Their Targets. *Journal of Medicinal Chemistry*, **2016**, *59* (6), 2312-2327.
344. Whitty, A.; Zhong, M.; Viarengo, L.; Beglov, D.; Hall, D. R.; Vajda, S., Quantifying the chameleonic properties of macrocycles and other high-molecular-weight drugs. *Drug Discovery Today*, **2016**, *21* (5), 712-717.
345. Egbert, M.; Whitty, A.; Keserú, G. M.; Vajda, S., Why Some Targets Benefit from beyond Rule of Five Drugs. *Journal of Medicinal Chemistry*, **2019**, *62* (22), 10005-10025.
346. Pajouhesh, H.; Lenz, G. R., Medicinal chemical properties of successful central nervous system drugs. *NeuroRX*, **2005**, *2* (4), 541-553.

347. Wager, T. T.; Hou, X.; Verhoest, P. R.; Villalobos, A., Central Nervous System Multiparameter Optimization Desirability: Application in Drug Discovery. *ACS Chemical Neuroscience*, **2016**, *7* (6), 767-775.
348. Hu, Q.; Feng, M.; Lai, L.; Pei, J., Prediction of Drug-Likeness Using Deep Autoencoder Neural Networks. *Frontiers in Genetics*, **2018**, *9* (585).
349. Mochizuki, M.; Suzuki, S. D.; Yanagisawa, K.; Ohue, M.; Akiyama, Y., QEX: target-specific druglikeness filter enhances ligand-based virtual screening. *Molecular Diversity*, **2019**, *23* (1), 11-18.
350. Yusof, I.; Segall, M. D., Considering the impact drug-like properties have on the chance of success. *Drug Discovery Today*, **2013**, *18* (13-14), 659-666.
351. Machado, D.; Girardini, M.; Viveiros, M.; Pieroni, M., Challenging the Drug-Likeness Dogma for New Drug Discovery in Tuberculosis. *Frontiers in Microbiology*, **2018**, *9* (1367).
352. Gomez-Orellana, I., Strategies to improve oral drug bioavailability. *Expert Opinion on Drug Delivery*, **2005**, *2* (3), 419-433.
353. Bruno, A.; Costantino, G.; Sartori, L.; Radi, M., The *In Silico* Drug Discovery Toolbox: Applications in Lead Discovery and Optimization. *Current Medicinal Chemistry*, **2019**, *26* (21), 3838-3873.
354. Jia, C.-Y.; Li, J.-Y.; Hao, G.-F.; Yang, G.-F., A drug-likeness toolbox facilitates ADMET study in drug discovery. *Drug Discovery Today*, **2020**, *25* (1), 248-258.
355. Agoni, C.; Olotu, F. A.; Ramharack, P.; Soliman, M. E., Druggability and drug-likeness concepts in drug design: are biomodelling and predictive tools having their say? *Journal of Molecular Modeling*, **2020**, *26* (6).
356. Dhanda, S. K.; Singla, D.; Mondal, A. K.; Raghava, G. P., DrugMint: a webserver for predicting and designing of drug-like molecules. *Biology Direct*, **2013**, *8* (1), 28.
357. Lagorce, D.; Bouslama, L.; Becot, J.; Miteva, M. A.; Villoutreix, B. O., FAF-Drugs4: free ADME-tox filtering computations for chemical biology and early stages drug discovery. *Bioinformatics*, **2017**, *33* (22), 3658-3660.
358. Bocci, G.; Carosati, E.; Vayer, P.; Arrault, A.; Lozano, S.; Cruciani, G., ADME-Space: a new tool for medicinal chemists to explore ADME properties. *Scientific Reports*, **2017**, *7* (1), 6359.
359. Dong, J.; Wang, N.-N.; Yao, Z.-J.; Zhang, L.; Cheng, Y.; Ouyang, D.; Lu, A.-P.; Cao, D.-S., ADMETlab: a platform for systematic ADMET evaluation based on a comprehensively collected ADMET database. *Journal of Cheminformatics*, **2018**, *10*, 29.
360. Yang, H.; Lou, C.; Sun, L.; Li, J.; Cai, Y.; Wang, Z.; Li, W.; Liu, G.; Tang, Y., admetSAR 2.0: web-service for prediction and optimization of chemical ADMET properties. *Bioinformatics*, **2019**, *35* (6), 1067-1069.
361. Lauria, A.; Mannino, S.; Gentile, C.; Mannino, G.; Martorana, A.; Peri, D., DRUDIT: web-based DRUGs Discovery Tools to design small molecules as modulators of biological targets. *Bioinformatics*, **2020**, *36* (5), 1562-1569.

362. Daina, A.; Michielin, O.; Zoete, V., SwissADME: a free web tool to evaluate pharmacokinetics, drug-likeness and medicinal chemistry friendliness of small molecules. *Scientific Reports*, **2017**, *7* (1), 42717.
363. Martin, Y. C., A Bioavailability Score. *Journal of Medicinal Chemistry*, **2005**, *48* (9), 3164-3170.
364. Brenk, R.; Schipani, A.; James, D.; Krasowski, A.; Gilbert, I. H.; Frearson, J.; Wyatt, P. G., Lessons Learnt from Assembling Screening Libraries for Drug Discovery for Neglected Diseases. *ChemMedChem*, **2008**, *3* (3), 435-444.
365. Baell, J. B.; Nissink, J. W. M., Seven Year Itch: Pan-Assay Interference Compounds (PAINS) in 2017—Utility and Limitations. *ACS Chemical Biology*, **2018**, *13* (1), 36-44.
366. Gilberg, E.; Stumpfe, D.; Bajorath, J., Activity profiles of analog series containing pan assay interference compounds. *RSC Advances*, **2017**, *7* (57), 35638-35647.
367. Dantas, R. F.; Evangelista, T. C. S.; Neves, B. J.; Senger, M. R.; Andrade, C. H.; Ferreira, S. B.; Silva-Junior, F. P., Dealing with frequent hitters in drug discovery: a multidisciplinary view on the issue of filtering compounds on biological screenings. *Expert Opinion on Drug Discovery*, **2019**, *14* (12), 1269-1282.
368. David, L.; Walsh, J.; Sturm, N.; Feierberg, I.; Nissink, J. W. M.; Chen, H.; Bajorath, J.; Engkvist, O., Identification of Compounds That Interfere with High-Throughput Screening Assay Technologies. *ChemMedChem*, **2019**, *14* (20), 1795-1802.
369. Wildman, S. A.; Crippen, G. M., Prediction of Physicochemical Parameters by Atomic Contributions. *Journal of Chemical Information and Computer Sciences*, **1999**, *39* (5), 868-873.
370. Ertl, P.; Rohde, B.; Selzer, P., Fast Calculation of Molecular Polar Surface Area as a Sum of Fragment-Based Contributions and Its Application to the Prediction of Drug Transport Properties. *Journal of Medicinal Chemistry*, **2000**, *43* (20), 3714-3717.
371. Daina, A.; Zoete, V., A BOILED-Egg To Predict Gastrointestinal Absorption and Brain Penetration of Small Molecules. *ChemMedChem*, **2016**, *11* (11), 1117-1121.
372. Medvedev, A.; Kopylov, A.; Buneeva, O.; Kurbatov, L.; Tikhonova, O.; Ivanov, A.; Zgoda, V., A Neuroprotective Dose of Isatin Causes Multilevel Changes Involving the Brain Proteome: Prospects for Further Research. *International Journal of Molecular Sciences*, **2020**, *21* (11), 4187.
373. Alegre-Requena, J. V.; Marqués-López, E.; Herrera, R. P., Introduction: Multicomponent Strategies. In *Multicomponent Reactions: Concepts and Applications for Design and Synthesis*, Herrera, R. P.; Marqués-López, E., Eds. John Wiley & Sons, New Jersey, USA, **2015**, pp 1-15.
374. Strecker, A., Ueber die künstliche Bildung der Milchsäure und einen neuen, dem Glycocoll homologen Körper. *Annalen der Chemie und Pharmacie*, **1850**, *75* (1), 27-45.
375. Hantzsch, A., Ueber die Synthese pyridinartiger Verbindungen aus Acetessigäther und Aldehydammoniak. *Justus Liebig's Annalen der Chemie*, **1882**, *215* (1), 1-82.

376. Biginelli, P., Aldureides of ethylic acetoacetate and ethylic oxaloacetate. *Gazzetta Chimica Italiana*, **1893**, 23, 360-416.
377. Mannich, C.; Krösche, W., Ueber ein Kondensationsprodukt aus Formaldehyd, Ammoniak und Antipyrin. *Archiv der Pharmazie*, **1912**, 250 (1), 647-667.
378. Passerini, M.; Simone, L., Composto del p-isonitrilazobenzolo con acetone e acido acetico. *Gazzetta Chimica Italiana*, **1921**, 51, 126-129.
379. Bergs, H. Verfahren Zur Darstellung von Hydantoinen, **1929**, DE566094C.
380. Bucherer, H.; Fischbeck, H., Hexahydrodiphenylamine and its derivatives. *Journal für Praktische Chemie*, **1934**, 140 (69).
381. Kabachnik, M.; Medved, T., New synthesis of aminophosphonic acids. *Proceedings of the USSR Academy of Sciences*, **1952**, 83, 689-692.
382. Fields, E. K., The Synthesis of Esters of Substituted Amino Phosphonic Acids. *Journal of the American Chemical Society*, **1952**, 74 (6), 1528-1531.
383. Asinger, F., Über die gemeinsame einwirkung von schwefel und ammoniak auf ketone. *Angewandte Chemie*, **1956**, 68 (12), 413.
384. Ugi, I.; Meyr, R.; Fetzer, U.; Steinbruckner, C., Studies on isonitriles. *Angewandte Chemie*, **1959**, 71, 373-388.
385. Gewalt, K.; Schinke, E.; Böttcher, H., Heterocyclen aus CH-aciden Nitrilen, VIII. 2-Amino-thiophene aus methylenaktiven Nitrilen, Carbonylverbindungen und Schwefel. *Chemische Berichte*, **1966**, 99 (1), 94-100.
386. Khand, I. U.; Knox, G. R.; Pauson, P. L.; Watts, W. E., A cobalt induced cleavage reaction and a new series of arenecobalt carbonyl complexes. *Journal of the Chemical Society D: Chemical Communications*, **1971**, (1), 36a.
387. Pauson, P. L.; Khand, I. U., Uses of Cobalt-Carbonyl Acetylene Complexes in Organic Synthesis. *Annals of the New York Academy of Sciences*, **1977**, 295 (1), 2-14.
388. Larsen, S. D.; Grieco, P. A., Aza Diels-Alder reactions in aqueous solution: cyclocondensation of dienes with simple iminium salts generated under Mannich conditions. *Journal of the American Chemical Society*, **1985**, 107 (6), 1768-1769.
389. Petasis, N. A.; Akritopoulou, I., The boronic acid mannich reaction: A new method for the synthesis of geometrically pure allylamines. *Tetrahedron Letters*, **1993**, 34 (4), 583-586.
390. Groebke, K.; Hunziker, J.; Fraser, W.; Peng, L.; Diederichsen, U.; Zimmermann, K.; Holzner, A.; Leumann, C.; Eschenmoser, A., Warum Pentose- und nicht Hexose-Nucleinsäuren? Teil V. (Purin-Purin)-Basenpaarung in der homo-DNS-Reihe: Guanin, Isoguanin, 2,6-Diaminopurin und Xanthin. *Helvetica Chimica Acta*, **1998**, 81 (3-4), 375-474.
391. Blackburn, C.; Guan, B.; Fleming, P.; Shiosaki, K.; Tsai, S., Parallel synthesis of 3-aminoimidazo[1,2-a]pyridines and pyrazines by a new three-component condensation. *Tetrahedron Letters*, **1998**, 39 (22), 3635-3638.
392. Bienaymé, H.; Bouzid, K., A New Heterocyclic Multicomponent Reaction For the Combinatorial Synthesis of Fused 3-Aminoimidazoles. *Angewandte Chemie International Edition*, **1998**, 37 (16), 2234-2237.

393. Bon, R. S.; Hong, C.; Bouma, M. J.; Schmitz, R. F.; De Kanter, F. J. J.; Lutz, M.; Spek, A. L.; Orru, R. V. A., Novel Multicomponent Reaction for the Combinatorial Synthesis of 2-Imidazolines. *Organic Letters*, **2003**, 5 (20), 3759-3762.
394. Zarganes-Tzitzikas, T.; Chandgude, A. L.; Dömling, A., Multicomponent Reactions, Union of MCRs and Beyond. *The Chemical Record*, **2015**, 15 (5), 981-996.
395. Ganem, B., Strategies for Innovation in Multicomponent Reaction Design. *Accounts of Chemical Research*, **2009**, 42 (3), 463-472.
396. Dömling, A.; Wang, W.; Wang, K., Chemistry and Biology Of Multicomponent Reactions. *Chemical Reviews*, **2012**, 112 (6), 3083-3135.
397. Rotstein, B. H.; Zaretsky, S.; Rai, V.; Yudin, A. K., Small Heterocycles in Multicomponent Reactions. *Chemical Reviews*, **2014**, 114 (16), 8323-8359.
398. Cioc, R. C.; Ruijter, E.; Orru, R. V. A., Multicomponent reactions: advanced tools for sustainable organic synthesis. *Green Chemistry*, **2014**, 16 (6), 2958-2975.
399. Longo Jr, L.; Craveiro, M., Deep Eutectic Solvents as Unconventional Media for Multicomponent Reactions. *Journal of the Brazilian Chemical Society*, **2018**.
400. Gu, Y., Multicomponent reactions in unconventional solvents: state of the art. *Green Chemistry*, **2012**, 14 (8), 2091.
401. Simon, M.-O.; Li, C.-J., Green chemistry oriented organic synthesis in water. *Chemical Society Reviews*, **2012**, 41 (4), 1415-1427.
402. Cukalovic, A.; Monbaliu, J.-C. M. R.; Stevens, C. V., Microreactor Technology as an Efficient Tool for Multicomponent Reactions. In *Synthesis of Heterocycles via Multicomponent Reactions I*, Orru, R. V. A.; Ruijter, E., Eds. Springer Berlin Heidelberg, Berlin, Germany, **2010**, pp 161-198.
403. Van Mileghem, S.; Veryser, C.; De Borggraeve, W. M., Flow-Assisted Synthesis of Heterocycles via Multicomponent Reactions. In *Flow Chemistry for the Synthesis of Heterocycles*, Sharma, U. K.; Van der Eycken, E. V., Eds. Springer International Publishing, **2018**, pp 133-159.
404. Bariwal, J. B.; Trivedi, J. C.; Van der Eycken, E. V., Microwave Irradiation and Multicomponent Reactions. In *Synthesis of Heterocycles via Multicomponent Reactions II*, Orru, R. V. A.; Ruijter, E., Eds. Springer Berlin Heidelberg, Berlin, Germany, **2010**, pp 169-230.
405. Dolzhenko, A. V., Chapter 3 - Microwave-assisted multicomponent reactions. In *Green Sustainable Process for Chemical and Environmental Engineering and Science*, Inamuddin, A.; Boddula, R.; Asiri, A. M., Eds. Elsevier: **2021**, pp 205-229.
406. Dandia, A.; Singh, R.; Bhaskaran, S., Multicomponent Reactions and Ultrasound: A Synergistic Approach for the Synthesis of Bioactive Heterocycles. *Current Green Chemistry*, **2014**, 1 (1), 17-39.
407. Penteadó, F.; Monti, B.; Sancineto, L.; Perin, G.; Jacob, R. G.; Santi, C.; Lenardão, E. J., Ultrasound-Assisted Multicomponent Reactions, Organometallic and Organochalcogen Chemistry. *Asian Journal of Organic Chemistry*, **2018**, 7 (12), 2368-2385.

408. Machado, I. V.; Dos Santos, J. R. N.; Januario, M. A. P.; Corrêa, A. G., Greener organic synthetic methods: sonochemistry and heterogeneous catalysis promoted multicomponent reactions. *Ultrasonics Sonochemistry*, **2021**, 105704.
409. Leonardi, M.; Villacampa, M.; Menéndez, J. C., Multicomponent mechanochemical synthesis. *Chemical Science*, **2018**, 9 (8), 2042-2064.
410. Hamada, T.; Yamashita, S.; Omichi, M.; Yoshimura, K.; Ueki, Y.; Seko, N.; Kakuchi, R., Multicomponent-Reaction-Ready Biomass-Sourced Organic Hybrids Fabricated via the Surface Immobilization of Polymers with Lignin-Based Compounds. *ACS Sustainable Chemistry & Engineering*, **2019**, 7 (8), 7795-7803.
411. Xu, J.; Fan, W.; Popowycz, F.; Queneau, Y.; Gu, Y., Multicomponent Reactions: A New Strategy for Enriching the Routes of Value-Added Conversions of Bio-platform Molecules. *Chinese Journal of Organic Chemistry*, **2019**, 39 (8), 2131-2138.
412. Climent, M. J.; Corma, A.; Iborra, S., Homogeneous and heterogeneous catalysts for multicomponent reactions. *RSC Advances*, **2012**, 2 (1), 16-58.
413. Jumbam, N. D.; Masamba, W., Bio-Catalysis in Multicomponent Reactions. *Molecules*, **2020**, 25 (24), 5935.
414. Chen, M.-N.; Mo, L.-P.; Cui, Z.-S.; Zhang, Z.-H., Magnetic nanocatalysts: Synthesis and application in multicomponent reactions. *Current Opinion in Green and Sustainable Chemistry*, **2019**, 15, 27-37.
415. Biggs-Houck, J. E.; Younai, A.; Shaw, J. T., Recent advances in multicomponent reactions for diversity-oriented synthesis. *Current Opinion in Chemical Biology*, **2010**, 14 (3), 371-382.
416. Schreiber, S. L., Target-Oriented and Diversity-Oriented Organic Synthesis in Drug Discovery. *Science*, **2000**, 287 (5460), 1964-1969.
417. Liu, R.; Li, X.; Lam, K. S., Combinatorial chemistry in drug discovery. *Current Opinion in Chemical Biology*, **2017**, 38, 117-126.
418. Spandl, R. J.; Díaz-Gavilán, M.; O'Connell, K. M. G.; Thomas, G. L.; Spring, D. R., Diversity-oriented synthesis. *The Chemical Record*, **2008**, 8 (3), 129-142.
419. Burke, M. D.; Schreiber, S. L., A Planning Strategy for Diversity-Oriented Synthesis. *Angewandte Chemie International Edition*, **2004**, 43 (1), 46-58.
420. O'Connell, K. M. G.; Galloway, W. R. J. D.; Spring, D. R., The Basics of Diversity-Oriented Synthesis. In *Diversity-Oriented Synthesis*, Trabocchi, A. Ed., John Wiley & Sons, Inc., New Jersey, USA, **2013**, pp 1-26.
421. Galloway, W. R. J. D.; Isidro-Llobet, A.; Spring, D. R., Diversity-oriented synthesis as a tool for the discovery of novel biologically active small molecules. *Nature Communications*, **2010**, 1 (1), 1-13.
422. Spring, D. R., Diversity-oriented synthesis; a challenge for synthetic chemists. *Organic & Biomolecular Chemistry*, **2003**, 1 (22), 3867.
423. Dandapani, S.; Marcaurelle, L. A., Current strategies for diversity-oriented synthesis. *Current Opinion in Chemical Biology*, **2010**, 14 (3), 362-370.

424. Gerry, C. J.; Schreiber, S. L., Chemical probes and drug leads from advances in synthetic planning and methodology. *Nature Reviews Drug Discovery*, **2018**, *17* (5), 333-352.
425. Ruijter, E.; Orru, R. V. A., Multicomponent reactions – opportunities for the pharmaceutical industry. *Drug Discovery Today: Technologies*, **2013**, *10* (1), e15-e20.
426. Zarganes-Tzitzikas, T.; Dömling, A., Modern multicomponent reactions for better drug syntheses. *Organic Chemistry Frontiers*, **2014**, *1* (7), 834-837.
427. Younus, H. A.; Al-Rashida, M.; Hameed, A.; Uroos, M.; Salar, U.; Rana, S.; Khan, K. M., Multicomponent reactions (MCR) in medicinal chemistry: a patent review (2010-2020). *Expert Opinion on Therapeutic Patents*, **2021**, *31* (3), 267-289.
428. Bossert, F.; Water, W. 4-Aryl-1,4-dihydropyridanes. **1969**, US3485847A.
429. Bridgwood, K. L.; Veitch, G. E.; Ley, S. V., Magnesium nitride as a convenient source of ammonia: preparation of dihydropyridines. *Organic Letters*, **2008**, *10* (16), 3627-9.
430. Baumann, M.; Baxendale, I. R., An overview of the synthetic routes to the best selling drugs containing 6-membered heterocycles. *Beilstein Journal of Organic Chemistry*, **2013**, *9*, 2265-319.
431. Weigert, W. M.; Offermanns, H.; Scherberich, P., D-Penicillamine-production and properties. *Angewandte Chemie International Edition*, **1975**, *14* (5), 330-6.
432. Chakrabarti, J. K.; Hotten, T. M.; Tupper, D. E. Process for preparing 2-methyl-thienobenzodiazepine. **1998**, US6008216A
433. Kothakonda, K. K.; CheBhaskar, D.; Guntoori, R. Processes for the synthesis of olanzapine. **2011**, US7863442B2.
434. Sugiyama, S.; Arai, S.; Kiriya, M.; Ishii, K., A convenient synthesis of immunosuppressive agent FTY720 using the petasis reaction. *Chemical & Pharmaceutical Bulletin*, **2005**, *53* (1), 100-2.
435. Zhangyong, H.; Zeming, C.; Kui, Y. J., W. Novel method for synthesis of anti-influenza medicament zanamivir. **2013**, CN104744415A.
436. Kalinski, C.; Lemoine, H.; Schmidt, J.; Burdack, C.; Kolb, J.; Umkehrer, M.; Ross, G., Multicomponent Reactions as a Powerful Tool for Generic Drug Synthesis. *Synthesis*, **2008**, *2008* (24), 4007-4011.
437. Znabet, A.; Polak, M. M.; Janssen, E.; de Kanter, F. J.; Turner, N. J.; Orru, R. V.; Ruijter, E., A highly efficient synthesis of telaprevir by strategic use of biocatalysis and multicomponent reactions. *Chemical Communications*, **2010**, *46* (42), 7918-7920.
438. Cioc, R. C.; van Riepst, L. S.; Schuckman, P.; Ruijter, E.; Orru, R. V. A., Ugi Four-Center Three-Component Reaction as a Direct Approach to Racetams. *Synthesis*, **2016**, *49* (07), 1664-1674.
439. Wehlan, H.; Oehme, J.; Schäfer, A.; Rossen, K., Development of Scalable Conditions for the Ugi Reaction—Application to the Synthesis of (*R*)-Lacosamide. *Organic Process Research & Development*, **2015**, *19* (12), 1980-1986.
440. Dömling, A.; Ugi, I., Multicomponent Reactions with Isocyanides. *Angewandte Chemie International Edition*, **2000**, *39* (18), 3168-3210.

441. Zarganes-Tzitzikas, T.; Neochoritis, C. G.; Domling, A., Atorvastatin (Lipitor) by MCR. *ACS Medicinal Chemistry Letters*, **2019**, *10* (3), 389-392.
442. Rossen, K.; Pye, P. J.; DiMichele, L. M.; Volante, R. P.; Reider, P. J., An efficient asymmetric hydrogenation approach to the synthesis of the Crixivan® piperazine intermediate. *Tetrahedron Letters*, **1998**, *39* (38), 6823-6826.
443. Borase, B. B.; Godbole, H. M.; Singh, G. P.; Upadhyay, P. R.; Trivedi, A.; Bhat, V.; Shenoy, G. G., Application of Ugi three component reaction for the synthesis of quinapril hydrochloride. *Synthetic Communications*, **2019**, *50* (1), 48-55.
444. Cao, H.; Liu, H.; Domling, A., Efficient multicomponent reaction synthesis of the schistosomiasis drug praziquantel. *Chemistry – A European Journal*, **2010**, *16* (41), 12296-8.
445. Liu, H.; William, S.; Herdtweck, E.; Botros, S.; Domling, A., MCR synthesis of praziquantel derivatives. *Chemical Biology & Drug Design*, **2012**, *79* (4), 470-477.
446. Popovici-Muller, J.; Lemieux, R. M.; Artin, E.; Saunders, J. O.; Salituro, F. G.; Travins, J.; Cianchetta, G.; Cai, Z.; Zhou, D.; Cui, D.; Chen, P.; Straley, K.; Tobin, E.; Wang, F.; David, M. D.; Penard-Lacronique, V.; Quivoron, C.; Saada, V.; De Botton, S.; Gross, S.; Dang, L.; Yang, H.; Utley, L.; Chen, Y.; Kim, H.; Jin, S.; Gu, Z.; Yao, G.; Luo, Z.; Lv, X.; Fang, C.; Yan, L.; Olaharski, A.; Silverman, L.; Biller, S.; Su, S.-S. M.; Yen, K., Discovery of AG-120 (Ivosidenib): A First-in-Class Mutant IDH1 Inhibitor for the Treatment of IDH1 Mutant Cancers. *ACS Medicinal Chemistry Letters*, **2018**, *9* (4), 300-305.
447. Malaquin, S.; Jida, M.; Gesquiere, J.-C.; Deprez-Poulain, R.; Deprez, B.; Laconde, G., Ugi reaction for the synthesis of 4-aminopiperidine-4-carboxylic acid derivatives. Application to the synthesis of carfentanil and remifentanil. *Tetrahedron Letters*, **2010**, *51* (22), 2983-2985.
448. Slobbe, P.; Ruijter, E.; Orru, R. V. A., Recent applications of multicomponent reactions in medicinal chemistry. *MedChemComm*, **2012**, *3* (10), 1189-1218.
449. Graebin, C. S.; Ribeiro, F. V.; Rogério, K. R.; Kümmerle, A. E., Multicomponent Reactions for the Synthesis of Bioactive Compounds: A Review. *Current Organic Synthesis*, **2019**, *16* (6), 855-899.
450. Insuasty, D.; Castillo, J.; Becerra, D.; Rojas, H.; Abonia, R., Synthesis of Biologically Active Molecules through Multicomponent Reactions. *Molecules*, **2020**, *25* (3), 505.
451. Brandão, P.; Burke, A. J.; Pineiro, M., Reações Multicomponente – Uma Ferramenta Valiosa na Descoberta e Produção de Fármacos. *Química*, **2020**, *44* (159), 264-276.
452. Dömling, A., The discovery of new isocyanide-based multi-component reactions. *Current Opinion in Chemical Biology*, **2000**, *4* (3), 318-323.
453. Rudick, J. G.; Shaabani, S.; Dömling, A., Editorial: Isocyanide-Based Multicomponent Reactions. *Frontiers in Chemistry*, **2020**, *7*, 918.
454. Golantsov, N. E.; Nguyen, H. M.; Golubenkova, A. S.; Varlamov, A. V.; Van der Eycken, E. V.; Voskressensky, L. G., Three-Component Reaction of 3-Arylidene-3H-Indolium Salts, Isocyanides, and Alcohols. *Frontiers in Chemistry*, **2019**, *7*, 345.
455. Shaaban, S.; Abdel-Wahab, B. F., Groebke–Blackburn–Bienaymé multicomponent reaction: emerging chemistry for drug discovery. *Molecular Diversity*, **2016**, *20* (1), 233-254.

456. Dömling, A., Recent Developments in Isocyanide Based Multicomponent Reactions in Applied Chemistry. *Chemical Reviews*, **2006**, *106* (1), 17-89.
457. Ugi, I.; Werner, B.; Dömling, A., The Chemistry of Isocyanides, their Multicomponent Reactions and their Libraries. *Molecules*, **2003**, *8* (1), 53-66.
458. Massarotti, A.; Brunelli, F.; Aprile, S.; Giustiniano, M.; Tron, G. C., Medicinal Chemistry of Isocyanides. *Chemical Reviews*, **2021**, *121* (17), 10742-10788.
459. Patil, P.; Ahmadian-Moghaddam, M.; Dömling, A., Isocyanide 2.0. *Green Chemistry*, **2020**, *22* (20), 6902-6911.
460. Ugi, I.; Fetzer, U.; Eholzer, U.; Knupfer, H.; Offermann, K., Isonitrile Syntheses. *Angewandte Chemie International Edition*, **1965**, *4* (6), 472-484.
461. Fouad, M. A.; Abdel-Hamid, H.; Ayoup, M. S., Two decades of recent advances of Ugi reactions: synthetic and pharmaceutical applications. *RSC Advances*, **2020**, *10* (70), 42644-42681.
462. Bryan, M. C.; Dunn, P. J.; Entwistle, D.; Gallou, F.; Koenig, S. G.; Hayler, J. D.; Hickey, M. R.; Hughes, S.; Kopach, M. E.; Moine, G.; Richardson, P.; Roschangar, F.; Steven, A.; Weiberth, F. J., Key Green Chemistry research areas from a pharmaceutical manufacturers' perspective revisited. *Green Chemistry*, **2018**, *20* (22), 5082-5103.
463. Valeur, E.; Bradley, M., Amide bond formation: beyond the myth of coupling reagents. *Chemical Society Reviews*, **2009**, *38* (2), 606-631.
464. Joullie, M. M.; Lassen, K. M., Evolution of amide bond formation. *Arkivoc*, **2010**, *2010* (8), 189-250.
465. Pattabiraman, V. R.; Bode, J. W., Rethinking amide bond synthesis. *Nature*, **2011**, *480* (7378), 471-479.
466. De Figueiredo, R. M.; Suppo, J.-S.; Campagne, J.-M., Nonclassical Routes for Amide Bond Formation. *Chemical Reviews*, **2016**, *116* (19), 12029-12122.
467. Massolo, E.; Pirola, M.; Benaglia, M., Amide Bond Formation Strategies: Latest Advances on a Dateless Transformation. *European Journal of Organic Chemistry*, **2020**, *2020* (30), 4641-4651.
468. Brown, D. G.; Boström, J., Analysis of Past and Present Synthetic Methodologies on Medicinal Chemistry: Where Have All the New Reactions Gone? *Journal of Medicinal Chemistry*, **2016**, *59* (10), 4443-4458.
469. Roughley, S. D.; Jordan, A. M., The Medicinal Chemist's Toolbox: An Analysis of Reactions Used in the Pursuit of Drug Candidates. *Journal of Medicinal Chemistry*, **2011**, *54* (10), 3451-3479.
470. Ertl, P.; Altmann, E.; McKenna, J. M., The Most Common Functional Groups in Bioactive Molecules and How Their Popularity Has Evolved over Time. *Journal of Medicinal Chemistry*, **2020**, *63* (15), 8408-8418.
471. Alvim, H. G. O.; da Silva Júnior, E. N.; Neto, B. A. D., What do we know about multicomponent reactions? Mechanisms and trends for the Biginelli, Hantzsch, Mannich, Passerini and Ugi MCRs. *RSC Advances*, **2014**, *4* (97), 54282-54299.

472. Rodrigues, M. O.; Eberlin, M. N.; Neto, B. A. D., How and Why to Investigate Multicomponent Reactions Mechanisms? A Critical Review. *The Chemical Record*, **2021**, *21* (10), 2762-2781.
473. Liu, Z.-Q., Ugi and Passerini Reactions as Successful Models for Investigating Multicomponent Reactions. *Current Organic Chemistry*, **2014**, *18* (6), 719-739.
474. Ugi, I.; Heck, S., The multicomponent reactions and their libraries for natural and preparative chemistry. *Combinatorial Chemistry & High Throughput Screening*, **2001**, *4* (1), 1-34.
475. Medeiros, G. A.; da Silva, W. A.; Bataglion, G. A.; Ferreira, D. A. C.; de Oliveira, H. C. B.; Eberlin, M. N.; Neto, B. A. D., Probing the mechanism of the Ugi four-component reaction with charge-tagged reagents by ESI-MS(/MS). *Chemical Communications*, **2014**, *50* (3), 338-340.
476. Chéron, N.; Ramozzi, R.; Kaïm, L. E.; Grimaud, L.; Fleurat-Lessard, P., Challenging 50 Years of Established Views on Ugi Reaction: A Theoretical Approach. *The Journal of Organic Chemistry*, **2012**, *77* (3), 1361-1366.
477. Rocha, R. O.; Rodrigues, M. O.; Neto, B. A. D., Review on the Ugi Multicomponent Reaction Mechanism and the Use of Fluorescent Derivatives as Functional Chromophores. *ACS Omega*, **2020**, *5* (2), 972-979.
478. Wang, Q.; Wang, D.-X.; Wang, M.-X.; Zhu, J., Still Unconquered: Enantioselective Passerini and Ugi Multicomponent Reactions. *Accounts of Chemical Research*, **2018**, *51* (5), 1290-1300.
479. Zhang, J.; Yu, P.; Li, S.-Y.; Sun, H.; Xiang, S.-H.; Wang, J.; Houk, K. N.; Tan, B., Asymmetric phosphoric acid-catalyzed four-component Ugi reaction. *Science*, **2018**, *361* (6407), eaas8707.
480. Shaabani, S.; Dömling, A., The Catalytic Enantioselective Ugi Four-Component Reactions. *Angewandte Chemie International Edition*, **2018**, *57* (50), 16266-16268.
481. Riva, R., Enantioselective four-component Ugi reactions. *Science*, **2018**, *361* (6407), 1072-1073.
482. Brandão, P.; Burke, A. J., Catalytic Ugi reactions: current advances, future challenges - Part 1. *Chimica Oggi - Chemistry Today (Monographic special issue: Catalysis & Biocatalysis)*, **2019**, *37* (4), 21-25.
483. Brandão, P.; Burke, A. J., Catalytic Ugi reactions: Current advances, future challenges - Part 2. *Chimica Oggi - Chemistry Today*, **2019**, *37* (4), 18-21.
484. Ibarra-Rivera, T. R.; Rentería-Gómez, M. A.; Nieto-Sepúlveda, E.; Gámez-Montaño, R.; Rivas Galindo, V. M.; Hernandez-Fernandez, E., Synthesis of novel tetrahydroindeno[1,2-*b*]pyrrolidines via Ugi multicomponent and palladium-catalyzed aerobic oxidative cyclization. *Synthetic Communications*, **2016**, *46* (6), 509-515.
485. Polindara-García, L. A.; Montesinos-Miguel, D.; Vazquez, A., An efficient microwave-assisted synthesis of cotinine and iso-cotinine analogs from an Ugi-4CR approach. *Organic & Biomolecular Chemistry*, **2015**, *13* (34), 9065-9071.

486. Polindara-García, L. A.; Juaristi, E., Synthesis of Ugi 4-CR and Passerini 3-CR Adducts under Mechanochemical Activation. *European Journal of Organic Chemistry*, **2016**, 2016 (6), 1095-1102.
487. Flores-Constante, G.; Sánchez-Chávez, A. C.; Polindara-García, L. A., A Convenient Synthesis of 1,2-Disubstituted-cis-3,4-Dihydropyrrrolidines via an Ugi-Four-Component-Reaction/Cycloisomerization/Dihydroxylation Protocol. *European Journal of Organic Chemistry*, **2018**, 2018 (33), 4586-4591.
488. Patil, P.; Zhang, J.; Kurpiewska, K.; Kalinowska-Tłuścik, J.; Dömling, A., Hydrazine in the Ugi Tetrazole Reaction. *Synthesis*, **2016**, 48 (8), 1122-1130.
489. Barreto, A. D. F. S.; Santos, V. A. D.; Andrade, C. K. Z., Consecutive hydrazino-Ugi-azide reactions: synthesis of acylhydrazines bearing 1,5-disubstituted tetrazoles. *Beilstein Journal of Organic Chemistry*, **2017**, 13, 2596-2602.
490. Angyal, A.; Demjén, A.; Wéber, E.; Kovács, A. K.; Wölfling, J.; Puskás, L. G.; Kanizsai, I., Lewis Acid-Catalyzed Diastereoselective Synthesis of Multisubstituted *N*-Acylaziridine-2-carboxamides from 2*H*-Azirines via Joullié-Ugi Three-Component Reaction. *The Journal of Organic Chemistry*, **2018**, 83 (7), 3570-3581.
491. Chandgude, A. L.; Dömling, A., *N*-Hydroxyimide Ugi Reaction toward α -Hydrazino Amides. *Organic Letters*, **2017**, 19 (5), 1228-1231.
492. Ren, Z.-L.; He, P.; Lu, W.-T.; Sun, M.; Ding, M.-W., Synthesis of iminoisindolinones via a cascade of the three-component Ugi reaction, palladium catalyzed isocyanide insertion, hydroxylation and an unexpected rearrangement reaction. *Organic & Biomolecular Chemistry*, **2018**, 16 (34), 6322-6331.
493. Foley, C.; Shaw, A.; Hulme, C., Two-Step Route to Diverse *N*-Functionalized Peptidomimetic-like Isatins through an Oxidation/Intramolecular Oxidative-Amidation Cascade of Ugi Azide and Ugi Three-Component Reaction Products. *Organic Letters*, **2016**, 18 (19), 4904-4907.
494. Song, G.-T.; Xu, Z.-G.; Tang, D.-Y.; Li, S.-Q.; Xie, Z.-G.; Zhong, H.-L.; Yang, Z.-W.; Zhu, J.; Zhang, J.; Chen, Z.-Z., Facile microwave-assisted synthesis of benzimidazole scaffolds via Ugi-type three-component condensation (3CC) reactions. *Molecular Diversity*, **2016**, 20 (2), 575-580.
495. Milen, M.; Dancsó, A.; Földesi, T.; Volk, B., Study on the propylphosphonic anhydride (T3P®) mediated Ugi-type three-component reaction. Efficient synthesis of an α -amino amide library. *Tetrahedron*, **2017**, 73 (1), 70-77.
496. Madej, A.; Paprocki, D.; Koszelewski, D.; Źądło-Dobrowolska, A.; Brzozowska, A.; Walde, P.; Ostaszewski, R., Efficient Ugi reactions in an aqueous vesicle system. *RSC Advances*, **2017**, 7 (53), 33344-33354.
497. Rostamnia, S.; Jafari, M., Metal-organic framework of amine-MIL-53(Al) as active and reusable liquid-phase reaction inductor for multicomponent condensation of Ugi-type reactions. *Applied Organometallic Chemistry*, **2017**, 31 (4), e3584.

498. Chacko, P.; Shivashankar, K., Nano structured spinel Co_3O_4 -catalyzed four component reaction: A novel synthesis of Ugi adducts from aryl alcohols as a key reagent. *Chinese Chemical Letters*, **2017**, *28* (7), 1619-1624.
499. Żądło-Dobrowolska, A.; Kłossowski, S.; Koszelewski, D.; Paprocki, D.; Ostaszewski, R., Enzymatic Ugi Reaction with Amines and Cyclic Imines. *Chemistry – A European Journal*, **2016**, *22* (46), 16684-16689.
500. Wilk, M.; Brodzka, A.; Koszelewski, D.; Madej, A.; Paprocki, D.; Żądło-Dobrowolska, A.; Ostaszewski, R., The influence of the isocyanoesters structure on the course of enzymatic Ugi reactions. *Bioorganic Chemistry*, **2019**, *93*, 102817.
501. Madej, A.; Koszelewski, D.; Paprocki, D.; Brodzka, A.; Ostaszewski, R., The sustainable synthesis of peptidomimetics via chemoenzymatic tandem oxidation–Ugi reaction. *RSC Advances*, **2018**, *8* (50), 28405-28413.
502. Chauhan, K. K.; Frost, C. G., Advances in indium-catalysed organic synthesis. *Journal of the Chemical Society, Perkin Transactions 1*, **2000**, *18*, 3015-3019.
503. Ranu, Brindaban C., Indium Metal and Its Halides in Organic Synthesis. *European Journal of Organic Chemistry*, **2000**, *2000*, 2347-2356.
504. Frost, C. G.; Hartley, J. P., New Applications of Indium Catalysts in Organic Synthesis. *Mini-Reviews in Organic Chemistry*, **2004**, *1* (1), 1-7.
505. Augé, J.; Lubin-Germain, N.; Uziel, J., Recent Advances in Indium-Promoted Organic Reactions. *Synthesis*, **2007**, *2007* (12), 1739-1764.
506. Yadav, J. S.; Antony, A.; George, J.; Subba Reddy, B. V., Recent Developments in Indium Metal and Its Salts in Organic Synthesis. *European Journal of Organic Chemistry*, **2010**, *2010* (4), 591-605.
507. Brandão, P.; Burke, A. J.; Pineiro, M., A Decade of Indium-Catalyzed Multicomponent Reactions (MCRs). *European Journal of Organic Chemistry*, **2020**, *2020* (34), 5501-5513.
508. Pitts, M., Endangered elements. *Chemical Engineer*, **2011**, *844*, 48-51.
509. Poliakoff, M.; Tang, S., The periodic table: icon and inspiration. *Philosophical Transactions of the Royal Society A: Mathematical, Physical and Engineering Sciences*, **2015**, *373* (2037), 20140211.
510. Ciacci, L.; Werner, T. T.; Vassura, I.; Passarini, F., Backlighting the European Indium Recycling Potentials. *Journal of Industrial Ecology*, **2019**, *23* (2), 426-437.
511. Pirrung, M. C.; Sarma, K. D., Multicomponent Reactions are Accelerated in Water. *Journal of the American Chemical Society*, **2004**, *126* (2), 444-445.
512. Azizi, N.; Dezfooli, S.; Hashemi, M. M., A sustainable approach to the Ugi reaction in deep eutectic solvent. *Comptes Rendus Chimie*, **2013**, *16* (12), 1098-1102.
513. Heublein, N.; Moore, J. S.; Smith, C. D.; Jensen, K. F., Investigation of Petasis and Ugi reactions in series in an automated microreactor system. *RSC Advances*, **2014**, *4* (109), 63627-63631.

514. Vasconcelos, S. N. S.; Fornari, E.; Caracelli, I.; Stefani, H. A., Synthesis of α -amino-1,3-dicarbonyl compounds via Ugi flow chemistry reaction: access to functionalized 1,2,3-triazoles. *Molecular Diversity*, **2017**, *21* (4), 893-902.
515. Salvador, C. E. M.; Pieber, B.; Neu, P. M.; Torvisco, A.; Kleber Z. Andrade, C.; Kappe, C. O., A Sequential Ugi Multicomponent/Cu-Catalyzed Azide–Alkyne Cycloaddition Approach for the Continuous Flow Generation of Cyclic Peptoids. *The Journal of Organic Chemistry*, **2015**, *80* (9), 4590-4602.
516. Marcaccini, S.; Torroba, T., The use of the Ugi four-component condensation. *Nature Protocols*, **2007**, *2* (3), 632-639.
517. Heravi, M. M.; Mohammadkhani, L., Synthesis of various *N*-heterocycles using the four-component Ugi reaction. *Advances in Heterocyclic Chemistry*, **2020**, *131*, 351-403.
518. El Kaïm, L.; Grimaud, L., The Ugi–Smiles and Passerini–Smiles Couplings: A Story About Phenols in Isocyanide-Based Multicomponent Reactions. *European Journal of Organic Chemistry*, **2014**, *2014* (35), 7749-7762.
519. Flores-Reyes, J. C.; Islas-Jácome, A.; González-Zamora, E., The Ugi-Three Component Reaction and its Variants. *Organic Chemistry Frontiers*, **2021**, *8*, 5460-5515.
520. Tripolitsiotis, N. P.; Thomaidi, M.; Neochoritis, C. G., The Ugi Three-Component Reaction; a Valuable Tool in Modern Organic Synthesis. *European Journal of Organic Chemistry*, **2020**, *2020* (42), 6525-6554.
521. Sun, X.; Janvier, P.; Zhao, G.; Bienaymé, H.; Zhu, J., A Novel Multicomponent Synthesis of Polysubstituted 5-Aminooxazole and Its New Scaffold-Generating Reaction to Pyrrolo[3,4-*b*]pyridine. *Organic Letters*, **2001**, *3* (6), 877-880.
522. Gazzotti, S.; Rainoldi, G.; Silvani, A., Exploitation of the Ugi–Joullié reaction in drug discovery and development. *Expert Opinion on Drug Discovery*, **2019**, *14* (7), 639-652.
523. Nazeri, M. T.; Farhid, H.; Mohammadian, R.; Shaabani, A., Cyclic Imines in Ugi and Ugi-Type Reactions. *ACS Combinatorial Science*, **2020**, *22* (8), 361-400.
524. Boltjes, A.; Dömling, A., The Groebke-Blackburn-Bienaymé Reaction. *European Journal of Organic Chemistry*, **2019**, *2019* (42), 7007-7049.
525. Kysil, V.; Khvat, A.; Tsirolnikov, S.; Tkachenko, S.; Williams, C.; Churakova, M.; Ivachtchenko, A., General Multicomponent Strategy for the Synthesis of 2-Amino-1,4-diazaheterocycles: Scope, Limitations, and Utility. *European Journal of Organic Chemistry*, **2010**, *2010* (8), 1525-1543.
526. La Spisa, F.; Meneghetti, F.; Pozzi, B.; Tron, G. C., Synthesis of Heteroarylogous 1*H*-Indole-3-carboxamidines via a Three-Component Interrupted Ugi Reaction. *Synthesis*, **2014**, *47* (4), 489-496.
527. Kielland, N.; Lavilla, R., Recent Developments in Reissert-Type Multicomponent Reactions. In *Synthesis of Heterocycles via Multicomponent Reactions II*, Orru, R. V. A.; Ruijter, E., Eds. Springer Berlin Heidelberg, Berlin, Germany, **2010**, pp 127-168.
528. Mohammadkhani, L.; Heravi, M. M., Synthesis of Various *N*-heterocycles Using the Ugi Four-Center Three-Component Reaction. *ChemistrySelect*, **2019**, *4* (34), 10187-10196.

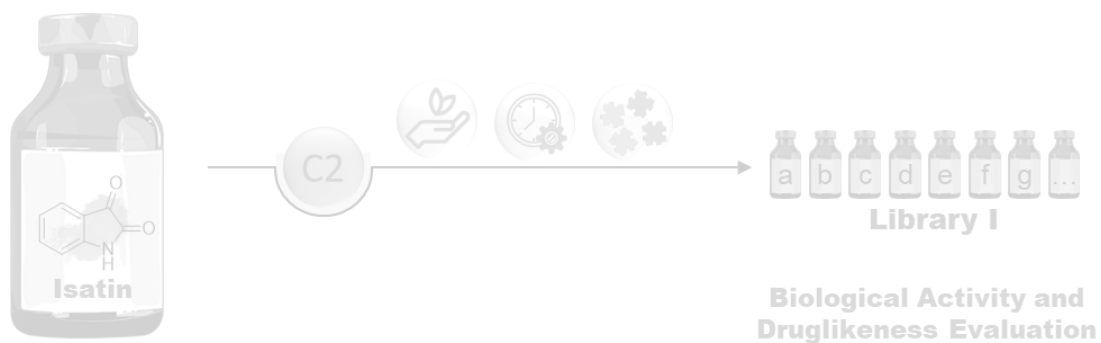
529. Giustiniano, M.; Moni, L.; Sangaletti, L.; Pelliccia, S.; Basso, A.; Novellino, E.; Tron, G. C., Interrupted Ugi and Passerini Reactions: An Underexplored Treasure Island. *Synthesis*, **2018**, *50* (18), 3549-3570.
530. Pelliccia, S.; Alfano, I. A.; Galli, U.; Novellino, E.; Giustiniano, M.; Tron, G. C., α -Amino Acids as Synthons in the Ugi-5-Centers-4-Components Reaction: Chemistry and Applications. *Symmetry*, **2019**, *11* (6), 798.
531. Tao, Y.; Wang, Z.; Tao, Y., Polypeptoids synthesis based on Ugi reaction: Advances and perspectives. *Biopolymers*, **2019**, *110* (6), e23288.
532. Yang, B.; Zhao, Y.; Wei, Y.; Fu, C.; Tao, L., The Ugi reaction in polymer chemistry: syntheses, applications and perspectives. *Polymer Chemistry*, **2015**, *6* (48), 8233-8239.
533. Monk, J. P.; Brogden, R. N., Naftifine - a review of its antimicrobial activity and therapeutic use in superficial dermatomycoses. *Drugs*, **1991**, *42* (4), 659-672.
534. Flick, A. C.; Leverett, C. A.; Ding, H. X.; McInturff, E.; Fink, S. J.; Helal, C. J.; O'Donnell, C. J., Synthetic Approaches to the New Drugs Approved During 2017. *Journal of Medicinal Chemistry*, **2019**, *62* (16), 7340-7382.
535. Petasis, N. A.; Boral, S., One-step three-component reaction among organoboronic acids, amines and salicylaldehydes. *Tetrahedron Letters*, **2001**, *42* (4), 539-542.
536. Guerrero, C. A.; Ryder, T. R., The Petasis Borono-Mannich Multicomponent Reaction. In *Boron Reagents in Synthesis*, Coca, A. Ed.; Oxford University Press, Washington DC, USA, **2016**, Vol. 1236, pp 275-311.
537. Candeias, N. R.; Montalbano, F.; Cal, P. M. S. D.; Gois, P. M. P., Boronic Acids and Esters in the Petasis-Borono Mannich Multicomponent Reaction. *Chemical Reviews*, **2010**, *110* (10), 6169-6193.
538. Souza, R. Y.; Bataglion, G. A.; Ferreira, D. A. C.; Gatto, C. C.; Eberlin, M. N.; Neto, B. A. D., Insights on the Petasis Borono-Mannich multicomponent reaction mechanism. *RSC Advances*, **2015**, *5* (93), 76337-76341.
539. Filho, J. F. A.; Lemos, B. C.; De Souza, A. S.; Pinheiro, S.; Greco, S. J., Multicomponent Mannich reactions: General aspects, methodologies and applications. *Tetrahedron*, **2017**, *73* (50), 6977-7004.
540. Wu, P.; Givskov, M.; Nielsen, T. E., Reactivity and Synthetic Applications of Multicomponent Petasis Reactions. *Chemical Reviews*, **2019**, *119* (20), 11245-11290.
541. Wu, P.; Nielsen, T. E., Petasis three-component reactions for the synthesis of diverse heterocyclic scaffolds. *Drug Discovery Today: Technologies*, **2018**, *29*, 27-33.
542. NobelPrize.org, Press release: The Nobel Prize in Chemistry 2021, available in <https://www.nobelprize.org/prizes/chemistry/2021/press-release/> (accessed 06/10/2021).
543. Lou, S.; Schaus, S. E., Asymmetric Petasis Reactions Catalyzed by Chiral Biphenols. *Journal of the American Chemical Society*, **2008**, *130* (22), 6922-6923.
544. Han, W.-Y.; Wu, Z.-J.; Zhang, X.-M.; Yuan, W.-C., Enantioselective Organocatalytic Three-Component Petasis Reaction among Salicylaldehydes, Amines, and Organoboronic Acids. *Organic Letters*, **2012**, *14* (4), 976-979.

545. Han, W.-Y.; Zuo, J.; Zhang, X.-M.; Yuan, W.-C., Enantioselective Petasis reaction among salicylaldehydes, amines, and organoboronic acids catalyzed by BINOL. *Tetrahedron*, **2013**, *69* (2), 537-541.
546. Jiang, Y.; Schaus, S. E., Asymmetric Petasis Borono-Mannich Allylation Reactions Catalyzed by Chiral Biphenols. *Angewandte Chemie International Edition*, **2017**, *56* (6), 1544-1548.
547. Marques, C. S.; McArdle, P.; Erxleben, A.; Burke, A. J., Accessing New 5- α -(3,3-Disubstituted Oxindole)-Benzylamine Derivatives from Isatin: Stereoselective Organocatalytic Three Component Petasis Reaction. *European Journal of Organic Chemistry*, **2020**, *2020* (24), 3622-3634.
548. Brunel, J. M., BINOL: A Versatile Chiral Reagent. *Chemical Reviews*, **2005**, *105* (3), 857-898.
549. Akiyama, T.; Itoh, J.; Fuchibe, K., Recent Progress in Chiral Brønsted Acid Catalysis. *Advanced Synthesis & Catalysis*, **2006**, *348* (9), 999-1010.
550. Nguyen, T.; Chen, P.-A.; Setthakarn, K.; May, J., Chiral Diol-Based Organocatalysts in Enantioselective Reactions. *Molecules*, **2018**, *23* (9), 2317.
551. Brandão, P.; Marques, C. S.; Carreiro, E. P.; Pineiro, M.; Burke, A. J., Engaging Isatins in Multicomponent Reactions (MCRs) – Easy Access to Structural Diversity. *The Chemical Record*, **2021**, *21* (4), 924-1037.
552. Brandão, P.; Marques, C.; Burke, A. J.; Pineiro, M., The application of isatin-based multicomponent-reactions in the quest for new bioactive and druglike molecules. *European Journal of Medicinal Chemistry*, **2021**, *211*, 113102.
553. Esmaeili, A. A.; Amini Ghalandarabad, S.; Jannati, S., A novel and efficient synthesis of 3,3-disubstituted indol-2-ones via Passerini three-component reactions in the presence of 4Å molecular sieves. *Tetrahedron Letters*, **2013**, *54* (5), 406-408.
554. Kaicharla, T.; Yetra, S. R.; Roy, T.; Biju, A. T., Engaging isatins in solvent-free, sterically congested Passerini reaction. *Green Chemistry*, **2013**, *15* (6), 1608.
555. Lesma, G.; Meneghetti, F.; Sacchetti, A.; Stucchi, M.; Silvani, A., Asymmetric Ugi 3CR on isatin-derived ketimine: synthesis of chiral 3,3-disubstituted 3-aminoxindole derivatives. *Beilstein Journal of Organic Chemistry*, **2014**, *10*, 1383-1389.
556. Rainoldi, G.; Lesma, G.; Picozzi, C.; Lo Presti, L.; Silvani, A., One step access to oxindole-based β -lactams through Ugi four-center three-component reaction. *RSC Advances*, **2018**, *8* (61), 34903-34910.
557. Beyrati, M.; Hasaninejad, A., One-pot, three-component synthesis of spiroindoloquinazoline derivatives under solvent-free conditions using ammonium acetate as a dual activating catalyst. *Tetrahedron Letters*, **2017**, *58* (20), 1947-1951.
558. Yavari, I.; Askarian-Amiri, M., A synthesis of spiroindolo[2,1-*b*]quinazoline-6,2'-pyrido[2,1-*b*][1,3]oxazines from tryptanthrins and Huisgen zwitterions. *Synthetic Communications*, **2021**, *51* (10), 1602-1608.

559. Filatov, A. S.; Knyazev, N. A.; Shmakov, S. V.; Bogdanov, A. A.; Ryazantsev, M. N.; Shtyrov, A. A.; Starova, G. L.; Molchanov, A. P.; Larina, A. G.; Boitsov, V. M.; Stepanov, A. V., Concise Synthesis of Tryptanthrin Spiro Analogues with *In Vitro* Antitumor Activity Based on One-Pot, Three-Component 1,3-Dipolar Cycloaddition of Azomethine Ylides to Cyclopropenes. *Synthesis*, **2019**, 51 (03), 713-729.
560. Beyrati, M.; Forutan, M.; Hasaninejad, A.; Rakovský, E.; Babaei, S.; Maryamabadi, A.; Mohebbi, G., One-pot, four-component synthesis of spiroindoloquinazoline derivatives as phospholipase inhibitors. *Tetrahedron*, **2017**, 73 (34), 5144-5152.

Chapter 2

In the Quest for New Bioactive Oxindole Derivatives: Engaging Isatin in the U4CR



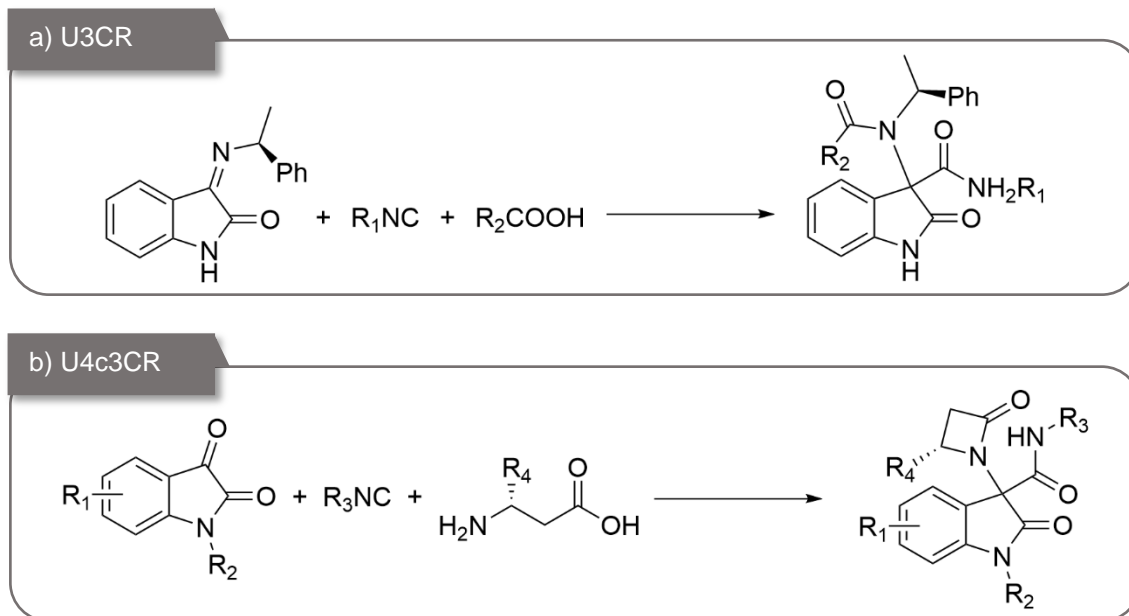
2.1. Introduction

MCRs are a valuable tool for the diversity-oriented synthesis of bioactive and druglike compounds. This approach, which allows high structural diversity in short synthetic pathways, make them a highly endorsed methodology in drug discovery for the generation and identification of hit compounds, as well as for hit-to-lead optimization processes, and even for the synthesis of APIs. They present several advantages, since the synthesis of new molecules occurs at a fast pace, and often at a lower cost when compared to more time-consuming and more laborious (and often troublesome) synthetic routes.¹⁻³ Several bioactive molecules have been synthesized using different MCRs, or even combination of different MCRs, highlighting their relevance for the discovery of new potential drug candidates, as recently reviewed in the literature.^{4, 5} Another feature of MCRs that intensifies their interest in modern medicinal and organic chemistry, is their inherent sustainability, since the green chemistry principles are intrinsically fulfilled in the vast majority of these reactions.⁶

Among the different MCRs available in the synthetic chemists toolbox, isocyanide-based MCRs play a pivotal role in several synthetic approaches. The Ugi reaction emerges of this class of MCRs as one of the most versatile examples. As already explored in Chapter 1, the Ugi reaction, classically involving aldehydes (although it can be replaced by other carbonyl compounds), a primary amine, a carboxylic acid and an isocyanide, leads to the formation of α -amino acyl amide derivatives, often designated as Ugi adducts or peptoids, due to the generation of two new amide bonds in the final product.^{7, 8}

Isatin, a key building block for the synthesis of compounds bearing the oxindole core, a known privileged structure in medicinal chemistry, is the central focus of attention of this Chapter. Despite the vast number of publications reporting the synthetic relevance and versatility of isatin,^{9, 10} including its use as starting material in MCRs,¹¹⁻¹³ there are only two very recent examples of isatin-based Ugi reaction, reported by the group of Silvani and co-workers. In the first example, a stereoselective U3CR was carried out using a chiral isatin-derived ketimine as starting material, and combining it with isocyanides and carboxylic acids (**Scheme 2.1 a**).¹⁴ In the second example, a Ugi four-center three component reaction (U4c3CR) was established, using isatin, isocyanides and β -amino acid reagents (**Scheme 2.1 b**).¹⁵ More attention will be given to this second approach in Chapter 3. Despite the interest of oxindole derivatives in the field of medicinal chemistry and drug discovery, for the library achieved using U3CR no biological activity was reported, whereas the oxindole- β -lactam derivatives obtained using U4c3CR was evaluated in what concerns their antibacterial activity, but no relevant

effect was observed. These results are quite underwhelming, considering the privileged structure nature of the oxindole core.



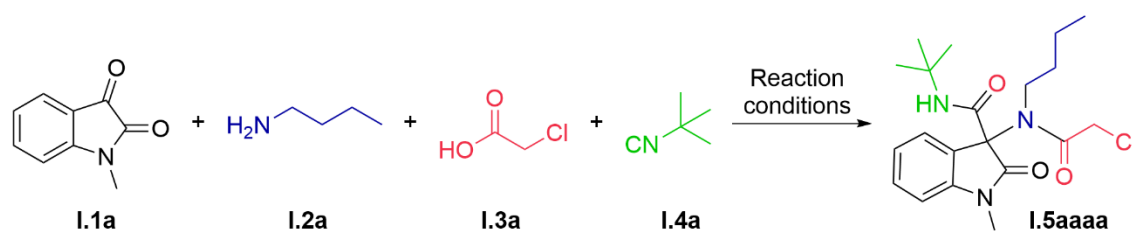
Scheme 2.1. Reported examples of isatin-based U3CR (a) and U4c3CR (b).

Furthermore, no examples of isatin-based U4CR were found in the literature, despite this scaffold being widely applied in diverse MCRs in the quest for new bioactive compounds, as recently reviewed by our group.^{12, 13} With this in mind, we decided to explore the possibility to apply isatin in the U4CR, with the goal to achieve new druglike compounds with relevant biological activity.

2.2. Isatin-Based U4CR

2.2.1. Reaction Conditions Optimization

The U4CR is a very complex MCR, as already thoroughly described and discussed in Chapter 1. Initially, the isatin-based U4CR was optimized by investigating the effect of several variables, such as solvent, catalyst, activation technique, stoichiometry, and temperature. To explore the impact of these variables, the reaction involving *N*-methylisatin (**I.1a**), *n*-butylamine (**I.2a**), chloroacetic acid (**I.3a**), and *tert*-butyl isocyanide (**I.4a**) was selected as the model reaction. The tested conditions are summarized in **Table 2.1**.

Table 2.1. Optimization of the U4CR conditions.

Entry ^a	Solvent	Catalyst (10 mol%)	Activation technique	Stoichiometry (1.1a:1.2a:1.3a:1.4a)	Temp. (°C)	Yield ^b (%)
1	MeOH	-	Stirring	1:1:1:1	rt	15
2	MeOH	-	Stirring	1:1:1:1	70	<15
3	DES	-	Stirring	1:1:1:1	rt	Trace
4	DES	-	Ultrasounds	1:1:1:1	rt	Trace
5	DES	-	Ultrasounds	1:1:1:1	70	Trace
6	MeOH	InCl ₃	Stirring	1:1:1:1	rt	19
7	MeOH	InCl ₃	Stirring	1:1.2:1:1.2	rt	47
8	ACN	InCl ₃	Stirring	1:1.2:1:1.2	rt	37
9	2-MeTHF	InCl ₃	Stirring	1:1.2:1:1.2	rt	32
10	CH ₂ Cl ₂	InCl ₃	Stirring	1:1.2:1:1.2	rt	17
11	TFE	InCl ₃	Stirring	1:1.2:1:1.2	rt	50 ^c
12	MeOH	ZnCl ₂	Stirring	1:1.2:1:1.2	rt	44
13	MeOH	K ₃ PO ₄	Stirring	1:1.2:1:1.2	rt	21
14	MeOH	H ₃ PO ₄	Stirring	1:1.2:1:1.2	rt	45
15	MeOH	-	MAOS	1:1.2:1:1.2	70	<15
16	MeOH	-	MAOS	1:1.2:1:1.2	100	Trace
17	MeOH	InCl ₃	MAOS	1:1.2:1:1.2	70	15
18	MeOH	InCl ₃ ^d	MAOS	1:1.2:1:1.2	70	15
19	-	InCl ₃	HSBM ^e	1:1.2:1:1.2	rt	Trace
20	LAG ^f	InCl ₃	HSBM ^e	1:1.2:1:1.2	rt	Trace
21	- ^g	InCl ₃	HSBM ^e	1:1.2:1:1.2	rt	<15
22	MeOH	InCl ₃	Stirring	1:1.5:1.5:1.5	rt	65
23	MeOH	-	Stirring	1:1.5:1.5:1.5	rt	34 ^h

^aReaction conditions: **1a** (200 mg, 1.24 mmol, 1 equiv) was dissolved in 1 mL of solvent in the presence of 150 mg of molecular sieves (MS) 3Å and the remaining components (**2a**, **3a** and **4a**) were added to the reaction vessel and allowed to stir at the indicated condition for 48 h. ^bIsolated yield. ^cThe reaction was allowed to proceed for 72 h. ^d20 mol% of InCl₃ were used. ^eMolecular sieves were not used in the HSBM experiments. ^f100 μL of MeOH were added to the reactor. ^gIn the presence of Na₂SO₄. ^hThe reaction was allowed to proceed for 72 h. DES=deep eutectic solvent urea:choline chloride. LAG=liquid-assisted grinding. MAOS=microwave-assisted organic synthesis. HSBM=high-speed ball-milling.

In the first attempt, classic Ugi reaction conditions were applied (**Table 2.1**, entry 1), using methanol as solvent at room temperature, and equimolar quantities of the four components. The expected Ugi product **1.5aaaa** was obtained, however in low yield (15%). Next, an experiment at higher temperature was performed, but no improvement

in the reaction yield was observed (**Table 2.1**, entry 2). Recent reports explored the utility of DESs in MCRs,¹⁶ including in the Ugi reaction.¹⁷ For this reason, it was decided to include de DES urea:choline chloride in the reaction conditions screening. Unfortunately, only trace amounts of the Ugi reaction product were detected (**Table 2.1**, entry 3). Due to the poor solubility of **I.1a** in the selected DES, a different activation technique was evaluated, by attempting to perform the reaction under sonication at both room temperature and 70 °C, but similar results were achieved (**Table 2.1**, entries 4 and 5, respectively).

Due to this failure in promoting the reaction using DES, we looked to recent application of catalysts in the Ugi reaction reported in the literature.^{18, 19} For catalyst screening, methanol under conventional stirring at room temperature were selected as reaction conditions. First, indium(III) trichloride was selected for initial assessment, as this Lewis acid is easy to handle, cheap, safe, stable to air and moisture, and already proved to be very useful in a wide range of MCRs.²⁰ In equimolar conditions for the four components, a slight improvement in reaction yield (19%) was observed (**Table 2.1**, entry 6). However, as in every reaction condition tested until this point, the reaction reached steady state without total consumption of **I.1a**. For this reason, an attempt was performed using slight excess of the amine and isocyanide components (**Table 2.1**, entry 7), and a considerable improvement in the observed yield was attained (47%).

With these conditions in hand, a solvent screening study was performed, using solvents with different polarities and properties. As expected for the Ugi reaction, polar protic solvents such as 2,2,2-trifluoroethanol (TFE) (**Table 2.1**, entry 11) afforded better results than polar aprotic and non-polar solvents, such as acetonitrile, 2-methyltetrahydrofuran and dichloromethane (**Table 2.1**, entries 8-10, respectively). To further proceed with exploring the reaction conditions, methanol was chosen over TFE, because the reaction was faster in this solvent.

The catalyst screening proceeded with other Lewis acids, as well as other commonly used catalysts in the Ugi reaction, being evaluated. Despite improvements being observed with all of them (**Table 2.1**, entries 12-14) when comparing with the catalyst-free procedure, InCl₃ emerged as the best option.

In order to consolidate the sustainability aspect of this MCR process, it was decided to explore eco-friendly activation techniques, namely microwave-assisted organic synthesis (MAOS) (**Table 2.1**, entries 15-18) and high-speed ball-milling (HSBM) (**Table 2.1**, entries 19-21), but only trace amounts and low yields of the desired compound **I.5aaaa** were observed.

Finally, an excess of the amine, carboxylic acid and isocyanide components was tested, with considerable improvement in the yield being achieved (**Table 2.1**, entry 22).

This reaction condition was considered as a good compromise between reaction performance and process sustainability, and therefore used for substrate scope screening. Performing the reaction in the absence of the catalyst significantly dropped the reaction yield (**Table 2.1**, entry 23).

2.2.2. Library I Synthesis

With the optimized reaction conditions in hands, efforts were made to study the substrate scope, in order to generate a structurally diverse library (**Figure 2.1**). Several *N*-substituted and *N*-unsubstituted isatins were screened (**I.1a- I.1j**), as well as different primary amines (**I.2a- I.2i**), carboxylic acids (**I.3a- I.3i**) and isocyanides (**I.4a- I.4e**).

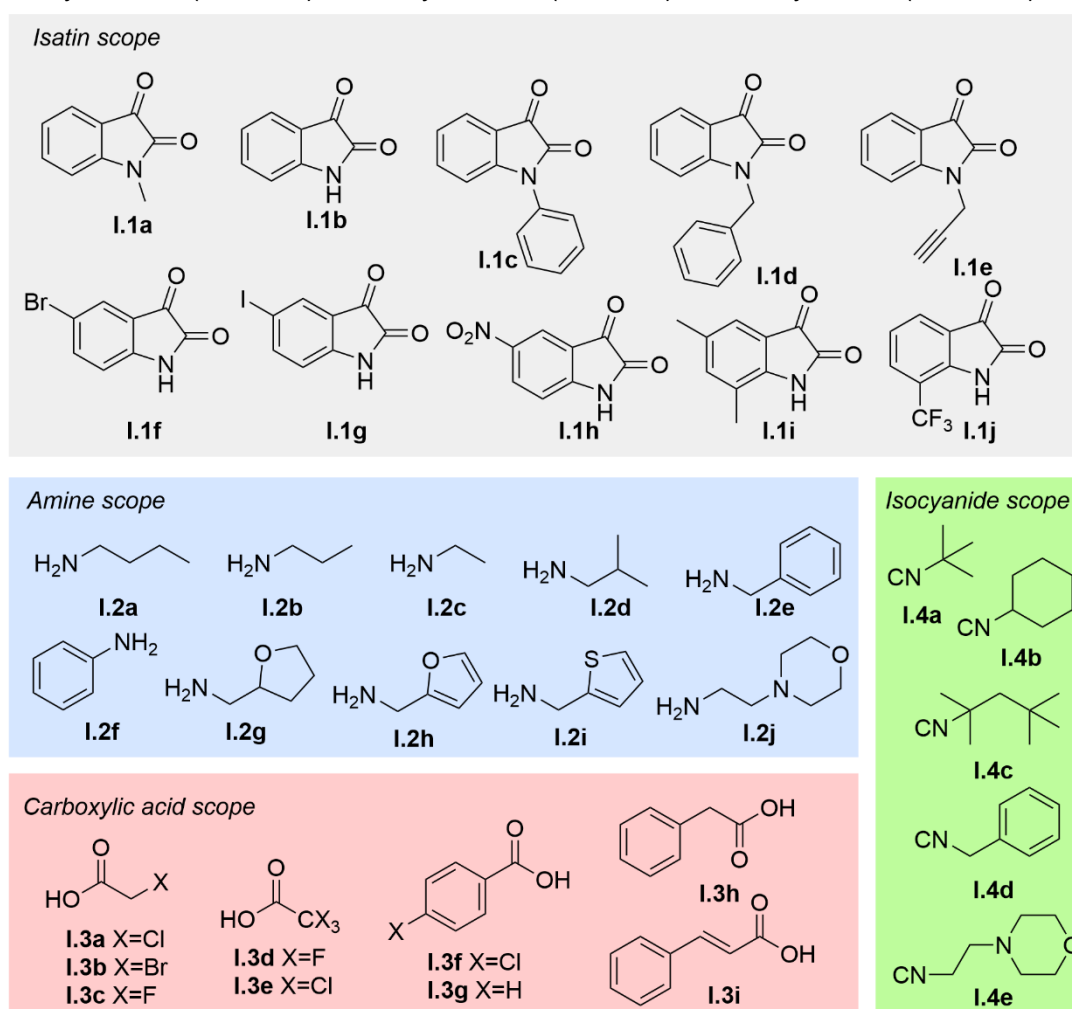


Figure 2.1. Reagent scope for the U4CR.

A total of 37 derivatives were obtained, showcasing the versatility of this approach to efficiently attain structural diversity (**Figure 2.2**). The following code was developed to identify the compounds: I.5 indicates Ugi adduct, the first letter corresponds to the isatin reactant, the second to the amine precursor, the third letter indicates the carboxylic acid

and the fourth letter the isocyanide component. The developed methodology could accommodate *N*-substituted and *N*-unsubstituted isatins, with different substitution patterns, with success. Another advantage found with this approach was that, for some of the synthesized compounds, the pure final Ugi reaction product could be isolated in a simple, chromatography-free process, with considerable impact on the sustainability of the process.

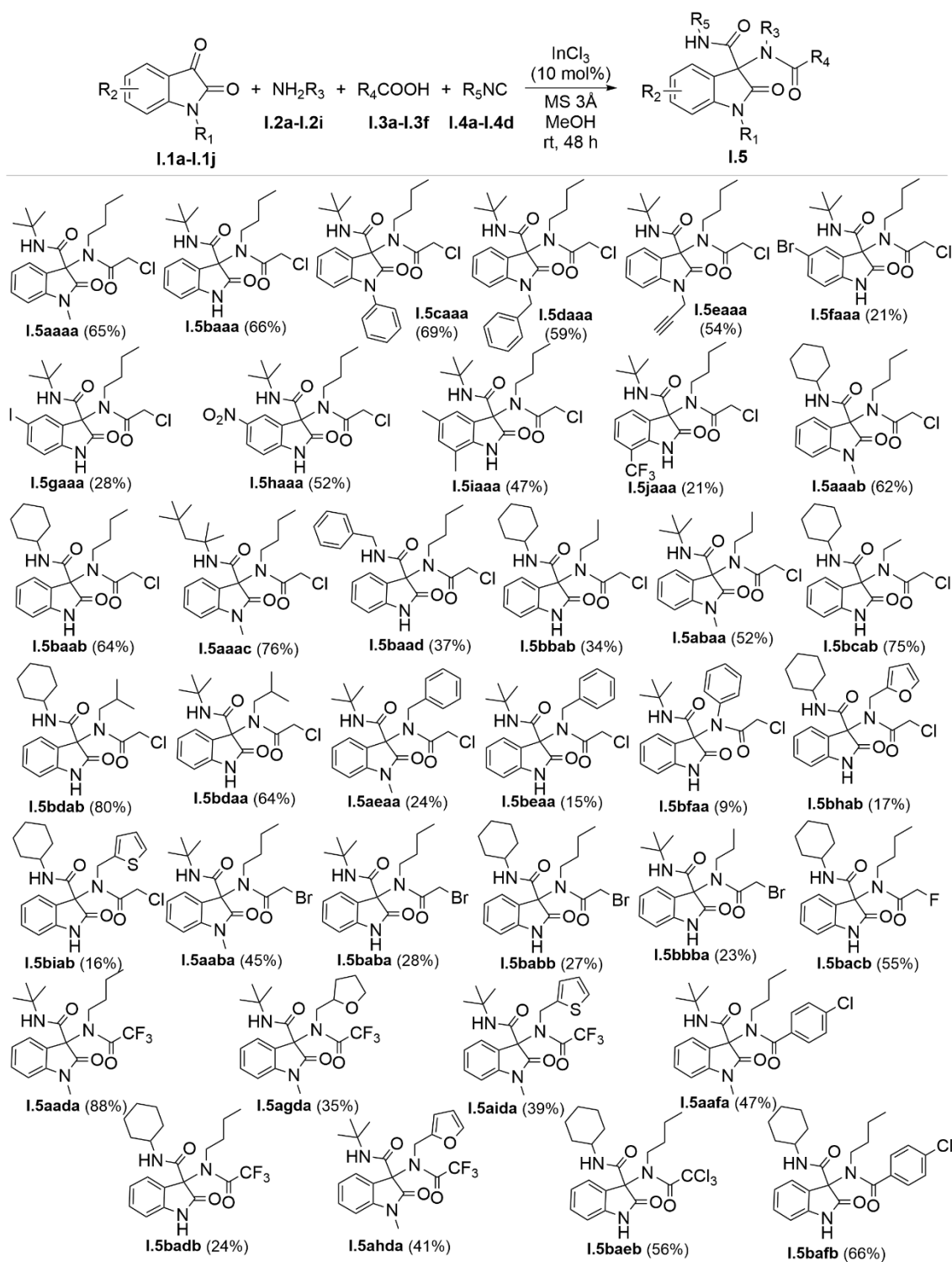
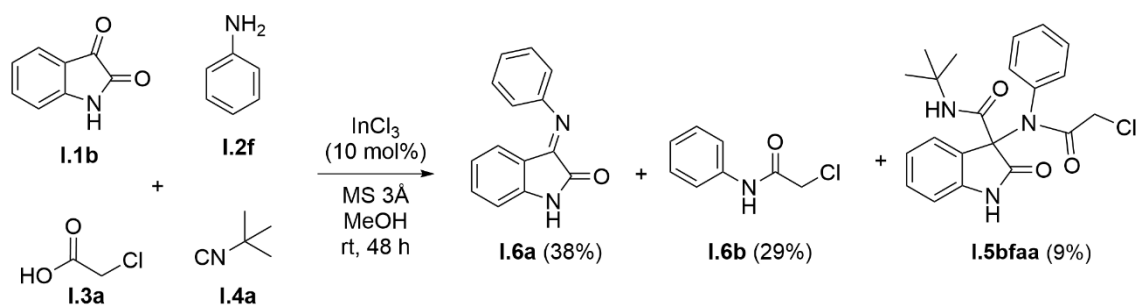


Figure 2.2. Library of oxindole derivatives obtained via U4CR.

Concerning the isatin scope, it was noticeable that when using isatins **I.1f**, **I.1g** and **I.1j**, a considerable decrease in yield was observed. This can be explained by the poor solubility exhibited by **I.1f** and **I.1g** in methanol, as well as in the other evaluated Ugi reaction solvents, namely TFE whereas **I.1j** displayed a polarity similar to the one displayed by the Ugi adduct, making the purification process more challenging.

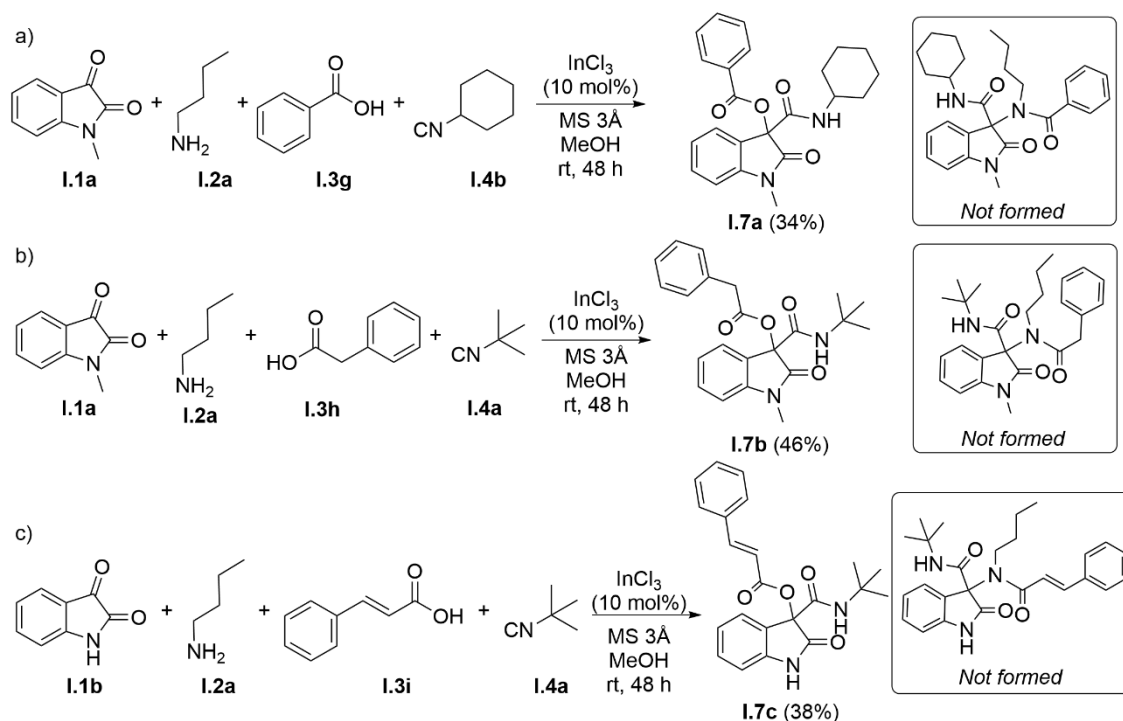
Analyzing the amine scope, linear aliphatic primary amines (**I.2a**- **I.2c**) and branched aliphatic amines (**I.2d**) were successfully used in this approach, achieving the desired U4CR products with moderate to very good yields. However, the presence of an aromatic moiety (**I.2e**, **I.2h**, and **I.2i**) led to a relevant decrease in the observed yields. It is hypothesized that this occurs due to steric effects, or even electronic effects, such as possible π - π interaction between the aromatic ring of the amine component and the isatin core. Aniline **I.2f** led to the lowest isolated yield of the library (**I.5faaa**). In this case, the U4CR is not the most promoted reaction, as two other products were successfully isolated from the reaction: (*E*)-3-(phenylimino)indolin-2-one (**I.6a**) was isolated as the main product, indicating that the imine intermediate was highly stable and therefore the progress of the U4CR was considerably halted at this stage; and 2-chloro-*N*-phenylacetamide (**I.6b**), another secondary product, with its formation leading to the consumption of two components in this secondary reaction (**Scheme 2.2**). When **I.2j** was employed as the primary amine, no reaction occurred and therefore we could not introduce the morpholine unit into the U4CR products using this methodology.



Scheme 2.2. Side-products attained when aniline is used in this isatin-based U4CR.

Another attempt to include the morpholine moiety in the U4CR was performed using isocyanide **I.4e**. The reaction did not occur, indicating that the morpholine unit might prevent the U4CR. This might be due to the basic nature of this heterocycle, as the pH of the reaction media can play a crucial role in this chemical transformation, as will be discussed later in this work. In what concerns the remaining isocyanides screened (**I.4a**-**I.4d**), all of them were successfully employed in the U4CR, with aliphatic isocyanides (**I.4a**-**I.4c**) generating overall good yields, whereas benzyl isocyanide (**I.4d**) leads to a considerable decrease in the reaction yield.

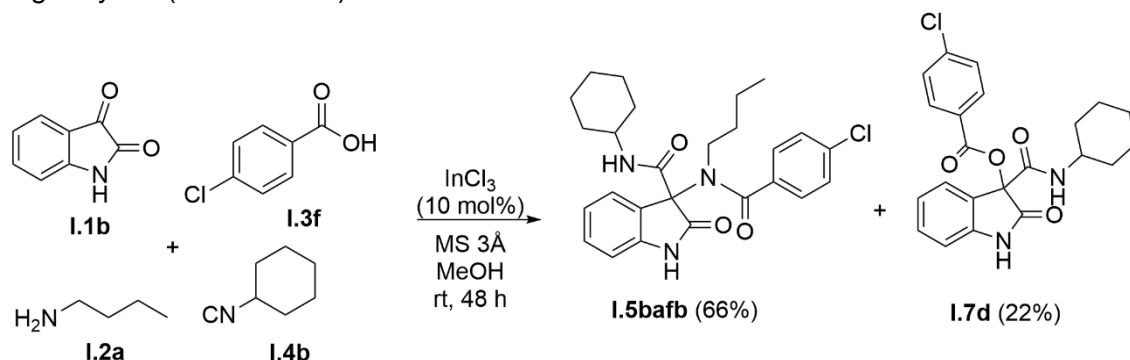
The impact of the carboxylic acid component in the U4CR outcome was greater than the one observed for any other component. Monohaloacetic acids **I.3a-I.3c** proved to be suitable to be applied for this reaction under our standard conditions. The size of the halogen atom might contribute to the reaction success, as bromoacetic acid (**I.3b**) led to overall lower yields than the chloro- and fluoroacetic acid counterparts. Trihaloacetic acids **I.3d** and **I.3e** were also successfully used in the developed U4CR. For example, using trifluoroacetic acid (**I.3d**) allowed improved yields, even when amines bearing aromatic rings were employed as substrates. Next, we attempted to introduce an aromatic ring in the carboxylic acid moiety of this U4CR, using benzoic acid (**I.3g**). Surprisingly, instead of an Ugi adduct, a Passerini adduct (**I.7a**) (product resulting from the reaction between a carbonyl component, a carboxylic acid and an isocyanide) was obtained from this reaction (**Scheme 2.3 a**). Initially, the hypothesis that this outcome was due to steric effects created by the proximity of the aromatic ring with the carboxylic acid functional group was explored, and the use of phenylacetic acid (**I.3h**) and cinnamic acid (**I.3i**) was evaluated, in order to increase this distance. However, the outcome was similar, with the formation of the Passerini reaction products **I.7b** and **I.7c** (**Scheme 2.3 b and c**).



Scheme 2.3. Passerini adducts obtained when screening benzoic acid, phenylacetic acid and cinnamic acid as carboxylic acid component of the U4CR.

With these intriguing findings, it was important to further explore what was the cause for this change in the reactivity in what concerns the carboxylic acid component. As detailed previously, a remarkable improvement in yield was observed when

trihaloacetic acids were used as the carboxylic acid component. Since these trihaloacetic acids display a very low pK_a value, it was hypothesized that this property of the carboxylic acid component could effectively be relevant for the U4CR outcome. To evaluate this hypothesis, *p*-chlorobenzoic acid (**I.3f**) was selected, as it keeps the close proximity between the carboxylic acid functional group but, at the same time, presents a lower pK_a value than **I.3g-I.3i**. Interestingly, in this reaction, both the Ugi adduct (**I.5bafb**) and the Passerini product (**I.7d**) were successfully isolated, with the former being produced in higher yield (**Scheme 2.4**).



Scheme 2.4. Exploring the U4CR using *p*-chlorobenzoic acid achieves both the Ugi and Passerini adducts of isatin.

Gathering all this information together, it is noteworthy that for the reaction conditions explored, isatin-based Ugi adduct formation is modulated by the pK_a of the carboxylic acid component, with less acidic carboxylic acids leading to the formation of the corresponding Passerini adducts, whereas highly acidic carboxylic acids generate exclusively the Ugi adducts. The experiments with *p*-chlorobenzoic acid, which displays a pK_a of 3.98 and affords both adducts, indicate that carboxylic acid components with pK_a around 4 will enable the formation of both the Ugi and Passerini adducts, whereas less acidic compounds will form the Passerini adduct exclusively, and more acidic compounds will generate the Ugi adduct (**Figure 2.3**). This finding might also explain the failure to accomplish this reaction with components bearing the morpholine unit, due to its basic nature.

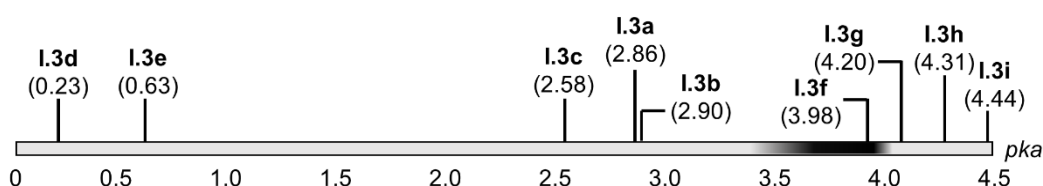


Figure 2.3. pK_a scale of the carboxylic acid components²¹ used in the screening of the U4CR (the darker area indicates the potential region where both Ugi and Passerini adducts are formed).

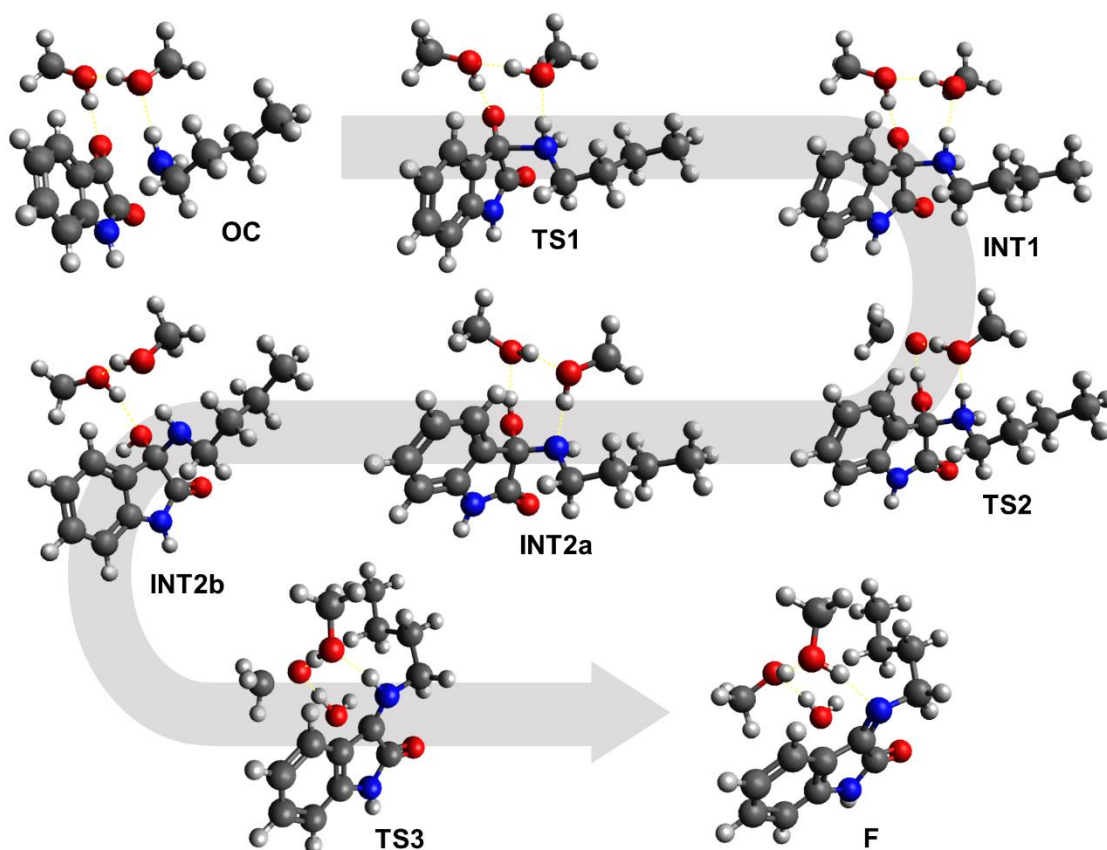
It is well established that the carboxylic acid component plays a crucial role in the Ugi reaction mechanism, including in the activation of the imine intermediate, the reversible addition to the nitrilium ion, and also for the success of the irreversible Mumm rearrangement.²² However, taking a look to recent literature exploring this effect of the pK_a on the Ugi reaction, only one example could be considered as slightly related. Okandeji and Sello, while exploring the Passerini reaction, noticed that when strong carboxylic acids were employed ($pK_a < 2$), instead of observing the formation of the expected α -acyloxyamide Passerini derivatives, α -aminoacyl amide derivatives (typical Ugi reaction products) were observed in higher yields. This would result of the *in situ* Brønsted acid-catalyzed reaction between the isocyanide and the aldehyde components, affording an imine that would undergo the typical Ugi reaction.²³ In the case reported in this work, such reaction was not observed, otherwise two units of the isocyanide component would be present in the final product isolated, which is not supported by the structural elucidation of the isolated compounds. This might also be due to isatin unique structural features, that despite allowing the carbonyl at position 3 to undergo Passerini or Ugi transformations, it does not possess the same reactivity as aldehydes and simpler ketones more commonly explored in the U4CR.

2.2.3. Theoretical Study: Insights into Isatin-Imine Formation

As highlighted in Chapter 1, there is a vast number of reports on the application of isatin-based MCRs.¹² However, the information about the isatin-based Ugi reaction is scarce.^{14, 15} Therefore, we decided to investigate the reactivity of isatin in this process at the C3 position. While in the classical approaches, the Ugi reaction uses an aldehyde, in our approach we explored the reactivity of the C3 carbonyl group of the isatin scaffold, vicinal to the carbonyl group of the cyclic amide. Expecting to understand the reactivity of isatin towards the primary amine in the isatin-imine formation process, theoretical density functional theory (DFT) calculations were performed for the first step of the Ugi reaction (*i.e.*, condensation of *n*-butylamine with isatin to attain 3-(butylimino)indolin-2-one).

The analysis started with the formation of a pre-reaction orientation complex (**OC**), involving isatin, *n*-butylamine and two methanol molecules interconnected via hydrogen bonds and van der Waals interactions. Previously, it has been reported that two solvent molecules (methanol in our case) are crucial for the correct description of the mechanism of imine formation from amines and carbonyl compounds.²⁴ In the first step of the reaction, a new C–N bond is formed between the C3 carbonyl atom of isatin and the

amine, to give a zwitterionic intermediate (**INT1**) via transition state **TS1** (**Figure 2.4**). The distance between C3 and the nitrogen atom of *n*-butylamine is 2.480 Å for **OC**, and reduces to 1.878 Å in **TS1**, reaching 1.608 Å in **TS1**, when C3 assumes a quaternary conformation. The formation step of **TS1** is virtually barrierless. A slightly lower Gibbs free energy of **TS1** relative to **OC** (by 0.5 kcal/mol) may be explained by the fact that the optimization of geometry was carried out on the total energy surface rather than on the Gibbs free energy surface. The formed zwitterionic intermediate **INT1** is exergonic by 3.7 kcal/mol relative to **OC** (**Scheme 2.5**).



Scheme 2.5. Ball-and-stick representation of **OC**, transition states, intermediaries and **F**.

Next, a hydrogen transfer from the amino group to the carbonyl in **INT1** leads to the formation of carbinolamine (**INT2a**) through transition state **TS2**. This transfer is indirect, as the two methanol molecules play the role of a proton shuttle significantly facilitating the hydrogen transfer compared to the process without any assistance from the solvent molecules.²⁴ It is noticeable for the fact that in **TS2** the protons promoting the hydrogen bonds are located almost halfway between the oxygen atoms or the oxygen and nitrogen atoms. Intermediate **INT2a** is quite stable being 10.8 kcal/mol lower in energy than initial orientation complex **OC** and its formation occurs with a very low

activation barrier of only 1.1 kcal/mol. At this intermediate, the distance between C3 and the oxygen and nitrogen atoms is now very similar (1.389 Å and 1.462 Å, respectively) and the first proton transfer is completed.

The final step includes the generation of complex **INT2b** which is isomeric with **INT2a** but with a different H-bond network, allowing the second methanol-assisted proton transfer from the imine moiety to the OH group via **TS3** to provide the final product **F**. This proton transfer is accompanied by the C3–O bond cleavage and elimination of a water molecule. At this stage, the C–N distance is established at 1.271 Å, with the double bond being formed and C3 returns to its planar configuration. The third reaction step is the rate-limiting one with an activation barrier of 27.5 kcal/mol, which qualitatively correlates with the experimental conditions used in this experiment. This information will be of great interest in Chapter 4, where it will be clear the importance of the unique reactivity displayed by isatin's C3 carbonyl group. The 3-(butylimino)indolin-2-one intermediate further reacts with chloroacetic acid and *tert*-butyl isocyanide to yield the final Ugi reaction product.

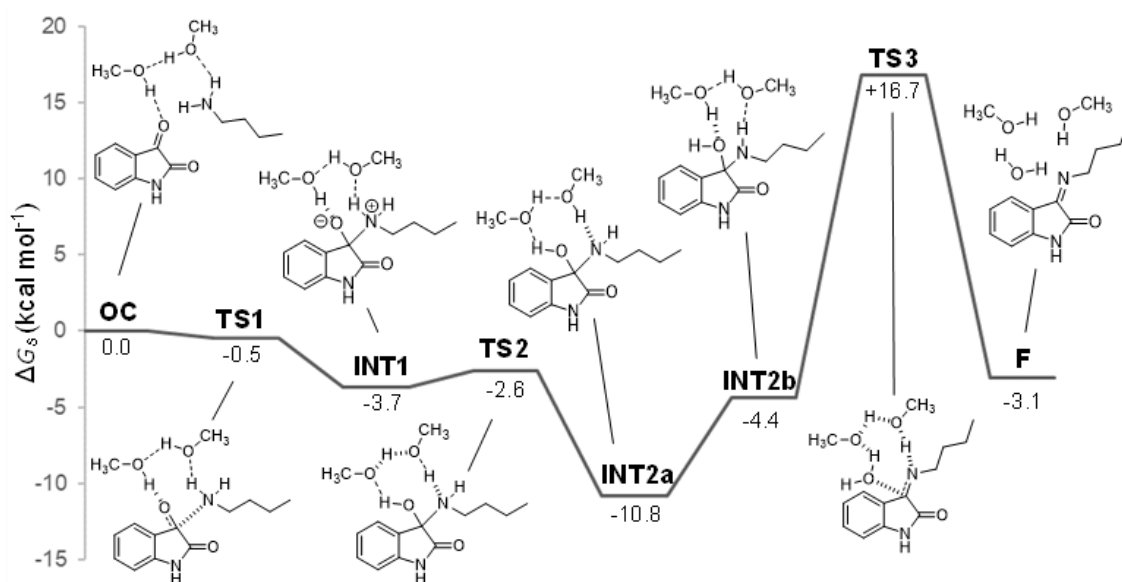


Figure 2.4. Energy profile of imine formation (relative Gibbs free energies are indicated for each level in kcal/mol).

2.2.4. Druglikeness Evaluation

With the library of U4CR products in hand, *in silico* evaluation of the druglikeness profiles of these new oxindole derivatives was performed using SwissADME®. This evaluation is relevant in early stages of drug discovery, because despite not being golden

rules, they remain good statistical indicators, as proved by the fact that most small-molecule drugs approved over the past decade fit within the parameters established by these druglikeness filters.²⁵⁻²⁷

Three important descriptors for druglikeness compliance are the number of hydrogen bond acceptors and donors (HBA and HBD, respectively) and the number of rotatable bonds (RB). These parameters are considered (totally or partially) in the Lipinski (HBA \leq 10, HBD \leq 5), Muegge (HBA \leq 10, HBD \leq 5, and RB \leq 15) and Veber (RB \leq 10) filters. All our synthesized compounds comply with the Lipinski and Muegge filters in what concerns their parameters, whilst compounds **I.5daaa** and **I.5aaac** were non-compliant with the Veber filter, as both possess 11 RBs (**Figure 2.5**).

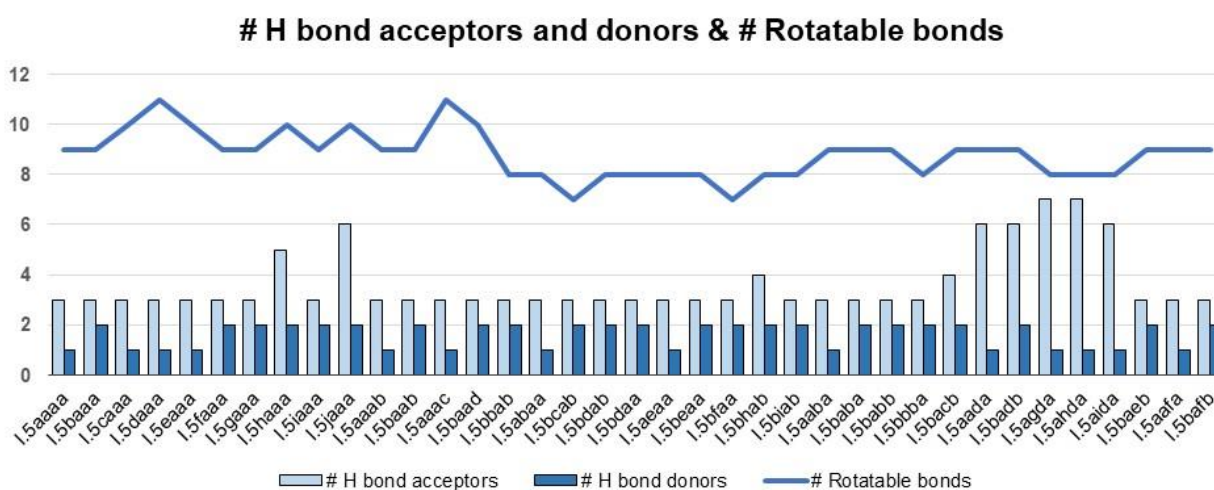


Figure 2.5. Calculated HBA, HBD and RB for the new oxindole-peptoid hybrids.

MW and lipophilicity (considering the value calculated by SwissADME® for consensus partition coefficient, CLogP, which takes into account five different LogP calculations – iLogP, XLogP3, WLogP, MLogP, SILICOS-IT) are two other physical-chemical properties taken in consideration by several of the druglikeness filters, including the Lipinski filter (MW \leq 500 Da, MLogP \leq 5), the Ghose filter (160 \leq MW \leq 480 Da, -0.4 \leq WLogP \leq 5.6), the Muegge filter (200 \leq MW \leq 600 Da, -2 \leq XLogP \leq 5), and the Egan filter (WLogP \leq 5.88). **Figure 2.6** correlates these two properties for the newly synthesized compounds which, with rare exceptions, comply with the druglikeness limits established by the mentioned filters. Exception for compound **I.5gaaa**, which displays a MW slightly superior to the upper limit of the Ghose and Lipinski filters, and compounds **I.5aaac** and **I.5bafb**, which although presenting a XLogP3 slightly above the limit established for the Muegge rule (WLogP3 for both compounds is 5.08), their CLogP, is within the desired interval.

are very close to the upper limit established by the filter, and furthermore, all the remaining LogP calculation methodologies display values well within this range.

Table 2.2. Compliance of the synthesized oxindole derivatives with the five evaluated druglikeness filters (green color means full compliance with the filter, while red color determines a non-compliance, with the number representing the number of violations).

		U4CR oxindole derivatives																		
		I.5aaaa	I.5baaa	I.5caaa	I.5daaa	I.5eaaa	I.5faaa	I.5gaaa	I.5haaa	I.5iaaa	I.5jaaa	I.5aaab	I.5baab	I.5aaac	I.5baad	I.5bbab	I.5abaa	I.5bcab	I.5bdab	I.5bdaa
Filters	Lipinski																			
	Ghose			1	1			1												
	Veber				1									1						
	Egan																			
	Muegge													1						
		U4CR oxindole derivatives																		
		I.5aea	I.5bea	I.5bfa	I.5bh	I.5bia	I.5aab	I.5ba	I.5ba	I.5bb	I.5bac	I.5aad	I.5ba	I.5ag	I.5ah	I.5aid	I.5bae	I.5aaf	I.5baf	
Filters	Lipinski																			
	Ghose																	1	1	
	Veber																			
	Egan																			
	Muegge																			1

The identification of PAINS in the synthesized library was also performed. None of the new compounds displayed alerts for PAINS, and therefore the exploration of their bioactive potential became of utmost importance.

2.2.5. Biological Activity Evaluation

Natural and synthetic oxindole derivatives are known for their wide potential as bioactive agents, as detailed in Chapter 1. Due to the intrinsic nature of oxindoles as privileged structures, our approach consisted in the use of a phenotypic assay to determine their potential as antiproliferative agents. These tests were performed by Professor José Padrón group, at the BioLab, Universidad de La Laguna, Spain.

Six tumor cell lines were selected for the screening, namely two breast cancer cell lines (HBL-100 and T-47D), one lung cancer cell line (A549), one colon cancer cell line (WiDr), one brain cancer cell line (SH-SY5Y), and one cervical cancer cell line (HeLa). The concentration to inhibit 50% of cell growth (GI_{50}) was determined and the obtained values are depicted in **Table 2.3**, and the range of antiproliferative activity shown in

Figure 2.8. The anticancer drugs cisplatin (CDDP) and paclitaxel (PTX) were used as reference standards for comparison purposes.

Table 2.3. GI_{50} obtained for the new oxindole derivatives obtained via U4CR
(n.t.=not tested).

	GI_{50} (μ M)					
	<i>A549</i>	<i>HBL-100</i>	<i>HeLa</i>	<i>SH-SY5Y</i>	<i>T-47D</i>	<i>WiDr</i>
I.5aaaa	3.0±0.5	1.4±0.3	1.7±0.4	1.1±0.2	3.3±0.6	2.3±0.1
I.5baaa	2.1±0.6	0.75±0.26	0.20±0.04	0.18±0.03	1.6±0.5	0.33±0.05
I.5caaa	2.7±0.5	2.1±0.7	1.8±0.3	1.3±0.01	2.4±0.4	2.0±0.4
I.5daaa	1.9±0.4	0.93±0.09	0.86±0.27	0.36±0.14	1.8±0.3	2.1±0.5
I.5eaaa	2.9±0.3	2.3±0.2	1.8±0.1	1.3±0.2	3.4±0.5	1.7±0.2
I.5faaa	1.2±0.4	0.19±0.04	0.0063± 0.0010	0.12±0.02	0.0094± 0.0035	0.014±0.003
I.5gaaa	1.0±0.2	0.000097± 0.000012	0.0065± 0.0031	0.052±0.019	1.4±0.2	0.0054± 0.0010
I.5haaa	1.4±0.4	0.69±0.10	0.23±0.01	0.16±0.04	1.3±0.6	0.30±0.09
I.5iaaa	1.0±0.4	0.029±0.012	0.023±0.003	0.17±0.05	0.066±0.023	0.054±0.020
I.5jaaa	2.2±0.3	1.3±0.4	1.0±0.01	0.50±0.18	2.7±0.7	0.41±0.13
I.5aaab	2.7±0.5	1.1±0.2	1.1±0.2	1.5±0.1	1.5±0.4	2.4±0.3
I.5baab	1.4±0.7	0.82±0.26	0.13±0.06	0.16±0.03	1.3±0.2	0.27±0.04
I.5aac	2.0±0.1	0.82±0.32	0.30±0.12	0.22±0.04	1.5±0.5	0.22±0.10
I.5baad	2.8±0.9	0.74±0.23	0.33±0.04	0.26±0.05	2.1±0.5	0.16±0.03
I.5bbab	1.6±0.4	0.20±0.06	0.25±0.10	0.29±0.05	0.21±0.08	0.13±0.01
I.5abaa	4.6±1.0	2.8±1.0	2.4±0.5	1.2±0.1	3.3±0.7	2.1±0.5
I.5bcab	1.8±0.3	0.43±0.13	0.57±0.18	0.20±0.01	1.4±0.3	0.27±0.09
I.5bdab	3.3±0.8	0.45±0.22	0.88±0.27	1.8±0.3	2.2±0.8	0.30±0.13
I.5bdaa	16±1.0	0.63±0.25	4.5±0.9	1.9±0.9	3.4±0.5	2.0±0.2
I.5aeaa	2.7±0.8	2.4±1.0	1.6±0.5	1.3±0.1	2.6±0.7	2.0±0.3
I.5beaa	2.1±0.4	0.70±0.12	0.28±0.07	0.71±0.31	2.1±0.5	0.39±0.15
I.5bfaa	1.6±0.5	0.16±0.06	0.29±0.11	0.23±0.05	0.72±0.34	0.27±0.08
I.5bhab	3.1±0.6	0.89±0.42	0.60±0.19	1.2±0.01	0.80±0.23	0.21±0.02
I.5biab	2.0±0.4	1.2±0.4	0.40±0.05	0.68±0.03	2.2±0.1	0.19±0.04
I.5aaba	1.9±0.7	0.78±0.27	0.84±0.32	0.18±0.05	2.7±0.9	1.9±0.1
I.5baba	1.6±0.1	0.24±0.08	0.18±0.08	0.18±0.02	1.4±0.1	0.21±0.01
I.5babb	2.2±0.3	0.89±0.27	0.13±0.01	0.31±0.10	1.4±0.5	0.029±0.004
I.5bbba	1.7±0.2	0.29±0.07	0.23±0.10	0.18±0.01	0.97±0.47	0.16±0.08
I.5bacb	4.4±0.9	78±33	4.4±0.04	27±8.7	32±13	28±8.6
I.5aada	65±23	91±13	54±21	23±0.3	80±24	51±1.3
I.5badb	8.1±2.8	16±3.9	8.1±2.7	16±0.2	11±4.7	4.8±1.4
I.5agda	>100	>100	>100	n.t.	>100	>100
I.5ahda	81±32	>100	91±15	n.t.	>100	99±1.6
I.5aida	85±13	>100	68±16	n.t.	>100	93±12
I.5baeb	5.0±2.0	15±5.4	9.2±3.4	3.8±0.7	10±3.9	8.0±2.3
I.5aafa	25±1.3	33±0.7	23±1.8	n.t.	25±0.4	20±2.9
I.5bafb	2.5±0.6	10±3.8	4.9±2.3	8.0±0.4	7.0±2.2	3.2±1.2
CDDP	4.9±0.2	1.9±0.2	1.8±0.5	n.t.	17±3.3	23±4.3
PTX	n.t.	0.000015± 0.000004	0.0023± 0.0003	n.t.	0.00015± 0.00002	0.00032± 0.00002

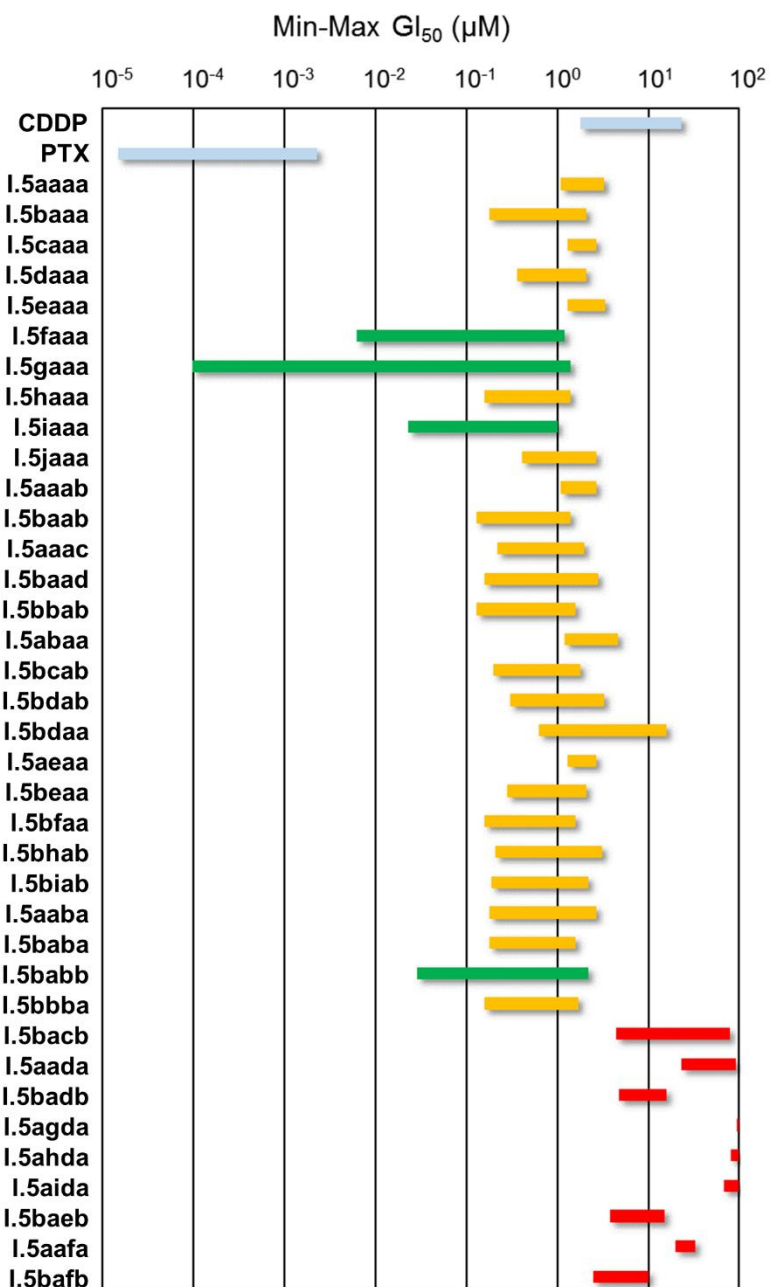


Figure 2.8. GI₅₀ range plot against human solid tumor cell lines. Green bars indicate the most active compounds, whilst red bars point the less active derivatives.

The overall results show great potential of these compounds as antiproliferative agents. Compound **I.5gaaa** exhibited a GI₅₀ value as low as 97 picomolar against HBL-100 cell line and in the low nanomolar range against HeLa and WiDr cell lines (6.5 nM and 5.4 nM, respectively). It appears that the iodine atom at position 5 of the oxindole core can be responsible for this high antiproliferative effect, since replacing it with other halogen, bromine, in compound **I.5faaa**, also led to considerable biological activity but with a different pattern. While **I.5gaaa** showed higher activity against HBL-100 cell line, **I.5faaa** displayed the weaker activity against this cell line (although still reaching a good

result of 0.19 μM), exhibiting better results against the other three cell lines, at the low nanomolar range (6.3 nM, 9.4 nM and 14 nM against HeLa, T-47D, and WiDr cell lines, respectively).

On the other end of the biological activity evaluation, compound **I.5agda** exhibited no relevant antiproliferative activity against the five cell lines tested ($>100 \mu\text{M}$). Two other compounds, **I.5ahda** and **I.5aida**, also exhibited no activity against the two breast cancer cell lines tested, and very weak antiproliferative activity against the other three cell lines evaluated ($>68 \mu\text{M}$). Other compound with weak antiproliferative activity is **I.5aada**, displaying antiproliferative activity in the ranges of 51-91 μM . These four compounds share structural similarities, and the presence of the trifluoromethyl group, provided by the use of trifluoroacetic acid as the carboxylic acid component of the U4CR, might be a good indicator for this poor antiproliferative activity. The compound bearing this structural motif displaying higher potential is **I.5badb**, which possesses antiproliferative activity against the six tested cell lines in the range 4.8-16.0 μM .

This allows to introduce a new level in the structure-activity relationship of the synthesized library. Direct comparison between **I.5badb** and **I.5aada**, which both possess the trifluoroacetic and *n*-butyl groups introduced in the U4CR, present a considerable different antiproliferative activity, with both compounds being most active against WiDr cell line, but the first exhibiting a higher activity by more than 10-fold. This difference can be induced by two structural features a) the methyl group at position 1 of the oxindole core, present in **I.5aada** but absent in **I.5badb** and/or: b) the presence of the cyclohexyl group *versus* the *tert*-butyl group. Other pairs of compounds that can be included in this comparison are **I.5aafa** and **I.5bafb**, with antiproliferative activities ranging between 20.0-33.0 μM and 2.5-10.0 μM , respectively, and **I.5abaa** and **I.5bbab** (2.1-4.6 μM and 0.13-1.60 μM , respectively). The antiproliferative activity of these compounds indicate that the methyl group at position 1 of the oxindole core, as well as *tert*-butyl group (*versus* cyclohexyl group) introduced by the isocyanide component of the U4CR tend to lead to less active compounds. Direct comparison between the pairs **I.5aaaa** and **I.5baaa**, **I.5aaab** and **I.5baab**, **I.5aaba** and **I.5baba**, help to consolidate the observation of *N*-unprotected oxindole derivatives display more potent antiproliferative activity than their *N*-methyl counterparts. Indeed, in a broader perspective, when *N*-unsubstituted isatins were used in the U4CR, more active compounds were achieved.

Checking with more detail the effect of the isocyanide component in the antiproliferative activity of the U4CR adducts, three pairs of compounds can be selected to establish this direct comparison, **I.5baab** and **I.5baaa**, **5bdab** and **I.5bdaa**, and **I.5babb** and **I.5baba**. With few exceptions, the derivative bearing the cyclohexyl exhibits higher antiproliferative in the six tested cell lines than its counterpart bearing the *tert*-

butyl moiety. The *tert*-octyl group present in compound **I.5aaac** seems to lead to more active compounds, in direct comparison with derivatives **I.5aaaa** and **I.5aaab**. On the other hand, the introduction of the benzyl group in the isocyanide component (**I.5baad**) of the U4CR leads to compounds slightly less active (when compared to **I.5baaa** and **I.5baab**), except for HBL-100 and WiDr cell lines, although we need to take into account that the compounds are highly active and for these three derivatives, antiproliferative activity under 1 μ M was observed for these two cell lines.

Considering the evaluated substituents in the aromatic ring of the oxindole core, and besides the already mentioned two most active compounds bearing the iodine (**I.5gaaa**) and bromine (**I.5faaa**) atom at position five, it is noticeable that compound **I.5iaaa** displays antiproliferative activity in the nanomolar range for five of the six cell lines screened, ranging between 23-170 nM. These results indicate the potential of the application of the 5,7-dimethylisatin in the U4CR to attain drug candidates with good antiproliferative profile. The nitro group at position 5 displayed by compound **I.5haaa** tends to lead to compounds with slightly more activity than the unsubstituted oxindole counterpart (**I.5baaa**), whereas compound **I.5jaaa**, bearing the trifluoromethyl group at position 7 of the oxindole core, appears to be less active than all the other *N*-unsubstituted oxindole counterparts.

Analyzing the impact of the amine component used in the U4CR, when linear alkyl amines are used, no significant change is observed, although smaller chain introduced by ethylamine (**I.5bcab**) appearing to exhibit less activity than the longer *n*-butyl chain (**I.5baab**). Ramified alkyl chains (**I.5bdab**) seem to slightly decrease the antiproliferative activity, similarly to what occurs when heteroaromatic groups are introduced (**I.5bhab** and **I.5biab**). Comparing the *n*-butyl group (**I.5baaa**) with benzyl or phenyl groups (**I.5beaa** and **I.5bfaa**, respectively), it is noticeable that when benzylamine was used in the U4CR, similarly or slightly less active compounds were achieved, whereas when aniline was used, slightly more potent compounds were found. However, taking into account the already described synthetic constraints of using aniline in the reported U4CR, more effective synthetic pathways might be required in the future, to further explore this potential.

To assess the effect of the carboxylic acid component of the U4CR in the antiproliferative activity of the reaction products, a comparison between compounds **I.5baab**, **I.5babb**, **I.5bacb**, **I.5badb**, and **I.5bafb** is established. The three monohaloacetic acids tested led to the generation of bioactive compounds, but while chloroacetic acid and bromoacetic acid formed products with similar bioactivities (**I.5baab** exhibits GI₅₀ in the range 0.13-1.40 μ M, and **I.5babb** in the range 29.0 nM-2.20 μ M), fluoroacetic acid led to less antiproliferative effect (**I.5bacb**, 4.40 μ M against A549

and HeLa cell lines, and $>27 \mu\text{M}$ against the remaining four cell lines screened). When using trifluoroacetic acid and *p*-chlorobenzoic acid for the U4CR, the products (**I.5badb** and **I.5bafb**, respectively) presented good antiproliferative activity, but were less potent than the compounds bearing the chloromethyl and bromomethyl groups. Trichloroacetic acid afforded compound **I.5baeb** which is significantly less active than its counterpart **I.5baab**.

Figure 2.9 shows some of the most interesting findings for the synthesized library of Ugi adducts of isatin in what concerns the structure-antiproliferative activity relationship, as well as the bioavailability radars for some of the most active compounds. These results have been published in the Asian Journal of Organic Chemistry (**Appendix 9**).²⁸

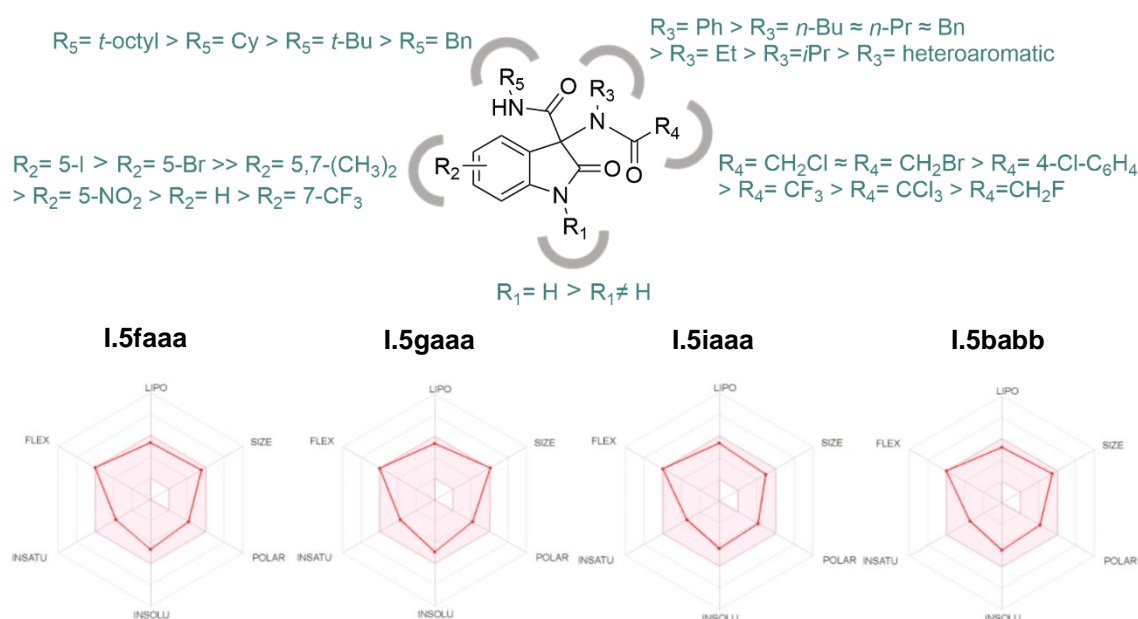


Figure 2.9. Structure-activity relationship for the synthesized library obtained via U4CR and bioavailability radar of the most active compounds.

The remarkable antiproliferative activity exhibited by the vast majority of the newly described oxindole derivatives, and even the structure-activity relationship discussed, needs to be considered carefully. First, we performed a phenotypic assay, which does not provide information in what concerns the type and number of targets the compound is interacting with. It also does not provide information about possible mechanism of action, cell death type, etc., and therefore, and due to the wide structural diversity, we need to keep in mind that different compounds might be interacting with different targets, which are expressed at different rates by the different cell lines evaluated. Further studies are required to have a more reliable knowledge of the potential of these new U4CR adducts as anticancer drug candidates, including their selectivity towards tumor cell lines

versus healthy cells. The chloroacetamide moiety, present in several compounds displaying higher activity, are electrophiles known for interacting selectively with cysteine residues of proteins, due to its strongly nucleophilic thiol side chain.²⁹ While on one hand the presence of the chloroacetamide moiety can lead to lack of selectivity towards different cysteine containing proteins, the tridimensional structure of the compounds can determine selectivity towards selective targets, as the cysteine residue is not abundant in the proteome and therefore covalent chemical modifications can be oriented to a single cysteine residue at a predetermined site.³⁰ For these reasons, chloroacetamide-bearing compounds continue to be explored over recent years as potential molecular probes and covalent drug candidates.³¹⁻³⁴

But considering the widespread presence of halogens in the library, and I, Br, and Cl in particular, might be of great value for further development of these molecules as drug candidates due to the ability for these three halogen atoms to engage in halogen bonding with therapeutic targets.³⁵⁻³⁷ And while organofluorine compounds are widely known for their potential in drug discovery programs³⁸ (hence the importance for us to also explore fluorine-bearing compounds) the impact of the other halogens should not be overlooked. Not only the percentage of drugs launched in the market bearing an halogen atom is as high as 25%, it is also remarkable that heavier halogens tend to be resilient through the drug discovery and development pipeline, with the ratio X/F (with X=Cl, Br or I) increasing from 0.9 at preclinical stages to 1.7 in launched drugs. Among the halogens, chlorine takes over fluoride only after Phase III clinical trials as the most popular halogen.³⁹ The inclusion of halogen atoms during hit or lead optimization used to be highly focused on potential steric effects, changing the ability for small molecules to interact with certain binding pockets of the target. However, the ability to generate intermolecular halogen bonds in the ligand-target interaction, made the inclusion of halogens in drug discovery libraries more rational and intentional, since these interactions can often improve binding affinity and even influence binding selectivity.^{37,}

40, 41

This knowledge will therefore be needed to take in consideration, when further exploring the potential mechanism of action underlying the antiproliferative activity of several compounds in Library I.

2.2.6. The Passerini Adducts – Druglikeness and Biological Activity

As discussed in section 2.2.2 of this Chapter, four Passerini adducts (**1.7a-d**) were successfully isolated while screening carboxylic acids for the U4CR. These compounds

were also evaluated in what concerns their antiproliferative activity, as shown in **Table 2.4**.

Table 2.4. GI₅₀ obtained for the Passerini adducts isolated.

	GI ₅₀ (μM)				
	A549	HBL-100	HeLa	T-47D	WiDr
I.7a	6.80±0.53	14.0±2.1	19.0±4.8	28.0±4.3	30.0±4.0
I.7b	>100	>100	88.0±21.0	98.0±3.7	90.0±16.0
I.7c	23.0±0.36	30.0±0.98	27.0±4.2	35.0±2.0	47.0±1.3
I.7d	33.0±9.0	70.0±27.0	30.0±5.4	39.0±11.0	39.0±10.0

The best result was observed for compound **7a** against A549 cell line, with the remaining compounds exhibiting moderate to no antiproliferative activity against the cell lines screened. These compounds are significantly less potent than most of the compounds prepared via U4CR. Isatin has been previously engaged in the Passerini reaction,⁴² although no bioactivity has been reported in literature to date about these derivatives. For this reason, a SwissADME® evaluation was performed for these four derivatives, in order to evaluate their druglike potential. The four compounds were compliant with the five druglikeness filters evaluated and do not exhibit PAINS alerts. **Figure 2.10** shows the BOILED-Egg model for these four Passerini derivatives, as well as the bioavailability radar for compound **I.7a**, which displays excellent physico-chemical properties for a drug candidate.

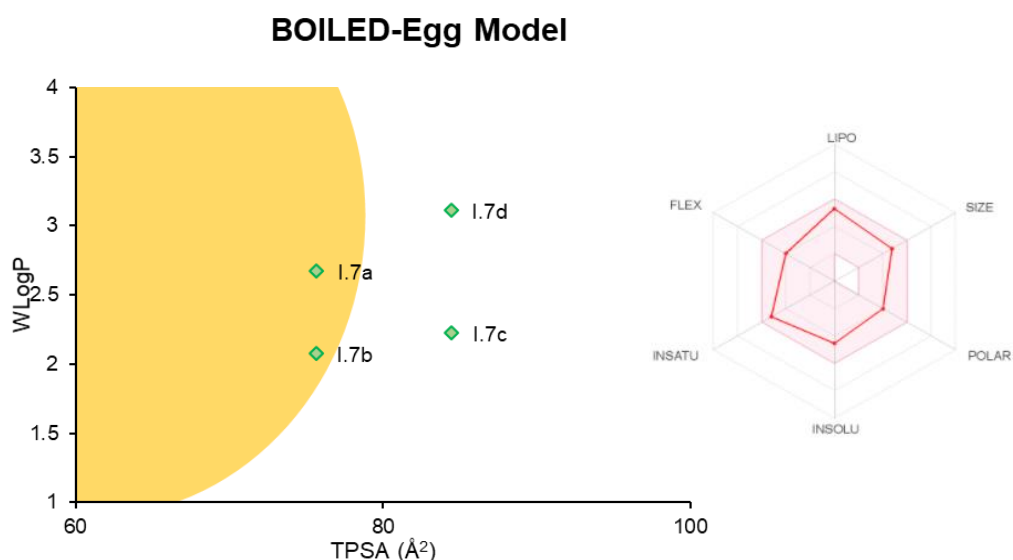


Figure 2.10. BOILED-Egg model of Passerini adducts **I.7a-d** and bioavailability radar of compound **I.7a**.

As shown in **Figure 2.10**, derivatives **I.7a** and **I.7b** are predictably capable of crossing the BBB, whereas the other two are not. Nevertheless, the four compounds are placed within the yellow and white areas, being good drug candidates for oral

administration. This might indicate that Passerini adducts of isatin might constitute a relevant focus for further studies in drug discovery.

2.3. Conclusions

In this Chapter, the first example of an isatin-based U4CR has been developed and reported. The main conclusions that can be drawn from the findings herein presented (**Figure 2.11**) are:

- The synthesis of a library of new oxindole derivatives was successfully achieved, using InCl_3 as an efficient catalyst and methanol at room temperature.

- The synthetic methodology proved to be suitable for a wide diversity of substrate scope for the four components taking part in this complex chemical transformation. It was observed that for the isatin component, a wide range of *N*-unsubstituted, *N*-substituted and aryl substituted isatins could be employed in the U4CR successfully. Several primary amines were also suitable for the chemical transformation, including linear and ramified aliphatic amines, (hetero)aromatic amines and even aniline, despite poor yields were observed in this last example. Primary amines carrying the morpholine unit failed to achieve an U4CR adduct. The same was observed for isocyanides bearing this moiety, nevertheless, other commercially available isocyanides afforded the desired compounds. The carboxylic acid component scope proved to be more limited for the explored chemical transformation, with the outcome being dependent on the $\text{p}K_a$ – carboxylic acids with low $\text{p}K_a$ afforded the desired U4CR adducts, whereas higher values of $\text{p}K_a$ led to Passerini adducts. Intermediate $\text{p}K_a$ values led to the isolation of both products, showcasing a limitation of this synthetic procedure.

- Computational studies indicate the relevance of the imine intermediate formation to achieve a successful U4CR using isatin as starting material. The mechanism of imine formation is stepwise involving a zwitterionic adduct and carbinolamine as intermediates. The rate limiting step of this process is the transformation of carbinolamine into imine via the hydrogen transfer which is facilitated by direct participation of the solvent (MeOH) molecules playing the role of a proton shuttle.

- The synthetic process herein reported allowed the preparation of structurally diverse new oxindole derivatives, bearing three amide groups, which possess relevant antiproliferative activity against six tumor cell lines (two breast cancer cell lines - HBL-100 and T-47D; one lung cancer cell line - A549; one colon cancer cell line – WiDr; one brain cancer cell line – SH-SY5Y; and one cervical cancer cell line – HeLa).

- The new library also exhibits overall good druglike properties and predictably favorable physico-chemical properties, which makes these compounds good candidates for further studies.

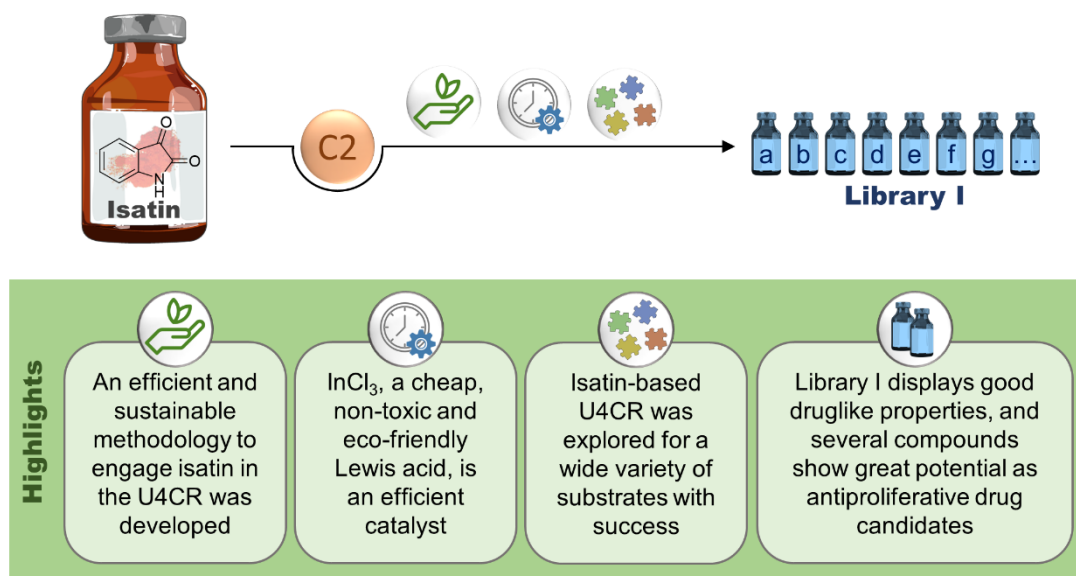


Figure 2.11. Summary of the main results of this Chapter.

2.4. References

1. Biggs-Houck, J. E.; Younai, A.; Shaw, J. T., Recent advances in multicomponent reactions for diversity-oriented synthesis. *Current Opinion in Chemical Biology*, **2010**, *14* (3), 371-382.
2. Zarganes-Tzitzikas, T.; Dömling, A., Modern multicomponent reactions for better drug syntheses. *Organic Chemistry Frontiers*, **2014**, *1* (7), 834-837.
3. Zarganes-Tzitzikas, T.; Chandgude, A. L.; Dömling, A., Multicomponent Reactions, Union of MCRs and Beyond. *The Chemical Record*, **2015**, *15* (5), 981-996.
4. Graebin, C. S.; Ribeiro, F. V.; Rogério, K. R.; Kümmerle, A. E., Multicomponent Reactions for the Synthesis of Bioactive Compounds: A Review. *Current Organic Synthesis*, **2019**, *16* (6), 855-899.
5. Insuasty, D.; Castillo, J.; Becerra, D.; Rojas, H.; Abonia, R., Synthesis of Biologically Active Molecules through Multicomponent Reactions. *Molecules*, **2020**, *25* (3), 505.
6. Cioc, R. C.; Ruijter, E.; Orru, R. V. A., Multicomponent reactions: advanced tools for sustainable organic synthesis. *Green Chemistry*, **2014**, *16* (6), 2958-2975.
7. Liu, Z.-Q., Ugi and Passerini Reactions as Successful Models for Investigating Multicomponent Reactions. *Current Organic Chemistry*, **2014**, *18* (6), 719-739.
8. Rocha, R. O.; Rodrigues, M. O.; Neto, B. A. D., Review on the Ugi Multicomponent Reaction Mechanism and the Use of Fluorescent Derivatives as Functional Chromophores. *ACS Omega*, **2020**, *5* (2), 972-979.
9. Moradi, R.; Ziarani, G. M.; Lashgari, N., Recent applications of isatin in the synthesis of organic compounds. *Arkivoc*, **2017**, (part i), 148-201.
10. Varun; Sonam; Kakkar, R., Isatin and its derivatives: a survey of recent syntheses, reactions, and applications. *MedChemComm*, **2019**, *10* (3), 351-368.
11. Liu, Y. Y.; Wang, H.; Wan, J. P., Recent Advances in Diversity Oriented Synthesis through Isatin-based Multicomponent Reactions. *Asian Journal of Organic Chemistry*, **2013**, *2* (5), 374-386.
12. Brandão, P.; Marques, C. S.; Carreiro, E. P.; Pineiro, M.; Burke, A. J., Engaging Isatins in Multicomponent Reactions (MCRs) – Easy Access to Structural Diversity. *The Chemical Record*, **2021**, *21*, 924-1037.
13. Brandão, P.; Marques, C.; Burke, A. J.; Pineiro, M., The application of isatin-based multicomponent-reactions in the quest for new bioactive and druglike molecules. *European Journal of Medicinal Chemistry*, **2021**, *211*, 113102.
14. Lesma, G.; Meneghetti, F.; Sacchetti, A.; Stucchi, M.; Silvani, A., Asymmetric Ugi 3CR on isatin-derived ketimine: synthesis of chiral 3,3-disubstituted 3-aminooxindole derivatives. *Beilstein Journal of Organic Chemistry*, **2014**, *10*, 1383-1389.
15. Rainoldi, G.; Lesma, G.; Picozzi, C.; Lo Presti, L.; Silvani, A., One step access to oxindole-based -lactams through Ugi four-center three-component reaction. *RSC Advances*, **2018**, *8* (61), 34903-34910.

16. Longo Jr., L. S.; Craveiro, M. V., Deep Eutectic Solvents as Unconventional Media for Multicomponent Reactions. *Journal of the Brazilian Chemical Society*, **2018**, *29*, 1999-2025.
17. Azizi, N.; Dezfooli, S.; Hashemi, M. M., A sustainable approach to the Ugi reaction in deep eutectic solvent. *Comptes Rendus Chimie*, **2013**, *16* (12), 1098-1102.
18. Brandão, P.; Burke, A. J., Catalytic Ugi reactions: current advances, future challenges - Part 1. *Chimica Oggi - Chemistry Today (Monographic special issue: Catalysis & Biocatalysis)*, **2019**, *37* (4), 21-25.
19. Brandão, P.; Burke, A. J., Catalytic Ugi reactions: Current advances, future challenges - Part 2. *Chimica Oggi - Chemistry Today*, **2019**, *37* (4), 18-21.
20. Brandão, P.; Burke, A. J.; Pineiro, M., A decade of Indium-catalyzed multicomponent reactions (MCRs). *European Journal of Organic Chemistry*, **2020**, *2020* (34), 5501-5513.
21. Rappoport, Z., *CRC Handbook of Tables for Organic Compound Identification*. 3rd edition ed.; CRC Press/Taylor and Francis, Boca Raton, FL, USA, **1984**.
22. Chandgude, A. L.; Dömling, A., *N*-Hydroxyimide Ugi Reaction toward α -Hydrazino Amides. *Organic Letters*, **2017**, *19* (5), 1228-1231.
23. Okandeji, B. O.; Sello, J. K., Brønsted Acidity of Substrates Influences the Outcome of Passerini Three-Component Reactions. *The Journal of Organic Chemistry*, **2009**, *74* (14), 5067-5070.
24. Hall, N. E.; Smith, B. J., High-Level ab Initio Molecular Orbital Calculations of Imine Formation. *The Journal of Physical Chemistry A*, **1998**, *102* (25), 4930-4938.
25. Agoni, C.; Olotu, F. A.; Ramharack, P.; Soliman, M. E., Druggability and drug-likeness concepts in drug design: are biomodelling and predictive tools having their say? *Journal of Molecular Modeling*, **2020**, *26* (6), 120.
26. Brown, D. G.; Wobst, H. J., A Decade of FDA-Approved Drugs (2010–2019): Trends and Future Directions. *Journal of Medicinal Chemistry*, **2021**, *64* (5), 2312-2338.
27. Brown, D. G.; Boström, J., Analysis of Past and Present Synthetic Methodologies on Medicinal Chemistry: Where Have All the New Reactions Gone? *Journal of Medicinal Chemistry*, **2016**, *59* (10), 4443-4458.
28. Brandão, P.; Puerta, A.; Padrón, J. M.; Kuznetsov, M. L.; Burke, A. J.; Pineiro, M., Ugi adducts of isatin as promising antiproliferative agents with druglike properties. *Asian Journal of Organic Chemistry*, **2021**, *in press*.
29. Chalker, J. M.; Bernardes, G. J. L.; Lin, Y. A.; Davis, B. G., Chemical Modification of Proteins at Cysteine: Opportunities in Chemistry and Biology. *Chemistry - An Asian Journal*, **2009**, *4* (5), 630-640.
30. Go, Y.-M.; Chandler, J. D.; Jones, D. P., The cysteine proteome. *Free Radical Biology and Medicine*, **2015**, *84*, 227-245.
31. Olszewska, A.; Pohl, R.; Brázdová, M.; Fojta, M.; Hocek, M., Chloroacetamide-Linked Nucleotides and DNA for Cross-Linking with Peptides and Proteins. *Bioconjugate Chemistry*, **2016**, *27* (9), 2089-2094.

32. Eaton, J. K.; Furst, L.; Ruberto, R. A.; Moosmayer, D.; Hillig, R. C.; Hilpmann, A.; Zimmermann, K.; Ryan, M. J.; Niehues, M.; Badock, V.; Kramm, A.; Chen, S.; Clemons, P. A.; Gradl, S.; Montagnon, C.; Lazarski, K. E.; Christian, S.; Bajrami, B.; Neuhaus, R.; Eheim, A. L.; Viswanathan, V. S.; Schreiber, S. L., Selective covalent targeting of GPX4 using masked nitrile-oxide electrophiles. *Nature Chemical Biology*, **2020**, *16*, 497-506.
33. Fumarola, C.; Bozza, N.; Castelli, R.; Ferlenghi, F.; Marseglia, G.; Lodola, A.; Bonelli, M.; La Monica, S.; Cretella, D.; Alfieri, R.; Minari, R.; Galetti, M.; Tiseo, M.; Ardizzoni, A.; Mor, M.; Petronini, P. G., Expanding the Arsenal of FGFR Inhibitors: A Novel Chloroacetamide Derivative as a New Irreversible Agent With Anti-proliferative Activity Against FGFR1-Amplified Lung Cancer Cell Lines. *Frontiers in Oncology*, **2019**, *9*, 179-179.
34. Machado, G. D. R. M.; Fernandes De Andrade, S.; Pippi, B.; Bergamo, V. Z.; Jacobus Berlitz, S.; Lopes, W.; Lavorato, S. N.; Clemes Kulkamp Guerreiro, I.; Vainstein, M. H.; Teixeira, M. L.; Alves, R. J.; Fuentefria, A. M., Chloroacetamide derivatives as a promising topical treatment for fungal skin infections. *Mycologia*, **2019**, *111* (4), 612-623.
35. Wilcken, R.; Zimmermann, M. O.; Lange, A.; Joerger, A. C.; Boeckler, F. M., Principles and Applications of Halogen Bonding in Medicinal Chemistry and Chemical Biology. *Journal of Medicinal Chemistry*, **2013**, *56* (4), 1363-1388.
36. Hernandez, M. Z.; Cavalcanti, S. M.; Moreira, D. R.; de Azevedo Junior, W. F.; Leite, A. C., Halogen atoms in the modern medicinal chemistry: hints for the drug design. *Current Drug Targets*, **2010**, *11* (3), 303-14.
37. Lu, Y.; Liu, Y.; Xu, Z.; Li, H.; Liu, H.; Zhu, W., Halogen bonding for rational drug design and new drug discovery. *Expert Opinion on Drug Discovery*, **2012**, *7* (5), 375-383.
38. Inoue, M.; Sumii, Y.; Shibata, N., Contribution of Organofluorine Compounds to Pharmaceuticals. *ACS Omega*, **2020**, *5* (19), 10633-10640.
39. Xu, Z.; Yang, Z.; Liu, Y.; Lu, Y.; Chen, K.; Zhu, W., Halogen Bond: Its Role beyond Drug-Target Binding Affinity for Drug Discovery and Development. *Journal of Chemical Information and Modeling*, **2014**, *54* (1), 69-78.
40. Ho, P. S., Halogen bonding in medicinal chemistry: from observation to prediction. *Future Medicinal Chemistry*, **2017**, *9* (7), 637-640.
41. Heidrich, J.; Sperl, L. E.; Boeckler, F. M., Embracing the Diversity of Halogen Bonding Motifs in Fragment-Based Drug Discovery—Construction of a Diversity-Optimized Halogen-Enriched Fragment Library. *Frontiers in Chemistry*, **2019**, *7*, 9.
42. Kaicharla, T.; Yetra, S. R.; Roy, T.; Biju, A. T., Engaging isatins in solvent-free, sterically congested Passerini reaction. *Green Chemistry*, **2013**, *15* (6), 1608-1614.
43. Shaabani, S.; Dömling, A., The Catalytic Enantioselective Ugi Four-Component Reactions. *Angewandte Chemie International Edition*, **2018**, *57* (50), 16266-16268.
44. Zhang, J.; Yu, P.; Li, S.-Y.; Sun, H.; Xiang, S.-H.; Wang, J.; Houk, K. N.; Tan, B., Asymmetric phosphoric acid-catalyzed four-component Ugi reaction. *Science*, **2018**, *361* (6407), eaas8707.

45. Wang, Q.; Wang, D.-X.; Wang, M.-X.; Zhu, J., Still Unconquered: Enantioselective Passerini and Ugi Multicomponent Reactions. *Accounts of Chemical Research*, **2018**, *51* (5), 1290-1300.

Chapter 3

U4c3CR as an Efficient Tool for Oxindole-Lactam Hybrids in Drug Discovery



3.1. Introduction

An important approach used in medicinal chemistry is molecular hybridization, which consists in combining two or more drugs, or pharmacophores present in bioactive scaffolds into one single chemical framework, which displays improved therapeutic efficacy and activity. Several advantages can emerge from this approach. The new molecular architecture can i) interact with different binding pockets of the therapeutic target, or even interact with different targets (multitarget) increasing the efficacy and activity of the drug; ii) improve the safety profile of the drug candidate, by decreasing the side-effects; iii) improve therapeutic compliance, by reducing the number of medicines taken by patients; iv) generate molecules with improved pharmacokinetic and pharmacodynamic profiles (**Figure 3.1**). This approach is, therefore, a cornerstone of polypharmacology and multitarget drug discovery.¹⁻⁶

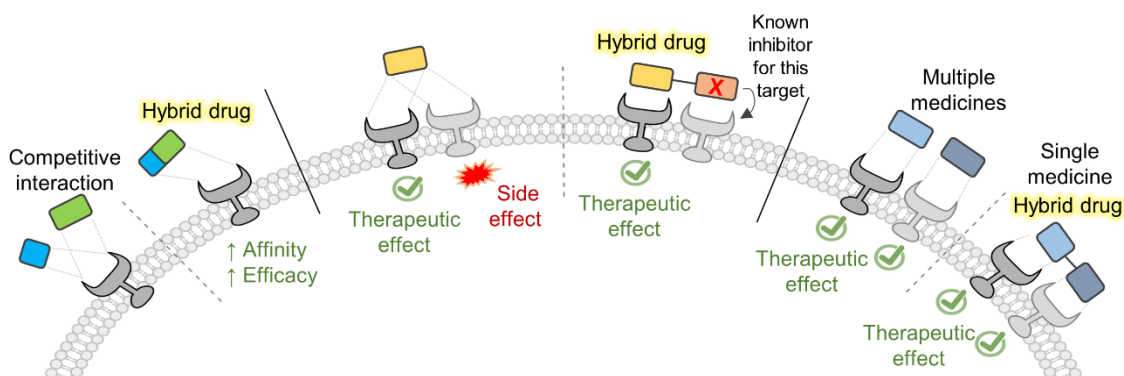


Figure 3.1. Examples of advantages of the application of molecular hybridization in drug discovery.

Several new drug candidates successfully emerged from this approach. Their application has been reported for the potential treatment of several complex pathologies, such as cancer, infectious diseases, and CNS diseases, including Alzheimer's disease.⁷⁻¹⁴

Alzheimer's disease is a very complex and multifactorial pathology with a heavy socio-economic burden associated. Being the most common cause of dementia (60-80% of cases), combined with ageing populations and improvement in the life expectancy, it is desirable, and expected, that a great deal of effort is being placed to treat this disease. Although it presents a multifactorial pathophysiology, and despite the efforts made by several research groups, the therapeutic options are still limited.¹⁵⁻¹⁷ Since multiple processes can be targeted, Alzheimer's disease is a pivotal candidate for polypharmacology approach and hybrid drug candidates.

Among the hybrid drug candidates reported in the literature, most examples incorporate in their structure the scaffolds of known cholinesterase inhibitors, including tacrine. Tacrine plays an interesting role in the treatment of Alzheimer's disease, since it was the first central acting cholinesterase inhibitor approved by the FDA for the treatment of this pathology. This molecule possesses the ability to inhibit both acetylcholinesterase (AChE) and butyrylcholinesterase (BuChE) and hence its therapeutic desirability. However, it also binds to several other targets, including CNS muscarinic receptors, brain histamine-*N*-methyltransferase, and it also inhibits the uptake of several neurotransmitters (noradrenaline, dopamine, and serotonin), monoamine oxidase activity, as well as it blocks neuronal potassium and sodium ion channels. Besides the possible side effects driven by all these "off-target" effects, tacrine was discontinued from clinical practice due to the hepatotoxicity observed at therapeutic doses.¹⁸⁻²¹ Despite these possible drawbacks attributed to the tacrine scaffold, recent efforts have been made in order to include it in hybrids for the treatment of Alzheimer's disease. Other common approaches are molecular hybridization involving one of the currently approved drugs for the treatment of Alzheimer's disease, donepezil, galantamine (both AChE inhibitors), and rivastigmine (AChE and BuChE inhibitor).²²⁻²⁵

Over the past 15 years, dozens of drug candidates for the treatment of Alzheimer's disease which successfully passed phase II clinical trials, failed phase III and did not reach the market. Several of them attempted to target different components of the pathophysiological process of this disease, such as amyloid- β ($A\beta$) aggregation, and β -secretase inhibition.²⁶ However, and despite cholinesterase inhibition is not capable to change the progression of the disease, it can ameliorate symptoms and remains a good therapeutic strategy. The adverse effects displayed with the current therapeutic options (including gastrointestinal and cardiovascular effects) however, create the need of novel drug candidates for this field. Moreover, increasing evidence show that BuChE levels are increased in patients with severe Alzheimer's disease, while depletion of the AChE levels occurs with disease progression, creating the chance to develop new agents targeting selectively BuChE activity.²⁷⁻³⁰

The need to look to different scaffolds which can inhibit these relevant targets, or even operate as multi-target agents is, therefore, of major importance. In our group, oxindole derivatives possessing valuable ChE inhibition activity, in particular targeting BuChE, have been reported in recent years (**Figure 3.2**).³¹⁻³³ Other oxindole derivatives have been reported in the literature with such activity, including some obtained using MCRs (**Figure 3.2**).^{34,35} On the other hand, recent accounts reporting lactam-derivatives, including β -lactam antibiotics, as agents for the treatment of Alzheimer's disease, open new opportunities for drug development (**Figure 3.2**).³⁶⁻⁴³ It is also well established that

lactams, in particular β - and γ -lactams, display a wide diversity of biological activities and are present in multiple approved drugs and drug candidates.⁴⁴⁻⁴⁷

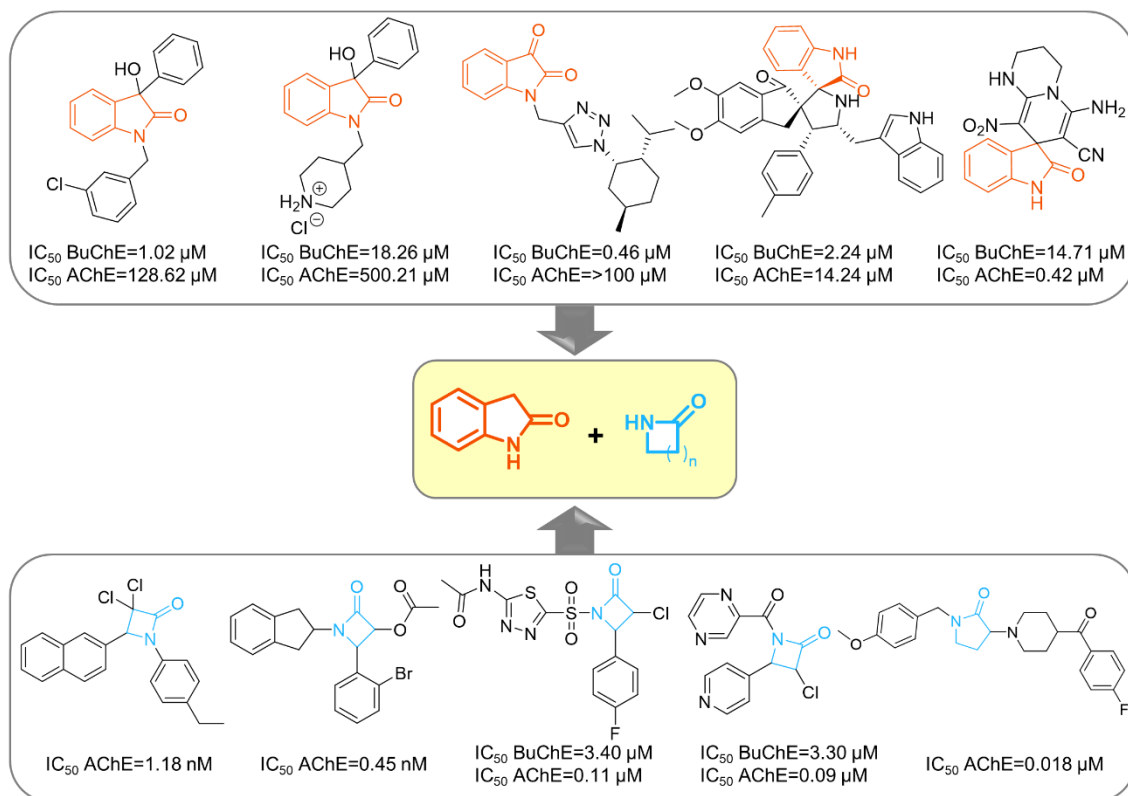


Figure 3.2. Examples of oxindole and lactam derivatives with ChE inhibition activity as the base for the rationale of oxindole-lactam hybrids.

For the synthesis of oxindole-lactam hybrids with potential cholinesterase inhibition activity, the use of the Ugi reaction would be of major importance. The U4c3CR in particular, has showed over the past two decades as a valuable tool for the synthesis of the lactam ring. This can be accomplished by using bifunctional components, such as β -amino acids or β -keto acids for β -lactams,⁴⁸⁻⁵³ or, as described more recently, γ -amino acids and levulinic acid for γ -lactams.⁵⁴⁻⁵⁶ Other ketoacids have also been described for the synthesis of γ - and δ -lactams.⁵⁷ Post-Ugi transformation can also afford lactam rings.^{58, 59}

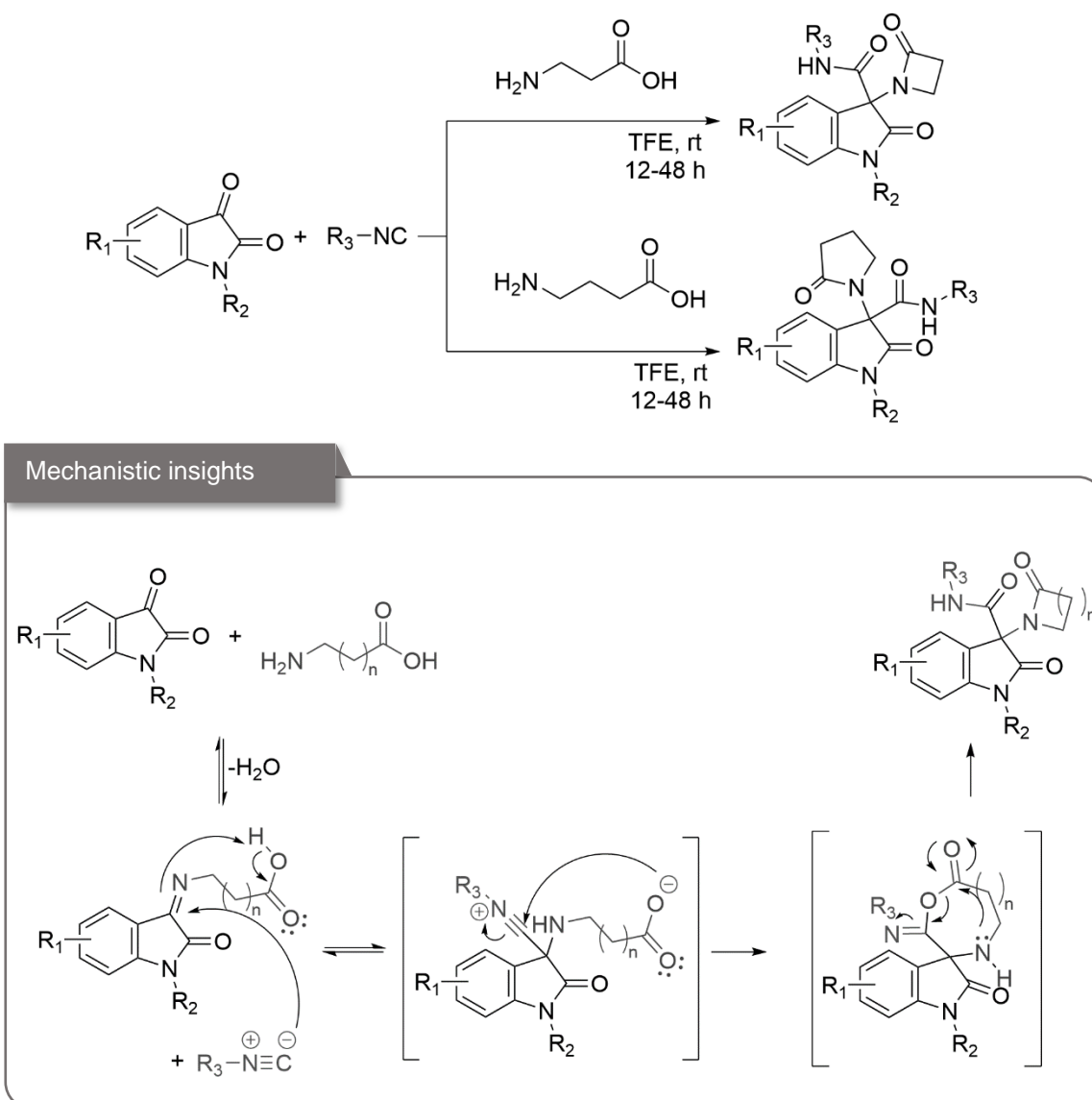
3.2. U4c3CR for the Synthesis of Oxindole-Lactam Hybrids

Concerning the generation of oxindole-lactam hybrids via U4c3CR a recent example reported by Silvani and co-workers, published while the research work herein described was being developed, was used as starting point. In their work, the obtained library was screened against four bacterial strains, with poor results (the best compound

displayed weak antibacterial activity against *Streptococcus mutans*, generating a slight inhibition zone at 0.81 mM). Moreover, the synthesized library was highly focused on the application of *N*-substituted isatins as starting materials.

Using the optimized reaction conditions reported for the one-step, one-pot U4c3CR,⁵² we expanded the reaction scope for the chemical diversity of oxindole-lactam hybrids, especially using *N*-unsubstituted isatins as starting material and, at the same time, attempt to increase the size of the lactam ring.

The overall synthetic approach to attain the different oxindole-lactam hybrids is depicted in **Scheme 3.1**, as well as the proposed mechanism.



Scheme 3.1. Synthetic approach for the U4c3CR to attain oxindole-lactam hybrids.

The commonly accepted mechanism comprises the condensation of the amino acid with the carbonyl group of isatin, affording the corresponding imine, which can be protonated by the acidic hydrogen. This intermediate further reacts with the isocyanide

to generate the corresponding seven-membered ring intermediate, which undergoes Mumm rearrangement to afford the final lactam.

The components used as starting material are depicted in **Figure 3.3**.

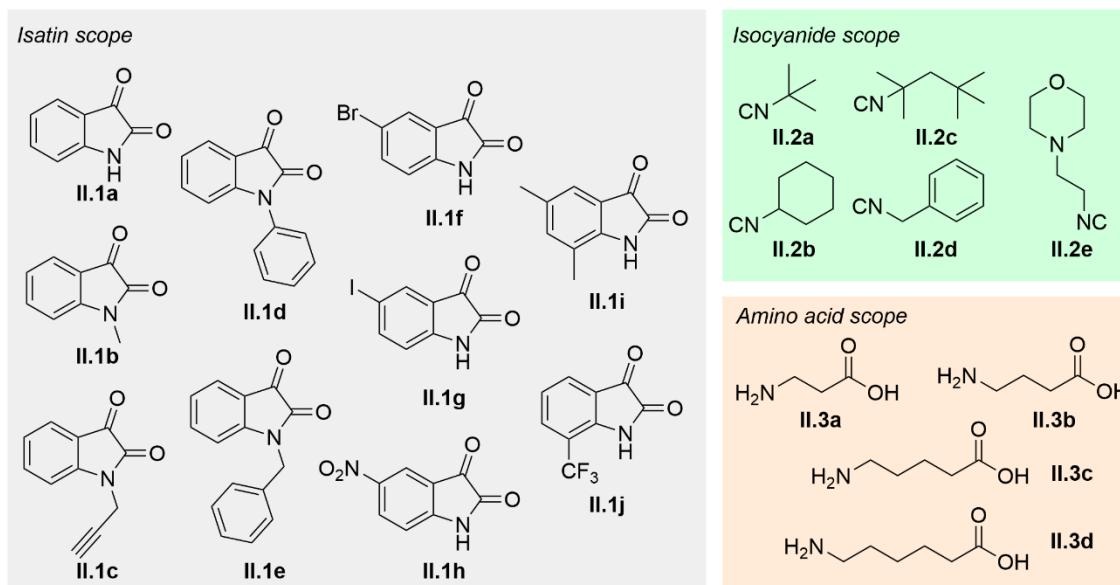


Figure 3.3. Isatin, isocyanide and amino acid components scope for the U4c3CR.

All the isatins evaluated were suitable to undergo the U4c3CR, while in what concerns the isocyanide scope, 2-morpholinoethyl isocyanide (**II.2e**) did not enable the formation of the desired product. Four different amino acids were also screened, with 3-aminopropanoic acid (or β -alanine **II.3a**) and 4-aminobutanoic acid (or γ -aminobutyric acid **II.3b**) affording the corresponding β - and γ -lactam rings, respectively. However, while attempting to generate larger lactam rings by employing 5-aminopentanoic acid (or 5-aminovaleric acid **II.3c**) and 6-aminohexanoic acid (or ϵ -aminocaproic acid **II.3d**) in the U4c3CR, the corresponding δ - and ϵ -lactam derivatives were not observed. Although the solvent used in this approach, TFE is known as an acidic and protic solvent,⁶⁰ when using isatin (as it is less reactive than aldehydes in the Ugi reaction), the acidity is crucial to promote the reaction, and whereas in the previous Chapter, the presence of a Lewis acid and highly acidic carboxylic acids promoted the U4CR, in the approach herein reported, that acidity of the reaction media was not possible to modulate. Attempts to generate the larger lactams in the presence of InCl_3 and ZnCl_2 were performed, but the same outcome was observed. Changing the solvent to methanol also did not afford the desired outcome. These findings might indicate that increasing the size of the amino acid derivative prevents the intramolecular cyclization, with the proton transfer being promoted only when smaller amino acids are used due to the proximity of the atoms during the reaction.

The generated library and respective isolated yields are depicted in **Figure 3.4**.

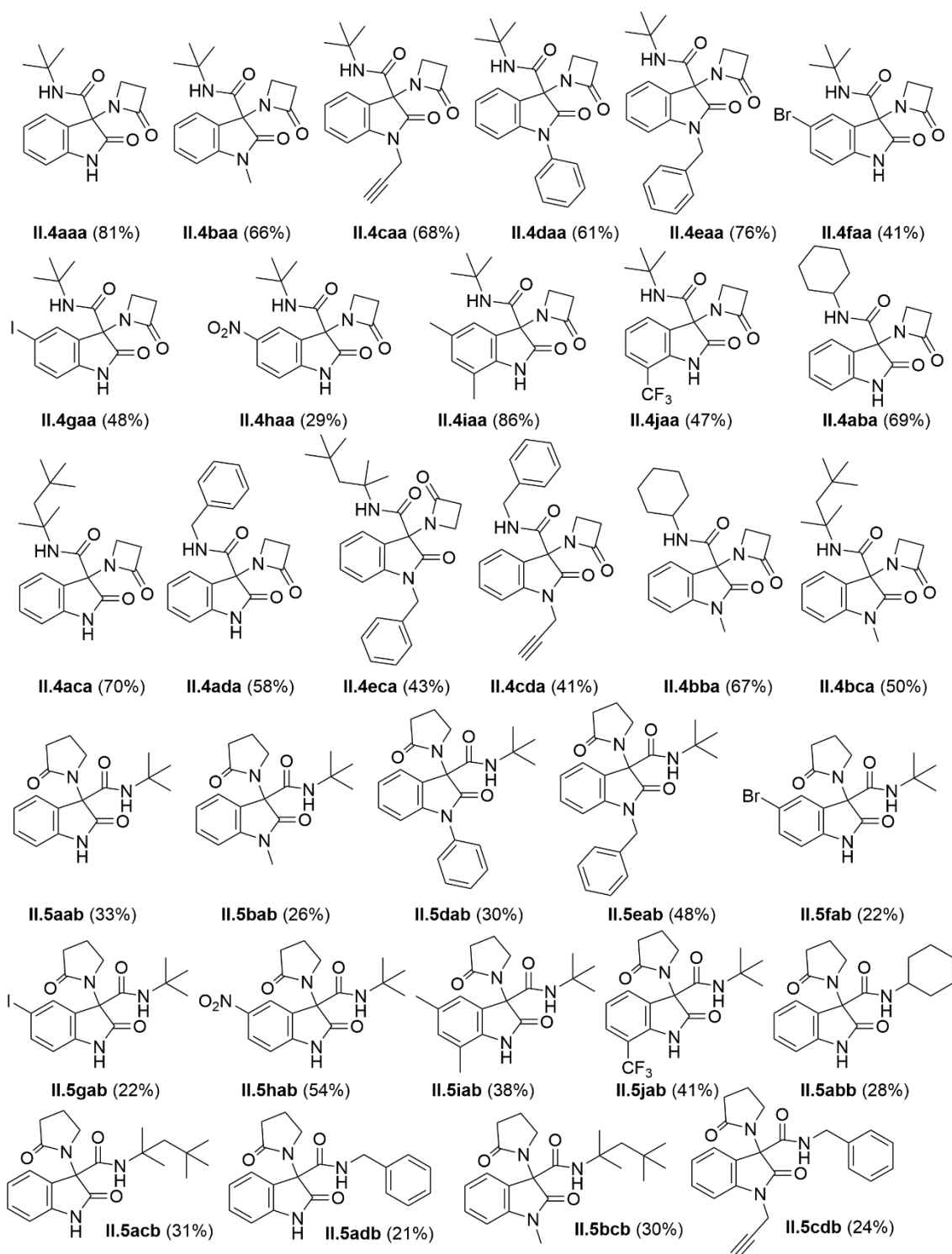


Figure 3.4. Library of oxindole- β -lactam and oxindole- γ -lactam hybrids.

Comparing both libraries, it is noteworthy that the overall yields attained for the oxindole- β -lactam hybrids are higher than the ones achieved for oxindole- γ -lactam hybrids. We can hypothesize, once again, that the proximity of the carboxylic acid moiety to the imine in the first synthetic intermediate, or even the stability/reactivity of the seven-

membered oxazepinone synthetic intermediate, might lead to the better yields of the oxindole- β -lactam hybrids, lowering the yields for their oxindole- γ -lactam hybrids counterparts. Analyzing the influence of the different components in the reaction outcome, we can verify that the yield is mostly influenced by the substituents at the aromatic ring of isatin, while *N*-substituted isatins allow similar yields, comparatively to the ones obtained using *N*-unsubstituted isatin. The influence of the substituents in the aromatic ring might be due to electronic effects or, most likely, solubility issues of the reagent in the reaction media. The different alkyl isocyanides tested did not lead to significant differences in the yields, although aliphatic isocyanides tend to display higher ones. A total of 17 oxindole- β -lactam hybrids (13 of them never described in the literature before), and 14 new oxindole- γ -lactam hybrids were successfully prepared using this approach.

3.3. Druglikeness Evaluation

With the library of oxindole-lactams in hand, it is important to access their potential as drug candidates, including their druglikeness. Three important descriptors are the number of hydrogen bond acceptors and receptors, as well as the number of rotatable bonds. **Figure 3.5** shows the results for all the synthesized compounds which, gratifyingly, fell within the specifications established by three of the key druglikeness filters which take these parameters into account (Lipinski, Muegge and Veber filters).

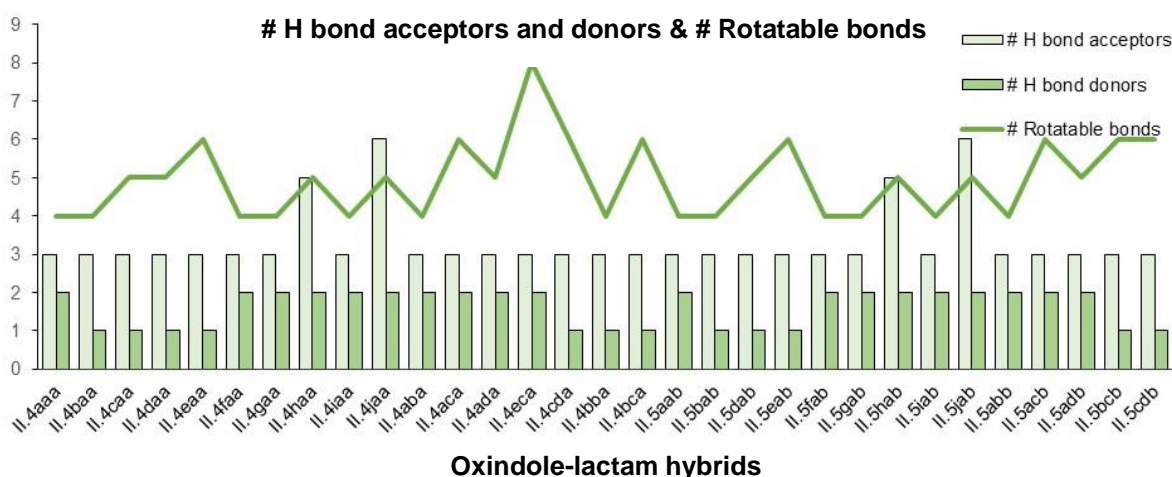


Figure 3.5. Calculated hydrogen bond acceptors, hydrogen bond donors, and rotatable bonds for the synthesized library of oxindole-lactam hybrids.

A series of other relevant parameters are presented in **Table 3.1** for the synthesized library. MW, taken in consideration in the Lipinski, Ghose and Muegge filter,

ranges between 301.34-447.57 Da for the oxindole-lactam hybrids herein described, and therefore are in accordance with the limits established by the filters.

Table 3.1. *In silico* calculation of several physical-chemical properties of the synthesized oxindole-lactam hybrids.

Compounds	MW (Da)	MR	TPSA (Å ²) ^{a)}	CLogP ^{b)}	LogS ^{c)}
II.4aaa	301.34	88.01	78.51	1.17	-2.22
II.4baa	315.37	92.91	69.72	1.36	-2.22
II.4caa	339.39	100.69	69.72	1.67	-2.34
II.4daa	377.44	113.15	69.72	2.58	-3.84
II.4eaa	391.46	117.40	69.72	2.58	-3.78
II.4faa	380.24	95.71	78.51	1.76	-2.93
II.4gaa	427.24	100.73	78.51	1.79	-2.89
II.4haa	346.34	96.83	124.33	0.46	-3.00
II.4iaa	329.39	97.94	78.51	1.82	-2.97
II.4jaa	369.34	93.01	78.51	2.32	-3.13
II.4aba	327.38	95.47	78.51	1.59	-2.50
II.4aca	357.45	106.98	78.51	2.43	-3.99
II.4ada	335.36	98.04	78.51	1.57	-2.75
II.4eca	447.57	136.37	69.72	3.73	-5.55
II.4cda	373.40	110.72	69.72	2.03	-2.87
II.4bba	341.40	100.37	69.72	1.72	-2.51
II.4bca	371.47	111.88	69.72	2.54	-4.00
II.5aab	315.37	92.82	78.51	1.33	-2.59
II.5bab	329.39	97.72	69.72	1.59	-2.59
II.5dab	391.46	117.96	69.72	2.78	-4.21
II.5eab	405.49	122.21	69.72	2.73	-4.14
II.5fab	394.26	100.52	78.51	1.87	-3.31
II.5gab	441.26	105.53	78.51	1.92	-3.26
II.5hab	360.36	101.64	124.33	0.59	-3.37
II.5iab	343.42	102.75	78.51	1.96	-3.34
II.5jab	383.36	97.82	78.51	2.35	-3.50
II.5abb	341.40	100.28	78.51	1.67	-2.87
II.5acb	371.47	111.79	78.51	2.44	-4.36
II.5adb	349.38	102.85	78.51	1.69	-3.12
II.5bcb	385.50	116.69	69.72	2.73	-4.37
II.5cdb	387.43	115.52	69.72	2.15	-3.24

a) Calculated in accordance to ref.⁶¹

b) SwissADME provides 5 LogP values and ClogP is an average of these calculations.

c) Calculated in accordance to ref.⁶²

The lipophilicity of these compounds (evaluated as CLogP) is also in agreement with the limits established by the filters which take this parameter into consideration (Lipinski, Ghose, Egan, and Muegge filters). The same positive outcome is observed for

MR and TPSA values calculated. The water solubility of the synthesized compounds, evaluated as LogS, ranges between -5.55 and -2.22, meaning the compounds can be classified as moderately soluble ($-6 \leq \text{LogS} \leq -4$) or soluble ($-4 \leq \text{LogS} \leq -2$). A correlation between the CLogP and the MW is depicted in **Figure 3.6**, showing the dispersion achieved with this structurally diverse library.

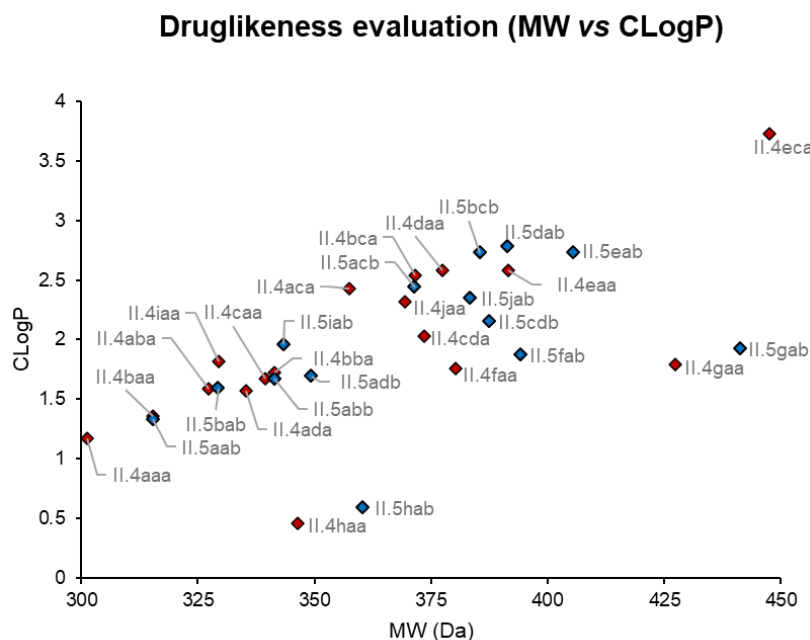


Figure 3.6. Relation between MW and CLogP of the synthesized hybrids (red = oxindole- β -lactam hybrids; blue = oxindole- γ -lactam hybrids).

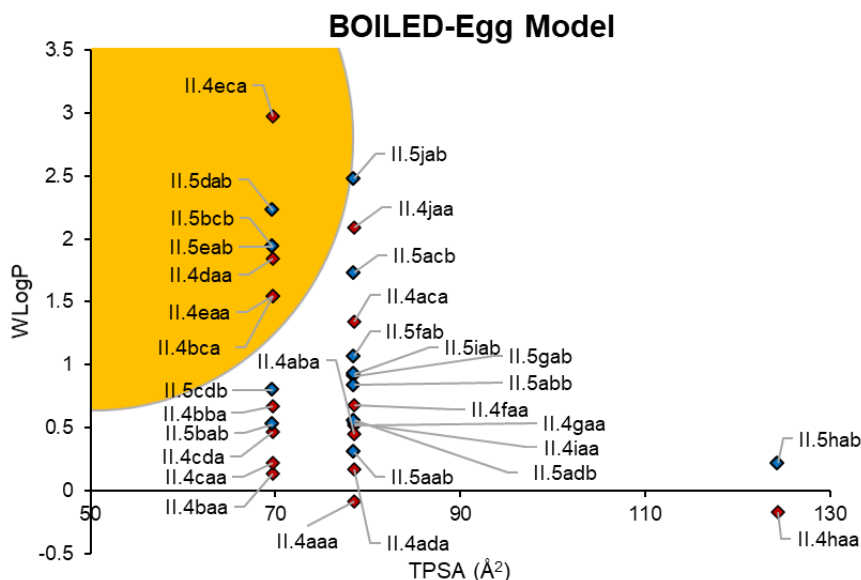


Figure 3.7. BOILED-Egg model for the oxindole-lactam hybrids obtained *via* U4c3CR.

The BOILED-Egg model,⁶³ depicted in **Figure 3.7**, achieved using SwissADME®, is a quick way to predict new compounds ability to cross the gastrointestinal barrier through passive diffusion (white area), making them suitable candidates for oral

administration, as well as their capability to cross the BBB (yellow/yolk area), making them more likely to reach targets in the CNS. The fact that all the oxindole-lactam hybrids are placed within the area delineated by this model, indicates that all the compounds exhibit good predictive gastrointestinal absorption, making them suitable candidates for oral administration. However, BBB permeation via passive diffusion is expected only for some of the *N*-substituted oxindole derivatives, including *N*-phenyl (**II.4daa**, **II.5dab**), *N*-benzyl-oxindole (**II.4eaa**, **II.4eca**, **4eab**), and *N*-methyl oxindole derivatives bearing very hydrophobic amide side-chains, such as **II.4bca** and **II.5bcb**. Nevertheless, the close proximity of the vast majority of the remaining derivatives to the yellow region might indicate that small structural modification of these compounds can lead to a higher BBB permeation.

The detection of possible PAINS, also performed by this web-based tool, did not detect any alert for the oxindole-lactam hybrids library, and the compliance with the five filters evaluated was also complete. All these results make evident the potential of the synthesized compounds as potential new drug candidates, and therefore their bioactivity evaluation could proceed for the entire library.

3.4. Biological Activity Evaluation

3.4.1. Cholinesterase Inhibition

Since these compounds were designed to be suitable cholinesterase inhibitors bearing two relevant heterocyclic cores, the oxindole and the lactam units, the evaluation of their biological activity started using model cholinesterase, namely AChE (*Electrophorus electricus*) and BuChE (equine serum). These results were obtained by Professor Óscar López, at the University of Seville, and are summarized in **Table 3.2**. In what concerns AChE inhibition, only one compound, **II.5hab**, exhibited moderate inhibition ($IC_{50} = 45 \mu\text{M}$), with the remaining compounds being inactive. More promising results were achieved against BuChE.

The tested compounds can be categorized in three different groups according to their potency towards BuChE: inactive ($IC_{50} > 100 \mu\text{M}$), moderate inhibitors ($18 \mu\text{M} < IC_{50} < 94 \mu\text{M}$), or strong inhibitors ($IC_{50} < 10 \mu\text{M}$). The latter group of compounds (**II.4eca**, **II.5dab**, **II.5acb**) are the most promising ones, all of them behaving as mixed inhibitors, meaning they can bind both the free enzyme and the E-I complex. Furthermore, compound **II.4eca** was slightly more potent than galantamine ($IC_{50} = 3.9$

μM), one the current cholinesterase inhibitors in clinical use against Alzheimer's disease, and used herein as a positive control (**Table 3.2**).

Table 3.2. ChE inhibition results (IC_{50} and K_i for the most promising compounds).

Inhibition of cholinesterases (IC_{50} , μM) ^{a,b}			
Compound	AChE (<i>Electrophorus electricus</i>)	BuChE (equine serum)	K_i (μM)
II.4aaa	>100	>100	-
II.4baa			
II.4caa			
II.4daa			
II.4eaa			
II.4faa			
II.4gaa			
II.4haa			
II.4iaa			
II.4jaa			
II.4aba			
II.4aca			
II.4ada			
II.4eca			
II.4cda	>100	>100	-
II.4bba			
II.4bca			
II.5aab			
II.5bab			
II.5dab	45 \pm 5	6.2 \pm 0.3	$K_{ia} = 6.1\pm 1.1$ $K_{ib} = 18\pm 6$ (Mixed inhibition)
II.5eab		32 \pm 3	-
II.5fab		>100	
II.5gab		68 \pm 13	
II.5hab		94 \pm 3	>100
II.5iab			
II.5jab			
II.5abb			
II.5acb	>100	8.4 \pm 0.1	$K_{ia} = 7.4\pm 1.8$ $K_{ib} = 15\pm 1$ (Mixed inhibition)
II.5adb		71 \pm 3	-
II.5bcb		18 \pm 1	
II.5cdb		>100	
Galantamine	2.7 \pm 0.2	3.9 \pm 0.3	-

^a[S] = 112 μM .

^bA set of 5-6 different inhibitor concentrations was used, and the data were obtained in duplicate and expressed as the mean \pm SD.

The results displayed in **Table 3.2** show a considerable selectivity of several compounds, towards BuChE, in particular compounds **II.4eca**, **II.5dab** and **II.5acb**. This is a very remarkable finding, as the quest for new selective BuChE inhibitors is becoming a popular field in drug discovery, with several efforts being undertaken in recent years aiming this target.⁶⁴⁻⁶⁶

No selective inhibitor of BuChE is currently available in the market, and from the drugs available as therapeutic options for Alzheimer's, only rivastigmine and, at a smaller extension, galantamine, work as dual inhibitor (AChE and BuChE). Furthermore, it is becoming clear that BuChE plays a major role in the pathophysiology of Alzheimer's disease, and in other CNS diseases. Moreover, BuChE is present in high concentrations in severe/late stages of the Alzheimer's disease, while AChE is depleted at this stage, and therefore its inhibition is more effective in the early stages of the disease, which sometimes are more difficult to diagnose. Hence the interest to discover these new drug candidates, as they can open the doors for new therapeutic options.⁶⁷⁻⁷¹

Taking a closer look to the structures of the synthesized library and respective exhibited ChE inhibition activity, a pattern can be detected. The γ -lactam derivative is always more active than the β -lactam counterpart, which is either less active, or inactive (e. g., **II.5dab** versus **II.4daa**, **II.5acb** versus **II.4aca**, **II.5eab** versus **II.4eaa**, etc.). Furthermore, oxindoles bearing substituents in the aromatic ring exhibit weak to no activity, and that alkyl isocyanides, in particular *t*-octyl isocyanide, tend to achieve more active compounds, while benzyl isocyanide leads to weak inhibitors or inactive compounds. The substitution at position 1 of the oxindole core is also crucial for the bioactivity shown by these derivatives. Propargyl and methyl derivatives leads to inactive compounds (except in the case of **II.5bcb**, which possesses good BuChE inhibition activity probably due to the combination of *t*-octyl and γ -lactam ring), whereas *N*-phenyl or *N*-benzyl oxindoles tend to exhibit promising activity (**Figure 3.8**). Integrating these results with the BOILED-Egg model prediction, we verify that out of the three most active compounds, the two most active (**II.4eca** and **II.5dab**) predictably possess activity to cross the BBB, which is of great importance for the treatment of Alzheimer's disease.

3.4.2. Monoamine Oxidase Inhibition

In a quest to identify further potential of these new compounds, we decided to perform a preliminary screening on their ability to interact with monoamine oxidase (MAO) A and MAO B. These tests were performed by Professor Holger Stark, at the Heinrich-Heine-Universitaet Duesseldorf.

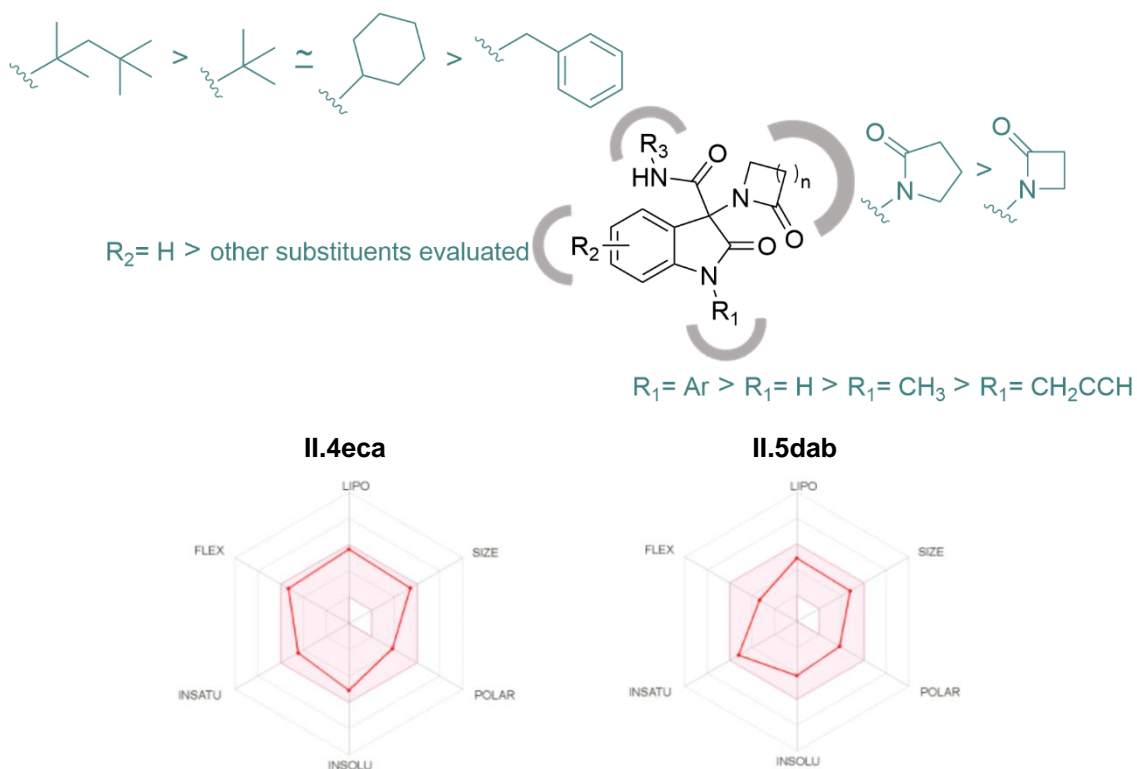


Figure 3.8. Structure-activity relationship of the oxindole-lactam hybrids as selective BuChE inhibitors, and bioavailability radars of the two most promising compounds.

MAO inhibitors emerged in therapeutics for the treatment of depression. However, their side-effect profile is not ideal, and they exhibit a lot of interaction with food and with other drugs, and therefore currently it remains a therapeutic option for patients who are refractory to other available medicines. Nevertheless, these compounds are gaining ground in what concerns neurodegenerative diseases, and some examples (selegiline and rasagiline, **Figure 3.9**) are currently used to treat Parkinson's disease.⁷²⁻⁷⁵ These drugs, as well as several molecules found in literature as possessing good MAO inhibition activity (**Figure 3.9**), exhibit in their structure the propargyl side-chain.⁷⁶⁻⁷⁹

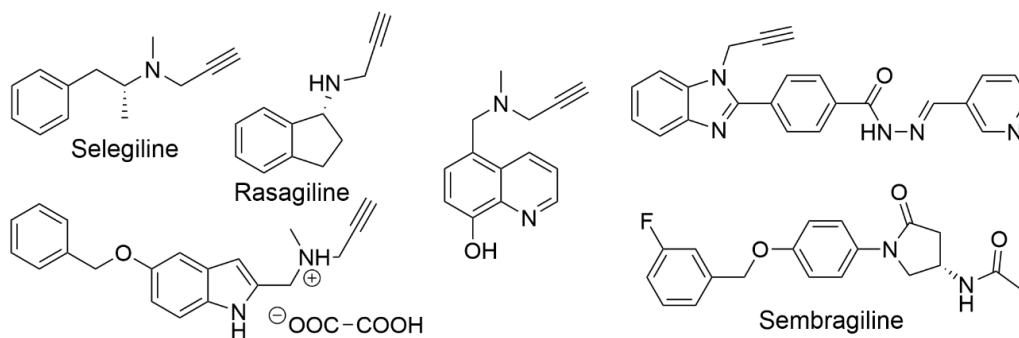


Figure 3.9. Structures of known MAO inhibitors.

Recently, sembragiline (**Figure 3.9**), reported as a selective MAO-B inhibitor, underwent Phase II clinical trials for the treatment of moderate Alzheimer's disease. However, despite showing a good safety profile, the drug failed to meet the desired efficacy, and therefore its development was halted at this stage for this pathology.^{80, 81} Interestingly, this compound possesses a lactam ring in its structure, but no propargyl unit.

With this information in mind, we selected compounds which we expected would possess higher chances to interact with MAO: **II.4caa**, **II.4cda**, and **II.5cbd**. **Table 3.3** shows the results obtained for these compounds bearing the propargyl unit. Unfortunately, no relevant MAO inhibition was observed. The best result was achieved by compound **II.5cdb**, which inhibited 13.2% of MAO A activity, at 1 μ M. This compound exhibits the lowest potential to inhibit MAO B activity (6.1%), comparing to the other two, but only by a bit over 1%. After these results, we decided to not pursue further studies of these targets for the remaining oxindole-lactam hybrids, at this stage.

Table 3.3. MAO A and MAO B preliminary screening for compounds **II.4caa**, **II.4cda** and **II.5cdb**. (n=4)

Compounds	MAO A		MAO B	
	% remaining activity	% inhibition	% remaining activity	% inhibition
No inhibitor	100.0 \pm 0.8	0.0 \pm 0.8	100.0 \pm 2.9	0.0 \pm 2.9
Clorgyline	-0.4 \pm 0.9	100.4 \pm 0.9	71.8 \pm 14.0	28.2 \pm 14.0
Safinamide	101.6 \pm 3.3	-1.6 \pm 3.3	3.0 \pm 0.4	97.0 \pm 0.4
II.4caa	94.1 \pm 7.1	5.9 \pm 7.1	92.6 \pm 1.5	7.4 \pm 1.5
II.4cda	91.1 \pm 0.7	8.9 \pm 0.7	92.4 \pm 4.7	7.6 \pm 4.7
II.5cdb	86.8 \pm 3.8	13.2 \pm 3.8	93.9 \pm 7.0	6.1 \pm 7.0

The results herein discussed have been published in ACS Medicinal Chemistry Letters (see **Appendix 10**).⁸²

3.4.3. Antibacterial Activity

Due to the well-established use of lactams as antibiotics, in particular β -lactams, and with the growing concerns on antibiotic resistance, side-effects and lack of therapeutic options, associated with a stagnant antibiotic discovery pipeline,⁸³⁻⁸⁵ we decided to perform a preliminary evaluation of some of the synthesized compounds on their antibacterial potential. These studies were performed in the Faculty of Pharmacy at the University of Coimbra, under the supervision of Professor Gabriela Jorge da Silva.

The selected compounds to be evaluated were oxindole-lactam hybrids **II.4aaa**, **II.4baa**, **II.4faa**, **II.4gaa**, **II.4haa**, and **II.5aab**. Gram-positive bacteria (*Enterococcus faecalis* and *Staphylococcus aureus*) and Gram-negative bacteria (*Acinetobacter baumannii*, *Escherichia coli*, and *Pseudomonas aeruginosa*) were selected for this evaluation, using disc diffusion method (with bacterial dispersions of 1.5×10^8 CFU/mL, corresponding to 0.5 at the MacFarland scale) to verify the antibacterial potential of the selected hybrids (using a concentration of 20 $\mu\text{g}/\mu\text{L}$). After incubation at 37 °C for 24 hours, the compounds shown no inhibition against the tested bacteria, presenting same result as the control (DMSO), while known antibiotics (ciprofloxacin and ampicillin), inhibited the growth of the bacteria, as expected, validating these assays.

3.5. Conclusions

In this Chapter, the application of a recently reported isatin-based U4c3CR for the synthesis of oxindole-lactam hybrids with potential to be applied in the treatment of Alzheimer's disease has been reported. Several conclusions emerge from the findings herein reported (**Figure 3.10**), such as:

- The synthesis of several oxindole-lactam hybrids was achieved, and the methodology was successfully applied to a broad scope of starting materials, including *N*-unsubstituted isatins, which were poorly explored in previous reports.
- The synthetic methodology proved to be suitable for the synthesis of not only β -lactam ring, but also γ -lactam ring, generating the first reported library of oxindole- γ -

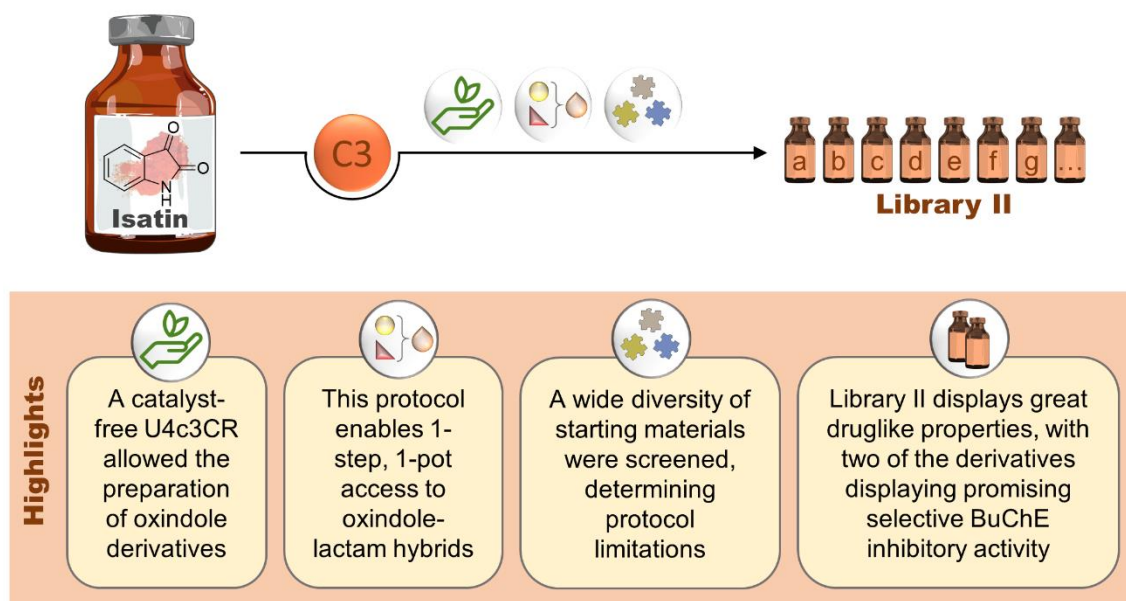


Figure 3.10. Summary of the main results for Chapter 3.

lactam hybrids. Larger lactam rings could not be synthesized under the explored reaction conditions, and therefore it remains a challenge for the future.

- Herein, we describe the first relevant bioactivity results for this family of compounds, with potential to be applied as selective BuChE inhibitors.

- The druglike properties of the designed compounds, especially compounds **II.4eca** and **II.5dab**, which predictably possess good BBB permeation, makes them great candidates for further development.

3.6. References

1. Viegas-Junior, C.; Danuello, A.; da Silva Bolzani, V.; Barreiro, E. J.; Fraga, C. A., Molecular hybridization: a useful tool in the design of new drug prototypes. *Current Medicinal Chemistry*, **2007**, *14* (17), 1829-1852.
2. Anighoro, A.; Bajorath, J.; Rastelli, G., Polypharmacology: challenges and opportunities in drug discovery. *Journal of Medicinal Chemistry*, **2014**, *57* (19), 7874-7887.
3. Bérubé, G., An overview of molecular hybrids in drug discovery. *Expert Opinion on Drug Discovery*, **2016**, *11* (3), 281-305.
4. Oliveira Pedrosa, M. d.; Duarte da Cruz, R. M.; Oliveira Viana, J. d.; de Moura, R. O.; Ishiki, H. M.; Barbosa Filho, J. M.; Diniz, M. F. F. M.; Scotti, M. T.; Scotti, L.; Bezerra Mendonca, F. J., Hybrid Compounds as Direct Multitarget Ligands: A Review. *Current Topics in Medicinal Chemistry*, **2017**, *17* (9), 1044-1079.
5. Ramsay, R. R.; Popovic-Nikolic, M. R.; Nikolic, K.; Uliassi, E.; Bolognesi, M. L., A perspective on multi-target drug discovery and design for complex diseases. *Clinical and Translational Medicine*, **2018**, *7* (1), 3.
6. Sampath Kumar, H. M.; Herrmann, L.; Tsogoeva, S. B., Structural hybridization as a facile approach to new drug candidates. *Bioorganic & Medicinal Chemistry Letters*, **2020**, *30* (23), 127514.
7. Tsogoeva, S. B., Recent Progress in the Development of Synthetic Hybrids of Natural or Unnatural Bioactive Compounds for Medicinal Chemistry. *Mini-Reviews in Medicinal Chemistry*, **2010**, *10* (9), 773-793.
8. Mishra, M.; Mishra, V. K.; Kashaw, V.; Iyer, A. K.; Kashaw, S. K., Comprehensive review on various strategies for antimalarial drug discovery. *European Journal of Medicinal Chemistry*, **2017**, *125*, 1300-1320.
9. Kerru, N.; Singh, P.; Koobanally, N.; Raj, R.; Kumar, V., Recent advances (2015–2016) in anticancer hybrids. *European Journal of Medicinal Chemistry*, **2017**, *142*, 179-212.
10. Bolognesi, M. L.; Cavalli, A., Multitarget Drug Discovery and Polypharmacology. *ChemMedChem*, **2016**, *11* (12), 1190-1192.
11. Ivasiv, V.; Albertini, C.; Gonçalves, A. E.; Rossi, M.; Bolognesi, M. L., Molecular Hybridization as a Tool for Designing Multitarget Drug Candidates for Complex Diseases. *Current Topics in Medicinal Chemistry*, **2019**, *19* (19), 1694-1711.
12. Saadeh, H. A.; Mubarak, M. S., Hybrid Drugs as Potential Combatants Against Drug-Resistant Microbes: A Review. *Current Topics in Medicinal Chemistry*, **2017**, *17* (8), 895-906.
13. Anusionwu, C. G.; Aderibigbe, B. A.; Mbianda, X. Y., Hybrid Molecules Development: A Versatile Landscape for the Control of Antifungal Drug Resistance: A Review. *Mini-Reviews in Medicinal Chemistry*, **2019**, *19* (6), 450-464.
14. Michalska, P.; Buendia, I.; Del Barrio, L.; Leon, R., Novel Multitarget Hybrid Compounds for the Treatment of Alzheimer's Disease. *Current Topics in Medicinal Chemistry*, **2017**, *17* (9), 1027-1043.

15. Farlow, M. R.; Cummings, J. L., Effective Pharmacologic Management of Alzheimer's Disease. *The American Journal of Medicine*, **2007**, *120* (5), 388-397.
16. Marasco, R. A., Current and evolving treatment strategies for the Alzheimer disease continuum. *The American Journal of Managed Care*, **2020**, *26* (Suppl 8), S167-S176.
17. Cummings, J.; Lee, G.; Ritter, A.; Zhong, K., Alzheimer's disease drug development pipeline: 2018. *Alzheimer's & Dementia: Translational Research & Clinical Interventions*, **2018**, *4* (1), 195-214.
18. Freeman, S. E.; Dawson, R. M., Tacrine: A pharmacological review. *Progress in Neurobiology*, **1991**, *36* (4), 257-277.
19. Wagstaff, A. J.; McTavish, D., Tacrine. *Drugs & Aging*, **1994**, *4* (6), 510-540.
20. Park, B. K.; Madden, S.; Spaldin, V.; Woolf, T. F.; Pool, W. F., Tacrine transaminitis: Potential mechanisms. *Alzheimer Disease and Associated Disorders*, **1994**, *8* (Suppl 2), S39-S49.
21. McEneny-King, A.; Osman, W.; Edginton, A. N.; Rao, P. P. N., Cytochrome P450 binding studies of novel tacrine derivatives: Predicting the risk of hepatotoxicity. *Bioorganic & Medicinal Chemistry Letters*, **2017**, *27* (11), 2443-2449.
22. Fancellu, G.; Chand, K.; Tomás, D.; Orlandini, E.; Piemontese, L.; Silva, D. F.; Cardoso, S. M.; Chaves, S.; Santos, M. A., Novel tacrine-benzofuran hybrids as potential multi-target drug candidates for the treatment of Alzheimer's Disease. *Journal of Enzyme Inhibition and Medicinal Chemistry*, **2020**, *35* (1), 211-226.
23. Li, K.; Jiang, Y.; Li, G.; Liu, T.; Yang, Z., Novel Multitarget Directed Tacrine Hybrids as Anti-Alzheimer's Compounds Improved Synaptic Plasticity and Cognitive Impairment in APP/PS1 Transgenic Mice. *ACS Chemical Neuroscience*, **2020**, *11* (24), 4316-4328.
24. Czarnecka, K.; Girek, M.; Wójtowicz, P.; Kręcisz, P.; Skibiński, R.; Jończyk, J.; Łątka, K.; Bajda, M.; Walczak, A.; Galita, G.; Kabziński, J.; Majsterek, I.; Szymczyk, P.; Szymański, P., New Tetrahydroacridine Hybrids with Dichlorobenzoic Acid Moieties Demonstrating Multifunctional Potential for the Treatment of Alzheimer's Disease. *International Journal of Molecular Sciences*, **2020**, *21* (11), 3765.
25. Singh, M.; Kaur, M.; Chadha, N.; Silakari, O., Hybrids: a new paradigm to treat Alzheimer's disease. *Molecular Diversity*, **2016**, *20* (1), 271-297.
26. Bachurin, S. O.; Bovina, E. V.; Ustyugov, A. A., Drugs in Clinical Trials for Alzheimer's Disease: The Major Trends. *Medicinal Research Reviews*, **2017**, *37* (5), 1186-1225.
27. Nordberg, A.; Ballard, C.; Bullock, R.; Darreh-Shori, T.; Somogyi, M., A review of butyrylcholinesterase as a therapeutic target in the treatment of Alzheimer's disease. *The Primary Care Companion for CNS Disorders*, **2013**, *15* (2), PCC.12r01412.
28. Andrisano, V.; Naldi, M.; De Simone, A.; Bartolini, M., A patent review of butyrylcholinesterase inhibitors and reactivators 2010–2017. *Expert Opinion on Therapeutic Patents*, **2018**, *28* (6), 455-465.
29. Li, Q.; Yang, H.; Chen, Y.; Sun, H., Recent progress in the identification of selective butyrylcholinesterase inhibitors for Alzheimer's disease. *European Journal of Medicinal Chemistry*, **2017**, *132*, 294-309.

30. Haake, A.; Nguyen, K.; Friedman, L.; Chakkampambal, B.; Grossberg, G. T., An update on the utility and safety of cholinesterase inhibitors for the treatment of Alzheimer's disease. *Expert Opinion on Drug Safety*, **2020**, *19* (2), 147-157.
31. Totobenazara, J.; Bacalhau, P.; Juan, A. A. S.; Marques, C. S.; Fernandes, L.; Goth, A.; Caldeira, A. T.; Martins, R.; Burke, A. J., Design, Synthesis and Bioassays of 3-Substituted-3-Hydroxyoxindoles for Cholinesterase Inhibition. *ChemistrySelect*, **2016**, *1* (13), 3580-3588.
32. Marques, C. S.; López, Ó.; Bagetta, D.; Carreiro, E. P.; Petralla, S.; Bartolini, M.; Hoffmann, M.; Alcaro, S.; Monti, B.; Bolognesi, M. L.; Decker, M.; Fernández-Bolaños, J. G.; Burke, A. J., *N*-1,2,3-triazole-isatin derivatives for cholinesterase and β -amyloid aggregation inhibition: A comprehensive bioassay study. *Bioorganic Chemistry*, **2020**, *98*, 103753.
33. Bacalhau, P.; Fernandes, L.; Rosário Martins, M.; Candeias, F.; Carreiro, E. P.; López, Ó.; Teresa Caldeira, A.; Totobenazara, J.; Guedes, R. C.; Burke, A. J., *In silico*, NMR and pharmacological evaluation of an hydroxyoxindole cholinesterase inhibitor. *Bioorganic & Medicinal Chemistry*, **2019**, *27* (2), 354-363.
34. Kumar, R. S.; Almansour, A. I.; Arumugam, N.; Basiri, A.; Kia, Y.; Kumar, R. R., Ionic Liquid-Promoted Synthesis and Cholinesterase Inhibitory Activity of Highly Functionalized Spiropyrrolidines. *Australian Journal of Chemistry*, **2015**, *68* (6), 863-871.
35. Maryamabadi, A.; Hasaninejad, A.; Nowrouzi, N.; Mohebbi, G.; Asghari, B., Application of PEG-400 as a green biodegradable polymeric medium for the catalyst-free synthesis of spiro-dihydropyridines and their use as acetyl and butyrylcholinesterase inhibitors. *Bioorganic & Medicinal Chemistry*, **2016**, *24* (6), 1408-1417.
36. Masoud, M.; Ali, A.; Ghareeb, D.; Nasr, N., Synthesis and characterization of cephradine metal complexes as Alzheimer disease therapeutic agent: An *in vitro* kinetic study on acetylcholinesterase and monoamine oxidase. *Journal of Chemical and Pharmaceutical Research*, **2013**, *5*, 1325-1334.
37. Elumalai, K.; Ali, M. A.; Elumalai, M.; Eluri, K.; Srinivasan, S., Acetylcholinesterase inhibitor and cytotoxic activity of some novel acetazolamide cyclocondensed azetidinones. *Journal of Acute Medicine*, **2014**, *4* (1), 20-25.
38. Turan, B.; Şendil, K.; Şengül, E.; Gültekin, M. S.; Taslimi, P.; Gülçin, İ.; Supuran, C. T., The synthesis of some β -lactams and investigation of their metal-chelating activity, carbonic anhydrase and acetylcholinesterase inhibition profiles. *Journal of Enzyme Inhibition and Medicinal Chemistry*, **2016**, *31* (Sup. 1), 79-88.
39. Elumalai, K.; Ashraf Ali, M.; Munusamy, S.; Elumalai, M.; Eluri, K.; Srinivasan, S., Novel pyrazinamide condensed azetidinones inhibit the activities of cholinesterase enzymes. *Journal of Taibah University for Science*, **2016**, *10* (5), 643-650.
40. Genç, H.; Kalin, R.; Köksal, Z.; Sadeghian, N.; Kocyigit, U.; Zengin, M.; Gülçin, İ.; Özdemir, H., Discovery of Potent Carbonic Anhydrase and Acetylcholinesterase Inhibitors: 2-Aminoindan β -Lactam Derivatives. *International Journal of Molecular Sciences*, **2016**, *17* (10), 1736.

41. Türkan, F.; Huyut, Z.; Taslimi, P.; Gülçin, İ., The effects of some antibiotics from cephalosporin groups on the acetylcholinesterase and butyrylcholinesterase enzymes activities in different tissues of rats. *Archives of Physiology and Biochemistry*, **2019**, *125* (1), 12-18.
42. Gupta, M.; Ojha, M.; Yadav, D.; Pant, S.; Yadav, R., Novel Benzylated (Pyrrolidin-2-one)/(Imidazolidin-2-one) Derivatives as Potential Anti-Alzheimer's Agents: Synthesis and Pharmacological Investigations. *ACS Chemical Neuroscience*, **2020**, *11* (18), 2849-2860.
43. Kumari, S.; Deshmukh, R., β -lactam antibiotics to tame down molecular pathways of Alzheimer's disease. *European Journal of Pharmacology*, **2021**, *895*, 173877.
44. Fisher, J. F.; Mobashery, S., Chapter 3 The β -Lactam (Azetidin-2-one) as a Privileged Ring in Medicinal Chemistry. In *Privileged Scaffolds in Medicinal Chemistry: Design, Synthesis, Evaluation*, Bräse S. Ed., The Royal Society of Chemistry, **2016**, pp. 64-97.
45. Szostak, M.; Aubé, J., Chemistry of Bridged Lactams and Related Heterocycles. *Chemical Reviews*, **2013**, *113* (8), 5701-5765.
46. Kaur, R.; Singh, R.; Ahlawat, P.; Kaushik, P.; Singh, K., Contemporary advances in therapeutic portfolio of 2-Azetidinones. *Chemical Biology Letters*, **2020**, *7* (1), 13-26.
47. Caruano, J.; Muccioli, G. G.; Robiette, R., Biologically active γ -lactams: synthesis and natural sources. *Organic & Biomolecular Chemistry*, **2016**, *14* (43), 10134-10156.
48. Gedey, S.; Eycken, J. V. d.; Fulop, F., Synthesis of Alicyclic β -lactams via the Ugi Reaction on a Solid Support. *Letters in Organic Chemistry*, **2004**, *1* (3), 215-220.
49. Szakonyi, Z.; Sillanpää, R.; Fülöp, F., Synthesis of conformationally constrained tricyclic β -lactam enantiomers through Ugi four-center three-component reactions of a monoterpene-based β -amino acid. *Molecular Diversity*, **2010**, *14* (1), 59-65.
50. Vishwanatha, T. M.; Narendra, N.; Sureshbabu, V. V., Synthesis of β -lactam peptidomimetics through Ugi MCR: first application of chiral N^β -Fmoc amino alkyl isocyanides in MCRs. *Tetrahedron Letters*, **2011**, *52* (43), 5620-5624.
51. Cheibas, C.; Cordier, M.; Li, Y.; El Kaïm, L., A Ugi Straightforward Access to Bis- β -lactam Derivatives. *European Journal of Organic Chemistry*, **2019**, *2019* (27), 4457-4463.
52. Rainoldi, G.; Lesma, G.; Picozzi, C.; Lo Presti, L.; Silvani, A., One step access to oxindole-based β -lactams through Ugi four-center three-component reaction. *RSC Advances*, **2018**, *8* (61), 34903-34910.
53. Pirrung, M. C.; Sarma, K. D., β -Lactam Synthesis by Ugi Reaction of β -Keto Acids in Aqueous Solution. *Synlett*, **2004**, *2004* (8), 1425-1427.
54. Khalesi, M.; Ziyaei Halimehjani, A.; Martens, J., Synthesis of a novel category of pseudo-peptides using an Ugi three-component reaction of levulinic acid as bifunctional substrate, amines, and amino acid-based isocyanides. *Beilstein Journal of Organic Chemistry*, **2019**, *15*, 852-857.
55. Suć Sajko, J.; Ljoljić Bilić, V.; Kosalec, I.; Jerić, I., Multicomponent Approach to a Library of *N*-Substituted γ -Lactams. *ACS Combinatorial Science*, **2019**, *21* (1), 28-34.

56. Cioc, R. C.; Schaepekens van Riepst, L.; Schuckman, P.; Ruijter, E.; Orru, R. V. A., Ugi Four-Center Three-Component Reaction as a Direct Approach to Racetams. *Synthesis*, **2017**, *49* (7), 1664-1674.
57. Musonda, C. C.; Gut, J.; Rosenthal, P. J.; Yardley, V.; Carvalho de Souza, R. C.; Chibale, K., Application of multicomponent reactions to antimalarial drug discovery. Part 2: New antiplasmodial and antitrypanosomal 4-aminoquinoline gamma- and delta-lactams via a 'catch and release' protocol. *Bioorganic & Medicinal Chemistry*, **2006**, *14* (16), 5605-5615.
58. Boltjes, A.; Liao, G. P.; Zhao, T.; Herdtweck, E.; Dömling, A., Ugi 4-CR synthesis of γ - and δ -lactams providing new access to diverse enzyme interactions, a PDB analysis. *MedChemComm*, **2014**, *5* (7), 949-952.
59. Gao, X.; Shan, C.; Chen, Z.; Liu, Y.; Zhao, X.; Zhang, A.; Yu, P.; Galons, H.; Lan, Y.; Lu, K., One-pot synthesis of β -lactams by the Ugi and Michael addition cascade reaction. *Organic & Biomolecular Chemistry*, **2018**, *16* (33), 6096-6105.
60. Dandia, A.; Singh, R.; Joshi, J.; Kumari, S., 2,2,2-Trifluoroethanol as Green Solvent in Organic Synthesis: A Review. *Mini-Reviews in Organic Chemistry*, **2014**, *11* (4), 462-476.
61. Ertl, P.; Rohde, B.; Selzer, P., Fast Calculation of Molecular Polar Surface Area as a Sum of Fragment-Based Contributions and Its Application to the Prediction of Drug Transport Properties. *Journal of Medicinal Chemistry*, **2000**, *43* (20), 3714-3717.
62. Ali, J.; Camilleri, P.; Brown, M. B.; Hutt, A. J.; Kirton, S. B., *In Silico* Prediction of Aqueous Solubility Using Simple QSPR Models: The Importance of Phenol and Phenol-like Moieties. *Journal of Chemical Information and Modeling*, **2012**, *52* (11), 2950-2957.
63. Daina, A.; Zoete, V., A BOILED-Egg To Predict Gastrointestinal Absorption and Brain Penetration of Small Molecules. *ChemMedChem*, **2016**, *11* (11), 1117-1121.
64. Brus, B.; Košak, U.; Turk, S.; Pišlar, A.; Coquelle, N.; Kos, J.; Stojan, J.; Colletier, J.-P.; Gobec, S., Discovery, Biological Evaluation, and Crystal Structure of a Novel Nanomolar Selective Butyrylcholinesterase Inhibitor. *Journal of Medicinal Chemistry*, **2014**, *57* (19), 8167-8179.
65. Kumar, A.; Pintus, F.; Di Petrillo, A.; Medda, R.; Caria, P.; Matos, M. J.; Viña, D.; Pieroni, E.; Delogu, F.; Era, B.; Delogu, G. L.; Fais, A., Novel 2-pheynlbenzofuran derivatives as selective butyrylcholinesterase inhibitors for Alzheimer's disease. *Scientific Reports*, **2018**, *8*, 4424.
66. Williams, A.; Zhou, S.; Zhan, C.-G., Discovery of potent and selective butyrylcholinesterase inhibitors through the use of pharmacophore-based screening. *Bioorganic & Medicinal Chemistry Letters*, **2019**, *29* (24), 126754.
67. Guillozet, A. L.; Mesulam, M. M.; Smiley, J. F.; Mash, D. C., Butyrylcholinesterase in the life cycle of amyloid plaques. *Annals of Neurology*, **1997**, *42* (6), 909-918.
68. Darvesh, S.; Hopkins, D. A.; Geula, C., Neurobiology of butyrylcholinesterase. *Nature Reviews Neuroscience*, **2003**, *4* (2), 131-138.

69. Tasker, A.; Perry, E. K.; Ballard, C. G., Butyrylcholinesterase: impact on symptoms and progression of cognitive impairment. *Expert Review of Neurotherapeutics*, **2005**, 5 (1), 101-106.
70. Lane, R. M.; He, Y., Butyrylcholinesterase genotype and gender influence Alzheimer's disease phenotype. *Alzheimer's & Dementia*, **2013**, 9 (2), e17-e73.
71. Wang, H.; Zhang, H., Reconsideration of Anticholinesterase Therapeutic Strategies against Alzheimer's Disease. *ACS Chemical Neuroscience*, **2019**, 10 (2), 852-862.
72. Riederer, P., Monoamine Oxidase-B Inhibition in Alzheimer's Disease. *NeuroToxicology*, **2004**, 25 (1-2), 271-277.
73. Cai, Z., Monoamine oxidase inhibitors: Promising therapeutic agents for Alzheimer's disease (Review). *Molecular Medicine Reports*, **2014**, 9 (5), 1533-1541.
74. Manzoor, S.; Hoda, N., A comprehensive review of monoamine oxidase inhibitors as Anti-Alzheimer's disease agents: A review. *European Journal of Medicinal Chemistry*, **2020**, 206, 112787.
75. Finberg, J. P. M.; Rabey, J. M., Inhibitors of MAO-A and MAO-B in Psychiatry and Neurology. *Frontiers in Pharmacology*, **2016**, 7, 340.
76. Samadi, A.; De Los Ríos, C.; Bolea, I.; Chioua, M.; Iriepa, I.; Moraleda, I.; Bartolini, M.; Andrisano, V.; Gálvez, E.; Valderas, C.; Unzeta, M.; Marco-Contelles, J., Multipotent MAO and cholinesterase inhibitors for the treatment of Alzheimer's disease: Synthesis, pharmacological analysis and molecular modeling of heterocyclic substituted alkyl and cycloalkyl propargyl amine. *European Journal of Medicinal Chemistry*, **2012**, 52, 251-262.
77. Bolea, I.; Gella, A.; Unzeta, M., Propargylamine-derived multitarget-directed ligands: fighting Alzheimer's disease with monoamine oxidase inhibitors. *Journal of Neural Transmission*, **2013**, 120 (6), 893-902.
78. Can, Ö. D.; Osmaniye, D.; Demir Özkay, Ü.; Sağlık, B. N.; Levent, S.; İlgin, S.; Baysal, M.; Özkay, Y.; Kaplancıklı, Z. A., MAO enzymes inhibitory activity of new benzimidazole derivatives including hydrazone and propargyl side chains. *European Journal of Medicinal Chemistry*, **2017**, 131, 92-106.
79. Tripathi, A. C.; Upadhyay, S.; Paliwal, S.; Saraf, S. K., Privileged scaffolds as MAO inhibitors: Retrospect and prospects. *European Journal of Medicinal Chemistry*, **2018**, 145, 445-497.
80. Borroni, E.; Bohrmann, B.; Grueninger, F.; Prinssen, E.; Nave, S.; Loetscher, H.; Chinta, S. J.; Rajagopalan, S.; Rane, A.; Siddiqui, A.; Ellenbroek, B.; Messer, J.; Pähler, A.; Andersen, J. K.; Wyler, R.; Cesura, A. M., Sembragiline: A Novel, Selective Monoamine Oxidase Type B Inhibitor for the Treatment of Alzheimer's Disease. *Journal of Pharmacology and Experimental Therapeutics*, **2017**, 362 (3), 413-423.
81. Nave, S.; Doody, R. S.; Boada, M.; Grimmer, T.; Savola, J.-M.; Delmar, P.; Pauly-Evers, M.; Nikolcheva, T.; Czech, C.; Borroni, E.; Ricci, B.; Dukart, J.; Mannino, M.; Carey, T.; Moran, E.; Gilaberte, I.; Muelhardt, N. M.; Gerlach, I.; Santarelli, L.; Ostrowitzki, S.; Fontoura, P., Sembragiline in Moderate Alzheimer's Disease: Results of a Randomized,

- Double-Blind, Placebo-Controlled Phase II Trial (MAYfLOWer RoAD). *Journal of Alzheimer's Disease*, **2017**, 58 (4), 1217-1228.
- 82.Brandão, P.; López, Ó.; Leitzbach, L.; Stark, H.; Fernández-Bolaños, J. G.; Burke, A. J.; Pineiro, M., Ugi Reaction Synthesis of Oxindole–Lactam Hybrids as Selective Butyrylcholinesterase Inhibitors. *ACS Medicinal Chemistry Letters*, **2021**, 12 (11), 1718-1725.
- 83.Kong, K.-F.; Schneper, L.; Mathee, K., Beta-lactam antibiotics: from antibiosis to resistance and bacteriology. *APMIS*, **2010**, 118 (1), 1-36.
- 84.Vardakas, K. Z.; Kalimeris, G. D.; Triarides, N. A.; Falagas, M. E., An update on adverse drug reactions related to β -lactam antibiotics. *Expert Opinion on Drug Safety*, **2018**, 17 (5), 499-508.
- 85.Butler, M. S.; Paterson, D. L., Antibiotics in the clinical pipeline in October 2019. *The Journal of Antibiotics*, **2020**, 73 (6), 329-364.

Chapter 4

A New Route to Tryptanthrin and its Petasis Adducts



4.1. Introduction

Tryptanthrin (indolo[2,1-*b*]quinazoline-6,12-dione) is a tetracyclic alkaloid with remarkable scientific relevance. As contextualized in Chapter 1, this yellow compound already presents almost two centuries of history, enriching the knowledge on several subjects, from natural product chemistry, synthetic organic chemistry, and medicinal chemistry. The interest over this molecule is driven by its myriad of applications and its widespread presence in different sources. Having been isolated from different natural sources, including several different plants and fungi, it has been identified as an important component in several natural products used in folklore medicine. With natural products often being a great source of inspiration for drug discovery, the study of tryptanthrin and its derivatives became an important task for several research groups. The diversity of reactivity key-points that can be introduced in the aromatic rings of the quinazoline and/or indole cores, as well as the chemical transformations which can be undertaken in the carbonyl groups, makes tryptanthrin a great starting point for the discovery of new drug candidates.¹⁻³

In this work, tryptanthrin emerged out of serendipity, a valuable, yet polarizing topic in nowadays scientific context. Nevertheless, serendipity has been playing a major role in changing the face of Science, including in the field of drug discovery, e.g., through the discovery of penicillin in 1928, which enabled the antibiotic revolution and therefore changed the landscape of infectious disease therapeutics, a topic which is in the spotlight with the emergence of multi-resistant microorganisms and new pathogenic agents.^{4,5}

Serendipity is much more than sheer luck, and serendipity in Science is almost a form of “art”. It requires the ability to keep an open mind and critical assessment over observation, and identifying valuable outputs out of unexpected results.⁶

During the first semester of the PhD studies reported in this thesis, a small research project was undertaken for the curricular unit “Introduction to Interdisciplinary Research”. Originally, the project aimed the synthesis and photophysical characterization of *cis-N,N'*-alkylindigo derivatives, obtained through a methodology adapted from one example reported in the literature, as discussed later in this Chapter (see section 4.2). However, it was observed the formation of an unexpected yellow compound while attempting to synthesize the aforementioned *cis-N,N'*-alkylindigo derivatives, which was identified as tryptanthrin. Out of this discovery, it was decided to further expand the scope of this work navigating around the potential of tryptanthrin, which is a molecule so closely related to isatin.

This Chapter will address two main achievements: a) a new synthetic route to prepare tryptanthrin and; b) the first example of tryptanthrin-based Petasis MCR.

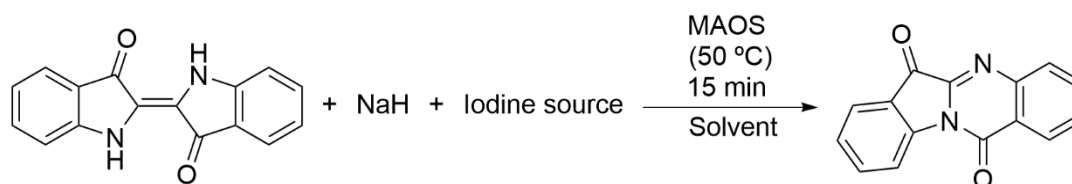
4.2. A New Route for the Synthesis of Tryptanthrin from Indigo and Isatin

As mentioned in the introduction of this Chapter, the starting point was a methodology reported in the literature,⁷ for the synthesis of alkylindigos by promoting the reaction between indigo and a diiodoalkane in the presence of a base in dimethylformamide (DMF). In order to improve the sustainability of the process and reduce reaction times, we decided to use microwave irradiation to promote the reaction (50 °C, 15 min). Different diiodoalkanes were evaluated. In our first attempt, using diiodomethane (**Table 4.1**, entry 1), trace amounts of *N*-iodomethylindigo were isolated, as well as a yellow compound. Predicting that the *cis-N,N'*-alkylindigo derivative could not be obtained due to the size of the diiodoalkane, we decided to use 1,3-diiodopropane in our next attempt (**Table 4.1**, entry 2), under the same conditions. A complex mixture was obtained, including the same yellow compound. When we switched the diiodoalkane for 1,2-diiodoethane (**Table 4.1**, entry 3), we observed that the yellow compound was the major product. This product was isolated and identified as tryptanthrin, when compared with nuclear magnetic resonance (NMR) data reported in the literature.⁸ A gas-chromatography-mass spectrometry (GC-MS) analysis of the reaction medium after 15 min of microwave irradiation showed the presence of tryptanthrin, unreacted indigo, and two very important compounds for the understanding of the mechanism of this reaction, isatin and isatoic anhydride (**Figure 4.1**).

As this product was unexpected, we decided to further explore this reaction. Conducting the reaction under conventional heating (50 °C, 15 min), tryptanthrin was obtained in very low yield (5%). With this information, we decided to further optimize the reaction under microwave irradiation, exploring different conditions and the influence of different parameters.

To verify the influence of the diiodoalkane, the reaction was performed in the absence of an iodine source (**Table 4.1**, entry 4). Under these experimental conditions, only indigo was observed after 15 min, showing the crucial role played by the iodine source for the reactivity.

Knowing that the reaction would involve oxidation of indigo to isatin, followed by its oxidative cyclization, based on the GC-MS identification of isatin and isatoic anhydride as synthetic intermediates, we hypothesized that atmospheric oxygen would be the oxidant of this reaction. To verify this premise, we performed the reaction under a nitrogen saturated atmosphere (**Table 4.1**, entry 5), which showed formation of tryptanthrin at similar levels as the ones observed under an atmosphere of air, thus showing that oxygen is not the oxidant in these conditions.

Table 4.1. Microwave-assisted tryptanthrin synthesis using indigo^{a)} as starting material.

Entry	NaH	Iodine source ^{a)}	Solvent	% Tryptanthrin ^{b)}
1	2 equiv	CH ₂ I ₂	DMF (2 mL)	9
2	2 equiv	C ₃ H ₆ I ₂	DMF (2 mL)	2
3	2 equiv	C ₂ H ₄ I ₂	DMF (2 mL)	23 (22 ^{c)})
4	2 equiv	-	DMF (2 mL)	0
5	2 equiv	C ₂ H ₄ I ₂	DMF (2 mL)	24
6	2 equiv	C ₂ H ₄ I ₂	Cyrene (1.8 mL) + DMF (0.2 mL)	Trace
7	2 equiv	C ₂ H ₄ I ₂	2-MeTHF (2 mL)	2
8	2 equiv	C ₂ H ₄ I ₂	2-MeTHF (2 mL) + DMF (58 μL)	7
9	4 equiv	C ₂ H ₄ I ₂	ThioDMF (2 mL)	0
10	-	C ₂ H ₄ I ₂	DMF (2 mL)	0
11	4 equiv	C ₂ H ₄ I ₂	DMF (2 mL)	83
12	2 equiv	I ₂	DMF (2 mL)	69 (64 ^{c)})

^{a)} All reactions were performed using 100 mg (1 equiv) of indigo and 2 equiv. of iodine source.

^{b)} Yields determined by GC-MS.

^{c)} Isolated yields.

As DMF is not considered the most environmentally friendly option, we decided to evaluate its role as oxygen source using greener options as solvents. Cyrene (dihydrolevoglucosenone), usually described as a good alternative to DMF, and 2-methyltetrahydrofuran (2-MeTHF) were chosen. Due to the well-known decomposition of Cyrene under basic conditions,⁹ we performed the reaction using stoichiometric amount of NaH, in the presence of 200 μL of DMF, followed by the addition of 1,2-diiodoethane in 1.8 mL of Cyrene (**Table 4.1**, entry 6), obtaining only trace amounts of tryptanthrin under these conditions. Replacing the solvent by 2-MeTHF, a small amount of tryptanthrin was detected (**Table 4.1**, entry 7), as well as traces of isatin and considerable quantity of 1,2-diiodoethane. With the addition of two equivalents (58 μL) of DMF (**Table 4.1**, entry 8), an increased amount of isatin and tryptanthrin were observed, pointing to the involvement of DMF in the indigo oxidation to isatin and consecutive oxidative cyclization. To verify this hypothesis, a solvent with similar properties and structure – dimethylthioformamide – was selected to perform the reaction under the optimized conditions (**Table 4.1**, entry 9). Under these conditions, no tryptanthrin was detected, only unreacted indigo, indicating that the reaction does not occur. This attempt allowed us to infer that dissolved oxygen, water traces or hydroxyl anions eventually present in the solvent are not responsible for the oxidative process.

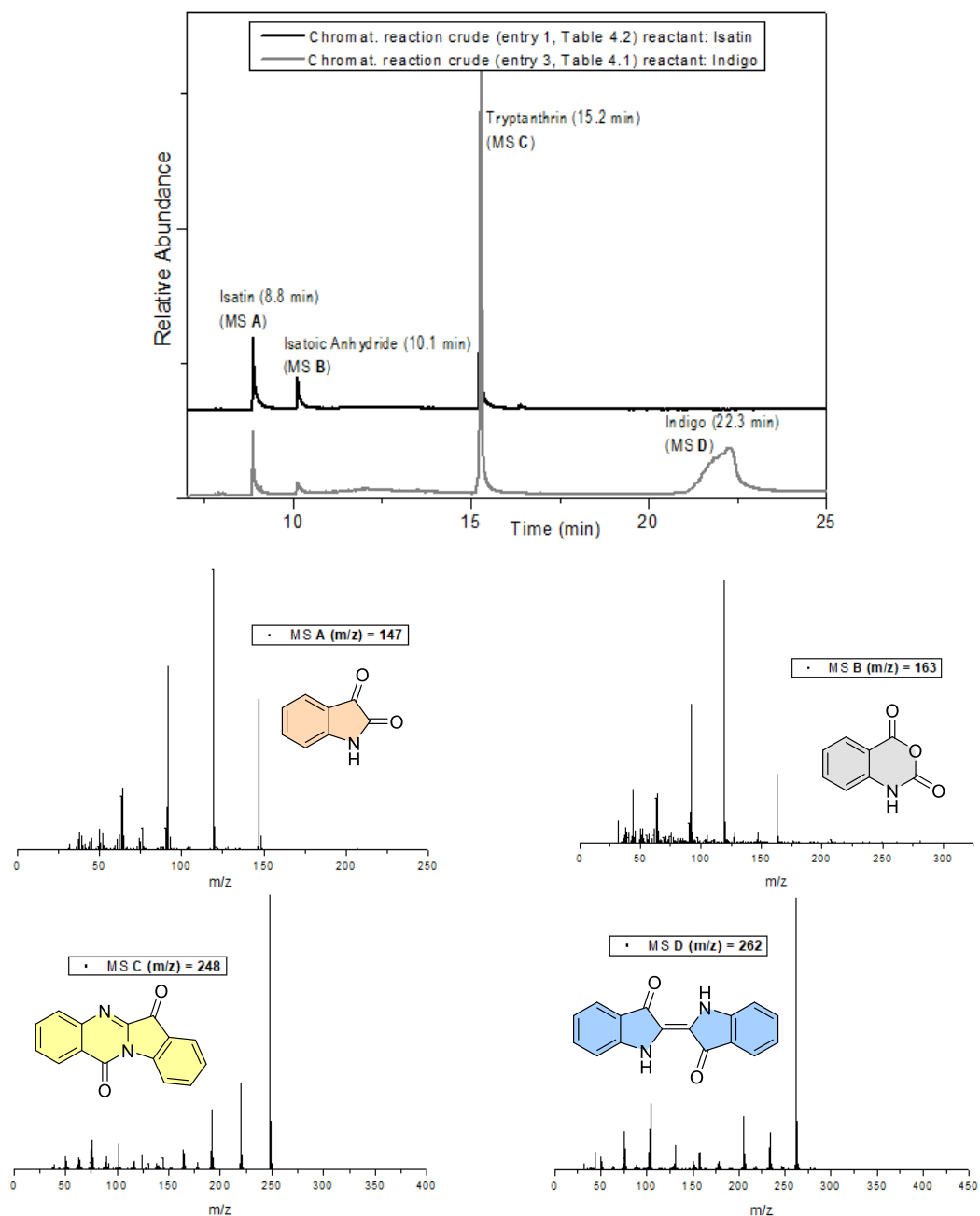


Figure 4.1. GC-MS chromatograms of the products obtained for the synthesis of tryptanthrin from indigo and isatin, and the mass spectra of the four relevant compounds (A = isatin; B = isatoic anhydride; C = tryptanthrin; D = indigo).

When a mixture of DMF and dimethylthioformamide (1:1) was used as solvent, tryptanthrin was detected showing, once again, the importance of DMF as oxygen source under the conditions described.

To evaluate the impact of NaH on the mechanism, two reactions were performed using DMF as solvent, one without the presence of NaH (**Table 4.1**, entry 10), and other with doubled equivalents (**Table 4.1**, entry 11). Under these reaction conditions, for the first case only unreacted indigo was detected in the GC-MS profile, while a dramatic

increase in the tryptanthrin formation was verified in the second case, showcasing the relevance of NaH to the success of the reaction. This yield increase might be due to several contributions: (i) the involvement of NaH in the decomposition of the dihaloalkane and production of reactive oxidant species; (ii) the need to have deprotonated indigo to promote the reaction; (iii) to the existence of a secondary reaction that might take place between NaH and DMF, as described in the literature, in which DMF can be decomposed to a dimethylamine salt, which can be alkylated in the presence of the dihaloalkane;^{10, 11} (iv) it might be involved in an acid-base reaction with isatin increasing its nucleophilicity; and (v) the use of excess hydride might promote this reaction that facilitates the formation of tryptanthrin.

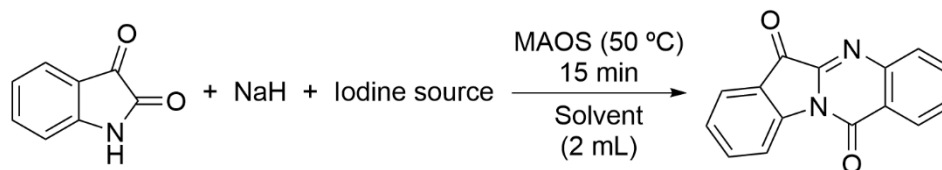
Since we observed the formation of a gas immediately after the addition of the 1,2-diiodoethane, we conducted a headspace GC-MS analysis in the closed microwave reactor. The result showed the presence of ethylene, indicating the decomposition of 1,2-diiodoethane under basic conditions. This leads to the formation of iodine or iodide radicals. Iodine is a universal oxidizing agent and a mild and non-toxic Lewis base catalyst, vastly used in the synthesis of heterocyclic compounds.¹²⁻¹⁵ For these reasons, we presumed it to be the oxidant in our reaction.

To further explore this hypothesis, we conducted the same reaction using molecular iodine (**Table 4.1**, entry 12). A considerable amount of tryptanthrin was detected under this reaction conditions, as well as isatin and isatoic anhydride, indicating once again their character as reaction intermediates/side-products. This information allowed us to infer that the presence of iodine (molecular iodine or organic iodide), combined with DMF and NaH, were determinant for the formation of tryptanthrin from indigo.

Since isatin and isatoic anhydride have been detected in many of the explored reaction conditions, we decided to verify if the reactant *trio* played a crucial role only in the oxidation of indigo to isatin/isatoic anhydride, or if it was also pivotal for the second step of the oxidative cyclization. To achieve this goal, we performed a series of reactions, but using isatin as starting material, instead of indigo (**Table 4.2**). The first test consisted of the reaction between isatin, NaH and 1,2-diiodoethane in 2 mL of DMF (**Table 4.2**, entry 1 and **Figure 4.1**). Tryptanthrin was formed in considerable yield, as expected, while this compound was not formed in the absence of iodine (**Table 4.2**, entry 2). This shows the crucial role played by iodine to not only generate isatin from indigo, but also to promote the oxidative cyclization to afford tryptanthrin. When switching to catalytic amounts of iodine (0.2 equivalents), the reaction did not occur after 15 minutes (**Table 4.2**, entry 3). By using molecular iodine in excess (2 equivalents), tryptanthrin could be detected in moderate yields (**Table 4.2**, entry 4). The removal of NaH (**Table 4.2**, entry

5) or replacement of DMF by 2-MeTHF (**Table 4.2**, entry 6) failed to afford tryptanthrin after 15 minutes reaction time under microwave irradiation.

Table 4.2. Microwave-assisted tryptanthrin synthesis using isatin^{a)} as starting material.



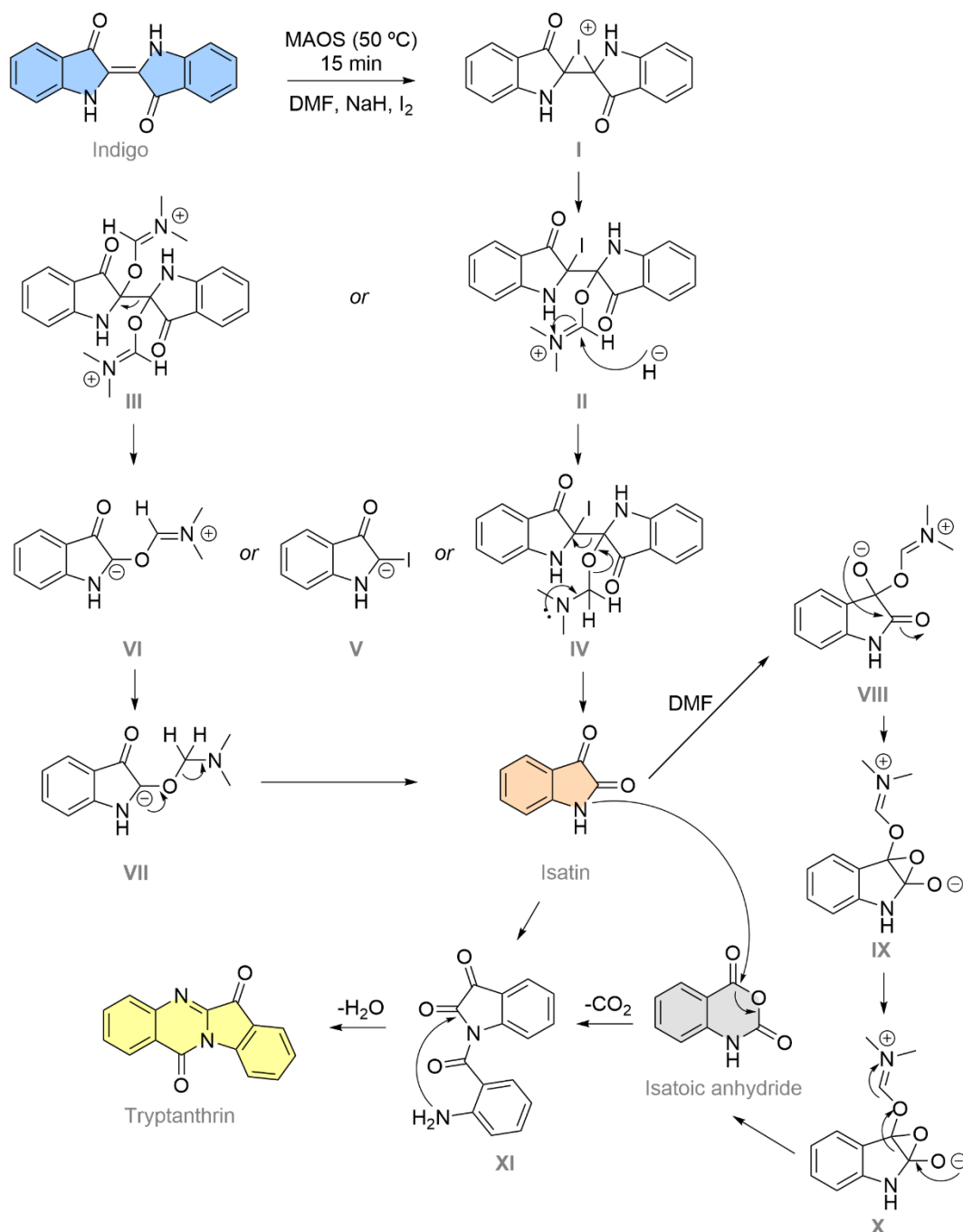
Entry	NaH	Iodine source ^{a)}	Solvent	% Tryptanthrin ^{b)}
1	1 equiv	C ₂ H ₄ I ₂ (2 equiv)	DMF	56
2	1 equiv	-	DMF	0
3	1.5 equiv	I ₂ (0.2 equiv)	DMF	0
4	4 equiv	I ₂ (2 equiv)	DMF	39
5	-	C ₂ H ₄ I ₂ (2 equiv)	DMF	0
6	1 equiv	C ₂ H ₄ I ₂ (2 equiv)	2-MeTHF	0

^{a)} All reactions were performed using 100 mg (1 equiv) of isatin.

^{b)} Yields determined by GC-MS.

After gathering all this information and taking in consideration previous reports found in the literature on the tryptanthrin synthesis and the DMF capability to act as oxygen source, we proposed a mechanism for the indigo transformation to isatin and isatoic anhydride (**Scheme 4.1**). The addition of iodine to indigo double bond (I) followed by the addition of DMF as proposed by Sudalai and co-workers, should lead to the formation of intermediate II.¹⁶ The iodine atom could be further substituted by DMF, generating intermediate III, as proposed by Liu *et al.*¹⁷ At the next stage, addition-elimination processes with hydride acting as the nucleophile,¹⁸ should form isatin precursors IV-VII. After the formation of isatin, this molecule could be oxidized to isatoic anhydride via DMF addition, intramolecular cyclization (analogous to the one reported for the oxidation with peroxide by Wu and co-workers¹⁹) and hydride addition-elimination (VIII-X). The condensation of the two detected synthetic intermediates (isatin and isatoic anhydride) would generate the target compound tryptanthrin through a well-established mechanism, via the condensation of these two molecules via intermediate XI.^{3, 20-22}

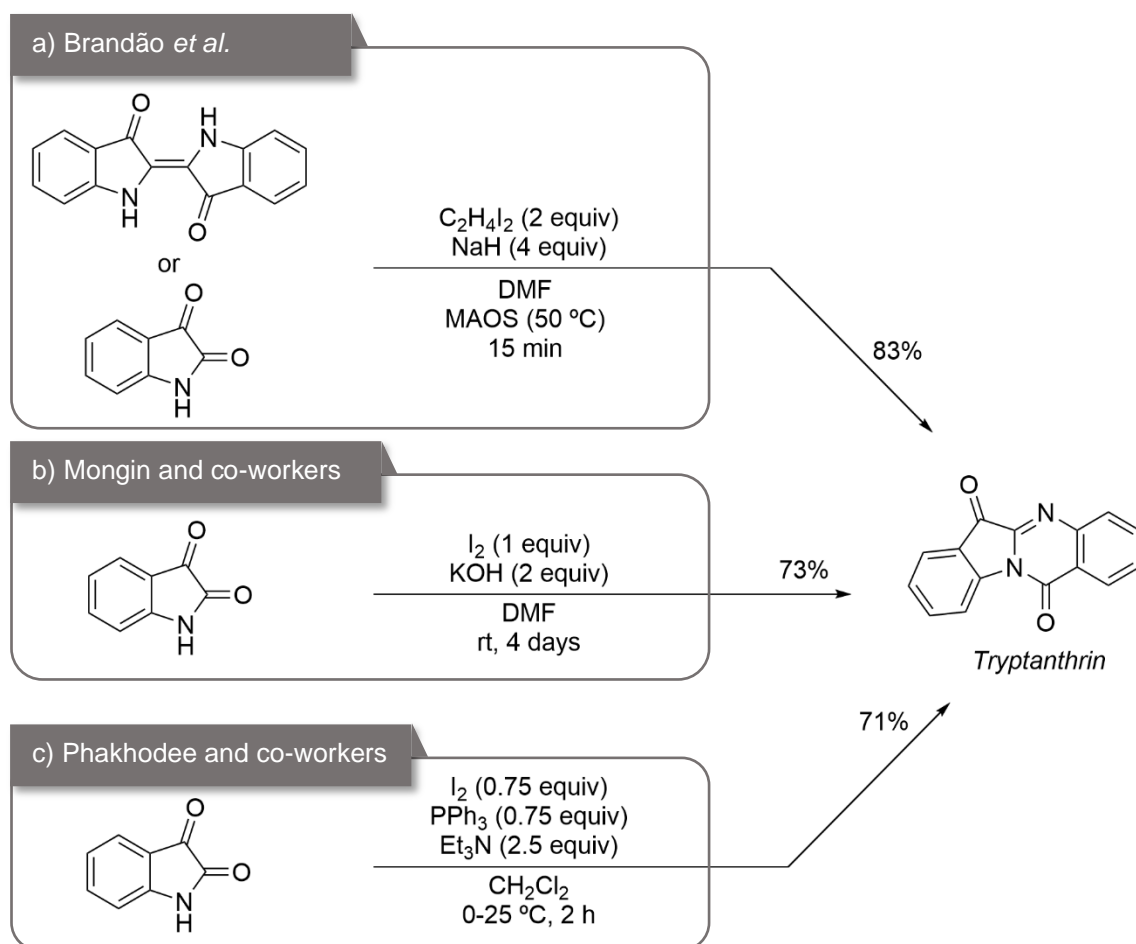
The developed methodology was further attested in the synthesis of bromine derivatives, in a collaborative work. Using two relevant dyes – 6,6'-dibromoindigo (Tyrian Purple) and 5,5',7,7'-tetrabromoindigo (Tina Blue), the corresponding di- and tetrabromotryptanthrin derivatives were isolated in 36 and 18% yield, respectively. The lower yields are likely to be due to the lower solubility exhibited by these dyes in DMF, when compared to indigo.



Scheme 4.1. Proposed mechanism for the indigo transformation to isatin and further oxidation to isatoic anhydride.

The results herein discussed have been published in the *Journal Dyes and Pigments* (**Appendix 11**) (**Scheme 4.2 a**).²³ Noteworthy, almost simultaneously, two other papers were published, concerning the I₂ promoted synthesis of tryptanthrin and its derivatives, by two different research groups. Mongin and co-workers reported a room temperature procedure where tryptanthrin and substituted versions were obtained from isatin, in the presence of equimolar amounts of molecular iodine and an excess of KOH, in DMF (a total of 8 examples, 15-80% yield; in some examples, the procedure required

a reaction time of 4-8 days at room temperature and increase in temperature to 100 °C for 3 or 19 hours) (**Scheme 4.2 b**). In this example, no exhaustive optimization of the reaction conditions was reported.²⁴ Phakhodee and co-workers reported the synthesis of tryptanthrin and 5 derivatives (40-84% yield), in the presence of molecular iodine, triphenylphosphine (Ph_3P) and triethylamine in dichloromethane (**Scheme 4.2 c**).²⁵ These contemporary approaches, despite sharing the iodine promoted synthesis of tryptanthrin with our approach, present several differences. The main findings and advantages of this newly developed approach are i) different iodine sources (molecular iodine and organic iodine) can promote tryptanthrin synthesis; ii) considerable reaction time reduction (15 minutes *versus* hours or days); iii) the use of the sustainability inherent to microwave irradiation (as evidenced in the *E*-factor calculation) ; iv) the other approaches are limited to the use of isatin as starting material, whereas the procedure herein reported withstands indigo and isatin as starting materials and; v) it is one of the



Scheme 4.2. Contemporary iodine-promoted approaches for the synthesis of tryptanthrin (the yields and reaction conditions depicted are relative to the best reaction conditions).

rare examples found in literature concerning the use of DMF as a “building block activating agent”, playing a dual role – oxygen source and solvent.

Taking into account the three synthetic methodologies described in **Scheme 4.2**, a comparison regarding sustainability was performed, using green metrics in order to evaluate the eco-friendliness of these processes. Atom economy, E-factor and EcoScale, discussed in Chapter 1, were the metrics selected for this evaluation.²⁶⁻³⁰

Considering the terminology used in **Scheme 4.2**, the following labels were attributed for the different approaches: *a-is* for the approach reported in our work, using isatin as starting material; *a-in* for the one we reported using indigo as starting material; *b* for the protocol established by Mongin and co-workers and; *c* for Phakhodee and co-workers methodology. The green metrics results are depicted in **Figure 4.2**. Considering the E-factor, where the lower the value the greener the process, the ratio between the mass of waste and the mass of product is evaluated (please note that the isolation was not considered for the calculation, since we did not possess all the required data). The best result was achieved in our approach, using indigo as starting material (*a-in*), with a great impact on this value being achieved by using microwave irradiation and by the improvement on the reaction yield. We can assume that fine-tuning of the reaction condition using isatin as starting material (*a-is*), could lead to yield improvement and consequent reduction on the E-factor value achieved. As regards atom economy, which only takes into account the molar mass of the reactants and the stoichiometry of the reaction, and therefore the higher the value the better, the best result was achieved by method *b*. However, it is necessary to keep in mind that for our methodology, DMF is taken into account in the calculation as a reactant, while its use in method *b* is not considered. For the EcoScale, the value achieved by *a-is* was not calculated, since the lower yield displayed in this not optimized approach would have a negative impact in the evaluation. For this metric system, isolation was taken into account, as quantities are not required for the assessment. Once again, method *b* proved to be slightly better than the remaining protocols. The higher yield obtained using our method was not enough to compensate characteristics of the selected base, with KOH being considered less dangerous than NaH used in our protocol. Nevertheless, the overall evaluation shows that our process, especially the one using indigo as starting material, possesses greater or comparable eco-friendliness to the ones described by the other research groups. Unfortunately, direct comparison with other methods using indigo as starting material to prepare tryptanthrin was not possible, as the original references do not provide the information required to thoroughly perform such an evaluation.

This work opened the door to a series of other relevant studies on the properties and applications of tryptanthrin, from the synthetic and medicinal chemistry point-of-view,

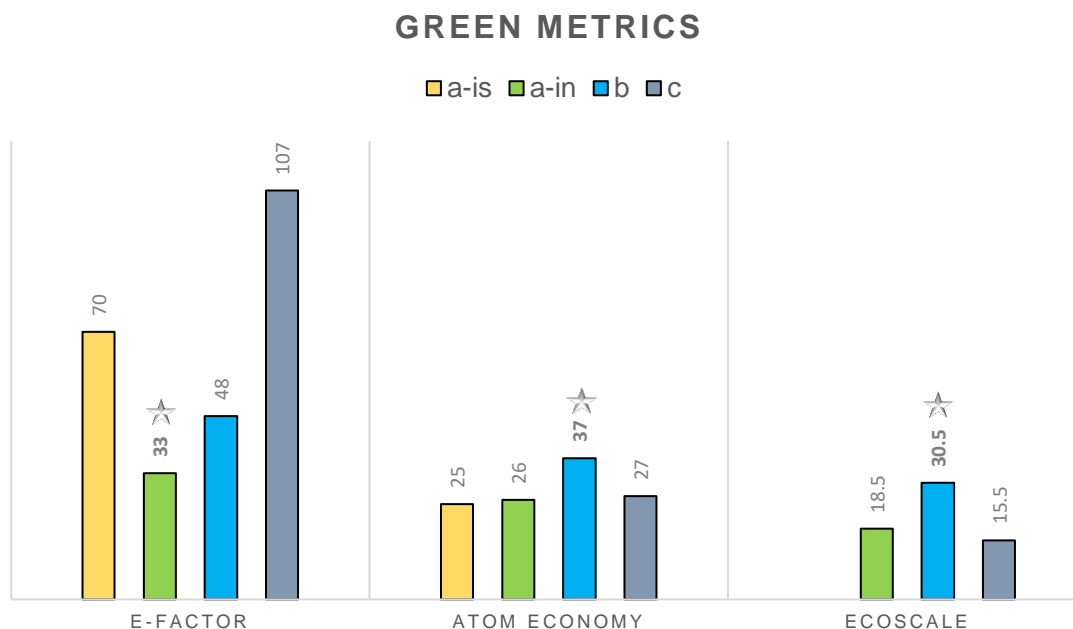


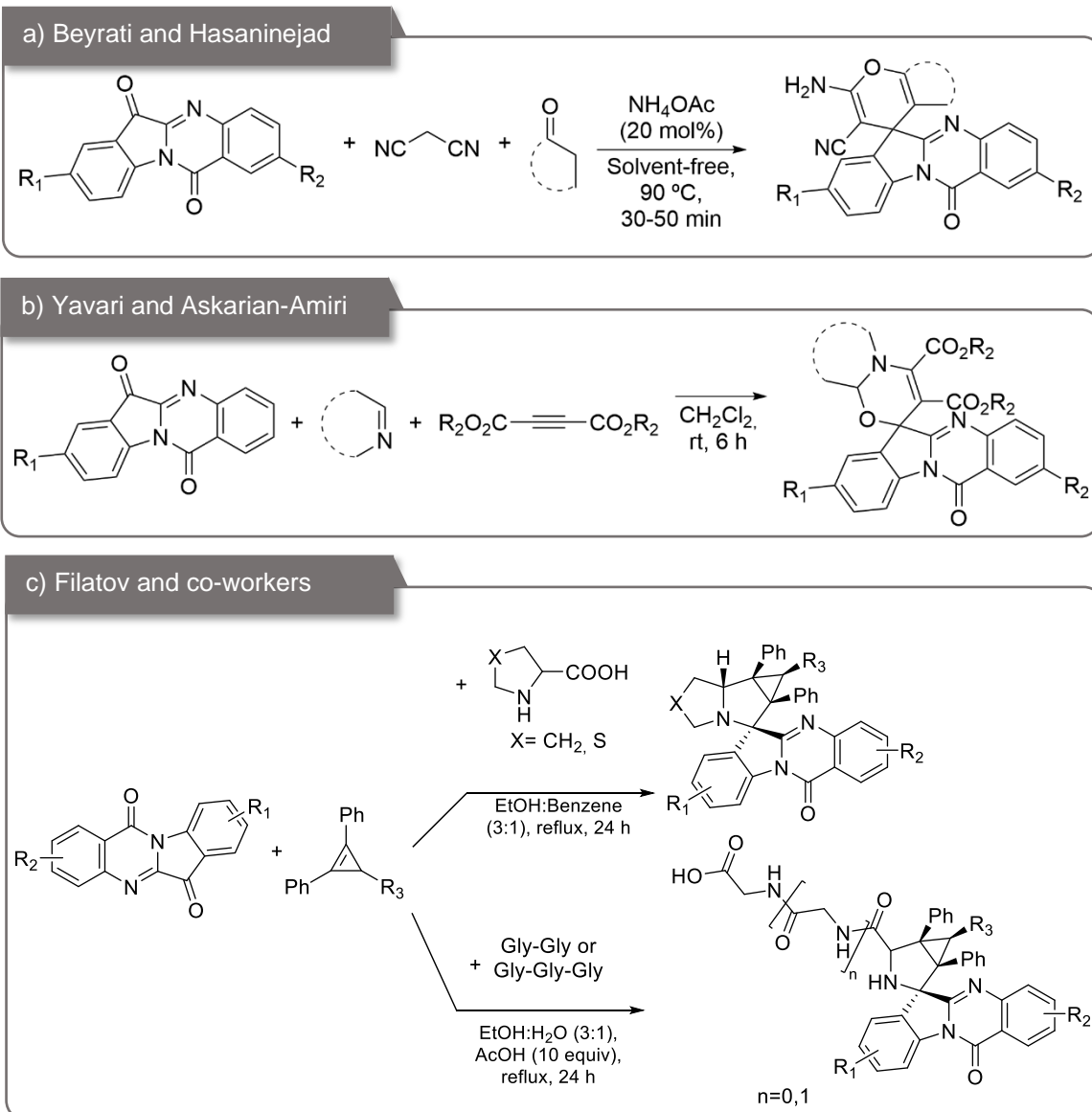
Figure 4.2. Green metrics evaluation of contemporary approaches using iodine-promoted synthesis of tryptanthrin.

as will be discussed in the next sections of this Chapter, but also in the studies of photophysical properties and potential application of tryptanthrin for energy storage (work developed in the Photochemistry Group@UC).^{31, 32}

4.3. What's Next? Engaging Tryptanthrin in MCRs

The developments achieved in the synthesis of tryptanthrin open the way for the sustainable synthesis of a new family of potentially bioactive compounds through MCRs. Considering the notorious knowledge already published in the literature about this molecule in what concerns its potential pharmacological applications, as already explored in the introduction of this thesis, surprisingly, tryptanthrin-based MCRs remain relatively unexplored. At the moment, only three examples were found. The first, reported by Beyrati and Hasaninejad, consists in the 3-MCR between tryptanthrin, C-H activated carbonyl compounds and malononitrile (**Scheme 4.3 a**). This solvent-free protocol, catalyzed by ammonium acetate, allowed the synthesis of a library of 20 spiro-tryptanthrin derivatives in very good to excellent yields (83-96%).³³ More recently, another example was published on a 3-MCR involving tryptanthrin, developed by Yavari and Askarian-Amiri. The tetracycle intercepts the Huisgen zwitterionic intermediate generated *in situ* from *N*-heterocycles and acetylenic esters (**Scheme 4.3 b**). A new family of spiro-tryptanthrin derivatives (10 examples) were obtained in very good yields

(70-85%) under catalyst-free conditions.³⁴ A third example, reported by Filatov and co-workers, consisted in the three component reaction between tryptanthrin, cyclopropenes and α -amino acids or simple peptides (glycine-based di- and tripeptides). The reaction occurs via 1,3-dipolar cycloaddition of the *in situ* formed azomethine ylide to cyclopropenes, leading to the formation of spiro analogs (25 examples) in moderate to very good yields (**Scheme 4.3 c**).³⁵



Scheme 4.3. Reported examples of tryptanthrin-based MCRs.

4.3.1. Tryptanthrin and the Ugi Reaction

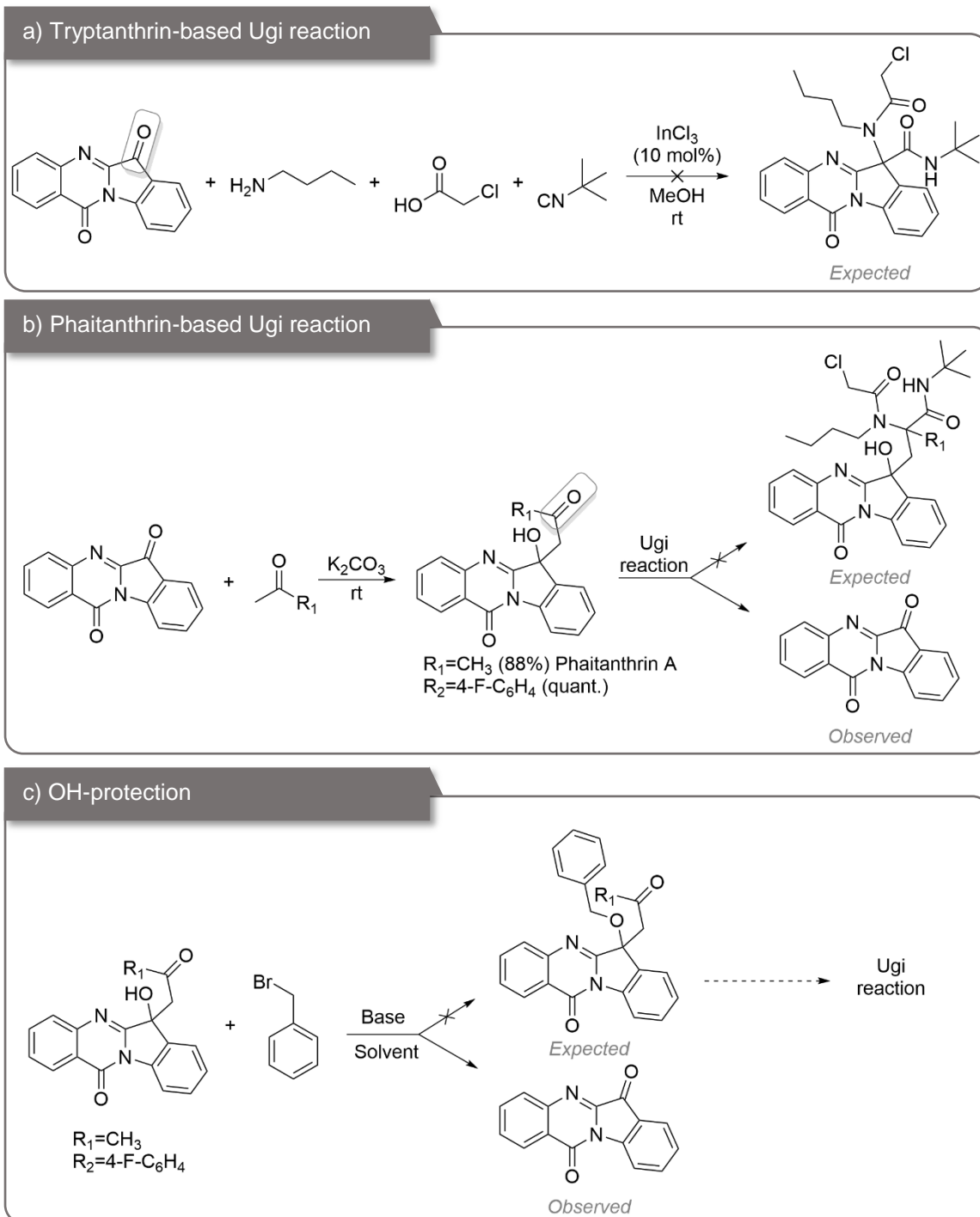
Taking into consideration the landscape of the state-of-the-art of tryptanthrin-based MCRs, we decided there was a great opportunity to further explore the potential of this molecule. With the expertise described in the previous Chapters, our first intention was to engage tryptanthrin in the Ugi reaction. It was assumed that the carbonyl group at

position 6 of the tryptanthrin core would react in a similar fashion to the one observed with the carbonyl group at position 3 of the isatin core (as discussed in Chapters 2 and 3). To achieve this goal, we started by using the best reaction conditions described in Chapter 2, promoting the reaction between tryptanthrin, *n*-butylamine, chloroacetic acid and *tert*-butyl isocyanide, in the presence of InCl_3 , using methanol as solvent. No reaction occurred at room temperature or even when the temperature was increased to 65 °C (**Scheme 4.4 a**).

Intrigued by this result, we decided to further explore this approach. Phaitanthrins are a class of natural products which can be easily obtained from tryptanthrin, via aldol reaction at position 6 of the tryptanthrin core. The phaitanthrins and their synthetic derivatives have been shown to be bioactive.^{3, 36-38} We decided to investigate the synthesis of phaitanthrin A and another phaitanthrin derivative, in order to achieve acyclic carbonyl groups (ketones), which could further be used as the Ugi reaction carbonyl component. The synthetic approach has been widely described in the literature, and consists in the aldol reaction between tryptanthrin and a ketone in the presence of a base.³⁹⁻⁴¹ We selected two ketones (acetone and 4'-fluoroacetophenone), which are liquids at room temperature, so they could play a dual role as solvent and reagent, and potassium carbonate as the base. The resulting phaitanthrins were obtained in very high to quantitative yields. However, on attempting the Ugi reaction under the conditions mentioned previously, we only observed a retro-aldol reaction forming tryptanthrin in a quantitative yield (**Scheme 4.4 b**).

To avoid the retro-aldol reaction, we performed some assays to attempt to protect the alcohol group with benzyl bromide. We looked at the optimizing the base/solvent system, and studied the following combinations: K_2CO_3 /acetone, NaH/N -methylmorpholine, NaH/N -methyl-2-pyrrolidine, NaH/THF , $\text{K}_2\text{CO}_3/\text{THF}$, KOH/THF , NEt_3/THF :acetone (**Scheme 4.4 c**), as well as a tandem reaction, where we attempted to generate phaitanthrin A *in situ* from tryptanthrin, while promoting the consecutive benzyl protection of the alcohol group. None of these experiments gave the desired *O*-protected derivative, with tryptanthrin being obtained in the first approach, whilst in the tandem reaction, phaitanthrin A was formed but the reaction did not proceed any further.

Knowing that the Ugi reaction mechanism starts with the formation of the imine intermediate, and as the reaction proceeds when isatin is used as starting material, we decided to verify if the imine was formed with tryptanthrin, phaitanthrin A or phaitanthrin derivative. In order to do this study, the reaction was carried out with *n*-butylamine in methanol, in the presence and absence of the catalyst, InCl_3 . No imine derivative was observed, and both phaitanthrins were observed to revert back to tryptanthrin. As a

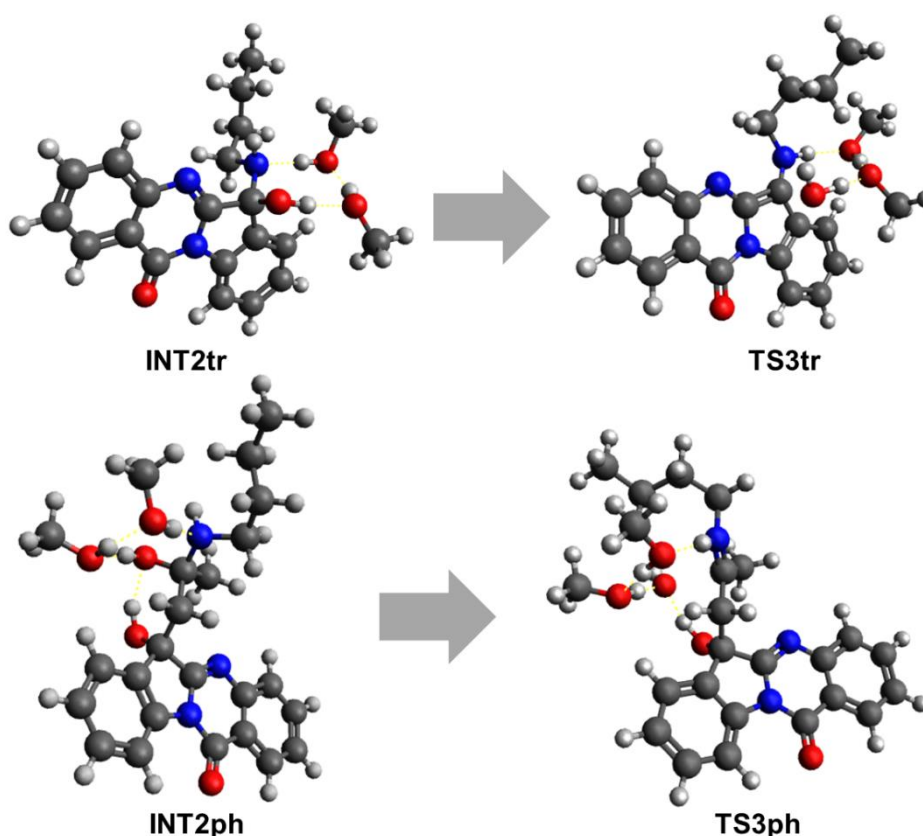


Scheme 4.4. Attempted approaches at performing the Ugi reaction on tryptanthrin and phaitantrins.

consequence, we decided to perform some computational studies, in order to understand the underlying mechanism for the formation of the imine intermediate.

DFT calculation studies, already showcased in Chapter 2 for the isatin-based U4CR, were performed for the tryptanthrin and phaitanthrin-based imine-formation step. For isatin, it was found that the rate-limiting step of the imine formation is the conversion of a carbinolamine intermediate into imine via the second H-transfer involving transition

state **TS3** ($\Delta G_s^\ddagger = 27.5$ kcal/mol). Therefore, analyzing the reactivity of tryptanthrin and phaitanthrin, we focused our attention at this reaction step. For these two reactants, the carbinolamine intermediates **INT2tr** and **INT2ph** and transition states **TS3tr** and **TS3ph** corresponding to the formation of the imines were calculated (**Scheme 4.5**).



Scheme 4.5. Optimized structures of **INT2tr**, **TS3tr**, **INT2ph** and **TS3ph**.

The calculated activation barrier of imine formation for tryptanthrin is 28.6 kcal/mol (in terms of Gibbs free energy) that is by 1.1 kcal/mol higher than for the isatin. Note that this energy difference corresponds to the ratio of the reaction rates *ca.* 6.4 allowing the interpretation of the different behavior of isatin and tryptanthrin in the Ugi reaction.

The calculated activation barrier of the imine formation for phaitanthrin A is much lower ($\Delta G_s^\ddagger = 17.9$ kcal/mol). However, due to the presence of the OH group in phaitanthrin, addition of a base (amine) to the reaction mixture should promote the retroaldol reaction leading to conversion of this reagent into tryptanthrin before the formation of imine species. We can also hypothesize, in the case of phaitanthrin A, that the presence of an intramolecular hydrogen bond between the hydroxy group and the keto group in the side chain can hinder the imine formation reaction.

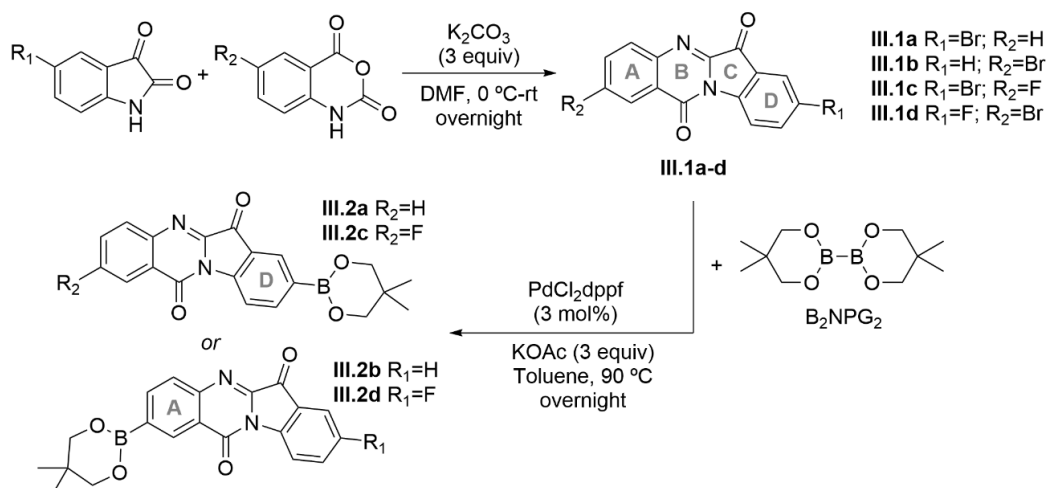
4.3.2. Engaging Tryptanthrin in the Petasis MCR

4.3.2.1. Library III Synthesis

Since the attempts made to perform the Ugi reaction at the C6 position of the tryptanthrin scaffold failed, due to differences of reactivity when compared to the C3 position of isatin, it was decided to evaluate alternatives to perform MCRs in the tryptanthrin unit. Aryl bromide derivatives emerged as a suitable candidate, in particular for the Petasis reaction, a versatile MCR never reported for tryptanthrin, which enables the formation of a C-C and a C-N bonds in a single step,⁴²⁻⁴⁴ and which was recently applied for the synthesis of new 3,3-disubstituted oxindole derivatives.⁴⁵

To achieve such a goal, a three-step pathway was established, consisting of i) synthesis of brominated tryptantrins; ii) borylation of the synthesized tryptantrins and; iii) Petasis MCR. For the synthesis of four different brominated tryptantrins, we selected the classic condensation between isatins and isatoic anhydrides in the presence of a base (K_2CO_3), since we aimed to afford mono-brominated tryptanthrin derivatives (monobromo-indigo is not commercially available). The reaction proceeds smoothly, overnight at room temperature, and the desired brominated tryptantrins are isolated in good to excellent yields (74-95%), which could be used in the next synthetic step without tedious work-up or purification procedures. In the next step, the brominated tryptantrins were borylated using bis(neopentyl glycolato)diboron (B_2NPG_2), in the presence of $PdCl_2(dppf)$ ($dppf = [1,1'$ -bis(diphenylphosphino)ferrocene]) and potassium acetate, in toluene at 90 °C, overnight.⁴⁶ The four borylated tryptanthrin derivatives were obtained in very good to excellent yields (80%-quantitative) and could be used in the Petasis MCR without tedious work-up, relevant for the overall sustainability of the synthetic process. The borylation reaction is selective for the aromatic position substituted with bromine, with no borylation occurring at the fluorine position. The two described synthetic steps are depicted in **Scheme 4.6**.

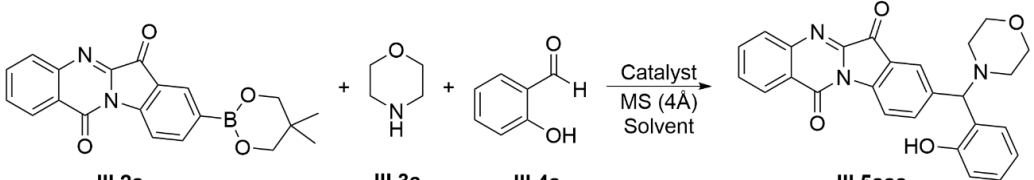
The Petasis reaction was fully optimized by studying different solvents, catalysts and temperatures. For the model reaction, borylated tryptanthrin **III.2a**, morpholine (**III.3a**) and salicylaldehyde (**III.4a**) were selected, and several reaction conditions were evaluated for optimization (**Table 4.3**). Different non-polar, polar aprotic and polar protic solvents were evaluated, namely those typically employed in the Petasis reaction, including benzotrifluoride,⁴⁷ considered a green alternative for dichloromethane. Although acetonitrile and 1,2-dichloroethane led to slightly higher yields than chloroform, we chose the latter, as it allowed a more straightforward work-up, lower operating



Scheme 4.6. Tryptanthrin synthesis from isatin and consecutive borylation.

temperature, and the components exhibited superior solubilities, even at room temperature. With the solvent selected, we attempted to improve the reactivity by screening different metal-based catalysts and organocatalysts. Our first attempt consisted in the use of CuBr/bpy (bpy = 4,4'-bipyridine) (**Table 4.3**, entry 8), based on a methodology described in the literature, which failed to afford the desired product.⁴⁸ Next, different Lewis acids were also screened in the Petasis reaction, including Fe(OTf)₂, Yb(OTf)₃ and InCl₃ (**Table 4.3**, entries 9-11), but no improvement in the reaction yield was observed.⁴⁹ Moreover, *N,N'*-diphenylthiourea (DTPU) only allowed a modest improvement in the yield (**Table 4.3**, entry 12). The best result was achieved using another organocatalyst, (±)-BINOL (**Table 4.3**, entry 13), affording a yield of 66% for compound **III.5aaa**.

With the best reaction conditions in hand, we moved on to study the reaction scope (**Figure 4.3**). The reactions between the four previously described borylated tryptanthrins (**III.2a-III.2d**), different secondary amines (cyclic, aliphatic and disubstituted amines **III.3a-III.3k**) and aldehydes (**III.4a-III.4l**) were evaluated. We verified that the four borylated tryptanthrins were successfully converted into the corresponding Petasis products. Furthermore, we also verified that the multicomponent BINOL-catalyzed reaction is successful when *ortho*-hydroxybenzaldehydes are used, while it does not proceed with other aldehydes (**III.4j-III.4l**), which is in agreement with literature precedence.⁴⁵ In the case of the amines, cyclic secondary amines (exception for **III.3b**), as well as *N*-substituted benzylamine **III.3e** could be successfully used, whereas aromatic amines (**III.3f** and **III.3g**) and aliphatic amines (**III.3h-III.3k**) failed to achieve the desired products.

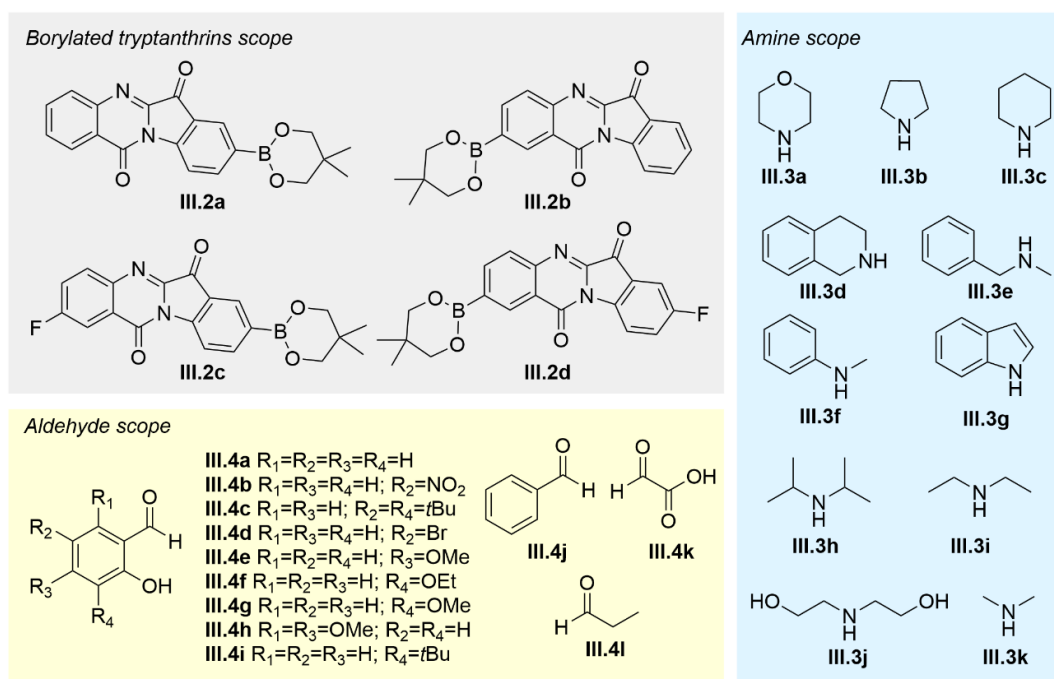
Table 4.3. Optimization of the Petasis reaction conditions.


Entry ^{a)}	Catalyst	Solvent	Temperature (°C)	Time (h)	Yield (%) ^{b)}					
1	-	CHCl ₃	70	24	24					
2	-	Toluene	90	15	14					
3	-	BFT	110	24	<10					
4	-	CH ₂ Cl ₂	50	24	0					
5	-	MeOH	90	24	10					
6	-	CH ₃ CN	90	24	36					
7	-	DCE	90	24	38					
8	CuBr/bpy	DMF	70	36	0					
9	Fe(OTf) ₂	CHCl ₃	70	24	22					
10	Yb(OTf) ₃	CHCl ₃	70	24	23					
11	InCl ₃	CHCl ₃	70	24	22					
12	DPTU	CHCl ₃	70	24 </tr <tr> <td>13</td> <td>BINOL</td> <td>CHCl₃</td> <td>70</td> <td>24</td> <td>66</td> </tr>	13	BINOL	CHCl ₃	70	24	66
13	BINOL	CHCl ₃	70	24	66					

^{a)} Reaction conditions: **III.2a** (0.3 mmol), **III.3a** (1.1 mmol), **III.4a** (0.9 mmol), catalyst (20 mol%), MS 4Å (200 mg) and solvent (3 mL) were added to a Radley's® 12 position carousel reactor tube under nitrogen atmosphere and stirred at the indicated temperature for a certain time.

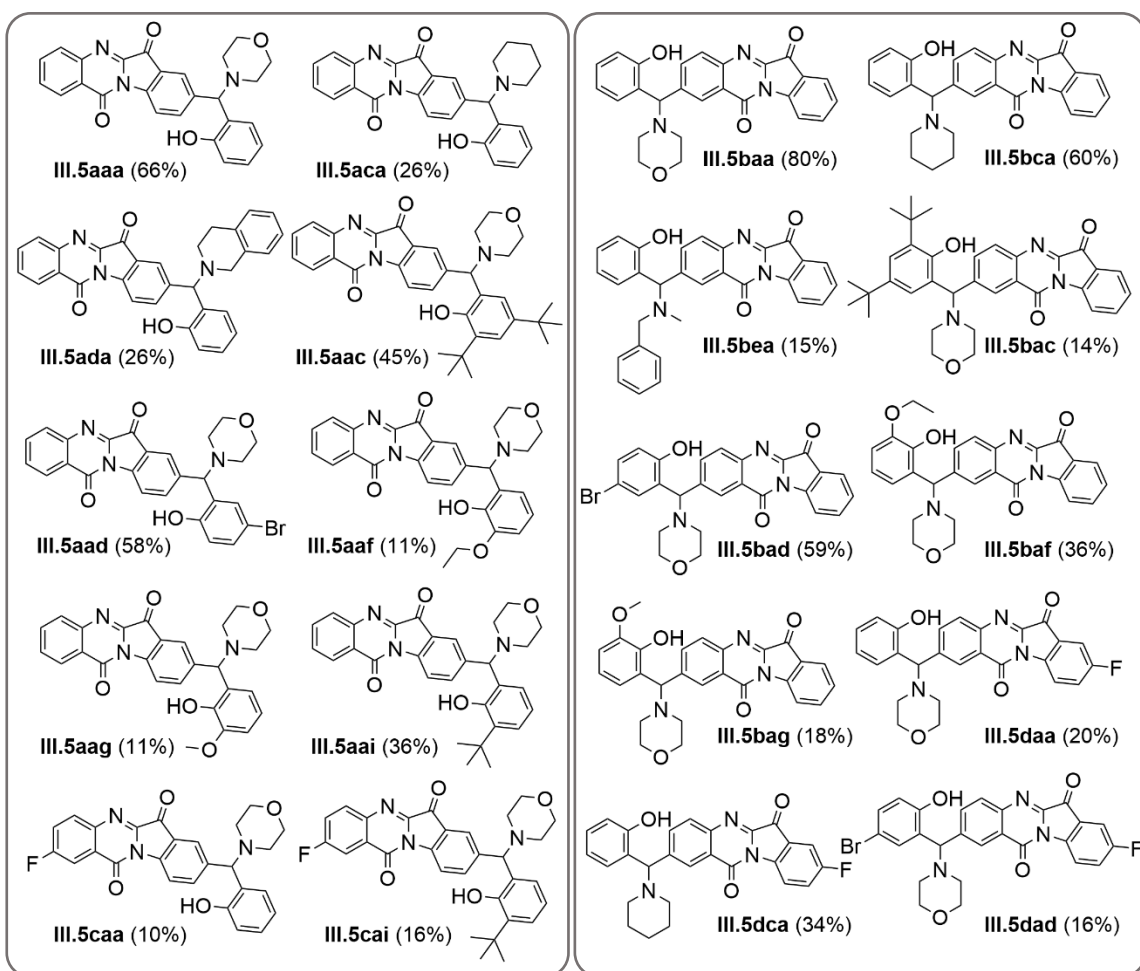
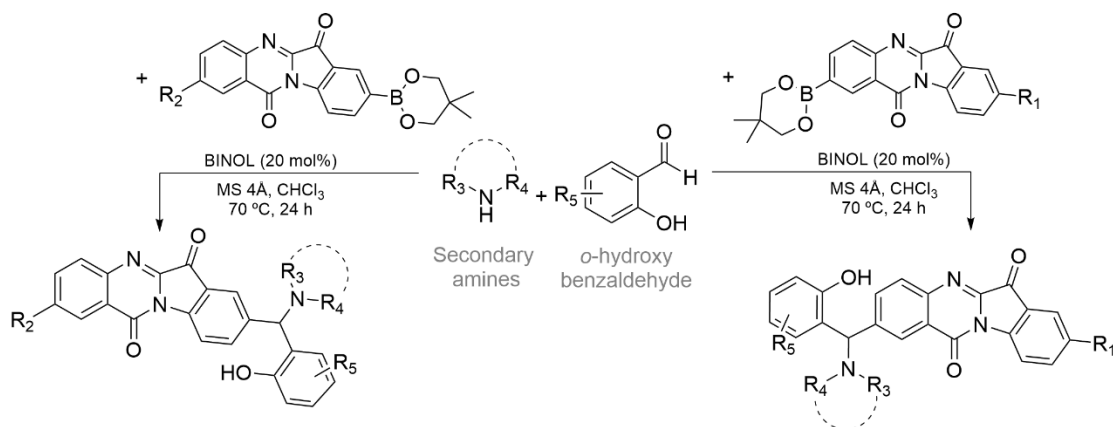
^{b)} Isolated yield.

BTF=benzotrifluoride. DPTU=*N,N'*-diphenylthiourea. BINOL=(±)-1,1'-Bi-2-naphthalene-2,2'-diol.

**Figure 4.3.** Reagent scope for the Petasis multicomponent reaction.

A new route to tryptanthrin and its Petasis adducts

A library of new tryptanthrin derivatives was obtained using the BINOL-catalyzed Petasis MCR (**Scheme 4.7**). Despite the high variability observed in the yields (11-80%), we verified that this chemical transformation is suitable to occur in both the A and the D rings of the tryptanthrin core. In most cases, higher yields were observed when the reaction occurred at position 2 of the tryptanthrin core, as opposed to those reactions at position 8. The only exceptions occurred when aldehydes **III.4c** and **III.4d** were used. The yields observed when fluorinated tryptanthrins were used were also significantly



Scheme 4.7. Library of tryptanthrin derivatives obtained via a Petasis MCR.

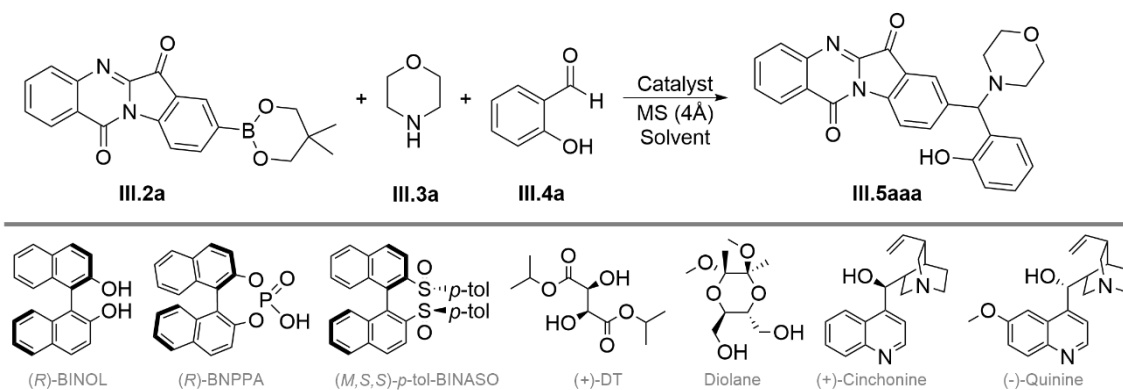
lower on maintaining the same amine/aldehyde components, which might be an indication of some form of deactivating effect.

4.3.2.2. Enantioselective Version of the Tryptanthrin-based Petasis Reaction

Motivated with the results obtained for the synthesis of the library of tryptanthrin-based Petasis adducts, we decided to take this work further and explore the potential of an asymmetric version. Our first efforts were focused on the catalyst which already afforded good results in the racemic version, BINOL.^{50, 51} For this assay, (*R*)-BINOL was selected, affording remarkable enantioselectivity (99% *ee*) (**Table 4.4**, entry 1). Two other chiral BINOL organocatalysts, namely the phosphoric acid derivative (*R*)-BNPPA (**Table 4.4**, entry 2) and the disulfoxide derivative (*M, S, S*)-*p*-Tol-BINASO⁵² (**Table 4.4**, entry 3) were evaluated, as well as two other chiral diols, diisopropyl tartrate (DT) (**Table 4.4**, entry 4) and 2,3-dimethoxy-2,3-dimethyl-5,6-bis(hydroxymethyl) dioxane (Diolane) (**Table 4.4**, entry 5). The hydroxyl bearing alkaloids (+)-cinchonine (**Table 4.4**, entry 6) and (-)-quinine (**Table 4.4**, entry 7) were also evaluated.

Besides the excellent results attained by (*R*)-BINOL, it was observed that the other diol organocatalysts evaluated, (+)-DT and Diolane, also allowed significant enantioselectivities (86% and 59% respectively), which allow us to infer that these diol organocatalysts are the most effective in the Petasis MCR. The remaining organocatalysts led to no significant enantioselectivity. Using smaller amounts of the secondary amine and aldehyde components (**Table 4.4**, entry 8) generated lower yield and enantioselectivity.

The stereochemical configuration of the product was assigned as *S*, on the basis of literature precedence.^{45, 53, 54} We hypothesize the mechanistic pathway showed in **Scheme 4.8**, in which after rapid generation of an iminium intermediate from nucleophilic addition of **III.3a** and **III.4a**, this ion is attacked by the *in situ* generated BINOL-boronic ester on the *Re*-face of the iminium intermediate. The final product is then obtained with the *S*-configuration, while the BINOL catalyst is then presumably recovered by hydrolysis.

Table 4.4. Asymmetric Petasis 3-MCR using borylated tryptanthrin (**III.2a**), morpholine (**III.3a**) and salicylaldehyde (**III.4a**): catalyst evaluation.


Entry ^{a)}	Catalyst	Yield (%) ^{b)}	ee (%) ^{c)}
1	(<i>R</i>)-BINOL	71	99
2	(<i>R</i>)-BNPPA	41	<10
3	(<i>M,S,S</i>)- <i>p</i> -Tol-BINASO	32	<5
4	<i>L</i> -(+)-DT	40	86 ^e
5	Diolane	32	59 ^e
6	(+)-Cinchonine	42	<5
7	(-)-Quinine	29	<5
8 ^{d)}	(<i>R</i>)-BINOL	53	75

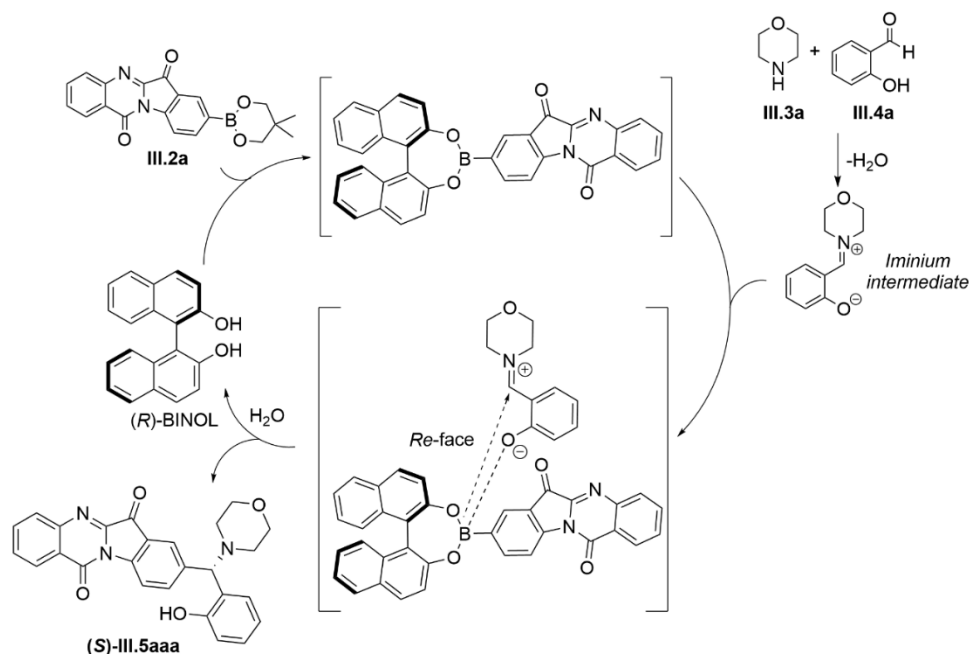
^{a)} Reaction conditions: **III.2a** (0.3 mmol), **III.3a** (1.1 mmol), **III.4a** (0.9 mmol), catalyst (20 mol%), MS 4Å (200 mg) and CHCl₃ (3 mL) were added to a Radley's® 12 position carousel reactor tube under nitrogen atmosphere and stirred at the indicated temperature for a certain time.

^{b)} Isolated yield.

^{c)} Determined by chiral HPLC (see experimental section for further details).

^{d)} reaction performed with 1.2 equiv of (**III.3a**) and 1.2 equiv of (**III.4a**).

^{e)} The major enantiomer has (*R*)-configuration.


Scheme 4.8. Proposed mechanism for the (*R*)-BINOL-catalyzed asymmetric reaction.

4.3.2.3. Druglikeness Evaluation

As already observed in previous Chapters of this thesis, in the context of drug discovery the determination of different physico-chemical properties of drug candidates, as well as their pharmacokinetic profile is of paramount importance. Therefore, we decided to study the same properties (*in silico*) for our newly synthesized tryptanthrin derivatives.

Among the features evaluated by the five filters selected and already described in Chapter 1, the number of hydrogen bond acceptors, donors and the number of rotatable bonds are amongst the easiest to be accessed and are summarized in **Figure 4.4**. As shown, all the compounds are within the established limits by the filters which take these features into account in the druglikeness evaluation.

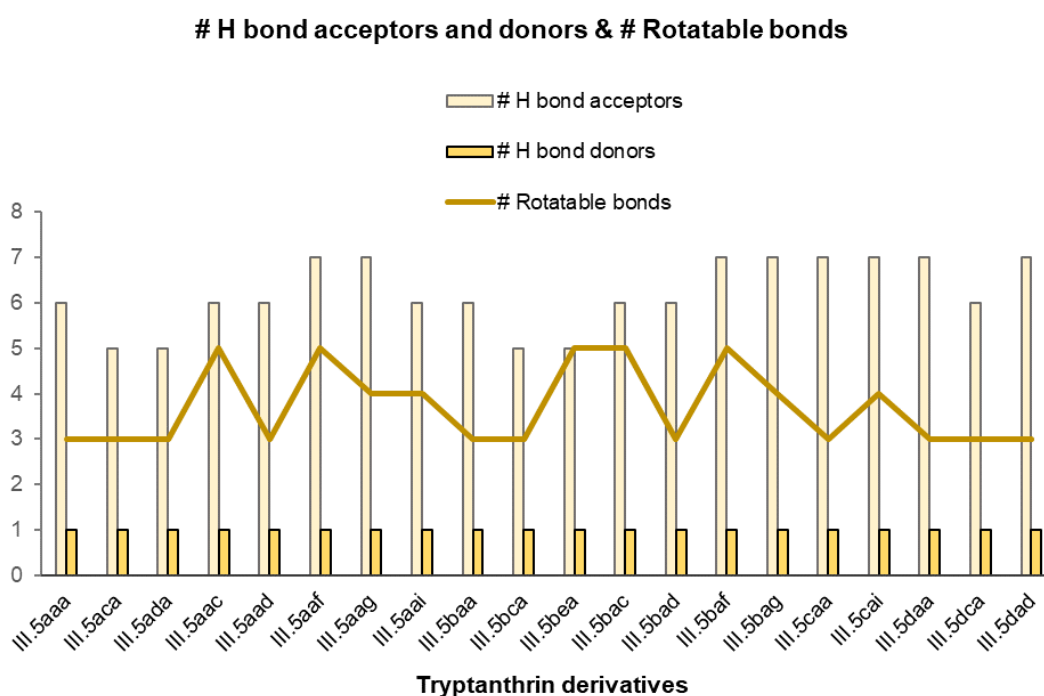


Figure 4.4. Calculated hydrogen bond acceptors, hydrogen bond donors, and rotatable bonds for the synthesized tryptanthrin derivatives.

Other physico-chemical properties predicted and calculated by the selected tool are molecular weight (MW), calculated partition coefficient (ClogP), molar refractivity (MR), topological polar surface area (TPSA), and water solubility (LogS). The results for this library are summarized in **Table 4.5**.

Table 4.5. *In silico* calculation of several physical-chemical properties of the synthesized tryptanthrin derivatives.

Compounds	MW (Da)	MR	TPSA (Å ²) ^{a)}	CLogP ^{b)}	LogS ^{c)}
III.5aaa	439.46	127.26	84.66	2.79	-4.29
III.5aca	437.49	130.98	75.43	3.65	-5.36
III.5ada	485.53	146.01	75.43	4.20	-6.07
III.5aac	551.68	165.80	84.66	5.13	-7.76
III.5aad	518.36	134.96	84.66	3.34	-5.00
III.5aaf	483.52	138.56	93.89	3.10	-4.83
III.5aag	469.49	133.75	93.89	2.78	-4.45
III.5aai	495.57	146.53	84.66	3.97	-6.03
III.5baa	439.46	127.26	84.66	2.87	-4.29
III.5bca	437.49	130.98	75.43	3.73	-5.36
III.5bea	473.52	139.25	75.43	4.21	-6.03
III.5bac	551.68	165.80	84.66	5.23	-7.76
III.5bad	518.36	134.96	84.66	3.49	-5.00
III.5baf	483.52	138.56	93.89	3.19	-4.83
III.5bag	469.49	133.75	93.89	2.85	-4.45
III.5caa	457.45	127.22	84.66	3.09	-4.45
III.5cai	513.56	146.49	84.66	4.27	-6.13
III.5daa	457.45	127.22	84.66	3.17	-4.39
III.5dca	455.48	130.94	75.43	4.04	-5.46
III.5dad	536.35	134.92	84.66	3.79	-5.12

a) Calculated in accordance to ref. ⁵⁵.

b) SwissADME provides 5 LogP values and ClogP is an average of these calculations.

c) Calculated in accordance to ref. ⁵⁶.

Checking these results in detail and keeping in mind the ranges established by the filters for each one of them, several conclusions can be drawn. In what concerns the MW, our library spanned the range $437.49 \leq MW \leq 551.68$ Da. This means six of these new compounds are not compliant with the Lipinski parameterization. However, it is well-established that compounds can violate one of the Lipinski's parameters, but still be compliant with the Lipinski filter and even end up as a successful drug. All the compounds fall within the parameterization established in the Muegge filter, whereas several are not compliant with the Ghose filter for this property. MR is taken into account only by the Ghose filter ($40 \leq MR \leq 130$). With our library spanning in the interval $127.22 \leq MR \leq 165.80$, it means several of these compounds are beyond the upper limit of this filter. The TPSA is a parameter considered in the Veber, Egan and Muegge filters. With the library displaying TPSAs ranging from 75.43 \AA^2 to 93.89 \AA^2 , it is concluded that the compounds are compliant with the three filters in what concerns this parameter. Lipophilicity is another relevant physico-chemical property to be evaluated for new drug candidates, as it will determine several aspects of their pharmacokinetic behavior, especially absorption

and distribution, as it determines the rate at which a molecule crosses the cell membrane and distributes across different tissues. This parameter is considered by the Lipinski, Ghose, Egan and Muegge filters and the library of tryptanthrin derivatives was in accordance with the ranges established by Ghose and Egan filters. Compounds **III.5aac** and **III.5bac** display values slightly above the ranges established for the Lipinski and Muegge filters. This finding is driven by the presence of the two *tert*-butyl groups, which significantly increases the lipophilicity of these two compounds. The correlation between LogP and MW is often considered as a good indicator of compounds druglikeness and leadlikeness. **Figure 4.5** displays this correlation, as well as the upper limits imposed by the different filters.

The water solubility of new drug candidates, although it is not considered in any of the five filters evaluated, also plays a very important role in drug discovery and development. The library synthesized in this work display a LogS value between -7.76 and -4.29, being classified as poorly soluble ($-10 \leq \text{LogS} \leq -6$) or moderately soluble ($-6 \leq \text{LogS} \leq -4$).

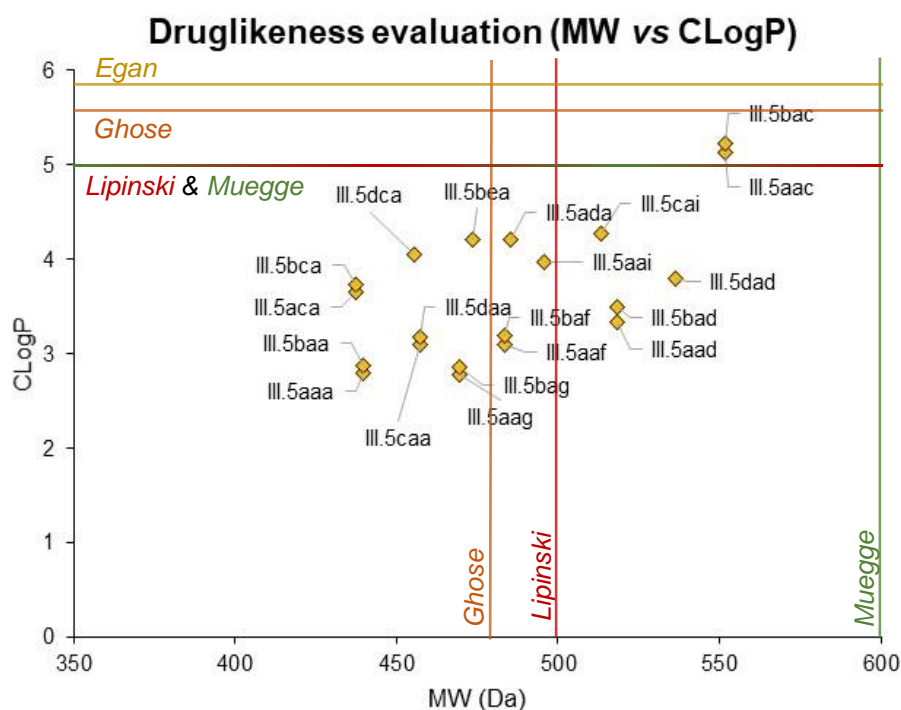


Figure 4.5. MW and CLogP correlation of the synthesized compounds and their placement according to the main filters upper limits.

The BOILED-Egg model for the library prepared in this work is depicted in **Figure 4.6**.

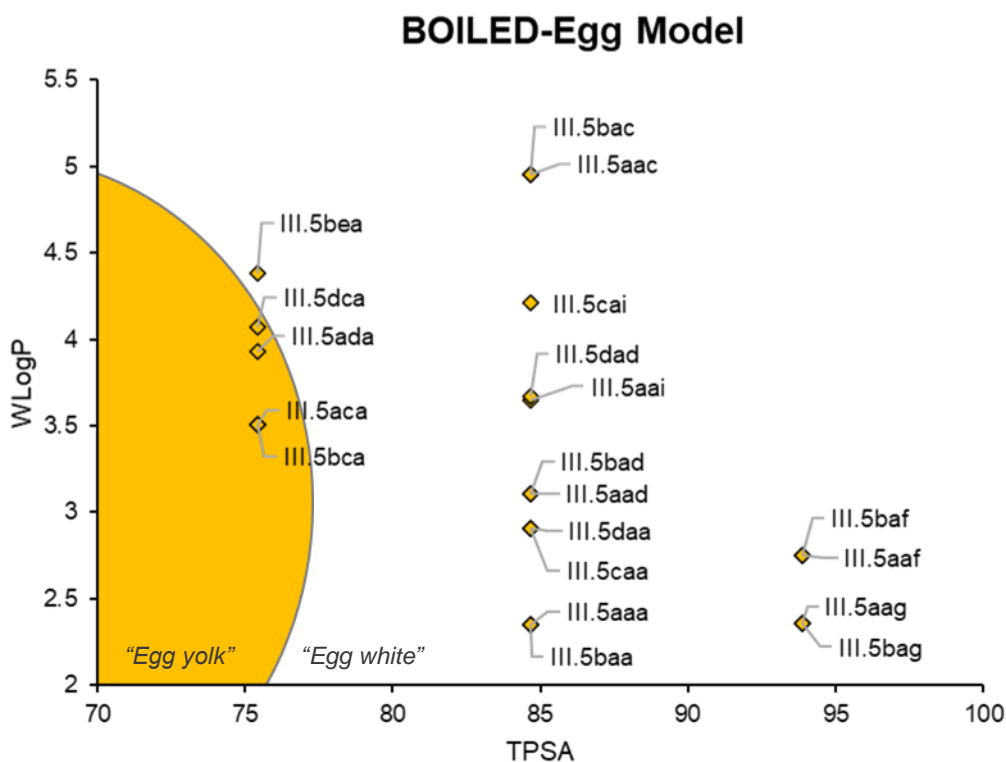


Figure 4.6. BOILED-Egg model for the new tryptanthrin derivatives.

Taking into account this model, it is interesting to verify that four of the newly synthesized compounds (**III.5dca**, **III.5ada**, **III.5aca**, and **III.5bca**) possess, predictably, the ability to cross the BBB. Detailed analysis of their structural features, we can infer that compounds bearing a piperidine or a 1,2,3,4-tetrahydroisoquinoline moiety integrated as the secondary amine component have a lower TPSA value. The remaining derivatives are distributed in the "egg white" area, and therefore display the potential to cross the gastrointestinal barrier via passive diffusion, and therefore are suitable candidates for oral drug administration.

Another interesting feature evaluated by the SwissADME tool is the identification of possible PAINS. According to the web-based tool, all our compounds display a phenolic Mannich base unit, which raises the PAINS flag. Even though this can become a drawback for further drug development of these molecules, we also need to take into account that several compounds bearing this structural feature exhibit significant bioactivity, and therefore with hindsight their early removal from the drug discovery pipeline would have been a gross mistake.⁵⁷ This theory can be illustrated by the example of the drug Lurbinectedin (commercialized as Zepzelca®). This drug was granted an accelerated approval by the FDA in 2020 for the treatment of metastatic small cell lung cancer and bears a phenolic Mannich base in its structure.^{58, 59} In addition, recent studies suggest that the removal of potential-PAINS compounds from drug

discovery pipeline require further data than the simple presence of these structural features, as their PAINS influence is highly dependent on the overall molecular structure.⁶⁰ With this knowledge, we have to admit that more studies will be required in order to verify if the phenolic Mannich bases present in this new library will determine their fate in the drug discovery pipeline.

Table 4.6. Druglikeness filters compliance for the new tryptanthrin derivatives (the number in the red squares indicate the number of rules breached).

		Tryptanthrin derivatives																					
		III.5aaa	III.5aca	III.5ada	III.5aac	III.5aad	III.5aaf	III.5aag	III.5aai	III.5baa	III.5bca	III.5bea	III.5bac	III.5bad	III.5baf	III.5bag	III.5caa	III.5cai	III.5daa	III.5dca	III.5dad		
Filters	Lipinski																						
	Ghose		1	2	3	2	2	1	2		1	1	3	2	2	1		2		1	2		
	Veber																						
	Egan																						
	Muegge				1								1										

Note: A green score stipulates a compliance with the filter, while a red score means the compounds does not comply with the designated filter.

The overall compliance of the synthesized tryptanthrin-based Petasis adducts with the five filters evaluated is depicted in **Table 4.6**. All these new compounds are compliant with the Lipinski, Veber, and Egan filters. With the Muegge filter, only compounds **III.5aac** and **III.5bac** are not compliant, due to their high lipophilicity, displayed due to the presence of the two *tert*-butyl substituents in the salicylaldehyde component. The Ghose filter is, by far, the one which this library is less compliant with, with only compounds **III.5aaa**, **III.5baa**, **III.5caa**, and **III.5daa** achieving the “green light”. The violations of the Ghose filter are mostly due to the high MRs (16 compounds), followed by the high MWs (10 compounds) and, for compounds **III.5aac** and **III.5bac**, which display three violations of this filter, the number of atoms is also an issue, as they are above 70. The overall scores showcase a good druglikeness profile for the newly synthesized library, especially because for the compounds not compliant with the Ghose and Muegge filters, the values are just outside the upper-limits.

All the collected data, combined with the potential displayed by tryptanthrin derivatives, enticed us to search for possible pharmacological applications of these new compounds.

4.3.2.4. Biological Activity Evaluation

As extensively discussed in the Chapter 1 of this thesis, tryptanthrin, as well as its derivatives, possess a wide range of interesting biological activities. Among them, antibacterial and antifungal activity are among the ones most commonly reported for this family of compounds.⁶¹⁻⁶⁴ With this in mind, and taking into account that the synthesized library is the first example of tryptanthrin-based Petasis adducts to be described, and none of the other examples of MCR-based tryptanthrin libraries have been screened for biological activity, we decided to check their antibacterial and antifungal activity. This decision was based on the fact that from all the bioactivities commonly described for tryptanthrin and its derivatives, antimicrobial is one of the most described and therefore we expected it to be a good starting point. This work was performed via a collaboration established with Professor Eugénia Pinto, from the Laboratory of Microbiology, Faculty of Pharmacy, University of Porto.

The antifungal activity was evaluated against nine fungal strains: two yeasts (*Candida albicans* and *Candida krusei*); three filamentous fungi (*Aspergillus fumigatus*, *Aspergillus niger*, and *Mucor* spp.); four dermatophyte species (*Trichophyton rubrum*, *Trichophyton mentagrophytes*, *Microsporum canis*, and *Nannizzia gypsea*). The antibacterial activity was evaluated against a Gram-negative bacteria, *Escherichia coli*, and a Gram-positive bacteria, *Staphylococcus aureus*.

The minimum inhibitory concentrations (MICs) and minimal lethal concentrations (MLCs) were used for defining the antimicrobial activity in agreement with the references of the Clinical and Laboratory Standards Institute (CLSI).⁶⁵ MIC was determined as the lowest concentration leading to 100% growth inhibition, in comparison to the sample-free control, and the MLC was defined as the lowest concentration required so that no colonies grew after incubation.

The library of new tryptanthrin derivatives, as well as the enantiomeric pure version of **III.5aaa**, did not display antibacterial activity against the two bacterial strains evaluated, at 512 µg/mL. For this reason, at this stage, we decided to halt the antibacterial activity evaluation for these compounds.

The evaluation of the antifungal properties gave mixed findings. While all the compounds were found to be inactive against the two yeasts and the three filamentous fungi tested, more promising results were achieved when screening the library against dermatophyte fungi (**Table 4.7**). These findings are very important, as dermatophyte are responsible for many infectious clinical manifestations, especially skin infections, in human health and veterinary settings, being often agents of zoonotic diseases. The

elimination of such pathogens can also be extremely challenging, due to their resistance mechanisms against current therapeutic options.^{66, 67}

Table 4.7. Antifungal activity (MIC and MLC) of the tryptanthrin derivatives against dermatophytes fungi strains.

Compounds	MIC / MLC ($\mu\text{g/mL}$)			
	<i>Trichophyton mentagrophytes</i>	<i>Trichophyton rubrum</i>	<i>Microsporum canis</i>	<i>Nannizzia gypsea</i>
III.5aaa	>512 / >512	>512 / >512	>512 / >512	>512 / >512
III.5aca	>512 / >512	>512 / >512	>512 / >512	>512 / >512
III.5ada	>512 / >512	>512 / >512	>512 / >512	>512 / >512
III.5aac	256 / 256	256 / >512	256 / >512	512 / >512
III.5aad	>512 / >512	>512 / >512	>512 / >512	>512 / >512
III.5aaf	>512 / >512	>512 / >512	>512 / >512	>512 / >512
III.5aag	>512 / >512	>512 / >512	>512 / >512	>512 / >512
III.5aai	>512 / >512	>512 / >512	>512 / >512	>512 / >512
III.5baa	>512 / >512	>512 / >512	>512 / >512	>512 / >512
III.5bca	256 / >512	512 / >512	512 / >512	>512 / >512
III.5bea	64 / 64	64 / 128	64 / 64	256 / >512
III.5bac	512 / 512	256 / >512	512 / >512	>512 / >512
III.5bad	>512 / >512	>512 / >512	>512 / >512	>512 / >512
III.5baf	>512 / >512	>512 / >512	>512 / >512	>512 / >512
III.5bag	>512 / >512	>512 / >512	>512 / >512	>512 / >512
III.5caa	>512 / >512	>512 / >512	>512 / >512	>512 / >512
III.5cai	>512 / >512	>512 / >512	>512 / >512	>512 / >512
III.5daa	>512 / >512	>512 / >512	>512 / >512	>512 / >512
III.5dca	>512 / >512	>512 / >512	>512 / >512	>512 / >512
III.5dad	>512 / >512	>512 / >512	>512 / >512	>512 / >512
(S)- III.5aaa	>512 / >512	>512 / >512	>512 / >512	>512 / >512

Compound **III.5bea** displayed moderate activity against the four dermatophytes tested, being the most promising derivative from the screened library. The best results were obtained against *T. mentagrophytes* and *M. canis*, with MIC/MLC values of 64 $\mu\text{g/mL}$, and *T. rubrum*, with MIC/MLC values of 64/128 $\mu\text{g/mL}$. This indicates that, against these three strains, this compound possesses fungicidal activity. This compound was also the most active against *N. gypsea*, but with weak activity (256 $\mu\text{g/mL}$ MIC value and 512 $\mu\text{g/mL}$ MLC value). Compounds **III.5bac**, **III.5bac**, and **III.5bca** also displayed weak antifungal activity against these four dermatophytes, in most cases with a fungistatic effect. Noteworthy is also the fact that the results achieved by the racemic mixture **III.5aaa** and **(S)-III.5aaa** were identical. Overall, these findings indicate that our compounds showed some degree of selectivity, particularly **III.5bea**, towards dermatophyte fungal infections.

Structurally, these findings provide important information for future drug development and hit-to-lead optimization. One information that stands out is that the only example of an acyclic secondary amine translated into the most active compound against dermatophyte fungal strains. Those compounds based on the aldehyde **III.4c** unit, showed activity, regardless of the structure of the tryptanthrin ring (compounds **III.5aac** and **III.5bac**). The presence of two *tert*-butyl groups also seems to be conducive of biological activity, as compounds bearing only one *tert*-butyl group (**III.5aai** and **III.5cai**) do not display antifungal activity. By comparing compounds **III.5bca** and **III.5aca**, we see that the location of the MCR-formed benzylamine moiety on the tryptanthrin ring has a bearing on the biological activity, since **III.5bca** possesses some antifungal activity, and **III.5aca** none. Also comparing compounds **III.5bea** and **III.5ada**, we can also hypothesize that using less rigid benzylamines as starting material (**III.3e** versus the rigid **III.3d**), is crucial for the antifungal activity observed.

Integrating the knowledge obtained from the druglikeness evaluation and the antifungal studies, we observe that the most active compound (**III.5bea**) complies with all the five rules. Compounds **III.5aac** and **III.5bac**, despite being the least compliant against the druglikeness filters, can still be considered for further studies, as dermatophyte fungal infections usually only require local/topical treatment, and therefore systemic pharmacokinetic behavior/oral bioavailability is not a crucial parameter to take into consideration. Taking a closer look to **Figures 4.5** and **4.6**, we can also infer that it appears to exist a correlation between the LogP value displayed by these new tryptanthrin derivatives and their antifungal activity, with the most active compounds being amongst those with higher LogP values.

The results herein discussed have been published in the *New Journal of Chemistry* (**Appendix 12**).⁶⁸

4.4. Conclusions

In this Chapter, through serendipity we found a new route for the synthesis of tryptanthrin, as well as the integration of this valuable tetracyclic alkaloid in MCRs as can be seen with the Petasis reaction. Several conclusions can be drawn from this work (**Figure 4.7**):

- A new, sustainable, microwave-assisted synthetic route for the preparation of tryptanthrin from indigo and isatin is herein described, based on the use of NaH/DMF/Iodine (as oxidant) trio.

- Our studies show this synthetic route as one of the rare examples found in the literature where DMF works as an oxygen transfer reagent (oxidant).

- Tryptanthrin and phaitanthrin A possess remarkable differences in their reactivity when compared to isatin, and therefore cannot undergo the Ugi reaction using the conditions described in Chapter 2. Computational studies combined with experimental evidence indicate that the imine formation step, the starting point for any Ugi reaction was the limiting step. In the case of tryptanthrin, it was verified the energetic barrier to be higher than the one observed for isatin. In the case of phaitanthrin, it was susceptible to undergo retro-aldol reaction, in the presence of a base.

- A new family of tryptanthrin derivatives obtained via Petasis MCR was successfully synthesized. This approach is one of the few examples reported in the literature of tryptanthrin-based MCR and the first using the Petasis MCR, as well as the first leading to non-spiro derivatives.

- A (*R*)-BINOL-catalyzed enantioselective version was also developed, proving to be suitable for attaining a Petasis adduct of tryptanthrin in excellent ee.

- The synthesized Petasis adducts display interesting druglike properties, making them suitable candidates for further drug development.

- Some of the new tryptanthrin derivatives exhibit interesting antifungal activity against dermatophytes fungi strains, especially compound **III.5bea**.

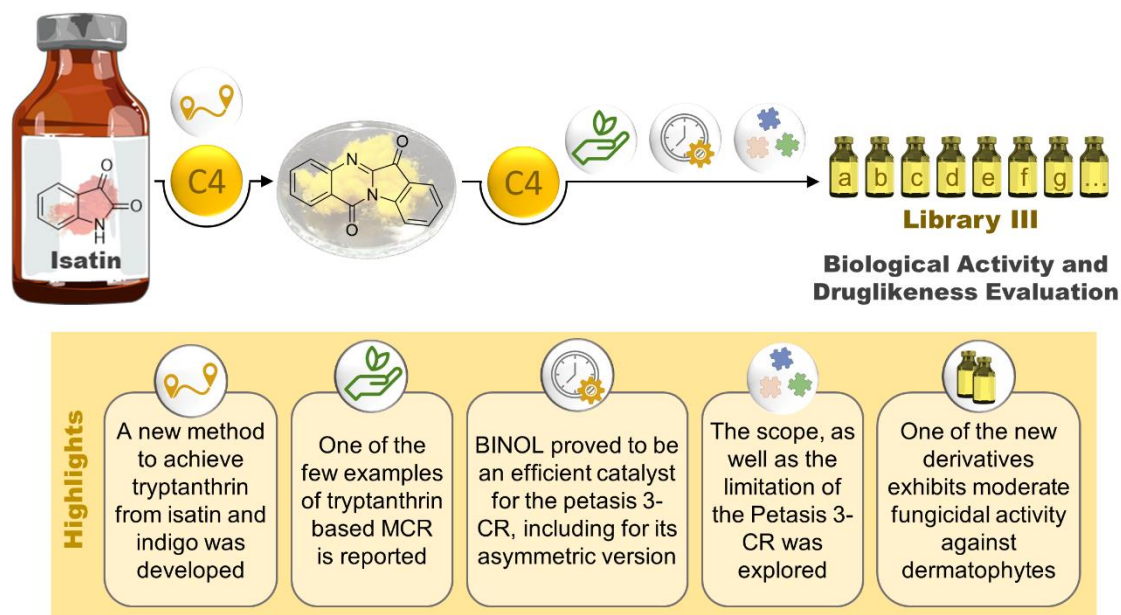


Figure 4.7. Highlights of Chapter 4.

4.5. References

1. Tucker, A. M.; Grundt, P., The chemistry of tryptanthrin and its derivatives. *Arkivoc*, **2012**, (part i), 546-569.
2. Jahng, Y., Progress in the studies on tryptanthrin, an alkaloid of history. *Archives of Pharmacal Research*, **2013**, 36 (5), 517-535.
3. Kaur, R.; Manjal, S. K.; Rawal, R. K.; Kumar, K., Recent synthetic and medicinal perspectives of tryptanthrin. *Bioorganic & Medicinal Chemistry*, **2017**, 25 (17), 4533-4552.
4. Ban, T. A., The role of serendipity in drug discovery. *Dialogues in Clinical Neuroscience*, **2006**, 8 (3), 335-344.
5. Foletti, A.; Fais, S., Unexpected Discoveries Should Be Reconsidered in Science—A Look to the Past? *International Journal of Molecular Sciences*, **2019**, 20 (16), 3973.
6. Copeland, S., On serendipity in science: discovery at the intersection of chance and wisdom. *Synthese*, **2019**, 196 (6), 2385-2406.
7. Setsune, J.-I., Synthesis and application of heteroaromatic compounds with unusual structure and function. *Journal of Synthetic Organic Chemistry*, **1988**, 46 (7), 681-692.
8. Antony, J.; Saikia, M.; V, V.; Nath, L. R.; Katiki, M. R.; Murty, M. S. R.; Paul, A.; A, S.; Chandran, H.; Joseph, S. M.; S, N. K.; Panakkal, E. J.; V, S. I.; V, S. I.; Ran, S.; S, S.; Rajan, E.; Anto, R. J., DW-F5: A novel formulation against malignant melanoma from *Wrightia tinctoria*. *Scientific Reports*, **2015**, 5 (1), 11107.
9. Camp, J. E., Bio-available Solvent Cyrene: Synthesis, Derivatization, and Applications. *ChemSusChem*, **2018**, 11 (18), 3048-3055.
10. Muzart, J., N,N-Dimethylformamide: much more than a solvent. *Tetrahedron*, **2009**, 65 (40), 8313-8323.
11. Heseck, D.; Lee, M.; Noll, B. C.; Fisher, J. F.; Mobashery, S., Complications from Dual Roles of Sodium Hydride as a Base and as a Reducing Agent. *The Journal of Organic Chemistry*, **2009**, 74 (6), 2567-2570.
12. Veisi, H., Molecular Iodine: Recent Application in Heterocyclic Synthesis. *Current Organic Chemistry*, **2011**, 15 (14), 2438-2468.
13. Finkbeiner, P.; Nachtsheim, B. J., Iodine in Modern Oxidation Catalysis. *Synthesis*, **2013**, 45 (8), 979-999.
14. Yusubov, M. S.; Zhdankin, V. V., Iodine catalysis: A green alternative to transition metals in organic chemistry and technology. *Resource-Efficient Technologies*, **2015**, 1 (1), 49-67.
15. Dandia, A.; Gupta, S. L.; Maheshwari, S., Molecular Iodine: Mild, Green, and Nontoxic Lewis Acid Catalyst for the Synthesis of Heterocyclic Compounds. In *Green Chemistry: Synthesis of Bioactive Heterocycles*, Ameta, K. L.; Dandia, A., Eds. Springer, New Delhi, India, **2014**, pp 277-327.
16. Prasad, P. K.; Reddi, R. N.; Sudalai, A., Oxidant controlled regio- and stereodivergent azidohydroxylation of alkenes via I₂ catalysis. *Chemical Communications*, **2015**, 51 (51), 10276-10279.

17. Liu, W.; Chen, C.; Zhou, P., *N,N*-Dimethylformamide (DMF) as a Source of Oxygen To Access α -Hydroxy Arones via the α -Hydroxylation of Arones. *The Journal of Organic Chemistry*, **2017**, *82* (4), 2219-2222.
18. Jin, C. H.; Lee, H. Y.; Lee, S. H.; Kim, I. S.; Jung, Y. H., Direct Etherification of Alkyl Halides by Sodium Hydride in the Presence of *N,N*-Dimethylformamide. *Synlett*, **2007**, *2007* (17), 2695-2698.
19. Jia, F.-C.; Zhou, Z.-W.; Xu, C.; Wu, Y.-D.; Wu, A.-X., Divergent Synthesis of Quinazolin-4(3*H*)-ones and Tryptanthrins Enabled by a *tert*-Butyl Hydroperoxide/ K_3PO_4 -Promoted Oxidative Cyclization of Isatins at Room Temperature. *Organic Letters*, **2016**, *18* (12), 2942-2945.
20. Hou, H.; Li, H.; Han, Y.; Yan, C., Synthesis of visible-light mediated tryptanthrin derivatives from isatin and isatoic anhydride under transition metal-free conditions. *Organic Chemistry Frontiers*, **2018**, *5* (1), 51-54.
21. Reissenweber, G.; Mangold, D., Oxidation of Isatins to Isatoic Anhydrides and 2,3-Dioxo-1,4-benzoxazines. *Angewandte Chemie International Edition*, **1980**, *19* (3), 222-223.
22. Abe, T.; Itoh, T.; Choshi, T.; Hibino, S.; Ishikura, M., One-pot synthesis of tryptanthrin by the Dakin oxidation of indole-3-carbaldehyde. *Tetrahedron Letters*, **2014**, *55* (38), 5268-5270.
23. Brandão, P.; Pinheiro, D.; Sérgio Seixas De Melo, J.; Pineiro, M., $I_2/NaH/DMF$ as oxidant trio for the synthesis of tryptanthrin from indigo or isatin. *Dyes and Pigments*, **2020**, *173*, 107935.
24. Amara, R.; Awad, H.; Chaker, D.; Bentabed-Ababsa, G.; Lassagne, F.; Erb, W.; Chevallier, F.; Roisnel, T.; Dorcet, V.; Fajloun, Z.; Vidal, J.; Mongin, F., Conversion of Isatins to Tryptanthrins, Heterocycles Endowed with a Myriad of Bioactivities. *European Journal of Organic Chemistry*, **2019**, *2019* (31-32), 5302-5312.
25. Pattarawarapan, M.; Wiriya, N.; Hongsibsong, S.; Phakhodee, W., Divergent Synthesis of Methylisatoid and Tryptanthrin Derivatives by Ph_3P-I_2 -Mediated Reaction of Isatins with and without Alcohols. *The Journal of Organic Chemistry*, **2020**, *85* (23), 15743-15751.
26. Trost, B., The atom economy - a search for synthetic efficiency. *Science*, **1991**, *254* (5037), 1471-1477.
27. Dicks, A. P.; Hent, A., Atom Economy and Reaction Mass Efficiency. In *Green Chemistry Metrics: A Guide to Determining and Evaluating Process Greenness*, Springer, London, UK, **2015**, pp 17-44.
28. Dicks, A. P.; Hent, A., The E Factor and Process Mass Intensity. In *Green Chemistry Metrics: A Guide to Determining and Evaluating Process Greenness*, Springer, London, UK, **2015**, pp 45-67.
29. Sheldon, R. A., The E factor 25 years on: the rise of green chemistry and sustainability. *Green Chemistry*, **2017**, *19* (1), 18-43.
30. Sheldon, R. A., Metrics of Green Chemistry and Sustainability: Past, Present, and Future. *ACS Sustainable Chemistry & Engineering*, **2018**, *6* (1), 32-48.

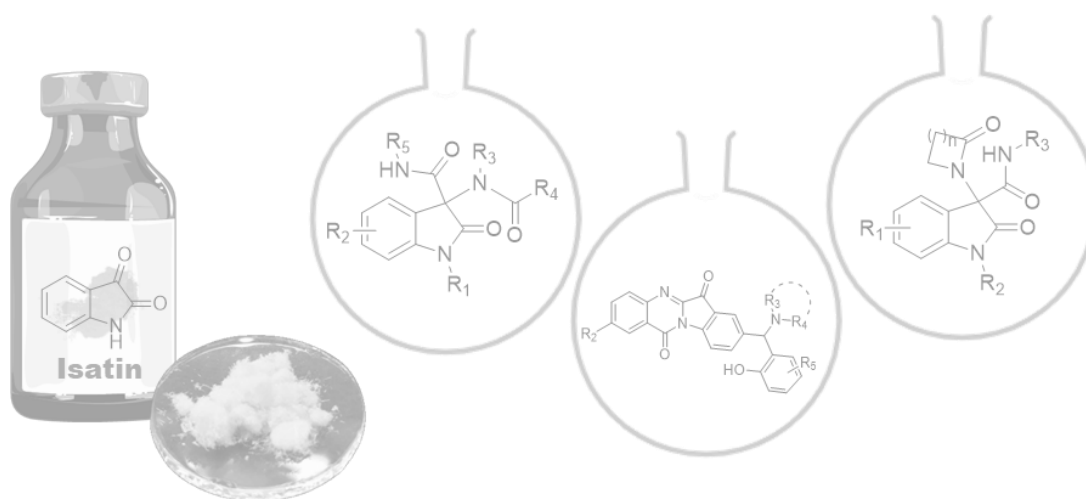
31. Pinheiro, D.; Pineiro, M.; Pina, J.; Brandão, P.; Galvão, A. M.; de Melo, J. S. S., Tryptanthrin from indigo: Synthesis, excited state deactivation routes and efficient singlet oxygen sensitization. *Dyes and Pigments*, **2020**, *175*, 108125.
32. Pinheiro, D.; Pineiro, M.; de Melo, J. S. S., Sulfonated tryptanthrin anolyte increases performance in pH neutral aqueous redox flow batteries. *Communications Chemistry*, **2021**, *4* (1), 89.
33. Beyrati, M.; Hasaninejad, A., One-pot, three-component synthesis of spiroindoloquinazoline derivatives under solvent-free conditions using ammonium acetate as a dual activating catalyst. *Tetrahedron Letters*, **2017**, *58* (20), 1947-1951.
34. Yavari, I.; Askarian-Amiri, M., A synthesis of spiroindolo[2,1-*b*]quinazoline-6,2'-pyrido[2,1-*b*][1,3]oxazines from tryptanthrins and Huisgen zwitterions. *Synthetic Communications*, **2021**, 1-7.
35. Filatov, A. S.; Knyazev, N. A.; Shmakov, S. V.; Bogdanov, A. A.; Ryazantsev, M. N.; Shtyrov, A. A.; Starova, G. L.; Molchanov, A. P.; Larina, A. G.; Boitsov, V. M.; Stepanov, A. V., Concise Synthesis of Tryptanthrin Spiro Analogues with In Vitro Antitumor Activity Based on One-Pot, Three-Component 1,3-Dipolar Cycloaddition of Azomethine Ylides to Cyclopropenes. *Synthesis*, **2019**, *51* (03), 713-729.
36. Jao, C.-W.; Lin, W.-C.; Wu, Y.-T.; Wu, P.-L., Isolation, Structure Elucidation, and Synthesis of Cytotoxic Tryptanthrin Analogues from *Phaius mishmensis*. *Journal of Natural Products*, **2008**, *71* (7), 1275-1279.
37. Chang, C.-F.; Hsu, Y.-L.; Lee, C.-Y.; Wu, C.-H.; Wu, Y.-C.; Chuang, T.-H., Isolation and Cytotoxicity Evaluation of the Chemical Constituents from *Cephalantheropsis gracilis*. *International Journal of Molecular Sciences*, **2015**, *16* (2), 3980-3989.
38. Deryabin, P. I.; Moskovkina, T. V.; Shevchenko, L. S.; Kalinovskii, A. I., Synthesis and antimicrobial activity of tryptanthrin adducts with ketones. *Russian Journal of Organic Chemistry*, **2017**, *53* (3), 418-422.
39. Vaidya, S. D.; Argade, N. P., Aryne Insertion Reactions Leading to Bioactive Fused Quinazolinones: Diastereoselective Total Synthesis of Cruciferane. *Organic Letters*, **2013**, *15* (15), 4006-4009.
40. Krivogorsky, B.; Nelson, A. C.; Douglas, K. A.; Grundt, P., Tryptanthrin derivatives as *Toxoplasma gondii* inhibitors—structure–activity-relationship of the 6-position. *Bioorganic & Medicinal Chemistry Letters*, **2013**, *23* (4), 1032-1035.
41. Kang, G.; Luo, Z.; Liu, C.; Gao, H.; Wu, Q.; Wu, H.; Jiang, J., Amino Acid Salts Catalyzed Asymmetric Aldol Reaction of Tryptanthrin: A Straightforward Synthesis of Phaitanthrin A and Its Derivatives. *Organic Letters*, **2013**, *15* (18), 4738-4741.
42. Candeias, N. R.; Montalbano, F.; Cal, P. M. S. D.; Gois, P. M. P., Boronic Acids and Esters in the Petasis-Borono Mannich Multicomponent Reaction. *Chemical Reviews*, **2010**, *110* (10), 6169-6193.
43. Wu, P.; Nielsen, T. E., Petasis three-component reactions for the synthesis of diverse heterocyclic scaffolds. *Drug Discovery Today: Technologies*, **2018**, *29*, 27-33.

44. Wu, P.; Givskov, M.; Nielsen, T. E., Reactivity and Synthetic Applications of Multicomponent Petasis Reactions. *Chemical Reviews*, **2019**, *119* (20), 11245-11290.
45. Marques, C. S.; McArdle, P.; Erxleben, A.; Burke, A. J., Accessing New 5- α -(3,3-Disubstituted Oxindole)-Benzylamine Derivatives from Isatin: Stereoselective Organocatalytic Three Component Petasis Reaction. *European Journal of Organic Chemistry*, **2020**, *2020* (24), 3622-3634.
46. Ishiyama, T.; Murata, M.; Miyaura, N., Palladium(0)-Catalyzed Cross-Coupling Reaction of Alkoxydiboron with Haloarenes: A Direct Procedure for Arylboronic Esters. *The Journal of Organic Chemistry*, **1995**, *60* (23), 7508-7510.
47. Ogawa, A.; Curran, D. P., Benzotrifluoride: A Useful Alternative Solvent for Organic Reactions Currently Conducted in Dichloromethane and Related Solvents. *The Journal of Organic Chemistry*, **1997**, *62* (3), 450-451.
48. Frauenlob, R.; García, C.; Bradshaw, G. A.; Burke, H. M.; Bergin, E., A Copper-Catalyzed Petasis Reaction for the Synthesis of Tertiary Amines and Amino Esters. *The Journal of Organic Chemistry*, **2012**, *77* (9), 4445-4449.
49. Li, Y.; Xu, M.-H., Lewis Acid Promoted Highly Diastereoselective Petasis Borono-Mannich Reaction: Efficient Synthesis of Optically Active β,γ -Unsaturated α -Amino Acids. *Organic Letters*, **2012**, *14* (8), 2062-2065.
50. Lou, S.; Schaus, S. E., Asymmetric Petasis Reactions Catalyzed by Chiral Biphenols. *Journal of the American Chemical Society*, **2008**, *130* (22), 6922-6923.
51. Jiang, Y.; Schaus, S. E., Asymmetric Petasis Borono-Mannich Allylation Reactions Catalyzed by Chiral Biphenols. *Angewandte Chemie International Edition*, **2017**, *56* (6), 1544-1548.
52. Carmen Carreño, M.; Hernández-Torres, G.; Ribagorda, M.; Urbano, A., Enantiopure sulfoxides: recent applications in asymmetric synthesis. *Chemical Communications*, **2009**, (41), 6129-6144.
53. Han, W.-Y.; Wu, Z.-J.; Zhang, X.-M.; Yuan, W.-C., Enantioselective Organocatalytic Three-Component Petasis Reaction among Salicylaldehydes, Amines, and Organoboronic Acids. *Organic Letters*, **2012**, *14* (4), 976-979.
54. Han, W.-Y.; Zuo, J.; Zhang, X.-M.; Yuan, W.-C., Enantioselective Petasis reaction among salicylaldehydes, amines, and organoboronic acids catalyzed by BINOL. *Tetrahedron*, **2013**, *69* (2), 537-541.
55. Ertl, P.; Rohde, B.; Selzer, P., Fast Calculation of Molecular Polar Surface Area as a Sum of Fragment-Based Contributions and Its Application to the Prediction of Drug Transport Properties. *Journal of Medicinal Chemistry*, **2000**, *43* (20), 3714-3717.
56. Ali, J.; Camilleri, P.; Brown, M. B.; Hutt, A. J.; Kirton, S. B., Revisiting the general solubility equation: in silico prediction of aqueous solubility incorporating the effect of topographical polar surface area. *Journal of Chemical Information and Modeling*, **2012**, *52* (2), 420-428.
57. Roman, G., Mannich bases in medicinal chemistry and drug design. *European Journal of Medicinal Chemistry*, **2015**, *89*, 743-816.

58. Trigo, J.; Subbiah, V.; Besse, B.; Moreno, V.; López, R.; Sala, M. A.; Peters, S.; Ponce, S.; Fernández, C.; Alfaro, V.; Gómez, J.; Kahatt, C.; Zeaiter, A.; Zaman, K.; Boni, V.; Arrondeau, J.; Martínez, M.; Delord, J.-P.; Awada, A.; Kristeleit, R.; Olmedo, M. E.; Wannesson, L.; Valdivia, J.; Rubio, M. J.; Anton, A.; Sarantopoulos, J.; Chawla, S. P.; Mosquera-Martinez, J.; D'Arcangelo, M.; Santoro, A.; Villalobos, V. M.; Sands, J.; Paz-Ares, L., Lurbinectedin as second-line treatment for patients with small-cell lung cancer: a single-arm, open-label, phase 2 basket trial. *The Lancet Oncology*, **2020**, *21* (5), 645-654.
59. Food and Drug Administration, FDA grants accelerated approval to lurbinectedin for metastatic small cell lung cancer, available in <https://www.fda.gov/drugs/drug-approvals-and-databases/fda-grants-accelerated-approval-lurbinectedin-metastatic-small-cell-lung-cancer> (accessed 09/02/2021).
60. Gilberg, E.; Stumpfe, D.; Bajorath, J., Activity profiles of analog series containing pan assay interference compounds. *RSC Advances*, **2017**, *7* (57), 35638-35647.
61. Costa, D. C. M.; de Azevedo, M. M. B.; Silva, D. O. E.; Romanos, M. T. V.; Souto-Padron, T.; Alviano, C. S.; Alviano, D. S., *In vitro* anti-MRSA activity of *Couroupita guianensis* extract and its component Tryptanthrin. *Natural Product Research*, **2017**, *31* (17), 2077-2080.
62. Hesse-Macabata, J.; Morgner, B.; Elsner, P.; Hipler, U. C.; Wiegand, C., Tryptanthrin promotes keratinocyte and fibroblast responses *in vitro* after infection with *Trichophyton benhamiae* DSM6916. *Scientific Reports*, **2020**, *10* (1), 1863.
63. Hwang, J. M.; Oh, T.; Kaneko, T.; Upton, A. M.; Franzblau, S. G.; Ma, Z. K.; Cho, S. N.; Kim, P., Design, Synthesis, and Structure-Activity Relationship Studies of Tryptanthrins As Antitubercular Agents. *Journal of Natural Products*, **2013**, *76* (3), 354-367.
64. Lin, C.-J.; Chang, Y.-L.; Yang, Y.-L.; Chen, Y.-L., Natural alkaloid tryptanthrin exhibits novel anticryptococcal activity. *Medical Mycology*, **2021**, *59* (6), 545-556.
65. CLSI. Clinical and Laboratory Standard Institute, Reference Method for Dilution Antimicrobial Susceptibility Tests. Wayne, PA. Clin. Lab. Stand. Inst. 28. CLSI Document M07-A8 for bacteria, M27-A3 for yeasts and M38-A2 for filamentous fungi.
66. Martinez-Rossi, N. M.; Bitencourt, T. A.; Peres, N. T. A.; Lang, E. A. S.; Gomes, E. V.; Quaresimin, N. R.; Martins, M. P.; Lopes, L.; Rossi, A., Dermatophyte Resistance to Antifungal Drugs: Mechanisms and Prospectus. *Frontiers in Microbiology*, **2018**, *9*, 1108.
67. Gnat, S.; Łagowski, D.; Nowakiewicz, A., Major challenges and perspectives in the diagnostics and treatment of dermatophyte infections. *Journal of Applied Microbiology*, **2020**, *129* (2), 212-232.
68. Brandão, P.; Marques, C.; Pinto, E.; Pineiro, M.; Burke, A. J., Petasis adducts of tryptanthrin – synthesis, biological activity evaluation and druglikeness assessment. *New Journal of Chemistry*, **2021**, *45* (32), 14633-14649.

Chapter 5

Final Remarks and Future Perspectives



With this work, the use of isatin as a valuable starting material for MCRs in sustainable drug discovery takes center stage.

In Chapters 2 and 3, the application of one of the most versatile MCRs, the Ugi reaction (U4CR and U4c3CR, respectively), lead to the discovery of compounds with potential biological activity. In Chapter 4, the transformation of isatin to tryptanthrin, an alkaloid with a wide range of applications, in a fast and efficient manner, is reported, as well as the generation of a library of Petasis adducts of tryptanthrin with prospective pharmacological applications.

The novelty of this work relies not only in the preparation of new compounds with potential biological activity, but also in the sustainable approaches used for the preparation of each library. The inherent sustainability of MCRs makes the approaches herein reported eco-friendly and efficient ways to obtain new druglike candidates with promising biological activity. The use of druglikeness filters and *in silico* evaluation of several physico-chemical properties also enable a rational approach for the design of new molecules.

In Chapter 2, Library I was successfully obtained by engaging isatin in the U4CR, which was never reported in the literature before. The selected catalyst, InCl_3 , as well as the fact that the reactions proceed at room temperature and several products were isolated using chromatography-free procedures, are relevant features for the overall process eco-friendliness. The diversity of the substrate scope for all the components, the identification of process limitations (namely the carboxylic acid $\text{p}K_a$), combined with computational calculations, allowed to collect further information on the potential of this chemical transformation. *In vitro* evaluation of Library I antiproliferative activity, combined with their druglike profile, indicate great potential for these compounds as antitumor drug candidates. These findings open the door to new research questions, including unveiling the mechanism of action of these compounds at a molecular level using target-based screenings, studying their selectivity towards tumor cells *versus* healthy cells, and even testing the less active compounds towards different pharmacological activities. From the synthetic point of view, the exploration of more reaction conditions, in order to further expand the substrate scope, namely by allowing the selective U4CR when using carboxylic acids with higher $\text{p}K_a$ values, remains a challenge. The reaction mechanism also requires further studies to justify the observed differences in what concerns the $\text{p}K_a$ of the carboxylic acid component, and the absence of the reaction in the presence of components bearing the morpholine core. The development of an asymmetric version would also be desirable, as this option remains a scientific challenge at present times (Figure 5.1).

In Chapter 3, the application of the U4c3CR enabled the fast preparation of a wide range of oxindole-lactam hybrids (Library II), in a molecular hybridization approach to obtain new potential cholinesterase inhibitors for the treatment of Alzheimer's disease. Two compounds in particular display great potential as selective BuChE inhibitors, with optimal druglike properties, including potential to cross the BBB. Hit-to-lead optimization of the most promising compounds, as well as their evaluation against other relevant targets of Alzheimer's disease pathophysiology would be of great interest for a polypharmacological approach in the future. From the synthetic point of view, the main challenge remaining is the ability to generate larger lactam rings using this MCR approach (**Figure 5.1**).

The discovery of a new synthetic pathway to attain tryptanthrin from indigo and isatin described in Chapter 4, was the driving force for the efforts therein described. The new synthetic route established for this valuable alkaloid is time- and cost-efficient, with good sustainability scores, and constitutes one of the few literature examples of the application of DMF as an oxygen transfer reagent. Then, the report of one of the few examples of tryptanthrin-based MCR, and the first using the Petasis reaction and not leading to spiro derivatives, led to the synthesis of Library III with good structural diversity. The BINOL organocatalyzed asymmetric version of the reaction was also successfully attained. One of the obtained tryptanthrin derivatives exhibit promising fungicidal activity, selective against dermatophytes, and therefore can be a good starting point for further development. Future endeavors can include efforts to unveil potential molecular targets, further exploration of the potential biological activity of the obtained

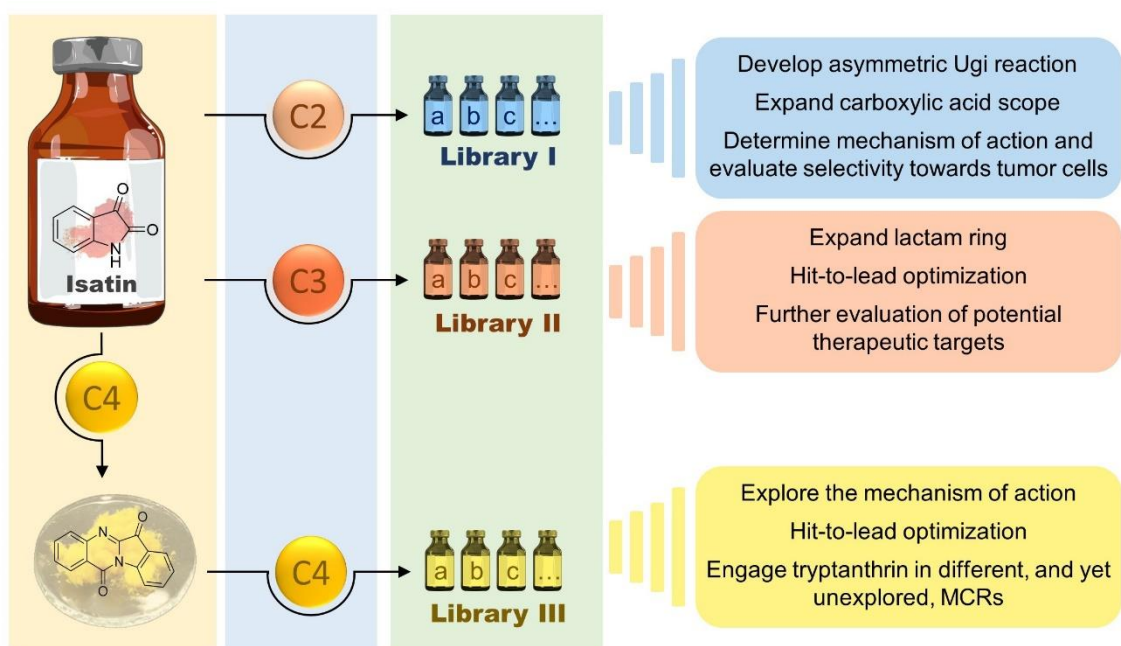


Figure 5.1. Examples of research opportunities created by the work reported in this thesis.

derivatives, as well as to continue efforts to engage tryptanthrin in MCRs, as this field remains considerably unexplored and can constitute a great opportunity to expand the chemical space occupied by tryptanthrin-based frameworks (**Figure 5.1**).

In a nutshell, the work reported in the thesis constitute a valuable effort to implement sustainable approaches in drug discovery and medicinal chemistry, with MCRs and green catalysts taking a central role.

Chapter 6

Experimental Section



6.1. General Remarks

6.1.1. Solvents and reagents

All the solvents used in this work were purified and dried under an inert atmosphere using common laboratory techniques.¹ All the reagents were purchased from Sigma-Aldrich, Merck, Fluorochem, Acros, Fluka and Alfa Aesar, and used as received.

6.1.2. Detection, characterization and purification of the synthesized compounds and other relevant equipment

Thin-layer chromatography (TLC) was carried out on aluminum-backed Kieselgel 60 F254 plates (Merck and Machery Nagel). Plates were visualized either by UV light or with phosphomolybdic acid in ethanol.

Melting points (m.p.) were determined using a Melting Point Device Falc R132467 (open capillary method).

NMR spectra were recorded with a Bruker Avance III and a Bruker DRX-400 spectrometer, both operating at 400.13 MHz for ¹H and 100.61 MHz for ¹³C. The chemical shifts (δ) were quoted in parts per million (ppm) with respect to the solvent (CDCl₃, ¹H: δ = 7.26 ppm, ¹³C: δ = 77.2 ppm; [d₆]DMSO, ¹H: δ = 2.50 ppm, ¹³C: δ = 39.5 ppm; (CD₃)₂CO, ¹H: δ = 2.05 ppm, ¹³C: δ = 29.84 and 206.26 ppm), using tetramethylsilane (TMS) as internal standard. Coupling constants (*J*) are reported in Hz and refer to apparent peak multiplicities. Splitting patterns are reported as s, singlet; d, doublet; dd, doublet of doublets; t, triplet; q, quadruplet; m, multiplet; br, broad.

High-resolution mass spectra (HRMS) were recorded on a Mass spectrometer MICRO-MASS Q-TOF (Waters), or on a TOF VG Autospect M spectrometer with electrospray ionization (ESI), or on a Orbitrap Q-exactive focus (Thermo scientific) coupled with a HPLC vanquish (thermo scientific) with ESI. Elemental analysis was carried out with an Elemental Vario MicroCube analyzer.

Gas chromatography-mass spectrometry (GC-MS) analyses were performed on a Hewlett-Packard 5973 MSD spectrometer, using EI (70 eV), coupled to a Hewlett-Packard Agilent 6890 chromatographer, equipped with a HP-5 MS column (30 m x 0.25 mm x 0.25 μ m) and high-purity helium as carrier gas.

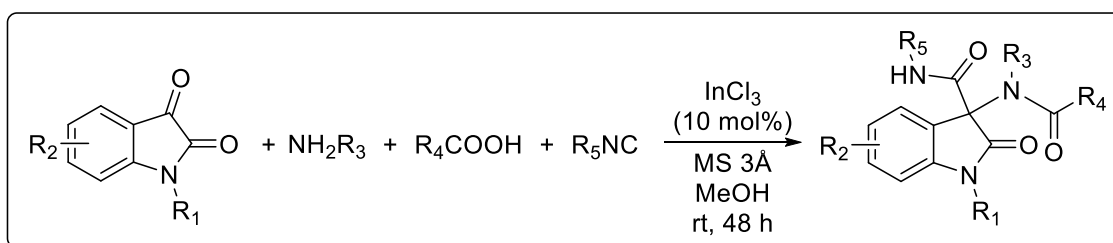
Fourier transform infrared spectroscopy – attenuated total reflectance (ATR-FTIR) spectra were recorded in a Fourier Transform spectrometer coupled with a diamond Attenuated Total Reflectance ATR sampling accessory (Agilent Cary 630).

High-performance liquid chromatographic (HPLC) analysis was carried out with a Hitachi Primaide instrument, equipped with a 1410 series UV detector. Daicel Chiralpak IA column was used as stationary phase, n-hexane/ethanol as mobile phase and 254 nm was used as wavelength in the UV light detector.

Microwave-assisted reactions were performed in a CEM Discover S-Class single-mode microwave reactor, featuring continuous temperature, pressure and microwave power monitoring.

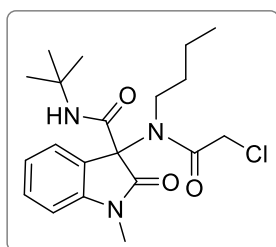
6.2. General Procedures

6.2.1. General procedure for the synthesis of 3,3-disubstituted oxindoles obtained via Ugi four component reaction (U4CR) (Chapter 2 – Library I)



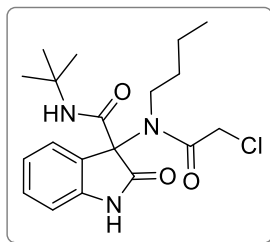
To a reaction vessel charged with isatin (200 mg, 1 equiv) and InCl_3 (10 mol%), 150 mg of MS 3Å and methanol (1 mL) were added. Next, the primary amine (1.5 equiv), isocyanide (1.5 equiv) and carboxylic acid (1.5 equiv) components were added, and the reaction was allowed to stir at room temperature for 48 h. The reaction was monitored by TLC. Upon completion, or when no change was detected, ethyl acetate (10 mL) was added, and the mixture was filtered through a pad of celite. The solvent was then removed under reduced pressure and the purification performed as required (direct precipitation/crystallization of the compound, column chromatography (CC), and/or preparative TLC).

6.2.1.1. Synthesis of *N*-(*tert*-butyl)-3-(*N*-butyl-2-chloroacetamido)-1-methyl-2-oxoindoline-3-carboxamide (1.5aaaa):

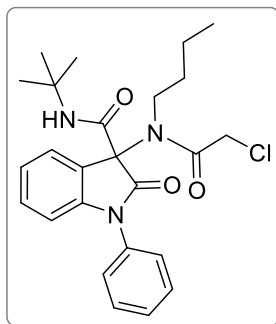


Prepared using *N*-methylisatin (**I.1a**), *n*-butylamine (**I.2a**), chloroacetic acid (**I.3a**), and *tert*-butyl isocyanide (**I.4a**). After 48 hours, ethyl acetate was added (10 mL) and the mixture filtered through a pad of celite. After solvent removal under reduced pressure, the crude product was crystallized from ethanol. The corresponding **I.5aaaa** was obtained as a white solid (316.8 mg, 65% yield). m.p.= 144.1-145.0 °C. ¹H NMR (CDCl₃, 400 MHz): δ 7.48 (d, *J*=7.0 Hz, 1H), 7.32 (td, *J*=7.7, 1.1, 1H), 7.18 (br s, 1H), 7.10 (td, *J*=7.6, 0.7 Hz, 1H), 6.84 (d, *J*=7.8 Hz, 1H), 4.09 (dd, *J*=13.0 Hz, 2H), 3.69-3.3.61 (m, 1H), 3.59-3.50 (m, 1H), 3.26 (s, 3H), 1.94-1.84 (m, 1H), 1.74-1.63 (m, 1H), 1.36-1.30 (m, 11H), 0.95 (t, *J*=7.4 Hz, 3H). ¹³C NMR (CDCl₃, 100 MHz): δ 173.8, 166.7, 161.5, 143.8, 129.4, 126.1 (2C), 123.3, 108.4, 72.0, 52.2, 47.2, 41.7, 33.8, 28.3 (3C), 27.0, 20.1, 13.6. HRMS (ESI) calculated for C₂₀H₂₉ClN₃O₃ [MH]⁺ 394.1892, found 394.1891. ATR-FTIR (cm⁻¹): 3342, 2961, 2927, 2861, 1714, 1658, 1612, 1526, 1406, 1364, 1351, 1262, 1217, 1092, 799, 756.

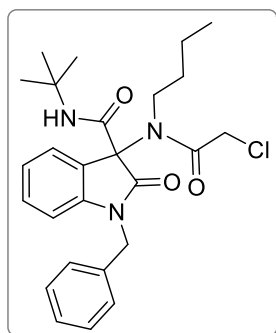
6.2.1.2. Synthesis of *N*-(*tert*-butyl)-3-(*N*-butyl-2-chloroacetamido)-2-oxoindoline-3-carboxamide (**I.5baaa**):



Prepared using isatin (**I.1b**), *n*-butylamine (**I.2a**), chloroacetic acid (**I.3a**), and *tert*-butyl isocyanide (**I.4a**). After 48 hours, ethyl acetate was added (10 mL) and the mixture filtered through a pad of celite. After solvent removal under reduced pressure, the crude product was crystallized from ethanol/diethyl ether. The corresponding **I.5baaa** was obtained as a beige solid (341.0 mg, 66% yield). m.p.= 187.2 °C (decomp.). ¹H NMR (CDCl₃, 400 MHz): δ 8.06 (br s, 1H), 7.44 (d, *J*=7.5 Hz, 1H), 7.23 (td, *J*=7.8, 1.2 Hz, 1H), 7.11 (br s, 1H), 7.07 (td, *J*=7.6, 0.9 Hz, 1H), 6.82 (d, *J*=7.7 Hz), 4.12 (dd, *J*=12.9 Hz, 2H), 3.72-3.64 (m, 1H), 3.60-3.52 (m, 1H), 1.95-1.90 (m, 1H), 1.73-1.69 (m, 1H), 1.37, 1.31 (m, 11H), 0.96 (t, *J*=7.4 Hz, 3H). ¹³C NMR (CDCl₃, 100 MHz): δ 175.2, 166.9, 161.2, 140.9, 129.4, 126.5, 126.3, 123.2, 110.2, 72.4, 52.2, 47.2, 41.6, 33.8, 28.2 (3C), 20.2, 13.6. HRMS (ESI) calculated for C₁₉H₂₇ClN₃O₃ [MH]⁺ 380.17355, found 380.17242. ATR-FTIR (cm⁻¹): 3264, 2962, 2935, 2872, 1727, 1653, 1619, 1539, 1473, 1458, 1362, 1262, 1222, 1202, 997, 752, 688.

6.2.1.3. Synthesis of *N*-(*tert*-butyl)-3-(*N*-butyl-2-chloroacetamido)-2-oxo-1-phenylindoline-3-carboxamide (I.5caaa):

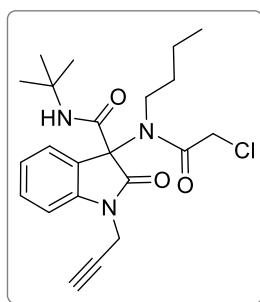
Prepared using *N*-phenylisatin (**I.1c**), *n*-butylamine (**I.2a**), chloroacetic acid (**I.3a**), and *tert*-butyl isocyanide (**I.4a**). After 48 hours, ethyl acetate was added (10 mL) and the mixture filtered through a pad of celite. After solvent removal under reduced pressure, the crude product was crystallized from ethanol. The corresponding **I.5caaa** was obtained as a white solid (281.6 mg, 69% yield). m.p.= 145.3-146.2 °C. ¹H NMR (CDCl₃, 400 MHz): δ 7.55-7.41 (m, 6H), 7.31 (br s, 1H), 7.23 (td, *J*=7.8, 1.0 Hz, 1H), 7.13 (t, *J*=7.4 Hz, 1H), 6.73 (d, *J*=7.8 Hz, 1H), 4.12 (s, 2H), 3.76-3.59 (m, 2H), 2.04-1.92 (m, 1H), 1.86-1.75 (m, 1H), 1.39-1.36 (m, 11H), 0.99 (t, *J*=7.4 Hz, 3H). ¹³C NMR (CDCl₃, 100 MHz): δ 173.7, 166.8, 161.3, 144.2, 134.4, 129.7 (2C), 129.3, 128.5, 126.9 (2C), 126.3, 125.6, 123.6, 109.5, 72.2, 52.3, 47.3, 41.5, 34.0, 28.3, 20.2, 13.7. HRMS (ESI) calculated for C₂₅H₃₁ClN₃O₃ [MH]⁺ 456.2048, found 456.2042. ATR-FTIR (cm⁻¹): 3371, 3340, 2962, 2929, 1731, 1664, 1518, 1498, 1365, 1206, 1107, 758, 748, 700.

6.2.1.4. Synthesis of 1-Benzyl-*N*-(*tert*-butyl)-3-(*N*-butyl-2-chloroacetamido)-2-oxoindoline-3-carboxamide (I.5daaa):

Prepared using *N*-benzylisatin (**I.1d**), *n*-butylamine (**I.2a**), chloroacetic acid (**I.3a**), and *tert*-butyl isocyanide (**I.4a**). After 48 hours, ethyl acetate was added (10 mL) and the mixture filtered through a pad of celite. After solvent removal under reduced pressure, the crude product was crystallized from ethanol/diethyl ether. The corresponding **I.5daaa** was obtained as a pale-yellow solid (233.8 mg, 59% yield). m.p.= 155.0-155.4 °C. ¹H

NMR (CDCl₃, 400 MHz): δ 7.47 (d, $J=6.8$ Hz, 1H), 7.31-7.24 (m, 5H), 7.20 (td, $J=7.8$, 1.1 Hz, 1H), 7.12 (br s, 1H), 7.07 (td, $J=7.6$, 0.6 Hz, 1H), 6.71 (d, $J=7.8$ Hz, 1H), 5.19 (d, $J=15.8$ Hz, 1H), 4.73 (d, $J=15.8$ Hz, 1H), 4.12 (s, 2H), 3.74-3.66 (m, 1H), 3.60-3.52 (m, 1H), 1.93-1.82 (m, 1H), 1.75-1.64 (m, 1H), 1.35-1.30 (m, 11H), 0.94 (t, $J=7.4$ Hz, 3H). ¹³C NMR (CDCl₃, 100 MHz): δ 173.9, 166.8, 161.5, 142.5, 135.6, 129.3, 128.8 (2C), 127.7, 127.1 (2C), 126.4, 125.9, 123.4, 109.2, 72.5, 52.2, 47.3, 44.3, 41.6, 33.8, 28.2 (3C), 20.1, 13.6. HRMS (ESI) calculated for C₂₆H₃₃ClN₃O₃ [MH]⁺ 470.2205, found 470.2209. ATR-FTIR (cm⁻¹): 3366, 2959, 2932, 1698, 1680, 1610, 1516, 1464, 1453, 1360, 1188, 1131, 799, 755, 732, 697.

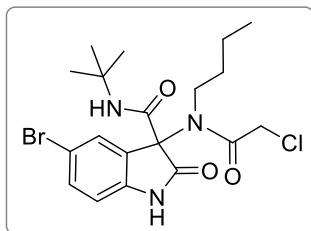
6.2.1.5. Synthesis of *N*-(*tert*-butyl)-3-(*N*-butyl-2-chloroacetamido)-2-oxo-1-(prop-2-yn-1-yl)indoline-3-carboxamide (**I.5eaaa**):



N-propargylisatin was synthesized as described in the literature.² Briefly, to a solution of isatin (**I.1b**, 1.0 g, 1 equiv) in DMF kept at 0 °C, sodium hydride (1.5 equiv) was slowly added and allowed to stir until the gas production ceased. Then, propargyl bromide (1.4 equiv) was added dropwise and the mixture was allowed to proceed with stirring at room temperature overnight. The DMF was then removed under reduced pressure. Water was added and the aqueous mixture extracted with ethyl acetate (3 x 30 mL), and the combined organic layers were washed with brine, dried with anhydrous Na₂SO₄ and evaporated to afford the desired product, which was used in the next step without further purification. **I.5eaaa** was prepared using *N*-propargylisatin (**I.1e**), *n*-butylamine (**I.2a**), chloroacetic acid (**I.3a**), and *tert*-butyl isocyanide (**I.4a**). After 48 hours, ethyl acetate was added (10 mL) and the mixture filtered through a pad of celite. After solvent removal under reduced pressure, the crude mixture was purified by column chromatography (hexane:AcOEt from 4:1 to 7:3). The corresponding **I.5eaaa** was obtained as a white solid (241.9 mg, 54% yield). m.p.= 164.5-164.9 °C. ¹H NMR (CDCl₃, 400 MHz): δ 7.50 (d, $J=7.2$ Hz, 1H), 7.34 (td, $J=7.8$, 1.0 Hz, 1H), 7.13 (td, $J=7.7$, 0.6 Hz, 1H), 7.06 (d, $J=7.8$ Hz, 1H), 6.97 (br s, 1H), 4.66 (dd, $J=17.7$, 2.4 Hz, 1H), 4.42 (dd, $J=17.7$, 2.4 Hz, 1H), 4.08 (s, 2H), 3.72-3.64 (m, 1H), 3.59-3.47 (m, 1H), 2.26 (t, $J=2.5$ Hz, 1H), 1.89-1.78 (m, 1H), 1.70-1.63 (m, 1H), 1.36-1.29 (m, 11H), 0.94 (t, $J=7.3$ Hz, 3H).

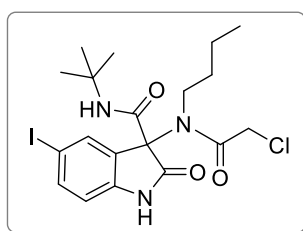
^{13}C NMR (CDCl_3 , 100 MHz): δ 172.8, 166.9, 161.2, 141.9, 129.5, 126.2 (2C), 123.7, 109.3, 76.5, 72.6, 72.2, 52.2, 47.2, 41.5, 33.6, 30.1, 28.2 (3C), 20.1, 13.6. HRMS (ESI) calculated for $\text{C}_{22}\text{H}_{29}\text{ClN}_3\text{O}_3$ $[\text{MH}]^+$ 418.1892, found 418.1894. ATR-FTIR (cm^{-1}): 3359, 3249, 2959, 2930, 1729, 1674, 1654, 1612, 1526, 1468, 1354, 1269, 1199, 1177, 1112, 934, 748, 730.

6.2.1.6. Synthesis of 5-Bromo-*N*-(*tert*-butyl)-3-(*N*-butyl-2-chloroacetamido)-2-oxoindoline-3-carboxamide (**I.5faaa**):



Prepared using 5-bromoisatin (**I.1f**), *n*-butylamine (**I.2a**), chloroacetic acid (**I.3a**), and *tert*-butyl isocyanide (**I.4a**). After 48 hours, ethyl acetate was added (10 mL) and the mixture filtered through a pad of celite. After solvent removal under reduced pressure, the crude mixture was purified by CC (hexane:AcOEt from 4:1 to 7:3) and further purified by preparative TLC (hexane:AcOEt 3:5). The corresponding **I.5faaa** was obtained as a pale-yellow solid (85.6 mg, 21% yield). m.p.= 124.6-125.3 °C. ^1H NMR (CDCl_3 , 400 MHz): δ 8.14 (br s, 1H), 7.52 (d, $J=1.8$ Hz, 1H), 7.35 (dd, $J=8.3, 2.0$ Hz, 1H), 7.17 (br s, 1H), 6.69 (d, $J=8.3$ Hz, 1H), 4.18 (d, $J=13.1$ Hz, 1H), 4.10 (d, $J=13.1$ Hz, 1H), 3.70-3.62 (m, 1H), 3.59-3.50 (m, 1H), 1.99-1.88 (m, 1H), 1.79-1.68 (m, 1H), 1.39-1.34 (m, 11H), 0.99 (t, $J=7.3$ Hz, 3H). ^{13}C NMR (CDCl_3 , 100 MHz): δ 175.0, 167.0, 160.5, 140.0, 132.2, 129.4, 128.3, 115.8, 111.7, 72.3, 52.4, 47.2, 41.6, 33.9, 28.2 (3C), 20.1, 13.6. HRMS (ESI) calculated for $\text{C}_{19}\text{H}_{26}\text{BrClN}_3\text{O}_3$ $[\text{MH}]^+$ 458.0841, found 458.0840. ATR-FTIR (cm^{-1}): 3252, 2961, 2930, 2872, 1719, 1654, 1618, 1534, 1473, 1364, 1265, 1200, 1120, 817.

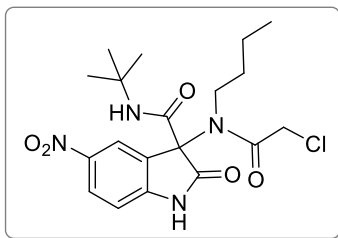
6.2.1.7. Synthesis of *N*-(*tert*-butyl)-3-(*N*-butyl-2-chloroacetamido)-5-iodo-2-oxoindoline-3-carboxamide (**I.5gaaa**):



Prepared using 5-iodoisatin (**I.1g**), *n*-butylamine (**I.2a**), chloroacetic acid (**I.3a**), and *tert*-butyl isocyanide (**I.4a**). After 48 hours, ethyl acetate was added (10 mL) and the

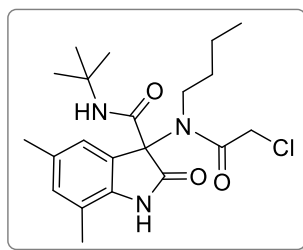
mixture filtered through a pad of celite. After solvent removal under reduced pressure, the crude mixture was purified by column chromatography (hexane:AcOEt from 4:1 to 7:3) and further purified by preparative TLC (hexane:AcOEt 3:5). The corresponding **I.5gaaa** was obtained as a yellow solid (102.9 mg, 28% yield). m.p.= 108.5-109.7 °C. ¹H NMR (CDCl₃, 400 MHz): δ 8.11 (br s, 1H), 7.68 (d, *J*=1.6 Hz, 1H), 7.54 (dd, *J*=8.2, 1.7 Hz, 1H), 7.17 (br s, 1H), 6.60 (d, *J*=8.2 Hz, 1H), 4.17 (d, *J*=13.2 Hz, 1H), 4.10 (d, *J*=13.1 Hz, 1H), 3.70-3.62 (m, 1H), 3.58-3.50 (m, 1H), 1.97-1.86 (m, 1H), 1.78-1.67 (m, 1H), 1.37-1.30 (m, 11H), 0.99 (t, *J*=7.3 Hz, 3H). ¹³C NMR (CDCl₃, 100 MHz): δ 174.8, 167.0, 160.5, 140.7, 138.2, 134.9, 128.6, 112.2, 85.9, 72.2, 52.4, 47.2, 41.6, 33.9, 28.2 (3C), 20.1, 13.6. HRMS (ESI) calculated for C₁₉H₂₆ClIN₃O₃ [MH]⁺ 506.0702, found 506.0700. ATR-FTIR (cm⁻¹): 3236, 2957, 2927, 1718, 1655, 1527, 1469, 1364, 1199, 1121, 813.

6.2.1.8. Synthesis of *N*-(*tert*-butyl)-3-(*N*-butyl-2-chloroacetamido)-5-nitro-2-oxoindoline-3-carboxamide (**I.5haaa**):



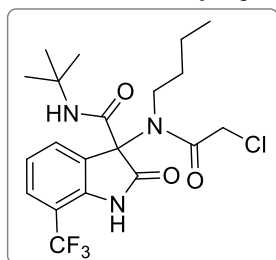
Prepared using 5-nitroisatin (**I.1h**), *n*-butylamine (**I.2a**), chloroacetic acid (**I.3a**), and *tert*-butyl isocyanide (**I.4a**). After 48 hours, ethyl acetate was added (10 mL) and the mixture filtered through a pad of celite. After solvent removal under reduced pressure, the crude mixture was purified by column chromatography (hexane:AcOEt from 4:1 to 3:2). The corresponding **I.5haaa** was obtained as a white solid (230.7 mg, 52% yield). m.p.= 179.5-179.8 °C. ¹H NMR (CDCl₃, 400 MHz): δ 8.67 (br s, 1H), 8.29 (d, *J*=2.2 Hz, 1H), 8.21 (dd, *J*=8.6, 2.3 Hz, 1H), 7.16 (br s, 1H), 6.90 (d, *J*=8.6 Hz, 1H), 4.24 (d, *J*=13.3 Hz, 1H), 4.12 (d, *J*=13.3 Hz, 1H), 3.76-3.68 (m, 1H), 3.66-3.58 (m, 1H), 2.10-1.99 (m, 1H), 1.88-1.76 (m, 1H), 1.42 (q, *J*=7.4 Hz, 2H), 1.35 (s, 9H), 1.04 (t, *J*=7.3 Hz, 3H). ¹³C NMR (CDCl₃, 100 MHz): δ 175.6, 167.5, 159.5, 146.7, 144.0, 127.1, 126.2, 122.2, 110.2, 71.9, 52.7, 47.3, 41.4, 34.0, 28.2 (3C), 20.2, 13.6. HRMS (ESI) calculated for C₁₉H₂₆ClN₄O₅ [MH]⁺ 425.1586, found 425.1585. ATR-FTIR (cm⁻¹): 3342, 2955, 2937, 1744, 1646, 1606, 1515, 1450, 1331, 1191, 1123, 1073, 900, 836, 749, 669.

6.2.1.9. Synthesis of *N*-(*tert*-butyl)-3-(*N*-butyl-2-chloroacetamido)-5,7-dimethyl-2-oxoindoline-3-carboxamide (**I.5iaaa**):



Prepared using 5,7-dimethylisatin (**I.1i**), *n*-butylamine (**I.2a**), chloroacetic acid (**I.3a**), and *tert*-butyl isocyanide (**I.4a**). After 48 hours, ethyl acetate was added (10 mL) and the mixture filtered through a pad of celite. After solvent removal under reduced pressure, the crude mixture was purified by column chromatography (hexane:AcOEt from 9:1 to 7:3). The corresponding **I.5iaaa** was obtained as a white solid (217.0 mg, 47% yield). m.p.= 153.5-154.6 °C. ¹H NMR (CDCl₃, 400 MHz): δ 8.02 (br s, 1H), 7.15 (br s, 1H), 7.07 (s, 1H), 6.87 (s, 1H), 4.15 (d, *J*=13.0 Hz, 1H), 4.10 (d, *J*=13.0 Hz, 1H), 3.70-3.62 (m, 1H), 3.58-3.47 (m, 1H), 2.29 (s, 3H), 2.15 (s, 3H), 1.94-1.86 (m, 1H), 1.76-1.68 (m, 1H), 1.37-1.31 (m, 11H), 0.96 (t, *J*=7.4 Hz, 3H). ¹³C NMR (CDCl₃, 100 MHz): δ 175.5, 166.8, 161.5, 137.1, 132.5, 131.5, 126.2, 124.3, 118.7, 72.9, 52.2, 47.1, 41.7, 33.7, 28.2 (3C), 21.2, 20.1, 16.1, 13.6. HRMS (ESI) calculated for C₂₁H₃₁ClN₃O₃ [MH]⁺ 408.2048, found 408.2050. ATR-FTIR (cm⁻¹): 3238, 2959, 2933, 2876, 1714, 1654, 1540, 1482, 1268, 1206, 1145, 866, 781, 732, 714.

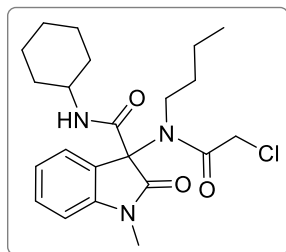
6.2.1.10. Synthesis of *N*-(*tert*-butyl)-3-(*N*-butyl-2-chloroacetamido)-2-oxo-7-(trifluoromethyl)indoline-3-carboxamide (**I.5jaaa**):



Prepared using 7-trifluoromethylisatin (**I.1j**), *n*-butylamine (**I.2a**), chloroacetic acid (**I.3a**), and *tert*-butyl isocyanide (**I.4a**). After 48 hours, ethyl acetate was added (10 mL) and the mixture filtered through a pad of celite. After solvent removal under reduced pressure, the crude mixture was purified by column chromatography (hexane:AcOEt from 4:1 to 7:3). The corresponding **I.5jaaa** was obtained as a beige solid (86.7 mg, 21% yield). m.p.= 107.3-108.5 °C. ¹H NMR (CDCl₃, 400 MHz): δ 7.86 (br s, 1H), 7.60 (d, *J*=7.4 Hz, 1H), 7.46 (d, *J*=8.0 Hz, 1H), 7.18 (t, *J*=7.9 Hz, 1H), 7.12 (br s, 1H), 4.10 (dd, *J*=17.4, 13.0 Hz, 2H), 3.71-3.53 (m, 2H), 2.00-1.89 (m, 1H), 1.80-1.71 (m, 1H), 1.39-1.36 (m, 11H), 0.99 (t, *J*=7.3 Hz, 3H). ¹³C NMR (CDCl₃, 100 MHz): δ 175.0, 167.0, 160.2, 138.0, 129.8, 128.2, 126.2, 126.2, 123.1, 112.4, 112.1, 71.4, 52.6, 47.2, 41.3, 34.1, 28.2 (3C),

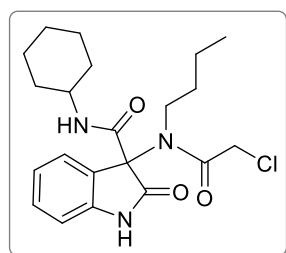
20.1, 13.6. HRMS (ESI) calculated for $C_{20}H_{26}ClF_3N_3O_3$ $[MH]^+$ 448.1609, found 448.1608. ATR-FTIR (cm^{-1}): 3341, 2965, 2874, 1719, 1654, 1624, 1524, 1457, 1339, 1319, 1198, 1163, 1111, 1067, 750.

6.2.1.11. Synthesis of 3-(*N*-butyl-2-chloroacetamido)-*N*-cyclohexyl-1-methyl-2-oxoindoline-3-carboxamide (**1.5a**):



Prepared using *N*-methylisatin (**1.1a**), *n*-butylamine (**1.2a**), chloroacetic acid (**1.3a**), and cyclohexyl isocyanide (**1.4b**). After 48 hours, ethyl acetate was added (10 mL) and the mixture filtered through a pad of celite. After solvent removal under reduced pressure, the crude product was crystallized from ethanol/diethyl ether. The corresponding **1.5a** was obtained as a white solid (324.8 mg, 62% yield). m.p.= 186.8-187.9 °C. 1H NMR ($CDCl_3$, 400 MHz): δ 7.49 (dd, $J=7.5$, 0.7 Hz, 1H), 7.32 (td, $J=7.8$, 1.2 Hz, 1H), 7.17 (d, $J=7.4$ Hz, 1H), 7.10 (td, $J=7.6$, 0.8 Hz, 1H), 6.83 (d, $J=7.8$ Hz, 1H), 4.09 (dd, $J=13.0$, 14.7 Hz, 2H), 3.75-3.64 (m, 2H), 3.55-3.46 (m, 1H), 3.26 (s, 3H), 1.96-1.59 (m, 7H), 1.38-1.15 (m, 7H), 0.95 (t, $J=7.3$ Hz, 3H). ^{13}C NMR ($CDCl_3$, 100 MHz): δ 173.6, 166.6, 161.7, 143.8, 1295, 126.0 (2C), 123.3, 108.4, 71.5, 49.3, 47.2, 41.7, 33.7, 32.3, 27.0, 25.4, 24.6, 24.5, 20.2, 13.6. HRMS (ESI) calculated for $C_{22}H_{31}ClN_3O_3$ $[MH]^+$ 420.2048, found 420.2046. ATR-FTIR (cm^{-1}): 3338, 2924, 2847, 1728, 1655, 1606, 1527, 1474, 1350, 1265, 1250, 1190, 1088, 1027, 797, 756, 729.

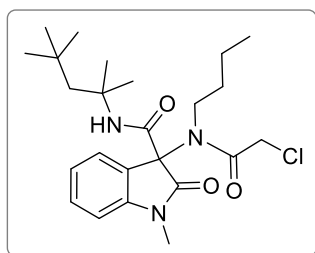
6.2.1.12. Synthesis of 3-(*N*-butyl-2-chloroacetamido)-*N*-cyclohexyl-2-oxoindoline-3-carboxamide (**1.5b**):



Prepared using isatin (**1.1b**), *n*-butylamine (**1.2a**), chloroacetic acid (**1.3a**), and cyclohexyl isocyanide (**1.4b**). After 48 hours, ethyl acetate was added (10 mL) and the mixture filtered through a pad of celite. After solvent removal under reduced pressure, the crude product was crystallized from ethanol/diethyl ether. The corresponding **1.5b**

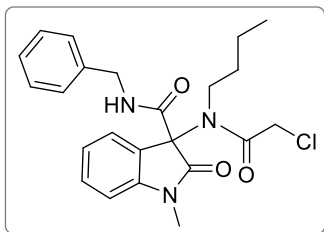
was obtained as a white solid (351.7 mg, 64% yield). m.p.= 110.3-111.2 °C. ¹H NMR (CDCl₃, 400 MHz): δ 7.89 (br s, 1H), 7.47 (d, *J*=7.4 Hz, 1H), 7.24 (td, *J*= 7.7, 1.0 Hz, 1H), 7.10-7.06 (m, 2H), 6.82 (d, *J*=7.7 Hz, 1H), 4.14 (d, *J*=12.9 Hz, 1H), 4.10 (d, *J*=12.9 Hz, 1H), 3.77-3.65 (m, 2H), 3.56-3.47 (m, 1H), 1.95-1.56 (m, 7H), 1.38-1.16 (m, 7H), 0.95 (t, *J*=7.3 Hz, 3H). ¹³C NMR (CDCl₃, 100 MHz): δ 174.9, 166.8, 161.5, 140.8, 129.5, 126.5, 126.3, 123.3, 110.1, 71.8, 49.3, 47.2, 41.6, 33.7, 32.3, 25.4, 24.6, 20.2, 13.6. HRMS (ESI) calculated for C₂₁H₂₉ClN₃O₃ [MH]⁺ 406.1892, found 406.1892. ATR-FTIR (cm⁻¹): 3330, 2925, 2849, 1743, 1656, 1616, 1529, 1477, 1402, 1251, 1188, 1112, 757, 730.

6.2.1.13. Synthesis of 3-(*N*-butyl-2-chloroacetamido)-1-methyl-2-oxo-*N*-(2,4,4-trimethylpentan-2-yl)indoline-3-carboxamide (I.5aaac):



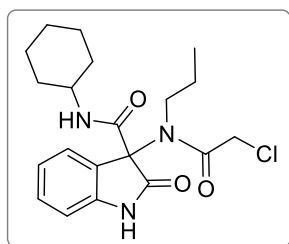
Prepared using *N*-methylisatin (**I.1a**), *n*-butylamine (**I.2a**), chloroacetic acid (**I.3a**), and 1,1,3,3-tetramethylbutyl isocyanide (**I.4c**). After 48 hours, ethyl acetate was added (10 mL) and the mixture filtered through a pad of celite. After solvent removal under reduced pressure, the crude mixture was purified by column chromatography (hexane:AcOEt 7:3). The corresponding **I.5aaac** was obtained as a white solid (425.8 mg, 76% yield). m.p.= 115.3-116.1 °C. ¹H NMR (CDCl₃, 400 MHz): δ 7.47 (d, *J*=7.4 Hz, 1H), 7.31 (td, *J*=7.7, 1.1 Hz, 1H), 7.12-7.08 (m, 2H), 6.82 (d, *J*=7.8 Hz, 1H), 4.11 (d, *J*=12.9 Hz, 1H), 4.07 (d, *J*=12.9 Hz, 1H), 3.71-3.63 (m, 1H), 3.59-3.51 (m, 1H), 3.23 (s, 3H), 1.96-1.88 (m, 2H), 1.76-1.66 (m, 1H), 1.42 (s, 3H), 1.39 (s, 3H), 1.37-1.31 (m, 3H), 0.96 (t, *J*=7.3 Hz, 3H), 0.86 (s, 9H). ¹³C NMR (CDCl₃, 100 MHz): δ 173.6, 166.6, 160.9, 143.5, 129.4, 126.3, 125.9, 123.4, 108.2, 72.4, 56.1, 51.6, 47.2, 41.7, 33.8, 31.5, 31.1, 28.4, 28.3, 26.7, 20.1, 13.6. HRMS (ESI) calculated for C₂₄H₃₇ClN₃O₃ [MH]⁺ 450.2518, found 450.2516. ATR-FTIR (cm⁻¹): 3397, 3378, 2949, 2871, 1698, 1669, 1609, 1525, 1460, 1365, 1352, 1256, 1205, 1128, 1092, 798, 778, 748, 696, 664.

6.2.1.14. Synthesis of *N*-benzyl-3-(*N*-butyl-2-chloroacetamido)-1-methyl-2-oxoindoline-3-carboxamide (I.5baad):



Prepared using isatin (**I.1b**), *n*-butylamine (**I.2a**), chloroacetic acid (**I.3a**), and benzyl isocyanide (**I.4d**). After 48 hours, ethyl acetate was added (10 mL) and the mixture filtered through a pad of celite. After solvent removal under reduced pressure, the crude mixture was purified by column chromatography (hexane:AcOEt from 7:3 to 1:1). The corresponding **I.5baad** was obtained as a pale-yellow solid (205.6 mg, 37% yield). m.p.= 123.0-124.4 °C. ¹H NMR (CDCl₃, 400 MHz): δ 8.28 (br s, 1H), 7.50 (d, *J*=7.4 Hz, 1H), 7.42 (t, *J*=5.3 Hz, 1H), 7.32-7.22 (m, 6H), 7.07 (td, *J*=7.6, 0.8 Hz, 1H), 6.82 (d, *J*=7.7 Hz, 1H), 4.48 (dd, *J*=14.6, 5.9 Hz, 1H), 4.33 (dd, *J*= 14.6, 5.6 Hz, 1H), 4.11 (dd, *J*=19.5, 13 Hz, 2H), 3.65-3.57 (m, 1H), 3.42-3.33 (m, 1H), 1.79-1.68 (m, 1H), 1.58-1.47 (m, 1H), 1.22-1.12 (m, 2H), 0.85 (t, *J*=7.3 Hz, 3H). ¹³C NMR (CDCl₃, 100 MHz): δ 174.6, 167.1, 162.9, 140.9, 137.1, 129.7, 128.8 (2C), 128.1 (2C), 127.8, 126.3 (2C), 123.4, 110.4, 71.8, 47.2, 44.4, 41.7, 33.4, 20.0, 13.5. HRMS (ESI) calculated for C₂₂H₂₅ClN₃O₃ [MH]⁺ 414.1579, found 414.1569. ATR-FTIR (cm⁻¹): 3416, 3176, 2958, 2868, 1745, 1655, 1618, 1510, 1469, 1421, 1399, 1198, 1126, 1109, 932, 752, 735, 693, 660.

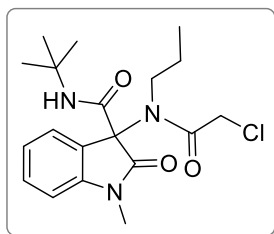
6.2.1.15. Synthesis of 3-(2-chloro-*N*-propylacetamido)-*N*-cyclohexyl-2-oxoindoline-3-carboxamide (**I.5bbab**):



Prepared using isatin (**I.1b**), *n*-propylamine (**I.2b**), chloroacetic acid (**I.3a**), and cyclohexyl isocyanide (**I.4b**). After 48 hours, ethyl acetate was added (10 mL) and the mixture filtered through a pad of celite. After solvent removal under reduced pressure, the crude mixture was purified by column chromatography (hexane:AcOEt from 9:1 to 4:1). The corresponding **I.5bbab** was obtained as a white solid (178.5 mg, 34% yield). m.p.= 108.6-109.0 °C. ¹H NMR (CDCl₃, 400 MHz): δ 8.04 (br s, 1H), 7.46 (d, *J*=7.5 Hz, 1H), 7.24 (td, *J*=7.7, 1.1 Hz, 1H), 7.09-7.05 (m, 2H), 6.82 (d, *J*=7.7 Hz, 1H), 4.13 (dd, *J*=18.9, 13.0 Hz, 2H), 3.77-3.71 (m, 1H), 3.70-3.62 (m, 1H), 3.52-3.44 (m, 1H), 1.96-1.88 (m, 2H), 1.79-1.68 (m, 4H), 1.60-1.56 (m, 1H), 1.38-1.13 (m, 5H), 0.93 (t, *J*=7.4 Hz, 3H).

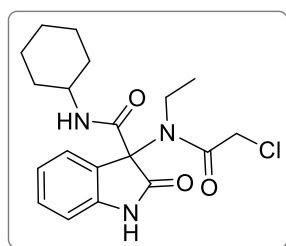
^{13}C NMR (CDCl_3 , 100 MHz): δ 175.0, 167.0, 161.6, 140.9, 129.5, 126.4, 126.2, 123.2, 110.2, 71.8, 49.3, 49.0, 41.6, 32.3, 25.4, 25.0, 24.6, 24.5, 11.2. HRMS (ESI) calculated for $\text{C}_{20}\text{H}_{27}\text{ClN}_3\text{O}_3$ $[\text{MH}]^+$ 392.1735, found 392.1752. ATR-FTIR (cm^{-1}): 3531, 3469, 3349, 2945, 2854, 1712, 1665, 1629, 1518, 1473, 1415, 1209, 1109, 945, 828, 745, 697.

6.2.1.16. Synthesis of *N*-(*tert*-butyl)-3-(2-chloro-*N*-propylacetamido)-1-methyl-2-oxoindoline-3-carboxamide (I.5abaa):



Prepared using *N*-methylisatin (**I.1a**), *n*-propylamine (**I.2b**), chloroacetic acid (**I.3a**), and *tert*-butyl isocyanide (**I.4a**). After 48 hours, ethyl acetate was added (10 mL) and the mixture filtered through a pad of celite. After solvent removal under reduced pressure, the crude was crystallized from ethanol. The corresponding **I.5abaa** was obtained as a white solid (243.8 mg, 52% yield). m.p.= 146.7-148.2 °C. ^1H NMR (CDCl_3 , 400 MHz): δ 7.47 (dd, $J=5.0, 0.6$ Hz, 1H), 7.32 (td, $J=7.7, 1.2$ Hz, 1H), 7.19 (br s, 1H), 7.10 (td, $J=7.6, 0.8$ Hz, 1H), 6.84 (d, $J=7.8$ Hz, 1H), 4.09 (dd, $J=15.8, 12.9$ Hz, 2H), 3.66-3.58 (m, 1H), 3.55-3.47 (m, 1H), 3.26 (s, 3H), 1.98-1.88 (m, 1H), 1.79-1.70 (m, 1H), 1.34 (s, 9H), 0.93 (t, $J=7.4$ Hz, 3H). ^{13}C NMR (CDCl_3 , 100 MHz): δ 173.8, 166.7, 161.4, 143.8, 129.4, 126.1, 126.1, 123.3, 108.4, 72.0, 52.2, 48.9, 41.7, 28.2 (3C), 27.0, 25.1, 11.1. HRMS (ESI) calculated for $\text{C}_{19}\text{H}_{27}\text{ClN}_3\text{O}_3$ $[\text{MH}]^+$ 380.1735, found 380.1740. ATR-FTIR (cm^{-1}): 3349, 2965, 1728, 1664, 1608, 1524, 1472, 1347, 1217, 1087, 1023, 752.

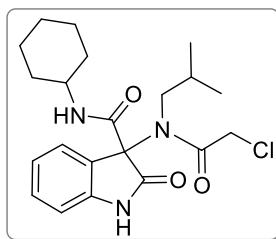
6.2.1.17. Synthesis of 3-(2-chloro-*N*-ethylacetamido)-*N*-cyclohexyl-2-oxoindoline-3-carboxamide (I.5bcab):



Prepared using isatin (**I.1b**), ethylamine (**I.2c**), chloroacetic acid (**I.3a**), and cyclohexyl isocyanide (**I.4b**). After 48 hours, ethyl acetate was added (10 mL) and the mixture filtered through a pad of celite. After solvent removal under reduced pressure, the crude mixture was purified by column chromatography (hexane:AcOEt 3:2). The

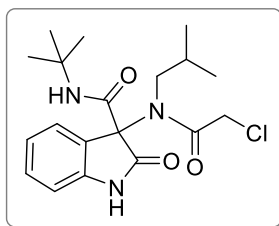
corresponding **I.5bcab** was obtained as a white solid (384.7 mg, 75% yield). m.p.= 125.1-126.6 °C. ^1H NMR (CDCl_3 , 400 MHz): δ 7.93 (br s, 1H), 7.47 (d, $J=7.5$ Hz, 1H), 7.24 (td, $J=7.8$, 1.2 Hz, 1H), 7.11 (br s, 1H), 7.08 (td, $J=7.6$, 0.9 Hz, 1H), 6.82 (d, $J=7.8$ Hz, 1H), 4.15 (d, $J=12.9$ Hz, 1H), 4.10 (d, $J=12.9$ Hz, 1H), 3.88-3.70 (m, 1H), 3.68-3.59 (m, 1H), 1.96-1.93 (m, 1H), 1.80-1.77 (m, 1H), 1.72-1.63 (m, 2H), 1.58-1.55 (m, 1H), 1.41 (t, $J=7.1$ Hz, 3H), 1.34-1.14 (m, 5H). ^{13}C NMR (CDCl_3 , 100 MHz): δ 174.9, 166.8, 161.5, 140.8, 129.5, 126.4, 126.2, 123.3, 110.1, 71.8, 49.3, 42.0, 41.6, 32.3, 25.4, 24.5, 17.0. HRMS (ESI) calculated for $\text{C}_{19}\text{H}_{25}\text{ClN}_3\text{O}_3$ $[\text{MH}]^+$ 378.1579, found 378.1587. ATR-FTIR (cm^{-1}): 3526, 3458, 3345, 2948, 2854, 1713, 1664, 1627, 1525, 1474, 1415, 1212, 1109, 829, 745, 694.

6.2.1.18. Synthesis of 3-(2-chloro-*N*-isobutylacetamido)-*N*-cyclohexyl-2-oxoindoline-3-carboxamide (**I.5bdab**):



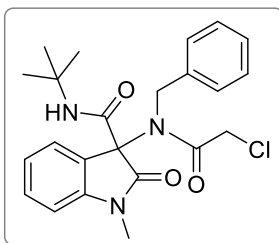
Prepared using isatin (**I.1b**), isobutylamine (**I.2d**), chloroacetic acid (**I.3a**), and cyclohexyl isocyanide (**I.4b**). After 48 hours, ethyl acetate was added (10 mL) and the mixture filtered through a pad of celite. After solvent removal under reduced pressure, the crude mixture was purified by column chromatography (hexane:AcOEt from 9:1 to 7:1). The corresponding **I.5bdab** was obtained as a white solid (441.9 mg, 80% yield). m.p.= 188.8 °C (decomp.). ^1H NMR (CDCl_3 , 400 MHz): δ 7.88 (br s, 1H), 7.48 (d, $J=7.5$ Hz, 1H), 7.25 (td, $J=7.7$, 1.1 Hz, 1H), 7.07 (td, $J=7.6$, 0.8 Hz, 1H), 6.86 (br s, 1H), 6.83 (d, $J=7.7$ Hz, 1H), 4.20 (d, $J=13.1$ Hz, 1H), 4.16 (d, $J=13.0$ Hz, 1H), 3.75-3.59 (m, 2H), 3.42-3.36 (m, 1H), 2.10-1.91 (m, 2H), 1.79-1.76 (m, 1H), 1.70-1.63 (m, 2H), 1.57-1.55 (m, 1H), 1.39-1.28 (m, 2H), 1.26-1.10 (3H), 0.95 (d, $J=6.6$ Hz, 3H), 0.89 (d, $J=6.6$ Hz, 3H). ^{13}C NMR (CDCl_3 , 100 MHz): δ 174.5, 167.6, 161.7, 140.7, 129.5, 126.8, 126.6, 123.3, 110.2, 71.9, 54.2, 49.3, 42.0, 32.3 (2C), 29.2, 25.4, 24.5 (2C), 19.9 (2C). HRMS (ESI) calculated for $\text{C}_{21}\text{H}_{29}\text{ClN}_3\text{O}_3$ $[\text{MH}]^+$ 406.1892, found 406.1897. ATR-FTIR (cm^{-1}): 3328, 3273, 2934, 2851, 1727, 1681, 1639, 1524, 1471, 1407, 1203, 754, 743, 710.

6.2.1.19. Synthesis of *N*-(*tert*-butyl)-3-(2-chloro-*N*-isobutylacetamido)-2-oxoindoline-3-carboxamide (**I.5bdaa**):



Prepared using isatin (**I.1b**), isobutylamine (**I.2d**), chloroacetic acid (**I.3a**), and *tert*-butyl isocyanide (**I.4a**). After 48 hours, ethyl acetate was added (10 mL) and the mixture filtered through a pad of celite. After solvent removal under reduced pressure, the crude mixture was purified by column chromatography (hexane:AcOEt 3:2). The corresponding **I.5bdaa** was obtained as a yellow solid (328.1 mg, 64% yield). m.p.= 169.7-169.9 °C. ¹H NMR (CDCl₃, 400 MHz): δ 8.21 (br s, 1H), 7.45 (d, *J*=7.5 Hz, 1H), 7.24 (td, *J*=7.7, 0.7 Hz, 1H), 7.07 (td, *J*=7.5, 0.3 Hz, 1H), 6.92 (br s, 1H), 6.84 (d, *J*=7.8 Hz, 1H), 4.23 (d, *J*=13.0 Hz, 1H), 4.16 (d, *J*=13.0 Hz, 1H), 3.58-3.44 (m, 2H), 2.17-2.05 (m, 1H), 1.32 (s, 9H), 0.96 (d, *J*=6.7 Hz, 3H), 0.89 (d, *J*=6.6 Hz, 3H). ¹³C NMR (CDCl₃, 100 MHz): δ 174.8, 167.6, 161.3, 140.9, 129.4, 126.7, 126.7, 123.2, 110.4, 72.6, 54.2, 52.2, 42.1, 29.3, 28.2 (3C), 19.9 (2C). Elemental analysis calculated for C₁₉H₂₆ClN₃O₃ C (60.07%), H (6.90%) and N (11.06%), found C (60.17%), H (7.26%) and N (10.87%). ATR-FTIR (cm⁻¹): 3258, 2958, 1726, 1687, 1643, 1619, 1538, 1471, 1203, 1134, 991, 757, 714.

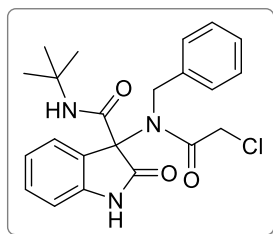
6.2.1.20. Synthesis of 3-(*N*-benzyl-2-chloroacetamido)-*N*-(*tert*-butyl)-1-methyl-2-oxoindoline-3-carboxamide (**I.5aeaa**):



Prepared using *N*-methylisatin (**I.1a**), benzylamine (**I.2e**), chloroacetic acid (**I.3a**), and *tert*-butyl isocyanide (**I.4a**). After 48 hours, ethyl acetate was added (10 mL) and the mixture filtered through a pad of celite. After solvent removal under reduced pressure, the crude mixture was purified by column chromatography (hexane:AcOEt 7:3). The corresponding **I.5aeaa** was obtained as a white solid (125.0 mg, 24% yield). m.p.= 214.6-215.0 °C. ¹H NMR (CDCl₃, 400 MHz): δ 7.49-7.28 (m, 7H), 7.15-7.11 (m, 2H), 6.82 (d, *J*=7.8 Hz, 1H), 5.13 (d, *J*=18.8 Hz, 1H), 4.97 (d, *J*=18.9 Hz, 1H), 3.98 (d, *J*=12.9 Hz, 1H), 3.87 (d, *J*=12.9 Hz, 1H), 3.26 (s, 3H), 0.97 (s, 9H). ¹³C NMR (CDCl₃, 100 MHz): δ 173.8,

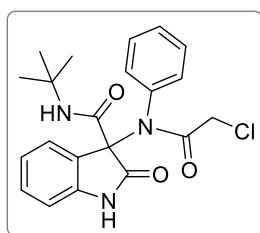
167.6, 161.2, 143.8, 137.1, 129.6, 129.0 (2C), 127.8, 125.8 (2C), 125.6, 125.6, 123.3, 108.4, 71.8, 52.0, 49.6, 41.8, 27.6 (3C), 27.0. HRMS (ESI) calculated for $C_{23}H_{27}ClN_3O_3$ $[MH]^+$ 428.1735, found 428.1743. ATR-FTIR (cm^{-1}): 3360, 2984, 1699, 1670, 1612, 1532, 1467, 1458, 1360, 1212, 1132, 974, 869, 799, 746, 729, 696.

6.2.1.21. Synthesis of 3-(*N*-benzyl-2-chloroacetamido)-*N*-(*tert*-butyl)-2-oxoindoline-3-carboxamide (**I.5beaa**):



Prepared using isatin (**I.1b**), benzylamine (**I.2e**), chloroacetic acid (**I.3a**), and *tert*-butyl isocyanide (**I.4a**). After 48 hours, ethyl acetate was added (10 mL) and the mixture filtered through a pad of celite. After solvent removal under reduced pressure, the crude mixture was purified by column chromatography (hexane:AcOEt 7:3). The corresponding **I.5beaa** was obtained as a white solid (86.3 mg, 15% yield). m.p.= 187.4-188.2 °C. 1H NMR ($CDCl_3$, 400 MHz): δ 7.84 (br s, 1H), 7.50-7.41 (m, 5H), 7.32 (t, J = 7.0 Hz, 1H), 7.26-7.23 (m, 1H), 7.12-7.08 (m, 2H), 6.80 (d, J =7.7 Hz, 1H), 5.15 (d, J =18.9 Hz, 1H), 5.00 (d, J =18.8 Hz, 1H), 3.98 (d, J =12.9 Hz, 1H), 3.89 (d, J =12.9 Hz, 1H), 0.96 (s, 9H). ^{13}C NMR ($CDCl_3$, 100 MHz): δ 175.2, 167.7, 160.9, 140.8, 137.1, 129.6, 129.2 (2C), 127.8, 126.2, 126.0, 125.5 (2C), 123.2, 110.2, 72.1, 52.0, 49.5, 41.7, 27.6 (3C). HRMS (ESI) calculated for $C_{22}H_{25}ClN_3O_3$ $[MH]^+$ 414.1579, found 414.1575. ATR-FTIR (cm^{-1}): 3329, 3251, 2953, 1722, 1661, 1620, 1551, 1463, 1391, 1221, 1199, 997, 964, 864, 797, 756, 694.

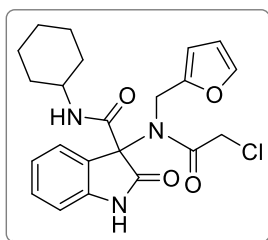
6.2.1.22. Synthesis of *N*-(*tert*-butyl)-3-(2-chloro-*N*-phenylacetamido)-2-oxoindoline-3-carboxamide (**I.5bfaa**):



Prepared using isatin (**I.1b**), aniline (**I.2f**), chloroacetic acid (**I.3a**), and *tert*-butyl isocyanide (**I.4a**). After 48 hours, ethyl acetate was added (10 mL) and the mixture filtered through a pad of celite. After solvent removal under reduced pressure, the crude

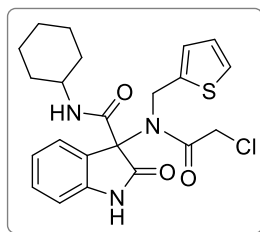
mixture was purified by column chromatography (hexane:AcOEt from 4:1 to 7:3) and further purified by preparative TLC (CH₂Cl₂:acetone 7:1). The corresponding **I.5bfaa** was obtained as a white solid (50.0 mg, 9% yield). m.p.= 195.9-196.7 °C. ¹H NMR (CDCl₃, 400 MHz): δ 8.00 (br s, 1H), 7.70 (d, *J*=7.4 Hz, 1H), 7.60-7.47 (m, 5H), 7.27 (td, *J*=7.7, 1.1 Hz, 1H), 7.15 (td, *J*=7.6, 0.7 Hz, 1H), 6.92 (br s, 1H), 6.85 (d, *J*=7.7 Hz, 1H), 3.78 (d, *J*=13.9 Hz, 1H), 3.68 (d, *J*=13.9 Hz, 1H), 0.91 (s, 9H). ¹³C NMR (CDCl₃, 100 MHz): δ 175.6, 166.5, 159.6, 141.0, 137.9, 131.5, 131.2, 129.9, 129.5, 129.4, 126.4, 123.3, 110.3, 73.2, 51.7, 42.5, 27.7 (3C). HRMS (ESI) calculated for C₂₁H₂₃ClN₃O₃ [MH]⁺ 400.1422, found 400.1428. ATR-FTIR (cm⁻¹): 3291, 2943, 1721, 1672, 1538, 1470, 1366, 1250, 1223, 755, 700, 690.

6.2.1.23. Synthesis of 3-(2-Chloro-*N*-(furan-2-ylmethyl)acetamido)-*N*-cyclohexyl-2-oxindoline-3-carboxamide (I.5bhab**):**



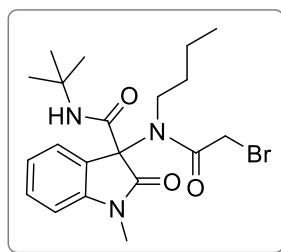
Prepared using isatin (**I.1b**), 2-furfurylamine (**I.2h**), chloroacetic acid (**I.3a**), and cyclohexyl isocyanide (**I.4b**). After 48 hours, ethyl acetate was added (10 mL) and the mixture filtered through a pad of celite. After solvent removal under reduced pressure, the crude mixture was purified by column chromatography (CH₂Cl₂:AcOEt 7:1). The corresponding **I.5bhab** was obtained as a white solid (96.7 mg, 17% yield). m.p.= 157.1-157.3 °C. ¹H NMR (CDCl₃, 400 MHz): δ 7.68 (br s, 1H), 7.36 (d, *J*=1.1 Hz, 1H), 7.21 (td, *J*=7.6, 1.5 Hz, 1H), 7.00-6.91 (m, 3H), 6.79 (d, *J*=7.8 Hz, 1H), 6.42 (d, *J*=3.0 Hz, 1H), 6.35-6.34 (m, 1H), 4.97 (d, *J*=17.9 Hz, 1H), 4.82 (d, *J*=17.9 Hz, 1H), 4.33 (s, 2H), 3.72-3.63 (m, 1H), 1.80-1.72 (m, 2H), 1.64-1.60 (m, 2H), 1.55-1.53 (m, 1H), 1.35-1.24 (m, 2H), 1.16-0.98 (m, 3H). ¹³C NMR (CDCl₃, 100 MHz): δ 174.1, 167.5, 161.5, 149.8, 142.8, 140.8, 129.6, 126.3, 126.0, 123.2, 110.8, 109.9, 109.3, 71.6, 49.2, 43.4, 42.0, 32.2, 32.0, 25.4, 24.5, 15.3. HRMS (ESI) calculated for C₂₂H₂₅ClN₃O₄ [MH]⁺ 430.1528, found 430.1531. ATR-FTIR (cm⁻¹): 3401, 3164, 2935, 2855, 1745, 1713, 1663, 1514, 1472, 1392, 1237, 1190, 1174, 1145, 1014, 795, 759, 724, 697.

6.2.1.24. Synthesis of 3-(2-Chloro-*N*-(thiophen-2-ylmethyl)acetamido)-*N*-cyclohexyl-2-oxindoline-3-carboxamide (I.5biab**):**



Prepared using isatin (**I.1b**), 2-thiophenemethylamine (**I.2i**), chloroacetic acid (**I.3a**), and cyclohexyl isocyanide (**I.4b**). After 48 hours, ethyl acetate was added (10 mL) and the mixture filtered through a pad of celite. After solvent removal under reduced pressure, the crude mixture was purified by column chromatography (CH₂Cl₂:AcOEt from 9:1 to 7:1). The corresponding **I.5biab** was obtained as a white solid (96.4 mg, 16% yield). m.p.= 171.1-172.3 °C. ¹H NMR (CDCl₃, 400 MHz): δ 7.95 (br s, 1H), 7.35 (d, *J*=7.5 Hz, 1H), 7.26-7.22 (m, 2H), 7.18 (br s, 1H), 7.06 (td, *J*=7.6, 0.8 Hz, 1H), 6.97 (dd, *J*=5.0, 3.6 Hz, 1H), 6.90 (d, *J*=7.4 Hz, 1H), 6.80 (d, *J*=7.8 Hz, 1H), 5.25 (d, *J*=18.2 Hz, 1H), 5.06 (d, *J*=18.3 Hz, 1H), 4.17 (d, *J*=13.0 Hz, 1H), 4.10 (d, *J*=13.0 Hz, 1H), 3.59-3.52 (m, 1H), 1.74-1.71 (m, 1H), 1.58-1.42 (m, 4H), 1.28-1.00 (m, 4H), 0.84-0.74 (m, 1H). ¹³C NMR (CDCl₃, 100 MHz): δ 174.5, 167.5, 161.6, 140.9, 140.1, 129.7, 127.2, 126.2, 126.1, 125.8, 125.5, 123.3, 110.1, 71.6, 49.3, 45.9, 41.8, 32.2, 31.5, 25.3, 24.4, 24.4. HRMS (ESI) calculated for C₂₂H₂₅ClN₃O₃S [MH]⁺ 446.1300, found 446.1307. ATR-FTIR (cm⁻¹): 3405, 3190, 2935, 2860, 1741, 1683, 1661, 1520, 1473, 1396, 1235, 1200, 1183, 1114, 943, 771, 727, 695.

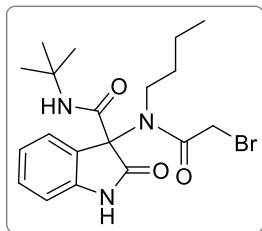
6.2.1.25. Synthesis of 3-(2-Bromo-*N*-butylacetamido)-*N*-(*tert*-butyl)-1-methyl-2-oxoindoline-3-carboxamide (**I.5aaba**):



Prepared using *N*-methylisatin (**I.1a**), *n*-butylamine (**I.2a**), bromoacetic acid (**I.3b**), and *tert*-butyl isocyanide (**I.4a**). After 48 hours, ethyl acetate was added (10 mL) and the mixture filtered through a pad of celite. After solvent removal under reduced pressure, the crude mixture was purified by column chromatography (hexane:AcOEt from 4:1 to 7:3). The corresponding **I.5aaba** was obtained as a white solid (243.2 mg, 45% yield). m.p.= 120.3-121.0 °C. ¹H NMR (CDCl₃, 400 MHz): δ 7.49 (dd, *J*=7.5, 0.7 Hz, 1H), 7.32 (td, *J*=7.8, 1.2 Hz, 1H), 7.13-7.08 (m, 2H), 6.83 (d, *J*=7.8 Hz, 1H), 3.86 (d, *J*=11.0 Hz, 1H), 3.82 (d, *J*=11.0 Hz, 1H), 3.73-3.64 (m, 1H), 3.60-3.52 (m, 1H), 3.26 (s, 3H), 1.91-

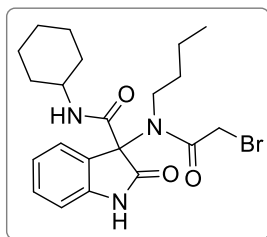
1.80 (m, 1H), 1.76-1.65 (m, 1H), 1.34-1.29 (m, 11H), 0.94 (t, $J=7.3$ Hz, 3H). ^{13}C NMR (CDCl_3 , 100 MHz): δ 173.7, 167.0, 161.6, 143.8, 129.4, 126.2, 126.1, 123.3, 108.3, 72.1, 52.1, 47.7, 33.9, 28.3 (3C), 27.0, 26.6, 20.1, 13.6. HRMS (ESI) calculated for $\text{C}_{20}\text{H}_{29}\text{BrN}_3\text{O}_3$ $[\text{MH}]^+$ 438.1387, found 438.1381. ATR-FTIR (cm^{-1}): 3359, 2959, 2926, 2873, 1718, 1661, 1609, 1523, 1471, 1347, 1260, 1211, 1085, 1023, 752.

6.2.1.26. Synthesis of 3-(2-Bromo-*N*-butylacetamido)-*N*-(*tert*-butyl)-2-oxoindoline-3-carboxamide (I.5baba):



Prepared using isatin (**I.1b**), *n*-butylamine (**I.2a**), bromoacetic acid (**I.3b**), and *tert*-butyl isocyanide (**I.4a**). After 48 hours, ethyl acetate was added (10 mL) and the mixture filtered through a pad of celite. After solvent removal under reduced pressure, the crude mixture was purified by column chromatography (hexane:AcOEt from 4:1 to 7:3). The corresponding **I.5baba** was obtained as a white solid (160.5 mg, 28% yield). m.p.= 157.9 °C (decomp.). ^1H NMR (CDCl_3 , 400 MHz): δ 7.79 (br s, 1H), 7.45 (d, $J=7.5$ Hz, 1H), 7.24 (td, $J=7.7, 1.2$ Hz, 1H), 7.10-7.06 (m, 2H), 6.82 (d, $J=7.7$ Hz, 1H), 3.87 (s, 2H), 3.74-3.66 (m, 1H), 3.62-3.54 (m, 1H), 1.96-1.85 (m, 1H), 1.80-1.69 (m, 1H), 1.39-1.30 (m, 11H), 0.96 (t, $J=7.3$ Hz, 3H). ^{13}C NMR (CDCl_3 , 100 MHz): δ 175.0, 167.1, 161.3, 140.7, 129.4, 126.6, 126.3, 123.2, 110.1, 72.4, 52.2, 47.7, 33.9, 28.2 (3C), 26.5, 20.1, 13.6. HRMS (ESI) calculated for $\text{C}_{19}\text{H}_{27}\text{BrN}_3\text{O}_3$ $[\text{MH}]^+$ 424.1230, found 424.1248. ATR-FTIR (cm^{-1}): 3335, 2959, 2935, 2872, 1720, 1652, 1619, 1527, 1471, 1365, 1204, 1099, 887, 747, 737, 682.

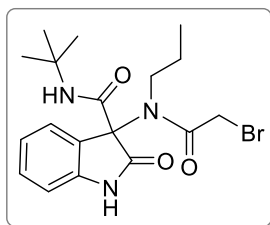
6.2.1.27. Synthesis of 3-(2-Bromo-*N*-butylacetamido)-*N*-cyclohexyl-2-oxoindoline-3-carboxamide (I.5babb):



Prepared using isatin (**I.1b**), *n*-butylamine (**I.2a**), bromoacetic acid (**I.3b**), and cyclohexyl isocyanide (**I.4b**). After 48 hours, ethyl acetate was added (10 mL) and the

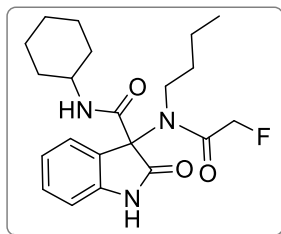
mixture filtered through a pad of celite. After solvent removal under reduced pressure, the crude mixture was purified by column chromatography (CH₂Cl₂:AcOEt 4:1). The corresponding **I.5babb** was obtained as a white solid (163.2 mg, 27% yield). m.p.= 156.6-157.1 °C. ¹H NMR (CDCl₃, 400 MHz): δ 8.01 (br s, 1H), 7.46 (d, *J*=7.5 Hz, 1H), 7.24 (td, *J*=7.7, 1.0 Hz, 1H), 7.09-7.05 (m, 2H), 6.81 (d, *J*=7.7 Hz, 1H), 3.88 (s, 2H), 3.76-3.68 (m, 2H), 3.58-3.47 (m, 1H), 1.95-1.55 (m, 7H), 1.38-1.15 (m, 7H), 0.95 (t, *J*=7.3 Hz, 3H). ¹³C NMR (CDCl₃, 100 MHz): δ 174.9, 167.1, 161.7, 140.9, 129.4, 126.5, 126.2, 123.2, 110.1, 71.8, 49.3, 47.8, 47.2, 41.6, 33.7, 32.3, 26.5, 25.4, 24.6, 24.5, 20.2, 13.6. HRMS (ESI) calculated for C₂₁H₂₉BrN₃O₃ [MH]⁺ 450.1387, found 450.1397. ATR-FTIR (cm⁻¹): 3320, 3261, 2930, 2853, 1726, 1643, 1618, 1438, 1199, 1100, 943, 891, 752, 743, 687.

6.2.1.28. Synthesis of 3-(2-Bromo-*N*-propylacetamido)-*N*-(*tert*-butyl)-2-oxindoline-3-carboxamide (**I.5bbba**):



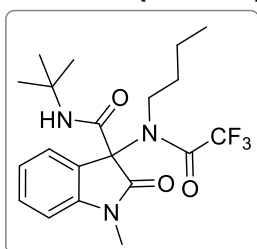
Prepared using isatin (**I.1b**), *n*-propylamine (**I.2b**), bromoacetic acid (**I.3b**), and *tert*-butyl isocyanide (**I.4a**). After 48 hours, ethyl acetate was added (10 mL) and the mixture filtered through a pad of celite. After solvent removal under reduced pressure, the crude mixture was purified by column chromatography (hexane:AcOEt from 4:1 to 7:3). The corresponding **I.5bbba** was obtained as a white solid (127.4 mg, 23% yield). m.p.= 169.3 °C (decomp.). ¹H NMR (CDCl₃, 400 MHz): δ 7.95 (br s, 1H), 7.44 (d, *J*=7.5 Hz, 1H), 7.24 (t, *J*=7.7 Hz, 1H), 7.11-7.05 (m, 2H), 6.82 (d, *J*=7.7 Hz, 1H), 3.88 (s, 2H), 3.71-3.60 (m, 1H), 3.58-3.47 (m, 1H), 1.99-1.90 (m, 1H), 1.83-1.73 (m, 1H), 1.34 (s, 9H), 0.94 (t, *J*=7.4 Hz, 3H). ¹³C NMR (CDCl₃, 100 MHz): δ 175.1, 167.1, 161, 4, 140.8, 129.4, 126.6, 126.3, 123.2, 110.2, 72.4, 52.2, 49.5, 28.2 (3C), 26.6, 25.2, 11.1. HRMS (ESI) calculated for C₁₈H₂₅BrN₃O₃ [MH]⁺ 410.1074, found 410.1075. ATR-FTIR (cm⁻¹): 3288, 2963, 2931, 1721, 1678, 1648, 1620, 1528, 1431, 1361, 1208, 1101, 854, 748, 736, 682.

6.2.1.29. Synthesis of 3-(*N*-butyl-2-fluoroacetamido)-*N*-cyclohexyl-2-oxindoline-3-carboxamide (**I.5bacb**):



Prepared using isatin (**I.1b**), *n*-butylamine (**I.2a**), fluoroacetic acid (**I.3c**), and cyclohexyl isocyanide (**I.4b**). After 48 hours, ethyl acetate was added (10 mL) and the mixture filtered through a pad of celite. After solvent removal under reduced pressure, the crude mixture was purified by column chromatography (hexane:AcOEt from 7:3 to 3:2). The corresponding **I.5bacb** was obtained as a white solid (289.3 mg, 55% yield). m.p.= 165.9-167.1 °C. ¹H NMR (CDCl₃, 400 MHz): δ 8.14 (br s, 1H), 7.48 (d, *J*=7.5 Hz, 1H), 7.24 (td, *J*=7.7, 1.0 Hz, 1H), 7.09-7.05 (m, 2H), 6.82 (d, *J*=7.8 Hz, 1H), 5.05 (q, *J*=14.2 Hz, 1H), 4.94 (q, *J*=14.2 Hz, 1H), 3.77-3.70 (m, 1H), 3.57-3.49 (m, 1H), 3.41-3.33 (m, 1H), 1.94-1.76 (m, 3H), 1.72-1.63 (m, 2H), 1.61-1.55 (m, 2H), 1.38-1.12 (m, 7H), 0.94 (t, *J*=7.3 Hz, 3H). ¹³C NMR (CDCl₃, 100 MHz): δ 175.0, 167.1, 161.4, 140.9, 129.6, 126.4, 126.3, 123.2, 110.2, 80.0, 78.2, 71.5, 49.3, 45.8, 33.5, 32.3, 25.4, 24.6, 24.5, 20.1, 13.6. HRMS (ESI) calculated for C₂₁H₂₉FN₃O₃ [MH]⁺ 390.2187, found 390.2187. ATR-FTIR (cm⁻¹): 3349, 3178, 2929, 2858, 1711, 1664, 1619, 1520, 1470, 1227, 1211, 1073, 1046, 761, 752.

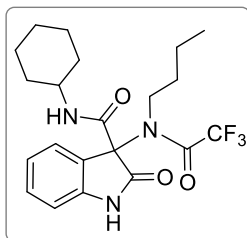
6.2.1.30. Synthesis of *N*-(*tert*-butyl)-3-(*N*-butyl-2,2,2-trifluoroacetamido)-1-methyl-2-oxoindoline-3-carboxamide (**I.5aada**):



Prepared using *N*-methylisatin (**I.1a**), *n*-butylamine (**I.2a**), trifluoroacetic acid (**I.3d**), and *tert*-butyl isocyanide (**I.4a**). After 48 hours, ethyl acetate was added (10 mL) and the mixture filtered through a pad of celite. After solvent removal under reduced pressure, the crude mixture was purified by column chromatography (hexane:AcOEt 7:3). The corresponding **I.5aada** was obtained as a white solid (452.0 mg, 88% yield). m.p.= 98.5-99.7 °C. ¹H NMR (CDCl₃, 400 MHz): δ 7.52 (d, *J*=7.5 Hz, 1H), 7.35 (td, *J*=7.8, 0.8 Hz, 1H), 7.16-7.12 (m, 2H), 6.86 (d, *J*=7.8 Hz, 1H), 3.84-3.76 (m, 1H), 3.66-3.57 (m, 1H), 3.27 (s, 3H), 2.01-1.92 (m, 1H), 1.70-1.59 (m, 1H), 1.34-1.26 (m, 11H), 0.93 (t, *J*=7.3 Hz, 3H). ¹³C NMR (CDCl₃, 100 MHz): δ 173.1, 160.3, 157.2, 143.9, 129.8, 126.4, 125.1,

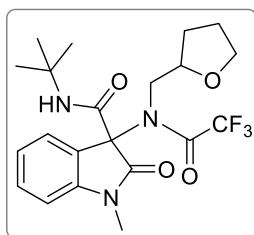
123.6, 120.3, 116.0, 108.5, 72.3, 52.4, 46.8, 33.6, 28.2 (3C), 27.1, 19.9, 13.5. HRMS (ESI) calculated for $C_{20}H_{27}F_3N_3O_3$ $[MH]^+$ 414.1999, found 414.1998. ATR-FTIR (cm^{-1}): 3335, 2975, 2881, 1751, 1218, 1085, 1047, 1020, 881.

6.2.1.31. Synthesis of 3-(*N*-butyl-2,2,2-trifluoroacetamido)-*N*-cyclohexyl-2-oxoindoline-3-carboxamide (**I.5badb**):



Prepared using isatin (**I.1b**), *n*-butylamine (**I.2a**), trifluoroacetic acid (**I.3d**), and cyclohexyl isocyanide (**I.4b**). After 48 hours, ethyl acetate was added (10 mL) and the mixture filtered through a pad of celite. After solvent removal under reduced pressure, the crude mixture was purified by column chromatography (CH_2Cl_2 :AcOEt from 9:1 to 7:1). The corresponding **I.5badb** was obtained as a white solid (137.9 mg, 24% yield). m.p.= 145.8-146.9 °C. 1H NMR ($CDCl_3$, 400 MHz): δ 8.09 (br s, 1H), 7.30-7.24 (m, 2H), 7.11 (td, $J=7.6$, 0.8 Hz, 1H), 6.80 (d, $J=7.8$ Hz, 1H), 5.25 (s, 1H), 3.58-3.51 (m, 1H), 3.21-3.13 (m, 1H), 2.63-2.57 (m, 1H), 2.32-2.22 (m, 1H), 2.12-2.06 (m, 1H), 1.86-1.78 (m, 3H), 1.70-1.67 (m, 1H), 1.62-1.59 (m, 1H), 1.32-0.96 (m, 7H), 0.64 (t, $J=6.9$ Hz, 3H). ^{13}C NMR ($CDCl_3$, 100 MHz): δ 175.5, 167.0, 141.2, 130.2, 126.5, 125.1, 123.9, 122.2, 111.0, 97.3, 75.3, 58.4, 54.8, 44.3, 31.2, 29.2, 29.1, 26.1, 26.0, 25.1, 19.7, 18.3, 13.5. HRMS (ESI) calculated for $C_{21}H_{27}F_3N_3O_3$ $[MH]^+$ 426.1999, found 426.1997. ATR-FTIR (cm^{-1}): 2936, 2858, 1688, 1619, 1428, 1366, 1259, 1170, 1141, 943, 755, 728.

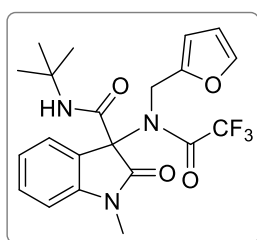
6.2.1.32. Synthesis of *N*-(*tert*-butyl)-1-methyl-2-oxo-3-(2,2,2-trifluoro-*N*-((tetrahydrofuran-2-yl)methyl)acetamido)indoline-3-carboxamide (**I.5agda**):



Prepared using *N*-methylisatin (**I.1a**), 2-(aminomethyl)tetrahydrofuran (**I.2g**), trifluoroacetic acid (**I.3d**), and *tert*-butyl isocyanide (**I.4a**). After 48 hours, ethyl acetate was added (10 mL) and the mixture filtered through a pad of celite. After solvent removal under reduced pressure, the crude mixture was purified by CC (hexane:AcOEt 7:3). The

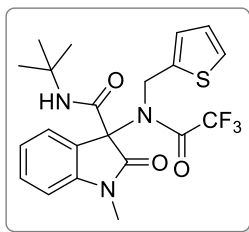
corresponding **I.5agda** was obtained as a white solid (189.3 mg, 35% yield). m.p.= 108.2-109.4 °C. ¹H NMR (CDCl₃, 400 MHz): δ 7.63 (dd, *J*=7.6, 0.7 Hz, 1H), 7.35 (td, *J*=7.8, 1.1 Hz, 1H), 7.14 (td, *J*=7.6, 0.9 Hz, 1H), 6.86 (d, *J*=7.8 Hz, 1H), 6.77 (br s, 1H), 4.29-4.21 (m, 1H), 3.90-3.83 (m 1H), 3.74-3.68 (m, 3H), 3.25 (s, 3H), 2.04-1.96 (m, 1H), 1.90-1.84 (m, 2H), 1.48-1.41 (m, 1H), 1.30 (s, 9H). ¹³C NMR (CDCl₃, 100 MHz): δ 172.1, 161.1, 158.0, 144.0, 129.8, 126.9, 125.5, 123.6, 116.1, 108.4, 76.8, 72.9, 68.2, 52.2, 50.5, 29.3, 28.2 (3C), 27.1, 25.7. HRMS (ESI) calculated for C₂₁H₂₇F₃N₃O₄ [MH]⁺ 442.1948, found 442.1936. ATR-FTIR (cm⁻¹): 3422, 2969, 2876, 1704, 1688, 1613, 1510, 1360, 1196, 1163, 1148, 1069, 953, 748.

6.2.1.33. Synthesis of *N*-(*tert*-butyl)-1-methyl-2-oxo-3-(2,2,2-trifluoro-*N*-(furan-2-ylmethyl)acetamido)indoline-3-carboxamide (I.ahda):



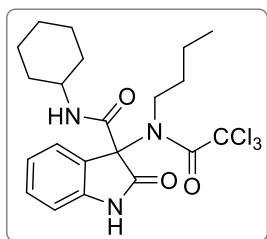
Prepared using *N*-methylisatin (**I.1a**), 2-furfurylamine (**I.2h**), trifluoroacetic acid (**I.3d**), and *tert*-butyl isocyanide (**I.4a**). After 48 hours, ethyl acetate was added (10 mL) and the mixture filtered through a pad of celite. After solvent removal under reduced pressure, the crude mixture was purified by column chromatography (hexane:AcOEt 7:3). The corresponding **I.5ahda** was obtained as a white solid (223.7 mg, 41% yield). m.p.= 126.4-126.9 °C. ¹H NMR (CDCl₃, 400 MHz): δ 7.27 (td, *J*=7.7, 1.3 Hz, 1H), 7.17 (br s, 1H), 7.09 (d, *J*=7.3 Hz, 1H), 7.02 (td, *J*=7.5, 0.8 Hz, 1H), 6.73 (d, *J*=7.8 Hz, 1H), 6.36 (br s, 1H), 6.21-6.18 (m, 2H), 5.03 (d, *J*=17.4 Hz, 1H), 4.91 (d, *J*=17.4 Hz, 1H), 3.18 (s, 3H), 1.24 (s, 9H). ¹³C NMR (CDCl₃, 100 MHz): δ 171.2, 161.0, 158.0, 148.2, 143.7, 142.7, 129.9, 126.5, 125.1, 123.7, 116.0, 110.4, 109.8, 108.4, 72.2, 52.2, 42.9, 28.1 (3C), 27.0. Elemental analysis calculated for C₂₁H₂₂F₃N₃O₄ C (57.66%), H (5.07%) and N (9.61%), found C (57.44%), H (5.28%) and N (9.56%). ATR-FTIR (cm⁻¹): 3397, 2981, 1703, 1617, 1515, 1459, 1368, 1205, 1147, 1134, 1074, 1011, 746, 683.

6.2.1.34. Synthesis of *N*-(*tert*-butyl)-1-methyl-2-oxo-3-(2,2,2-trifluoro-*N*-(thiophen-2-ylmethyl)acetamido)indoline-3-carboxamide (I.5aida):



Prepared using *N*-methylisatin (**I.1a**), 2-thiophenemethylamine (**I.2i**), trifluoroacetic acid (**I.3d**), and *tert*-butyl isocyanide (**I.4a**). After 48 hours, ethyl acetate was added (10 mL) and the mixture filtered through a pad of celite. After solvent removal under reduced pressure, the crude mixture was purified by column chromatography (hexane:AcOEt 7:3). The corresponding **I.5aia** was obtained as a white solid (216.9 mg, 39% yield). m.p.= 135.3-135.6 °C. ¹H NMR (CDCl₃, 400 MHz): δ 7.34-7.26 (m, 2H), 7.13 (dd, *J*=5.0, 1.0 Hz, 1H), 7.05 (td, *J*=7.6, 0.8 Hz, 1H), 6.88-6.86 (m, 1H), 6.82-6.80 (m, 1H), 6.66 (d, *J*=7.8 Hz, 1H), 6.20 (br s, 1H), 5.31 (d, *J*=17.4 Hz, 1H), 5.10 (d, *J*=17.4 Hz, 1H), 3.09 (s, 3H), 1.20 (s, 9H). ¹³C NMR (CDCl₃, 100 MHz): δ 171.0, 161.4, 157.9, 143.7, 137.7, 130.1, 127.6, 126.7, 126.3, 126.3, 125.6, 123.7, 117.6, 108.4, 71.9, 52.2, 45.0, 28.1 (3C), 26.8. Elemental analysis calculated for C₂₁H₂₂F₃N₃O₃S (55.62%), H (4.89%), N (9.27%) and S (7.07%), found C (55.25%), H (4.50%), N (9.23%) and S (7.06%). ATR-FTIR (cm⁻¹): 3354, 2979, 1722, 1675, 1609, 1523, 1473, 1352, 1212, 1183, 1149, 1128, 919, 824, 759, 712.

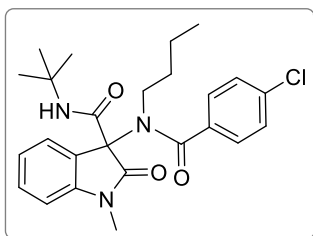
6.2.1.35. Synthesis of 3-(*N*-butyl-2,2,2-trichloroacetamido)-*N*-cyclohexyl-2-oxoindoline-3-carboxamide (**I.5baeb**):



Prepared using isatin (**I.1b**), *n*-butylamine (**I.2a**), trichloroacetic acid (**I.3e**), and cyclohexyl isocyanide (**I.4b**). After 48 hours, ethyl acetate was added (10 mL) and the mixture filtered through a pad of celite. After solvent removal under reduced pressure, the crude mixture was purified by column chromatography (hexane:AcOEt from 4:1 to 7:3). The corresponding **I.5baeb** was obtained as a pale-yellow solid (362.7 mg, 56% yield). m.p.= 106.2-107.4 °C. ¹H NMR (CDCl₃, 400 MHz): δ 7.86 (br s, 1H), 7.56 (d, *J*=7.6 Hz, 1H), 7.29 (td, *J*=7.7, 1.0 Hz, 1H), 7.11 (td, *J*=7.6, 0.6 Hz, 1H), 6.86 (d, *J*=7.7 Hz, 1H), 6.70 (br s, 1H), 4.17-4.09 (m, 1H), 3.99-3.91 (m, 1H), 3.77-3.70 (m, 1H), 1.96-1.62 (m, 6H), 1.57-1.53 (m, 1H), 1.37-1.14 (m, 7H), 0.88 (t, *J*=7.4 Hz, 3H). ¹³C NMR (CDCl₃, 100

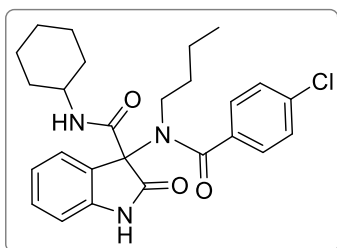
MHz): δ 173.7, 161.3, 161.0, 140.6, 129.8, 126.6, 126.5, 123.6, 110.3, 92.9, 73.5, 49.3, 48.7, 32.4, 32.3, 25.4, 24.5, 24.5, 19.9, 13.6. HRMS (ESI) calculated for $C_{21}H_{27}Cl_3N_3O_3$ $[MH]^+$ 474.1113, found 474.1122. ATR-FTIR (cm^{-1}): 3229, 2931, 2854, 1724, 1672, 1619, 1509, 1470, 1388, 1195, 1109, 838, 810, 749.

6.2.1.36. Synthesis of *N*-(*tert*-butyl)-3-(*N*-butyl-4-chlorobenzamido)-1-methyl-2-oxoindoline-3-carboxamide (I.5aafa):



Prepared using *N*-methylisatin (**I.1a**), *n*-butylamine (**I.2a**), 4-chlorobenzoic acid (**I.3f**), and *tert*-butyl isocyanide (**I.4a**). After 48 hours, ethyl acetate was added (10 mL) and the mixture filtered through a pad of celite. After solvent removal under reduced pressure, the crude mixture was purified by column chromatography (hexane:AcOEt from 4:1 to 7:3). The corresponding **I.5aafa** was obtained as a white solid (263.7 mg, 47% yield). m.p.= 166.2-167.4 °C. 1H NMR ($CDCl_3$, 400 MHz): δ 7.64 (d, $J=7.5$ Hz, 1H), 7.37-7.31 (m, 5H), 7.15 (td, $J=7.6, 0.7$ Hz, 1H), 7.07 (br s, 1H), 6.86 (d, $J=7.8$ Hz, 1H), 3.61-3.45 (m, 2H), 3.28 (s, 3H), 1.66-1.58 (m, 1H), 1.49-1.42 (m, 1H), 1.34 (s, 9H), 1.07-0.97 (m, 2H), 0.68 (t, $J=7.3$ Hz, 3H). ^{13}C NMR ($CDCl_3$, 100 MHz): δ 174.0, 171.6, 161.9, 143.9, 135.8, 134.4, 129.4, 128.7 (2C), 128.2 (2C), 126.9, 126.3, 123.4, 108.4, 71.9, 52.1, 48.5, 33.4, 28.3 (3C), 27.0, 19.8, 13.4. Elemental analysis calculated for $C_{25}H_{30}ClN_3O_3$ C (65.85%), H (6.63%) and N (9.22%), found C (65.90%), H (6.66%) and N (9.22%). ATR-FTIR (cm^{-1}): 3329, 2958, 2931, 2874, 1702, 1647, 1542, 1468, 1356, 1235, 1091, 1012, 933, 844, 751, 697.

6.2.1.37. Synthesis of 3-(*N*-butyl-4-chlorobenzamido)-*N*-cyclohexyl-2-oxoindoline-3-carboxamide (I.5bafb):

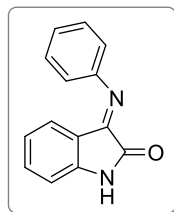


Prepared using *N*-methylisatin (**I.1a**), *n*-butylamine (**I.2a**), 4-chlorobenzoic acid (**I.3f**), and cyclohexyl isocyanide (**I.4b**). After 48 hours, ethyl acetate was added (10 mL)

and the mixture filtered through a pad of celite. After solvent removal under reduced pressure, the crude mixture was purified by column chromatography (hexane:AcOEt from 7:3 to 3:1). The corresponding **I.5bafb** was obtained as a beige solid (421.0 mg, 66% yield). m.p.= 110.0-111.3 °C. ¹H NMR (CDCl₃, 400 MHz): δ 7.92 (br s, 1H), 7.63 (d, *J*=7.4 Hz, 1H), 7.37 (s, 4H), 7.28-7.24 (m, 1H), 7.11 (td, *J*=7.6, 0.5 Hz, 1H), 6.90 (d, *J*=7.6 Hz, 1H), 6.82 (d, *J*=7.7 Hz, 1H), 3.79-3.69 (m, 1H), 3.65-3.57 (m, 1H), 3.52-3.44 (m, 1H), 1.94-1.88 (m, 1H), 1.83-1.76 (m, 1H), 1.70-1.62 (m, 2H), 1.56-1.42 (m, 2H), 1.41-0.98 (m, 8H), 0.68 (t, *J*=7.3 Hz, 3H). ¹³C NMR (CDCl₃, 100 MHz): δ 175.0, 171.8, 162.1, 140.8, 136.0, 134.3, 129.5, 128.7, 128.3, 127.3, 126.4, 123.4, 110.1, 71.6, 49.2, 48.6, 33.4, 32.4, 25.4, 24.6, 24.5, 19.8, 13.4. HRMS (ESI) calculated for C₂₆H₃₁ClN₃O₃ [MH]⁺ 468.2048, found 468.2069. ATR-FTIR (cm⁻¹): 3192, 2931, 2857, 1718, 1654, 1618, 1470, 1399, 1297, 1189, 1091, 1013, 842, 751.

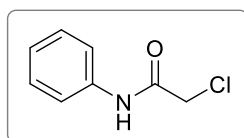
6.2.2. Identification of side products isolated during the synthesis of I.5bfaa

6.2.2.1. Side product (*E*)-3-(Phenylimino)indolin-2-one (I.6a):



Compound obtained as a yellow solid (38% yield). ¹H NMR (CDCl₃, 400 MHz): δ 9.28 (br s, 1H), 7.46-7.42 (m, 2H), 7.31 (td, *J*=7.7, 1.2 Hz, 1H), 7.28-7.24 (m, 1H), 7.05-7.02 (m, 2H), 6.93 (d, *J*=7.8 Hz, 1H), 6.74 (td, *J*=7.7, 0.8 Hz, 1H), 6.65 (d, *J*=7.3 Hz, 1H). ¹³C NMR (CDCl₃, 100 MHz): δ 165.2, 154.6, 150.1, 145.6, 134.4, 129.5, 126.4, 125.5, 122.8, 117.9, 116.2, 111.7. Compound previously described in the literature.³

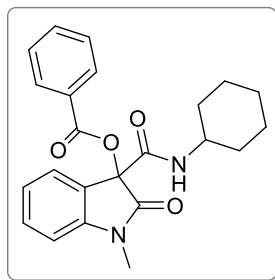
6.2.2.2. Side product 2-Chloro-*N*-phenylacetamide (I.6b):



Compound obtained as a white solid (29% yield). ¹H NMR (CDCl₃, 400 MHz): δ 8.22 (br s, 1H), 7.55 (d, *J*= 8.7, 2H), 7.39-7.35 (m, 2H), 7.20-7.16 (m, 1H), 4.20 (s, 2H). ¹³C NMR (CDCl₃, 100 MHz): δ 163.7, 136.7, 129.2, 125.3, 120.1, 42.9. Compound previously described in the literature.⁴

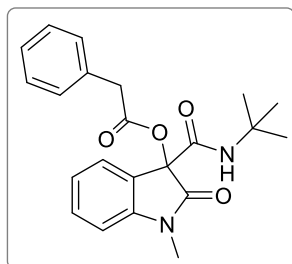
6.2.3. Identification of Passerini adducts

6.2.3.1. Passerini adduct 3-(Cyclohexylcarbamoyl)-1-methyl-2-oxoindolin-3-yl benzoate (I.7a):



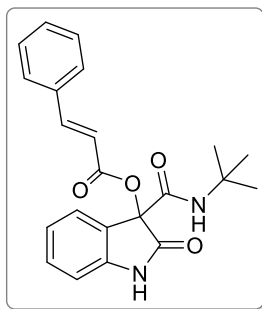
Unexpected synthesis of a Passerini adduct. Compound obtained as a white solid (34% yield). ^1H NMR (CDCl_3 , 400 MHz): δ 7.98 (d, $J=7.1$ Hz, 2H), 7.60 (t, $J=7.5$ Hz, 1H), 7.48–7.44 (m, 2H), 7.40–7.34 (m, 2H), 7.06 (t, $J=7.6$ Hz, 1H), 6.91 (d, $J=7.8$ Hz, 1H), 6.77 (d, $J=7.0$ Hz, 1H), 3.86–3.79 (m, 1H), 3.32 (s, 3H), 2.03–1.19 (m, 10H). ^{13}C NMR (CDCl_3 , 100 MHz): δ 171.4, 163.7, 163.2, 145.1, 133.9, 130.7, 129.9 (2C), 128.7 (2C), 128.6, 125.0, 124.2, 123.2, 108.8, 80.9, 48.9, 32.8, 32.6, 26.9, 25.5, 24.7, 24.6. Compound previously reported in the literature.⁵

6.2.3.2. Passerini adduct 3-(*tert*-Butylcarbamoyl)-1-methyl-2-oxoindolin-3-yl 2-phenylacetate (I.7b):



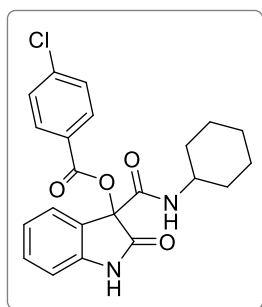
Unexpected synthesis of a Passerini adduct. Compound obtained as a white solid (46% yield). m.p.= 202.9–204.1 °C. ^1H NMR (CDCl_3 , 400 MHz): δ 7.38–7.25 (m, 6H), 7.08–7.00 (m, 2H), 6.84 (d, $J=7.8$ Hz, 1H), 6.28 (br s, 1H), 3.74 (d, $J=16.2$ Hz, 1H), 3.70 (d, $J=16.2$ Hz, 1H), 3.24 (s, 3H), 1.27 (s, 9H). ^{13}C NMR (CDCl_3 , 100 MHz): δ 171.2, 167.9, 163.2, 145.3, 133.1, 130.7, 129.3 (2C), 128.9 (2C), 127.5, 125.2, 123.0 (2C), 108.8, 81.0, 51.9, 41.0, 28.5 (3C), 26.8. HRMS (ESI) calculated for $\text{C}_{22}\text{H}_{35}\text{N}_2\text{O}_4$ $[\text{MH}]^+$ 381.1809, found 381.1811. ATR-FTIR (cm^{-1}): 3383, 2972, 2937, 1760, 1726, 1671, 1607, 1540, 1351, 1218, 1149, 1076, 1021, 1009, 750, 711.

6.2.3.3. Passerini adduct 3-(*tert*-Butylcarbamoyl)-2-oxoindolin-3-yl cinnamate (I.7c):



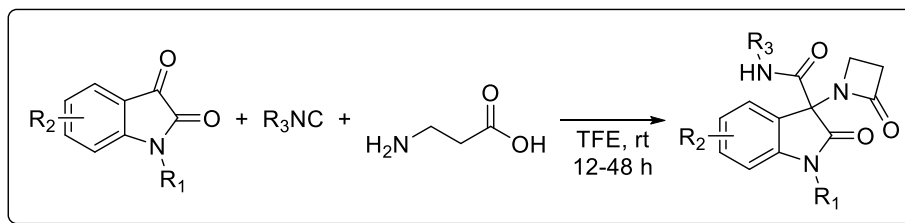
Unexpected synthesis of a Passerini adduct. Compound obtained as a white solid (38% yield). m.p.= 210.2-211.6 °C. ^1H NMR (CDCl_3 , 400 MHz): δ 7.75 (br s, 1H), 7.67 (d, $J=16.0$ Hz, 1H), 7.53-7.50 (m, 2H), 7.42-7.38 (m, 3H), 7.31-7.27 (m, 2H), 7.05 (t, $J=7.6$ Hz, 1H), 6.89 (d, $J=8.4$ Hz, 1H), 6.68 (br s, 1H), 6.51 (d, $J=15.9$ Hz, 1H), 1.42 (s, 9H). ^{13}C NMR (CDCl_3 , 100 MHz): δ 172.7, 164.0, 163.1, 147.8, 142.1, 133.8, 131.0, 130.6, 129.0 (2C), 128.4 (2C), 125.8, 124.0, 123.1, 115.6, 110.5, 81.1, 52.1, 28.6 (3C). HRMS (ESI) calculated for $\text{C}_{22}\text{H}_{23}\text{N}_2\text{O}_4$ $[\text{MH}]^+$ 379.1652, found 379.1648. ATR-FTIR (cm^{-1}): 3376, 3146, 2962, 1726, 1681, 1637, 1520, 1474, 1333, 1310, 1200, 1148, 1116, 973, 854, 767, 746.

6.2.3.4. Passerini adduct 3-(Cyclohexylcarbamoyl)-2-oxindolin-3-yl 4-chlorobenzoate (I.7d):



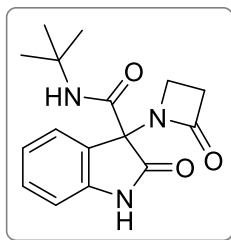
Unexpected synthesis of a Passerini adduct. Compound obtained as a white solid (22% yield). m.p.= 208.1-209.2 °C. ^1H NMR (CDCl_3 , 400 MHz): δ 7.94-7.91 (m, 2H), 7.78 (br s, 1H), 7.46-7.43 (m, 2H), 7.35-7.29 (m, 2H), 7.05 (td, $J=7.6$, 0.7 Hz, 1H), 6.91 (d, $J=7.8$ Hz, 1H), 6.66 (d, $J=7.7$ Hz, 1H), 3.88-3.79 (m, 1H), 2.03-1.93 (m, 2H), 1.77-1.70 (m, 2H), 1.65-1.59 (m, 1H), 1.43-1.21 (m, 5H). ^{13}C NMR (CDCl_3 , 100 MHz): δ 172.3, 163.1, 162.8, 141.9, 140.6, 131.3 (2C), 130.8, 129.1 (2C), 126.9, 125.1, 124.7, 123.3, 110.5, 81.0, 48.9, 32.8, 32.5, 25.4, 24.6, 24.6. HRMS (ESI) calculated for $\text{C}_{22}\text{H}_{22}\text{ClN}_2\text{O}_4$ $[\text{MH}]^+$ 413.1263, found 413.1262. ATR-FTIR (cm^{-1}): 3341, 2928, 2858, 1743, 1731, 1657, 1534, 1470, 1273, 1177, 1089, 1012, 848, 754.

6.2.4. General procedure for the synthesis of β -lactam-oxindole hybrids obtained via Ugi4c3CR (Chapter 3 – Library II)



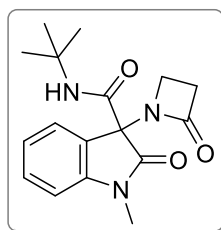
To a stirring solution of isatin derivative (100 mg, 1.0 equiv) and 3-aminopropanoic acid (1.0 equiv) in TFE (1 mL), isocyanide (1.0 equiv) was added. The reaction was allowed to stir at room temperature and the progress monitored by TLC. Upon completion, the solvent was evaporated under reduced pressure and the crude reaction mixture was purified by column chromatography (CC) using the eluent indicated in each case.

6.2.4.1. Synthesis of *N*-(*tert*-Butyl)-2-oxo-3-(2-oxoazetididin-1-yl)indoline-3-carboxamide (II.4aaa):



Prepared using isatin, 3-aminopropanoic acid and *tert*-butyl isocyanide. CC: Hexane:EtOAc 2:1. The corresponding **II.4aaa** was obtained as a beige solid (165.2 mg, 81% yield). m.p.= 173.0-174.2 °C. ¹H NMR (CDCl₃, 400 MHz): δ 8.61 (br s, 1H), 7.66 (d, *J*=8 Hz, 1H), 7.35 (br s, 1H), 7.26 (t, *J*=8 Hz, 1H), 7.09 (t, *J*=8 Hz, 1H), 6.83 (d, *J*=8 Hz, 1H), 3.62-3.59 (m, 1H), 3.42-3.38 (m, 1H), 2.96-2.92 (m, 2H), 1.37 (s, 9H). ¹³C NMR (CDCl₃, 100 MHz): δ 172.6, 167.3, 162.1, 140.7, 130.1, 126.6, 126.0, 123.4, 110.8, 68.2, 52.3, 39.5, 35.9, 28.5. Compound previously described in the literature.⁶

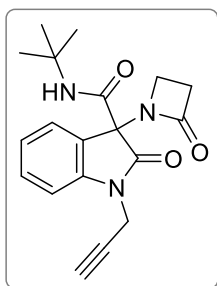
6.2.4.2. Synthesis of *N*-(*tert*-Butyl)-1-methyl-2-oxo-3-(2-oxoazetididin-1-yl)indoline-3-carboxamide (II.4baa):



Prepared using *N*-methylisatin, 3-aminopropanoic acid and *tert*-butyl isocyanide. CC: Hexane:EtOAc 2:1. The corresponding **II.4baa** was obtained as a white solid (128.7

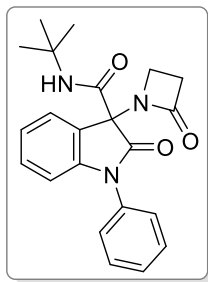
mg, 66% yield). m.p.= 117.8-119.0 °C. ¹H NMR (CDCl₃, 400 MHz): δ 7.72 (d, *J*=8, 1H), 7.39-7.35 (m, 2H), 7.14 (td, *J*= 8, 4 Hz, 1H), 6.87 (d, *J*=8 Hz, 1H), 3.54-3.51 (m, 1H), 3.35-3.31 (m, 1H), 3.27 (s, 3H), 2.90 (t, *J*=4 Hz, 2H), 1.37 (s, 9H). ¹³C NMR (CDCl₃, 100 MHz): δ 171.4, 166.9, 162.1, 143.3, 130.1, 126.7, 125.4, 123.7, 108.8, 68.0. 52.2, 39.2, 36.0, 28.5 (3C), 26.8. Compound previously described in the literature.⁶

6.2.4.3. Synthesis of *N*-(*tert*-Butyl)-2-oxo-3-(2-oxoazetidin-1-yl)-1-(prop-2-yn-1-yl)indoline-3-carboxamide (II.4caa):



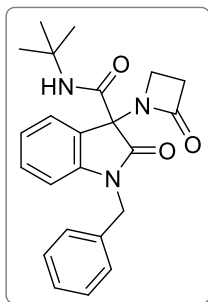
N-propargylisatin was synthesized as described in the literature.² Briefly, to a solution of isatin (1.0 g, 1 equiv) in DMF kept at 0 °C, sodium hydride (1.5 equiv) was slowly added and allowed to stir until the gas production ceased. Then, propargyl bromide (1.4 equiv) was added dropwise and the mixture was allowed to proceed with stirring at room temperature overnight. The DMF was then removed under reduced pressure. Water was added and the aqueous mixture extracted with ethyl acetate (3 x 30 mL), and the combined organic layers were washed with brine, dried with anhydrous Na₂SO₄ and evaporated to afford the desired product, which was used in the next step without further purification. The lactam-oxindole hybrid **II.4caa** was prepared using *N*-propargylisatin, 3-aminopropanoic acid and *tert*-butyl isocyanide. CC: Hexane:EtOAc 2:1. The corresponding **II.4caa** was obtained as a beige solid (124.0 mg, 68% yield). m.p.= 130.5-131.9 °C. ¹H NMR (CDCl₃, 400 MHz): δ 7.73 (d, *J*=8 Hz, 1H), 7.39 (t, *J*=8 Hz, 1H), 7.25 (br s, 1H), 7.17 (t, *J*=8 Hz, 1H), 7.09 (d, *J*=8, 1H), 4.54 (d, *J*=4 Hz, 2H), 3.54-3.51 (m, 1H), 3.33-3.29 (m, 1H), 2.91 (t, *J*=4 Hz, 2H), 2.27 (t, *J*=4 Hz, 1H), 1.37 (s, 9H). ¹³C NMR (CDCl₃, 100 MHz): δ 170.4, 167.2, 162.0, 141.5, 130.2, 126.7, 125.4, 124.0, 109.8, 76.1, 72.9, 68.3, 52.3, 39.1, 36.0, 29.9, 28.5 (3C). HRMS (ESI) calculated for C₁₉H₂₂N₃O₃ [MH]⁺ 340.1656, found 340.1653; and calculated for C₁₉H₂₁N₃NaO₃ [MNa]⁺ 362.1475, found 362.1462.

6.2.4.4. Synthesis of *N*-(*tert*-Butyl)-2-oxo-3-(2-oxoazetidin-1-yl)-1-phenylindoline-3-carboxamide (II.4daa):



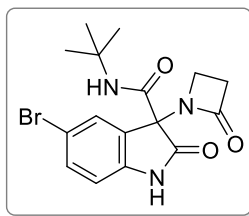
Prepared using *N*-phenylisatin, 3-aminopropanoic acid and *tert*-butyl isocyanide. CC: Hexane:EtOAc 2.5:1. The corresponding **II.4daa** was obtained as a white solid (102.8 mg, 61% yield). m.p.= 180.2-181.5 °C. ¹H NMR (CDCl₃, 400 MHz): δ 7.79 (d, *J*=8 Hz, 1H), 7.57-7.53 (m, 2H), 7.49-7.43 (m, 4H), 7.28 (td, *J*=8, 4 Hz, 1H), 7.17 (t, *J*=8 Hz, 1H), 6.81 (d, *J*=8 Hz, 1H), 3.64-3.60 (m, 1H), 3.45-3.41 (m, 1H), 3.00-2.90 (m, 2H), 1.39 (s, 9H). ¹³C NMR (CDCl₃, 100 MHz): δ 171.0, 166.8, 161.8, 143.5, 133.7, 130.0, 129.8 (2C), 128.7, 127.0, 126.7 (2C), 125.3, 124.0, 110.0, 67.7, 52.3, 39.2, 36.1, 28.5 (3C). HRMS (ESI) calculated for C₂₂H₂₃N₃NaO₃ [MNa]⁺ 400.1632, found 400.1624.

6.2.4.5. Synthesis of 1-Benzyl-*N*-(*tert*-butyl)-2-oxo-3-(2-oxoazetidino-1-yl)indoline-3-carboxamide (**II.4eaa**):



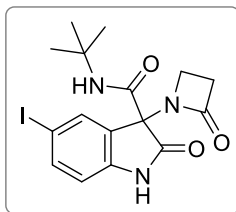
Prepared using *N*-benzylisatin, 3-aminopropanoic acid and *tert*-butyl isocyanide. CC: Hexane:EtOAc 1.5:1. The corresponding **II.4eaa** was obtained as a white solid (125.7 mg, 76% yield). m.p.= 119.2-120.3 °C. ¹H NMR (CDCl₃, 400 MHz): δ 7.70 (d, *J*=8 Hz, 1H), 7.35-7.21 (m, 7H), 7.10 (t, *J*=8 Hz, 1H), 6.71 (d, *J*=8 Hz, 1H), 5.03 (d, *J*=16 Hz, 1H), 4.89 (d, *J*=16 Hz, 1H), 3.60-3.57 (m, 1H), 3.38-3.34 (m, 1H), 2.94 (t, *J*=4, 2H), 1.38 (s, 9H). ¹³C NMR (CDCl₃, 100 MHz): δ 171.6, 167.0, 162.0, 142.3, 134.9, 130.0, 128.9 (2C), 127.8, 127.2 (2C), 126.7, 125.6, 123.7, 109.9, 68.2, 52.2, 44.3, 39.3, 36.1, 28.5 (3C). Compound previously described in the literature.⁶

6.2.4.6. Synthesis of 5-Bromo-*N*-(*tert*-butyl)-2-oxo-3-(2-oxoazetidino-1-yl)indoline-3-carboxamide (**II.4faa**):



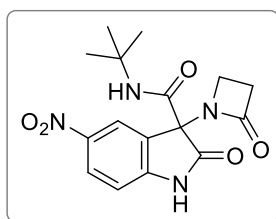
Prepared using 5-bromoisatin, 3-aminopropanoic acid and *tert*-butyl isocyanide. CC: Hexane:EtOAc 2:1. The corresponding **II.4faa** was obtained as a white solid (68.9 mg, 41% yield). m.p.= 197.6-198.1 °C. ¹H NMR (CDCl₃, 400 MHz): δ 8.85 (br s, 1H), 7.78 (d, *J*=2.0 Hz, 1H), 7.38 (m, 2H), 6.69 (d, *J*=8.3 Hz, 1H), 3.62 (m, 1H), 3.43 (m, 1H), 2.97 (m, 2H), 1.37 (s, 9H). ¹³C NMR (CDCl₃, 100 MHz): δ 172.2, 167.2, 161.0, 139.8, 133.0, 129.6, 127.8, 116.1, 112.4, 67.6, 52.4, 39.6, 35.9, 28.4 (3C). HRMS (ESI) calculated for C₁₆H₁₉BrN₃O₃ [MH]⁺ 380.0604, found 360.0605.

6.2.4.7. Synthesis of *N*-(*tert*-Butyl)-5-iodo-2-oxo-3-(2-oxoazetidin-1-yl)indoline-3-carboxamide (**II.4gaa**):



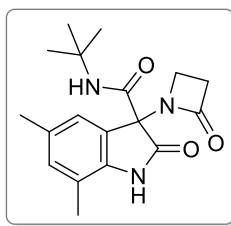
Prepared using 5-iodoisatin, 3-aminopropanoic acid and *tert*-butyl isocyanide. CC: Hexane:EtOAc 2:1. The corresponding **II.4gaa** was obtained as a white solid (75.5 mg, 48% yield). m.p.= 204.0-205.3 °C. ¹H NMR (CDCl₃, 400 MHz): δ 8.58 (br s, 1H), 7.94 (d, *J*=1.7 Hz, 1H), 7.58 (dd, *J*=8.2 Hz, 1.8, 1H), 7.35 (br s, 1H), 6.60 (d, *J*=8.2 Hz, 1H), 3.62-3.59 (m, 1H), 3.43-3.40 (m, 1H), 3.03-2.91 (m, 2H), 1.37 (s, 9H). ¹³C NMR (CDCl₃, 100 MHz): δ 172.0, 167.0, 161.0, 140.3, 139.0, 135.2, 128.0, 112.8, 86.1, 67.4, 52.4, 39.6, 36.0, 28.4 (3C). HRMS (ESI) calculated for C₁₆H₁₉IN₃O₃ [MH]⁺ 428.0466, found 428.0463; and calculated for C₁₆H₁₉IN₃NaO₃ [MNa]⁺ 450.0285, found 450.0283.

6.2.4.8. Synthesis of *N*-(*tert*-Butyl)-5-nitro-2-oxo-3-(2-oxoazetidin-1-yl)indoline-3-carboxamide (**II.4haa**):



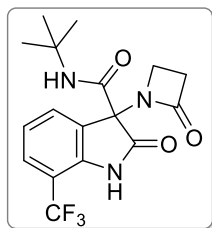
Prepared using 5-nitroisatin, 3-aminopropanoic acid and *tert*-butyl isocyanide. CC: Hexane:EtOAc 2:1. The corresponding **II.4haa** was obtained as a white solid (52.0 mg, 29% yield). m.p.= 199.2-200.7 °C. ¹H NMR ((CD₃)₂CO, 400 MHz): δ 8.50 (d, *J*=2.4 Hz, 1H), 8.29 (dd, *J*=8.7, 2.4 Hz, 1H), 7.37 (br s, 1H), 7.20 (d, *J*=8.7, 1H), 3.64-3.60 (m, 1H), 3.56-3.52 (m, 1H), 2.95-2.92 (m, 2H), 1.38 (s, 9H). ¹³C NMR ((CD₃)₂CO, 100 MHz): δ 175.1, 169.3, 164.0, 150.6, 145.6, 129.9, 1247, 124.5, 112.7, 70.7, 54.2, 41.3, 38.3, 30.1 (3C). HRMS (ESI) calculated for C₁₆H₁₉N₄O₅ [MH]⁺ 347.1350, found 347.1343; and calculated for C₁₆H₁₈N₄NaO₅ [MNa]⁺ 369.1169, found 369.1159.

6.2.4.9. Synthesis of *N*-(*tert*-Butyl)-5,7-dimethyl-2-oxo-3-(2-oxoazetidin-1-yl)indoline-3-carboxamide (II.4iaa):



Prepared using 5,7-dimethylisatin, 3-aminopropanoic acid and *tert*-butyl isocyanide. CC: Hexane:EtOAc 1:1. The corresponding **II.4iaa** was obtained as a white solid (161.7 mg, 86% yield). m.p.= 179.8-181.1 °C. ¹H NMR (CDCl₃, 400 MHz): δ 8.37 (br s, 1H), 7.38 (br s, 1H), 7.30 (s, 1H), 6.90 (s, 1H), 3.57-3.56 (m, 1H), 3.37-3.35 (m, 1H), 2.94-2.92 (m, 2H), 2.31 (s, 3H), 2.12 (s, 3H), 1.37 (s, 9H). ¹³C NMR (CDCl₃, 100 MHz): δ 173.0, 167.1, 162.1, 136.7, 133.0, 132.1, 125.8, 1247, 119.4, 68.8, 52.2, 39.3, 35.9, 28.5, 21.1, 16.2. HRMS (ESI) calculated for C₁₈H₂₃N₃NaO₃ [MNa]⁺ 352.1632, found 352.1624.

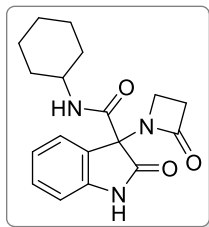
6.2.4.10. Synthesis of *N*-(*tert*-Butyl)-2-oxo-3-(2-oxoazetidin-1-yl)-7-(trifluoromethyl)indoline-3-carboxamide (II.4jaa):



Prepared using 7-trifluoromethylisatin, 3-aminopropanoic acid and *tert*-butyl isocyanide. CC: Hexane:EtOAc 2:1. The corresponding **II.4jaa** was obtained as a white solid (80.4 mg, 47% yield). m.p.= 106.0-107.3 °C. ¹H NMR (CDCl₃, 400 MHz): δ 8.13 (br s, 1H), 7.88 (d, *J*=8 Hz, 1H), 7.52 (d, *J*=8 Hz, 1H), 7.23 (t, *J*=8 Hz, 1H), 7.18 (br s, 1H),

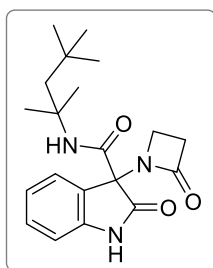
3.57-3.54 (m, 1H), 3.40-3.38 (m, 1H), 2.96 (t, $J=4$ Hz, 2H), 1.38 (s, 9H). ^{13}C NMR (CDCl_3 , 100 MHz): δ 172.4, 166.9, 160.8, 137.6, 130.8, 127.3, 127.0, 126.9, 123.5, 113.0, 112.6, 67.1, 52.5, 39.4, 36.2, 28.4 (3C). HRMS (ESI) calculated for $\text{C}_{17}\text{H}_{18}\text{F}_3\text{N}_3\text{NaO}_3$ $[\text{MNa}]^+$ 392.1192, found 392.1183.

6.2.4.11. Synthesis of *N*-Cyclohexyl-2-oxo-3-(2-oxoazetidin-1-yl)indoline-3-carboxamide (II.4aba):



Prepared using isatin, 3-aminopropanoic acid and cyclohexyl isocyanide. CC: Hexane:EtOAc 2:1. The corresponding **II.4aba** was obtained as a pale yellow solid (152.7 mg, 69% yield). m.p.= 187.8-189.1 °C. ^1H NMR (CDCl_3 , 400 MHz): δ 8.65 (br s, 1H), 7.66 (d, $J=8$ Hz, 1H), 7.35 (d, $J=4$ Hz, 1H), 7.26 (t, $J=8$ Hz, 1H), 7.09 (t, $J=8$ Hz, 1H), 6.83 (d, $J=8$ Hz, 1H), 3.79-3.74 (m, 1H), 3.62-3.58 (m, 1H), 3.40-3.36 (m, 1H), 2.94-2.92 (m, 1H), 1.96-1.16 (m, 10H). ^{13}C NMR (CDCl_3 , 100 MHz): δ 172.4, 167.5, 162.6, 140.8, 130.2, 126.5, 126.0, 123.4, 110.8, 68.1, 49.1, 39.5, 35.9, 32.6, 32.4, 25.4, 24.6. HRMS (ESI) calculated for $\text{C}_{18}\text{H}_{21}\text{N}_3\text{NaO}_3$ $[\text{MNa}]^+$ 350.1475, found 350.1467.

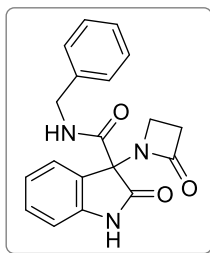
6.2.4.12. Synthesis of 2-Oxo-3-(2-oxoazetidin-1-yl)-*N*-(2,4,4-trimethylpentan-2-yl)indoline-3-carboxamide (II.4aca):



Prepared using isatin, 3-aminopropanoic acid and *tert*-octyl isocyanide. CC: Hexane:EtOAc 1.5:1. The corresponding **II.4aca** was obtained as a white solid (170.7 mg, 70% yield). m.p.= 139.8-140.7 °C. ^1H NMR (CDCl_3 , 400 MHz): δ 8.51 (br s, 1H), 7.67 (d, $J=8$ Hz, 1H), 7.26 (td, $J=8$, 4 Hz, 1H), 7.15 (br s, 1H), 7.09 (td, $J=7.6$, 0.9 Hz, 1H), 6.82 (d, $J=8$ Hz, 1H), 3.65-3.61 (m, 1H), 3.44-3.40 (m, 1H), 2.95-2.92 (m, 2H), 1.83 (d, $J=15$ Hz, 1H), 1.56 (d, $J=15$ Hz, 1H), 1.44 (s, 3H), 1.43 (s, 3H), 0.94 (9H). ^{13}C NMR (CDCl_3 , 100 MHz): δ 172.4, 167.3, 161.8, 140.7, 130.1, 126.7, 126.0, 123.4, 110.7, 68.5,

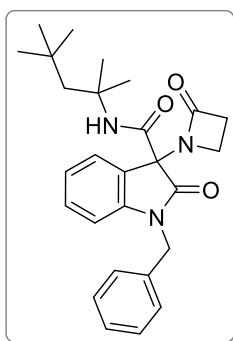
56.3, 52.1, 39.6, 36.0, 31.6, 31.3 (3C), 28.6, 28.5. HRMS (ESI) calculated for $C_{20}H_{27}N_3NaO_3$ [MNa]⁺ 380.1945, found 380.1935.

6.2.4.13. Synthesis of *N*-Benzyl-2-oxo-3-(2-oxoazetid-1-yl)indoline-3-carboxamide (II.4ada):



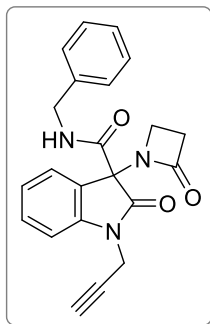
Prepared using isatin, 3-aminopropanoic acid and benzyl isocyanide. CC: Hexane:EtOAc 1.5:1. The corresponding **II.4ada** was obtained as a white solid (131.2 mg, 58% yield). m.p.= 172.2-173.0 °C. ¹H NMR (CDCl₃, 400 MHz): δ 8.32 (br s, 1H), 7.69-7.66 (m, 2H), 7.34-7.26 (m, 6H), 7.10 (t, *J*=8 Hz, 1H), 6.84 (d, *J*=8 Hz, 1H), 4.56-4.39 (m, 2H), 3.58-3.54 (m, 1H), 3.34-3.30 (m, 1H), 2.92 (t, *J*=4 Hz, 2H). ¹³C NMR (CDCl₃, 100 MHz): δ 172.0, 167.6, 163.7, 140.6, 137.3, 130.4, 128.8 (2C), 127.8 (2C), 127.7, 126.7, 125.8, 123.6, 110.8, 68.2, 44.2, 39.5, 36.1. HRMS (ESI) calculated for $C_{19}H_{17}N_3NaO_3$ [MNa]⁺ 358.1162, found 358.1153.

6.2.4.14. Synthesis of 1-Benzyl-2-oxo-3-(2-oxoazetid-1-yl)-*N*-(2,4,4-trimethylpentan-2-yl)indoline-3-carboxamide (II.4eca):



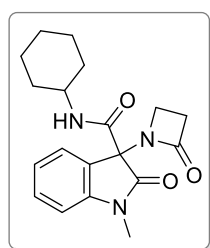
Prepared using *N*-benzylisatin, 3-aminopropanoic acid and *tert*-octyl isocyanide. CC: Hexane:EtOAc 1.5:1. The corresponding **II.4eca** was obtained as a white solid (80.6 mg, 43% yield). m.p.= 113.1-113.9 °C. ¹H NMR (CDCl₃, 400 MHz): δ 7.73 (d, *J*=8 Hz, 1H), 7.35-7.21 (m, 6H), 7.12-7.08 (m, 2H), 6.73 (d, *J*=8 Hz, 1H), 4.98 (d, *J*=16, 1H), 4.92 (d, *J*=16, 1H), 3.63-3.60 (m, 1H), 3.39-3.36 (m, 1H), 2.93 (t, *J*=4 Hz, 2H), 1.83 (d, *J*=16 Hz, 1H), 1.53 (d, *J*=16 Hz, 1H), 1.44 (s, 3H), 1.43 (s, 3H), 0.92 (s, 9H). Compound previously described in the literature.⁶

6.2.4.15. Synthesis of *N*-Benzyl-2-oxo-3-(2-oxoazetid-1-yl)-1-(prop-2-yn-1-yl)indoline-3-carboxamide (II.4cda):



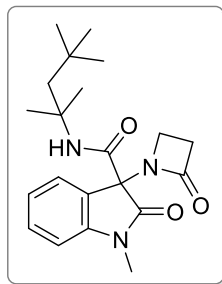
Prepared using *N*-propargylisatin, 3-aminopropanoic acid and benzyl isocyanide. CC: Hexane:EtOAc 2:1. The corresponding **II.4cda** was obtained as a beige solid (82.7 mg, 41% yield). m.p.= 167.3-168.1 °C. ¹H NMR (CDCl₃, 400 MHz): δ 7.76 (d, *J*=8 Hz, 1H), 7.58 (br s, 1H), 7.40 (td, *J*=8, 4 Hz, 1H), 7.35-7.26 (m, 5H), 7.18 (td, *J*=7.6, 0.8 Hz, 1H), 7.08 (d, *J*=8 Hz, 1H), 4.58-4.39 (m, 4H), 3.53-3.49 (m, 1H), 3.27-3.24 (m, 1H), 2.93-2.90 (m, 2H), 2.25 (t, *J*=2.5, 1H). ¹³C NMR (CDCl₃, 100 MHz): δ 170.0, 167.5, 163.6, 141.6, 137.3, 130.4, 128.8 (2C), 127.8 (2C), 127.6, 126.8, 125.1, 124.1, 109.9, 76.0, 73.0, 68.1, 44.2, 39.2, 36.2, 29.9. HRMS (ESI) calculated for C₂₂H₁₉N₃NaO₃ [MNa]⁺ 396.1319, found 396.1311.

6.2.4.16. Synthesis of *N*-Cyclohexyl-1-methyl-2-oxo-3-(2-oxoazetid-1-yl)indoline-3-carboxamide (II.4bba):



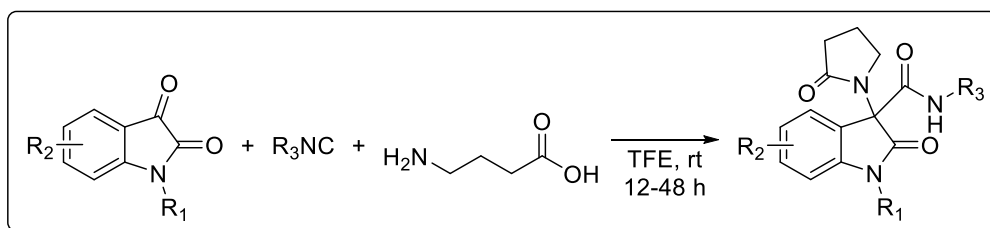
Prepared using *N*-methylisatin, 3-aminopropanoic acid and cyclohexyl isocyanide. CC: Hexane:EtOAc 1.5:1. The corresponding **II.4bba** was obtained as a white solid (141.6 mg, 67% yield). m.p.= 158.2-159.1 °C. ¹H NMR (CDCl₃, 400 MHz): δ 7.73 (d, *J*=8 Hz, 1H), 7.39-7.27 (m, 2H), 7.14 (td, *J*=7.6, 0.9 Hz, 1H), 6.86 (d, *J*=8 Hz, 1H), 3.79-3.73 (m, 1H), 3.54-3.49 (m, 1H), 3.34-3.30 (m, 1H), 3.26 (s, 3H), 2.90 (t, *J*=4.3, 2H), 1.97-1.94 (m, 1H), 1.85-1.81 (m, 1H), 1.74-1.66 (m, 2H), 1.61-1.56 (m, 1H), 1.39-1.19 (m, 5H). ¹³C NMR (CDCl₃, 100 MHz): δ 171.2, 167.1, 162.4, 143.3, 130.2, 126.7, 125.3, 123.7, 108.8, 67.7, 49.1, 39.2, 16.0, 32.6, 32.4, 26.8, 25.4, 24.6. HRMS (ESI) calculated for C₁₉H₂₃N₃NaO₃ [MNa]⁺ 364.1632, found 364.1622.

6.2.4.17. Synthesis of 1-Methyl-2-oxo-3-(2-oxoazetid-1-yl)-*N*-(2,4,4-trimethylpentan-2-yl)indoline-3-carboxamide (II.4bca):



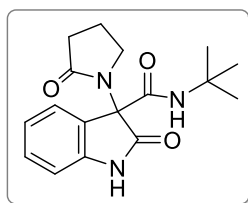
Prepared using *N*-methylisatin, 3-aminopropanoic acid and *tert*-octyl isocyanide. CC: Hexane:EtOAc 1.5:1. The corresponding **II.4bca** was obtained as a white solid (114.2 mg, 50% yield). m.p.= 107.2-108.5 °C. ¹H NMR (CDCl₃, 400 MHz): δ 7.73 (d, *J*=8 Hz, 1H), 7.36 (td, *J*=7.7, 1.2 Hz, 1H), 7.16-7.12 (m, 2H), 6.86 (d, *J*=8 Hz, 1H), 3.58-3.55 (m, 1H), 3.36-3.32 (m, 1H), 3.25 (s, 3H), 2.90 (t, *J*=4.3 Hz, 2H), 1.80 (d, *J*=15 Hz, 1H), 1.55 (d, *J*=15 Hz, 1H), 1.44 (s, 3H), 1.43 (s, 3H), 0.95 (s, 9H). ¹³C NMR (CDCl₃, 100 MHz): δ 171.2, 167.0, 161.8, 143.2, 130.1, 126.8, 125.5, 123.6, 108.7, 68.4, 56.2, 52.2, 39.3, 36.0, 31.6, 31.3 (3C), 28.6, 28.4, 26.7. HRMS (ESI) calculated for C₂₁H₂₉N₃NaO₃ [MNa]⁺ 394.2101, found 394.2092.

6.2.5. General procedure for the synthesis of γ -lactam-oxindole hybrids obtained via Ugi4c3CR (Chapter 3 – Library II)



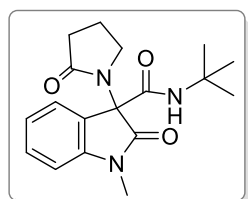
To a stirring solution of isatin derivative (100 mg, 1.0 equiv) and 4-aminobutanoic acid (1.0 equiv) in TFE (1 mL), isocyanide (1.0 equiv) was added. The reaction was allowed to stir at room temperature and the progress monitored by TLC. Upon completion, or when no change was detected, the magnetic stir bar was removed, and the solvent evaporated under reduced pressure. The crude reaction mixture was purified by column chromatography (CC).

6.2.5.1. Synthesis of *N*-(*tert*-Butyl)-2-oxo-3-(2-oxopyrrolidin-1-yl)indoline-3-carboxamide (**II.5aab**):

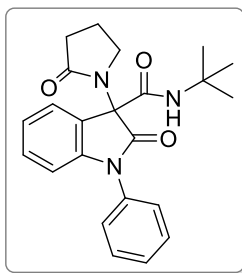


Prepared using isatin, 4-aminobutanoic acid and *tert*-butyl isocyanide. CC: Hexane:EtOAc 2:1. The corresponding **II.5aab** was obtained as a pale yellow solid (71.6 mg, 33% yield). m.p.= 235.0 °C (decomp.). ¹H NMR (CDCl₃, 400 MHz): δ 8.51 (br s, 1H), 7.50 (d, *J*=7.0 Hz, 1H), 7.34 (br s, 1H), 7.22 (td, *J*=7.7, 1.0 Hz, 1H), 7.06 (td, *J*=7.6, 0.7 Hz, 1H), 6.77 (d, *J*=7.8 Hz, 1H), 3.87-3.81 (m, 1H), 3.70-3.64 (m, 1H), 2.48-2.40 (m, 1H), 2.34-2.26 (m, 1H), 2.19-2.12 (m, 2H), 1.35 (s, 9H). ¹³C NMR (CDCl₃, 100 MHz): δ 175.1, 174.8, 161.6, 141.2, 129.6, 126.4, 126.2, 123.1, 110.5, 67.7, 52.1, 46.7, 30.7, 28.4 (3C), 18.8. HRMS (ESI) calculated for C₁₇H₂₂N₃O₃ [MH]⁺ 316.1656, found 316.1659; and calculated for C₁₇H₂₁N₃NaO₃ [MNa]⁺ 338.1475, found 338.1477.

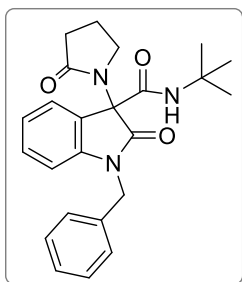
6.2.5.2. Synthesis of *N*-(*tert*-Butyl)-1-methyl-2-oxo-3-(2-oxopyrrolidin-1-yl)indoline-3-carboxamide (**II.5bab**):



Prepared using *N*-methylisatin, 4-aminobutanoic acid and *tert*-butyl isocyanide. CC: Hexane:EtOAc 2:1. The corresponding **II.5bab** was obtained as a white solid (52.9 mg, 26% yield). m.p.= 179.2-180.1 °C. ¹H NMR (CDCl₃, 400 MHz): δ 7.55 (d, *J*=7.4 Hz, 1H), 7.35-7.31 (m, 2H), 7.11 (t, *J*=7.5 Hz, 1H), 6.85 (d, *J*=7.8 Hz, 1H), 3.81-3.75 (m, 1H), 3.65-3.59 (m, 1H), 3.28 (s, 3H), 2.41-2.33 (m, 1H), 2.28-2.19 (m, 1H), 2.17-2.07 (m, 2H), 1.37 (s, 9H). ¹³C NMR (CDCl₃, 100 MHz): δ 174.9, 173.5, 161.9, 143.9, 129.7, 126.3, 125.8, 123.3, 108.4, 67.4, 52.1, 46.4, 30.4, 28.4 (3C), 27.0, 18.8. HRMS (ESI) calculated for C₁₈H₂₃N₃NaO₃ [MNa]⁺ 352.1632, found 352.1622.

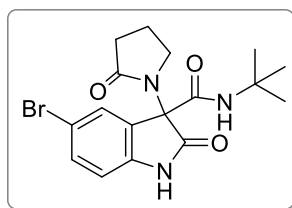
6.2.5.3. Synthesis of *N*-(*tert*-Butyl)-2-oxo-3-(2-oxopyrrolidin-1-yl)-1-phenylindoline-3-carboxamide (II.5dab):

Prepared using *N*-phenylisatin, 4-aminobutanoic acid and *tert*-butyl isocyanide. CC: Hexane:EtOAc 2:1. The corresponding **II.5dab** was obtained as a beige solid (52.3 mg, 30% yield). m.p.= 185.7-186.3 °C. ¹H NMR (CDCl₃, 400 MHz): δ 7.61 (dd, *J*=7.4, 0.9 Hz, 1H), 7.56-7.41 (m, 6H), 7.24 (td, *J*=7.8, 1.3 Hz, 1H), 7.13 (td, *J*=7.6, 1.0 Hz, 1H), 6.75 (d, *J*=7.8 Hz, 1H), 3.89-3.83 (m, 1H), 3.75-3.69 (m, 1H), 2.44-2.40 (m, 1H), 2.32-2.16 (m, 3H), 1.38 (s, 9H). ¹³C NMR (CDCl₃, 100 MHz): δ 175.0, 173.2, 161.7, 144.3, 134.4, 129.7 (2C), 129.6, 128.5, 126.9 (2C), 126.6, 125.3, 123.6, 109.6, 67.3, 52.2, 46.4, 30.4, 28.4 (3C), 19.0. HRMS (ESI) calculated for C₂₃H₂₅N₃NaO₃ [MNa]⁺ 414.1788, found 414.1779.

6.2.5.4. Synthesis of 1-Benzyl-*N*-(*tert*-butyl)-2-oxo-3-(2-oxopyrrolidin-1-yl)indoline-3-carboxamide (II.5eab):

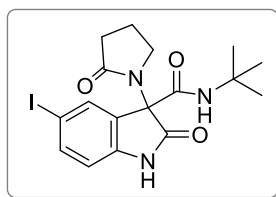
Prepared using *N*-benzylisatin, 4-aminobutanoic acid and *tert*-butyl isocyanide. CC: Hexane:EtOAc 1.5:1. The corresponding **II.5eab** was obtained as a white solid (81.4 mg, 48% yield). m.p.= 201.1-202.3 °C. ¹H NMR (CDCl₃, 400 MHz): δ 7.54 (dd, *J*=7.4, 0.8 Hz, 1H), 7.37-7.23 (m, 6H), 7.18 (td, *J*=7.8, 1.2 Hz, 1H), 7.06 (td, *J*=7.6, 0.8 Hz, 1H), 6.66 (d, *J*=7.8 Hz, 1H), 4.98 (s, 2H), 3.85-3.79 (m, 1H), 3.68-3.62 (m, 1H), 2.47-2.39 (m, 1H), 2.34-2.25 (m, 1H), 2.19-2.10 (m, 2H), 1.37 (s, 9H). ¹³C NMR (CDCl₃, 100 MHz): δ 174.9, 173.6, 161.8, 142.7, 135.3, 129.5, 128.8 (2C), 127.6, 127.1 (2C), 126.3, 125.9, 123.4, 109.5, 67.9, 52.1, 46.6, 44.5, 30.5, 28.4 (3C), 18.9. HRMS (ESI) calculated for C₂₄H₂₇N₃NaO₃ [MNa]⁺ 428.1945, found 428.1936.

6.2.5.5. Synthesis of 5-Bromo-*N*-(*tert*-butyl)-2-oxo-3-(2-oxopyrrolidin-1-yl)indoline-3-carboxamide (**II.5fab**):



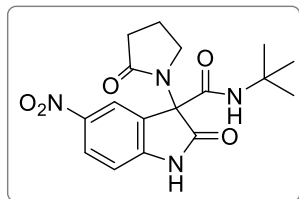
Prepared using 5-bromoisatin, 4-aminobutanoic acid and *tert*-butyl isocyanide. CC: Hexane:EtOAc 1.5:1. The corresponding **II.5fab** was obtained as a beige solid (38.0 mg, 22% yield). m.p.= 240.1-241.3 °C. ^1H NMR (CDCl_3 , 400 MHz): δ 8.40 (br s, 1H), 7.62 (d, $J=1.8$ Hz, 1H), 7.35 (dd, $J=8.3$, 2.0 Hz, 1H), 7.33 (br s, 1H), 6.67 (d, $J=8.3$ Hz, 1H), 3.84-3.78 (m, 1H), 3.70-3.64 (m, 1H), 2.49-2.41 (m, 1H), 2.37-2.28 (m, 1H), 2.21-2.14 (m, 2H), 1.36 (s, 9H). ^{13}C NMR (CDCl_3 , 100 MHz): δ 175.2, 174.5, 160.9, 140.2, 132.4, 129.6, 128.0, 115.8, 111.8, 67.5, 52.3, 46.6, 30.5, 28.4 (3C), 18.8. HRMS (ESI) calculated for $\text{C}_{17}\text{H}_{21}\text{N}_3\text{O}_3\text{Br}$ $[\text{MH}]^+$ 394.0761, found 394.0756; and calculated for $\text{C}_{17}\text{H}_{20}\text{BrN}_3\text{NaO}_3$ $[\text{MNa}]^+$ 416.0580, found 416.0573.

6.2.5.6. Synthesis of *N*-(*tert*-Butyl)-5-iodo-2-oxo-3-(2-oxopyrrolidin-1-yl)indoline-3-carboxamide (**II.5gab**):



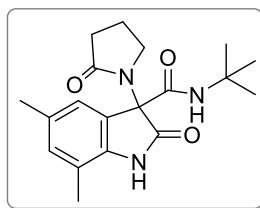
Prepared using 5-iodoisatin, 4-aminobutanoic acid and *tert*-butyl isocyanide. CC: Hexane:EtOAc 1.5:1. The corresponding **II.5gab** was obtained as a white solid (34.8 mg, 22% yield). m.p.= 239.5-241.0 °C. ^1H NMR (CDCl_3 , 400 MHz): δ 8.19 (br s, 1H), 7.78 (d, $J=1.6$ Hz, 1H), 7.55 (dd, $J=8.2$, 1.8 Hz, 1H), 7.31 (br s, 1H), 6.58 (d, $J=8.2$ Hz, 1H), 3.83-3.77 (m, 1H), 3.68-3.63 (m, 1H), 2.48-2.40 (m, 1H), 2.36-2.28 (m, 1H), 2.21-2.13 (m, 2H), 1.36 (s, 9H). ^{13}C NMR (CDCl_3 , 100 MHz): δ 175.2, 174.3, 160.9, 140.8, 138.4, 135.2, 128.2, 112.3, 85.8, 67.4, 52.3, 46.6, 30.5, 28.4 (3C), 18.8. HRMS (ESI) calculated for $\text{C}_{17}\text{H}_{20}\text{IN}_3\text{NaO}_3$ $[\text{MNa}]^+$ 464.0442, found 464.0436.

6.2.5.7. Synthesis of *N*-(*tert*-Butyl)-5-nitro-2-oxo-3-(2-oxopyrrolidin-1-yl)indoline-3-carboxamide (**II.5hab**):



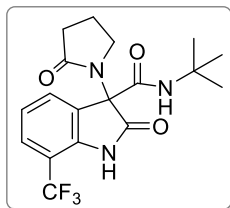
Prepared using 5-nitroisatin, 4-aminobutanoic acid and *tert*-butyl isocyanide. CC: Hexane:EtOAc 2:1. The corresponding **II.5hab** was obtained as a beige solid (101.0 mg, 54% yield). m.p.= 218.5 (decomp.). ^1H NMR (CDCl_3 , 400 MHz): δ 9.00 (br s, 1H), 8.38 (d, $J=2.2$ Hz, 1H), 8.22-8.19 (m, 1H), 7.26-7.23 (m, 1H), 6.86 (dd, $J=8.6, 3.1$ Hz, 1H), 3.95-3.89 (m, 1H), 3.78-3.73 (m, 1H), 2.54-2.45 (m, 1H), 2.40-2.32 (m, 1H), 2.28-2.23 (m, 2H), 1.36 (s, 9H). ^{13}C NMR (CDCl_3 , 100 MHz): δ 175.7, 175.1, 160.0, 146.9, 143.9, 126.9, 126.4, 122.6, 110.3, 67.2, 52.6, 46.8, 30.4, 28.3 (3C), 18.8. HRMS (ESI) calculated for $\text{C}_{17}\text{H}_{20}\text{N}_4\text{NaO}_5$ $[\text{MNa}]^+$ 383.1326, found 383.1320.

6.2.5.8. Synthesis of *N*-(*tert*-Butyl)-5,7-dimethyl-2-oxo-3-(2-oxopyrrolidin-1-yl)indoline-3-carboxamide (**II.5iab**):



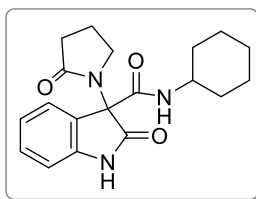
Prepared using 5,7-dimethylisatin, 4-aminobutanoic acid and *tert*-butyl isocyanide. CC: Hexane:EtOAc 1.5:1. The corresponding **II.5iab** was obtained as a beige solid (73.6 mg, 38% yield). m.p.= 231.4-232.7 °C. ^1H NMR (CDCl_3 , 400 MHz): δ 7.87 (br s, 1H), 7.31 (br s, 1H), 7.15 (s, 1H), 6.88 (s, 1H), 3.83-3.77 (m, 1H), 3.65-3.60 (m, 1H), 2.46-2.37 (m, 1H), 2.33-2.25 (m, 1H), 2.29 (s, 3H), 2.17-2.10 (m, 2H), 2.14 (s, 3H), 1.36 (s, 9H). ^{13}C NMR (CDCl_3 , 100 MHz): δ 175.0, 174.9, 161.9, 137.0, 132.6, 131.7, 125.9, 124.6, 118.7, 68.2, 52.0, 46.5, 30.5, 28.4 (3C), 21.1, 18.8, 16.2. HRMS (ESI) calculated for $\text{C}_{19}\text{H}_{25}\text{N}_3\text{NaO}_3$ $[\text{MNa}]^+$ 366.1788, found 366.1781.

6.2.5.9. Synthesis of *N*-(*tert*-Butyl)-2-oxo-3-(2-oxopyrrolidin-1-yl)-7-(trifluoromethyl)indoline-3-carboxamide (**II.5jab**):

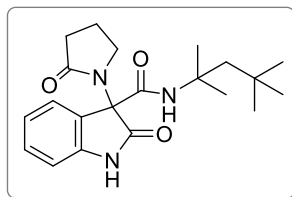


Prepared using 7-trifluoromethylisatin, 4-aminobutanoic acid and *tert*-butyl isocyanide. CC: Hexane:EtOAc 2:1. The corresponding **II.5jab** was obtained as a white solid (72.8 mg, 41% yield). m.p.= 169.8-171.2 °C. ¹H NMR (CDCl₃, 400 MHz): δ 7.95 (br s, 1H), 7.68 (d, *J*=7.5 Hz, 1H), 7.48 (d, *J*=8.0 Hz, 1H), 7.20-7.17 (m, 2H), 3.83-3.77 (m, 1H), 3.68-3.62 (m, 1H), 2.46-2.38 (m, 1H), 2.32-2.24 (m, 1H), 2.21-2.12 (m, 2H), 1.38 (s, 9H). ¹³C NMR (CDCl₃, 100 MHz): δ 175.2, 174.6, 160.7, 138.1, 130.2, 127.9, 126.5, 126.4, 123.1, 112.5, 112.2, 66.7, 52.4, 46.4, 30.2, 28.4 (3C), 19.0. HRMS (ESI) calculated for C₁₈H₂₀F₃N₃NaO₃ [MNa]⁺ 406.1349, found 406.1340.

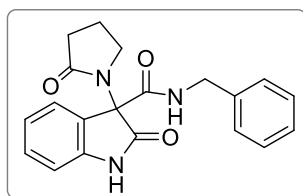
6.2.5.10. Synthesis of *N*-Cyclohexyl-2-oxo-3-(2-oxopyrrolidin-1-yl)indoline-3-carboxamide (**II.5abb**):



Prepared using isatin, 4-aminobutanoic acid and cyclohexyl isocyanide. CC: Hexane:EtOAc 2:1. The corresponding **II.5abb** was obtained as a white solid (65.7 mg, 28% yield). m.p.= 214.7-215.8 °C. ¹H NMR (CDCl₃, 400 MHz): δ 8.17 (br s, 1H), 7.53 (d, *J*=7.4 Hz, 1H), 7.28-7.22 (m, 2H), 7.07 (t, *J*=7.6 Hz, 1H), 6.80 (d, *J*=7.8 Hz, 1H), 3.84-3.72 (m, 2H), 3.64-3.58 (m, 1H), 2.45-2.38 (m, 1H), 2.35-2.26 (m, 1H), 2.17-2.09 (m, 2H), 1.97-1.94 (m, 1H), 1.80-1.65 (m, 3H), 1.39-1.14 (m, 6H). ¹³C NMR (CDCl₃, 100 MHz): δ 175.1, 174.6, 161.8, 141.0, 129.6, 126.5, 126.2, 123.2, 110.3, 67.3, 49.1, 46.8, 32.6, 32.3, 30.7, 25.4, 24.6, 24.5, 18.8. HRMS (ESI) calculated for C₁₉H₂₃N₃NaO₃ [MNa]⁺ 364.1632, found 364.1623.

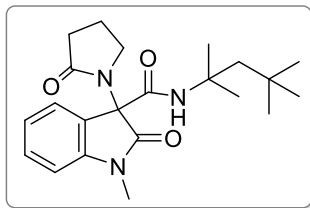
6.2.5.11. Synthesis of 2-Oxo-3-(2-oxopyrrolidin-1-yl)-N-(2,4,4-trimethylpentan-2-yl)indoline-3-carboxamide (II.5acb):


Prepared using isatin, 4-aminobutanoic acid and *tert*-octyl isocyanide. CC: Hexane:EtOAc 1.5:1. The corresponding **II.5acb** was obtained as a white solid (78.4 mg, 31% yield). m.p.= 198.5-199.2 °C. ^1H NMR (CDCl_3 , 400 MHz): δ 8.35 (br s, 1H), 7.51 (d, $J=7.4$ Hz, 1H), 7.25 (br s, 1H), 7.21 (td, $J=7.7$, 1.1 Hz, 1H), 7.06 (td, $J=7.6$, 0.8 Hz, 1H), 6.76 (d, $J=7.8$ Hz, 1H), 3.86-3.80 (m, 1H), 3.69-3.64 (m, 1H), 2.47-2.38 (m, 1H), 2.34-2.26 (m, 1H), 2.17-2.10 (m, 2H), 1.89 (d, $J=14.9$ Hz, 1H), 1.46-1.42 (m, 7H), 0.93 (s, 9H). ^{13}C NMR (CDCl_3 , 100 MHz): δ 175.1, 174.6, 161.2, 141.0, 129.5, 126.4, 126.3, 123.1, 110.4, 68.0, 56.1, 52.2, 46.7, 31.5, 31.3 (3C), 30.7, 28.6, 28.0, 18.9. HRMS (ESI) calculated for $\text{C}_{21}\text{H}_{29}\text{N}_3\text{NaO}_3$ $[\text{MNa}]^+$ 394.2101, found 394.2093.

6.2.5.12. Synthesis of N-Benzyl-2-oxo-3-(2-oxopyrrolidin-1-yl)indoline-3-carboxamide (II.5adb):


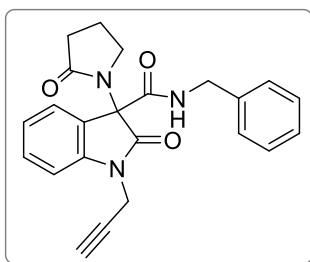
Prepared using isatin, 4-aminobutanoic acid and benzyl isocyanide. CC: Hexane:EtOAc 2:1. The corresponding **II.5adb** was obtained as a white solid (48.7 mg, 21% yield). m.p.= 215.8-217.1 °C. ^1H NMR (CDCl_3 , 400 MHz): δ 8.08 (br s, 1H), 7.57-7.56 (m, 2H), 7.31-7.23 (m, 6H), 7.08 (td, $J=7.6$, 0.9 Hz, 1H), 6.81 (d, $J=7.8$ Hz, 1H), 4.52 (dd, $J=14.7$, 5.9 Hz, 1H), 4.40 (dd, $J=14.7$, 5.7 Hz, 1H), 3.76-3.70 (m, 1H), 3.47-3.42 (m, 1H), 2.44-2.26 (m, 2H), 2.11-2.04 (m, 2H). ^{13}C NMR (CDCl_3 , 100 MHz): δ 175.3, 174.1, 163.2, 140.9, 137.3, 129.9, 128.8 (2C), 127.9 (2C), 127.7, 126.6, 126.0, 123.4, 110.4, 67.5, 46.7, 44.2, 30.6, 18.7. HRMS (ESI) calculated for $\text{C}_{20}\text{H}_{19}\text{N}_3\text{NaO}_3$ $[\text{MNa}]^+$ 372.1319, found 372.1311.

6.2.5.13. Synthesis of 1-Methyl-2-oxo-3-(2-oxopyrrolidin-1-yl)-*N*-(2,4,4-trimethylpentan-2-yl)indoline-3-carboxamide (II.5bcb):



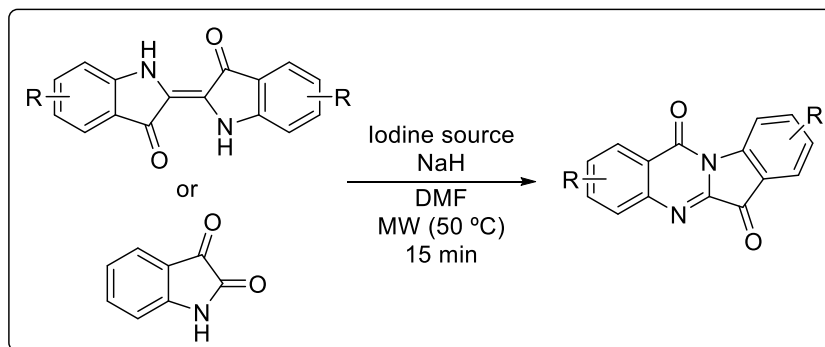
Prepared using *N*-methylisatin, 4-aminobutanoic acid and *tert*-octyl isocyanide. CC: Hexane:EtOAc 2:1. The corresponding **II.5bcb** was obtained as a beige solid (70.8 mg, 30% yield). m.p.= 152.7-153.8 °C. ¹H NMR (CDCl₃, 400 MHz): δ 7.55 (dd, *J*=7.4, 0.8 Hz, 1H), 7.32 (td, *J*=7.8, 1.2 Hz, 1H), 7.29 (br s, 1H), 7.10 (td, *J*=7.6, 0.8 Hz, 1H), 6.83 (d, *J*=7.8 Hz, 1H), 3.82-3.76 (m, 1H), 3.64-3.58 (m, 1H), 3.25 (s, 3H), 2.41-2.33 (m, 1H), 2.29-2.20 (m, 1H), 2.15-2.09 (m, 2H), 1.89 (d, *J*=15.0 Hz, 1H), 1.44-1.41 (m, 7H), 0.92 (s, 9H). ¹³C NMR (CDCl₃, 100 MHz): δ 175.0, 173.3, 161.4, 143.7, 129.6, 126.3, 126.0, 123.4, 108.3, 67.8, 56.0, 52.2, 46.6, 31.5, 31.2 (3C), 30.5, 28.6, 28.0, 26.8, 18.9. HRMS (ESI) calculated for C₂₂H₃₁N₃NaO₃ [MNa]⁺ 408.2258, found 408.2249.

6.2.5.14. Synthesis of *N*-Benzyl-2-oxo-3-(2-oxopyrrolidin-1-yl)-1-(prop-2-yn-1-yl)indoline-3-carboxamide (II.5cdb):



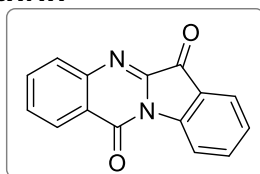
Prepared using *N*-propargylisatin, 4-aminobutanoic acid and benzyl isocyanide. CC: Hexane:EtOAc 2:1. The corresponding **II.5cdb** was obtained as a beige solid (50.2 mg, 24% yield). m.p.= 194.2 °C (decomp.). ¹H NMR (CDCl₃, 400 MHz): δ 7.62 (dd, *J*=7.5, 0.7 Hz, 1H), 7.52 (br s, 1H), 7.39-7.26 (m, 6H), 7.15 (td, *J*=7.6, 0.9 Hz, 1H), 7.07 (d, *J*=7.9 Hz, 1H), 4.63 (dd, *J*=17.7, 2.6 Hz, 1H), 4.54 (dd, *J*=14.8, 6.0 Hz, 1H), 4.47 (dd, *J*=17.7, 2.5 Hz, 1H), 4.39 (dd, *J*=14.8, 5.6 Hz, 1H), 3.72-3.67 (m, 1H), 3.42-3.37 (m, 1H), 2.39-2.22 (m, 3H), 2.10-2.02 (m, 2H). ¹³C NMR (CDCl₃, 100 MHz): δ 175.3, 172.0, 163.0, 142.0, 137.3, 129.9, 128.8 (2C), 127.9 (2C), 127.7, 126.5, 125.5, 123.9, 109.5, 76.2, 72.8, 67.3, 46.4, 44.2, 30.4, 30.1, 18.8. HRMS (ESI) calculated for C₂₃H₂₁N₃NaO₃ [MNa]⁺ 410.1475, found 410.1469.

6.2.6. General procedure for the synthesis of tryptanthrin and brominated tryptanthrins using iodine/DMF/NaH trio (Chapter 4)



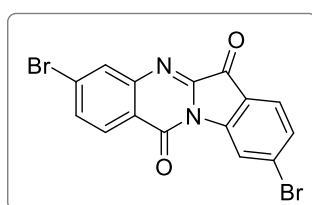
In a thick-glass microwave reactor charged with a magnetic stirring bar, indigo or isatin (100 mg, 0.381 mmol of Indigo or 0.68 mmol of isatin, 1 equiv) and sodium hydride (60% dispersion in mineral oil, stored in a dry box) were dissolved in 1 mL of the appropriate dry solvent. The iodine source was added, and solvent was added to a total volume of 2 mL. The resulting mixture was heated under microwave irradiation (CEM Discover S-Class single-mode microwave reactor) at 50 °C for 15 min. After cooling down to room temperature, a sample was collected, dissolved in 1 mL of dichloromethane and washed with 1 mL of water. The organic layer was analyzed by GC-MS.

6.2.6.1. Synthesis of tryptanthrin



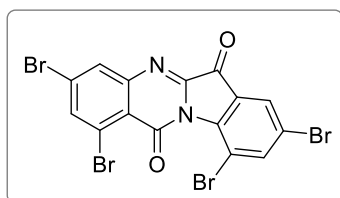
The corresponding was obtained as a yellow solid. ^1H NMR (CDCl_3 , 400 MHz): δ 8.61 (d, $J=8.1$ Hz, 1H), 8.42 (dd, $J=7.9$ Hz, $J=1.3$ Hz, 1H), 8.02 (d, $J=7.8$ Hz, 1H), 7.90 (d, $J=7.6$ Hz, 1H), 7.82-7.87 (m, 1H), 7.76-7.80 (m, 1H), 7.64-7.68 (m, 1H), 7.40-7.44 (m, $J=7.5$ Hz, $J=0.4$ Hz, 1H); ^{13}C NMR (CDCl_3 , 101 MHz) (ppm): δ 182.6 (C=O), 158.1 (C=O), 146.6, 146.4, 144.4, 138.3, 135.1, 130.8, 130.3, 127.6, 127.2, 125.4, 123.8, 122.0, 118.0; GC-MS: m/z [M^+] = 248.0; ESI-TOF-MS: m/z [$\text{M}+1$] $^+$ = 249.0659 for $\text{C}_{15}\text{H}_9\text{N}_2\text{O}_2$.

6.2.6.2. Synthesis of 3,9-dibromo-tryptanthrin



The 3,9-dibromo-tryptanthrin was obtained as a yellow solid (36% yield). ^1H NMR (CDCl_3 , 400 MHz) (ppm): δ 8.85 (d, $J=1.5$ Hz, 1H), 8.29 (d, $J=8.5$ Hz, 1H), 8.19 (d, $J=1.8$ Hz, 1H), 7.81-7.76 (m, 2H), 7.61 (dd, $J=8.1$ Hz, $J=1.6$ Hz, 1H). ^{13}C NMR (CDCl_3 , 101 MHz) (ppm): δ 180.03, 156.44, 146.49, 145.47, 143.94, 132.73, 132.69, 132.37, 129.85, 129.22, 127.90, 125.34, 121.26, 120.42, 119.52. HRMS (ESI-TOF-MS): (m/z) found 404.8866, calculated for $\text{C}_{15}\text{H}_7\text{Br}_2\text{N}_2\text{O}_2$ 404.8869 $[\text{M}+1]^+$.

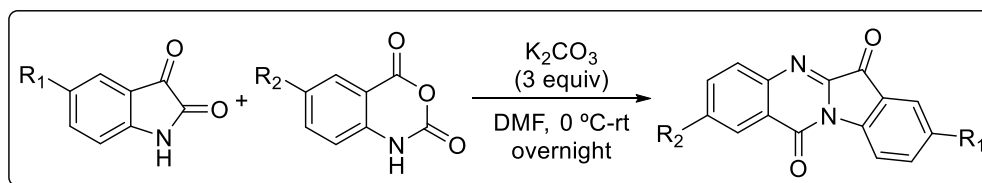
6.2.6.3. Synthesis of 2,4,8,10-tetrabromo-tryptanthrin



The 2,4,8,10-tetrabromo-tryptanthrin was obtained as a green solid (18% yield). ^1H NMR (CDCl_3 , 400 MHz) (ppm): δ 8.43 (d, $J = 2.1$ Hz, 1H), 8.22 (d, $J=2.2$ Hz, 1H), 8.15 (d, $J = 1.9$ Hz, 1H), 8.03 (d, $J=1.9$ Hz, 1H). ^{13}C NMR (CDCl_3 , 101 MHz) (ppm): δ 179.41, 154.72, 145.73, 144.58, 144.52, 143.01, 141.39, 130.04, 127.48, 127.25, 126.67, 126.53, 124.81, 121.96, 112.04. HRMS (ESI-TOF-MS): (m/z) found 560.7074, calculated for $\text{C}_{15}\text{H}_5\text{Br}_4\text{N}_2\text{O}_2$ 560.7079 $[\text{M}+1]^+$.

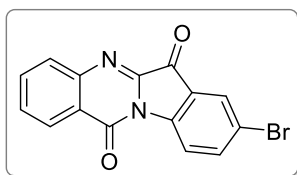
6.2.7. Procedures for the synthesis of precursors for the Petasis MCR

6.2.7.1. General procedure for the synthesis of brominated tryptanthrins (III.1a-1d)



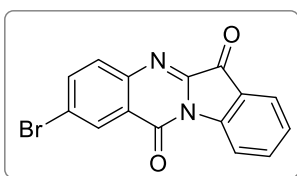
In a round-bottomed flask placed in an ice bath, (un)substituted isatin (1 equiv) was dissolved in DMF (20 mL). Potassium carbonate (3 equiv) was slowly added, and allowed to stir, leading to a colour change and hydrogen release. Once gas production ceased, the suspension was kept at room temperature and (un)substituted isatoic anhydride (1.2 equiv) was added. The reaction was allowed to proceed overnight, with stirring at room temperature and monitored by TLC. When the reaction was complete, the formed solid was washed with water (3 x 50 mL) and ethanol (2 x 20 mL) and the corresponding tryptanthrin used in the next step without further purification.

6.2.7.1.1. Synthesis of 8-Bromo-tryptanthrin (8-bromoindolo[2,1-*b*]quinazoline-6,12-dione) (III.1a)^{7,8}



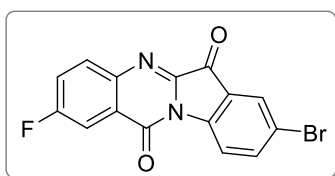
5-Bromo-isatin (1.0 g, 1 equiv), isatoic anhydride (0.866 g, 1.2 equiv), K_2CO_3 (1.830 g, 3 equiv) and DMF (20 mL) were used. The corresponding **III.1a** was obtained as a yellow solid (1.23 g, 85% yield).

6.2.7.1.2. Synthesis of 2-Bromo-tryptanthrin (2-bromoindolo[2,1-*b*]quinazoline-6,12-dione) (III.1b)^{7,8}



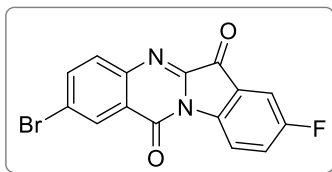
Isatin (0.75 g, 1 equiv), 5-bromoisatoic anhydride (1.48 g, 1.2 equiv), K_2CO_3 (2.11 g, 3 equiv) and DMF (20 mL) were used. The corresponding **III.1b** was obtained as a yellow solid (1.59 g, 95% yield).

6.2.7.1.3. Synthesis of 8-Bromo-2-fluoro-tryptanthrin (8-bromo-2-fluoroindolo[2,1-*b*]quinazoline-6,12-dione) (III.1c)



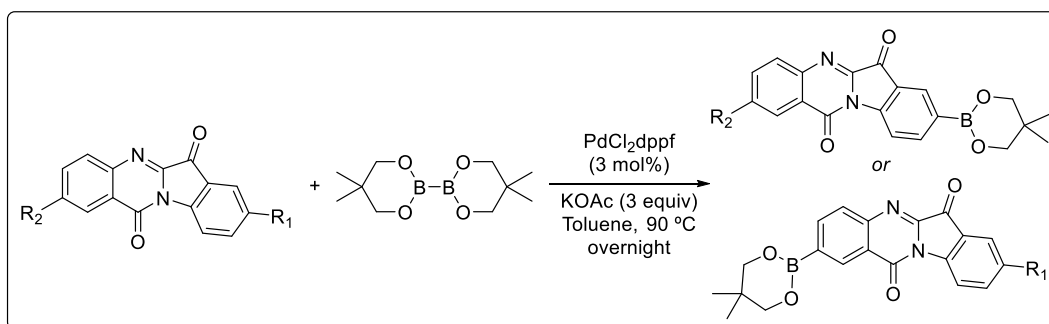
5-Bromoisatin (1.50 g, 1 equiv), 5-fluoroisatoic anhydride (1.44 g, 1.2 equiv), K_2CO_3 (2.75 g, 3 equiv) and DMF (20 mL) were used. The corresponding **III.1c** was obtained as a yellow solid (1.69 g, 74% yield).

6.2.7.1.4. Synthesis of 2-Bromo-8-fluoro-tryptanthrin (2-bromo-8-fluoroindolo[2,1-*b*]quinazoline-6,12-dione) (III.1d)



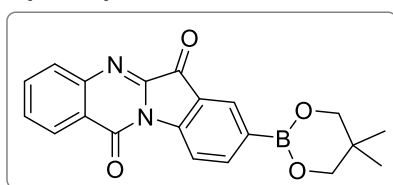
5-Fluoroisatin (1.0 g, 1 equiv), 5-bromoisatoic anhydride (1.76 g, 1.2 equiv), K_2CO_3 (2.75 g, 3 equiv) and DMF (20 mL) were used. The corresponding **III.1d** was obtained as a yellow solid (1.70 g, 81% yield).

6.2.7.2. General procedure for the synthesis of boronate-tryptanthrins (III.2a- III.2d)⁹



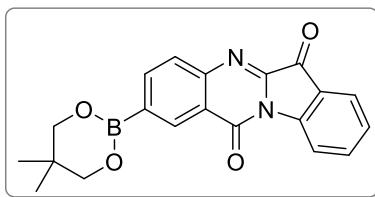
In a round-bottom flask or in a Radley's® 12 position carousel reactor tube under nitrogen atmosphere was added the halide derivatives, B_2NPG_2 (1.1 equiv), $PdCl_2(dppf)$ (3 mol%), KOAc (3 equiv) and toluene. The reaction was stirred at 90°C (in an oil bath when a round-bottom flask was used) overnight and monitored by TLC. The reaction was quenched with brine (30 mL) followed by extraction with $CHCl_3$ (3 x 30 mL). The combined organic phases were dried with $MgSO_4$, filtered and the solvent evaporated on the rotative evaporator. The crude mixture was filtered over a porous plate glass filter funnel packed with a layer of celite and a layer of SiO_2 and eluted with $CHCl_3$ until the washings became colourless. After evaporation of the solvent the corresponding product (**2**) was obtained and used in the next steps.

6.2.7.2.1. Synthesis of 8-(5,5-dimethyl-1,3,2-dioxaborinan-2-yl)indolo[2,1-*b*]quinazoline-6,12-dione (III.2a)



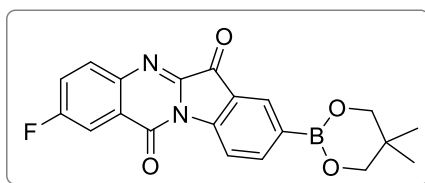
8-Bromoindolo[2,1-*b*]quinazoline-6,12-dione (**III.1a**) (301.7 mg, 0.92 mmol), B₂NPG₂ (228 mg, 1.0 mmol, 1.1 equiv), PdCl₂(dppf) (20.1 mg, 0.028 mmol, 3 mol%), KOAc (270 mg, 2.8 mmol, 3 equiv) and toluene (4 mL) were used. The corresponding **III.2a** was obtained as a yellow-green solid (275.2 mg, 87% yield). m.p.= >220°C. ¹H NMR (CDCl₃, 400 MHz): δ 1.04 (s, CH₃, 6H), 3.79 (s, CH₂, 4H), 7.63-7.67 (t, *J*= 8 Hz, Ar, 1H), 7.81-7.85 (t, *J*= 8 Hz, Ar, 1H), 8.00-8.02 (d, *J*= 8 Hz, Ar, 1H), 8.18-8.20 (d, *J*= 8 Hz, Ar, 1H), 8.34 (s, Ar, 1H), 8.41-8.43 (d, *J*= 8 Hz, Ar, 1H), 8.53-8.55 (d, *J*= 8 Hz, Ar, 1H). ¹³C NMR (CDCl₃, 100 MHz): δ 22.00, 32.08, 72.57, 117.02, 121.42, 123.84, 127.67, 130.24, 130.80, 131.27, 135.21, 144.21, 146.78, 147.90, 158.25, 182.80. HRMS (ESI-TOF) *m/z*: calcd. for C₂₀H₁₈BN₂O₄ [M]⁺ 361.1760, found 361.0960.

6.2.7.2.2. Synthesis of 2-(5,5-dimethyl-1,3,2-dioxaborinan-2-yl)indolo[2,1-*b*]quinazoline-6,12-dione (**III.2b**)



2-Bromoindolo[2,1-*b*]quinazoline-6,12-dione (**III.1b**) (373 mg, 0.9 mmol), B₂NPG₂ (228 mg, 1.0 mmol, 1.1 equiv), PdCl₂(dppf) (20.1 mg, 0.028 mmol, 3 mol%), KOAc (270 mg, 2.8 mmol, 3 equiv) and toluene (4 mL) were used. The corresponding **III.2b** was obtained as a yellow solid (369.6 mg, >99% yield). m.p.= >220°C. ¹H NMR (CDCl₃, 400 MHz): δ 1.05 (s, CH₃, 6H), 3.83 (s, CH₂, 4H), 7.39-7.43 (t, *J*= 8 Hz, Ar, 1H), 7.76-7.80 (t, *J*= 8 Hz, Ar, 1H), 7.90-7.91 (d, *J*= 8 Hz, Ar, 1H), 7.96-7.98 (d, *J*= 8 Hz, Ar, 1H), 8.22-8.24 (d, *J*= 8 Hz, Ar, 1H), 8.64-8.66 (d, *J*= 8 Hz, Ar, 1H), 8.88 (s, Ar, 1H). ¹³C NMR (CDCl₃, 100 MHz): δ 22.03, 32.11, 72.62, 118.18, 122.05, 122.91, 125.48, 127.20, 129.76, 133.75, 138.39, 140.28, 144.80, 146.60, 148.24, 158.44, 182.87. HRMS (ESI-TOF) *m/z*: calcd. for C₂₀H₁₈BN₂O₄ [M]⁺ 361.1760, found 361.0957.

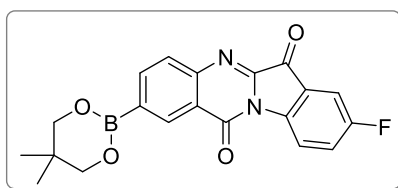
6.2.7.2.3. Synthesis of 8-(5,5-dimethyl-1,3,2-dioxaborinan-2-yl)-2-fluoroindolo[2,1-*b*]quinazoline-6,12-dione (**III.2c**)



8-Bromo-2-fluoroindolo[2,1-*b*]quinazoline-6,12-dione (**III.1c**) (332 mg, 0.8 mmol), B₂NPG₂ (216 mg, 0.9 mmol, 1.1 equiv), PdCl₂(dppf) (19.1 mg, 0.026 mmol, 3 mol%),

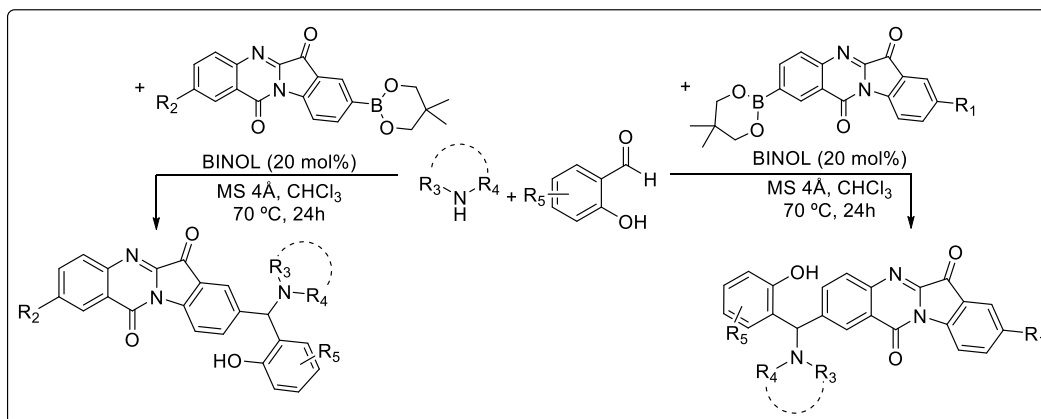
KOAc (256 mg, 2.6 mmol, 3 equiv) and toluene (4 mL) were used. The corresponding **III.2c** was obtained as a yellow solid (292.8 mg, 80% yield). m.p.= >220°C. ¹H NMR (CDCl₃, 400 MHz): δ 1.04 (s, CH₃, 6H), 3.80 (s, CH₂, 4H), 7.55-7.58 (m, Ar, 1H), 8.02-8.09 (m, Ar, 2H), 8.20-8.22 (d, *J* = 8 Hz, Ar, 1H), 8.36 (s, Ar, 1H), 8.54-8.56 (d, *J* = 8 Hz, Ar, 1H). ¹³C NMR (CDCl₃, 100 MHz): δ 22.01, 32.11, 72.60, 113.27, 113.55, 117.08, 118.17, 121.50, 123.37, 123.61, 125.65, 127.61, 131.37, 133.26, 138.48, 143.43, 144.27, 147.66, 157.34, 182.31. HRMS (ESI-TOF) *m/z*: calcd. for C₂₀H₁₇BFN₂O₄ [M]⁺ 379.1740, found 379.0864.

6.2.7.2.4. Synthesis of 2-(5,5-dimethyl-1,3,2-dioxaborinan-2-yl)-8-fluoroindolo[2,1-*b*]quinazoline-6,12-dione (**III.2d**)



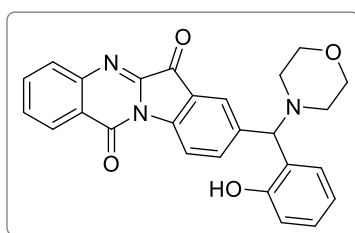
2-Bromo-8-fluoroindolo[2,1-*b*]quinazoline-6,12-dione (**III.1d**) (297 mg, 0.8 mmol), B₂NPG₂ (216 mg, 0.9 mmol, 1.1 equiv), PdCl₂(dppf) (19.1 mg, 0.026 mmol, 3 mol%), KOAc (256 mg, 2.6 mmol, 3 equiv) and toluene (4 mL) were used. The corresponding **III.2d** was obtained as a yellow solid (302 mg, 93% yield). m.p.= >220°C. ¹H NMR (CDCl₃, 400 MHz): δ 1.05 (s, CH₃, 6H), 3.83 (s, CH₂, 4H), 7.46-7.50 (t, *J* = 8 Hz, Ar, 1H), 7.56-7.58 (d, *J* = 8 Hz, Ar, 1H), 7.96-7.98 (d, *J* = 8 Hz, Ar, 1H), 8.23-8.25 (d, *J* = 8 Hz, Ar, 1H), 8.65-8.66 (m, Ar, 1H), 8.87 (s, Ar, 1H). ¹³C NMR (CDCl₃, 100 MHz): δ 22.03, 32.11, 72.62, 118.18, 122.05, 122.91, 124.31, 125.48, 127.20, 129.76, 132.72, 133.75, 138.39, 140.28, 144.80, 146.60, 148.24, 158.44, 182.87. MS (ESI) *m/z*: 333.09 (M-OHNa)⁺.

6.2.8. General procedure for the synthesis of tryptanthrin-based Petasis adducts (Chapter 4 – Library III)



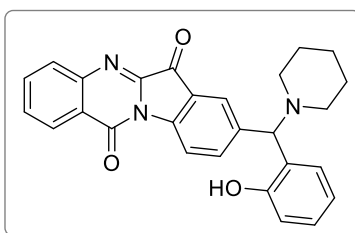
In a round-bottom flask or in a Radley's® 12 position carousel reactor tube was added the borylated tryptanthrin derivatives (2) (0.3 mmol, 1.0 equiv), the amine (3.9 equiv), the aldehyde (3.3 equiv), BINOL (20 mol%), MS 4Å (200 mg) and CHCl₃ (3 mL). The reaction was stirred at 70 °C for 24 hours. After cooling down, the reaction mixture was filtered with a porous plate glass funnel packed with a celite layer and washed with CHCl₃. The solvent was evaporated under reduced pressure and the crude product purified by silica gel flash chromatography using hexane/AcOEt from (5:1) to (1:1) as eluents.

6.2.8.1. Synthesis of 8-((2-hydroxyphenyl)(morpholino)methyl)indolo[2,1-b]quinazoline-6,12-dione (III.5aaa)



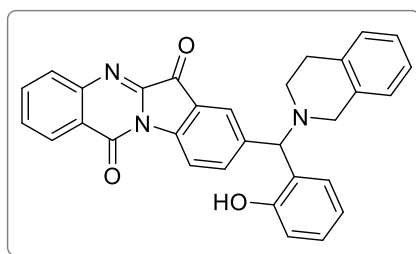
III.2a (112 mg, 0.3 mmol, 1 equiv), **III.3a** (0.1 mL, 1.1 mmol, 3.9 equiv), **III.4a** (0.1 mL, 0.9 mmol, 3.3 equiv), BINOL (15.9 mg, 0.06 mmol, 20 mol%), MS 4Å (200 mg) and CHCl₃ (3 mL) were used to obtain the corresponding **III.5aaa** as a yellow solid (89.9 mg, 66% yield). m.p.= >220°C. ¹H NMR (CDCl₃, 400 MHz): δ 2.48-2.51 (m, CH₂, 2H), 2.65 (s br, CH₂, 2H), 3.79 (s, CH₂, 4H), 4.50 (s, CH, 1H), 6.74-6.78 (t, *J*= 8 Hz, Ar, 1H), 6.88-6.90 (d, *J*= 8 Hz, Ar, 1H), 6.95-6.97 (d, *J*= 8 Hz, Ar, 1H), 7.14-7.18 (t, *J*= 8 Hz, Ar, 1H), 7.63-7.66 (t, Ar, 1H), 7.81-7.85 (t, *J*= 8 Hz, Ar, 1H), 7.87-7.89 (m, Ar, 1H), 7.96-8.00 (m, Ar, 2H), 8.38-8.40 (d, *J*= 8 Hz, Ar, 1H), 8.54-8.56 (d, *J*= 8 Hz, Ar, 1H), 11.29 (s br, OH, 1H). ¹³C NMR (CDCl₃, 100 MHz): δ 52.47, 66.86, 76.15, 117.12, 118.66, 120.21, 122.53, 123.70, 125.30, 127.71, 129.22, 129.52, 130.52, 130.92, 135.35, 138.36, 139.26, 144.39, 145.98, 146.63, 155.91, 157.99, 182.23. HRMS (ESI-TOF) *m/z*: calcd. for C₂₆H₂₂O₄N₃ [M]⁺ 440.16048, found 440.1597.

6.2.8.2. Synthesis of 8-((2-hydroxyphenyl)(piperidin-1-yl)methyl)indolo[2,1-b]quinazoline-6,12-dione (III.5aca)



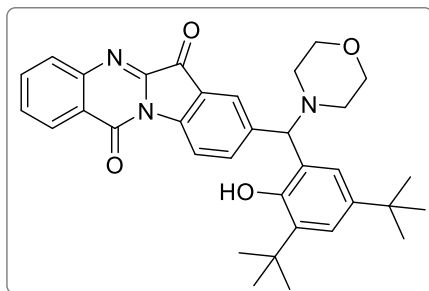
III.2a (100 mg, 0.3 mmol, 1 equiv), **III.3c** (0.1 mL, 1.1 mmol, 3.9 equiv), **III.4a** (0.1 mL, 0.9 mmol, 3.3 equiv), BINOL (15.9 mg, 0.06 mmol, 20 mol%), MS 4Å (200 mg) and CHCl₃ (3 mL) were used to obtain the corresponding **III.5aca** as a green solid (32.1 mg, 26% yield). m.p.= 216.8°C decomp. ¹H NMR (CDCl₃, 400 MHz): δ 1.49-1.67 (m, CH₂, 6H), 2.37-2.44 (m, CH₂, 4H), 4.55 (s, CH, 1H), 6.70-6.73 (t, Ar, 1H), 6.86-6.89 (m, Ar, 2H), 7.11-7.15 (t, *J*= 8 Hz, Ar, 1H), 7.61-7.64 (t, Ar, 1H), 7.79-7.84 (m, Ar, 2H), 7.92 (s, Ar, 1H), 7.97-7.99 (d, *J*= 8 Hz, Ar, 1H), 8.36-8.38 (d, *J*= 8 Hz, Ar, 1H), 8.51-8.53 (d, *J*= 8 Hz, Ar, 1H), 12.06 (s br, OH, 1H). ¹³C NMR (CDCl₃, 100 MHz): δ 24.08, 26.08, 52.84, 75.85, 117.51, 118.44, 119.62, 122.33, 123.71, 124.44, 125.47, 127.66, 128.96, 129.10, 130.42, 130.86, 135.27, 138.57, 139.57, 144.48, 145.81, 146.65, 156.86, 157.96, 182.43. HRMS (ESI-TOF) *m/z*: calcd. for C₂₇H₂₄O₃N₃ [M]⁺ 438.18122, found 438.1803.

6.2.8.3. Synthesis of 8-((3,4-dihydroisoquinolin-2(1H)-yl)(2-hydroxyphenyl)methyl)indolo[2,1-*b*]quinazoline-6,12-dione (**III.5ada**)



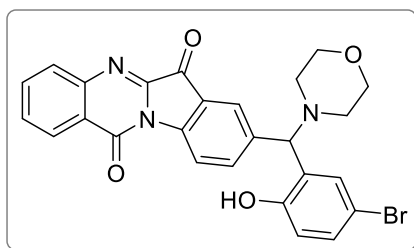
III.2a (122 mg, 0.3 mmol), **III.3d** (0.14 mL, 1.1 mmol, 3.9 equiv), **III.4a** (0.1 mL, 0.9 mmol, 3.3 equiv), BINOL (15.9 mg, 0.06 mmol, 20 mol%), MS 4Å (200 mg) and CHCl₃ (3 mL) were used to obtain the corresponding **III.5ada** as a yellow solid (19.1 mg, 12% yield). m.p.= 215°C decomp. ¹H NMR (CDCl₃, 400 MHz): δ 2.82-3.10 (m, CH₂, 4H), 3.71 (s, CH₂, 2H), 4.71 (s, CH, 1H), 6.76-6.80 (t, *J*= 8 Hz, Ar, 1H), 6.90-6.92 (m, Ar, 2H), 6.99-7.00 (m, Ar, 1H), 7.09-7.21 (m, Ar, 4H), 7.63-7.67 (t, *J*= 8 Hz, Ar, 2H), 7.81-7.85 (t, *J*= 8 Hz, Ar, 1H), 7.96-8.02 (m, Ar, 3H), 8.39-8.41 (d, *J*= 8 Hz, Ar, 1H), 8.56-8.58 (d, *J*= 8 Hz, Ar, 1H), 11.49 (s br, OH, 1H). ¹³C NMR (CDCl₃, 100 MHz): δ 28.59, 49.23, 54.62, 75.16, 117.81, 118.70, 119.98, 122.51, 123.74, 124.34, 125.22, 126.27, 126.92, 127.02, 127.71, 128.78, 129.05, 129.38, 130.48, 130.92, 132.94, 133.44, 135.32, 138.24, 139.93, 144.47, 145.99, 146.67, 156.47, 158.01, 182.38. HRMS (ESI-TOF) *m/z*: calcd. for C₃₁H₂₄O₃N₃ [M]⁺ 486.18122, found 486.1805.

6.2.8.4. Synthesis of 8-((3,5-di-tert-butyl-2-hydroxyphenyl)(morpholino)methyl)indolo[2,1-*b*]quinazoline-6,12-dione (III.5aac)



III.2a (88 mg, 0.3 mmol), **III.3a** (0.1 mL, 1.1 mmol, 3.9 equiv), **III.4c** (215 mg, 0.9 mmol, 3.3 equiv), BINOL (15.9 mg, 0.06 mmol, 20 mol%), MS 4 Å (200 mg) and CHCl₃ (3 mL) were used to obtain the corresponding **III.5aac** as a yellow solid (60.5 mg, 45% yield). m.p.= 217.2°C decomp. ¹H NMR (CDCl₃, 400 MHz): δ 1.21 (s, CH₃, 9H), 1.44 (s, CH₃, 9H), 2.50-2.60 (m, CH₂, 4H), 3.79 (s, CH₂, 4H), 4.46 (s, CH, 1H), 6.80 (s, Ar, 1H), 7.20 (s, Ar, 1H), 7.63-7.67 (t, *J*= 8 Hz, Ar, 1H), 7.81-7.85 (t, *J*= 8 Hz, Ar, 1H), 7.95-8.02 (m, Ar, 3H), 8.40-8.42 (d, *J*= 8 Hz, Ar, 1H), 8.54-8.56 (d, *J*= 8 Hz, Ar, 1H), 11.45 (s br, OH, 1H). ¹³C NMR (CDCl₃, 100 MHz): δ 29.68, 31.72, 34.33, 35.23, 66.82, 77.05, 118.69, 122.45, 122.83, 123.76, 125.46, 127.74, 130.46, 130.93, 135.31, 137.08, 138.44, 139.79, 141.72, 144.51, 145.92, 146.71, 152.35, 158.03, 182.44. HRMS (ESI-TOF) *m/z*: calcd. for C₃₄H₃₈O₄N₃ [M]⁺ 552.2857, found 552.2850.

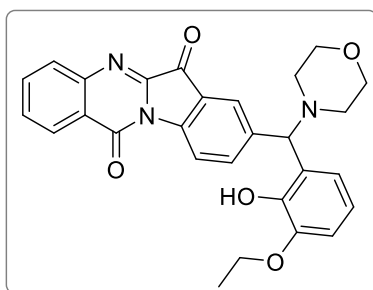
6.2.8.5. Synthesis of 8-((5-bromo-2-hydroxyphenyl)(morpholino)methyl)indolo[2,1-*b*]quinazoline-6,12-dione (III.5aad)



III.2a (177 mg, 0.5 mmol), **III.3a** (0.17 mL, 1.9 mmol, 3.9 equiv), **III.4d** (332 mg, 1.7 mmol, 3.3 equiv), BINOL (28.6 mg, 0.1 mmol, 20 mol%), MS 4 Å (300 mg) and CHCl₃ (5 mL) were used to obtain the corresponding **III.5aad** as a green solid (147.4 mg, 58% yield). m.p.= 170°C decomp. ¹H NMR (CDCl₃, 400 MHz): δ 2.29-2.62 (m, CH₂, 4H), 3.77 (s br, CH₂, 4H), 4.45 (s, CH, 1H), 6.77-6.79 (d, *J*= 8 Hz, Ar, 1H), 7.07 (s, Ar, 1H), 7.23-7.26 (m, Ar, 1H), 7.62-7.66 (t, *J*= 8 Hz, Ar, 1H), 7.82-7.84 (m, Ar, 2H), 7.93 (s, Ar, 1H), 7.97-7.99 (d, *J*= 8 Hz, Ar, 1H), 8.36-8.38 (d, *J*= 8 Hz, Ar, 1H), 8.55-8.57 (d, *J*= 8 Hz, Ar, 1H), 11.47 (s br, OH, 1H). ¹³C NMR (CDCl₃, 100 MHz): δ 66.77, 75.64, 111.78, 118.79,

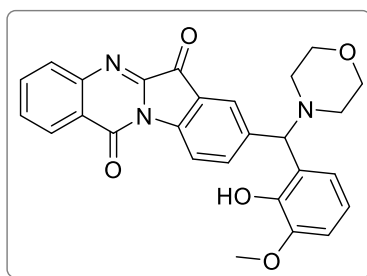
119.66, 122.64, 123.68, 125.24, 125.73, 127.74, 130.58, 130.95, 131.73, 132.32, 135.41, 138.28, 138.45, 144.31, 146.16, 146.61, 155.18, 158.00, 182.23. HRMS (ESI-TOF) m/z : calcd. for $C_{26}H_{21}O_4N_3Br$ $[M]^+$ 518.0710, found 518.0701.

6.2.8.6. Synthesis of 8-((3-ethoxy-2-hydroxyphenyl)(morpholino)methyl)indolo[2,1-*b*]quinazoline-6,12-dione (**III.5aaf**)



III.2a (93 mg, 0.3 mmol), **III.3a** (0.1 mL, 1.1 mmol, 3.9 equiv), **III.4f** (152 mg, 0.9 mmol, 3.3 equiv), BINOL (15.9 mg, 0.06 mmol, 20 mol%), MS 4Å (200 mg) and $CHCl_3$ (3 mL) were used to obtain the corresponding **III.5aaf** as a yellow solid (13.6 mg, 11% yield). m.p.= 137.5-138.2°C. 1H NMR ($CDCl_3$, 400 MHz): δ 1.47-1.50 (t, CH_3 , 3H), 2.48-2.62 (m, CH_2 , 4H), 3.77 (m, CH_2 , 4H), 4.05-4.12 (q, CH_2 , 2H), 4.58 (s, CH, 1H), 6.67-6.77 (m, Ar, 3H), 7.62-7.66 (t, $J=8$ Hz, Ar, 1H), 7.80-7.84 (t, $J=8$ Hz, Ar, 1H), 7.90-8.00 (m, Ar, 3H), 8.37-8.39 (d, $J=8$ Hz, Ar, 2H), 8.51-8.53 (d, $J=8$ Hz, Ar, 1H), 10.27 (s br, OH, 1H). ^{13}C NMR ($CDCl_3$, 100 MHz): δ 15.01, 52.48, 64.40, 66.96, 73.93, 111.84, 118.54, 119.91, 120.47, 122.35, 123.70, 124.51, 125.31, 127.67, 130.45, 130.87, 135.30, 138.35, 139.97, 144.44, 145.05, 145.80, 146.61, 147.62, 157.95, 182.42. HRMS (ESI-TOF) m/z : calcd. for $C_{28}H_{26}O_5N_3$ $[M]^+$ 484.1867, found 484.1858.

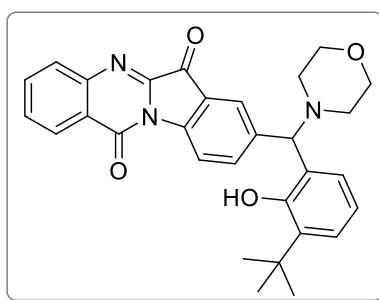
6.2.8.7. Synthesis of 8-((2-hydroxy-3-methoxyphenyl)(morpholino)methyl)indolo[2,1-*b*]quinazoline-6,12-dione (**III.5aag**)



III.2a (121 mg, 0.3 mmol), **III.3a** (0.1 mL, 1.1 mmol, 3.9 equiv), **III.4g** (140 mg, 0.9 mmol, 3.3 equiv), BINOL (15.9 mg, 0.06 mmol, 20 mol%), MS 4Å (200 mg) and $CHCl_3$ (3 mL) were used to obtain the corresponding **III.5aag** as a yellow solid (18.0 mg, 11% yield). m.p.= 165.2-167°C. 1H NMR ($CDCl_3$, 400 MHz): δ 2.49-2.64 (m, CH_2 , 4H), 3.78 (s

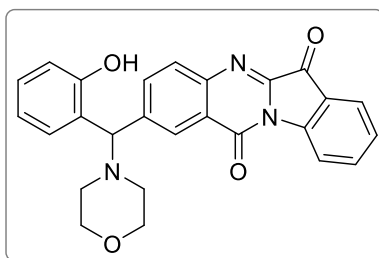
br, CH₂, 4H), 3.88 (s, OMe, 3H), 4.57 (s, CH, 1H), 6.66 (m, Ar, 1H), 6.74-6.78 (t, *J* = 8 Hz, Ar, 2H), 7.62-7.66 (t, *J* = 8 Hz, Ar, 1H), 7.80-7.84 (t, *J* = 8 Hz, Ar, 1H), 7.89-8.00 (m, Ar, 3H), 8.36-8.38 (d, *J* = 8 Hz, Ar, 1H), 8.51-8.53 (m, Ar, 1H), 10.75 (s br, OH, 1H). ¹³C NMR (CDCl₃, 100 MHz): δ 52.45, 56.00, 66.94, 74.51, 110.81, 118.61, 119.98, 120.63, 122.37, 123.68, 125.32, 127.68, 130.48, 130.88, 135.32, 138.36, 144.39, 145.00, 146.60, 157.95, 182.36. HRMS (ESI-TOF) *m/z*: calcd. for C₂₇H₂₄O₅N₃ [M]⁺ 470.1711, found 470.1702.

6.2.8.8. Synthesis of 8-((3-(tert-butyl)-2-hydroxyphenyl)(morpholino)methyl)indolo[2,1-*b*]quinazoline-6,12-dione (III.5aai)



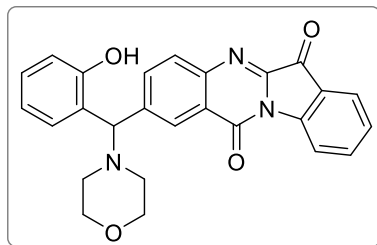
III.2a (102 mg, 0.3 mmol), **III.3a** (0.1 mL, 1.1 mmol, 3.9 equiv), **III.4i** (163 mg, 0.9 mmol, 3.3 equiv), BINOL (15.9 mg, 0.06 mmol, 20 mol%), MS 4 Å (200 mg) and CHCl₃ (3 mL) were used to obtain the corresponding **III.5aai** as a yellow solid (50 mg, 36% yield). m.p.= 254°C decomp. ¹H NMR (CDCl₃, 400 MHz): δ 1.43 (s, CH₃, 9H), 2.45-2.70 (m, CH₂, 4H), 3.80 (s, CH₂, 4H), 4.49 (s, CH, 1H), 6.68-6.72 (t, *J*=8 Hz, Ar, 1H), 6.82-6.84 (d, *J*= 8 Hz, Ar, 1H), 7.17-7.19 (d, *J*= 8 Hz, Ar, 1H), 7.65-7.69 (t, *J*= 8 Hz, Ar, 1H), 7.83-7.87 (t, *J*= 8 Hz, Ar, 1H), 7.92-8.03 (m, Ar, 3H), 8.41-8.43 (d, *J*= 8 Hz, Ar, 1H), 8.55-8.57 (d, *J*= 8 Hz, Ar, 1H), 11.73 (s, OH, 1H). ¹³C NMR (CDCl₃, 100 MHz): δ 29.40, 34.91, 66.68, 76.51, 118.54, 119.23, 123.54, 123.63, 125.25, 126.53, 127.08, 127.61, 130.35, 130.82, 135.20, 137.97, 138.16, 139.29, 145.82, 154.94, 163.24, 182.23. HRMS (ESI-TOF) *m/z*: calcd. for C₃₀H₂₉O₄N₃Na [M]⁺ 518.2050, found 518.2042.

6.2.8.9. Synthesis of 2-((2-hydroxyphenyl)(morpholino)methyl)indolo[2,1-*b*]quinazoline-6,12-dione (III.5baa)



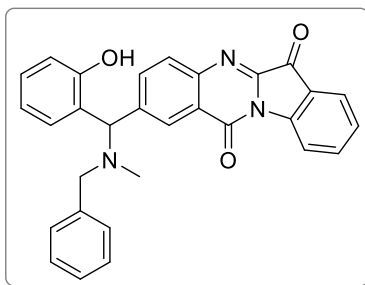
III.2b (103 mg, 0.3 mmol), **III.3a** (0.1 mL, 1.1 mmol, 3.9 equiv), **III.4a** (0.1 mL, 0.9 mmol, 3.3 equiv), BINOL (15.9 mg, 0.06 mmol, 20 mol%), MS 4Å (200 mg) and CHCl₃ (3 mL) were used to obtain the corresponding **III.5baa** as a yellow solid (100.9 mg, 80% yield). m.p.= 211.5°C decomp. ¹H NMR (CDCl₃, 400 MHz): δ 2.45-2.65 (m, CH₂, 4H), 3.71-3.76 (m, CH₂, 4H), 4.60 (s, CH, 1H), 6.71-6.74 (t, Ar, 1H), 6.85-6.87 (d, *J*= 8 Hz, Ar, 1H), 6.97-6.99 (m, Ar, 1H), 7.10-7.14 (t, *J*= 8 Hz, Ar, 1H), 7.37-7.41 (t, *J*= 8 Hz, Ar, 1H), 7.73-7.77 (t, *J*= 8 Hz, Ar, 1H), 7.85-7.87 (d, *J*= 8 Hz, Ar, 1H), 7.93-7.95 (d, *J*= 8 Hz, Ar, 2H), 7.99 (m, Ar, 1H), 8.39 (s, Ar, 1H), 8.55-8.58 (d, *J*= 8 Hz, Ar, 1H), 11.37 (s br, OH, 1H). ¹³C NMR (CDCl₃, 100 MHz): δ 52.55, 66.86, 76.41, 117.64, 118.08, 120.20, 122.06, 123.71, 124.02, 125.62, 127.47, 127.51, 129.45, 129.53, 131.87, 134.87, 138.48, 142.37, 144.62, 146.31, 146.52, 155.94, 157.95, 182.46. HRMS (ESI-TOF) *m/z*: calcd. for C₂₆H₂₂O₄N₃ [M]⁺ 440.1605, found 440.1598.

6.2.8.10. Synthesis of 2-((2-hydroxyphenyl)(piperidin-1-yl)methyl)indolo[2,1-*b*]quinazoline-6,12-dione (**III.5bca**)



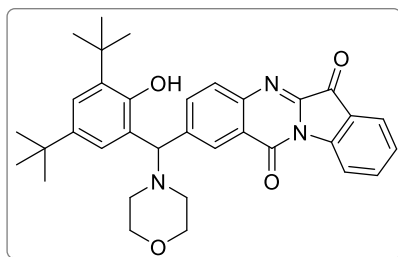
III.2b (85 mg, 0.3 mmol), **III.3c** (0.1 mL, 1.1 mmol, 3.9 equiv), **III.4a** (0.1 mL, 0.9 mmol, 3.3 equiv), BINOL (15.9 mg, 0.06 mmol, 20 mol%), MS 4Å (200 mg) and CHCl₃ (3 mL) were used to obtain the corresponding **III.5bca** as a green solid (61.8 mg, 60% yield). m.p.= 197.8°C decomp. ¹H NMR (CDCl₃, 400 MHz): δ 1.48 (s br, CH₂, 2H), 1.65 (s br, CH₂, 4H), 2.42-2.62 (m, CH₂, 4H), 4.65 (s, CH, 1H), 6.68-6.71 (t, Ar, 1H), 6.85-6.87 (d, *J*= 8 Hz, Ar, 1H), 6.90-6.92 (d, *J*= 8 Hz, Ar, 1H), 7.09-7.13 (t, *J*= 8 Hz, Ar, 1H), 7.35-7.39 (t, *J*= 8 Hz, Ar, 1H), 7.70-7.74 (t, *J*= 8 Hz, Ar, 1H), 7.84-7.85 (d, *J*= 4 Hz, Ar, 1H), 7.92-7.97 (m, Ar, 2H), 8.36 (s, Ar, 1H), 8.54-8.56 (d, *J*= 8 Hz, Ar, 1H), 11.90 (s br, OH, 1H). ¹³C NMR (CDCl₃, 100 MHz): δ 24.06, 26.06, 76.10, 117.38, 117.93, 119.53, 121.97, 123.75, 124.51, 125.45, 127.34, 127.44, 129.01, 129.14, 131.50, 138.32, 142.80, 144.40, 146.21, 146.22, 156.83, 157.95, 182.40. HRMS (ESI-TOF) *m/z*: calcd. for C₂₇H₂₄O₄N₃ [M]⁺ 438.1812, found 438.1802.

6.2.8.11. Synthesis of 2-((benzyl(methyl)amino)(2-hydroxyphenyl)methyl)indolo[2,1-*b*]quinazoline-6,12-dione (**III.5bea**)



III.2b (107 mg, 0.3 mmol), **III.3e** (0.14 mL, 1.1 mmol, 3.9 equiv), **III.4a** (0.1 mL, 0.9 mmol, 3.3 equiv), BINOL (15.9 mg, 0.06 mmol, 20 mol%), MS 4Å (200 mg) and CHCl₃ (3 mL) were used to obtain the corresponding **III.5bea** as a yellow solid (21.4 mg, 15% yield). m.p.= 194°C decomp. ¹H NMR (CDCl₃, 400 MHz): δ 2.21 (s, CH₃, 3H), 3.56-3.79 (m, CH₂, 2H), 4.86 (s, CH, 1H), 6.74-6.78 (t, *J*= 8 Hz, Ar, 1H), 6.93-6.99 (m, Ar, 2H), 7.15-7.19 (t, *J*= 8 Hz, Ar, 1H), 7.27-7.37 (m, Ar, 5H), 7.39-7.43 (t, *J*= 8 Hz, Ar, 1H), 7.75-7.79 (t, *J*= 8 Hz, Ar, 1H), 7.88-7.90 (d, *J*= 8 Hz, Ar, 1H), 7.99-8.01 (m, Ar, 1H), 8.09-8.11 (m, Ar, 1H), 8.46 (s, Ar, 1H), 8.59-8.61 (d, *J*= 8 Hz, Ar, 1H), 11.95 (s br, OH, 1H). ¹³C NMR (CDCl₃, 100 MHz): δ 39.67, 60.01, 75.32, 117.60, 118.06, 119.83, 122.05, 123.94, 124.51, 125.58, 127.45, 127.63, 127.95, 128.85, 129.13, 129.40, 129.46, 131.69, 135.16, 138.52, 138.44, 142.49, 144.56, 146.31, 146.44, 156.63, 158.01, 182.48. HRMS (ESI-TOF) *m/z*: calcd. for C₃₀H₂₄O₃N₃ [M]⁺ 474.1812, found 474.1804.

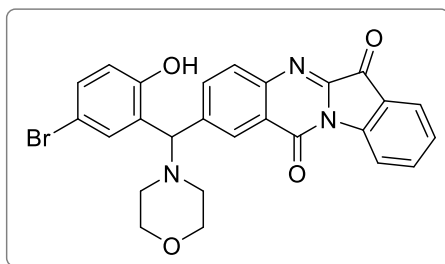
6.2.8.12. Synthesis of 2-((3,5-di-*tert*-butyl-2-hydroxyphenyl)(morpholino)methyl)indolo[2,1-*b*]quinazoline-6,12-dione (**III.5bac**)



III.2b (96 mg, 0.3 mmol), **III.3a** (0.1 mL, 1.1 mmol, 3.9 equiv), **III.4c** (215 mg, 0.9 mmol, 3.3 equiv), BINOL (15.9 mg, 0.06 mmol, 20 mol%), MS 4Å (200 mg) and CHCl₃ (3 mL) were used to obtain the corresponding **III.5bac** as a yellow solid (20.3 mg, 14% yield). m.p.= 115.3-117°C. ¹H NMR (CDCl₃, 400 MHz): δ 1.20 (s, CH₃, 9H), 1.45 (s, CH₃, 9H), 2.46-2.47 (m, CH₂, 4H), 3.74-3.78 (m, CH₂, 4H), 4.57 (s, CH, 1H), 6.83-6.84 (d, *J*= 8 Hz, Ar, 1H), 7.19-7.20 (d, *J*= 8 Hz, Ar, 1H), 7.38-7.41 (t, Ar, 1H), 7.72-7.77 (m, Ar, 1H), 7.87-7.88 (d, *J*= 4 Hz, Ar, 1H), 7.93-7.95 (d, *J*= 8 Hz, Ar, 1H), 8.05-8.09 (m, Ar, 1H), 8.46

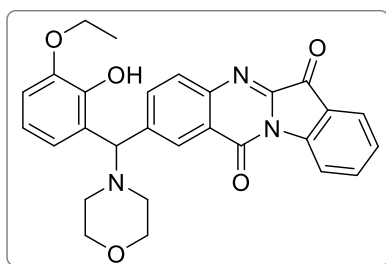
(s br, Ar, 1H), 8.57-8.59 (d, J = 8 Hz, Ar, 1H), 11.60 (s br, OH, 1H). ^{13}C NMR (CDCl_3 , 100 MHz): δ 29.67, 31.70, 34.29, 35.22, 66.83, 77.30, 118.04, 122.01, 122.81, 123.70, 123.91, 124.00, 125.55, 127.41, 127.59, 129.60, 131.74, 135.11, 136.95, 138.42, 141.55, 142.95, 144.48, 146.28, 146.31, 152.42, 158.01, 182.52. HRMS (ESI-TOF) m/z : calcd. for $\text{C}_{34}\text{H}_{38}\text{O}_4\text{N}_3$ $[\text{M}]^+$ 552.2857, found 552.2844.

6.2.8.13. Synthesis of 2-((5-bromo-2-hydroxyphenyl)(morpholino)methyl)indolo[2,1-*b*]quinazoline-6,12-dione (**III.5bad**)



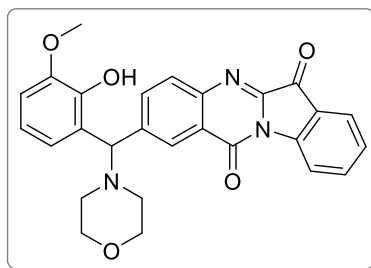
III.2b (95 mg, 0.3 mmol), **III.3a** (0.1 mL, 1.1 mmol, 3.9 equiv), **III.4d** (184 mg, 0.9 mmol, 3.3 equiv), BINOL (15.9 mg, 0.06 mmol, 20 mol%), MS 4\AA (200 mg) and CHCl_3 (3 mL) were used to obtain the corresponding **III.5bad** as a green solid (80.3 mg, 59% yield). m.p. = 179.1-183°C. ^1H NMR (CDCl_3 , 400 MHz): δ 2.45-2.64 (m, CH_2 , 4H), 3.77 (m, CH_2 , 4H), 4.55 (s, CH, 1H), 6.77-6.79 (d, J = 8 Hz, Ar, 1H), 7.09-7.10 (d, J = 4 Hz, Ar, 1H), 7.22-7.24 (d, J = 8 Hz, Ar, 1H), 7.40-7.44 (t, J = 8 Hz, Ar, 1H), 7.76-7.80 (t, J = 8 Hz, Ar, 1H), 7.88-7.90 (d, J = 8 Hz, Ar, 1H), 7.97-7.99 (m, Ar, 2H), 8.39 (s, Ar, 1H), 8.58-8.60 (d, J = 8 Hz, Ar, 1H), 11.56 (s br, OH, 1H). ^{13}C NMR (CDCl_3 , 100 MHz): δ 66.78, 75.91, 117.71, 118.06, 119.57, 121.99, 124.11, 125.63, 125.76, 127.45, 127.55, 131.89, 131.95, 132.27, 134.73, 138.52, 141.55, 144.71, 146.24, 146.68, 155.19, 157.83, 182.40. HRMS (ESI-TOF) m/z : calcd. for $\text{C}_{26}\text{H}_{21}\text{O}_4\text{N}_3\text{Br}$ $[\text{M}]^+$ 518.0710, found 518.0701.

6.2.8.14. Synthesis of 2-((3-ethoxy-2-hydroxyphenyl)(morpholino)methyl)indolo[2,1-*b*]quinazoline-6,12-dione (**III.5baf**)



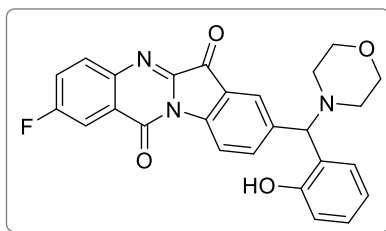
III.2b (99 mg, 0.3 mmol), **III.3a** (0.1 mL, 1.1 mmol, 3.9 equiv), **III.4f** (152 mg, 0.9 mmol, 3.3 equiv), BINOL (15.9 mg, 0.06 mmol, 20 mol%), MS 4Å (200 mg) and CHCl₃ (3 mL) were used to obtain the corresponding **III.5baf** as a yellow solid (47.7 mg, 36% yield). m.p.= 99.8-101.2°C. ¹H NMR (CDCl₃, 400 MHz): δ 1.44-1.48 (t, *J*= 8 Hz, CH₃, 3H), 2.44-2.63 (m, CH₂, 4H), 3.71-3.80 (m, CH₂, 4H), 4.02-4.07 (q, CH₂, 2H), 4.67 (s, CH, 1H), 6.68-6.75 (m, Ar, 3H), 7.34-7.38 (t, *J*= 8 Hz, Ar, 1H), 7.70-7.74 (t, *J*= 8 Hz, Ar, 1H), 7.82-7.84 (d, *J*= 8 Hz, Ar, 1H), 7.90-7.92 (d, *J*= 8 Hz, Ar, 1H), 8.02-8.06 (m, Ar, 1H), 8.38 (s, Ar, 1H), 8.52-8.54 (d, *J*= 8 Hz, Ar, 1H), 10.61 (s br, OH, 1H). ¹³C NMR (CDCl₃, 100 MHz): δ 14.95, 52.45, 64.29, 66.87, 74.51, 111.87, 117.90, 119.77, 120.71, 121.92, 123.73, 124.39, 125.44, 127.30, 127.33, 131.63, 134.75, 138.31, 142.93, 144.36, 145.09, 146.15, 146.20, 147.60, 157.86, 182.36. HRMS (ESI-TOF) *m/z*: calcd. for C₂₈H₂₆O₅N₃ [M]⁺ 484.1867, found 484.1859.

6.2.8.15. Synthesis of 2-((2-hydroxy-3-methoxyphenyl)(morpholino)methyl)indolo[2,1-*b*]quinazoline-6,12-dione (**III.5bag**)



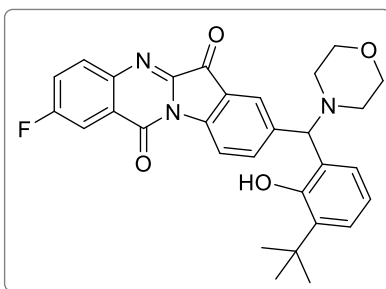
III.2b (94 mg, 0.3 mmol), **III.3a** (0.1 mL, 1.1 mmol, 3.9 equiv), **III.4g** (140 mg, 0.9 mmol, 3.3 equiv), BINOL (15.9 mg, 0.06 mmol, 20 mol%), MS 4Å (200 mg) and CHCl₃ (3 mL) were used to obtain the corresponding **III.5bag** as a yellow solid (22.3 mg, 18% yield). m.p.= 133.8-135°C. ¹H NMR (CDCl₃, 400 MHz): δ 2.46-2.66 (m, CH₂, 4H), 3.77-3.81 (m, CH₂, 4H), 3.87 (s, OMe, 3H), 4.67 (s, CH, 1H), 6.66-6.77 (m, Ar, 3H), 7.38-7.42 (t, *J*= 8 Hz, Ar, 1H), 7.74-7.78 (t, *J*= 8 Hz, Ar, 1H), 7.86 (m, Ar, 1H), 7.93-7.95 (d, *J*= 8 Hz, Ar, 1H), 8.03-8.08 (m, Ar, 1H), 8.39-8.40 (m, Ar, 1H), 8.57-8.59 (d, *J*= 8 Hz, Ar, 1H), 11.04 (s br, OH, 1H). ¹³C NMR (CDCl₃, 100 MHz): δ 52.50, 55.96, 66.92, 75.11, 110.83, 118.00, 119.90, 120.90, 121.99, 123.84, 124.24, 125.55, 127.41, 127.43, 129.57, 134.79, 138.42, 142.68, 144.48, 145.07, 146.24, 146.36, 148.42, 157.93, 182.44. HRMS (ESI-TOF) *m/z*: calcd. for C₂₇H₂₄O₅N₃ [M]⁺ 470.1711, found 470.1702.

6.2.8.16. Synthesis of 2-fluoro-8-((2-hydroxyphenyl)(morpholino)methyl)indolo[2,1-*b*]quinazoline-6,12-dione (**III.5caa**)



III.2c (108 mg, 0.26 mmol), **III.3a** (0.1 mL, 1.1 mmol, 3.9 equiv), **III.4a** (0.1 mL, 0.9 mmol, 3.3 equiv), BINOL (14.9 mg, 0.05 mmol, 20 mol%), MS 4Å (200 mg) and CHCl₃ (3 mL) were used to obtain the corresponding **III.5caa** as a yellow solid (12.7 mg, 10% yield). m.p.= 210.3°C decomp. ¹H NMR (CDCl₃, 400 MHz): δ 2.48-2.51 (m, CH₂, 2H), 2.65 (m, CH₂, 2H), 3.79 (m, CH₂, 4H), 4.51 (s, CH, 1H), 6.75-6.78 (t, Ar, 1H), 6.88-6.90 (d, *J*= 8 Hz, Ar, 1H), 6.96-6.98 (d, *J*= 8 Hz, Ar, 1H), 7.14-7.18 (t, *J*= 8 Hz, Ar, 1H), 7.52-7.57 (m, Ar, 1H), 7.89-7.91 (d, *J*= 8 Hz, Ar, 1H), 7.97-8.05 (m, Ar, 3H), 8.53-8.55 (d, *J*= 8 Hz, Ar, 1H), 11.29 (s br, OH, 1H). ¹³C NMR (CDCl₃, 100 MHz): δ 52.50, 66.84, 76.13, 113.36, 113.60, 117.75, 118.73, 120.26, 122.63, 123.48, 123.64, 123.72, 125.39, 125.56, 125.65, 129.11, 129.58, 133.31, 133.40, 138.39, 139.54, 143.25, 143.93, 145.73, 155.89, 157.13, 162.07, 164.60, 182.00. HRMS (ESI-TOF) *m/z*: calcd. for C₂₆H₂₁O₄N₃F [M]⁺ 458.1511, found 458.1503.

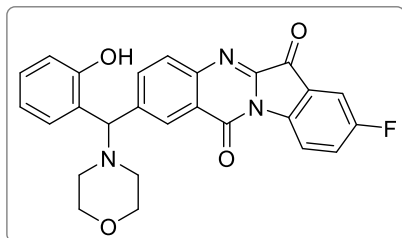
6.2.8.17. Synthesis of 8-((3-(tert-butyl)-2-hydroxyphenyl)(morpholino)methyl)-2-fluoroindolo[2,1-*b*]quinazoline-6,12-dione (**III.5cai**)



III.2c (100 mg, 0.26 mmol), **III.3a** (0.1 mL, 1.1 mmol, 3.9 equiv), **III.4i** (155 mg, 0.9 mmol, 3.3 equiv), BINOL (14.9 mg, 0.05 mmol, 20 mol%), MS 4Å (200 mg) and CHCl₃ (3 mL) were used to obtain the corresponding **III.5cai** as a yellow solid (21 mg, 16% yield). m.p.= 253°C decomp. ¹H NMR (CDCl₃, 400 MHz): δ 1.43 (s, CH₃, 9H), 2.51-2.66 (m, CH₂, 4H), 3.80 (s, CH₂, 4H), 4.49 (s, CH, 1H), 6.68-6.72 (t, *J*= 8 Hz, Ar, 1H), 6.81-6.83 (d, *J*= 8 Hz, Ar, 1H), 7.17-7.19 (d, *J*= 8 Hz, Ar, 1H), 7.53-7.57 (t, *J*= 8 Hz, Ar, 1H), 7.93-8.07 (m, Ar, 4H), 8.54-8.56 (d, *J*= 8 Hz, Ar, 1H), 11.71 (s, OH, 1H). ¹³C NMR (CDCl₃, 100 MHz): δ 29.39, 34.91, 66.67, 76.51, 113.23, 113.48,

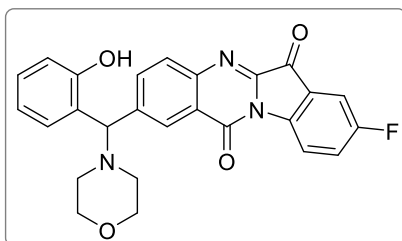
118.58, 119.25, 123.32, 123.50, 123.56, 125.32, 126.56, 127.07, 133.18, 133.27, 138.01, 138.18, 139.61, 143.19, 143.81, 143.84, 145.54, 154.93, 181.90. HRMS (ESI-TOF) m/z : calcd. for $C_{30}H_{27}O_4N_3F$ [M]⁻ 512.1991, found 512.1990.

6.2.8.18. Synthesis of 8-fluoro-2-((2-hydroxyphenyl)(morpholino)methyl)indolo[2,1-*b*]quinazoline-6,12-dione (III.5daa)



III.2d (90 mg, 0.26 mmol), **III.3a** (0.1 mL, 1.1 mmol, 3.9 equiv), **III.4a** (0.1 mL, 0.9 mmol, 3.3 equiv), BINOL (14.9 mg, 0.05 mmol, 20 mol%), MS 4Å (200 mg) and $CHCl_3$ (3 mL) were used to obtain the corresponding **III.5daa** as a yellow solid (22.1 mg, 20% yield). m.p.= 193.5°C decomp. ¹H NMR ($CDCl_3$, 400 MHz): δ 2.52-2.69 (m, CH_2 , 4H), 3.80 (m, CH_2 , 4H), 4.68 (s, CH, 1H), 6.74-6.78 (t, J = 8 Hz, Ar, 1H), 6.88-6.90 (d, J = 8 Hz, Ar, 1H), 7.05 (s, Ar, 1H), 7.13-7.17 (t, J = 8 Hz, Ar, 1H), 7.44-7.49 (m, Ar, 1H), 7.53-7.56 (m, Ar, 1H), 7.94-7.96 (d, J = 8 Hz, Ar, 1H), 8.07 (s, Ar, 1H), 8.41 (s, Ar, 1H), 8.57-8.60 (m, Ar, 1H), 11.45 (s br, OH, 1H). ¹³C NMR ($CDCl_3$, 100 MHz): δ 52.52, 66.64, 112.15, 112.40, 117.59, 119.71, 119.79, 120.28, 123.41, 123.49, 123.94, 124.89, 125.12, 127.46, 129.40, 129.61, 131.96, 134.98, 142.39, 144.56, 146.34, 155.82, 157.66, 160.04, 162.54, 181.54. HRMS (ESI-TOF) m/z : calcd. for $C_{26}H_{21}O_4N_3F$ [M]⁺ 458.1511, found 458.1501.

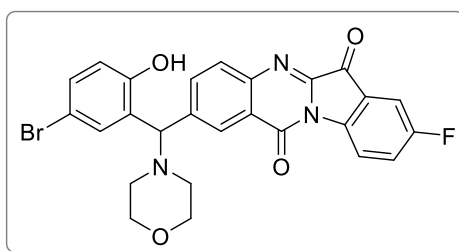
6.2.8.19. Synthesis of 8-fluoro-2-((2-hydroxyphenyl)(piperidin-1-yl)methyl)indolo[2,1-*b*]quinazoline-6,12-dione (III.5dca)



III.2d (77 mg, 0.26 mmol), **III.3c** (0.1 mL, 1.1 mmol, 3.9 equiv), **III.4a** (0.1 mL, 0.9 mmol, 3.3 equiv), BINOL (14.9 mg, 0.05 mmol, 20 mol%), MS 4Å (200 mg) and $CHCl_3$ (3 mL) were used to obtain the corresponding **III.5dca** as a yellow solid (32 mg, 34% yield). m.p.= 209.9°C decomp. ¹H NMR ($CDCl_3$, 400 MHz): δ 1.49-1.67 (m, CH_2 , 6H), 2.45 (m, CH_2 , 4H), 4.69 (s, CH, 1H), 6.69-6.73 (t, J = 8 Hz, Ar, 1H), 6.86-6.88 (d, J = 8 Hz,

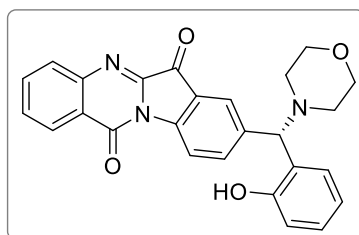
Ar, 1H), 6.95 (s, Ar, 1H), 7.10-7.14 (t, $J=8$ Hz, Ar, 1H), 7.43-7.48 (m, Ar, 1H), 7.53-7.55 (m, Ar, 1H), 7.93-7.95 (d, $J=8$ Hz, Ar, 1H), 8.02 (s, Ar, 1H), 8.37 (s, Ar, 1H), 8.57-8.61 (m, Ar, 1H), 12.13 (s br, OH, 1H). ^{13}C NMR (CDCl_3 , 100 MHz): δ 24.02, 25.94, 52.97, 75.89, 112.09, 112.34, 117.44, 119.70, 119.77, 113.43, 123.51, 123.78, 124.35, 124.83, 125.07, 127.47, 129.16, 131.73, 135.22, 142.41, 142.43, 143.06, 144.41, 146.16, 156.74, 157.78, 160.00, 162.49, 181.58. HRMS (ESI-TOF) m/z : calcd. for $\text{C}_{27}\text{H}_{23}\text{O}_3\text{N}_3\text{F}$ $[\text{M}]^+$ 456.1718, found 456.1709.

6.2.8.20. Synthesis of 2-((5-bromo-2-hydroxyphenyl)(morpholino) methyl)-8-fluoroindolo[2,1-*b*]quinazoline-6,12-dione (**III.5dad**)



III.2d (75 mg, 0.26 mmol), **III.3a** (0.1 mL, 1.1 mmol, 3.9 equiv), **III.4d** (172.5 mg, 0.9 mmol, 3.3 equiv), BINOL (14.9 mg, 0.05 mmol, 20 mol%), MS 4\AA (200 mg) and CHCl_3 (3 mL) were used to obtain the corresponding **III.5dad** as a yellow solid (16.5 mg, 16% yield). m.p.= 192.2-194°C. ^1H NMR (CDCl_3 , 400 MHz): δ 2.54-2.69 (m, CH_2 , 4H), 3.81 (s, CH_2 , 4H), 4.62 (s, CH, 1H), 6.81-6.83 (d, $J=8$ Hz, Ar, 1H), 7.17 (s br, Ar, 1H), 7.24 (s, Ar, 1H), 7.48-7.52 (m, Ar, 1H), 7.56-7.58 (m, Ar, 1H), 7.97-8.03 (m, Ar, 2H), 8.42 (s, Ar, 1H), 8.59-8.62 (m, Ar, 1H), 11.62 (s br, OH, 1H). ^{13}C NMR (CDCl_3 , 100 MHz): δ 52.53, 66.58, 75.71, 111.87, 112.26, 112.50, 119.60, 119.79, 119.87, 123.41, 123.49, 124.13, 125.01, 125.25, 127.51, 131.92, 132.15, 132.47, 142.39, 144.71, 146.61, 155.11, 157.61, 160.12, 162.61, 181.57. HRMS (ESI-TOF) m/z : calcd. for $\text{C}_{26}\text{H}_{20}\text{O}_4\text{N}_3\text{BrF}$ $[\text{M}]^+$ 536.0616, found 536.0609.

6.2.9. General procedure for the asymmetric version of the tryptanthrin-based Petasis adducts (Chapter 4 – (S)- **III.5aaa**)



In a round-bottom flask or in a Radley's® 12 position carousel reactor tube was added (**III.2a**) (0.3 mmol, 1.0 equiv), (**III.3a**) (3.9 equiv), (**III.4a**) (3.3 equiv), chiral organocatalyst (20 mol%), MS 4Å (200 mg) and solvent (3 mL). The reaction was stirred at the indicated temperature and monitored by TLC. After cooling down, the reaction mixture was filtered with a porous plate glass funnel packed with a celite layer and washed with CHCl₃. The solvent was evaporated under reduced pressure and the crude product purified by silica gel flash chromatography using hexane/AcOEt (5:1) to (1:1) as eluents. The product was analyzed by HPLC, using a Daicel Chiralpak IA column, using n-hexane/ethanol 70:30 as mobile phase, with a flow rate of 0.8 mL/min. The detector was set at 254 nm and the enantiomers were detected at 129.44 minutes ((*R*)-enantiomer, minor) and 142.827 minutes ((*S*)-enantiomer, major).

6.3. Biological activity assays

6.3.1. Antiproliferative activity evaluation

These assays were performed by Professor José Padrón and his team at the BioLab, Instituto Universitario de Bio-Orgánica Antonio González (IUBO-AG), Universidad de La Laguna, Spain.

Cells were seeded onto 96 well plates at a density of 2500 (A549, HBL-100, HeLa, and SH-SY5Y) or 5000 (T-47D and WiDr) cells/well. Stock solutions of **Library I** were prepared in DMSO at 40 mM (400 times the desired maximum test concentration, i.e. 100 μM). Compounds were tested at decimal dilutions starting at 100 μM. Control cells were exposed to an equivalent amount of DMSO (0.25% v/v, negative control). Cells were incubated with the test compounds for 48 h, after which time the SRB protocol was applied.¹⁰ Finally, in each well, the optical density (OD) was measured at 530 nm using the BioTeK Power Wave XS absorbance microplate reader. Values were corrected with the background OD of the wells containing the control. The antiproliferative activity of the extracts was expressed as the 50% reduction in cancer cell growth (GI₅₀).

6.3.2. Cholinesterase inhibition evaluation

These assays were performed by Professor Óscar López at the Departamento de Química Orgánica, Facultad de Química, Universidad de Sevilla, Spain.

Inhibition of AChE (electric eel) and BuChE (equine serum) was measured using the Ellman's colorimetric assay,¹¹ with the minor modifications reported by us.¹² DMSO (1.25% final concentration in cuvette) was used for preparing the stock inhibitor solutions. Enzymatic kinetics were monitored by UV–Vis spectroscopy using DTNB (5,5'-dithiobis(2-nitrobenzoic acid), 0.975 mM) as the chromogenic agent. Reaction took place in a buffered medium (50 μ M phosphate buffer, pH 8.0), $T = 25$ °C, being monitored for 125 s at 405 nm.

For determining the percentage of inhibition, the substrate concentration (acetylthiocholine iodide for AChE; S-butyrylthiocholine iodide for BuChE) was fixed at 121 μ M for AChE and 112 μ M for BuChE. IC_{50} values were calculated by plotting the percentage of inhibition vs. $\log[I]$ using 5-7 different inhibitor concentrations, and adjusting to a second-order equation. Cornish-Bowden plots ($1/V$ vs. $[I]$ and $[S]/V$ vs. $[I]$) were used for estimating the mode of action, and the kinetic parameters (K_M , $K_{M,app}$, V_{max} , $V_{max,app}$) were calculated using non-linear regression analysis (least squares fit) implemented in GraphPad Prism 8.01 software. Inhibition constants (K_i) were calculated using the same equations as previously.¹²

6.3.3. Monoamine oxidase inhibition evaluation

These studies were conducted by Professor Holger Stark at the Institute of Pharmaceutical and Medicinal Chemistry, Heinrich Heine University Düsseldorf, Germany.

Assessment of potential MAO A and B inhibition was conducted. One-point screening of compounds were carried out for both isoforms using a discontinuous fluorimetric assay as described previously.¹³ In brief, MAO inhibition assay was conducted using recombinant membrane-bound MAO A and MAO B (Sigma-Aldrich, MO, USA), Kynuramine was used as substrate in 2-fold K_M concentrations ($K_M = 30$ μ M for MAO A and $K_M = 20$ μ M for MAO B). After initiation of enzyme reaction by addition of kynuramine, mixture was incubated (20 min, 37 °C) and stopped by adding 35 μ L sodium hydroxide (2 N). Enzyme activity was measured by detection of 4-hydroxyquinoline ($\lambda_{Ex} = 320 \pm 20$ nm, $\lambda_{Em} = 405 \pm 20$ nm) using an infinite M1000 Pro microplate reader (Tecan Trading AG, Switzerland). Data of one-point measurements were calculated as percentage of control (product formation in absence of inhibitor) and expressed as mean \pm standard deviation (%) performing at least two independent experiments in duplicates. Clorgyline and Safinamide were used as references.

6.3.4. Antimicrobial activity evaluation

The antimicrobial activity studies were performed by Professor Eugénia Pinto at the Laboratório de Microbiologia, Departamento de Ciências Biológicas, Faculdade de Farmácia, Universidade do Porto, Portugal.

MICs and MLCs were used for defining the antimicrobial activity in agreement with the references of the Clinical and Laboratory Standards Institute (CLSI) for broth microdilution tests, with minor modifications:¹⁴ M27-A3 for yeasts, M38-A2 for filamentous fungi and dermatophytes and M100-A25 for bacteria.

A stock solution of the tryptanthrin derivatives was prepared in dimethylsulfoxide (DMSO, Sigma-Aldrich, St. Louis, MO, US). Two-fold serial dilutions in RPMI for fungi and in MHB2 for bacteria were prepared (concentration range 512–32 µg/mL) and distributed in sterile and disposable 96 flat bottom wells microtiter plates. The final concentration of DMSO, used in growth control, did not interfere on the bacterial/fungal growth. Furthermore, other two controls were performed: a sterility control and a quality control, performed with an ATCC reference strain, bacteria with gentamicin (Sigma-Aldrich, Seelze, Germany) and yeast with voriconazole (kindly provided by Pfizer). Equal volumes of cell suspension and sample dilutions were added in the wells.

MICs were determined as the lowest concentrations resulting in 100% growth inhibition, in comparison to the sample-free controls. From wells showing no visible growth, 10 µL of culture were collected and deposited on MHA plates (for bacteria) and SDA (for fungi) to evaluate the MLC, defined as the lowest concentration at which no colonies grew after an incubation of 16–18 h/35 °C for bacteria, 48 h/35 °C for yeasts, *Aspergillus* and *Mucor*, and 5 days/25 °C for dermatophytes.

The 20 new tryptanthrin-based Petasis adducts (**Library III**), as well as the enantiomeric pure version of (S)- **III.5aaa** were tested at least two times against bacterial and fungal strains.

6.4. Computational details

The full geometry optimization of all structures and transition states has been carried out at the DFT level of theory using the M06-2X functional¹⁵ and the 6-31G* basis set with the help of the Gaussian-09 program package.¹⁶ Single point calculations were performed on the basis of the equilibrium geometries found by using the 6-311+G** basis set. Cartesian d and f basis functions (6d, 10f) were used in all calculations. Ultrafine

integration grid was used for numerical integrations. No symmetry operations have been applied for any of the calculated structures.

The Hessian matrix was calculated analytically for the optimized structures to prove the location of correct minima (no imaginary frequencies) or saddle points (only one imaginary frequency), and to estimate the thermodynamic parameters, the latter being calculated at temperature 298.15 K. The nature of all transition states was investigated by the analysis of vectors associated with the imaginary frequency and by the calculations of the intrinsic reaction coordinates (IRC) using the Gonzalez-Schlegel method.¹⁷⁻²⁰

The total energies corrected for solvent effects (E_s) were estimated at the single-point calculations on the basis of gas-phase geometries at the SMD-M06-2X/6-311+G**//gas-M06-2X/6-31G* level of theory using the polarizable continuum model in the SMD version²¹ with methanol as solvent. The entropic term in methanol solution (S_s) was calculated according to the procedure described by Wertz²² and Cooper and Ziegler²³ using eqs. 1–4:

$$\Delta S_1 = R \ln V_{m,\text{liq}}^s / V_{m,\text{gas}} \quad (1)$$

$$\Delta S_2 = R \ln V_m^o / V_{m,\text{liq}}^s \quad (2)$$

$$\alpha = [S^{\circ,s}_{\text{liq}} - (S^{\circ,s}_{\text{gas}} + \Delta S_1)] / [S^{\circ,s}_{\text{gas}} + \Delta S_1] \quad (3)$$

$$S_s = S_g + \Delta S_{\text{sol}} = S_g + [\Delta S_1 + \alpha(S_g + \Delta S_1) + \Delta S_2] = S_g + [(-12.72 \text{ cal/mol}\cdot\text{K}) - 0.32(S_g - 12.72 \text{ cal/mol}\cdot\text{K}) + 6.37 \text{ cal/mol}\cdot\text{K}] \quad (4)$$

where S_g is the gas-phase entropy of solute, ΔS_{sol} is solvation entropy, $S^{\circ,s}_{\text{liq}}$, $S^{\circ,s}_{\text{gas}}$, and $V_{m,\text{liq}}^s$ are standard entropies and the molar volume of the solvent in liquid or gas phases (127.2 and 239.9 J/mol·K and 40.46 mL/mol, respectively, for MeOH), $V_{m,\text{gas}}$ is molar volume of the ideal gas at 25 °C (24450 mL/mol), V_m^o is molar volume of the solution corresponding to the standard conditions (1000 mL/mol). The enthalpies (H_s) and Gibbs free energies (G_s) in solution were estimated using the equations 5 and 6:

$$H_s = E_s(6-311+G^{**}) - E_g(6-311+G^{**}) + H_g(6-31+G^*) \quad (5)$$

$$G_s = H_s - TS_s \quad (6)$$

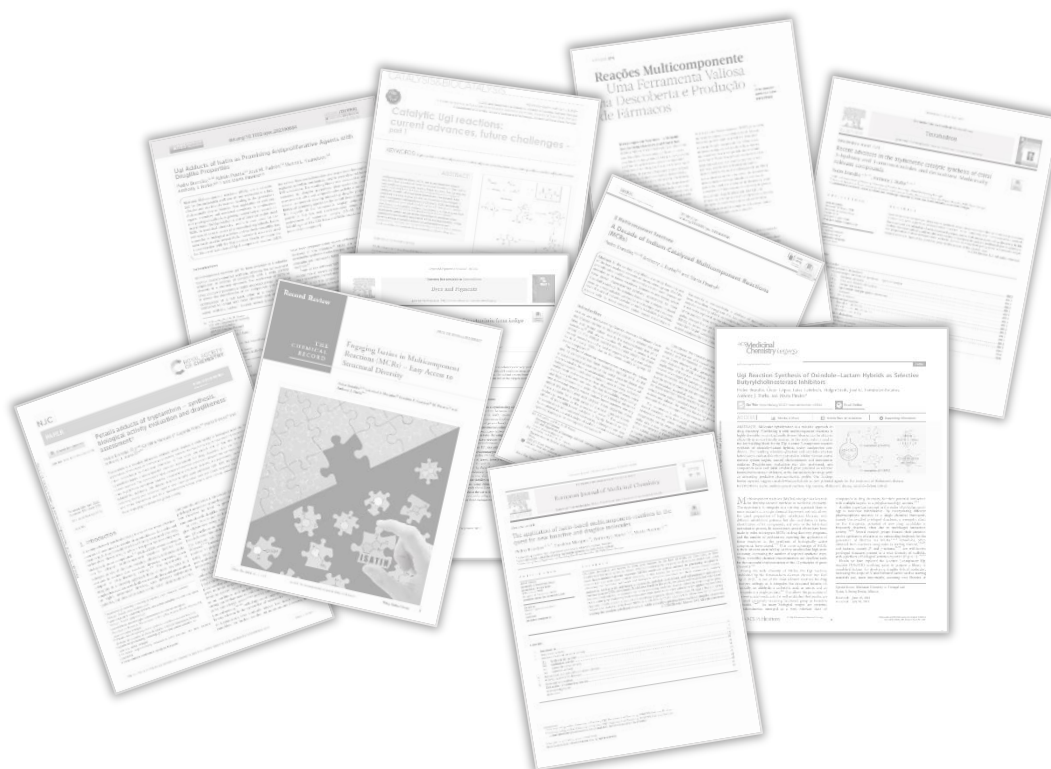
where E_s and E_g are the total energies in solution and the gas phase, and H_g is the gas-phase enthalpy calculated at the corresponding level. The Gibbs free energies in solution are discussed in this work.

6.5. References

1. Armarego, W. L. F.; Lin Chai, C. L., *Purification of Laboratory Chemicals*. 7th ed., Butterworth-Heinemann/Elsevier, Oxford, UK, **2013**.
2. Marques, C. S.; Burke, A. J., Enantioselective Rhodium(I)-Catalyzed Additions of Arylboronic Acids to *N*-1,2,3-Triazole-Isatin Derivatives: Accessing *N*-(1,2,3-Triazolmethyl)-3-hydroxy-3-aryloxindoles. *ChemCatChem*, **2016**, *8* (22), 3518-3526.
3. González, A.; Quirante, J.; Nieto, J.; Almeida, M. R.; Saraiva, M. J.; Planas, A.; Arsequell, G.; Valencia, G., Isatin derivatives, a novel class of transthyretin fibrillogenesis inhibitors. *Bioorganic & Medicinal Chemistry Letters*, **2009**, *19* (17), 5270-5273.
4. Kumar, S.; Wahi, A. K.; Singh, R., Synthesis and Preliminary Pharmacological Evaluation of 2-[4-(Aryl substituted)piperazin-1-yl]-*N*-phenylacetamides: Potential Antipsychotics. *Tropical Journal of Pharmaceutical Research*, **2011**, *10* (3), 265-272.
5. Kaicharla, T.; Yetra, S. R.; Roy, T.; Biju, A. T., Engaging isatins in solvent-free, sterically congested Passerini reaction. *Green Chemistry*, **2013**, *15* (6), 1608-1614.
6. Rainoldi, G.; Lesma, G.; Picozzi, C.; Lo Presti, L.; Silvani, A., One step access to oxindole-based -lactams through Ugi four-center three-component reaction. *RSC Advances*, **2018**, *8* (61), 34903-34910.
7. Kumar, A.; Tripathi, V. D.; Kumar, P., β -Cyclodextrin catalysed synthesis of tryptanthrin in water. *Green Chemistry*, **2011**, *13* (1), 51-54.
8. Onambele, L. A.; Riepl, H.; Fischer, R.; Pradel, G.; Prokop, A.; Aminake, M. N., Synthesis and evaluation of the antiparasmodial activity of tryptanthrin derivatives. *International Journal of Parasitology: Drugs and Drug Resistance*, **2015**, *5* (2), 48-57.
9. Ishiyama, T.; Murata, M.; Miyaura, N., Palladium(0)-Catalyzed Cross-Coupling Reaction of Alkoxydiboron with Haloarenes: A Direct Procedure for Arylboronic Esters. *The Journal of Organic Chemistry*, **1995**, *60* (23), 7508-7510.
10. Orellana, E. A.; Kasinski, A. L., Sulforhodamine B (SRB) Assay in Cell Culture to Investigate Cell Proliferation. *Bio-protocol*, **2016**, *6* (21), e1984.
11. Ellman, G. L.; Courtney, K. D.; Andres, V.; Featherstone, R. M., A new and rapid colorimetric determination of acetylcholinesterase activity. *Biochemical Pharmacology*, **1961**, *7* (2), 88-95.
12. Oliveira de Santana, Q. L.; Santos Evangelista, T. C.; Imhof, P.; Ferreira, S. B.; Fernández-Bolaños, J. G.; Sydnes, M. O.; Lopéz, Ó.; Lindbäck, E., Tacrine-sugar mimetic conjugates as enhanced cholinesterase inhibitors. *Organic & Biomolecular Chemistry*, **2021**, *19* (10), 2322-2337.
13. Affini, A.; Hagenow, S.; Zivkovic, A.; Marco-Contelles, J.; Stark, H., Novel indanone derivatives as MAO B/H₃R dual-targeting ligands for treatment of Parkinson's disease. *European Journal of Medicinal Chemistry*, **2018**, *148*, 487-497.
14. CLSI. Clinical and Laboratory Standard Institute, Reference Method for Dilution Antimicrobial Susceptibility Tests. Wayne, PA. Clin. Lab. Stand. Inst. 28. CLSI Document M07-A8 for bacteria, M27-A3 for yeasts and M38-A2 for filamentous fungi.

15. Zhao, Y.; Truhlar, D. G., The M06 suite of density functionals for main group thermochemistry, thermochemical kinetics, noncovalent interactions, excited states, and transition elements: two new functionals and systematic testing of four M06-class functionals and 12 other function. *Theoretical Chemistry Accounts*, **2008**, *120* (1-3), 215-241.
16. Frisch, M. J.; Trucks, G. W.; Schlegel, H. B.; Scuseria, G. E.; Robb, M. A.; Cheeseman, J. R.; Scalmani, V. B.; Mennucci, G. A. Petersson, H. Nakatsuji, M. Caricato, X. Li, H. P. Hratchian, A. F. Izmaylov, J. Bloino, G. Zheng, J. L. Sonnenberg, M. Hada, M. Ehara, K. Toyota, R. Fukuda, J. Hasegawa, M. Ishida, T. Nakajima, Y. Honda, O. Kitao, H. Nakai, T. Vreven, J. A. Montgomery, Jr., J. E. Peralta, F. Ogliaro, M. Bearpark, J. J. Heyd, E. Brothers, K. N. Kudin, V. N. Staroverov, R. Kobayashi, J. Normand, K. Raghavachari, A. Rendell, J. C. Burant, S. S. Iyengar, J. Tomasi, M. Cossi, N. Rega, J. M. Millam, M. Klene, J. E. Knox, J. B. Cross, V. Bakken, C. Adamo, J. Jaramillo, R. Gomperts, R. E. Stratmann, O. Yazyev, A. J. Austin, R. Cammi, C. Pomelli, J. W. Ochterski, R. L. Martin, K. Morokuma, V. G. Zakrzewski, G. A. Voth, P. Salvador, J. J. Dannenberg, S. Dapprich, A. D. Daniels, Ö. Farkas, J. B. Foresman, J. V. Ortiz, J. Cioslowski, and D. J. Fox, Gaussian 09, Revision D.01. *Gaussian 09, Revision D.01*, **2009**, Wallingford CT.
17. Fukui, K., The path of chemical reactions - the IRC approach. *Accounts of Chemical Research*, **1981**, *14* (12), 363-368.
18. Gonzalez, C.; Schlegel, H. B., An improved algorithm for reaction path following. *The Journal of Chemical Physics*, **1989**, *90* (4), 2154-2161.
19. Gonzalez, C.; Schlegel, H. B., Improved algorithms for reaction path following: Higher-order implicit algorithms. *The Journal of Chemical Physics*, **1991**, *95* (8), 5853-5860.
20. Gonzalez, C.; Schlegel, H. B., Reaction path following in mass-weighted internal coordinates. *The Journal of Physical Chemistry*, **1990**, *94* (14), 5523-5527.
21. Tomasi, J.; Persico, M., Molecular Interactions in Solution: An Overview of Methods Based on Continuous Distributions of the Solvent. *Chemical Reviews*, **1994**, *94* (7), 2027-2094.
22. Wertz, D. H., Relationship between the gas-phase entropies of molecules and their entropies of solvation in water and 1-octanol. *Journal of the American Chemical Society*, **1980**, *102* (16), 5316-5322.
23. Cooper, J.; Ziegler, T., A Density Functional Study of SN2 Substitution at Square-Planar Platinum(II) Complexes. *Inorganic Chemistry*, **2002**, *41* (25), 6614-6622.

Appendices



Appendix 1

Tetrahedron 74 (2018) 4927–4957



Contents lists available at ScienceDirect

Tetrahedron

journal homepage: www.elsevier.com/locate/tet

Tetrahedron report 1171

Recent advances in the asymmetric catalytic synthesis of chiral 3-hydroxy and 3-aminooxindoles and derivatives: Medicinally relevant compounds

Pedro Brandão ^{a, b, **}, Anthony J. Burke ^{b, c, *}

^a CQC and Department of Chemistry, University of Coimbra, Rua Larga, 3004-535 Coimbra, Portugal

^b Centro de Química de Évora, Institute for Research and Advanced Studies, University of Évora, Rua Romão Ramalho, 7000 Évora, Portugal

^c Department of Chemistry, School of Science and Technology, University of Évora, Rua Romão Ramalho, 7000 Évora, Portugal



ARTICLE INFO

Article history:

Received 29 March 2018

Received in revised form

1 June 2018

Accepted 5 June 2018

Available online 11 June 2018

Keywords:

3-Hydroxyoxindole

3-Aminooxindole

Asymmetric catalysis

Organocatalysis

ABSTRACT

Several oxindole derivatives, of natural or synthetic origin, have been identified as medicinally appealing compounds, with a plethora of bioactivities reported. Chiral 3-hydroxy and 3-aminooxindole scaffolds have captured the attention of several research groups, due to their importance in drug discovery. In this review, we systematically address the wide variety of asymmetric catalytic methodologies employed in the preparation of these relevant chiral scaffolds, present in many biologically active compounds and/or natural products. Special focus will be given to the nature of the catalyst used.

© 2018 Elsevier Ltd. All rights reserved.

Graphical abstract



Reproduced with the permission of Elsevier.

For further reading, please use the link:

<https://doi.org/10.1016/j.tet.2018.06.015>

Appendix 2

Triptantrina: da Natureza ao Laboratório

>
Daniela Pinheiro
Pedro Brandão
J. Sérgio Seixas de Melo
Marta Pineiro*

Tryptanthrin: from Nature to the Laboratory.
Tryptanthrin is an indoloquinazoline alkaloid, present in several natural sources, particularly in plants. Used since ancient times for its anti-inflammatory, antipyretic and analgesic activities, today its biological properties continue to be subject of intense study. The interest in the development of various applications of tryptanthrin has stimulated the growth of several synthetic pathways and the in-depth study of its unique photophysical, photochemical and redox properties. Tryptanthrin is an example of the many natural products with unique properties and relevant biological activity that demonstrates the importance of preserving natural sources, as guardians of knowledge.

A triptantrina é um alcaloide indoloquinazolinico, presente em diversas fontes naturais, especialmente em diversas espécies vegetais. Utilizada desde a antiguidade pela sua atividade anti-inflamatória, antipirética e analgésica, as suas propriedades biológicas continuam a ser alvo de intenso estudo. A investigação das diversas aplicações da triptantrina impulsionou o desenvolvimento de vários métodos de síntese e o estudo aprofundado das suas propriedades, nomeadamente fotofísicas, fotoquímicas e redox. A triptantrina é um exemplo das muitas moléculas presentes na natureza, com propriedades únicas e com atividade biológica relevante, o que demonstra a importância de se preservarem os recursos naturais.

Reproduced with the permission of Química – Boletim da Sociedade Portuguesa de Química.

For further reading, please use the link:

DOI: 10.52590/M3.P697.A30002440

Appendix 3

Reações Multicomponente – Uma Ferramenta Valiosa na Descoberta e Produção de Fármacos

>
Pedro Brandão*
Anthony J. Burke
Marta Piñeiro

Multicomponent Reactions – a Valuable Tool for Drug Discovery and Production.

Multicomponent reactions (MCRs) allow the combination, in one step, of three or more reactants in one product, being a very useful tool for the generation of new compound libraries since they lead to a wide structural diversity. These reactions are characterized by their high atom economy, hence being excellent models for sustainable chemistry methodologies throughout the drug discovery, development, and production process, inclusively being applied in the synthesis of commercialized drugs, with a considerable reduction in the number of synthetic steps. The application of MCRs in drug synthesis is clear with the large number of reports published recently, and herein we explore in further detail some of these examples.

As reações multicomponente (RMC) permitem, num único passo, a combinação de três ou mais reagentes num só produto, pelo que a sua aplicação na geração de bibliotecas de novos compostos é muito útil, uma vez que conduzem a uma grande diversidade estrutural. Estas reações são caracterizadas pela sua elevada economia atómica e são, por isso, excelentes ferramentas para o desenvolvimento de metodologias de química sustentável durante o processo de descoberta, desenvolvimento e produção de fármacos, podendo conduzir à síntese de fármacos, com considerável diminuição do número de passos reacionais. A aplicabilidade das RMC na síntese de fármacos é bem evidente no elevado número de exemplos que se encontram na literatura científica, alguns deles explorados em mais detalhe neste trabalho.

Reproduced with the permission of Química – Boletim da Sociedade Portuguesa de Química.

For further reading, please use the link:

DOI: 10.52590/M3.P694.A30002331

Appendix 4

CATALYSIS&BIOCATALYSIS

PEDRO BRANDÃO^{1,2}, ANTHONY J. BURKE³

1. CQC and Department of Chemistry, University of Coimbra, Coimbra, Portugal

2. Centro de Química de Évora, Institute for Research and Advanced Studies, University of Évora, Évora, Portugal

3. Department of Chemistry, School of Science and Technology, University of Évora, Évora, Portugal

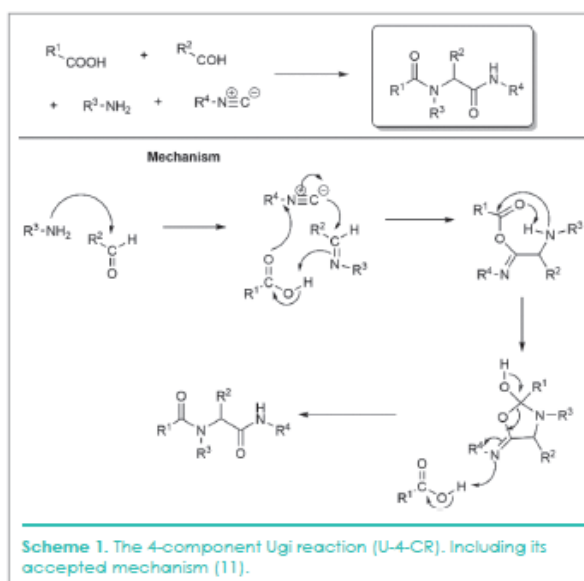


Catalytic Ugi reactions: current advances, future challenges - part 1

KEYWORDS: Ugi reaction, metal catalysis, non-metal catalysis, multicomponent reactions, peptides, sustainable processes.

ABSTRACT

Multicomponent reactions (MCRs) are a very important class of reactions that are used with ever increasing frequency in the hunt for new medicinal compounds. Among these reactions, the Ugi reaction holds a special place, as it can be catalyzed by various types of catalysts. As part 1 of a two series short review (the second to be published in a later review) we discuss advances in the catalytic 3- and 4-component Ugi reactions (U-3-CR and U-4-CR, respectively) using metal and non-metal catalytic systems (in the second review we discuss: nano-catalytic systems, biocatalysis and the progress that has been made to date in the development of the catalytic asymmetric version, as well as the application of continuous flow systems and the industrial application of this exciting reaction). In this review a strong emphasis is placed on sustainable and non-conventional methods, such as microwaves, unconventional solvents (such as water and deep-eutectic-solvents) and ball-milling, etc..



Reproduced with the permission of TKS.

For further reading, please use the link:

https://www.teknoscienze.com/tks_article/catalytic-ugi-reactions-current-advances-future-challenges-part-1/

Appendix 5

CATALYSIS & BIOCATALYSIS



PEDRO BRANDÃO^{1,2}, ANTHONY J. BURKE^{2,3*}

*Corresponding author

1. CQC and Department of Chemistry, Coimbra, Portugal

2. Centro de Química de Évora, Institute for Research and Advanced Studies, University of Évora, Évora, Portugal

3. Department of Chemistry, School of Science and Technology, University of Évora, Évora, Portugal

Catalytic Ugi reactions: Current advances, future challenges - Part 2

KEYWORDS: Ugi reaction, biocatalysis, enantioselectivity, continuous flow, chiral phosphoric acid organocatalysts.

ABSTRACT

Multicomponent reactions (MCRs) are a very important class of reactions that are considerably useful in the quest for new medicines and, within this category, the Ugi-MCR holds a special place. In part 2 of this series (the first was previously published) we discuss advances in the catalytic 3- and 4-component Ugi reactions (U-3-CR and U-4-CR, respectively) as regards to nanocatalysis, biocatalysis, asymmetric catalysis with organocatalysts, as well as continuous manufacturing methods such as, continuous-flow processes. Again, in this review there is a strong focus on green and sustainable versions of this important reaction. To conclude this report, the operation and implications (both presently and in the future) of this versatile and enabling reaction in the pharmaceutical industry are discussed.

Reproduced with the permission of TKS.

For further reading, please use the link:

https://www.teknoscienze.com/tks_article/recent-advances-in-toxicological-science-bioinformatics-and-biology-have-provided-means-to-transform-the-traditional-toxicology-based-mainly-on-animal-experimental-studies-into-a-predictiv/

Appendix 6

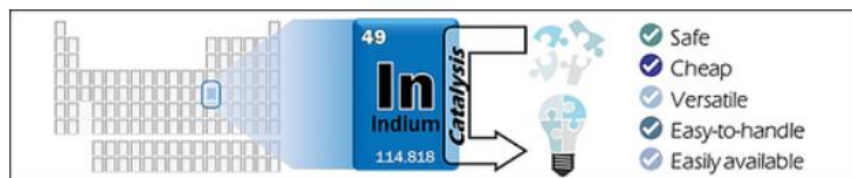
Multicomponent Reactions

A Decade of Indium-Catalyzed Multicomponent Reactions (MCRs)

Pedro Brandão,^{*[a,b]} Anthony J. Burke,^[b] and Marta Pineiro^[a]

Abstract: In the context of synthetic chemistry, Indium is one of the least explored elements of the notorious group 13 of the periodic table and has not attracted quite the same amount of attention as its fellow members, Aluminium and Boron, which have shown unprecedented synthetic applications for more than half a century. Nonetheless, Indium has emerged in recent years as a very valuable catalyst for multicomponent reactions. From the use of indium powder or easily accessible and cheap indium salts to more complex indium-based metal-organic

frameworks or nanoparticles, a plethora of applications has been described throughout this last decade, showcasing not only the versatility of indium catalysis but also how much there is still to be explored. In the aftermath of the international year of the periodic table of the chemical elements in 2019, we navigated through the large inventory of multicomponent reactions (MCRs) to encounter the types of useful reactions leading to important target compounds (many of which are biologically active) catalyzed by this *d*-block post-transition metal.



Reproduced with the permission of John Wiley and Sons.

For further reading, please use the link:

<https://doi.org/10.1002/ejoc.202000596>

Appendix 7

Record Review

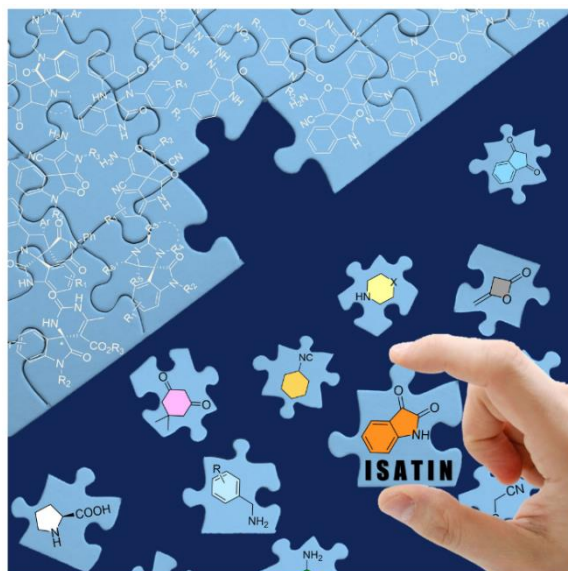
THE
CHEMICAL
RECORD

DOI: 10.1002/tcr.202000167

Engaging Isatins in Multicomponent
Reactions (MCRs) – Easy Access to
Structural DiversityPedro Brandão,^[a,b] Carolina S. Marques,^[b] Elisabete P. Carreiro,^[b] M. Pineiro,^[a] and
Anthony J. Burke^[b,c]

Abstract: Multicomponent reactions (MCRs) are a valuable tool in diversity-oriented synthesis. Its application to privileged structures is gaining relevance in the fields of organic and medicinal chemistry. Isatin, due to its unique reactivity, can undergo different MCRs, affording multiple interesting scaffolds, namely oxindole-derivatives (including spirooxindoles, bis-oxindoles and 3,3-disubstituted oxindoles) and even, under certain conditions, ring-opening reactions occur that leads to other heterocyclic compounds. Over the past few years, new methodologies have been described for the application of this important and easily available starting material in MCRs. In this review, we explore these novelties, displaying them according to the structure of the final products obtained.

Keywords: isatin, multicomponent reactions, spirooxindoles, bis-oxindoles, 3,3-disubstituted oxindoles, oxindole, sustainability, catalysis, nanocatalysts, diversity oriented synthesis



Reproduced with the permission of John Wiley and Sons.

For further reading, please use the link:

<https://doi.org/10.1002/tcr.202000167>

Appendix 8



Contents lists available at ScienceDirect

European Journal of Medicinal Chemistry

journal homepage: <http://www.elsevier.com/locate/ejmech>

Review article

The application of isatin-based multicomponent-reactions in the quest for new bioactive and druglike molecules

Pedro Brandão^{a, b, *}, Carolina Marques^b, Anthony J. Burke^{b, c}, Marta Pineiro^{a, **}^a University of Coimbra, CQC, Department of Chemistry, 3004-535, Coimbra, Portugal^b LAQV-REQUIMTE, University of Évora, Rua Romão Ramalho, 59, 7000, Évora, Portugal^c University of Évora, Department of Chemistry, Rua Romão Ramalho, 59, 7000, Évora, Portugal

ARTICLE INFO

Article history:

Received 16 November 2020

Received in revised form

9 December 2020

Accepted 10 December 2020

Available online 18 December 2020

Keywords:

Multicomponent reactions

Isatin

Oxindole

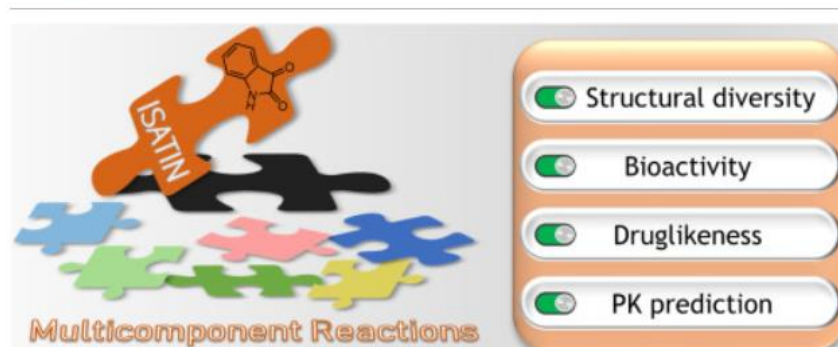
Bioactive compounds

ABSTRACT

Oxindole derivatives are known for their great interest in the field of Medicinal Chemistry, as they display vast biological activities. Recent efforts concerning the preparation of oxindole derivatives using isatin-based multicomponent reactions (MCRs) constitute a great advance in generating druglike libraries fast and with wide scaffold diversity. In this review, we address those recent developments, exploring the synthetic pathways and biological activities described for these compounds, namely antitumor, antibacterial, antifungal, antiparasitic, antiviral, antioxidant, anti-inflammatory and central nervous system (CNS) pathologies. To add new depth to this work, we used a well-established web-based free tool (SwissADME) to evaluate the most promising scaffolds in what concerns their druglike properties, namely by evaluating their compliance with some of the most valuable rules applied by medicinal chemists in both academia and industrial settings (Lipinski, Ghose, Veber, Egan, Muegge). The aim of this review is to endorse isatin-based MCRs as a valuable synthetic approach to attain new hit compounds bearing the oxindole privileged structure, while critically exploring these scaffolds' druglike properties.

© 2020 Elsevier Masson SAS. All rights reserved.

Graphical abstract



Reproduced with the permission of Elsevier.

For further reading, please use the link:

<https://doi.org/10.1016/j.ejmech.2020.113102>

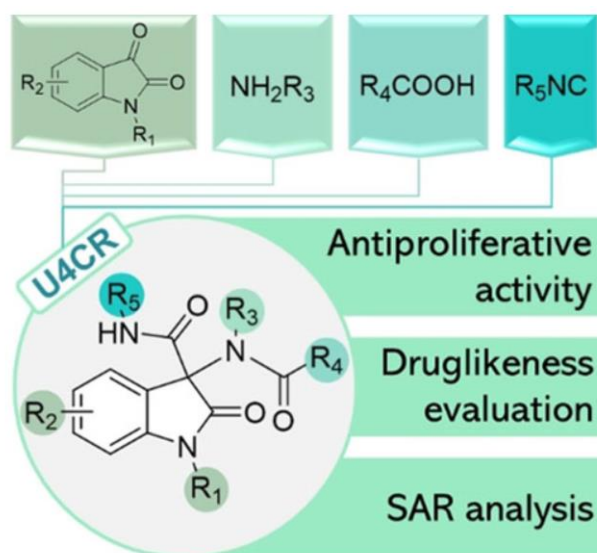
Appendix 9

Ugi Adducts of Isatin as Promising Antiproliferative Agents with Druglike Properties

Pedro Brandão,^[a, b] Adrián Puerta,^[c] José M. Padrón,^[c] Maxim L. Kuznetsov,^[d]
Anthony J. Burke,^{*[b, e]} and Marta Pineiro^{*[a]}

Abstract: Multicomponent reactions (MCRs) are a valuable tool for the sustainable synthesis of new molecules in a fast, effective and eco-friendly manner, leading to the generation of structurally diverse libraries. Their application in synthetic organic chemistry and medicinal chemistry, in combination with privileged scaffolds, is gaining momentum in recent years. The Ugi reaction is one of the most widely used MCRs in medicinal chemistry, and it is even used for the synthesis of several active pharmaceutical ingredients. Isatin, known for its biological activities and synthetic versatility, has been vastly used in several MCRs, however it was rarely used in combination with the Ugi reaction. Herein we report the first library of isatin-based Ugi 4 component reaction (U4CR)

derivatives. Reaction optimization and scope were thoroughly explored, as well as mechanistic insights were obtained using DFT calculations. The resulting library was evaluated in what concerns its druglike properties, pharmacokinetic profile assessment *in silico* and antiproliferative activity *in vitro*, with several compounds bearing interesting druglike properties. Biological screening against six tumor cell lines, showed that the majority of the compounds display antiproliferative activity in the low and sub-micromolar range, with the achievement of nanomolar activity (0.1 nM, 6.5 nM and 5.4 nM against HBL-100, HeLa and WiDr, respectively) for the more active compound.



Reproduced with the permission of John Wiley and Sons.

For further reading, please use the link:

<https://doi.org/10.1002/ajoc.202100684>

Appendix 10

Ugi Reaction Synthesis of Oxindole–Lactam Hybrids as Selective Butyrylcholinesterase Inhibitors

Pedro Brandão, Óscar López, Luisa Leitzbach, Holger Stark, José G. Fernández-Bolaños, Anthony J. Burke, and Marta Pineiro*

Cite This: <https://doi.org/10.1021/acsmedchemlett.1c00344>

Read Online

ACCESS |

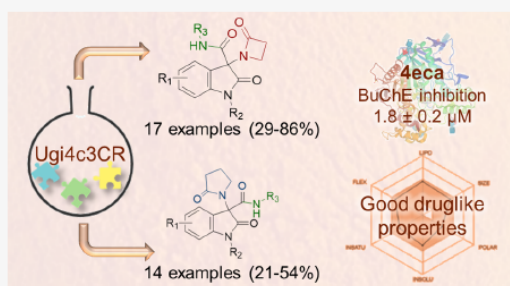
Metrics & More

Article Recommendations

Supporting Information

ABSTRACT: Molecular hybridization is a valuable approach in drug discovery. Combining it with multicomponent reactions is highly desirable, since structurally diverse libraries can be attained efficiently in an eco-friendly manner. In this work, isatin is used as the key building block for the Ugi 4-center 3-component reaction synthesis of oxindole–lactam hybrids, under catalyst-free conditions. The resulting oxindole– β -lactam and oxindole– γ -lactam hybrids were evaluated for their potential to inhibit relevant central nervous system targets, namely cholinesterases and monoamine oxidases. Druglikeness evaluation was also performed, and compounds 4eca and 5dab exhibited great potential as selective butyrylcholinesterase inhibitors, at the low micromolar range, with an interesting predictive pharmacokinetic profile. Our findings herein reported suggest oxindole–lactam hybrids as new potential agents for the treatment of Alzheimer's disease.

KEYWORDS: Isatin, multicomponent reactions, Ugi reaction, Alzheimer's disease, oxindole–lactam hybrids



Reproduced with the permission of American Chemical Society.

For further reading, please use the link:

<https://doi.org/10.1021/acsmedchemlett.1c00344>

Appendix 11



Contents lists available at ScienceDirect

Dyes and Pigments

journal homepage: <http://www.elsevier.com/locate/dyepig>

I₂/NaH/DMF as oxidant *trio* for the synthesis of tryptanthrin from indigo or isatin

Pedro Brandão^{a,b}, Daniela Pinheiro^a, J. Sérgio Seixas de Melo^a, Marta Pineiro^{a,*}

^a CQC and Department of Chemistry, University of Coimbra, Rua Larga, 3004-535, Coimbra, Portugal

^b Centro de Química de Évora, Institute for Research and Advanced Studies, University of Évora, Rua Romão Ramalho, 7000, Évora, Portugal

ARTICLE INFO

Keywords:
Tryptanthrin
DMF
Oxidation
Isatin
Indigo

ABSTRACT

Tryptanthrin, a product present in several natural sources used as colorants and very relevant in the field of Medicinal Chemistry, was synthesized from indigo and isatin under mild conditions using microwave irradiation. A plausible mechanism for the synthesis of tryptanthrin using the oxidant system formed by iodine, sodium hydride and DMF, the latter acting with dual activity as solvent and as the oxygen source, is proposed.

Graphical abstract



Reproduced with the permission of Elsevier.

For further reading, please use the link:

<https://doi.org/10.1016/j.dyepig.2019.107935>

Appendix 12


NJC

PAPER

View Article Online
View Journal

Cite this: DOI: 10.1039/d1nj02079j

Petasis adducts of tryptanthrin – synthesis, biological activity evaluation and druglikeness assessment†

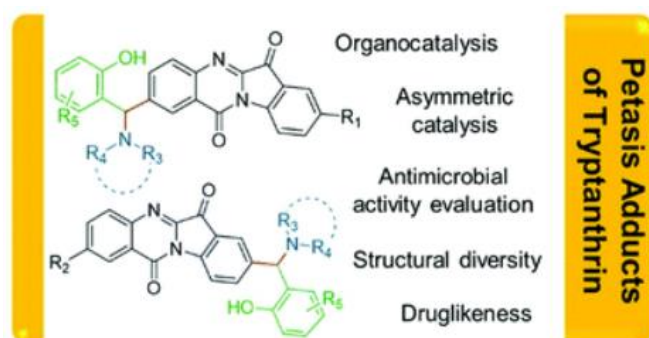
Pedro Brandão,[†]  ^{*,ab} Carolina Marques,[†]  ^b Eugénia Pinto,^{cd} Marta Pineiro^a and Anthony J. Burke  ^{*,be}

Tryptanthrin is a valuable tetracyclic alkaloid, which displays a wide variety of biological activities. The application of this type of scaffold as a starting material for the discovery of new drug candidates is of major importance in medicinal chemistry. In this work, we report one of the few examples of tryptanthrin-based multicomponent reaction approaches for drug discovery, and the first using the Petasis reaction. The optimized BINOL-catalyzed reaction conditions allowed the synthesis of a library of new tryptanthrin derivatives bearing considerable structural diversity. An asymmetric version was also established, achieving the desired enantiomerically pure derivative with 99% ee and 71% yield. The resulting library was screened against one Gram-positive and one Gram-negative bacteria, two yeasts, and three filamentous and four dermatophyte fungal strains with clinical relevance, with compound 5bea displaying moderate fungicidal activity.

Received 28th April 2021,
Accepted 30th June 2021

DOI: 10.1039/d1nj02079j

rsc.li/njc



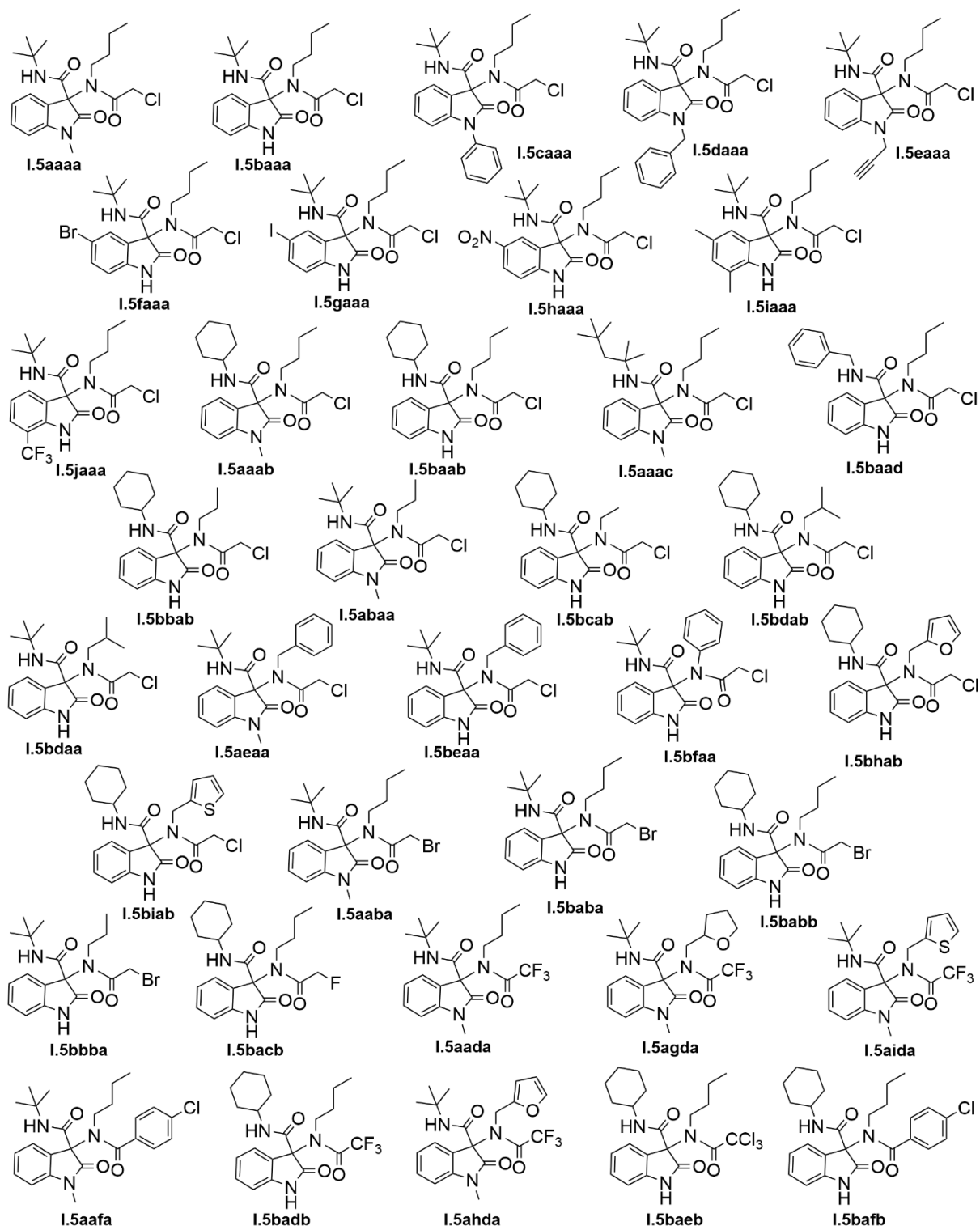
Reproduced with the permission of Centre National de la Recherche Scientifique (CNRS) and the Royal Society of Chemistry..

For further reading, please use the link:

<https://doi.org/10.1039/D1NJ02079J>

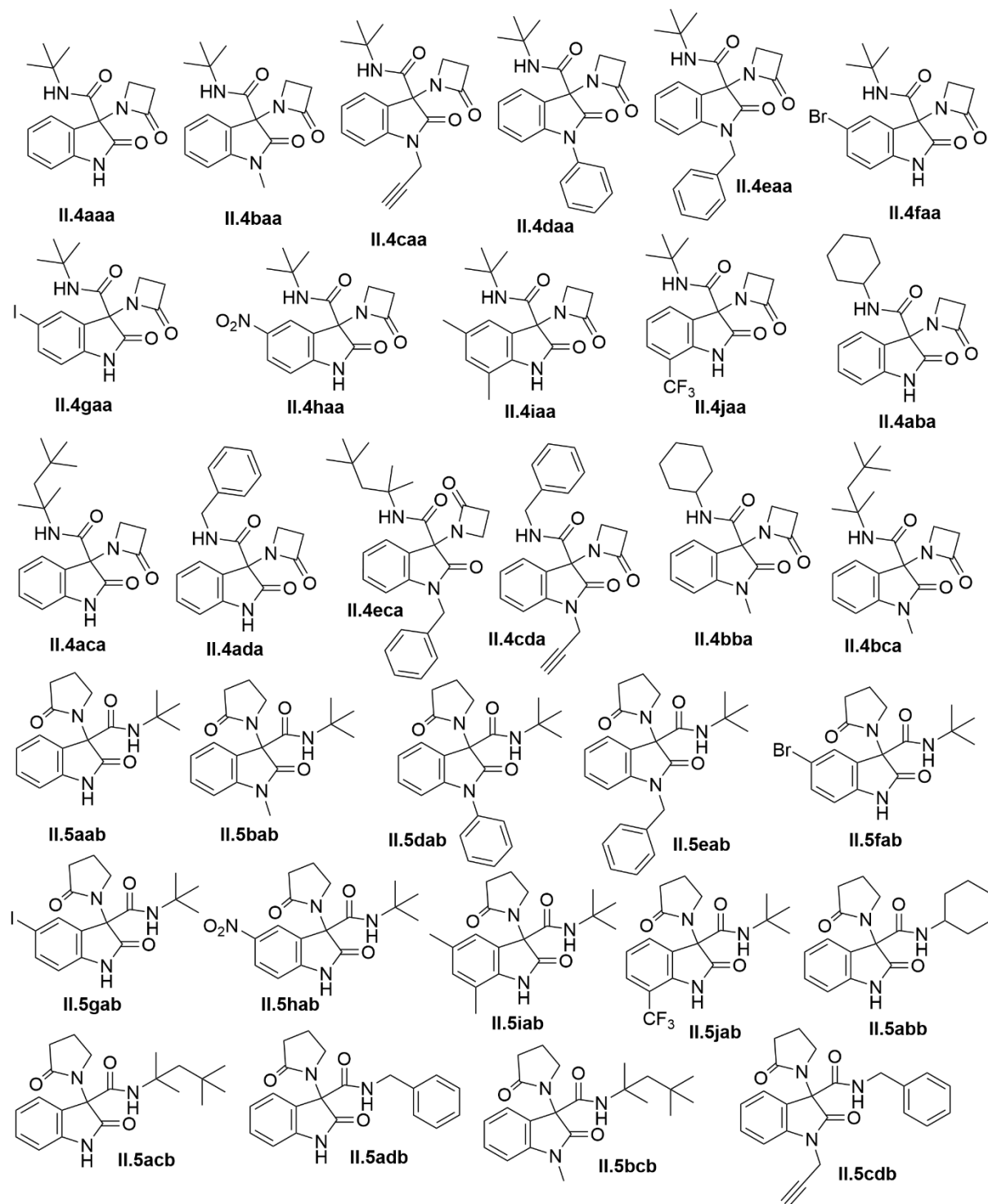
Appendix 13

Library I (Chapter 2)



Appendix 14

Library II (Chapter 3)



Appendix 15

Library III (Chapter 4)

